PARTICLE PHYSICS SUMMARY*

A Digest of the *1996 Review of Particle Physics*
Particle Data Group

R.M. Barnett, C.D. Carone, D.E. Groom, T.G. Trippe, and C.G. Wohl
Technical Associates: B. Armstrong, P.S. Gee, and G.S. Wagman†
Physics Division, Lawrence Berkeley National Laboratory, 1 Cyclotron Road, Berkeley, CA 94720, USA

F. James, M. Mangano, K. Mönig, and L. Montanet
CERN, European Laboratory for Particle Physics, CH-1211 Genève 23, Switzerland

J.L. Feng‡ and H. Murayama
Physics Division, Lawrence Berkeley National Laboratory, 1 Cyclotron Road, Berkeley, CA 94720, USA; and Department of Physics, University of California, Berkeley, CA 94720, USA

J.J. Hernández
IFIC — Instituto de Física Corpuscular, Universitat de València — C.S.I.C., E-46100 Burjassot, València, Spain; and CERN

A. Manohar
Department of Physics, University of California at San Diego, La Jolla, CA 92093, USA

M. Aguilar-Benitez
C.I.E.M.A.T., E-28040, Madrid, Spain; and CERN

C. Caso
Dipartimento di Fisica e INFN, Università di Genova, I-16146 Genova, Italy

R.L. Crawford
Department of Physics and Astronomy, University of Glasgow, Glasgow G12 8QQ, Scotland

M. Roos
Physics Department, PB 9, FIN-00014 University of Helsinki, Finland

N.A. Törnqvist
Research Institute of High Energy Physics, PB 9, FIN-00014 University of Helsinki, Finland

K.G. Hayes
Department of Physics, Hillsdale College, Hillsdale, MI 49242, USA

K. Hagiwara, K. Nakamura, and M. Tanabashi
KEK, National Laboratory for High Energy Physics, Oho, Tsukuba-shi, Ibaraki-ken 305, Japan

K. Olive
School of Physics and Astronomy, University of Minnesota, Minneapolis, MN 55455, USA

K. Honscheid
Department of Physics, Ohio State University, Columbus, OH 43210 USA

P.R. Burchat
Department of Physics, Stanford University, Stanford, CA 94305, USA

R.E. Shrock
Institute for Theoretical Physics, State University of New York, Stony Brook, NY 11794, USA

S. Eidelman
Institute of Nuclear Physics, SU-630090, Novosibirsk, Russia

R.H. Schindler
Stanford Linear Accelerator Center, Stanford, CA 94309, USA

A. Gurtu
Tata Institute of Fundamental Research, Bombay 400 005, India; and CERN

K. Hikasa
Physics Department, Tohoku University, Aoba-ku, Sendai 980-77, Japan

G. Conforto
Università degli Studi, I-61029 Urbino, Italy; Istituto Nazionale di Fisica Nucleare, Sezione di Firenze, I-50125 Firenze, Italy

R.L. Workman
Department of Physics, Virginia Polytechnic Institute and State University, Blacksburg, VA 24061, USA

C. Grab
Institute for High Energy Physics, ETH-Hönggerberg, CH-8093 Zürich, Switzerland

C. Amsler
Institute of Physics, University of Zürich, CH-8057 Zürich, Switzerland

Abstract

This report summarizes the highlights of the 1996 *Review of Particle Physics* (Phys. Rev. **D54**, 1 (1996)). Using data from previous editions, plus 1900 new measurements from 700 papers, we list, evaluate, and average measured properties of gauge bosons, leptons, quarks, mesons, and baryons. We summarize searches for hypothetical particles such as Higgs bosons, heavy neutrinos, and supersymmetric particles. We also give numerous reviews, tables, figures, and formulae. The present edition marks the apparent completion of the table of Standard Model quarks with the discovery of the top. A booklet is available containing the Summary Tables and abbreviated versions of some of the other sections of the full *Review.*

*The publication of the *Review of Particle Physics* is supported by the Director, Office of Energy Research, Office of High Energy and Nuclear Physics, the Division of High Energy Physics of the U.S. Department of Energy under Contract No. DE–AC03–76SF00098; by the U.S. National Science Foundation under Agreement No. PHY-9320551; by the European Laboratory for Particle Physics (CERN); by an implementing arrangement between the governments of Japan (Monbusho) and the United States (DOE) on cooperative research and development; and by the Italian National Institute of Nuclear Physics (INFN).

†Deceased. A tribute to Gary Wagman may be found in Phys. Rev. **D54**, 3 (1996) or visit our WWW memorial on `http://pdg.lbl.gov/wagman_memorial.html`.

‡Jonathan Feng acknowleges support from the Miller Institute for Basic Research in Science.

Special thanks are due to our administrative assistant at LBNL, Gail Harper, for her careful proofreading of the text, layout, and graphics in this *Review.*

TABLE OF CONTENTS

Introduction 614

The Particle Summary Tables
Gauge and Higgs Bosons 615
Leptons 617
Quarks 620
Mesons 621
Baryons 642
Searches 652
Tests of Conservation Laws 653

Constants, Units, Atomic and Nuclear Properties
Physical Constants (rev.) 655
Astrophysical Constants 656
Atomic and Nuclear Properties of Materials (rev.) 658

Standard Model and Related Topics
Quantum Chromodynamics (rev.) 660
Standard Model of Electroweak Interactions (rev.) 668
Cabibbo-Kobayashi-Maskawa Mixing Matrix (rev.) 677
Quark Model 681

Particle Properties
The Top Quark 685
Pseudoscalar-Meson Decay Constants 688
Production and Decay of b-flavored Hadrons 689
Quark Masses 693

Neutrino Physics
Solar Neutrinos 697

Hypothetical Particles
The Higgs Boson 699
Supersymmetry 701
Non-$q\bar{q}$ Mesons 706

Astrophysics and Cosmology
Big-bang Cosmology 708
Big-bang Nucleosynthesis (new) 710
The Hubble Constant (new) 713
Dark Matter (rev.) 717
Cosmic Background Radiation (new) 719
Cosmic Rays (new) 723

Cross-section Plots
Hadron Nucleon and γp 729

Rare/Hypothetical Processes and Particles
Rare Kaon Decays 730
CP Violation 732

INTRODUCTION

The *Review of Particle Physics* and the abbreviated version, the *Particle Physics Booklet,* are reviews of the field of Particle Physics. This complete *Review* includes a compilation/evaluation of data on particle properties, called the "Particle Listings." These Listings include 1900 new measurements from 700 papers, in addition to the 14,000 measurements from 4000 papers that first appeared in previous editions.

Both books include Summary Tables with our best values and limits for particle properties such as masses, widths or lifetimes, and branching fractions, as well as an extensive summary of searches for hypothetical particles. In addition, we give a long section of "Reviews, Tables, and Plots" on a wide variety of theoretical and experimental topics, a quick reference for the practicing particle physicist.

The *Review* and the *Booklet* are published in even-numbered years. This edition is an updating through December 1995 (and, in some areas, well into 1996). As described in the section "Using Particle Physics Databases" following this introduction, the content of this *Review* is available on the World-Wide Web, and is updated between printed editions (`http://pdg.lbl.gov/`).

The Summary Tables give our best values of the properties of the particles we consider to be well established, a summary of search limits for hypothetical particles, and a summary of experimental tests of conservation laws.

The Particle Listings contain all the data used to get the values given in the Summary Tables. Other measurements considered recent enough or important enough to mention, but which for one reason or another are not used to get the best values, appear separately just beneath the data we do use for the Summary Tables. The Particle Listings also give information on unconfirmed particles and on particle searches, as well as short "reviews" on subjects of particular interest or controversy.

The Particle Listings were once an archive of all published data on particle properties. This is no longer possible because of the large quantity of data. We refer interested readers to earlier editions for data now considered to be obsolete.

We organize the particles into six categories:

Gauge and Higgs bosons
Leptons
Quarks
Mesons
Baryons
Searches for monopoles,
supersymmetry, compositeness, *etc.*

The last category only includes searches for particles that do not belong to the previous groups; searches for heavy charged leptons and massive neutrinos, by contrast, are with the leptons.

The accuracy and usefulness of this *Review* depend in large part on interaction between its users and the authors. We appreciate comments, criticisms, and suggestions for improvements of any kind. Please send them to the appropriate author, or to the LBNL addresses below.

To order a copy of the *Review* or the *Particle Physics Booklet* from North and South America, Australia, and the Far East, write to

Particle Data Group, MS 50-308
Lawrence Berkeley National Laboratory
Berkeley, CA 94720, USA

or send e-mail to `PDG@LBL.GOV`.

To order more than one copy of the *Review* or booklet, write to

c/o Anne Fleming
Technical Information Division, MS 50B-4206
Lawrence Berkeley National Laboratory
Berkeley, CA 94720, USA

or send e-mail to `ASFLEMING@LBL.GOV`.

From all other areas, write to

CERN Scientific Information Service
CH-1211 Geneva 23
Switzerland

or via the WWW from CERN (`http://www.cern.ch`)
Scientific Information Service
Ordering CERN publications

SUMMARY TABLES OF PARTICLE PROPERTIES

July 1996

Particle Data Group

R.M. Barnett, C.D. Carone, D.E. Groom, T.G. Trippe, C.G. Wohl, B. Armstrong*, P.S. Gee*, G.S. Wagman*†, F. James, M. Mangano, K. Mönig, L. Montanet, J.L. Feng, H. Murayama, J.J. Hernández, A. Manohar, M. Aguilar-Benitez, C. Caso, R.L. Crawford, M. Roos, N.A. Törnqvist, K.G. Hayes, K. Hagiwara, K. Nakamura, M. Tanabashi, K. Olive, K. Honscheid, P.R. Burchat, R.E. Shrock, S. Eidelman, R.H. Schindler, A. Gurtu, K. Hikasa, G. Conforto, R.L. Workman, C. Grab, and C. Amsler

*Technical Associate

†Deceased

(Approximate closing date for data: January 1, 1996)

GAUGE AND HIGGS BOSONS

γ

$I(J^{PC}) = 0,1(1^{--})$

Mass $m < 6 \times 10^{-16}$ eV, CL = 99.7%
Charge $q < 5 \times 10^{-30}$ e
Mean life τ = Stable

g or gluon

$I(J^{P}) = 0(1^{-})$

Mass $m = 0$ [a]
SU(3) color octet

W

$J = 1$

Charge = ± 1 e
Mass $m = 80.33 \pm 0.15$ GeV
$m_Z - m_W = 10.85 \pm 0.15$ GeV
$m_{W^+} - m_{W^-} = -0.2 \pm 0.6$ GeV
Full width $\Gamma = 2.07 \pm 0.06$ GeV

W^- modes are charge conjugates of the modes below.

W^+ DECAY MODES		Fraction (Γ_i/Γ)	Confidence level	p (MeV/c)
$\ell^+\nu$	[b]	(10.8±0.4) %		40110
$e^+\nu$		(10.8±0.4) %		40110
$\mu^+\nu$		(10.4±0.6) %		40110
$\tau^+\nu$		(10.9±1.0) %		40110
hadrons		(67.9±1.5) %		–
$\pi^+\gamma$		$< 5 \times 10^{-4}$	95%	40110

Z

$J = 1$

Charge = 0
Mass $m = 91.187 \pm 0.007$ GeV [c]
Full width $\Gamma = 2.490 \pm 0.007$ GeV
$\Gamma(\ell^+\ell^-) = 83.83 \pm 0.27$ MeV [b]
Γ(invisible) $= 498.3 \pm 4.2$ MeV [d]
Γ(hadrons) $= 1740.7 \pm 5.9$ MeV
$\Gamma(\mu^+\mu^-)/\Gamma(e^+e^-) = 1.000 \pm 0.005$
$\Gamma(\tau^+\tau^-)/\Gamma(e^+e^-) = 0.998 \pm 0.005$ [e]

Average charged multiplicity

$\langle N_{charged} \rangle = 20.99 \pm 0.14$

Couplings to leptons

$g_V^\ell = -0.0376 \pm 0.0012$
$g_A^\ell = -0.5008 \pm 0.0008$
$g^{\nu_e} = 0.53 \pm 0.09$
$g^{\nu_\mu} = 0.502 \pm 0.017$

Asymmetry parameters [f]

$A_e = 0.156 \pm 0.008$ (S = 1.2)
$A_\tau = 0.145 \pm 0.009$
$A_c = 0.59 \pm 0.19$
$A_b = 0.89 \pm 0.11$

Charge asymmetry (%) at Z pole

$A_{FB}^{(0\ell)} = 1.59 \pm 0.18$
$A_{FB}^{(0s)} = 13 \pm 4$
$A_{FB}^{(0c)} = 7.22 \pm 0.67$
$A_{FB}^{(0b)} = 9.92 \pm 0.35$

Z DECAY MODES			Fraction (Γ_i/Γ)	Confidence level	p (MeV/c)
e^+e^-			(3.366±0.008) %		45600
$\mu^+\mu^-$			(3.367±0.013) %		45600
$\tau^+\tau^-$			(3.360±0.015) %		45600
$\ell^+\ell^-$		[b]	(3.366±0.006) %		45600
invisible			(20.01 ±0.16) %		–
hadrons			(69.90 ±0.15) %		–
$(u\bar{u}+c\bar{c})/2$			(9.6 ±1.3) %		–
$(d\bar{d}+s\bar{s}+b\bar{b})/3$			(16.9 ±0.9) %		–
$c\bar{c}$			(11.0 ±0.7) %		–
$b\bar{b}$			(15.46 ±0.14) %		–
$\pi^0\gamma$			$< 5.2 \times 10^{-5}$	95%	45600
$\eta\gamma$			$< 5.1 \times 10^{-5}$	95%	45600
$\omega\gamma$			$< 6.5 \times 10^{-4}$	95%	45600
$\eta'(958)\gamma$			$< 4.2 \times 10^{-5}$	95%	45600
$\gamma\gamma$			$< 5.2 \times 10^{-5}$	95%	45600
$\gamma\gamma\gamma$			$< 1.0 \times 10^{-5}$	95%	45600
$\pi^\pm W^\mp$		[g]	$< 7 \times 10^{-5}$	95%	10300
$\rho^\pm W^\mp$		[g]	$< 8.3 \times 10^{-5}$	95%	10300
$J/\psi(1S)X$			(3.80 ±0.27) $\times 10^{-3}$		–
$\psi(2S)X$			(1.60 ±0.33) $\times 10^{-3}$		–
$\chi_{c1}(1P)X$			(6.0 ±1.9) $\times 10^{-3}$		–
ΥX			(1.0 ±0.5) $\times 10^{-4}$		–
$(D^0/\bar{D}^0)X$			(20.7 ±2.0) %		–
$D^\pm X$			(12.2 ±1.7) %		–
$D^*(2010)^\pm X$		[g]	(11.4 ±1.3) %		–
$B_s^0 X$			seen		–
anomalous γ+ hadrons		[h]	$< 3.2 \times 10^{-3}$	95%	–
$e^+e^-\gamma$		[h]	$< 5.2 \times 10^{-4}$	95%	45600
$\mu^+\mu^-\gamma$		[h]	$< 5.6 \times 10^{-4}$	95%	45600
$\tau^+\tau^-\gamma$		[h]	$< 7.3 \times 10^{-4}$	95%	45600
$\ell^+\ell^-\gamma\gamma$		[i]	$< 6.8 \times 10^{-6}$	95%	45600
$q\bar{q}\gamma\gamma$		[i]	$< 5.5 \times 10^{-6}$	95%	–
$\nu\bar{\nu}\gamma\gamma$		[i]	$< 3.1 \times 10^{-6}$	95%	45600
$e^\pm\mu^\mp$	LF	[g]	$< 1.7 \times 10^{-6}$	95%	45600
$e^\pm\tau^\mp$	LF	[g]	$< 9.8 \times 10^{-6}$	95%	45600
$\mu^\pm\tau^\mp$	LF	[g]	$< 1.7 \times 10^{-5}$	95%	45600

Gauge & Higgs Boson Summary Table

Higgs Bosons — H^0 and $H^\pm$, Searches for

H^0 Mass $m >$ 58.4 GeV, CL = 95%

H_1^0 in Supersymmetric Models ($m_{H_1^0} < m_{H_2^0}$) [j]

Mass $m >$ 44 GeV, CL = 95%

A^0 Pseudoscalar Higgs Boson in Supersymmetric Models [j]

Mass $m >$ 24.3 GeV, CL = 95% $\tan\beta > 1$, $m_t < 200$ GeV

$H^\pm$ Mass $m >$ 43.5 GeV, CL = 95%

See the Particle Listings for a Note giving details of Higgs Bosons.

Heavy Bosons Other Than Higgs Bosons, Searches for

Additional W Bosons

W_R — right-handed W

Mass $m >$ 406 GeV, CL = 90%
(assuming light right-handed neutrino)

W' with standard couplings decaying to $e\nu$, $\mu\nu$

Mass $m >$ 652 GeV, CL = 95%

Additional Z Bosons

Z'_{SM} with standard couplings

Mass $m >$ 505 GeV, CL = 95% ($p\overline{p}$ direct search)

Mass $m >$ 779 GeV, CL = 95% (electroweak fit)

Z_{LR} of $SU(2)_L \times SU(2)_R \times U(1)$
(with $g_L = g_R$)

Mass $m >$ 445 GeV, CL = 95% ($p\overline{p}$ direct search)

Mass $m >$ 389 GeV, CL = 95% (electroweak fit)

Z_χ of $SO(10) \rightarrow SU(5) \times U(1)_\chi$
(coupling constant derived from G.U.T.)

Mass $m >$ 425 GeV, CL = 95% ($p\overline{p}$ direct search)

Mass $m >$ 321 GeV, CL = 95% (electroweak fit)

Z_ψ of $E_6 \rightarrow SO(10) \times U(1)_\psi$
(coupling constant derived from G.U.T.)

Mass $m >$ 415 GeV, CL = 95% ($p\overline{p}$ direct search)

Mass $m >$ 160 GeV, CL = 95% (electroweak fit)

Z_η of $E_6 \rightarrow SU(3) \times SU(2) \times U(1) \times U(1)_\eta$
(coupling constant derived from G.U.T.);
charges are $Q_\eta = \sqrt{3/8}Q_\chi - \sqrt{5/8}Q_\psi$)

Mass $m >$ 440 GeV, CL = 95% ($p\overline{p}$ direct search)

Mass $m >$ 182 GeV, CL = 95% (electroweak fit)

Scalar Leptoquarks

Mass $m >$ 116 GeV, CL = 95% (1st generation, pair prod.)

Mass $m >$ 230 GeV, CL = 95% (1st gener., single prod.)

Mass $m >$ 97 GeV, CL = 95% (2nd gener., pair prod.)

Mass $m >$ 73 GeV, CL = 95% (2nd gener., single prod.)

Mass $m >$ 45 GeV, CL = 95% (3rd gener., pair prod.)

(The second, fourth, and fifth limits above are for charge $-1/3$, weak isoscalar.)

Axions (A^0) and Other Very Light Bosons, Searches for

The standard Peccei-Quinn axion is ruled out. Variants with reduced couplings or much smaller masses are constrained by various data. The Particle Listings in the full *Review* contain a Note discussing axion searches.

The best limit for the half-life of neutrinoless double beta decay with Majoron emission is $> 7.2 \times 10^{24}$ years (CL = 90%).

NOTES

In this Summary Table:

When a quantity has "(S = ...)" to its right, the error on the quantity has been enlarged by the "scale factor" S, defined as $S = \sqrt{\chi^2/(N-1)}$, where N is the number of measurements used in calculating the quantity. We do this when $S > 1$, which often indicates that the measurements are inconsistent. When $S > 1.25$, we also show in the Particle Listings an ideogram of the measurements. For more about S, see the Introduction.

A decay momentum p is given for each decay mode. For a 2-body decay, p is the momentum of each decay product in the rest frame of the decaying particle. For a 3-or-more-body decay, p is the largest momentum any of the products can have in this frame.

[a] Theoretical value. A mass as large as a few MeV may not be precluded.

[b] ℓ indicates each type of lepton (e, μ, and τ), not sum over them.

[c] The Z-boson mass listed here corresponds to a Breit-Wigner resonance parameter. It lies approximately 34 MeV above the real part of the position of the pole (in the energy-squared plane) in the Z-boson propagator.

[d] This partial width takes into account Z decays into $\nu\overline{\nu}$ and any other possible undetected modes.

[e] This ratio has not been corrected for the τ mass.

[f] Here $A \equiv 2g_V g_A/(g_V^2+g_A^2)$.

[g] The value is for the sum of the charge states of particle/antiparticle states indicated.

[h] See the Z Particle Listings for the γ energy range used in this measurement.

[i] For $m_{\gamma\gamma} = (60 \pm 5)$ GeV.

[j] The limits assume no invisible decays.

LEPTONS

e

$J = \frac{1}{2}$

Mass $m = 0.51099907 \pm 0.00000015$ MeV [a]
$= (5.48579903 \pm 0.00000013) \times 10^{-4}$ u
$(m_{e^+} - m_{e^-})/m < 4 \times 10^{-8}$, CL = 90%
$|q_{e^+} + q_{e^-}|/e < 4 \times 10^{-8}$
Magnetic moment $\mu = 1.001159652193 \pm 0.000000000010\ \mu_B$
$(g_{e^+} - g_{e^-}) / g_{\text{average}} = (-0.5 \pm 2.1) \times 10^{-12}$
Electric dipole moment $d = (-0.3 \pm 0.8) \times 10^{-26}\ e$cm
Mean life $\tau > 4.3 \times 10^{23}$ yr, CL = 68% [b]

μ

$J = \frac{1}{2}$

Mass $m = 105.658389 \pm 0.000034$ MeV [c]
$= 0.113428913 \pm 0.000000017$ u
Mean life $\tau = (2.19703 \pm 0.00004) \times 10^{-6}$ s
$\tau_{\mu^+}/\tau_{\mu^-} = 1.00002 \pm 0.00008$
$c\tau = 658.654$ m
Magnetic moment $\mu = 1.001165923 \pm 0.000000008\ e\hbar/2m_\mu$
$(g_{\mu^+} - g_{\mu^-}) / g_{\text{average}} = (-2.6 \pm 1.6) \times 10^{-8}$
Electric dipole moment $d = (3.7 \pm 3.4) \times 10^{-19}\ e$cm

Decay parameters [d]

$\rho = 0.7518 \pm 0.0026$
$\eta = -0.007 \pm 0.013$
$\delta = 0.749 \pm 0.004$
$\xi P_\mu = 1.003 \pm 0.008$ [e]
$\xi P_\mu \delta/\rho > 0.99682$, CL = 90% [e]
$\xi' = 1.00 \pm 0.04$
$\xi'' = 0.7 \pm 0.4$
$\alpha/A = (0 \pm 4) \times 10^{-3}$
$\alpha'/A = (0 \pm 4) \times 10^{-3}$
$\beta/A = (4 \pm 6) \times 10^{-3}$
$\beta'/A = (2 \pm 6) \times 10^{-3}$
$\overline{\eta} = 0.02 \pm 0.08$

μ^+ modes are charge conjugates of the modes below.

μ^- DECAY MODES		Fraction (Γ_i/Γ)	Confidence level	p (MeV/c)
$e^- \overline{\nu}_e \nu_\mu$		$\approx 100\%$		53
$e^- \overline{\nu}_e \nu_\mu \gamma$		[f] (1.4±0.4) %		53
$e^- \overline{\nu}_e \nu_\mu e^+ e^-$		[g] $(3.4 \pm 0.4) \times 10^{-5}$		53
Lepton Family number (*LF*) violating modes				
$e^- \nu_e \overline{\nu}_\mu$	*LF*	[h] < 1.2 %	90%	53
$e^- \gamma$	*LF*	$< 4.9 \times 10^{-11}$	90%	53
$e^- e^+ e^-$	*LF*	$< 1.0 \times 10^{-12}$	90%	53
$e^- 2\gamma$	*LF*	$< 7.2 \times 10^{-11}$	90%	53

τ

$J = \frac{1}{2}$

Mass $m = 1777.00^{+0.30}_{-0.27}$ MeV
Mean life $\tau = (291.0 \pm 1.5) \times 10^{-15}$ s
$c\tau = 87.2\ \mu$m
Electric dipole moment $d < 5 \times 10^{-17}\ e$cm, CL = 95%

Weak dipole moment

$\text{Re}(d_\tau^W) < 7.8 \times 10^{-18}\ e$cm, CL = 95%
$\text{Im}(d_\tau^W) < 4.5 \times 10^{-17}\ e$cm, CL = 95%

Decay parameters

See the τ Particle Listings for a note concerning τ-decay parameters.

$\rho^\tau(e \text{ or } \mu) = 0.742 \pm 0.027$
$\rho^\tau(e) = 0.736 \pm 0.028$
$\rho^\tau(\mu) = 0.74 \pm 0.04$
$\xi^\tau(e \text{ or } \mu) = 1.03 \pm 0.12$
$\xi^\tau(e) = 1.03 \pm 0.25$
$\xi^\tau(\mu) = 1.23 \pm 0.24$
$\eta^\tau(e \text{ or } \mu) = -0.01 \pm 0.14$
$\eta^\tau(\mu) = -0.24 \pm 0.29$
$(\delta\xi)^\tau(e \text{ or } \mu) = 0.76 \pm 0.11$ (S = 1.3)
$(\delta\xi)^\tau(e) = 1.11 \pm 0.18$
$(\delta\xi)^\tau(\mu) = 0.71 \pm 0.15$
$\xi^\tau(\pi) = 0.99 \pm 0.06$
$\xi^\tau(\rho) = 1.04 \pm 0.07$
$\xi^\tau(a_1) = 1.01 \pm 0.04$
$\xi^\tau(\text{all hadronic modes}) = 1.011 \pm 0.027$

τ^+ modes are charge conjugates of the modes below. "$h^\pm$" stands for $\pi^\pm$ or $K^\pm$. "ℓ" stands for e or μ. "Neutral" means neutral hadron whose decay products include γ's and/or π^0's.

τ^- DECAY MODES		Fraction (Γ_i/Γ)	Scale factor/ Confidence level	p (MeV/c)
Modes with one charged particle				
particle$^- \geq 0$ neutrals $\geq 0K^0_L \nu_\tau$ ("1-prong")		(84.96± 0.14) %	S=1.3	–
particle$^- \geq 0$ neutrals $\geq 0K^0 \nu_\tau$		(85.53± 0.14) %	S=1.3	–
$\mu^- \overline{\nu}_\mu \nu_\tau$	[i]	(17.35± 0.10) %		885
$\mu^- \overline{\nu}_\mu \nu_\tau \gamma$ ($E_\gamma > 37$ MeV)		$(2.3 \pm 1.0) \times 10^{-3}$		–
$e^- \overline{\nu}_e \nu_\tau$	[i]	(17.83± 0.08) %		888
$h^- \geq 0$ neutrals $\geq 0K^0_L \nu_\tau$		(49.78± 0.17) %	S=1.2	–
$h^- \geq 0K^0_L \nu_\tau$		(12.51± 0.13) %	S=1.1	–
$h^- \nu_\tau$		(12.03± 0.14) %	S=1.1	–
$\pi^- \nu_\tau$	[i]	(11.31± 0.15) %	S=1.1	883
$K^- \nu_\tau$	[i]	$(7.1 \pm 0.5) \times 10^{-3}$		820
$h^- \geq 1\pi^0 \nu_\tau$		(36.97± 0.18) %	S=1.1	–
$h^- \pi^0 \nu_\tau$		(25.76± 0.15) %	S=1.1	–
$\pi^- \pi^0 \nu_\tau$	[i]	(25.24± 0.16) %	S=1.1	878
$\pi^- \pi^0$ non-$\rho(770) \nu_\tau$		$(3.0 \pm 3.2) \times 10^{-3}$		878
$K^- \pi^0 \nu_\tau$	[i]	$(5.2 \pm 0.5) \times 10^{-3}$		814
$h^- \geq 2\pi^0 \nu_\tau$		(10.95± 0.16) %	S=1.1	–
$h^- 2\pi^0 \nu_\tau$		(9.50± 0.14) %	S=1.1	–
$h^- 2\pi^0 \nu_\tau$ (ex.K^0)		(9.35± 0.14) %	S=1.1	–
$\pi^- 2\pi^0 \nu_\tau$ (ex.K^0)	[i]	(9.27± 0.14) %	S=1.1	862
$K^- 2\pi^0 \nu_\tau$ (ex.K^0)	[i]	$(8.1 \pm 2.7) \times 10^{-4}$		796
$h^- \geq 3\pi^0 \nu_\tau$		(1.46± 0.11) %	S=1.1	–
$h^- 3\pi^0 \nu_\tau$		(1.28± 0.10) %		–
$\pi^- 3\pi^0 \nu_\tau$ (ex.K^0)	[i]	(1.14± 0.14) %		836
$K^- 3\pi^0 \nu_\tau$ (ex.K^0)	[i]	$(5.0\ ^{+10.0}_{-3.3}) \times 10^{-4}$		766
$h^- 4\pi^0 \nu_\tau$ (ex.K^0)		$(1.8 \pm 0.6) \times 10^{-3}$		–
$h^- 4\pi^0 \nu_\tau$ (ex.K^0,η)	[i]	$(1.2 \pm 0.6) \times 10^{-3}$		–
$K^- \geq 1$ (π^0 or K^0) ν_τ		$(9.4 \pm 1.0) \times 10^{-3}$		–
Modes with K^0's				
$h^- \overline{K}^0 \geq 0$ neutrals $\geq 0K^0_L \nu_\tau$		(1.54± 0.10) %	S=1.3	–
$h^- \overline{K}^0 \nu_\tau$		$(9.2 \pm 0.8) \times 10^{-3}$	S=1.3	–
$\pi^- \overline{K}^0 \nu_\tau$	[i]	$(7.7 \pm 0.8) \times 10^{-3}$	S=1.3	812
$\pi^- \overline{K}^0$ (non-$K^*(892)^-$) ν_τ		$< 1.7 \times 10^{-3}$	CL=95%	812
$K^- K^0 \nu_\tau$	[i]	$(1.55 \pm 0.28) \times 10^{-3}$		737
$h^- \overline{K}^0 \pi^0 \nu_\tau$		$(5.5 \pm 0.5) \times 10^{-3}$		–
$\pi^- \overline{K}^0 \pi^0 \nu_\tau$	[i]	$(4.1 \pm 0.6) \times 10^{-3}$		794
$K^- K^0 \pi^0 \nu_\tau$	[i]	$(1.38 \pm 0.32) \times 10^{-3}$		685
$h^- K^0_S K^0_S \nu_\tau$		$(2.5 \pm 0.6) \times 10^{-4}$		–
$\pi^- K^0 \overline{K}^0 \nu_\tau$	[i]	$(1.01 \pm 0.23) \times 10^{-3}$		682
$K^- K^0 \geq 0$ neutrals ν_τ		$(2.9 \pm 0.4) \times 10^{-3}$		–
$K^- \geq 0\pi^0 \geq 0K^0 \nu_\tau$		(1.65± 0.10) %		–
K^0(particles)$^- \nu_\tau$		(1.58± 0.10) %	S=1.2	–
$K^0 h^+ h^- h^- \geq 0$ neut. ν_τ		$< 1.7 \times 10^{-3}$	CL=95%	–

Lepton Summary Table

Modes with three charged particles

$h^-h^-h^+ \geq$ 0neut. ν_τ ("3-prong")		(14.91 ± 0.14) %	S=1.3	–
$h^-h^-h^+ \geq 0$ neutrals ν_τ (ex. $K^0_S \to \pi^+\pi^-$)		(14.36 ± 0.14) %	S=1.3	–
$\pi^-\pi^+\pi^- \geq 0$ neutrals ν_τ		(14.09 ± 0.31) %		–
$h^-h^-h^+\nu_\tau$		(9.80 ± 0.10) %	S=1.1	–
$h^-h^-h^+\nu_\tau$(ex.K^0)		(9.48 ± 0.10) %	S=1.1	–
$h^-h^-h^+\nu_\tau$(ex.K^0,ω)	[i]	(9.44 ± 0.10) %	S=1.1	–
$h^-h^-h^+ \geq 1$ neutrals ν_τ		(5.08 ± 0.11) %	S=1.2	–
$h^-h^-h^+ \geq 1$ neutrals ν_τ(ex. $K^0_S \to \pi^+\pi^-$)		(4.88 ± 0.11) %	S=1.2	–
$h^-h^-h^+\pi^0\nu_\tau$		(4.44 ± 0.09) %	S=1.1	–
$h^-h^-h^+\pi^0\nu_\tau$(ex.K^0)		(4.25 ± 0.09) %	S=1.1	–
$h^-h^-h^+\pi^0\nu_\tau$(ex. K^0, ω)	[i]	(2.55 ± 0.09) %		–
$h^-(\rho\pi)^0\nu_\tau$		(2.84 ± 0.34) %		–
$(a_1(1260)h)^-\nu_\tau$		< 2.0 %	CL=95%	–
$h^-\rho\pi^0\nu_\tau$		(1.33 ± 0.20) %		–
$h^-\rho^+h^-\nu_\tau$		(4.4 ± 2.2) × 10^{-3}		–
$h^-\rho^-h^+\nu_\tau$		(1.15 ± 0.23) %		–
$h^-h^-h^+2\pi^0\nu_\tau$		(5.2 ± 0.5) × 10^{-3}		–
$h^-h^-h^+2\pi^0\nu_\tau$(ex.K^0)		(5.1 ± 0.5) × 10^{-3}		–
$h^-h^-h^+2\pi^0\nu_\tau$(ex.K^0,ω,η)	[i]	(1.0 ± 0.4) × 10^{-3}		–
$h^-h^-h^+ \geq 3\pi^0\nu_\tau$	[i]	(1.1 ± 0.6) × 10^{-3}		–
$K^-h^+h^- \geq 0$ neutrals ν_τ		< 6 × 10^{-3}	CL=90%	–
$K^-\pi^+\pi^- \geq 0$ neut. ν_τ		(3.9 $^{+1.9}_{-1.6}$) × 10^{-3}	S=1.5	–
$K^-\pi^+K^- \geq 0$ neut. ν_τ		< 9 × 10^{-4}	CL=95%	–
$K^-K^+\pi^- \geq 0$ neut. ν_τ		(1.5 $^{+0.9}_{-0.3}$) × 10^{-3}		–
$K^-K^+\pi^-\nu_\tau$		(2.2 $^{+1.8}_{-1.2}$) × 10^{-3}		685
$\phi\pi^-\nu_\tau$		< 3.5 × 10^{-4}	CL=90%	585
$K^-K^+K^- \geq 0$ neut. ν_τ		< 2.1 × 10^{-3}	CL=95%	–
$\pi^-K^+\pi^- \geq 0$ neut. ν_τ		< 2.5 × 10^{-3}	CL=95%	–
$e^-e^-e^+\overline{\nu}_e\nu_\tau$		(2.8 ± 1.5) × 10^{-5}		888
$\mu^-e^-e^+\overline{\nu}_\mu\nu_\tau$		< 3.6 × 10^{-5}	CL=90%	885

Modes with five charged particles

$3h^-2h^+ \geq 0$ neutrals ν_τ (ex. $K^0_S \to \pi^-\pi^+$) ("5-prong")		(9.7 ± 0.7) × 10^{-4}		–
$3h^-2h^+\nu_\tau$(ex.K^0)	[i]	(7.5 ± 0.7) × 10^{-4}		–
$3h^-2h^+\pi^0\nu_\tau$(ex.K^0)	[i]	(2.2 ± 0.5) × 10^{-4}		–
$3h^-2h^+2\pi^0\nu_\tau$		< 1.1 × 10^{-4}	CL=90%	–

Miscellaneous other allowed modes

$(5\pi)^-\nu_\tau$		(3.3 ± 0.7) × 10^{-3}		–
$4h^-3h^+ \geq 0$ neutrals ν_τ ("7-prong")		< 1.9 × 10^{-4}	CL=90%	–
$K^*(892)^- \geq 0(h^0 \neq K^0_S)\nu_\tau$		(1.94 ± 0.31) %		–
$K^*(892)^- \geq 0$ neutrals ν_τ		(1.33 ± 0.13) %		–
$K^*(892)^-\nu_\tau$		(1.28 ± 0.08) %		665
$K^*(892)^0K^- \geq 0$ neutrals ν_τ		(3.2 ± 1.4) × 10^{-3}		–
$K^*(892)^0K^-\nu_\tau$		(2.0 ± 0.6) × 10^{-3}		539
$\overline{K}^*(892)^0\pi^- \geq 0$ neutrals ν_τ		(3.8 ± 1.7) × 10^{-3}		–
$\overline{K}^*(892)^0\pi^-\nu_\tau$		(2.5 ± 1.1) × 10^{-3}		653
$K_1(1270)^-\nu_\tau$		(4 ± 4) × 10^{-3}		433
$K_1(1400)^-\nu_\tau$		(8 ± 4) × 10^{-3}		335
$K^*_2(1430)^-\nu_\tau$		< 3 × 10^{-3}	CL=95%	317
$\eta\pi^-\nu_\tau$		< 1.4 × 10^{-4}	CL=95%	798
$\eta\pi^-\pi^0\nu_\tau$	[i]	(1.71 ± 0.28) × 10^{-3}		778
$\eta\pi^-\pi^0\pi^0\nu_\tau$		< 4.3 × 10^{-4}	CL=95%	746
$\eta K^-\nu_\tau$		(2.6 ± 0.7) × 10^{-4}		720
$\eta\pi^+\pi^-\pi^- \geq 0$ neutrals ν_τ		< 3 × 10^{-3}	CL=90%	–
$\eta\eta\pi^-\nu_\tau$		< 1.1 × 10^{-4}	CL=95%	637
$\eta\eta\pi^-\pi^0\nu_\tau$		< 2.0 × 10^{-4}	CL=95%	559
$h^-\omega \geq 0$ neutrals ν_τ		(2.32 ± 0.11) %		–
$h^-\omega\nu_\tau$	[i]	(1.91 ± 0.09) %		–
$h^-\omega\pi^0\nu_\tau$	[i]	(4.1 ± 0.6) × 10^{-3}		–

Lepton Family number (*LF*), Lepton number (*L*), or Baryon number (*B*) violating modes
(In the modes below, ℓ means a sum over *e* and μ modes)

L means lepton number violation (*e.g.* $\tau^- \to e^+\pi^-\pi^-$). Following common usage, *LF* means lepton family violation *and not* lepton number violation (*e.g.* $\tau^- \to e^-\pi^+\pi^-$).

$e^-\gamma$	*LF*	< 1.1	× 10^{-4}	CL=90%	888
$\mu^-\gamma$	*LF*	< 4.2	× 10^{-6}	CL=90%	885
$e^-\pi^0$	*LF*	< 1.4	× 10^{-4}	CL=90%	883
$\mu^-\pi^0$	*LF*	< 4.4	× 10^{-5}	CL=90%	880
e^-K^0	*LF*	< 1.3	× 10^{-3}	CL=90%	819
μ^-K^0	*LF*	< 1.0	× 10^{-3}	CL=90%	815
$e^-\eta$	*LF*	< 6.3	× 10^{-5}	CL=90%	804
$\mu^-\eta$	*LF*	< 7.3	× 10^{-5}	CL=90%	800
$e^-\rho^0$	*LF*	< 4.2	× 10^{-6}	CL=90%	722
$\mu^-\rho^0$	*LF*	< 5.7	× 10^{-6}	CL=90%	718
$e^-K^*(892)^0$	*LF*	< 6.3	× 10^{-6}	CL=90%	663
$\mu^-K^*(892)^0$	*LF*	< 9.4	× 10^{-6}	CL=90%	657
$\pi^-\gamma$	*L*	< 2.8	× 10^{-4}	CL=90%	883
$\pi^-\pi^0$	*L*	< 3.7	× 10^{-4}	CL=90%	878
$e^-e^+e^-$	*LF*	< 3.3	× 10^{-6}	CL=90%	888
$e^-\mu^+\mu^-$	*LF*	< 3.6	× 10^{-6}	CL=90%	882
$e^+\mu^-\mu^-$	*LF*	< 3.5	× 10^{-6}	CL=90%	882
$\mu^-e^+e^-$	*LF*	< 3.4	× 10^{-6}	CL=90%	885
$\mu^+e^-e^-$	*L*	< 3.4	× 10^{-6}	CL=90%	885
$\mu^-\mu^+\mu^-$	*LF*	< 1.9	× 10^{-6}	CL=90%	873
$e^-\pi^+\pi^-$	*LF*	< 4.4	× 10^{-6}	CL=90%	877
$e^+\pi^-\pi^-$	*L*	< 4.4	× 10^{-6}	CL=90%	877
$\mu^-\pi^+\pi^-$	*LF*	< 7.4	× 10^{-6}	CL=90%	866
$\mu^+\pi^-\pi^-$	*L*	< 6.9	× 10^{-6}	CL=90%	866
$e^-\pi^+K^-$	*LF*	< 7.7	× 10^{-6}	CL=90%	813
$e^-\pi^-K^+$	*LF*	< 4.6	× 10^{-6}	CL=90%	813
$e^+\pi^-K^-$	*L*	< 4.5	× 10^{-6}	CL=90%	813
$\mu^-\pi^+K^-$	*LF*	< 8.7	× 10^{-6}	CL=90%	800
$\mu^-\pi^-K^+$	*LF*	< 1.5	× 10^{-5}	CL=90%	800
$\mu^+\pi^-K^-$	*L*	< 2.0	× 10^{-5}	CL=90%	800
$\overline{p}\gamma$	*L*,*B*	< 2.9	× 10^{-4}	CL=90%	641
$\overline{p}\pi^0$	*L*,*B*	< 6.6	× 10^{-4}	CL=90%	632
$\overline{p}\eta$	*L*,*B*	< 1.30	× 10^{-3}	CL=90%	475
$e^-\overline{K}^*(892)^0$	*LF*	< 1.1	× 10^{-5}	CL=90%	663
$\mu^-\overline{K}^*(892)^0$	*LF*	< 8.7	× 10^{-6}	CL=90%	657
e^- light boson	*LF*	< 2.7	× 10^{-3}	CL=95%	–
μ^- light boson	*LF*	< 5	× 10^{-3}	CL=95%	–

Heavy Charged Lepton Searches

$L^\pm$ – charged lepton

Mass $m >$ 42.7 GeV, CL = 95% $\quad m_\nu \approx 0$

$L^\pm$ – stable charged heavy lepton

Mass $m >$ 42.8 GeV, CL = 95%

Neutrinos

See the Particle Listings for a Note giving details of neutrinos, masses, mixing, and the status of experimental searches.

ν_e

$J = \frac{1}{2}$

Mass *m*: Unexplained effects have resulted in significantly negative m^2 in the new, precise tritium beta decay experiments. It is felt that a real neutrino mass as large as 10–15 eV would cause observable spectral distortions even in the presence of the end-point count excesses.

Mean life/mass, $\tau/m_{\nu_e} >$ 300 s/eV, CL = 90%

Magnetic moment $\mu < 1.8 \times 10^{-10}\ \mu_B$, CL = 90%

ν_μ

$J = \frac{1}{2}$

Mass $m <$ 0.17 MeV, CL = 90%

Mean life/mass, $\tau/m_{\nu_\mu} >$ 15.4 s/eV, CL = 90%

Magnetic moment $\mu < 7.4 \times 10^{-10}\ \mu_B$, CL = 90%

ν_τ

$J = \frac{1}{2}$

Mass $m <$ 24 MeV, CL = 95%
Magnetic moment $\mu < 5.4 \times 10^{-7}\ \mu_B$, CL = 90%

Number of Light Neutrino Types

(including ν_e, ν_μ, and ν_τ)
Number $N = 2.991 \pm 0.016$ (Standard Model fits to LEP data)
Number $N = 3.09 \pm 0.13$ (Direct measurement of invisible Z width)

Massive Neutrinos and Lepton Mixing, Searches for

For excited leptons, see Compositeness Limits below.

See the Particle Listings for a Note giving details of neutrinos, masses, mixing, and the status of experimental searches.

No direct, uncontested evidence for massive neutrinos or lepton mixing has been obtained. Sample limits are:
Mass $m >$ 45.0, CL = 95% (Dirac)
Mass $m >$ 39.5, CL = 95% (Majorana)

ν oscillation: $\nu_\mu \rightarrow \nu_e$ (θ = mixing angle)
Mass $m >$ 19.6 GeV, CL = 95% (all $|U_{\ell J}|^2$) (Dirac)
Mass $m >$ 45.7 GeV or $m <$ 25, CL = 95% ($|U_{\ell J}|^2 > 10^{-13}$ (Dirac)

ν oscillation: $\overline{\nu}_e \not\rightarrow \overline{\nu}_e$
$\Delta(m^2) < 0.0075\ \text{eV}^2$, CL = 90% (if $\sin^2 2\theta = 1$)
$\sin^2 2\theta < 0.02$, CL = 90% (if $\Delta(m^2)$ is large)

ν oscillation: $\nu_\mu \rightarrow \nu_e$ (θ = mixing angle)
$\Delta(m^2) < 0.09\ \text{eV}^2$, CL = 90% (if $\sin^2 2\theta = 1$)
$\sin^2 2\theta < 2.5 \times 10^{-3}$, CL = 90% (if $\Delta(m^2)$ is large)

NOTES

In this Summary Table:

When a quantity has "(S = ...)" to its right, the error on the quantity has been enlarged by the "scale factor" S, defined as $S = \sqrt{\chi^2/(N-1)}$, where N is the number of measurements used in calculating the quantity. We do this when S > 1, which often indicates that the measurements are inconsistent. When S > 1.25, we also show in the Particle Listings an ideogram of the measurements. For more about S, see the Introduction.

A decay momentum p is given for each decay mode. For a 2-body decay, p is the momentum of each decay product in the rest frame of the decaying particle. For a 3-or-more-body decay, p is the largest momentum any of the products can have in this frame.

[a] The uncertainty in the electron mass in unified atomic mass units (u) is ten times smaller than that given by the 1986 CODATA adjustment, quoted in the Table of Physical Contants (Section 1). The conversion to MeV via the factor 931.49432(28) MeV/u is more uncertain because of the electron charge uncertainty. Our value in MeV differs slightly from the 1986 CODATA result.

[b] This is the best "electron disappearance" limit. The best limit for the mode $e^- \rightarrow \nu\gamma$ is $> 2.35 \times 10^{25}$ yr (CL=68%).

[c] The muon mass is most precisely known in u (unified atomic mass units). The conversion factor to MeV via the factor 931.49432(28) MeV/u is more uncertain because of the electron charge uncertainty.

[d] See the "Note on Muon Decay Parameters" in the μ Particle Listings for definitions and details.

[e] P_μ is the longitudinal polarization of the muon from pion decay. In standard $V-A$ theory, $P_\mu = 1$ and $\rho = \delta = 3/4$.

[f] This only includes events with the γ energy > 10 MeV. Since the $e^-\overline{\nu}_e\nu_\mu$ and $e^-\overline{\nu}_e\nu_\mu\gamma$ modes cannot be clearly separated, we regard the latter mode as a subset of the former.

[g] See the μ Particle Listings for the energy limits used in this measurement.

[h] A test of additive vs. multiplicative lepton family number conservation.

[i] Basis mode for the τ.

Quark Summary Table

QUARKS

The u-, d-, and s-quark masses are estimates of so-called "current-quark masses," in a mass-independent subtraction scheme such as $\overline{\text{MS}}$ at a scale $\mu \approx 1$ GeV. The c- and b-quark masses are estimated from charmonium, bottomonium, D, and B masses. They are the "running" masses in the $\overline{\text{MS}}$ scheme. These can be different from the heavy quark masses obtained in potential models.

u

$I(J^P) = \frac{1}{2}(\frac{1}{2}^+)$

Mass $m = 2$ to 8 MeV [a] Charge $= \frac{2}{3}\,e$ $I_z = +\frac{1}{2}$
$m_u/m_d = 0.25$ to 0.70

d

$I(J^P) = \frac{1}{2}(\frac{1}{2}^+)$

Mass $m = 5$ to 15 MeV [a] Charge $= -\frac{1}{3}\,e$ $I_z = -\frac{1}{2}$
$m_s/m_d = 17$ to 25

s

$I(J^P) = 0(\frac{1}{2}^+)$

Mass $m = 100$ to 300 MeV [a] Charge $= -\frac{1}{3}\,e$ Strangeness $= -1$
$(m_s - (m_u + m_d)/2)/(m_d - m_u) = 34$ to 51

c

$I(J^P) = 0(\frac{1}{2}^+)$

Mass $m = 1.0$ to 1.6 GeV Charge $= \frac{2}{3}\,e$ Charm $= +1$

b

$I(J^P) = 0(\frac{1}{2}^+)$

Mass $m = 4.1$ to 4.5 GeV Charge $= -\frac{1}{3}\,e$ Bottom $= -1$

t

$I(J^P) = 0(\frac{1}{2}^+)$

Charge $= \frac{2}{3}\,e$ Top $= +1$

Mass $m = 180 \pm 12$ GeV (direct observation of top events)
Mass $m = 179 \pm 8^{+17}_{-20}$ GeV (Standard Model electroweak fit)

b′ (4^{th} Generation) Quark, Searches for

Mass $m > 85$ GeV, CL = 95% ($p\overline{p}$, charged current decays)
Mass $m > 46.0$ GeV, CL = 95% (e^+e^-, all decays)

Free Quark Searches

All searches since 1977 have had negative results.

NOTES

[a] The ratios m_u/m_d and m_s/m_d are extracted from pion and kaon masses using chiral symmetry. The estimates of u and d masses are not without controversy and remain under active investigation. Within the literature there are even suggestions that the u quark could be essentially massless. The s-quark mass is estimated from SU(3) splittings in hadron masses.

LIGHT UNFLAVORED MESONS ($S = C = B = 0$)

For $I = 1$ (π, b, ρ, a): $u\overline{d}$, $(u\overline{u}-d\overline{d})/\sqrt{2}$, $d\overline{u}$;
for $I = 0$ (η, η', h, h', ω, ϕ, f, f'): $c_1(u\overline{u} + d\overline{d}) + c_2(s\overline{s})$

$\pi^\pm$

$I^G(J^P) = 1^-(0^-)$

Mass $m = 139.56995 \pm 0.00035$ MeV
Mean life $\tau = (2.6033 \pm 0.0005) \times 10^{-8}$ s (S = 1.2)
$c\tau = 7.8045$ m

$\pi^\pm \to \ell^\pm \nu\gamma$ form factors [a]

$F_V = 0.017 \pm 0.008$
$F_A = 0.0116 \pm 0.0016$ (S = 1.3)
$R = 0.059^{+0.009}_{-0.008}$

π^- modes are charge conjugates of the modes below.

π^+ DECAY MODES		Fraction (Γ_i/Γ)	Confidence level	p (MeV/c)
$\mu^+\nu_\mu$	[b]	(99.98770±0.00004) %		30
$\mu^+\nu_\mu\gamma$	[c]	(1.24 ±0.25) × 10^{-4}		30
$e^+\nu_e$	[b]	(1.230 ±0.004) × 10^{-4}		70
$e^+\nu_e\gamma$	[c]	(1.61 ±0.23) × 10^{-7}		70
$e^+\nu_e\pi^0$		(1.025 ±0.034) × 10^{-8}		4
$e^+\nu_e e^+e^-$		(3.2 ±0.5) × 10^{-9}		70
$e^+\nu_e\nu\overline{\nu}$		< 5 × 10^{-6}	90%	70
Lepton Family number (LF) or Lepton number (L) violating modes				
$\mu^+\overline{\nu}_e$	L	[d] < 1.5 × 10^{-3}	90%	30
$\mu^+\nu_e$	LF	[d] < 8.0 × 10^{-3}	90%	30
$\mu^-e^+e^+\nu$	LF	< 1.6 × 10^{-6}	90%	30

π^0

$I^G(J^{PC}) = 1^-(0^{-+})$

Mass $m = 134.9764 \pm 0.0006$ MeV
$m_{\pi^\pm} - m_{\pi^0} = 4.5936 \pm 0.0005$ MeV
Mean life $\tau = (8.4 \pm 0.6) \times 10^{-17}$ s (S = 3.0)
$c\tau = 25.1$ nm

π^0 DECAY MODES		Fraction (Γ_i/Γ)	Scale factor/ Confidence level	p (MeV/c)
2γ		(98.798±0.032) %	S=1.1	67
$e^+e^-\gamma$		(1.198±0.032) %	S=1.1	67
γpositronium		(1.82 ±0.29) × 10^{-9}		67
$e^+e^+e^-e^-$		(3.14 ±0.30) × 10^{-5}		67
e^+e^-		(7.5 ±2.0) × 10^{-8}		67
4γ		< 2 × 10^{-8}	CL=90%	67
$\nu\overline{\nu}$	[e]	< 8.3 × 10^{-7}	CL=90%	67
$\nu_e\overline{\nu}_e$		< 1.7 × 10^{-6}	CL=90%	67
$\nu_\mu\overline{\nu}_\mu$		< 3.1 × 10^{-6}	CL=90%	67
$\nu_\tau\overline{\nu}_\tau$		< 2.1 × 10^{-6}	CL=90%	67
Charge conjugation (C) or Lepton Family number (LF) violating modes				
3γ	C	< 3.1 × 10^{-8}	CL=90%	67
$\mu^+e^- + e^-\mu^+$	LF	< 1.72 × 10^{-8}	CL=90%	26

η

$I^G(J^{PC}) = 0^+(0^{-+})$

Mass $m = 547.45 \pm 0.19$ MeV (S = 1.6)
Full width $\Gamma = 1.18 \pm 0.11$ keV [f] (S = 1.8)

C-nonconserving decay parameters [g]

$\pi^+\pi^-\pi^0$	Left-right asymmetry = $(0.09 \pm 0.17) \times 10^{-2}$
$\pi^+\pi^-\pi^0$	Sextant asymmetry = $(0.18 \pm 0.16) \times 10^{-2}$
$\pi^+\pi^-\pi^0$	Quadrant asymmetry = $(-0.17 \pm 0.17) \times 10^{-2}$
$\pi^+\pi^-\gamma$	Left-right asymmetry = $(0.9 \pm 0.4) \times 10^{-2}$
$\pi^+\pi^-\gamma$	β (D-wave) = 0.05 ± 0.06 (S = 1.5)

η DECAY MODES		Fraction (Γ_i/Γ)	Scale factor/ Confidence level	p (MeV/c)
neutral modes		(71.4 ±0.6) %	S=1.3	–
2γ	[f]	(39.25±0.31) %	S=1.3	274
$3\pi^0$		(32.1 ±0.4) %	S=1.2	180
$\pi^0 2\gamma$		(7.1 ±1.4) × 10^{-4}		258
other neutral modes		< 2.8 %	CL=90%	–
charged modes		(28.6 ±0.6) %	S=1.3	–
$\pi^+\pi^-\pi^0$		(23.2 ±0.5) %	S=1.3	175
$\pi^+\pi^-\gamma$		(4.78±0.12) %	S=1.2	236
$e^+e^-\gamma$		(4.9 ±1.1) × 10^{-3}		274
$\mu^+\mu^-\gamma$		(3.1 ±0.4) × 10^{-4}		253
e^+e^-		< 3 × 10^{-4}	CL=90%	274
$\mu^+\mu^-$		(5.8 ±0.8) × 10^{-6}		253
$\pi^+\pi^-e^+e^-$		(1.3 $^{+1.2}_{-0.8}$) × 10^{-3}		236
$\pi^+\pi^-2\gamma$		< 2.1 × 10^{-3}		236
$\pi^+\pi^-\pi^0\gamma$		< 6 × 10^{-4}	CL=90%	175
$\pi^0\mu^+\mu^-\gamma$		< 3 × 10^{-6}	CL=90%	211
Charge conjugation (C), Parity (P), or Charge conjugation × Parity (CP) violating modes				
$\pi^+\pi^-$	P,CP	< 1.5 × 10^{-3}		236
3γ	C	< 5 × 10^{-4}	CL=95%	274
$\pi^0e^+e^-$	C	[h] < 4 × 10^{-5}	CL=90%	258
$\pi^0\mu^+\mu^-$	C	[h] < 5 × 10^{-6}	CL=90%	211

$f_0(400\text{–}1200)$ [i] or σ

$I^G(J^{PC}) = 0^+(0^{++})$

The interpretation of this entry as a particle is controversial. See the "Note on scalar mesons" in the Particle Listings under the $f_0(1370)$.
Mass $m = (400\text{–}1200)$ MeV
Full width $\Gamma = (600\text{–}1000)$ MeV

$f_0(400\text{–}1200)$ DECAY MODES	Fraction (Γ_i/Γ)	p (MeV/c)
$\pi\pi$	dominant	–
$\gamma\gamma$	seen	–

$\rho(770)$ [j]

$I^G(J^{PC}) = 1^+(1^{--})$

Mass $m = 768.5 \pm 0.6$ MeV (S = 1.2)
Full width $\Gamma = 150.7 \pm 1.2$ MeV
$\Gamma_{ee} = 6.77 \pm 0.32$ keV

$\rho(770)$ DECAY MODES		Fraction (Γ_i/Γ)	Scale factor/ Confidence level	p (MeV/c)
$\pi\pi$		~ 100 %		358
$\rho(770)^\pm$ decays				
$\pi^\pm\gamma$		(4.5 ±0.5) × 10^{-4}	S=2.2	372
$\pi^\pm\eta$		< 6 × 10^{-3}	CL=84%	146
$\pi^\pm\pi^+\pi^-\pi^0$		< 2.0 × 10^{-3}	CL=84%	249
$\rho(770)^0$ decays				
$\pi^+\pi^-\gamma$		(9.9 ±1.6) × 10^{-3}		358
$\pi^0\gamma$		(7.9 ±2.0) × 10^{-4}		372
$\eta\gamma$		(3.8 ±0.7) × 10^{-4}		189
$\mu^+\mu^-$	[k]	(4.60±0.28) × 10^{-5}		369
e^+e^-	[k]	(4.48±0.22) × 10^{-5}		384
$\pi^+\pi^-\pi^0$		< 1.2 × 10^{-4}	CL=90%	319
$\pi^+\pi^-\pi^+\pi^-$		< 2 × 10^{-4}	CL=90%	246
$\pi^+\pi^-\pi^0\pi^0$		< 4 × 10^{-5}	CL=90%	252

$\omega(782)$

$I^G(J^{PC}) = 0^-(1^{--})$

Mass $m = 781.94 \pm 0.12$ MeV (S = 1.5)
Full width $\Gamma = 8.43 \pm 0.10$ MeV
$\Gamma_{ee} = 0.60 \pm 0.02$ keV

$\omega(782)$ DECAY MODES	Fraction (Γ_i/Γ)	Confidence level	p (MeV/c)
$\pi^+\pi^-\pi^0$	(88.8 ±0.7) %		327
$\pi^0\gamma$	(8.5 ±0.5) %		379
$\pi^+\pi^-$	(2.21±0.30) %		365
neutrals (excluding $\pi^0\gamma$)	(5.3 $^{+8.7}_{-3.5}$) × 10^{-3}		–
$\eta\gamma$	(8.3 ±2.1) × 10^{-4}		199
$\pi^0e^+e^-$	(5.9 ±1.9) × 10^{-4}		379
$\pi^0\mu^+\mu^-$	(9.6 ±2.3) × 10^{-5}		349

Meson Summary Table

e^+e^-		(7.15±0.19)	× 10^{-5}		391
$\pi^+\pi^-\pi^0\pi^0$		< 2	%	90%	261
$\pi^+\pi^-\gamma$		< 3.6	× 10^{-3}	95%	365
$\pi^+\pi^-\pi^+\pi^-$		< 1	× 10^{-3}	90%	256
$\pi^0\pi^0\gamma$		(7.2 ±2.5)	× 10^{-5}		367
$\mu^+\mu^-$		< 1.8	× 10^{-4}	90%	376
3γ		< 2	× 10^{-4}	90%	391
Charge conjugation (C)					
$\eta\pi^0$	C	< 1	× 10^{-3}	90%	162
$3\pi^0$	C	< 3	× 10^{-4}	90%	329

$\eta'(958)$

$I^G(J^{PC}) = 0^+(0^{-+})$

Mass m = 957.77 ± 0.14 MeV
Full width Γ = 0.201 ± 0.016 MeV (S = 1.3)

$\eta'(958)$ DECAY MODES	Fraction (Γ_i/Γ)	Scale factor/ Confidence level	p (MeV/c)
$\pi^+\pi^-\eta$	(43.7 ±1.5) %	S=1.1	232
$\rho^0\gamma$	(30.2 ±1.3) %	S=1.1	169
$\pi^0\pi^0\eta$	(20.8 ±1.3) %	S=1.2	239
$\omega\gamma$	(3.02±0.30) %		160
$\gamma\gamma$	(2.12±0.13) %	S=1.2	479
$3\pi^0$	(1.55±0.26) × 10^{-3}		430
$\mu^+\mu^-\gamma$	(1.04±0.26) × 10^{-4}		467
$\pi^+\pi^-\pi^0$	< 5 %	CL=90%	427
$\pi^0\rho^0$	< 4 %	CL=90%	118
$\pi^+\pi^-$	< 2 %	CL=90%	458
$\pi^0e^+e^-$	< 1.3 %	CL=90%	469
ηe^+e^-	< 1.1 %	CL=90%	322
$\pi^+\pi^+\pi^-\pi^-$	< 1 %	CL=90%	372
$\pi^+\pi^+\pi^-\pi^-$ neutrals	< 1 %	CL=95%	–
$\pi^+\pi^+\pi^-\pi^-\pi^0$	< 1 %	CL=90%	298
6π	< 1 %	CL=90%	189
$\pi^+\pi^-e^+e^-$	< 6	× 10^{-3} CL=90%	458
$\pi^0\pi^0$	< 9	× 10^{-4} CL=90%	459
$\pi^0\gamma\gamma$	< 8	× 10^{-4} CL=90%	469
$4\pi^0$	< 5	× 10^{-4} CL=90%	379
3γ	< 1.0	× 10^{-4} CL=90%	479
$\mu^+\mu^-\pi^0$	< 6.0	× 10^{-5} CL=90%	445
$\mu^+\mu^-\eta$	< 1.5	× 10^{-5} CL=90%	274
e^+e^-	< 2.1	× 10^{-7} CL=90%	479

$f_0(980)$ [l]

$I^G(J^{PC}) = 0^+(0^{++})$

Mass m = 980 ± 10 MeV
Full width Γ = 40 to 100 MeV

$f_0(980)$ DECAY MODES	Fraction (Γ_i/Γ)	Confidence level	p (MeV/c)
$\pi\pi$	(78.1 ±2.4) %		470
$K\overline{K}$	(21.9 ±2.4) %		–
$\gamma\gamma$	(1.19±0.33) × 10^{-5}		490
e^+e^-	< 3 × 10^{-7}	90%	490

$a_0(980)$ [l]

$I^G(J^{PC}) = 1^-(0^{++})$

Mass m = 983.5 ± 0.9 MeV
Full width Γ = 50 to 100 MeV

$a_0(980)$ DECAY MODES	Fraction (Γ_i/Γ)	p (MeV/c)
$\eta\pi$	dominant	321
$K\overline{K}$	seen	–
$\gamma\gamma$	seen	492

$\phi(1020)$

$I^G(J^{PC}) = 0^-(1^{--})$

Mass m = 1019.413 ± 0.008 MeV
Full width Γ = 4.43 ± 0.05 MeV
Γ_{ee} = 1.37 ± 0.05 keV

$\phi(1020)$ DECAY MODES	Fraction (Γ_i/Γ)	Scale factor/ Confidence level	p (MeV/c)
K^+K^-	(49.1 ±0.6) %	S=1.2	127
$K^0_LK^0_S$	(34.1 ±0.5) %	S=1.1	110
$\rho\pi$	(12.9 ±0.7) %		181
$\pi^+\pi^-\pi^0$	(2.7 ±0.9) %	S=1.1	462
$\eta\gamma$	(1.26±0.06) %	S=1.1	363
$\pi^0\gamma$	(1.31±0.13) × 10^{-3}		501
e^+e^-	(3.00±0.06) × 10^{-4}	S=1.1	510
$\mu^+\mu^-$	(2.48±0.34) × 10^{-4}		499
ηe^+e^-	(1.3 $^{+0.8}_{-0.6}$) × 10^{-4}		363
$\pi^+\pi^-$	(8 $^{+5}_{-4}$) × 10^{-5}	S=1.5	490
$\omega\gamma$	< 5 %	CL=84%	210
$\rho\gamma$	< 2 %	CL=84%	219
$\pi^+\pi^-\gamma$	< 7 × 10^{-3}	CL=90%	490
$\pi^0\pi^0\gamma$	< 1 × 10^{-3}	CL=90%	492
$\pi^+\pi^-\pi^+\pi^-$	< 8.7 × 10^{-4}	CL=90%	410
$\eta'(958)\gamma$	< 4.1 × 10^{-4}	CL=90%	60
$\pi^+\pi^+\pi^-\pi^-\pi^0$	< 1.5 × 10^{-4}	CL=95%	341
$\pi^0e^+e^-$	< 1.2 × 10^{-4}	CL=90%	501
$a_0(980)\gamma$	< 5 × 10^{-3}	CL=90%	36

$h_1(1170)$

$I^G(J^{PC}) = 0^-(1^{+-})$

Mass m = 1170 ± 20 MeV
Full width Γ = 360 ± 40 MeV

$h_1(1170)$ DECAY MODES	Fraction (Γ_i/Γ)	p (MeV/c)
$\rho\pi$	seen	310

$b_1(1235)$

$I^G(J^{PC}) = 1^+(1^{+-})$

Mass m = 1231 ± 10 MeV [l]
Full width Γ = 142 ± 8 MeV (S = 1.1)

$b_1(1235)$ DECAY MODES	Fraction (Γ_i/Γ)	Confidence level	p (MeV/c)
$\omega\pi$	dominant [D/S amplitude ratio = 0.26 ± 0.04]		348
$\pi^\pm\gamma$	(1.6±0.4) × 10^{-3}		608
$\eta\rho$	seen		–
$\pi^+\pi^+\pi^-\pi^0$	< 50 %	84%	536
$(K\overline{K})^\pm\pi^0$	< 8 %	90%	248
$K^0_SK^0_L\pi^\pm$	< 6 %	90%	238
$K^0_SK^0_S\pi^\pm$	< 2 %	90%	238
$\pi\phi$	< 1.5 %	84%	146

$a_1(1260)$ [m]

$I^G(J^{PC}) = 1^-(1^{++})$

Mass m = 1230 ± 40 MeV [l]
Full width Γ ~ 400 MeV

$a_1(1260)$ DECAY MODES	Fraction (Γ_i/Γ)	p (MeV/c)
$\rho\pi$	dominant	356
$\pi\gamma$	seen	607
$K\overline{K}^*(892)$	possibly seen	–

$f_2(1270)$

$I^G(J^{PC}) = 0^+(2^{++})$

Mass m = 1275 ± 5 MeV [l]
Full width Γ = 185 ± 20 MeV [l]

$f_2(1270)$ DECAY MODES	Fraction (Γ_i/Γ)	Scale factor/ Confidence level	p (MeV/c)
$\pi\pi$	(84.7 $^{+2.6}_{-1.2}$) %	S=1.3	622
$\pi^+\pi^-2\pi^0$	(7.2 $^{+1.4}_{-2.9}$) %	S=1.3	562
$K\overline{K}$	(4.6 ±0.5) %	S=2.8	403
$2\pi^+2\pi^-$	(2.8 ±0.4) %	S=1.2	559
$\eta\eta$	(4.5 ±1.0) × 10^{-3}	S=2.4	327
$4\pi^0$	(3.0 ±1.0) × 10^{-3}		564
$\gamma\gamma$	(1.32 $^{+0.18}_{-0.16}$) × 10^{-5}		637
$\eta\pi\pi$	< 8 × 10^{-3}	CL=95%	475
$K^0K^-\pi^+$ + c.c.	< 3.4 × 10^{-3}	CL=95%	293
e^+e^-	< 9 × 10^{-9}	CL=90%	637

$f_1(1285)$ $I^G(J^{PC}) = 0^+(1^{++})$

Mass $m = 1282.2 \pm 0.7$ MeV [l] (S = 1.7)
Full width $\Gamma = 24.8 \pm 1.3$ MeV [l] (S = 1.3)

$f_1(1285)$ DECAY MODES	Fraction (Γ_i/Γ)	Scale factor/ Confidence level	p (MeV/c)
4π	$(29 \pm 6)\%$		563
$\pi^0\pi^0\pi^+\pi^-$	$(15\ ^{+\ 9}_{-\ 8})\%$	S=1.1	566
$2\pi^+2\pi^-$	$(15 \pm 6)\%$		563
$\rho^0\pi^+\pi^-$	dominates $2\pi^+\ 2\pi^-$		340
$4\pi^0$	$< 7 \times 10^{-4}$	CL=90%	568
$\eta\pi\pi$	$(54 \pm 15)\%$		479
$a_0(980)\pi$ [ignoring $a_0(980) \to K\overline{K}$]	$(44 \pm 7)\%$	S=1.1	234
$\eta\pi\pi$ [excluding $a_0(980)\pi$]	$(10\ ^{+\ 7}_{-\ 6})\%$	S=1.1	–
$K\overline{K}\pi$	$(9.7 \pm 1.6)\%$	S=1.2	308
$K\overline{K}^*(892)$	not seen		–
$\gamma\rho^0$	$(6.6 \pm 1.3)\%$	S=1.5	410
$\phi\gamma$	$(8.0 \pm 3.1) \times 10^{-4}$		236

$\eta(1295)$ $I^G(J^{PC}) = 0^+(0^{-+})$

Mass $m = 1295 \pm 4$ MeV
Full width $\Gamma = 53 \pm 6$ MeV

$\eta(1295)$ DECAY MODES	Fraction (Γ_i/Γ)	p (MeV/c)
$\eta\pi^+\pi^-$	seen	488
$a_0(980)\pi$	seen	245

$\pi(1300)$ $I^G(J^{PC}) = 1^-(0^{-+})$

Mass $m = 1300 \pm 100$ MeV [l]
Full width $\Gamma = 200$ to 600 MeV

$\pi(1300)$ DECAY MODES	Fraction (Γ_i/Γ)	p (MeV/c)
$\rho\pi$	seen	406
$\pi(\pi\pi)_{S\text{-wave}}$	seen	612

$a_2(1320)$ $I^G(J^{PC}) = 1^-(2^{++})$

Mass $m = 1318.1 \pm 0.7$ MeV (S = 1.2)
Full width $\Gamma = 107 \pm 5$ MeV [l] ($K^\pm K^0_S$ and $\eta\pi$ modes)

$a_2(1320)$ DECAY MODES	Fraction (Γ_i/Γ)	Scale factor/ Confidence level	p (MeV/c)
$\rho\pi$	$(70.1 \pm 2.7)\%$	S=1.2	419
$\eta\pi$	$(14.5 \pm 1.2)\%$		535
$\omega\pi\pi$	$(10.6 \pm 3.2)\%$	S=1.3	362
$K\overline{K}$	$(4.9 \pm 0.8)\%$		437
$\eta'(958)\pi$	$(5.7 \pm 1.1) \times 10^{-3}$		287
$\pi^\pm\gamma$	$(2.8 \pm 0.6) \times 10^{-3}$		652
$\gamma\gamma$	$(9.7 \pm 1.0) \times 10^{-6}$		659
$\pi^+\pi^-\pi^-$	$< 8\ \%$	CL=90%	621
e^+e^-	$< 2.3 \times 10^{-7}$	CL=90%	659

$f_0(1370)$ [l] was $f_0(1300)$ $I^G(J^{PC}) = 0^+(0^{++})$

Mass $m = 1200$ to 1500 MeV
Full width $\Gamma = 300$ to 500 MeV

In two-particle decay modes the $\pi\pi$ decay is dominant. We include here the resonance observed in 4π under the same entry as the one decaying to 2 pseudoscalars. See also the minireview under non-$q\overline{q}$ candidates.

$f_0(1370)$ DECAY MODES	Fraction (Γ_i/Γ)	p (MeV/c)
$\pi\pi$	seen	–
4π	seen	–
$2\pi^+2\pi^-$	seen	–
$\pi^+\pi^-2\pi^0$	seen	–
$\eta\eta$	seen	–
$K\overline{K}$	seen	–
$\gamma\gamma$	seen	–
e^+e^-	not seen	–

$f_1(1420)$ [n] $I^G(J^{PC}) = 0^+(1^{++})$

Mass $m = 1426.8 \pm 2.3$ MeV (S = 1.3)
Full width $\Gamma = 53 \pm 5$ MeV

$f_1(1420)$ DECAY MODES	Fraction (Γ_i/Γ)	p (MeV/c)
$K\overline{K}\pi$	dominant	439
$\eta\pi\pi$	possibly seen	571

$\omega(1420)$ [o] $I^G(J^{PC}) = 0^-(1^{--})$

Mass $m = 1419 \pm 31$ MeV
Full width $\Gamma = 174 \pm 60$ MeV

$\omega(1420)$ DECAY MODES	Fraction (Γ_i/Γ)	p (MeV/c)
$\rho\pi$	dominant	488

$\eta(1440)$ [p] $I^G(J^{PC}) = 0^+(0^{-+})$

Mass $m = 1415 \pm 10$ MeV [l]
Full width $\Gamma = 60 \pm 20$ MeV [l]

$\eta(1440)$ DECAY MODES	Fraction (Γ_i/Γ)	p (MeV/c)
$K\overline{K}\pi$	seen	429
$\eta\pi\pi$	seen	564
$a_0(980)\pi$	seen	347
4π	seen	637

$\rho(1450)$ [q] $I^G(J^{PC}) = 1^+(1^{--})$

Mass $m = 1465 \pm 25$ MeV [l]
Full width $\Gamma = 310 \pm 60$ MeV [l]

$\rho(1450)$ DECAY MODES	Fraction (Γ_i/Γ)	Confidence level	p (MeV/c)
$\pi\pi$	seen		719
4π	seen		665
e^+e^-	seen		732
$\eta\rho$	$<4\ \%$		317
$\omega\pi$	$<2.0\ \%$	95%	512
$\phi\pi$	$<1\ \%$		358
$K\overline{K}$	$<1.6 \times 10^{-3}$	95%	541

$f_0(1500)$ [r] was $f_0(1525)$ and $f_0(1590)$ $I^G(J^{PC}) = 0^+(0^{++})$

Mass $m = 1503 \pm 11$ MeV
Full width $\Gamma = 120 \pm 19$ MeV

$f_0(1500)$ DECAY MODES	Fraction (Γ_i/Γ)	p (MeV/c)
$\eta\eta'(958)$	seen	–
$\eta\eta$	seen	515
$4\pi^0$	seen	690
$\pi^0\pi^0$	seen	739
$2\pi^+2\pi^-$	seen	686

$f_1(1510)$ $I^G(J^{PC}) = 0^+(1^{++})$

Mass $m = 1512 \pm 4$ MeV
Full width $\Gamma = 35 \pm 15$ MeV

$f_1(1510)$ DECAY MODES	Fraction (Γ_i/Γ)	p (MeV/c)
$K\overline{K}^*(892)+$ c.c.	seen	292

Meson Summary Table

$f_2'(1525)$

$I^G(J^{PC}) = 0^+(2^{++})$

Mass $m = 1525 \pm 5$ MeV [l]
Full width $\Gamma = 76 \pm 10$ MeV [l]

$f_2'(1525)$ DECAY MODES	Fraction (Γ_i/Γ)	p (MeV/c)
$K\overline{K}$	(88.8 ±3.1) %	581
$\eta\eta$	(10.3 ±3.1) %	531
$\pi\pi$	(8.2 ±1.5) × 10^{-3}	750
$\gamma\gamma$	(1.32±0.21) × 10^{-6}	763

$\omega(1600)$ [s]

$I^G(J^{PC}) = 0^-(1^{--})$

Mass $m = 1649 \pm 24$ MeV (S = 2.3)
Full width $\Gamma = 220 \pm 35$ MeV (S = 1.6)

$\omega(1600)$ DECAY MODES	Fraction (Γ_i/Γ)	p (MeV/c)
$\rho\pi$	seen	637
$\omega\pi\pi$	seen	601
e^+e^-	seen	824

$\omega_3(1670)$

$I^G(J^{PC}) = 0^-(3^{--})$

Mass $m = 1667 \pm 4$ MeV
Full width $\Gamma = 168 \pm 10$ MeV [l]

$\omega_3(1670)$ DECAY MODES	Fraction (Γ_i/Γ)	p (MeV/c)
$\rho\pi$	seen	647
$\omega\pi\pi$	seen	614
$b_1(1235)\pi$	possibly seen	359

$\pi_2(1670)$

$I^G(J^{PC}) = 1^-(2^{-+})$

Mass $m = 1670 \pm 20$ MeV [l]
Full width $\Gamma = 258 \pm 18$ MeV [l] (S = 1.7)
$\Gamma_{ee} = 1.35 \pm 0.26$ keV

$\pi_2(1670)$ DECAY MODES	Fraction (Γ_i/Γ)	p (MeV/c)
3π	(95.8±1.4) %	806
$f_2(1270)\pi$	(56.2±3.2) %	325
$\rho\pi$	(31 ±4) %	649
$f_0(1370)\pi$	(8.7±3.4) %	–
$K\overline{K}^*(892)+$ c.c.	(4.2±1.4) %	453
$\gamma\gamma$	(5.2±1.1) × 10^{-6}	835

$\phi(1680)$

$I^G(J^{PC}) = 0^-(1^{--})$

Mass $m = 1680 \pm 20$ MeV [l]
Full width $\Gamma = 150 \pm 50$ MeV [l]

$\phi(1680)$ DECAY MODES	Fraction (Γ_i/Γ)	p (MeV/c)
$K\overline{K}^*(892)+$ c.c.	dominant	463
$K_S^0 K\pi$	seen	620
$K\overline{K}$	seen	681
e^+e^-	seen	840
$\omega\pi\pi$	not seen	622

$\rho_3(1690)$

$I^G(J^{PC}) = 1^+(3^{--})$

J^P from the 2π and $K\overline{K}$ modes.
Mass $m = 1691 \pm 5$ MeV [l]
Full width $\Gamma = 160 \pm 10$ MeV [l] (S = 1.5)

$\rho_3(1690)$ DECAY MODES	Fraction (Γ_i/Γ)	Scale factor	p (MeV/c)
4π	(71.1 ± 1.9) %		788
$\pi^\pm\pi^+\pi^-\pi^0$	(67 ±22) %		788
$\pi\pi$	(23.6 ± 1.3) %		834
$\omega\pi$	(16 ± 6) %		656
$K\overline{K}\pi$	(3.8 ± 1.2) %		628
$K\overline{K}$	(1.58± 0.26) %	1.2	686
$\eta\pi^+\pi^-$	seen		728

$\rho(1700)$ [q]

$I^G(J^{PC}) = 1^+(1^{--})$

Mass $m = 1700 \pm 20$ MeV [l] ($\eta\rho^0$ and $\pi^+\pi^-$ modes)
Full width $\Gamma = 235 \pm 50$ MeV [l] ($\eta\rho^0$ and $\pi^+\pi^-$ modes)

$\rho(1700)$ DECAY MODES	Fraction (Γ_i/Γ)	p (MeV/c)
$\rho\pi\pi$	dominant	640
$\rho^0\pi^+\pi^-$	large	640
$\rho^\pm\pi^\mp\pi^0$	large	642
$2(\pi^+\pi^-)$	large	792
$\pi^+\pi^-$	seen	838
$K\overline{K}^*(892)+$ c.c.	seen	479
$\eta\rho$	seen	533
$K\overline{K}$	seen	692
e^+e^-	seen	850

$f_J(1710)$ [t]

$I^G(J^{PC}) = 0^+(\text{even}^{++})$

Mass $m = 1697 \pm 4$ MeV (S = 1.4)
Full width $\Gamma = 175 \pm 9$ MeV (S = 1.7)

$f_J(1710)$ DECAY MODES	Fraction (Γ_i/Γ)	p (MeV/c)
$K\overline{K}$	seen	690
$\eta\eta$	seen	648
$\pi\pi$	seen	837

$\phi_3(1850)$

$I^G(J^{PC}) = 0^-(3^{--})$

Mass $m = 1854 \pm 7$ MeV
Full width $\Gamma = 87^{+28}_{-23}$ MeV (S = 1.2)

$\phi_3(1850)$ DECAY MODES	Fraction (Γ_i/Γ)	p (MeV/c)
$K\overline{K}$	seen	785
$K\overline{K}^*(892)+$ c.c.	seen	602

$f_2(2010)$

$I^G(J^{PC}) = 0^+(2^{++})$

Seen by one group only.
Mass $m = 2011^{+60}_{-80}$ MeV
Full width $\Gamma = 202 \pm 60$ MeV

$f_2(2010)$ DECAY MODES	Fraction (Γ_i/Γ)	p (MeV/c)
$\phi\phi$	seen	–

$f_4(2050)$

$I^G(J^{PC}) = 0^+(4^{++})$

Mass $m = 2044 \pm 11$ MeV (S = 1.4)
Full width $\Gamma = 208 \pm 13$ MeV (S = 1.2)

$f_4(2050)$ DECAY MODES	Fraction (Γ_i/Γ)	p (MeV/c)
$\omega\omega$	(26 ±6) %	658
$\pi\pi$	(17.0±1.5) %	1012
$K\overline{K}$	($6.8^{+3.4}_{-1.8}$) × 10^{-3}	895
$\eta\eta$	(2.1±0.8) × 10^{-3}	863
$4\pi^0$	< 1.2 %	977

$f_2(2300)$

$I^G(J^{PC}) = 0^+(2^{++})$

Mass $m = 2297 \pm 28$ MeV
Full width $\Gamma = 149 \pm 40$ MeV

$f_2(2300)$ DECAY MODES	Fraction (Γ_i/Γ)	p (MeV/c)
$\phi\phi$	seen	529

$f_2(2340)$

$I^G(J^{PC}) = 0^+(2^{++})$

Mass $m = 2339 \pm 60$ MeV
Full width $\Gamma = 319^{+80}_{-70}$ MeV

$f_2(2340)$ DECAY MODES	Fraction (Γ_i/Γ)	p (MeV/c)
$\phi\phi$	seen	573

STRANGE MESONS ($S = \pm 1$, $C = B = 0$)

$K^+ = u\bar{s}$, $K^0 = d\bar{s}$, $\overline{K}^0 = \bar{d}s$, $K^- = \bar{u}s$, similarly for K^*'s

$K^\pm$

$I(J^P) = \frac{1}{2}(0^-)$

Mass $m = 493.677 \pm 0.016$ MeV [u] (S = 2.8)
Mean life $\tau = (1.2386 \pm 0.0024) \times 10^{-8}$ s (S = 2.0)
$c\tau = 3.713$ m

Slope parameter g [v]

(See Particle Listings for quadratic coefficients)
$K^+ \to \pi^+\pi^+\pi^- = -0.2154 \pm 0.0035$ (S = 1.4)
$K^- \to \pi^-\pi^-\pi^+ = -0.217 \pm 0.007$ (S = 2.5)
$K^\pm \to \pi^\pm\pi^0\pi^0 = 0.594 \pm 0.019$ (S = 1.3)

$K^\pm$ decay form factors [a,w]

K^+_{e3} $\lambda_+ = 0.0286 \pm 0.0022$
$K^+_{\mu3}$ $\lambda_+ = 0.033 \pm 0.008$ (S = 1.6)
$K^+_{\mu3}$ $\lambda_0 = 0.004 \pm 0.007$ (S = 1.6)
K^+_{e3} $|f_S/f_+| = 0.084 \pm 0.023$ (S = 1.2)
K^+_{e3} $|f_T/f_+| = 0.38 \pm 0.11$ (S = 1.1)
$K^+_{\mu3}$ $|f_T/f_+| = 0.02 \pm 0.12$
$K^+ \to e^+\nu_e\gamma$ $|F_A + F_V| = 0.148 \pm 0.010$
$K^+ \to \mu^+\nu_\mu\gamma$ $|F_A + F_V| < 0.23$, CL = 90%
$K^+ \to e^+\nu_e\gamma$ $|F_A - F_V| < 0.49$
$K^+ \to \mu^+\nu_\mu\gamma$ $|F_A - F_V| = -2.2$ to 0.3

K^- modes are charge conjugates of the modes below.

K^+ DECAY MODES		Fraction (Γ_i/Γ)	Scale factor/ Confidence level	p (MeV/c)
$\mu^+\nu_\mu$		(63.51±0.18) %	S=1.3	236
$e^+\nu_e$		(1.55±0.07) × 10^{-5}		247
$\pi^+\pi^0$		(21.16±0.14) %	S=1.1	205
$\pi^+\pi^+\pi^-$		(5.59±0.05) %	S=1.8	125
$\pi^+\pi^0\pi^0$		(1.73±0.04) %	S=1.2	133
$\pi^0\mu^+\nu_\mu$ Called $K^+_{\mu3}$.		(3.18±0.08) %	S=1.5	215
$\pi^0 e^+\nu_e$ Called K^+_{e3}.		(4.82±0.06) %	S=1.3	228
$\pi^0\pi^0 e^+\nu_e$		(2.1 ±0.4) × 10^{-5}		206
$\pi^+\pi^- e^+\nu_e$		(3.91±0.17) × 10^{-5}		203
$\pi^+\pi^-\mu^+\nu_\mu$		(1.4 ±0.9) × 10^{-5}		151
$\pi^0\pi^0\pi^0 e^+\nu_e$		< 3.5 × 10^{-6}	CL=90%	135
$\pi^+\gamma\gamma$	[x]	< 1 × 10^{-6}	CL=90%	227
$\pi^+ 3\gamma$	[x]	< 1.0 × 10^{-4}	CL=90%	227
$\mu^+\nu_\mu\nu\overline{\nu}$		< 6.0 × 10^{-6}	CL=90%	236
$e^+\nu_e\nu\overline{\nu}$		< 6 × 10^{-5}	CL=90%	247
$\mu^+\nu_\mu e^+ e^-$		(1.06±0.32) × 10^{-6}		236
$e^+\nu_e e^+ e^-$		(2.1 $^{+2.1}_{-1.1}$) × 10^{-7}		247
$\mu^+\nu_\mu\mu^+\mu^-$		< 4.1 × 10^{-7}	CL=90%	185
$\mu^+\nu_\mu\gamma$	[x,y]	(5.50±0.28) × 10^{-3}		236
$\pi^+\pi^0\gamma$	[x,y]	(2.75±0.15) × 10^{-4}		205
$\pi^+\pi^0\gamma$(DE)	[x,z]	(1.8 ±0.4) × 10^{-5}		205
$\pi^+\pi^+\pi^-\gamma$	[x,y]	(1.04±0.31) × 10^{-4}		125
$\pi^+\pi^0\pi^0\gamma$	[x,y]	(7.5 $^{+5.5}_{-3.0}$) × 10^{-6}		133
$\pi^0\mu^+\nu_\mu\gamma$	[x,y]	< 6.1 × 10^{-5}	CL=90%	215
$\pi^0 e^+\nu_e\gamma$	[x,y]	(2.62±0.20) × 10^{-4}		228
$\pi^0 e^+\nu_e\gamma$(SD)	[aa]	< 5.3 × 10^{-5}	CL=90%	228
$\pi^0\pi^0 e^+\nu_e\gamma$		< 5 × 10^{-6}	CL=90%	206

Lepton Family number (LF), Lepton number (L), $\Delta S = \Delta Q$ (SQ) violating modes, or $\Delta S = 1$ weak neutral current ($S1$) modes

$\pi^+\pi^+ e^-\overline{\nu}_e$	SQ	< 1.2	× 10^{-8}	CL=90%	203
$\pi^+\pi^+\mu^-\overline{\nu}_\mu$	SQ	< 3.0	× 10^{-6}	CL=95%	151
$\pi^+ e^+ e^-$	$S1$	(2.74±0.23)	× 10^{-7}		227
$\pi^+\mu^+\mu^-$	$S1$	< 2.3	× 10^{-7}	CL=90%	172
$\pi^+\nu\overline{\nu}$	$S1$	< 2.4	× 10^{-9}	CL=90%	227
$\mu^-\nu e^+ e^+$	LF	< 2.0	× 10^{-8}	CL=90%	236
$\mu^+\nu_e$	LF	[d] < 4	× 10^{-3}	CL=90%	236
$\pi^+\mu^+ e^-$	LF	< 2.1	× 10^{-10}	CL=90%	214
$\pi^+\mu^- e^+$	LF	< 7	× 10^{-9}	CL=90%	214
$\pi^-\mu^+ e^+$	L	< 7	× 10^{-9}	CL=90%	214
$\pi^- e^+ e^+$	L	< 1.0	× 10^{-8}	CL=90%	227
$\pi^-\mu^+\mu^+$	L	< 1.5	× 10^{-4}	CL=90%	172
$\mu^+\overline{\nu}_e$	L	[d] < 3.3	× 10^{-3}	CL=90%	236
$\pi^0 e^+\overline{\nu}_e$	L	[d] < 3	× 10^{-3}	CL=90%	228

K^0

$I(J^P) = \frac{1}{2}(0^-)$

50% K_S, 50% K_L
Mass $m = 497.672 \pm 0.031$ MeV
$m_{K^0} - m_{K^\pm} = 3.995 \pm 0.034$ MeV (S = 1.1)
$|m_{K^0} - m_{\overline{K}^0}| / m_{\text{average}} < 9 \times 10^{-19}$ [bb]

K^0_S

$I(J^P) = \frac{1}{2}(0^-)$

Mean life $\tau = (0.8927 \pm 0.0009) \times 10^{-10}$ s
$c\tau = 2.6762$ cm

CP-violation parameters [cc]

$\mathrm{Im}(\eta_{+-0}) = -0.015 \pm 0.030$
$\mathrm{Im}(\eta_{000})^2 < 0.1$, CL = 90%

K^0_S DECAY MODES		Fraction (Γ_i/Γ)	Scale factor/ Confidence level	p (MeV/c)
$\pi^+\pi^-$		(68.61±0.28) %	S=1.2	206
$\pi^0\pi^0$		(31.39±0.28) %	S=1.2	209
$\pi^+\pi^-\gamma$	[y,dd]	(1.78±0.05) × 10^{-3}		206
$\gamma\gamma$		(2.4 ±0.9) × 10^{-6}		249
$\pi^+\pi^-\pi^0$		(3.9 $^{+5.5}_{-1.9}$) × 10^{-7}		133
$3\pi^0$		< 3.7 × 10^{-5}	CL=90%	139
$\pi^\pm e^\mp\nu$	[ee]	(6.70±0.07) × 10^{-4}	S=1.3	229
$\pi^\pm\mu^\mp\nu$	[ee]	(4.69±0.06) × 10^{-4}	S=1.2	216
$\Delta S = 1$ weak neutral current ($S1$) modes				
$\mu^+\mu^-$	$S1$	< 3.2 × 10^{-7}	CL=90%	225
$e^+ e^-$	$S1$	< 2.8 × 10^{-6}	CL=90%	249
$\pi^0 e^+ e^-$	$S1$	< 1.1 × 10^{-6}	CL=90%	231

K^0_L

$I(J^P) = \frac{1}{2}(0^-)$

$m_{K_L} - m_{K_S} = (0.5304 \pm 0.0014) \times 10^{10}\ \hbar\ \mathrm{s}^{-1}$
$= (3.491 \pm 0.009) \times 10^{-12}$ MeV
Mean life $\tau = (5.17 \pm 0.04) \times 10^{-8}$ s (S = 1.1)
$c\tau = 15.51$ m

Slope parameter g [v]

(See Particle Listings for quadratic coefficients)
$K^0_L \to \pi^+\pi^-\pi^0 = 0.670 \pm 0.014$ (S = 1.6)

K_L decay form factors [w]

K^0_{e3} $\lambda_+ = 0.0300 \pm 0.0016$ (S = 1.2)
$K^0_{\mu3}$ $\lambda_+ = 0.034 \pm 0.005$ (S = 2.3)
$K^0_{\mu3}$ $\lambda_0 = 0.025 \pm 0.006$ (S = 2.3)
K^0_{e3} $|f_S/f_+| < 0.04$, CL = 68%
K^0_{e3} $|f_T/f_+| < 0.23$, CL = 68%
$K^0_{\mu3}$ $|f_T/f_+| = 0.12 \pm 0.12$
$K_L \to e^+ e^-\gamma$: $\alpha_{K^*} = -0.28 \pm 0.08$

Meson Summary Table

CP-violation parameters [cc]

$\delta = (0.327 \pm 0.012)\%$
$|\eta_{00}| = (2.275 \pm 0.019) \times 10^{-3}$ (S = 1.1)
$|\eta_{+-}| = (2.285 \pm 0.019) \times 10^{-3}$
$|\eta_{00}/\eta_{+-}| = 0.9956 \pm 0.0023$ [ff] (S = 1.8)
$\epsilon'/\epsilon = (1.5 \pm 0.8) \times 10^{-3}$ [ff] (S = 1.8)
$\phi_{+-} = (43.7 \pm 0.6)°$
$\phi_{00} = (43.5 \pm 1.0)°$
$\phi_{00} - \phi_{+-} = (-0.2 \pm 0.8)°$
j for $K_L^0 \to \pi^+\pi^-\pi^0 = 0.0011 \pm 0.0008$
$|\eta_{+-\gamma}| = (2.35 \pm 0.07) \times 10^{-3}$
$\phi_{+-\gamma} = (44 \pm 4)°$
$|\epsilon'_{+-\gamma}|/\epsilon < 0.3$, CL = 90%

$\Delta S = -\Delta Q$ in $K^0_{\ell 3}$ decay

Re $x = 0.006 \pm 0.018$ (S = 1.3)
Im $x = -0.003 \pm 0.026$ (S = 1.2)

CPT-violation parameters

Re $\Delta = 0.018 \pm 0.020$
Im $\Delta = 0.02 \pm 0.04$

K^0_L DECAY MODES		Fraction (Γ_i/Γ)	Scale factor/ Confidence level	p (MeV/c)
$3\pi^0$		(21.12 ±0.27) %	S=1.1	139
$\pi^+\pi^-\pi^0$		(12.56 ±0.20) %	S=1.7	133
$\pi^\pm\mu^\mp\nu$ Called $K^0_{\mu 3}$.	[gg]	(27.17 ±0.25) %	S=1.1	216
$\pi^\pm e^\mp\nu_e$ Called K^0_{e3}.	[gg]	(38.78 ±0.27) %	S=1.1	229
2γ		(5.92 ±0.15) $\times 10^{-4}$		249
3γ		< 2.4 $\times 10^{-7}$	CL=90%	249
$\pi^0 2\gamma$	[hh]	(1.70 ±0.28) $\times 10^{-6}$		231
$\pi^0\pi^\pm e^\mp\nu$	[gg]	(5.18 ±0.29) $\times 10^{-5}$		207
$(\pi\mu\text{atom})\nu$		(1.06 ±0.11) $\times 10^{-7}$		–
$\pi^\pm e^\mp\nu_e\gamma$	[y,gg,hh]	(1.3 ±0.8) %		229
$\pi^+\pi^-\gamma$	[y,hh]	(4.61 ±0.14) $\times 10^{-5}$		206
$\pi^0\pi^0\gamma$		< 5.6 $\times 10^{-6}$		209
Charge conjugation × Parity (CP, CPV) or Lepton Family number (LF) violating modes, or $\Delta S = 1$ weak neutral current (S1) modes				
$\pi^+\pi^-$	CPV	(2.067±0.035) $\times 10^{-3}$	S=1.1	206
$\pi^0\pi^0$	CPV	(9.36 ±0.20) $\times 10^{-4}$		209
$\mu^+\mu^-$	S1	(7.2 ±0.5) $\times 10^{-9}$	S=1.4	225
$\mu^+\mu^-\gamma$	S1	(3.23 ±0.30) $\times 10^{-7}$		225
e^+e^-	S1	< 4.1 $\times 10^{-11}$	CL=90%	249
$e^+e^-\gamma$	S1	(9.1 ±0.5) $\times 10^{-6}$		249
$e^+e^-\gamma\gamma$	S1 [hh]	(6.5 ±1.2) $\times 10^{-7}$		249
$\pi^+\pi^-e^+e^-$	S1	< 2.5 $\times 10^{-6}$	CL=90%	206
$\mu^+\mu^-e^+e^-$	S1	< 4.9 $\times 10^{-6}$	CL=90%	225
$e^+e^-e^+e^-$	S1 [ii]	(4.1 ±0.8) $\times 10^{-8}$	S=1.2	249
$\pi^0\mu^+\mu^-$	CP,S1 [jj]	< 5.1 $\times 10^{-9}$	CL=90%	177
$\pi^0 e^+e^-$	CP,S1 [jj]	< 4.3 $\times 10^{-9}$	CL=90%	231
$\pi^0\nu\overline{\nu}$	CP,S1 [kk]	< 5.8 $\times 10^{-5}$	CL=90%	231
$e^\pm\mu^\mp$	LF [gg]	< 3.3 $\times 10^{-11}$	CL=90%	238

$K^*(892)$ $I(J^P) = \frac{1}{2}(1^-)$

$K^*(892)^\pm$ mass $m = 891.59 \pm 0.24$ MeV (S = 1.1)
$K^*(892)^0$ mass $m = 896.10 \pm 0.28$ MeV (S = 1.4)
$K^*(892)^\pm$ full width $\Gamma = 49.8 \pm 0.8$ MeV
$K^*(892)^0$ full width $\Gamma = 50.5 \pm 0.6$ MeV (S = 1.1)

$K^*(892)$ DECAY MODES	Fraction (Γ_i/Γ)	Confidence level	p (MeV/c)
$K\pi$	~ 100 %		291
$K^0\gamma$	(2.30±0.20) $\times 10^{-3}$		310
$K^\pm\gamma$	(1.01±0.09) $\times 10^{-3}$		309
$K\pi\pi$	< 7 $\times 10^{-4}$	95%	224

$K_1(1270)$ $I(J^P) = \frac{1}{2}(1^+)$

Mass $m = 1273 \pm 7$ MeV [l]
Full width $\Gamma = 90 \pm 20$ MeV [l]

$K_1(1270)$ DECAY MODES	Fraction (Γ_i/Γ)	p (MeV/c)
$K\rho$	(42 ±6) %	76
$K_0^*(1430)\pi$	(28 ±4) %	–
$K^*(892)\pi$	(16 ±5) %	301
$K\omega$	(11.0±2.0) %	–
$Kf_0(1370)$	(3.0±2.0) %	–

$K_1(1400)$ $I(J^P) = \frac{1}{2}(1^+)$

Mass $m = 1402 \pm 7$ MeV
Full width $\Gamma = 174 \pm 13$ MeV (S = 1.6)

$K_1(1400)$ DECAY MODES	Fraction (Γ_i/Γ)	p (MeV/c)
$K^*(892)\pi$	(94 ±6) %	401
$K\rho$	(3.0±3.0) %	298
$Kf_0(1370)$	(2.0±2.0) %	–
$K\omega$	(1.0±1.0) %	285

$K^*(1410)$ $I(J^P) = \frac{1}{2}(1^-)$

Mass $m = 1412 \pm 12$ MeV (S = 1.1)
Full width $\Gamma = 227 \pm 22$ MeV (S = 1.1)

$K^*(1410)$ DECAY MODES	Fraction (Γ_i/Γ)	Confidence level	p (MeV/c)
$K^*(892)\pi$	> 40 %	95%	408
$K\pi$	(6.6±1.3) %		611
$K\rho$	< 7 %	95%	309

$K_0^*(1430)$ [l] $I(J^P) = \frac{1}{2}(0^+)$

Mass $m = 1429 \pm 6$ MeV
Full width $\Gamma = 287 \pm 23$ MeV

$K_0^*(1430)$ DECAY MODES	Fraction (Γ_i/Γ)	p (MeV/c)
$K\pi$	(93±10) %	621

$K_2^*(1430)$ $I(J^P) = \frac{1}{2}(2^+)$

$K_2^*(1430)^\pm$ mass $m = 1425.4 \pm 1.3$ MeV (S = 1.1)
$K_2^*(1430)^0$ mass $m = 1432.4 \pm 1.3$ MeV
$K_2^*(1430)^\pm$ full width $\Gamma = 98.4 \pm 2.3$ MeV
$K_2^*(1430)^0$ full width $\Gamma = 109 \pm 5$ MeV (S = 1.9)

$K_2^*(1430)$ DECAY MODES	Fraction (Γ_i/Γ)	Scale factor/ Confidence level	p (MeV/c)
$K\pi$	(49.7±1.2) %		622
$K^*(892)\pi$	(25.2±1.7) %		423
$K^*(892)\pi\pi$	(13.0±2.3) %		375
$K\rho$	(8.8±0.8) %	S=1.2	331
$K\omega$	(2.9±0.8) %		319
$K^+\gamma$	(2.4±0.5) $\times 10^{-3}$		627
$K\eta$	($1.4^{+2.8}_{-0.9}$) $\times 10^{-3}$	S=1.1	492
$K\omega\pi$	< 7.2 $\times 10^{-4}$	CL=95%	110
$K^0\gamma$	< 9 $\times 10^{-4}$	CL=90%	631

$K^*(1680)$

$I(J^P) = \frac{1}{2}(1^-)$

Mass $m = 1714 \pm 20$ MeV (S = 1.1)
Full width $\Gamma = 323 \pm 110$ MeV (S = 4.2)

$K^*(1680)$ DECAY MODES	Fraction (Γ_i/Γ)	p (MeV/c)
$K\pi$	(38.7±2.5) %	779
$K\rho$	$(31.4^{+4.7}_{-2.1})$ %	571
$K^*(892)\pi$	$(29.9^{+2.2}_{-4.7})$ %	615

$K_2(1770)$ [mm]

$I(J^P) = \frac{1}{2}(2^-)$

Mass $m = 1773 \pm 8$ MeV
Full width $\Gamma = 186 \pm 14$ MeV

$K_2(1770)$ DECAY MODES	Fraction (Γ_i/Γ)	p (MeV/c)
$K\pi\pi$		–
$K_2^*(1430)\pi$	dominant	287
$K^*(892)\pi$	seen	653
$Kf_2(1270)$	seen	–
$K\phi$	seen	441
$K\omega$	seen	608

$K_3^*(1780)$

$I(J^P) = \frac{1}{2}(3^-)$

Mass $m = 1770 \pm 10$ MeV (S = 1.7)
Full width $\Gamma = 164 \pm 17$ MeV (S = 1.1)

$K_3^*(1780)$ DECAY MODES	Fraction (Γ_i/Γ)	Scale factor/ Confidence level	p (MeV/c)
$K\rho$	(45 ±4) %	S=1.4	612
$K^*(892)\pi$	(27.3±3.2) %	S=1.5	651
$K\pi$	(19.3±1.0) %		810
$K\eta$	(8.0±1.5) %	S=1.4	715
$K_2^*(1430)\pi$	< 21 %	CL=95%	284

$K_2(1820)$ [nn]

$I(J^P) = \frac{1}{2}(2^-)$

Mass $m = 1816 \pm 13$ MeV
Full width $\Gamma = 276 \pm 35$ MeV

$K_2(1820)$ DECAY MODES	Fraction (Γ_i/Γ)	p (MeV/c)
$K\phi$	possibly seen	481
$K_2^*(1430)\pi$	seen	325
$K^*(892)\pi$	seen	680
$Kf_2(1270)$	seen	186
$K\omega$	seen	638

$K_4^*(2045)$

$I(J^P) = \frac{1}{2}(4^+)$

Mass $m = 2045 \pm 9$ MeV (S = 1.1)
Full width $\Gamma = 198 \pm 30$ MeV

$K_4^*(2045)$ DECAY MODES	Fraction (Γ_i/Γ)	p (MeV/c)
$K\pi$	(9.9±1.2) %	958
$K^*(892)\pi\pi$	(9 ±5) %	800
$K^*(892)\pi\pi\pi$	(7 ±5) %	764
$\rho K\pi$	(5.7±3.2) %	742
$\omega K\pi$	(5.0±3.0) %	736
$\phi K\pi$	(2.8±1.4) %	591
$\phi K^*(892)$	(1.4±0.7) %	363

CHARMED MESONS ($C = \pm 1$)

$D^+ = c\overline{d}$, $D^0 = c\overline{u}$, $\overline{D}^0 = \overline{c}u$, $D^- = \overline{c}d$, similarly for D^*'s

$D^\pm$

$I(J^P) = \frac{1}{2}(0^-)$

Mass $m = 1869.3 \pm 0.5$ MeV (S = 1.1)
Mean life $\tau = (1.057 \pm 0.015) \times 10^{-12}$ s
$c\tau = 317$ μm

CP-violation decay-rate asymmetries

$A_{CP}(K^+K^-\pi^\pm) = -0.03 \pm 0.07$
$A_{CP}(K^\pm K^{*0}) = -0.12 \pm 0.13$
$A_{CP}(\phi\pi^\pm) = 0.07 \pm 0.09$

$D^+ \to \overline{K}^*(892)^0\ell^+\nu_\ell$ form factors

$r_2 = 0.73 \pm 0.15$
$r_v = 1.90 \pm 0.25$
$\Gamma_L/\Gamma_T = 1.23 \pm 0.13$
$\Gamma_+/\Gamma_- = 0.16 \pm 0.04$

D^- modes are charge conjugates of the modes below.

D^+ DECAY MODES		Fraction (Γ_i/Γ)		Scale factor/ Confidence level	p (MeV/c)
Inclusive modes					
e^+ anything		(17.2 ±1.9) %			–
K^- anything		(24.2 ±2.8) %		S=1.4	–
$\overline{K}^0$ anything + K^0 anything		(59 ±7) %			–
K^+ anything		(5.8 ±1.4) %			–
η anything	[oo]	< 13	%	CL=90%	–
Leptonic and semileptonic modes					
$\mu^+\nu_\mu$		< 7.2	$\times 10^{-4}$	CL=90%	932
$\overline{K}^0\ell^+\nu_\ell$	[pp]	(6.7 ±0.8) %			868
$\overline{K}^0 e^+\nu_e$		(6.6 ±0.9) %			868
$\overline{K}^0\mu^+\nu_\mu$		(7.0 $^{+3.0}_{-2.0}$) %			865
$K^-\pi^+e^+\nu_e$		(4.2 $^{+0.9}_{-0.7}$) %			863
$\overline{K}^*(892)^0 e^+\nu_e$ × B($\overline{K}^{*0} \to K^-\pi^+$)		(3.2 ±0.33) %			720
$K^-\pi^+e^+\nu_e$ nonresonant		< 7	$\times 10^{-3}$	CL=90%	863
$K^-\pi^+\mu^+\nu_\mu$		(3.2 ±0.4) %		S=1.1	851
$\overline{K}^*(892)^0\mu^+\nu_\mu$ × B($\overline{K}^{*0} \to K^-\pi^+$)		(3.0 ±0.4) %			715
$K^-\pi^+\mu^+\nu_\mu$ nonresonant		(2.7 ±1.1)	$\times 10^{-3}$		851
$(\overline{K}^*(892)\pi)^0 e^+\nu_e$		< 1.2	%	CL=90%	714
$(\overline{K}\pi\pi)^0 e^+\nu_e$ non-$\overline{K}^*(892)$		< 9	$\times 10^{-3}$	CL=90%	846
$K^-\pi^+\pi^0\mu^+\nu_\mu$		< 1.4	$\times 10^{-3}$	CL=90%	825
$\pi^0\ell^+\nu_\ell$	[qq]	(5.7 ±2.2)	$\times 10^{-3}$		930

Fractions of some of the following modes with resonances have already appeared above as submodes of particular charged-particle modes.

$\overline{K}^*(892)^0\ell^+\nu_\ell$	[pp]	(4.8 ±0.4) %			720
$\overline{K}^*(892)^0 e^+\nu_e$		(4.8 ±0.5) %			720
$\overline{K}^*(892)^0\mu^+\nu_\mu$		(4.5 ±0.6) %		S=1.1	715
$\rho^0 e^+\nu_e$		< 3.7	$\times 10^{-3}$	CL=90%	776
$\rho^0\mu^+\nu_\mu$		(2.0 $^{+1.5}_{-1.3}$)	$\times 10^{-3}$		772
$\phi e^+\nu_e$		< 2.09	%	CL=90%	657
$\phi\mu^+\nu_\mu$		< 3.72	%	CL=90%	651
$\eta'(958)\mu^+\nu_\mu$		< 9	$\times 10^{-3}$	CL=90%	684
Hadronic modes with a $\overline{K}$ or $\overline{K}K\overline{K}$					
$\overline{K}^0\pi^+$		(2.74±0.29) %			862
$K^-\pi^+\pi^+$	[rr]	(9.1 ±0.6) %			845
$\overline{K}^*(892)^0\pi^+$ × B($\overline{K}^{*0} \to K^-\pi^+$)		(1.28±0.13) %			712
$\overline{K}_0^*(1430)^0\pi^+$ × B($\overline{K}_0^*(1430)^0 \to K^-\pi^+$)		(2.3 ±0.3) %			368
$\overline{K}^*(1680)^0\pi^+$ × B($\overline{K}^*(1680)^0 \to K^-\pi^+$)		(3.7 ±0.8)	$\times 10^{-3}$		65
$K^-\pi^+\pi^+$ nonresonant		(8.6 ±0.9) %			845

Meson Summary Table

$\overline{K}^0\pi^+\pi^0$	[rr]	(9.7 ±3.0) %	S=1.1	845
$\overline{K}^0\rho^+$		(6.6 ±2.5) %		680
$\overline{K}^*(892)^0\pi^+$ × B($\overline{K}^{*0}\to\overline{K}^0\pi^0$)		(6.4 ±0.6) × 10^{-3}		712
$\overline{K}^0\pi^+\pi^0$ nonresonant		(1.3 ±1.1) %		845
$K^-\pi^+\pi^+\pi^0$	[rr]	(6.4 ±1.1) %		816
$\overline{K}^*(892)^0\rho^+$ total × B($\overline{K}^{*0}\to K^-\pi^+$)		(1.4 ±0.9) %		423
$\overline{K}_1(1400)^0\pi^+$ × B($\overline{K}_1(1400)^0\to K^-\pi^+\pi^0$)		(2.2 ±0.6) %		390
$K^-\rho^+\pi^+$ total		(3.1 ±1.1) %		616
$K^-\rho^+\pi^+$ 3-body		(1.1 ±0.4) %		616
$\overline{K}^*(892)^0\pi^+\pi^0$ total × B($\overline{K}^{*0}\to K^-\pi^+$)		(4.5 ±0.9) %		687
$\overline{K}^*(892)^0\pi^+\pi^0$ 3-body × B($\overline{K}^{*0}\to K^-\pi^+$)		(2.8 ±0.9) %		687
$K^*(892)^-\pi^+\pi^+$ 3-body × B($K^{*-}\to K^-\pi^0$)		(7 ±3) × 10^{-3}		688
$K^-\pi^+\pi^+\pi^0$ nonresonant	[ss]	(1.2 ±0.6) %		816
$\overline{K}^0\pi^+\pi^+\pi^-$	[rr]	(7.0 ±1.0) %		814
$\overline{K}^0 a_1(1260)^+$ × B($a_1(1260)^+\to\pi^+\pi^+\pi^-$)		(4.0 ±0.9) %		328
$\overline{K}_1(1400)^0\pi^+$ × B($\overline{K}_1(1400)^0\to\overline{K}^0\pi^+\pi^-$)		(2.2 ±0.6) %		390
$K^*(892)^-\pi^+\pi^+$ 3-body × B($K^{*-}\to\overline{K}^0\pi^-$)		(1.4 ±0.6) %		688
$\overline{K}^0\rho^0\pi^+$ total		(4.2 ±0.9) %		614
$\overline{K}^0\rho^0\pi^+$ 3-body		(5 ±5) × 10^{-3}		614
$\overline{K}^0\pi^+\pi^+\pi^-$ nonresonant		(8 ±4) × 10^{-3}		814
$K^-\pi^+\pi^+\pi^+\pi^-$		(8.2 ±1.4) × 10^{-3}		772
$\overline{K}^*(892)^0\pi^+\pi^+\pi^-$ × B($\overline{K}^{*0}\to K^-\pi^+$)		(6.8 ±1.8) × 10^{-3}		642
$\overline{K}^*(892)^0\rho^0\pi^+$ × B($\overline{K}^{*0}\to K^-\pi^+$)		(5.1 ±2.2) × 10^{-3}		242
$K^-\pi^+\pi^+\pi^0\pi^0$		(2.2 $^{+5.0}_{-0.9}$) %		775
$\overline{K}^0\pi^+\pi^+\pi^-\pi^0$		(5.4 $^{+3.0}_{-1.4}$) %		773
$\overline{K}^0\pi^+\pi^+\pi^+\pi^-\pi^-$		(8 ±7) × 10^{-4}		714
$K^-\pi^+\pi^+\pi^+\pi^-\pi^0$		(2.0 ±1.8) × 10^{-3}		718
$\overline{K}^0\overline{K}^0K^+$		(1.8 ±0.8) %		545

Fractions of some of the following modes with resonances have already appeared above as submodes of particular charged-particle modes.

$\overline{K}^0\rho^+$		(6.6 ±2.5) %		680
$\overline{K}^0 a_1(1260)^+$		(8.1 ±1.7) %		328
$\overline{K}^0 a_2(1320)^+$		< 3 × 10^{-3}	CL=90%	199
$\overline{K}^*(892)^0\pi^+$		(1.92±0.19) %		712
$\overline{K}^*(892)^0\rho^+$ total		(2.1 ±1.4) %		423
$\overline{K}^*(892)^0\rho^+$ S-wave	[ss]	(1.7 ±1.6) %		423
$\overline{K}^*(892)^0\rho^+$ P-wave		< 1 × 10^{-3}	CL=90%	423
$\overline{K}^*(892)^0\rho^+$ D-wave		(10 ±7) × 10^{-3}		423
$\overline{K}^*(892)^0\rho^+$ D-wave longitudinal		< 7 × 10^{-3}	CL=90%	423
$\overline{K}_1(1270)^0\pi^+$		< 7 × 10^{-3}	CL=90%	487
$\overline{K}_1(1400)^0\pi^+$		(5.0 ±1.3) %		390
$\overline{K}^*(1410)^0\pi^+$		< 7 × 10^{-3}	CL=90%	382
$\overline{K}_0^*(1430)^0\pi^+$		(3.7 ±0.4) %		368
$\overline{K}^*(1680)^0\pi^+$		(1.45±0.31) %		65
$\overline{K}^*(892)^0\pi^+\pi^0$ total		(6.7 ±1.4) %		687
$\overline{K}^*(892)^0\pi^+\pi^0$ 3-body		(4.2 ±1.4) %		687
$K^*(892)^-\pi^+\pi^+$ 3-body		(2.1 ±0.9) %		688
$K^-\rho^+\pi^+$ total		(3.1 ±1.1) %		616
$K^-\rho^+\pi^+$ 3-body		(1.1 ±0.4) %		616
$\overline{K}^0\rho^0\pi^+$ total		(4.2 ±0.9) %	CL=90%	614
$\overline{K}^0\rho^0\pi^+$ 3-body		(5 ±5) × 10^{-3}		614
$\overline{K}^0 f_0(980)\pi^+$		< 5 × 10^{-3}	CL=90%	461
$\overline{K}^*(892)^0\pi^+\pi^+\pi^-$		(1.02±0.27) %		642
$\overline{K}^*(892)^0\rho^0\pi^+$		(7.7 ±3.3) × 10^{-3}		242

Pionic modes

$\pi^+\pi^0$		(2.5 ±0.7) × 10^{-3}		925
$\pi^+\pi^+\pi^-$		(3.2 ±0.6) × 10^{-3}		908
$\rho^0\pi^+$		< 1.4 × 10^{-3}	CL=90%	769
$\pi^+\pi^+\pi^-$ nonresonant		(2.5 ±0.7) × 10^{-3}		908
$\pi^+\pi^+\pi^-\pi^0$		(1.9 $^{+1.5}_{-1.2}$) %		882
$\eta\pi^+$ × B($\eta\to\pi^+\pi^-\pi^0$)		(1.8 ±0.6) × 10^{-3}		848
$\omega\pi^+$ × B($\omega\to\pi^+\pi^-\pi^0$)		< 6 × 10^{-3}	CL=90%	764
$\pi^+\pi^+\pi^+\pi^-\pi^-$		(1.0 $^{+0.8}_{-0.7}$) × 10^{-3}		845
$\pi^+\pi^+\pi^+\pi^-\pi^-\pi^0$		(2.9 $^{+2.9}_{-2.0}$) × 10^{-3}		799

Fractions of some of the following modes with resonances have already appeared above as submodes of particular charged-particle modes.

$\eta\pi^+$		(7.5 ±2.5) × 10^{-3}		848
$\rho^0\pi^+$		< 1.4 × 10^{-3}	CL=90%	769
$\omega\pi^+$		< 7 × 10^{-3}	CL=90%	764
$\eta\rho^+$		< 1.2 %	CL=90%	658
$\eta'(958)\pi^+$		< 9 × 10^{-3}	CL=90%	680
$\eta'(958)\rho^+$		< 1.5 %	CL=90%	355

Hadronic modes with a $K\overline{K}$ pair

$K^+\overline{K}^0$		(7.2 ±1.2) × 10^{-3}		792
$K^+K^-\pi^+$	[rr]	(8.9 ±0.8) × 10^{-3}		744
$\phi\pi^+$ × B($\phi\to K^+K^-$)		(3.0 ±0.3) × 10^{-3}		647
$K^+\overline{K}^*(892)^0$ × B($\overline{K}^{*0}\to K^-\pi^+$)		(2.8 ±0.4) × 10^{-3}		610
$K^+K^-\pi^+$ nonresonant		(4.6 ±0.9) × 10^{-3}		744
$K^0\overline{K}^0\pi^+$				741
$K^*(892)^+\overline{K}^0$ × B($K^{*+}\to K^0\pi^+$)		(2.0 ±0.9) %		611
$K^+K^-\pi^+\pi^0$				682
$\phi\pi^+\pi^0$ × B($\phi\to K^+K^-$)		(1.1 ±0.5) %		619
$\phi\rho^+$ × B($\phi\to K^+K^-$)		< 7 × 10^{-3}	CL=90%	268
$K^+K^-\pi^+\pi^0$ non-ϕ		(1.5 $^{+0.7}_{-0.6}$) %		682
$K^+\overline{K}^0\pi^+\pi^-$		< 2 %	CL=90%	678
$K^0K^-\pi^+\pi^+$		(1.0 ±0.6) %		678
$K^*(892)^+\overline{K}^*(892)^0$ × $B^2(K^*\to K\pi^+)$		(1.2 ±0.5) %		273
$K^0K^-\pi^+\pi^+$ non-$K^{*+}\overline{K}^{*0}$		< 7.9 × 10^{-3}	CL=90%	678
$K^+K^-\pi^+\pi^+\pi^-$				600
$\phi\pi^+\pi^+\pi^-$ × B($\phi\to K^+K^-$)		< 1 × 10^{-3}	CL=90%	565
$K^+K^-\pi^+\pi^+\pi^-$ nonresonant		< 3 %	CL=90%	600

Fractions of the following modes with resonances have already appeared above as submodes of particular charged-particle modes.

$\phi\pi^+$		(6.1 ±0.6) × 10^{-3}		647
$\phi\pi^+\pi^0$		(2.3 ±1.0) %		619
$\phi\rho^+$		< 1.5 %	CL=90%	268
$\phi\pi^+\pi^-$		< 2 × 10^{-3}	CL=90%	565
$K^+\overline{K}^*(892)^0$		(4.2 ±0.5) × 10^{-3}		610
$K^*(892)^+\overline{K}^0$		(3.0 ±1.4) %		611
$K^*(892)^+\overline{K}^*(892)^0$		(2.6 ±1.1) %		273

Doubly Cabibbo suppressed (DC) modes, $\Delta C = 1$ weak neutral current ($C1$) modes, or Lepton Family number (LF) or Lepton number (L) violating modes

$K^+\pi^+\pi^-$	DC		(6.5 ±2.6) × 10^{-4}		845
$K^+\rho^0$	DC	<	6 × 10^{-4}	CL=90%	681
$K^*(892)^0\pi^+$	DC	<	1.9 × 10^{-4}	CL=90%	712
$K^+K^+K^-$	DC	<	1.5 × 10^{-4}	CL=90%	550
ϕK^+	DC	<	1.3 × 10^{-4}	CL=90%	527
$\pi^+e^+e^-$	$C1$	<	6.6 × 10^{-5}	CL=90%	929
$\pi^+\mu^+\mu^-$	$C1$	<	1.8 × 10^{-5}	CL=90%	917
$\rho^+\mu^+\mu^-$	$C1$	<	5.6 × 10^{-4}	CL=90%	759
$K^+e^+e^-$		[tt] <	4.8 × 10^{-3}	CL=90%	869
$K^+\mu^+\mu^-$		[tt] <	3.2 × 10^{-4}	CL=90%	856
$\pi^+e^\pm\mu^\mp$	LF	[gg] <	3.8 × 10^{-3}	CL=90%	926
$\pi^+e^+\mu^-$	LF	<	3.3 × 10^{-3}	CL=90%	926
$\pi^+e^-\mu^+$	LF	<	3.3 × 10^{-3}	CL=90%	926
$K^+e^+\mu^-$	LF	<	3.4 × 10^{-3}	CL=90%	866
$K^+e^-\mu^+$	LF	<	3.4 × 10^{-3}	CL=90%	866
$\pi^-e^+e^+$	L	<	4.8 × 10^{-3}	CL=90%	929
$\pi^-\mu^+\mu^+$	L	<	2.2 × 10^{-4}	CL=90%	917
$\pi^-e^+\mu^+$	L	<	3.7 × 10^{-3}	CL=90%	926
$\rho^-\mu^+\mu^+$	L	<	5.6 × 10^{-4}	CL=90%	759
$K^-e^+e^+$	L	<	9.1 × 10^{-3}	CL=90%	869
$K^-\mu^+\mu^+$	L	<	3.2 × 10^{-4}	CL=90%	856
$K^-e^+\mu^+$	L	<	4.0 × 10^{-3}	CL=90%	866
$K^*(892)^-\mu^+\mu^+$	L	<	8.5 × 10^{-4}	CL=90%	703

D^0

$I(J^P) = \frac{1}{2}(0^-)$

Mass $m = 1864.5 \pm 0.5$ MeV (S = 1.1)
$|m_{D_1^0} - m_{D_2^0}| < 21 \times 10^{10}\ \hbar\ s^{-1}$, CL = 90% [uu]
$m_{D^\pm} - m_{D^0} = 4.78 \pm 0.10$ MeV
Mean life $\tau = (0.415 \pm 0.004) \times 10^{-12}$ s
$c\tau = 124.4\ \mu$m
$|\Gamma_{D_1^0} - \Gamma_{D_2^0}|/\Gamma_{D^0} < 0.17$, CL = 90% [uu]
$\frac{\Gamma(K^+\pi^- \text{or } K^+\pi^-\pi^+\pi^- (\text{via } \overline{D}^0))}{\Gamma(K^-\pi^+ \text{or } K^-\pi^+\pi^+\pi^-)} < 0.0037$, CL = 90%
$\Gamma(\mu^- X \text{ (via } \overline{D}^0))/\Gamma(\mu^+ X) < 0.0056$, CL = 90%

CP-violation decay-rate asymmetries

$A_{CP}(K^+K^-) = 0.06 \pm 0.05$
$A_{CP}(K_S^0\phi) = -0.03 \pm 0.09$
$A_{CP}(K_S^0\pi^0) = -0.018 \pm 0.030$

$\overline{D}^0$ modes are charge conjugates of the modes below.

D^0 DECAY MODES		Fraction (Γ_i/Γ)	Scale factor/ Confidence level	p (MeV/c)
Inclusive modes				
e^+ anything		(7.7 ±1.2) %	S=1.1	–
μ^+ anything	[vv]	(6.8 ±1.0) %		–
K^- anything		(53 ±4) %	S=1.3	–
$\overline{K}^0$ anything + K^0 anything		(42 ±5) %		–
K^+ anything		(3.4 $^{+0.6}_{-0.4}$) %		–
η anything	[oo]	< 13 %	CL=90%	–
Semileptonic modes				
$K^-\ell^+\nu_\ell$	[pp]	(3.48±0.16) %	S=1.1	867
$K^-e^+\nu_e$		(3.64±0.20) %	S=1.1	867
$K^-\mu^+\nu_\mu$		(3.23±0.19) %		863
$K^-\pi^0e^+\nu_e$		(1.6 $^{+1.3}_{-0.5}$) %		861
$\overline{K}^0\pi^-e^+\nu_e$		(2.8 $^{+1.7}_{-0.9}$) %		860
$\overline{K}^*(892)^-e^+\nu_e$ × B($K^{*-} \to \overline{K}^0\pi^-$)		(1.34±0.22) %		719
$K^-\pi^+\pi^-\mu^+\nu_\mu$		< 1.2 × 10^{-3}	CL=90%	821
$(\overline{K}^*(892)\pi)^-\mu^+\nu_\mu$		< 1.4 × 10^{-3}	CL=90%	693
$\pi^-e^+\nu_e$		(3.8 $^{+1.2}_{-1.0}$) × 10^{-3}		927
A fraction of the following resonance mode has already appeared above as a submode of a charged-particle mode.				
$K^*(892)^-e^+\nu_e$		(2.01±0.33) %		719
Hadronic modes with a $\overline{K}$ or $\overline{K}K\overline{K}$				
$K^-\pi^+$		(3.83±0.12) %		861
$\overline{K}^0\pi^0$		(2.11±0.21) %	S=1.1	860
$\overline{K}^0\pi^+\pi^-$	[rr]	(5.4 ±0.4) %	S=1.2	842
$\overline{K}^0\rho^0$		(1.20±0.17) %		676
$\overline{K}^0 f_0(980)$ × B($f_0 \to \pi^+\pi^-$)		(3.0 ±0.8) × 10^{-3}		549
$\overline{K}^0 f_2(1270)$ × B($f_2 \to \pi^+\pi^-$)		(2.3 ±0.9) × 10^{-3}		263
$\overline{K}^0 f_0(1370)$ × B($f_0 \to \pi^+\pi^-$)		(4.3 ±1.3) × 10^{-3}		–
$K^*(892)^-\pi^+$ × B($K^{*-} \to \overline{K}^0\pi^-$)		(3.3 ±0.3) %		711
$K_0^*(1430)^-\pi^+$ × B($K_0^*(1430)^- \to \overline{K}^0\pi^-$)		(6.4 ±1.6) × 10^{-3}		364
$\overline{K}^0\pi^+\pi^-$ nonresonant		(1.46±0.24) %		842
$K^-\pi^+\pi^0$	[rr]	(13.9 ±0.9) %	S=1.3	844
$K^-\rho^+$		(10.8 ±1.0) %		678
$K^*(892)^-\pi^+$ × B($K^{*-} \to K^-\pi^0$)		(1.7 ±0.2) %		711
$\overline{K}^*(892)^0\pi^0$ × B($\overline{K}^{*0} \to K^-\pi^+$)		(2.1 ±0.3) %		709
$K^-\pi^+\pi^0$ nonresonant		(6.9 ±2.5) × 10^{-3}		844
$\overline{K}^0\pi^0\pi^0$				843
$\overline{K}^*(892)^0\pi^0$ × B($\overline{K}^{*0} \to \overline{K}^0\pi^0$)		(1.0 ±0.2) %		709
$\overline{K}^0\pi^0\pi^0$ nonresonant		(7.8 ±2.0) × 10^{-3}		843
$K^-\pi^+\pi^+\pi^-$	[rr]	(7.5 ±0.4) %	S=1.1	812
$K^-\pi^+\rho^0$ total		(6.3 ±0.4) %		612
$K^-\pi^+\rho^0$ 3-body		(4.7 ±2.1) × 10^{-3}		612
$\overline{K}^*(892)^0\rho^0$ × B($\overline{K}^{*0} \to K^-\pi^+$)		(9.8 ±2.2) × 10^{-3}		418
$K^-a_1(1260)^+$ × B($a_1(1260)^+ \to \pi^+\pi^+\pi^-$)		(3.6 ±0.6) %		327
$\overline{K}^*(892)^0\pi^+\pi^-$ total × B($\overline{K}^{*0} \to K^-\pi^+$)		(1.5 ±0.4) %		683
$\overline{K}^*(892)^0\pi^+\pi^-$ 3-body × B($\overline{K}^{*0} \to K^-\pi^+$)		(9.5 ±2.1) × 10^{-3}		683
$K_1(1270)^-\pi^+$ × B($K_1(1270)^- \to K^-\pi^+\pi^-$)	[ss]	(3.6 ±1.0) × 10^{-3}		483
$K^-\pi^+\pi^+\pi^-$ nonresonant		(1.75±0.25) %		812
$\overline{K}^0\pi^+\pi^-\pi^0$	[rr]	(10.0 ±1.2) %		812
$\overline{K}^0\eta$ × B($\eta \to \pi^+\pi^-\pi^0$)		(1.6 ±0.3) × 10^{-3}		772
$\overline{K}^0\omega$ × B($\omega \to \pi^+\pi^-\pi^0$)		(1.9 ±0.4) %		670
$K^*(892)^-\rho^+$ × B($K^{*-} \to \overline{K}^0\pi^-$)		(4.0 ±1.6) %		422
$\overline{K}^*(892)^0\rho^0$ × B($\overline{K}^{*0} \to \overline{K}^0\pi^0$)		(4.9 ±1.1) × 10^{-3}		418
$K_1(1270)^-\pi^+$ × B($K_1(1270)^- \to \overline{K}^0\pi^-\pi^0$)	[ss]	(5.1 ±1.4) × 10^{-3}		483
$\overline{K}^*(892)^0\pi^+\pi^-$ 3-body × B($\overline{K}^{*0} \to \overline{K}^0\pi^0$)		(4.7 ±1.1) × 10^{-3}		683
$\overline{K}^0\pi^+\pi^-\pi^0$ nonresonant		(2.1 ±2.1) %		812
$K^-\pi^+\pi^0\pi^0$		(15 ±5) %		815
$K^-\pi^+\pi^+\pi^-\pi^0$		(4.0 ±0.4) %		771
$\overline{K}^*(892)^0\pi^+\pi^-\pi^0$ × B($\overline{K}^{*0} \to K^-\pi^+$)		(1.2 ±0.6) %		641
$\overline{K}^*(892)^0\eta$ × B($\overline{K}^{*0} \to K^-\pi^+$) × B($\eta \to \pi^+\pi^-\pi^0$)		(3.0 ±0.8) × 10^{-3}		580
$K^-\pi^+\omega$ × B($\omega \to \pi^+\pi^-\pi^0$)		(2.7 ±0.5) %		605
$\overline{K}^*(892)^0\omega$ × B($\overline{K}^{*0} \to K^-\pi^+$) × B($\omega \to \pi^+\pi^-\pi^0$)		(7 ±3) × 10^{-3}		406
$\overline{K}^0\pi^+\pi^+\pi^-\pi^-$		(5.8 ±1.6) × 10^{-3}		768
$\overline{K}^0\pi^+\pi^-\pi^0\pi^0(\pi^0)$		(10.6 $^{+7.3}_{-3.0}$) %		771
$\overline{K}^0K^+K^-$		(9.3 ±1.0) × 10^{-3}		544
$\overline{K}^0\phi$ × B($\phi \to K^+K^-$)		(4.2 ±0.5) × 10^{-3}		520
$\overline{K}^0K^+K^-$ non-ϕ		(5.0 ±0.8) × 10^{-3}		544
$K_S^0K_S^0K_S^0$		(9.7 ±2.3) × 10^{-4}		538
$K^+K^-K^-\pi^+$		(2.1 ±0.5) × 10^{-4}		434
$K^+K^-\overline{K}^0\pi^0$		(7.2 $^{+4.8}_{-3.5}$) × 10^{-3}		435
Fractions of many of the following modes with resonances have already appeared above as submodes of particular charged-particle modes. (Modes for which there are only upper limits and $\overline{K}^*(892)\rho$ submodes only appear below.)				
$\overline{K}^0\eta$		(7.0 ±1.0) × 10^{-3}		772
$\overline{K}^0\rho^0$		(1.20±0.17) %		676
$K^-\rho^+$		(10.8 ±1.0) %	S=1.2	678
$\overline{K}^0\omega$		(2.1 ±0.4) %		670
$\overline{K}^0\eta'(958)$		(1.70±0.26) %		565
$\overline{K}^0 f_0(980)$		(5.7 ±1.6) × 10^{-3}		549
$\overline{K}^0\phi$		(8.5 ±1.0) × 10^{-3}		520
$K^-a_1(1260)^+$		(7.3 ±1.1) %		327
$\overline{K}^0a_1(1260)^0$		< 1.9 %	CL=90%	322
$\overline{K}^0 f_2(1270)$		(4.1 ±1.5) × 10^{-3}		263
$\overline{K}^0 f_0(1370)$		(6.9 ±2.1) × 10^{-3}		–
$K^-a_2(1320)^+$		< 2 × 10^{-3}	CL=90%	197
$K^*(892)^-\pi^+$		(5.0 ±0.4) %	S=1.2	711
$\overline{K}^*(892)^0\pi^0$		(3.1 ±0.4) %		709
$\overline{K}^*(892)^0\pi^+\pi^-$ total		(2.3 ±0.5) %		683
$\overline{K}^*(892)^0\pi^+\pi^-$ 3-body		(1.42±0.32) %		683
$K^-\pi^+\rho^0$ total		(6.3 ±0.4) %		612
$K^-\pi^+\rho^0$ 3-body		(4.7 ±2.1) × 10^{-3}		612
$\overline{K}^*(892)^0\rho^0$		(1.47±0.33) %		418
$\overline{K}^*(892)^0\rho^0$ transverse		(1.5 ±0.5) %		418
$\overline{K}^*(892)^0\rho^0$ S-wave		(2.8 ±0.6) %		418
$\overline{K}^*(892)^0\rho^0$ S-wave long.		< 3 × 10^{-3}	CL=90%	418
$\overline{K}^*(892)^0\rho^0$ P-wave		< 3 × 10^{-3}	CL=90%	418
$\overline{K}^*(892)^0\rho^0$ D-wave		(1.9 ±0.6) %		418

Meson Summary Table

$K^*(892)^-\rho^+$		(6.0 ±2.4) %			422
$K^*(892)^-\rho^+$ longitudinal		(2.9 ±1.2) %			422
$K^*(892)^-\rho^+$ transverse		(3.2 ±1.8) %			422
$K^*(892)^-\rho^+$ P-wave		< 1.5	%	CL=90%	422
$K^-\pi^+ f_0(980)$		< 1.1	%	CL=90%	459
$\overline{K}^*(892)^0 f_0(980)$		< 7	$\times 10^{-3}$	CL=90%	–
$K_1(1270)^-\pi^+$	[ss]	(1.06±0.29) %			483
$K_1(1400)^-\pi^+$		< 1.2	%	CL=90%	386
$\overline{K}_1(1400)^0\pi^0$		< 3.7	%	CL=90%	387
$K^*(1410)^-\pi^+$		< 1.2	%	CL=90%	378
$K_0^*(1430)^-\pi^+$		(1.04±0.26) %			364
$K_2^*(1430)^-\pi^+$		< 8	$\times 10^{-3}$	CL=90%	367
$\overline{K}_2^*(1430)^0\pi^0$		< 4	$\times 10^{-3}$	CL=90%	363
$\overline{K}^*(892)^0\pi^+\pi^-\pi^0$		(1.8 ±0.9) %			641
$\overline{K}^*(892)^0\eta$		(1.9 ±0.5) %			580
$K^-\pi^+\omega$		(3.0 ±0.6) %			605
$\overline{K}^*(892)^0\omega$		(1.1 ±0.4) %			406
$K^-\pi^+\eta'(958)$		(7.0 ±1.8) $\times 10^{-3}$			479
$\overline{K}^*(892)^0\eta'(958)$		< 1.1	$\times 10^{-3}$	CL=90%	99

Pionic modes

$\pi^+\pi^-$		(1.52±0.11) $\times 10^{-3}$			922
$\pi^0\pi^0$		(8.4 ±2.2) $\times 10^{-4}$			922
$\pi^+\pi^-\pi^0$		(1.6 ±1.1) %		S=2.7	907
$\pi^+\pi^+\pi^-\pi^-$		(7.4 ±0.6) $\times 10^{-3}$			879
$\pi^+\pi^+\pi^-\pi^-\pi^0$		(1.9 ±0.4) %			844
$\pi^+\pi^+\pi^+\pi^-\pi^-\pi^-$		(4.0 ±3.0) $\times 10^{-4}$			795

Hadronic modes with a $K\overline{K}$ pair

K^+K^-		(4.33±0.27) $\times 10^{-3}$			791
$K^0\overline{K}^0$		(1.3 ±0.4) $\times 10^{-3}$			788
$K^0K^-\pi^+$		(6.4 ±1.0) $\times 10^{-3}$		S=1.1	739
$\overline{K}^*(892)^0K^0$ × B($\overline{K}^{*0}\to K^-\pi^+$)		< 1.1	$\times 10^{-3}$	CL=90%	605
$K^*(892)^+K^-$ × B($K^{*+}\to K^0\pi^+$)		(2.3 ±0.5) $\times 10^{-3}$			610
$K^0K^-\pi^+$ nonresonant		(2.3 ±2.3) $\times 10^{-3}$			739
$\overline{K}^0K^+\pi^-$		(4.9 ±1.0) $\times 10^{-3}$			739
$K^*(892)^0\overline{K}^0$ × B($K^{*0}\to K^+\pi^-$)		< 5	$\times 10^{-4}$	CL=90%	605
$K^*(892)^-K^+$ × B($K^{*-}\to \overline{K}^0\pi^-$)		(1.2 ±0.7) $\times 10^{-3}$			610
$\overline{K}^0K^+\pi^-$ nonresonant		(3.8 $^{+2.3}_{-1.9}$) $\times 10^{-3}$			739
$K^+K^-\pi^+\pi^-$	[ww]	(2.58±0.28) $\times 10^{-3}$			676
$\phi\pi^+\pi^-\times$ B($\phi\to K^+K^-$)		(5.3 ±1.4) $\times 10^{-4}$			614
$\phi\rho^0\times$ B($\phi\to K^+K^-$)		(5.3 ±1.4) $\times 10^{-4}$			260
$K^+K^-\rho^0$ 3-body		(9.0 ±2.3) $\times 10^{-4}$			309
$K^*(892)^0K^-\pi^+$ × B($K^{*0}\to K^+\pi^-$)		(2.1 ±0.9) $\times 10^{-3}$			528
$\overline{K}^*(892)^0K^+\pi^-$ × B($\overline{K}^{*0}\to K^-\pi^+$)		(1.1 ±0.8) $\times 10^{-3}$			528
$K^*(892)^0\overline{K}^*(892)^0$ × B^2($K^{*0}\to K^+\pi^-$)		(6 ±2) $\times 10^{-4}$			257
$K^+K^-\pi^+\pi^-$ non-ϕ		(1.7 ±0.5) $\times 10^{-3}$			676
$K^+K^-\pi^+\pi^-$ nonresonant		< 8	$\times 10^{-4}$	CL=90%	676
$K^0\overline{K}^0\pi^+\pi^-$		(6.8 ±2.7) $\times 10^{-3}$			673
$K^+K^-\pi^+\pi^-\pi^0$		(3.1 ±2.0) $\times 10^{-3}$			600

Fractions of most of the following modes with resonances have already appeared above as submodes of particular charged-particle modes.

$\overline{K}^*(892)^0K^0$	< 1.6	$\times 10^{-3}$	CL=90%	605
$K^*(892)^+K^-$	(3.5 ±0.8) $\times 10^{-3}$			610
$K^*(892)^0\overline{K}^0$	< 8	$\times 10^{-4}$	CL=90%	605
$K^*(892)^-K^+$	(1.8 ±1.0) $\times 10^{-3}$			610
$\phi\pi^0$	< 1.4	$\times 10^{-3}$	CL=90%	644
$\phi\eta$	< 2.8	$\times 10^{-3}$	CL=90%	489
$\phi\omega$	< 2.1	$\times 10^{-3}$	CL=90%	239
$\phi\pi^+\pi^-$	(1.07±0.29) $\times 10^{-3}$			614
$\phi\rho^0$	(1.07±0.29) $\times 10^{-3}$			260
$\phi\pi^+\pi^-$ 3-body	< 5	$\times 10^{-4}$	CL=90%	614
$K^*(892)^0K^-\pi^+$	(3.2 ±1.3) $\times 10^{-3}$			528
$\overline{K}^*(892)^0K^+\pi^-$	(1.7 ±1.2) $\times 10^{-3}$			528
$K^*(892)^0\overline{K}^*(892)^0$	(1.4 ±0.5) $\times 10^{-3}$			257

Doubly Cabibbo suppressed (*DC*) modes, $\Delta C = 2$ forbidden via mixing (*C2M*) modes, $\Delta C = 1$ weak neutral current (*C1*) modes, or Lepton Family number (*LF*) violating modes

$K^+\pi^-$	*DC*		(2.9 ±1.4) $\times 10^{-4}$			861
$K^+\pi^-$ (via $\overline{D}^0$)	*C2M*	< 1.9	$\times 10^{-4}$	CL=90%		861
$K^+\pi^-\pi^+\pi^-$	*DC*	< 1.4	$\times 10^{-3}$	CL=90%		812
$K^+\pi^-\pi^+\pi^-$ (via $\overline{D}^0$)	*C2M*	< 4	$\times 10^{-4}$	CL=90%		812
μ^- anything (via $\overline{D}^0$)	*C2M*	< 4	$\times 10^{-4}$	CL=90%		–
e^+e^-	*C1*	< 1.3	$\times 10^{-5}$	CL=90%		932
$\mu^+\mu^-$	*C1*	< 7.6	$\times 10^{-6}$	CL=90%		926
$\pi^0e^+e^-$	*C1*	< 4.5	$\times 10^{-5}$	CL=90%		927
$\pi^0\mu^+\mu^-$	*C1*	< 1.8	$\times 10^{-4}$	CL=90%		915
ηe^+e^-	*C1*	< 1.1	$\times 10^{-4}$	CL=90%		852
$\eta\mu^+\mu^-$	*C1*	< 5.3	$\times 10^{-4}$	CL=90%		838
$\rho^0e^+e^-$	*C1*	< 1.0	$\times 10^{-4}$	CL=90%		773
$\rho^0\mu^+\mu^-$	*C1*	< 2.3	$\times 10^{-4}$	CL=90%		756
ωe^+e^-	*C1*	< 1.8	$\times 10^{-4}$	CL=90%		768
$\omega\mu^+\mu^-$	*C1*	< 8.3	$\times 10^{-4}$	CL=90%		751
ϕe^+e^-	*C1*	< 5.2	$\times 10^{-5}$	CL=90%		654
$\phi\mu^+\mu^-$	*C1*	< 4.1	$\times 10^{-4}$	CL=90%		631
$\overline{K}^0e^+e^-$		[tt] < 1.1	$\times 10^{-4}$	CL=90%		866
$\overline{K}^0\mu^+\mu^-$		[tt] < 2.6	$\times 10^{-4}$	CL=90%		852
$\overline{K}^*(892)^0e^+e^-$		[tt] < 1.4	$\times 10^{-4}$	CL=90%		717
$\overline{K}^*(892)^0\mu^+\mu^-$		[tt] < 1.18	$\times 10^{-3}$	CL=90%		698
$\pi^+\pi^-\pi^0\mu^+\mu^-$	*C1*	< 8.1	$\times 10^{-4}$	CL=90%		863
$\mu^\pm e^\mp$	*LF*	[gg] < 1.9	$\times 10^{-5}$	CL=90%		929
$\pi^0e^\pm\mu^\mp$	*LF*	[gg] < 8.6	$\times 10^{-5}$	CL=90%		924
$\eta e^\pm\mu^\mp$	*LF*	[gg] < 1.0	$\times 10^{-4}$	CL=90%		848
$\rho^0e^\pm\mu^\mp$	*LF*	[gg] < 4.9	$\times 10^{-5}$	CL=90%		769
$\omega e^\pm\mu^\mp$	*LF*	[gg] < 1.2	$\times 10^{-4}$	CL=90%		764
$\phi e^\pm\mu^\mp$	*LF*	[gg] < 3.4	$\times 10^{-5}$	CL=90%		648
$\overline{K}^0e^\pm\mu^\mp$	*LF*	[gg] < 1.0	$\times 10^{-4}$	CL=90%		862
$\overline{K}^*(892)^0e^\pm\mu^\mp$	*LF*	[gg] < 1.0	$\times 10^{-4}$	CL=90%		712

$D^*(2007)^0$

$I(J^P) = \frac{1}{2}(1^-)$
I, *J*, *P* need confirmation.

Mass $m = 2006.7 \pm 0.5$ MeV (S = 1.1)
$m_{D^{*0}} - m_{D^0} = 142.12 \pm 0.07$ MeV
Full width $\Gamma < 2.1$ MeV, CL = 90%

$\overline{D}^*(2007)^0$ modes are charge conjugates of modes below.

$D^*(2007)^0$ DECAY MODES	Fraction (Γ_i/Γ)	p (MeV/c)
$D^0\pi^0$	(61.9±2.9) %	43
$D^0\gamma$	(38.1±2.9) %	137

$D^*(2010)^\pm$

$I(J^P) = \frac{1}{2}(1^-)$
I, *J*, *P* need confirmation.

Mass $m = 2010.0 \pm 0.5$ MeV (S = 1.1)
$m_{D^*(2010)^+} - m_{D^+} = 140.64 \pm 0.09$ MeV
$m_{D^*(2010)^+} - m_{D^0} = 145.42 \pm 0.05$ MeV
Full width $\Gamma < 0.131$ MeV, CL = 90%

$D^*(2010)^-$ modes are charge conjugates of the modes below.

$D^*(2010)^\pm$ DECAY MODES	Fraction (Γ_i/Γ)	p (MeV/c)
$D^0\pi^+$	(68.3±1.4) %	39
$D^+\pi^0$	(30.6±2.5) %	38
$D^+\gamma$	(1.1 $^{+2.1}_{-0.7}$) %	136

$D_1(2420)^0$

$I(J^P) = \frac{1}{2}(1^+)$
I, *J*, *P* need confirmation.

Mass $m = 2422.2 \pm 1.8$ MeV (S = 1.2)
Full width $\Gamma = 18.9^{+4.6}_{-3.5}$ MeV

$\overline{D}_1(2420)^0$ modes are charge conjugates of modes below.

$D_1(2420)^0$ DECAY MODES	Fraction (Γ_i/Γ)	p (MeV/c)
$D^*(2010)^+\pi^-$	seen	355
$D^+\pi^-$	not seen	474

$D_2^*(2460)^0$ $I(J^P) = \frac{1}{2}(2^+)$

$J^P = 2^+$ assignment strongly favored (ALBRECHT 89B).

Mass $m = 2458.9 \pm 2.0$ MeV (S = 1.2)
Full width $\Gamma = 23 \pm 5$ MeV

$\overline{D}_2^*(2460)^0$ modes are charge conjugates of modes below.

$D_2^*(2460)^0$ DECAY MODES	Fraction (Γ_i/Γ)	p (MeV/c)
$D^+\pi^-$	seen	503
$D^*(2010)^+\pi^-$	seen	387

$D_2^*(2460)^\pm$ $I(J^P) = \frac{1}{2}(2^+)$

$J^P = 2^+$ assignment strongly favored (ALBRECHT 89B).

Mass $m = 2459 \pm 4$ MeV (S = 1.7)
$m_{D_2^*(2460)^\pm} - m_{D_2^*(2460)^0} = 0.9 \pm 3.3$ MeV (S = 1.1)
Full width $\Gamma = 25^{+8}_{-7}$ MeV

$D_2^*(2460)^-$ modes are charge conjugates of modes below.

$D_2^*(2460)^\pm$ DECAY MODES	Fraction (Γ_i/Γ)	p (MeV/c)
$D^0\pi^+$	seen	508
$D^{*0}\pi^+$	seen	390

CHARMED, STRANGE MESONS ($C = S = \pm 1$)

$D_s^+ = c\overline{s}$, $D_s^- = \overline{c}s$, similarly for D_s^*'s

$D_s^\pm$ was $F^\pm$ $I(J^P) = 0(0^-)$

Mass $m = 1968.5 \pm 0.6$ MeV (S = 1.1)
$m_{D_s^\pm} - m_{D^\pm} = 99.2 \pm 0.5$ MeV (S = 1.1)
Mean life $\tau = (0.467 \pm 0.017) \times 10^{-12}$ s
$c\tau = 140$ μm

D_s^+ form factors

$r_2 = 1.6 \pm 0.4$
$r_V = 1.5 \pm 0.5$
$\Gamma_L/\Gamma_T = 0.72 \pm 0.18$

Branching fractions for modes with a resonance in the final state include all the decay modes of the resonance. D_s^- modes are charge conjugates of the modes below.

D_s^+ DECAY MODES	Fraction (Γ_i/Γ)	Confidence level	p (MeV/c)
Inclusive modes			
K^- anything	(13 $^{+14}_{-12}$) %		–
$\overline{K}^0$ anything + K^0 anything	(39 $\pm$28) %		–
K^+ anything	(20 $^{+18}_{-14}$) %		–
non-$K\overline{K}$ anything	(64 $\pm$17) %		–
e^+ anything	< 20 %	90%	–
Leptonic and semileptonic modes			
$\mu^+\nu_\mu$	(9 $\pm$ 4) $\times 10^{-3}$		981
$\phi\ell^+\nu_\ell$	[xx] (1.9 $\pm$ 0.5) %		–
$\eta\ell^+\nu_\ell$ + $\eta'(958)\ell^+\nu_\ell$	(3.3 $\pm$ 1.0) %		–
$\eta\ell^+\nu_\ell$	(2.5 $\pm$ 0.7) %		–
$\eta'(958)\ell^+\nu_\ell$	(8.7 $\pm$ 3.4) $\times 10^{-3}$		–
Hadronic modes with a $K\overline{K}$ pair (including from a ϕ)			
$K^+\overline{K}^0$	(3.6 $\pm$ 1.1) %		850
$K^+K^-\pi^+$	[rr,yy] (4.6 $\pm$ 1.2) %		805
$\phi\pi^+$	(3.6 $\pm$ 0.9) %		712
$K^+\overline{K}^*(892)^0$	(3.4 $\pm$ 0.9) %		682
$f_0(980)\pi^+$	(1.1 $\pm$ 0.4) %		732
$K^+\overline{K}_0^*(1430)^0$	(7 $\pm$ 4) $\times 10^{-3}$		186
$f_J(1710)\pi^+ \to K^+K^-\pi^+$	[zz] (1.5 $\pm$ 2.0) $\times 10^{-3}$		204
$K^+K^-\pi^+$ nonresonant	(9 $\pm$ 4) $\times 10^{-3}$		805
$K^0\overline{K}^0\pi^+$			802
$K^*(892)^+\overline{K}^0$	(4.3 $\pm$ 1.4) %		683
$K^+K^-\pi^+\pi^0$			748
$\phi\pi^+\pi^0$	(9 $\pm$ 5) %		687
$\phi\rho^+$	(6.7 $\pm$ 2.3) %		407
$\phi\pi^+\pi^0$ 3-body	< 2.6 %	90%	687
$K^+K^-\pi^+\pi^0$ non-ϕ	< 9 %	90%	748
$K^+\overline{K}^0\pi^+\pi^-$	< 2.8 %	90%	744
$K^0K^-\pi^+\pi^+$	(4.3 $\pm$ 1.5) %		744
$K^*(892)^+\overline{K}^*(892)^0$	(5.8 $\pm$ 2.5) %		412
$K^0K^-\pi^+\pi^+$ non-$K^{*+}\overline{K}^{*0}$	< 2.9 %	90%	744
$K^+K^-\pi^+\pi^+\pi^-$			673
$\phi\pi^+\pi^+\pi^-$	(1.8 $\pm$ 0.6) %		640
$K^+K^-\pi^+\pi^+\pi^-$ non-ϕ	(3.0 $^{+3.0}_{-2.0}$) $\times 10^{-3}$		673
Other hadronic modes (0, 1, or 3 K's)			
$\pi^+\pi^+\pi^-$	(1.4 $\pm$ 0.4) %		959
$\rho^0\pi^+$	< 2.9 $\times 10^{-3}$	90%	827
$f_0(980)\pi^+$	(1.2 $\pm$ 0.5) %		732
$\pi^+\pi^+\pi^-$ nonresonant	(1.0 $\pm$ 0.4) %		959
$\pi^+\pi^+\pi^-\pi^0$	< 12 %	90%	935
$\eta\pi^+$	(2.0 $\pm$ 0.6) %		902
$\omega\pi^+$	< 1.8 %	90%	822
$\pi^+\pi^+\pi^+\pi^-\pi^-$	(3.0 $^{+4.0}_{-3.0}$) $\times 10^{-3}$		899
$\pi^+\pi^+\pi^-\pi^0\pi^0$			902
$\eta\rho^+$	(10.3 $\pm$ 3.2) %		727
$\eta\pi^+\pi^0$ 3-body	< 3.0 %	90%	886
$\pi^+\pi^+\pi^+\pi^-\pi^-\pi^0$	(4.9 $\pm$ 3.2) %		856
$\eta'(958)\pi^+$	(4.9 $\pm$ 1.8) %		743
$\pi^+\pi^+\pi^+\pi^-\pi^-\pi^0\pi^0$			803
$\eta'(958)\rho^+$	(12 $\pm$ 4) %		470
$\eta'(958)\pi^+\pi^0$ 3-body	< 3.1 %	90%	720
$K^0\pi^+$	< 8 $\times 10^{-3}$	90%	916
$K^+\pi^+\pi^-$	(1.0 $\pm$ 0.4) %		900
$K^+\rho^0$	< 2.9 $\times 10^{-3}$	90%	747
$K^*(892)^0\pi^+$	(6.5 $\pm$ 2.8) $\times 10^{-3}$		773
$K^+K^+K^-$	< 6 $\times 10^{-4}$	90%	628
ϕK^+	< 5 $\times 10^{-4}$	90%	607
$\Delta C = 1$ weak neutral current ($C1$) modes, or Lepton number (L) violating modes			
$\pi^+\mu^+\mu^-$	[aaa] < 4.3 $\times 10^{-4}$	90%	968
$K^+\mu^+\mu^-$	$C1$ < 5.9 $\times 10^{-4}$	90%	909
$K^*(892)^+\mu^+\mu^-$	$C1$ < 1.4 $\times 10^{-3}$	90%	765
$\pi^-\mu^+\mu^+$	L < 4.3 $\times 10^{-4}$	90%	968
$K^-\mu^+\mu^+$	L < 5.9 $\times 10^{-4}$	90%	909
$K^*(892)^-\mu^+\mu^+$	L < 1.4 $\times 10^{-3}$	90%	765

Meson Summary Table

$D_s^{*\pm}$

$I(J^P) = ?(?^?)$

Mass $m = 2112.4 \pm 0.7$ MeV (S = 1.1)
$m_{D_s^{*\pm}} - m_{D_s^{\pm}} = 143.8 \pm 0.4$ MeV
Full width $\Gamma < 1.9$ MeV, CL = 90%

D_s^{*-} modes are charge conjugates of the modes below.

D_s^{*+} DECAY MODES	Fraction (Γ_i/Γ)	p (MeV/c)
$D_s^+\gamma$	seen	139
$D_s^+\pi^0$	seen	48

$D_{s1}(2536)^{\pm}$

$I(J^P) = 0(1^+)$
I, J, P need confirmation.

Mass $m = 2535.35 \pm 0.34$ MeV
Full width $\Gamma < 2.3$ MeV, CL = 90%

$D_{s1}(2536)^-$ modes are charge conjugates of the modes below.

$D_{s1}(2536)^+$ DECAY MODES	Fraction (Γ_i/Γ)	p (MeV/c)
$D^*(2010)^+K^0$	seen	150
$D^*(2007)^0K^+$	seen	169
D^+K^0	not seen	382
D^0K^+	not seen	392
$D_s^{*+}\gamma$	possibly seen	389

$D_{sJ}(2573)^{\pm}$

$I(J^P) = ?(?^?)$

J^P is natural, width and decay modes consistent with 2^{+2}.
Mass $m = 2573.5 \pm 1.7$ MeV
Full width $\Gamma = 15^{+5}_{-4}$ MeV

$D_{sJ}(2573)^-$ modes are charge conjugates of the modes below.

$D_{sJ}(2573)^+$ DECAY MODES	Fraction (Γ_i/Γ)	p (MeV/c)
D^0K^+	seen	436
$D^*(2007)^0K^+$	seen	245

BOTTOM MESONS ($B = \pm 1$)

$B^+ = u\overline{b}$, $B^0 = d\overline{b}$, $\overline{B}^0 = \overline{d}b$, $B^- = \overline{u}b$, similarly for B^*'s

B-particle organization

Many measurements of B decays involve admixtures of B hadrons. Previously we arbitrarily included such admixtures in the $B^{\pm}$ section, but because of their importance we have created two new sections: "$B^{\pm}/B^0$ Admixture" for $\Upsilon(4S)$ results and "$B^{\pm}/B^0/B_s^0$/b-baryon Admixture" for results at higher energies. Most inclusive decay branching fractions are found in the Admixture sections. B^0-$\overline{B}^0$ mixing data are found in the B^0 section, while B_s^0-$\overline{B}_s^0$ mixing data and B-$\overline{B}$ mixing data for a B^0/B_s^0 admixture are found in the B_s^0 section. CP-violation data are found in the B^0 section. b-baryons are found near the end of the Baryon section.

The organization of the B sections is now as follows, where bullets indicate particle sections and brackets indicate reviews.

[Production and Decay of b-flavored Hadrons]
[Semileptonic Decays of B Mesons]
- $B^{\pm}$
  - mass
  - mean life
  - branching fractions
- B^0
  - mass
  - mean life
  - branching fractions
  - polarization in B^0 decay
  - B^0-$\overline{B}^0$ mixing
  - [B^0-$\overline{B}^0$ Mixing and CP Violation in B Decay]
  - CP violation
- $B^{\pm}$ B^0 Admixtures
  - branching fractions
- $B^{\pm}/B^0/B_s^0/b$-baryon Admixtures
  - mean life
  - production fractions
  - branching fractions
- B^*
  - mass
- B_s^0
  - mass
  - mean life
  - branching fractions
  - polarization in B_s^0 decay
  - B_s^0-$\overline{B}_s^0$ mixing
  - B-$\overline{B}$ mixing (admixture of B^0, B_s^0)

At end of Baryon Listings:
- Λ_b
  - mass
  - mean life
  - branching fractions

$B^\pm$

$I(J^P) = \frac{1}{2}(0^-)$

I, J, P need confirmation. Quantum numbers shown are quark-model predictions.

Mass $m_{B^\pm} = 5278.9 \pm 1.8$ MeV
Mean life $\tau_{B^\pm} = (1.62 \pm 0.06) \times 10^{-12}$ s
$c\tau = 462\ \mu$m

B^- modes are charge conjugates of the modes below. Modes which do not identify the charge state of the B are listed in the $B^\pm/B^0$ ADMIXTURE section.

The branching fractions listed below assume 50% $B^0\overline{B}^0$ and 50% B^+B^- production at the $\Upsilon(4S)$. We have attempted to bring older measurements up to date by rescaling their assumed $\Upsilon(4S)$ production ratio to 50:50 and their assumed D, D_s, D^*, and ψ branching ratios to current values whenever this would affect our averages and best limits significantly.

Indentation is used to indicate a subchannel of a previous reaction. All resonant subchannels have been corrected for resonance branching fractions to the final state so the sum of the subchannel branching fractions can exceed that of the final state.

B^+ DECAY MODES	Fraction (Γ_i/Γ)	Scale factor/ Confidence level	p (MeV/c)
Semileptonic and leptonic modes			
$\ell^+\nu_\ell$ anything	[qq] (10.1 ±2.3) %		–
$\overline{D}^0\ell^+\nu_\ell$	[qq] (1.6 ±0.7) %		–
$\overline{D}^*(2007)^0\ell^+\nu_\ell$	[qq] (5.3 ±0.8) %		–
$\pi^0 e^+\nu_e$	< 2.2 × 10^{-3}	CL=90%	2638
$\omega\ell^+\nu_\ell$	[qq] < 2.1 × 10^{-4}	CL=90%	–
$\rho^0\ell^+\nu_\ell$	[qq] < 2.1 × 10^{-4}	CL=90%	–
$e^+\nu_e$	< 1.5 × 10^{-5}	CL=90%	2639
$\mu^+\nu_\mu$	< 2.1 × 10^{-5}	CL=90%	2638
$\tau^+\nu_\tau$	< 1.8 × 10^{-3}	CL=90%	2340
D, D^*, or D_s modes			
$\overline{D}^0\pi^+$	(5.3 ±0.5) × 10^{-3}		2308
$\overline{D}^0\rho^+$	(1.34±0.18) %		2238
$\overline{D}^0\pi^+\pi^+\pi^-$	(1.1 ±0.4) %		2289
$\overline{D}^0\pi^+\pi^+\pi^-$ nonresonant	(5 ±4) × 10^{-3}		2289
$\overline{D}^0\pi^+\rho^0$	(4.2 ±3.0) × 10^{-3}		2209
$\overline{D}^0 a_1(1260)^+$	(5 ±4) × 10^{-3}		2123
$D^*(2010)^-\pi^+\pi^+$	(2.1 ±0.6) × 10^{-3}		2247
$D^-\pi^+\pi^+$	< 1.4 × 10^{-3}	CL=90%	2299
$\overline{D}^*(2007)^0\pi^+$	(5.2 ±0.8) × 10^{-3}		2256
$\overline{D}^*(2007)^0\rho^+$	(1.55±0.31) %		2183
$\overline{D}^*(2007)^0\pi^+\pi^+\pi^-$	(9.4 ±2.6) × 10^{-3}		2236
$\overline{D}^*(2007)^0 a_1(1260)^+$	(1.9 ±0.5) %		2062
$D^*(2010)^-\pi^+\pi^+\pi^0$	(1.5 ±0.7) %		2235
$D^*(2010)^-\pi^+\pi^+\pi^+\pi^-$	< 1 %	CL=90%	2217
$\overline{D}_1^*(2420)^0\pi^+$	(1.5 ±0.6) × 10^{-3}	S=1.3	2081
$\overline{D}_1^*(2420)^0\rho^+$	< 1.4 × 10^{-3}	CL=90%	1997
$\overline{D}_2^*(2460)^0\pi^+$	< 1.3 × 10^{-3}	CL=90%	2064
$\overline{D}_2^*(2460)^0\rho^+$	< 4.7 × 10^{-3}	CL=90%	1979
$\overline{D}^0 D_s^+$	(1.7 ±0.6) %		1815
$\overline{D}^0 D_s^{*+}$	(1.2 ±1.0) %		1734
$\overline{D}^*(2007)^0 D_s^+$	(10 ±7) × 10^{-3}		1737
$\overline{D}^*(2007)^0 D_s^{*+}$	(2.3 ±1.4) %		1650
$D_s^+\pi^0$	< 2.0 × 10^{-4}	CL=90%	2270
$D_s^{*+}\pi^0$	< 3.3 × 10^{-4}	CL=90%	2214
$D_s^+\eta$	< 5 × 10^{-4}	CL=90%	2235
$D_s^{*+}\eta$	< 8 × 10^{-4}	CL=90%	2177
$D_s^+\rho^0$	< 4 × 10^{-4}	CL=90%	2198
$D_s^{*+}\rho^0$	< 5 × 10^{-4}	CL=90%	2139
$D_s^+\omega$	< 5 × 10^{-4}	CL=90%	2195
$D_s^{*+}\omega$	< 7 × 10^{-4}	CL=90%	2136
$D_s^+ a_1(1260)^0$	< 2.2 × 10^{-3}	CL=90%	2079
$D_s^{*+} a_1(1260)^0$	< 1.6 × 10^{-3}	CL=90%	2014
$D_s^+\phi$	< 3.2 × 10^{-4}	CL=90%	2141
$D_s^{*+}\phi$	< 4 × 10^{-4}	CL=90%	2079
$D_s^+\overline{K}^0$	< 1.1 × 10^{-3}	CL=90%	2241
$D_s^{*+}\overline{K}^0$	< 1.1 × 10^{-3}	CL=90%	2184
$D_s^+\overline{K}^*(892)^0$	< 5 × 10^{-4}	CL=90%	2171
$D_s^{*+}\overline{K}^*(892)^0$	< 4 × 10^{-4}	CL=90%	2110
$D_s^-\pi^+K^+$	< 8 × 10^{-4}	CL=90%	2222
$D_s^{*-}\pi^+K^+$	< 1.2 × 10^{-3}	CL=90%	2164
$D_s^-\pi^+K^*(892)^+$	< 6 × 10^{-3}	CL=90%	2137
$D_s^{*-}\pi^+K^*(892)^+$	< 8 × 10^{-3}	CL=90%	2075
Charmonium modes			
$J/\psi(1S)K^+$	(1.01±0.14) × 10^{-3}		1683
$J/\psi(1S)K^+\pi^+\pi^-$	(1.4 ±0.6) × 10^{-3}		1612
$J/\psi(1S)K^*(892)^+$	(1.7 ±0.5) × 10^{-3}		1571
$J/\psi(1S)\pi^-$	(4.4 ±2.4) × 10^{-5}		1727
$\psi(2S)K^+$	(6.9 ±3.1) × 10^{-4}	S=1.3	1284
$\psi(2S)K^*(892)^+$	< 3.0 × 10^{-3}	CL=90%	1115
$\psi(2S)K^*(892)^+\pi^+\pi^-$	(1.9 ±1.2) × 10^{-3}		909
$\chi_{c1}(1P)K^+$	(1.0 ±0.4) × 10^{-3}		1411
$\chi_{c1}(1P)K^*(892)^+$	< 2.1 × 10^{-3}	CL=90%	1265
K* or *K* **modes**			
$K^0\pi^+$	< 4.8 × 10^{-5}	CL=90%	2614
$K^+\pi^0$	< 1.4 × 10^{-5}	CL=90%	2615
$K^*(892)^0\pi^+$	< 4.1 × 10^{-5}	CL=90%	2561
$K^*(892)^+\pi^0$	< 9.9 × 10^{-5}	CL=90%	2562
$K^+\pi^-\pi^+$(no charm)	< 1.9 × 10^{-4}	CL=90%	2609
$K_1(1400)^0\pi^+$	< 2.6 × 10^{-3}	CL=90%	2451
$K_2^*(1430)^0\pi^+$	< 6.8 × 10^{-4}	CL=90%	2443
$K^+\rho^0$	< 1.9 × 10^{-5}	CL=90%	2559
$K^0\rho^+$	< 4.8 × 10^{-5}	CL=90%	2559
$K^*(892)^+\pi^+\pi^-$	< 1.1 × 10^{-3}	CL=90%	2556
$K^*(892)^+\rho^0$	< 9.0 × 10^{-4}	CL=90%	2505
$K_1(1400)^+\rho^0$	< 7.8 × 10^{-4}	CL=90%	2389
$K_2^*(1430)^+\rho^0$	< 1.5 × 10^{-3}	CL=90%	2382
$K^+K^-K^+$	< 3.1 × 10^{-4}	CL=90%	2522
$K^+\phi$	< 1.2 × 10^{-5}	CL=90%	2516
$K^*(892)^+K^+K^-$	< 1.6 × 10^{-3}	CL=90%	2466
$K^*(892)^+\phi$	< 7.0 × 10^{-5}	CL=90%	2460
$K_1(1400)^+\phi$	< 1.1 × 10^{-3}	CL=90%	2339
$K_2^*(1430)^+\phi$	< 3.4 × 10^{-3}	CL=90%	2332
$K^+ f_0(980)$	< 8 × 10^{-5}	CL=90%	2524
$K^*(892)^+\gamma$	(5.7 ±3.3) × 10^{-5}		2564
$K_1(1270)^+\gamma$	< 7.3 × 10^{-3}	CL=90%	2486
$K_1(1400)^+\gamma$	< 2.2 × 10^{-3}	CL=90%	2453
$K_2^*(1430)^+\gamma$	< 1.4 × 10^{-3}	CL=90%	2447
$K^*(1680)^+\gamma$	< 1.9 × 10^{-3}	CL=90%	2361
$K_3^*(1780)^+\gamma$	< 5.5 × 10^{-3}	CL=90%	2343
$K_4^*(2045)^+\gamma$	< 9.9 × 10^{-3}	CL=90%	2243
Light unflavored meson modes			
$\pi^+\pi^0$	< 1.7 × 10^{-5}	CL=90%	2636
$\pi^+\pi^+\pi^-$	< 1.9 × 10^{-4}	CL=90%	2630
$\rho^0\pi^+$	< 4.3 × 10^{-5}	CL=90%	2582
$\pi^+ f_0(980)$	< 1.4 × 10^{-4}	CL=90%	2547
$\pi^+ f_2(1270)$	< 2.4 × 10^{-4}	CL=90%	2483
$\pi^+\pi^0\pi^0$	< 8.9 × 10^{-4}	CL=90%	2631
$\rho^+\pi^0$	< 7.7 × 10^{-5}	CL=90%	2582
$\pi^+\pi^-\pi^+\pi^0$	< 4.0 × 10^{-3}	CL=90%	2621
$\rho^+\rho^0$	< 1.0 × 10^{-3}	CL=90%	2525
$a_1(1260)^+\pi^0$	< 1.7 × 10^{-3}	CL=90%	2494
$a_1(1260)^0\pi^+$	< 9.0 × 10^{-4}	CL=90%	2494
$\omega\pi^+$	< 4.0 × 10^{-4}	CL=90%	2580
$\eta\pi^+$	< 7.0 × 10^{-4}	CL=90%	2609
$\pi^+\pi^+\pi^+\pi^-\pi^-$	< 8.6 × 10^{-4}	CL=90%	2608
$\rho^0 a_1(1260)^+$	< 6.2 × 10^{-4}	CL=90%	2434
$\rho^0 a_2(1320)^+$	< 7.2 × 10^{-4}	CL=90%	2411
$\pi^+\pi^+\pi^+\pi^-\pi^-\pi^0$	< 6.3 × 10^{-3}	CL=90%	2592
$a_1(1260)^+ a_1(1260)^0$	< 1.3 %	CL=90%	2335
Baryon modes			
$p\overline{p}\pi^+$	< 1.6 × 10^{-4}	CL=90%	2439
$p\overline{p}\pi^+\pi^+\pi^-$	< 5.2 × 10^{-4}	CL=90%	2369
$p\overline{\Lambda}$	< 6 × 10^{-5}	CL=90%	2430
$p\overline{\Lambda}\pi^+\pi^-$	< 2.0 × 10^{-4}	CL=90%	2367
$\overline{\Delta}^0 p$	< 3.8 × 10^{-4}	CL=90%	2402
$\Delta^{++}\overline{p}$	< 1.5 × 10^{-4}	CL=90%	2402

Meson Summary Table

Lepton Family number (LF) or Lepton number (L) violating modes, or $\Delta B = 1$ weak neutral current ($B1$) modes					
$\pi^+ e^+ e^-$	$B1$	< 3.9	$\times 10^{-3}$	CL=90%	2638
$\pi^+ \mu^+ \mu^-$	$B1$	< 9.1	$\times 10^{-3}$	CL=90%	2633
$K^+ \mu^+ \mu^-$	$B1$	< 1.7	$\times 10^{-4}$	CL=90%	2612
$K^*(892)^+ e^+ e^-$	$B1$	< 6.9	$\times 10^{-4}$	CL=90%	2564
$K^*(892)^+ \mu^+ \mu^-$	$B1$	< 1.2	$\times 10^{-3}$	CL=90%	2560
$\pi^+ e^+ \mu^-$	LF	< 6.4	$\times 10^{-3}$	CL=90%	2637
$\pi^+ e^- \mu^+$	LF	< 6.4	$\times 10^{-3}$	CL=90%	2637
$K^+ e^+ \mu^-$	LF	< 6.4	$\times 10^{-3}$	CL=90%	2615
$K^+ e^- \mu^+$	LF	< 6.4	$\times 10^{-3}$	CL=90%	2615
$\pi^- e^+ e^+$	L	< 3.9	$\times 10^{-3}$	CL=90%	2638
$\pi^- \mu^+ \mu^+$	L	< 9.1	$\times 10^{-3}$	CL=90%	2633
$\pi^- e^+ \mu^+$	L	< 6.4	$\times 10^{-3}$	CL=90%	2637
$K^- e^+ e^+$	L	< 3.9	$\times 10^{-3}$	CL=90%	2616
$K^- \mu^+ \mu^+$	L	< 9.1	$\times 10^{-3}$	CL=90%	2612
$K^- e^+ \mu^+$	L	< 6.4	$\times 10^{-3}$	CL=90%	2615

B^0

$I(J^P) = \frac{1}{2}(0^-)$

I, J, P need confirmation. Quantum numbers shown are quark-model predictions.

Mass $m_{B^0} = 5279.2 \pm 1.8$ MeV

$m_{B^0} - m_{B^\pm} = 0.35 \pm 0.29$ MeV (S = 1.1)

Mean life $\tau_{B^0} = (1.56 \pm 0.06) \times 10^{-12}$ s

$c\tau = 468\ \mu$m

$\tau_{B^+}/\tau_{B^0} = 1.02 \pm 0.05$ (average of direct and inferred)

$\tau_{B^+}/\tau_{B^0} = 1.03 \pm 0.06$ (direct measurements)

$\tau_{B^+}/\tau_{B^0} = 0.93 \pm 0.22$ (inferred from branching fractions)

B^0-$\overline{B}^0$ mixing parameters

$\chi_d = 0.175 \pm 0.016$

$\Delta m_{B^0} = m_{B^0_H} - m_{B^0_L} = (0.474 \pm 0.031) \times 10^{12}\ \hbar\ \mathrm{s}^{-1}$

$x_d = \Delta m_{B^0}/\Gamma_{B^0} = 0.73 \pm 0.05$

CP violation parameters

$|\mathrm{Re}(\epsilon_{B^0})| < 0.045$

$\overline{B}^0$ modes are charge conjugates of the modes below. Reactions indicate the weak decay vertex and do not include mixing. Modes which do not identify the charge state of the B are listed in the $B^\pm/B^0$ ADMIXTURE section.

The branching fractions listed below assume 50% $B^0\overline{B}^0$ and 50% B^+B^- production at the $\Upsilon(4S)$. We have attempted to bring older measurements up to date by rescaling their assumed $\Upsilon(4S)$ production ratio to 50:50 and their assumed D, D_s, D^*, and ψ branching ratios to current values whenever this would affect our averages and best limits significantly.

Indentation is used to indicate a subchannel of a previous reaction. All resonant subchannels have been corrected for resonance branching fractions to the final state so the sum of the subchannel branching fractions can exceed that of the final state.

B^0 DECAY MODES		Fraction (Γ_i/Γ)	Scale factor/ Confidence level		p (MeV/c)
Semileptonic and leptonic modes					
$\ell^+ \nu_\ell$ anything	[qq]	(10.3 ±1.0) %			–
$D^- \ell^+ \nu_\ell$	[qq]	(1.9 ±0.5) %			–
$D^*(2010)^- \ell^+ \nu_\ell$	[qq]	(4.56±0.27) %			–
$\rho^- \ell^+ \nu_\ell$	[qq]	< 4.1	$\times 10^{-4}$	CL=90%	–
D, D^*, or D_s modes					
$D^- \pi^+$		(3.0 ±0.4)	$\times 10^{-3}$		2306
$D^- \rho^+$		(7.8 ±1.4)	$\times 10^{-3}$		2236
$\overline{D}^0 \pi^+ \pi^-$		< 1.6	$\times 10^{-3}$	CL=90%	2301
$D^*(2010)^- \pi^+$		(2.6 ±0.4)	$\times 10^{-3}$		2254
$D^- \pi^+ \pi^+ \pi^-$		(8.0 ±2.5)	$\times 10^{-3}$		2287
($D^- \pi^+ \pi^+ \pi^-$) nonresonant		(3.9 ±1.9)	$\times 10^{-3}$		2287
$D^- \pi^+ \rho^0$		(1.1 ±1.0)	$\times 10^{-3}$		2207
$D^- a_1(1260)^+$		(6.0 ±3.3)	$\times 10^{-3}$		2121
$D^*(2010)^- \pi^+ \pi^0$		(1.5 ±0.5) %			2247
$D^*(2010)^- \rho^+$		(7.3 ±1.5)	$\times 10^{-3}$		2181
$D^*(2010)^- \pi^+ \pi^+ \pi^-$		(7.6 ±1.7)	$\times 10^{-3}$	S=1.3	2235
($D^*(2010)^- \pi^+ \pi^+ \pi^-$) nonresonant		(0.0 ±2.5)	$\times 10^{-3}$		2235
$D^*(2010)^- \pi^+ \rho^0$		(5.7 ±3.1)	$\times 10^{-3}$		2151
$D^*(2010)^- a_1(1260)^+$		(1.30±0.27) %			2061
$D^*(2010)^- \pi^+ \pi^+ \pi^- \pi^0$		(3.4 ±1.8) %			2218
$\overline{D}_2^*(2460)^- \pi^+$		< 2.2	$\times 10^{-3}$	CL=90%	2064
$\overline{D}_2^*(2460)^- \rho^+$		< 4.9	$\times 10^{-3}$	CL=90%	1979
$D^- D_s^+$		(7 ±4)	$\times 10^{-3}$		1812
$D^*(2010)^- D_s^+$		(1.2 ±0.6) %			1735
$D^- D_s^{*+}$		(2.0 ±1.5) %			1731
$D^*(2010)^- D_s^{*+}$		(1.9 ±1.2) %			1649
$D_s^+ \pi^-$		< 2.8	$\times 10^{-4}$	CL=90%	2270
$D_s^{*+} \pi^-$		< 5	$\times 10^{-4}$	CL=90%	2214
$D_s^+ \rho^-$		< 7	$\times 10^{-4}$	CL=90%	2198
$D_s^{*+} \rho^-$		< 8	$\times 10^{-4}$	CL=90%	2139
$D_s^+ a_1(1260)^-$		< 2.6	$\times 10^{-3}$	CL=90%	2079
$D_s^{*+} a_1(1260)^-$		< 2.2	$\times 10^{-3}$	CL=90%	2014
$D_s^- K^+$		< 2.4	$\times 10^{-4}$	CL=90%	2242
$D_s^{*-} K^+$		< 1.7	$\times 10^{-4}$	CL=90%	2185
$D_s^- K^*(892)^+$		< 9.9	$\times 10^{-4}$	CL=90%	2172
$D_s^{*-} K^*(892)^+$		< 1.1	$\times 10^{-3}$	CL=90%	2112
$D_s^- \pi^+ K^0$		< 5	$\times 10^{-3}$	CL=90%	2221
$D_s^{*-} \pi^+ K^0$		< 3.1	$\times 10^{-3}$	CL=90%	2164
$D_s^- \pi^+ K^*(892)^0$		< 4	$\times 10^{-3}$	CL=90%	2136
$D_s^{*-} \pi^+ K^*(892)^0$		< 2.0	$\times 10^{-3}$	CL=90%	2074
$\overline{D}^0 \pi^0$		< 4.8	$\times 10^{-4}$	CL=90%	2308
$\overline{D}^0 \rho^0$		< 5.5	$\times 10^{-4}$	CL=90%	2238
$\overline{D}^0 \eta$		< 6.8	$\times 10^{-4}$	CL=90%	2274
$\overline{D}^0 \eta'$		< 8.6	$\times 10^{-4}$	CL=90%	2198
$\overline{D}^0 \omega$		< 6.3	$\times 10^{-4}$	CL=90%	2235
$\overline{D}^*(2007)^0 \pi^0$		< 9.7	$\times 10^{-4}$	CL=90%	2256
$\overline{D}^*(2007)^0 \rho^0$		< 1.17	$\times 10^{-3}$	CL=90%	2183
$\overline{D}^*(2007)^0 \eta$		< 6.9	$\times 10^{-4}$	CL=90%	2220
$\overline{D}^*(2007)^0 \eta'$		< 2.7	$\times 10^{-3}$	CL=90%	2141
$\overline{D}^*(2007)^0 \omega$		< 2.1	$\times 10^{-3}$	CL=90%	2180
Charmonium modes					
$J/\psi(1S) K^0$		(7.5 ±2.1)	$\times 10^{-4}$		1683
$J/\psi(1S) K^+ \pi^-$		(1.1 ±0.6)	$\times 10^{-3}$		1652
$J/\psi(1S) K^*(892)^0$		(1.58±0.27)	$\times 10^{-3}$		1570
$J/\psi(1S) \pi^0$		< 6.9	$\times 10^{-3}$	CL=90%	1728
$\psi(2S) K^0$		< 8	$\times 10^{-4}$	CL=90%	1283
$\psi(2S) K^+ \pi^-$		< 1	$\times 10^{-3}$	CL=90%	1238
$\psi(2S) K^*(892)^0$		(1.4 ±0.9)	$\times 10^{-3}$		1113
$\chi_{c1}(1P) K^0$		< 2.7	$\times 10^{-3}$	CL=90%	1411
$\chi_{c1}(1P) K^*(892)^0$		< 2.1	$\times 10^{-3}$	CL=90%	1263
K or K^* modes					
$K^+ \pi^-$		< 1.7	$\times 10^{-5}$	CL=90%	2615
$K^0 \pi^0$		< 4.0	$\times 10^{-5}$	CL=90%	2614
$K^+ K^-$		< 4	$\times 10^{-6}$	CL=90%	2593
$K^+ \rho^-$		< 3.5	$\times 10^{-5}$	CL=90%	2559
$K^0 \rho^0$		< 3.9	$\times 10^{-5}$	CL=90%	2559
$K^0 f_0(980)$		< 3.6	$\times 10^{-4}$	CL=90%	2523
$K^*(892)^+ \pi^-$		< 7.2	$\times 10^{-5}$	CL=90%	2562
$K^*(892)^0 \pi^0$		< 2.8	$\times 10^{-5}$	CL=90%	2562
$K_2^*(1430)^+ \pi^-$		< 2.6	$\times 10^{-3}$	CL=90%	2445
$K^0 K^+ K^-$		< 1.3	$\times 10^{-3}$	CL=90%	2522
$K^0 \phi$		< 8.8	$\times 10^{-5}$	CL=90%	2516
$K^- \pi^+ \pi^+ \pi^-$	[bbb]	< 2.1	$\times 10^{-4}$	CL=90%	2600
$K^*(892)^0 \pi^+ \pi^-$		< 1.4	$\times 10^{-3}$	CL=90%	2556
$K^*(892)^0 \rho^0$		< 4.6	$\times 10^{-4}$	CL=90%	2504
$K^*(892)^0 f_0(980)$		< 1.7	$\times 10^{-4}$	CL=90%	2467
$K_1(1400)^+ \pi^-$		< 1.1	$\times 10^{-3}$	CL=90%	2451
$K^- a_1(1260)^+$	[bbb]	< 3.9	$\times 10^{-4}$	CL=90%	2471
$K^*(892)^0 K^+ K^-$		< 6.1	$\times 10^{-4}$	CL=90%	2466
$K^*(892)^0 \phi$		< 4.3	$\times 10^{-5}$	CL=90%	2459
$K_1(1400)^0 \rho^0$		< 3.0	$\times 10^{-3}$	CL=90%	2389
$K_1(1400)^0 \phi$		< 5.0	$\times 10^{-3}$	CL=90%	2339
$K_2^*(1430)^0 \rho^0$		< 1.1	$\times 10^{-3}$	CL=90%	2380
$K_2^*(1430)^0 \phi$		< 1.4	$\times 10^{-3}$	CL=90%	2330
$K^*(892)^0 \gamma$		(4.0 ±1.9)	$\times 10^{-5}$		2564
$K_1(1270)^0 \gamma$		< 7.0	$\times 10^{-3}$	CL=90%	2486
$K_1(1400)^0 \gamma$		< 4.3	$\times 10^{-3}$	CL=90%	2453
$K_2^*(1430)^0 \gamma$		< 4.0	$\times 10^{-4}$	CL=90%	2445
$K^*(1680)^0 \gamma$		< 2.0	$\times 10^{-3}$	CL=90%	2361
$K_3^*(1780)^0 \gamma$		< 1.0	%	CL=90%	2343
$K_4^*(2045)^0 \gamma$		< 4.3	$\times 10^{-3}$	CL=90%	2244
$\phi\phi$		< 3.9	$\times 10^{-5}$	CL=90%	2435

Light unflavored meson modes

$\pi^+\pi^-$		< 2.0	$\times 10^{-5}$	CL=90%	2636
$\pi^0\pi^0$		< 9.1	$\times 10^{-6}$	CL=90%	2636
$\eta\pi^0$		< 2.5	$\times 10^{-4}$	CL=90%	2609
$\eta\eta$		< 4.1	$\times 10^{-4}$	CL=90%	2582
$\pi^+\pi^-\pi^0$		< 7.2	$\times 10^{-4}$	CL=90%	2631
$\rho^0\pi^0$		< 2.4	$\times 10^{-5}$	CL=90%	2582
$\rho^\mp\pi^\pm$	[gg]	< 8.8	$\times 10^{-5}$	CL=90%	2582
$\pi^+\pi^-\pi^+\pi^-$		< 2.8	$\times 10^{-4}$	CL=90%	2621
$\rho^0\rho^0$		< 2.8	$\times 10^{-4}$	CL=90%	2525
$a_1(1260)^\mp\pi^\pm$	[gg]	< 4.9	$\times 10^{-4}$	CL=90%	2494
$a_2(1320)^\mp\pi^\pm$	[gg]	< 3.0	$\times 10^{-4}$	CL=90%	2473
$\pi^+\pi^-\pi^0\pi^0$		< 3.1	$\times 10^{-3}$	CL=90%	2622
$\rho^+\rho^-$		< 2.2	$\times 10^{-3}$	CL=90%	2525
$a_1(1260)^0\pi^0$		< 1.1	$\times 10^{-3}$	CL=90%	2494
$\omega\pi^0$		< 4.6	$\times 10^{-4}$	CL=90%	2580
$\pi^+\pi^+\pi^-\pi^-\pi^0$		< 9.0	$\times 10^{-3}$	CL=90%	2609
$a_1(1260)^+\rho^-$		< 3.4	$\times 10^{-3}$	CL=90%	2434
$a_1(1260)^0\rho^0$		< 2.4	$\times 10^{-3}$	CL=90%	2434
$\pi^+\pi^+\pi^+\pi^-\pi^-\pi^-$		< 3.0	$\times 10^{-3}$	CL=90%	2592
$a_1(1260)^+a_1(1260)^-$		< 2.8	$\times 10^{-3}$	CL=90%	2336
$\pi^+\pi^+\pi^+\pi^-\pi^-\pi^-\pi^0$		< 1.1	%	CL=90%	2572

Baryon modes

$p\overline{p}$		< 3.4	$\times 10^{-5}$	CL=90%	2467
$p\overline{p}\pi^+\pi^-$		< 2.5	$\times 10^{-4}$	CL=90%	2406
$p\overline{\Lambda}\pi^-$		< 1.8	$\times 10^{-4}$	CL=90%	2401
$\Delta^0\overline{\Delta}^0$		< 1.5	$\times 10^{-3}$	CL=90%	2334
$\Delta^{++}\Delta^{--}$		< 1.1	$\times 10^{-4}$	CL=90%	2334
$\overline{\Sigma}_c^{--}\Delta^{++}$		< 1.2	$\times 10^{-3}$	CL=90%	1839

Lepton Family number (*LF*) violating modes, or $\Delta B = 1$ weak neutral current (*B1*) modes

$\gamma\gamma$	*B1*		< 3.9	$\times 10^{-5}$	CL=90%	2640
e^+e^-	*B1*		< 5.9	$\times 10^{-6}$	CL=90%	2640
$\mu^+\mu^-$	*B1*		< 5.9	$\times 10^{-6}$	CL=90%	2637
$K^0e^+e^-$	*B1*		< 3.0	$\times 10^{-4}$	CL=90%	2616
$K^0\mu^+\mu^-$	*B1*		< 3.6	$\times 10^{-4}$	CL=90%	2612
$K^*(892)^0e^+e^-$	*B1*		< 2.9	$\times 10^{-4}$	CL=90%	2564
$K^*(892)^0\mu^+\mu^-$	*B1*		< 2.3	$\times 10^{-5}$	CL=90%	2559
$e^\pm\mu^\mp$	*LF*	[gg]	< 5.9	$\times 10^{-6}$	CL=90%	2639
$e^\pm\tau^\mp$	*LF*	[gg]	< 5.3	$\times 10^{-4}$	CL=90%	2341
$\mu^\pm\tau^\mp$	*LF*	[gg]	< 8.3	$\times 10^{-4}$	CL=90%	2339

$B^\pm/B^0$ ADMIXTURE

The branching fraction measurements are for an admixture of B mesons at the $\Upsilon(4S)$. The values quoted assume that $B(\Upsilon(4S) \to B\overline{B}) = 100\%$.

For inclusive branching fractions, *e.g.*, $B \to D^\pm$ anything, the treatment of multiple D's in the final state must be defined. One possibility would be to count the number of events with one-or-more D's and divide by the total number of B's. Another possibility would be to count the total number of D's and divide by the total number of B's, which is the definition of average multiplicity. The two definitions are identical when only one of the specified particles is allowed in the final state. Even though the "one-or-more" definition seems sensible, for practical reasons inclusive branching fractions are almost always measured using the multiplicity definition. For heavy final state particles, authors call their results inclusive branching fractions while for light particles some authors call their results multiplicities. In the B sections, we list all results as inclusive branching fractions, adopting a multiplicity definition. This means that inclusive branching fractions can exceed 100% and that inclusive partial widths can exceed total widths, just as inclusive cross sections can exceed total cross sections.

$\overline{B}$ modes are charge conjugates of the modes below. Reactions indicate the weak decay vertex and do not include mixing.

***B* DECAY MODES**		Fraction (Γ_i/Γ)	Scale factor/ Confidence level	*p* (MeV/*c*)
Semileptonic and leptonic modes				
$e^+\nu_e$ anything	[ccc]	(10.4 ±0.4) %	S=1.3	–
$\overline{p}e^+\nu_e$ anything		< 1.6 $\times 10^{-3}$	CL=90%	–
$\mu^+\nu_\mu$ anything	[ccc]	(10.3 ±0.5) %		–
$\ell^+\nu_\ell$ anything	[qq,ccc]	(10.43±0.24) %		–
$D^-\ell^+\nu_\ell$ anything	[qq]	(2.7 ±0.8) %		–
$\overline{D}^0\ell^+\nu_\ell$ anything	[qq]	(7.0 ±1.4) %		–
$\overline{D}^{**}\ell^+\nu_\ell$	[qq,ddd]	(2.7 ±0.7) %		–
$\overline{D}(1)(2420)^0\ell^+\nu_\ell$ anything		seen		–
$\overline{D}(2)^*(2460)^0\ell^+\nu_\ell$ anything		not seen		–
$D^{*-}\pi^+\ell^+\nu_\ell$ anything		(1.00±0.34) %		–
$D_s^-\ell^+\nu_\ell$ anything	[qq]	< 9 $\times 10^{-3}$	CL=90%	–
$D_s^-\ell^+\nu_\ell K^+$ anything	[qq]	< 6 $\times 10^{-3}$	CL=90%	–
$D_s^-\ell^+\nu_\ell K^0$ anything	[qq]	< 9 $\times 10^{-3}$	CL=90%	–
$K^+\ell^+\nu_\ell$ anything	[qq]	(6.0 ±0.5) %		–
$K^-\ell^+\nu_\ell$ anything	[qq]	(10 ±4) $\times 10^{-3}$		–
$K^0/\overline{K}^0\ell^+\nu_\ell$ anything	[qq]	(4.4 ±0.5) %		–
***D*, *D**, or D_s modes**				
$D^\pm$ anything		(24.2 ±3.3) %		–
$D^0/\overline{D}^0$ anything		(58 ±5) %	S=1.1	–
$D^*(2010)^\pm$ anything		(23.1 ±3.3) %	S=1.1	–
$D_s^\pm$ anything	[gg]	(8.6 ±1.6) %		–
D_sD, D_s^*D, D_sD^*, or $D_s^*D^*$	[gg]	(4.9 ±1.1) %		–
$D^*(2010)\gamma$		< 1.1 $\times 10^{-3}$	CL=90%	–
$D_s^+\pi^-$, $D_s^{*+}\pi^-$, $D_s^+\rho^-$, $D_s^{*+}\rho^-$, $D_s^+\pi^0$, $D_s^{*+}\pi^0$, $D_s^+\eta$, $D_s^{*+}\eta$, $D_s^+\rho^0$, $D_s^{*+}\rho^0$, $D_s^+\omega$, $D_s^{*+}\omega$	[gg]	< 5 $\times 10^{-4}$	CL=90%	–
Charmonium modes				
$J/\psi(1S)$ anything		(1.14±0.06) %		–
$J/\psi(1S)$(direct) anything		(8.0 ±0.8) $\times 10^{-3}$		–
$\psi(2S)$ anything		(3.5 ±0.5) $\times 10^{-3}$		–
$\chi_{c1}(1P)$ anything		(4.2 ±0.7) $\times 10^{-3}$		–
$\chi_{c1}(1P)$(direct) anything		(3.7 ±0.7) $\times 10^{-3}$		–
$\chi_{c2}(1P)$ anything		< 3.8 $\times 10^{-3}$	CL=90%	–
$\eta_c(1S)$ anything		< 9 $\times 10^{-3}$	CL=90%	–
***K* or *K** modes**				
$K^\pm$ anything	[gg]	(78.9 ±2.5) %		–
K^+ anything		(66 ±5) %		–
K^- anything		(13 ±4) %		–
$K^0/\overline{K}^0$ anything	[gg]	(64 ±4) %		–
$K^*(892)^\pm$ anything		(18 ±6) %		–
$K^*(892)^0/\overline{K}^*(892)^0$ anything	[gg]	(14.6 ±2.6) %		–
$K_1(1400)\gamma$		< 4.1 $\times 10^{-4}$	CL=90%	–
$K_2^*(1430)\gamma$		< 8.3 $\times 10^{-4}$	CL=90%	–
$K_2(1770)\gamma$		< 1.2 $\times 10^{-3}$	CL=90%	–
$K_3^*(1780)\gamma$		< 3.0 $\times 10^{-3}$	CL=90%	–
$K_4^*(2045)\gamma$		< 1.0 $\times 10^{-3}$	CL=90%	–
$\overline{b} \to \overline{s}\gamma$		(2.3 ±0.7) $\times 10^{-4}$		–
Light unflavored meson modes				
$\pi^\pm$ anything	[gg,eee]	(359 ±7) %		–
ρ^0 anything		(21 ±5) %		–
ω anything		< 81 %	CL=90%	–
ϕ anything		(3.5 ±0.7) %	S=1.8	–
Baryon modes				
charmed-baryon anything		(6.4 ±1.1) %		–
$\overline{\Sigma}_c^{--}$ anything		(4.8 ±2.5) $\times 10^{-3}$		–
$\overline{\Sigma}_c^-$ anything		< 1.1 %	CL=90%	–
$\overline{\Sigma}_c^0$ anything		(5.2 ±2.5) $\times 10^{-3}$		–
$\overline{\Sigma}_c^0N$ (N = p or n)		< 1.7 $\times 10^{-3}$	CL=90%	–
$p/\overline{p}$ anything	[gg]	(8.0 ±0.4) %		–
$p/\overline{p}$(direct) anything	[gg]	(5.5 ±0.5) %		–
$\Lambda/\overline{\Lambda}$ anything	[gg]	(4.0 ±0.5) %		–
$\Xi^-/\overline{\Xi}^+$ anything	[gg]	(2.7 ±0.6) $\times 10^{-3}$		–
baryons anything		(6.8 ±0.6) %		–
$p\overline{p}$ anything		(2.47±0.23) %		–
$\Lambda\overline{p}/\overline{\Lambda}p$ anything	[gg]	(2.5 ±0.4) %		–
$\Lambda\overline{\Lambda}$ anything		< 5 $\times 10^{-3}$	CL=90%	–

Meson Summary Table

$\Delta B = 1$ weak neutral current ($B1$) modes						
e^+e^- anything	$B1$	<	2.4	$\times 10^{-3}$	CL=90%	–
$\mu^+\mu^-$ anything	$B1$	<	2.4	$\times 10^{-3}$	CL=90%	–

$B^\pm/B^0/B_s^0$/b-baryon ADMIXTURE

These measurements are for an admixture of bottom particles at high energy (LEP, Tevatron, S$p\overline{p}$S).

Mean life $\tau = (1.549 \pm 0.020) \times 10^{-12}$ s

Mean life $\tau = (1.72 \pm 0.10) \times 10^{-12}$ s Charged b-hadron admixture

Mean life $\tau = (1.58 \pm 0.14) \times 10^{-12}$ s Neutral b-hadron admixture

$\tau_{\text{charged } b\text{-hadron}}/\tau_{\text{neutral } b\text{-hadron}} = 1.09 \pm 0.13$

The branching fraction measurements are for an admixture of B mesons and baryons at energies above the $\Upsilon(4S)$. Only the highest energy results (LEP, Tevatron, S$p\overline{p}$S) are used in the branching fraction averages. The production fractions give our best current estimate of the admixture at LEP.

For inclusive branching fractions, *e.g.*, $B \to D^\pm$ anything, the treatment of multiple D's in the final state must be defined. One possiblity would be to count the number of events with one-or-more D's and divide by the total number of B's. Another possibility would be to count the total number of D's and divide by the total number of B's, which is the definition of average multiplicity. The two definitions are identical when only one of the specified particles is allowed in the final state. Even though the "one-or-more" definition seems sensible, for practical reasons inclusive branching fractions are almost always measured using the multiplicity definition. For heavy final state particles, authors call their results inclusive branching fractions while for light particles some authors call their results multiplicities. In the B sections, we list all results as inclusive branching fractions, adopting a multiplicity definition. This means that inclusive branching fractions can exceed 100% and that inclusive partial widths can exceed total widths, just as inclusive cross sections can exceed total cross sections.

The modes below are listed for a $\overline{b}$ initial state. b modes are their charge conjugates. Reactions indicate the weak decay vertex and do not include mixing.

$\overline{b}$ DECAY MODES		Fraction (Γ_i/Γ)	Confidence level	p (MeV/c)
PRODUCTION FRACTIONS				

The production fractions for weakly decaying b-hadrons at the Z have been calculated from the best values of mean lives, mixing parameters, and branching fractions in this edition by O. Hayes (CERN) and M. Jimack (U. Birmingham) as described in the note "Production and Decay of b-Flavored Hadrons" in the $B^\pm$ Particle Listings. Values assume

$\mathrm{B}(\overline{b} \to B^+) = \mathrm{B}(\overline{b} \to B^0)$

$\mathrm{B}(\overline{b} \to B^+) + \mathrm{B}(\overline{b} \to B^0) + \mathrm{B}(\overline{b} \to B_s^0) + \mathrm{B}(b \to \Lambda_b) = 100$ %.

The notation for production fractions varies in the literature (f_{B^0}, $f(b \to \overline{B}^0)$, $\mathrm{Br}(b \to \overline{B}^0)$). We use our own branching fraction notation here, $\mathrm{B}(\overline{b} \to B^0)$.

$\overline{b} \to B^+$	(37.8 ± 2.2) %		–
$\overline{b} \to B^0$	(37.8 ± 2.2) %		–
$\overline{b} \to B_s^0$	(11.2 $^{+\ 1.8}_{-\ 1.9}$) %		–
$b \to \Lambda_b$	(13.2 ± 4.1) %		–
DECAY MODES			
Semileptonic and leptonic modes			
$\overline{b} \to e^+\nu_e$ anything	[ccc]	(11.1 ± 1.0) %	–
$\overline{b} \to \mu^+\nu_\mu$ anything	[ccc]	(10.7 ± 0.7) %	–
$\overline{b} \to \ell^+\nu_\ell$ anything	[qq,ccc]	(11.13± 0.29) %	–
$\overline{b} \to D^-\ell^+\nu_\ell$ anything	[qq]	(2.01± 0.29) %	–
$\overline{b} \to \overline{D}^0\ell^+\nu_\ell$ anything	[qq]	(6.6 ± 0.6) %	–
$\overline{b} \to D^{*-}\ell^+\nu_\ell$ anything	[qq]	(2.76± 0.29) %	–
$\overline{b} \to \overline{D}_j^0\ell^+\nu_\ell$ anything	[qq,fff]	seen	–
$\overline{b} \to D_j^-\ell^+\nu_\ell$ anything	[qq,fff]	seen	–
$\overline{b} \to \overline{D}_2^*(2460)^0\ell^+\nu_\ell$ anything		seen	–
$\overline{b} \to D_2^*(2460)^-\ell^+\nu_\ell$ anything		seen	–
$\overline{b} \to \tau^+\nu_\tau$ anything		(2.7 ± 0.4) %	–
$\overline{b} \to \overline{b} \to \overline{c} \to \ell^-\overline{\nu}_\ell$ anything	[qq]	(7.9 ± 0.8) %	–
Charmonium modes			
$\overline{b} \to J/\psi(1S)$ anything		(1.16± 0.10) %	–
$\overline{b} \to \psi(2S)$ anything		(4.8 ± 2.4) $\times 10^{-3}$	–
$\overline{b} \to \chi_{c1}(1P)$ anything		(1.8 ± 0.5) %	–
K or K^* modes			
$\overline{b} \to \overline{s}\gamma$		< 1.2 $\times 10^{-3}$ 90%	–
$\overline{b} \to K^\pm$ anything		(88 ±19) %	–
$\overline{b} \to K_S^0$ anything		(29.0 ± 2.9) %	–
Baryon modes			
$\overline{b} \to p/\overline{p}$ anything		(14 ± 6) %	–
$\overline{b} \to \Lambda/\overline{\Lambda}$ anything		(5.9 ± 1.1) %	–
Other modes			
$\overline{b} \to$ charged anything	[eee]	(584 ±40) %	–
$\Delta B = 1$ weak neutral current ($B1$) modes			
$\overline{b} \to \mu^+\mu^-$ anything	$B1$	< 5.0 $\times 10^{-5}$ 90%	–
$\overline{b} \to \nu\overline{\nu}$ anything	$B1$	< 3.9 $\times 10^{-4}$	–

B^*

$I(J^P) = \frac{1}{2}(1^-)$

I, J, P need confirmation. Quantum numbers shown are quark-model predictions.

Mass $m_{B^*} = 5324.8 \pm 1.8$ MeV

$m_{B^*} - m_B = 45.7 \pm 0.4$ MeV

B^* DECAY MODES	Fraction (Γ_i/Γ)	p (MeV/c)
$B\gamma$	dominant	46

BOTTOM, STRANGE MESONS ($B = \pm 1, S = \mp 1$)

$B_s^0 = s\overline{b}$, $\overline{B}_s^0 = \overline{s}b$, similarly for B_s^*'s

B_s^0

$I(J^P) = 0(0^-)$

I, J, P need confirmation. Quantum numbers shown are quark-model predictions.

Mass $m_{B_s^0} = 5369.3 \pm 2.0$ MeV

Mean life $\tau = (1.61^{+0.10}_{-0.09}) \times 10^{-12}$ s

$c\tau = 483\ \mu$m

B_s^0-$\overline{B}_s^0$ mixing parameters

$\chi_s > 0.49$, CL = 95%

χ_B at high energy = $f_d\chi_d + f_s\chi_s = 0.126 \pm 0.008$

$\Delta m_{B_s^0} = m_{B_{sH}^0} - m_{B_{sL}^0} > 5.9 \times 10^{12}\ \hbar\ \mathrm{s}^{-1}$, CL = 95%

$x_s = \Delta m_{B_s^0}/\Gamma_{B_s^0} > 9.5$, CL = 95%

These branching fractions all scale with $\mathrm{B}(\overline{b} \to B_s^0)$, the LEP B_s^0 production fraction. The first four were evaluated using $\mathrm{B}(\overline{b} \to B_s^0) = (11.2^{+1.8}_{-1.9})$% and the rest assume $\mathrm{B}(\overline{b} \to B_s^0) = 12$%.

The branching fraction $\mathrm{B}(B_s^0 \to D_s^-\ell^+\nu_\ell$ anything) is not a pure measurement since the measured product branching fraction $\mathrm{B}(\overline{b} \to B_s^0) \times \mathrm{B}(B_s^0 \to D_s^-\ell^+\nu_\ell$ anything) was used to determine $\mathrm{B}(\overline{b} \to B_s^0)$, as described in the note on "Production and Decay of b-Flavored Hadrons."

B_s^0 DECAY MODES		Fraction (Γ_i/Γ)	Confidence level	p (MeV/c)
D_s^- anything		(87 ±31) %		–
$D_s^-\ell^+\nu_\ell$ anything	[ggg]	(7.6 ± 2.4) %		–
$D_s^-\pi^+$		< 12 %		2321
$J/\psi(1S)\phi$		< 6 $\times 10^{-3}$		1590
$\psi(2S)\phi$		seen		1122
$\pi^0\pi^0$		< 2.1 $\times 10^{-4}$	90%	2861
$\eta\pi^0$		< 1.0 $\times 10^{-3}$	90%	2655
$\eta\eta$		< 1.5 $\times 10^{-3}$	90%	2628
π^+K^-		< 2.6 $\times 10^{-4}$	90%	2660
K^+K^-		< 1.4 $\times 10^{-4}$	90%	2639
$\Delta B = 1$ weak neutral current ($B1$) modes				
$\gamma\gamma$	$B1$	< 1.48 $\times 10^{-4}$	90%	2685

$c\bar{c}$ MESONS

$\eta_c(1S)$ $I^G(J^{PC}) = 0^+(0^{-+})$

Mass $m = 2979.8 \pm 2.1$ MeV (S = 2.1)
Full width $\Gamma = 13.2^{+3.8}_{-3.2}$ MeV

$\eta_c(1S)$ DECAY MODES	Fraction (Γ_i/Γ)	Confidence level	p (MeV/c)
Decays involving hadronic resonances			
$\eta'(958)\pi\pi$	(4.1 ±1.7) %		1319
$\rho\rho$	(2.6 ±0.9) %		1275
$K^*(892)^0 K^-\pi^+$ + c.c.	(2.0 ±0.7) %		1273
$K^*(892)\overline{K}^*(892)$	(8.5 ±3.1) × 10^{-3}		1193
$\phi\phi$	(7.1 ±2.8) × 10^{-3}		1086
$a_0(980)\pi$	< 2 %	90%	1323
$a_2(1320)\pi$	< 2 %	90%	1193
$K^*(892)\overline{K}$ + c.c.	< 1.28 %	90%	1307
$f_2(1270)\eta$	< 1.1 %	90%	1142
$\omega\omega$	< 3.1 × 10^{-3}	90%	1268
Decays into stable hadrons			
$K\overline{K}\pi$	(5.5 ±1.7) %		1378
$\eta\pi\pi$	(4.9 ±1.8) %		1425
$\pi^+\pi^- K^+K^-$	(2.0 $^{+0.7}_{-0.6}$) %		1342
$2(K^+K^-)$	(2.1 ±1.2) %		1053
$2(\pi^+\pi^-)$	(1.2 ±0.4) %		1457
$p\overline{p}$	(1.2 ±0.4) × 10^{-3}		1157
$K\overline{K}\eta$	< 3.1 %	90%	1262
$\pi^+\pi^- p\overline{p}$	< 1.2 %	90%	1023
$\Lambda\overline{\Lambda}$	< 2 × 10^{-3}	90%	987
Radiative decays			
$\gamma\gamma$	(3.0 ±1.2) × 10^{-4}		1489

$J/\psi(1S)$ $I^G(J^{PC}) = 0^-(1^{--})$

Mass $m = 3096.88 \pm 0.04$ MeV
Full width $\Gamma = 87 \pm 5$ keV
$\Gamma_{ee} = 5.26 \pm 0.37$ keV (Assuming $\Gamma_{ee} = \Gamma_{\mu\mu}$)

$J/\psi(1S)$ DECAY MODES		Fraction (Γ_i/Γ)	Scale factor/ Confidence level	p (MeV/c)
hadrons		(87.7 ±0.5) %		–
virtual $\gamma \to$ hadrons		(17.0 ±2.0) %		–
e^+e^-		(6.02±0.19) %		1548
$\mu^+\mu^-$		(6.01±0.19) %		1545
Decays involving hadronic resonances				
$\rho\pi$		(1.28±0.10) %		1449
$\rho^0\pi^0$		(4.2 ±0.5) × 10^{-3}		1449
$a_2(1320)\rho$		(1.09±0.22) %		1125
$\omega\pi^+\pi^+\pi^-\pi^-$		(8.5 ±3.4) × 10^{-3}		1392
$\omega\pi^+\pi^-$		(7.2 ±1.0) × 10^{-3}		1435
$K^*(892)^0\overline{K}_2^*(1430)^0$ + c.c.		(6.7 ±2.6) × 10^{-3}		1005
$\omega K^*(892)\overline{K}$ + c.c.		(5.3 ±2.0) × 10^{-3}		1098
$\omega f_2(1270)$		(4.3 ±0.6) × 10^{-3}		1143
$K^+\overline{K}^*(892)^-$ + c.c.		(5.0 ±0.4) × 10^{-3}		1373
$K^0\overline{K}^*(892)^0$ + c.c.		(4.2 ±0.4) × 10^{-3}		1371
$\omega\pi^0\pi^0$		(3.4 ±0.8) × 10^{-3}		1436
$b_1(1235)^\pm\pi^\mp$	[gg]	(3.0 ±0.5) × 10^{-3}		1299
$\omega K^\pm K_S^0\pi^\mp$	[gg]	(3.0 ±0.7) × 10^{-3}		1210
$b_1(1235)^0\pi^0$		(2.3 ±0.6) × 10^{-3}		1299
$\phi K^*(892)\overline{K}$ + c.c.		(2.04±0.28) × 10^{-3}		969
$\omega K\overline{K}$		(1.9 ±0.4) × 10^{-3}		1268
$\omega f_J(1710) \to \omega K\overline{K}$		(4.8 ±1.1) × 10^{-4}		878
$\phi 2(\pi^+\pi^-)$		(1.60±0.32) × 10^{-3}		1318
$\Delta(1232)^{++}\overline{p}\pi^-$		(1.6 ±0.5) × 10^{-3}		1030
$\omega\eta$		(1.58±0.16) × 10^{-3}		1394
$\phi K\overline{K}$		(1.48±0.22) × 10^{-3}		1179
$\phi f_J(1710) \to \phi K\overline{K}$		(3.6 ±0.6) × 10^{-4}		875
$p\overline{p}\omega$		(1.30±0.25) × 10^{-3}	S=1.3	769
$\Delta(1232)^{++}\overline{\Delta}(1232)^{--}$		(1.10±0.29) × 10^{-3}		938
$\Sigma(1385)^-\overline{\Sigma}(1385)^+$ (or c.c.)	[gg]	(1.03±0.13) × 10^{-3}		692
$p\overline{p}\eta'(958)$		(9 ±4) × 10^{-4}	S=1.7	596
$\phi f_2'(1525)$		(8 ±4) × 10^{-4}	S=2.7	871
$\phi\pi^+\pi^-$		(8.0 ±1.2) × 10^{-4}		1365
$\phi K^\pm K_S^0\pi^\mp$	[gg]	(7.2 ±0.9) × 10^{-4}		1114
$\omega f_1(1420)$		(6.8 ±2.4) × 10^{-4}		1062
$\phi\eta$		(6.5 ±0.7) × 10^{-4}		1320
$\Xi(1530)^-\overline{\Xi}^+$		(5.9 ±1.5) × 10^{-4}		597
$pK^-\overline{\Sigma}(1385)^0$		(5.1 ±3.2) × 10^{-4}		645
$\omega\pi^0$		(4.2 ±0.6) × 10^{-4}	S=1.4	1447
$\phi\eta'(958)$		(3.3 ±0.4) × 10^{-4}		1192
$\phi f_0(980)$		(3.2 ±0.9) × 10^{-4}	S=1.9	1182
$\Xi(1530)^0\overline{\Xi}^0$		(3.2 ±1.4) × 10^{-4}		608
$\Sigma(1385)^-\overline{\Sigma}^+$ (or c.c.)	[gg]	(3.1 ±0.5) × 10^{-4}		857
$\phi f_1(1285)$		(2.6 ±0.5) × 10^{-4}	S=1.1	1032
$\rho\eta$		(1.93±0.23) × 10^{-4}		1398
$\omega\eta'(958)$		(1.67±0.25) × 10^{-4}		1279
$\omega f_0(980)$		(1.4 ±0.5) × 10^{-4}		1271
$\rho\eta'(958)$		(1.05±0.18) × 10^{-4}		1283
$p\overline{p}\phi$		(4.5 ±1.5) × 10^{-5}		527
$a_2(1320)^\pm\pi^\mp$	[gg]	< 4.3 × 10^{-3}	CL=90%	1263
$K\overline{K}_2^*(1430)$ + c.c.		< 4.0 × 10^{-3}	CL=90%	1159
$K_2^*(1430)^0\overline{K}_2^*(1430)^0$		< 2.9 × 10^{-3}	CL=90%	588
$K^*(892)^0\overline{K}^*(892)^0$		< 5 × 10^{-4}	CL=90%	1263
$\phi f_2(1270)$		< 3.7 × 10^{-4}	CL=90%	1036
$p\overline{p}\rho$		< 3.1 × 10^{-4}	CL=90%	779
$\phi\eta(1440) \to \phi\eta\pi\pi$		< 2.5 × 10^{-4}	CL=90%	946
$\omega f_2'(1525)$		< 2.2 × 10^{-4}	CL=90%	1003
$\Sigma(1385)^0\overline{\Lambda}$		< 2 × 10^{-4}	CL=90%	911
$\Delta(1232)^+\overline{p}$		< 1 × 10^{-4}	CL=90%	1100
$\Sigma^0\overline{\Lambda}$		< 9 × 10^{-5}	CL=90%	1032
$\phi\pi^0$		< 6.8 × 10^{-6}	CL=90%	1377
Decays into stable hadrons				
$2(\pi^+\pi^-)\pi^0$		(3.37±0.26) %		1496
$3(\pi^+\pi^-)\pi^0$		(2.9 ±0.6) %		1433
$\pi^+\pi^-\pi^0$		(1.50±0.20) %		1533
$\pi^+\pi^-\pi^0 K^+K^-$		(1.20±0.30) %		1368
$4(\pi^+\pi^-)\pi^0$		(9.0 ±3.0) × 10^{-3}		1345
$\pi^+\pi^- K^+K^-$		(7.2 ±2.3) × 10^{-3}		1407
$K\overline{K}\pi$		(6.1 ±1.0) × 10^{-3}		1440
$p\overline{p}\pi^+\pi^-$		(6.0 ±0.5) × 10^{-3}	S=1.3	1107
$2(\pi^+\pi^-)$		(4.0 ±1.0) × 10^{-3}		1517
$3(\pi^+\pi^-)$		(4.0 ±2.0) × 10^{-3}		1466
$n\overline{n}\pi^+\pi^-$		(4 ±4) × 10^{-3}		1106
$\Sigma\overline{\Sigma}$		(3.8 ±0.5) × 10^{-3}		992
$2(\pi^+\pi^-)K^+K^-$		(3.1 ±1.3) × 10^{-3}		1320
$p\overline{p}\pi^+\pi^-\pi^0$	[hhh]	(2.3 ±0.9) × 10^{-3}	S=1.9	1033
$p\overline{p}$		(2.14±0.10) × 10^{-3}		1232
$p\overline{p}\eta$		(2.09±0.18) × 10^{-3}		948
$p\overline{n}\pi^-$		(2.00±0.10) × 10^{-3}		1174
$n\overline{n}$		(1.9 ±0.5) × 10^{-3}		1231
$\Xi\overline{\Xi}$		(1.8 ±0.4) × 10^{-3}	S=1.8	818
$\Lambda\overline{\Lambda}$		(1.35±0.14) × 10^{-3}	S=1.2	1074
$p\overline{p}\pi^0$		(1.09±0.09) × 10^{-3}		1176
$\Lambda\overline{\Sigma}^-\pi^+$ (or c.c.)	[gg]	(1.06±0.12) × 10^{-3}		945
$pK^-\overline{\Lambda}$		(8.9 ±1.6) × 10^{-4}		876
$2(K^+K^-)$		(7.0 ±3.0) × 10^{-4}		1131
$pK^-\overline{\Sigma}^0$		(2.9 ±0.8) × 10^{-4}		820
K^+K^-		(2.37±0.31) × 10^{-4}		1468
$\Lambda\overline{\Lambda}\pi^0$		(2.2 ±0.7) × 10^{-4}		998
$\pi^+\pi^-$		(1.47±0.23) × 10^{-4}		1542
$K_S^0K_L^0$		(1.08±0.14) × 10^{-4}		1466
$\Lambda\overline{\Sigma}$ + c.c.		< 1.5 × 10^{-4}	CL=90%	1032
$K_S^0K_S^0$		< 5.2 × 10^{-6}	CL=90%	1466
Radiative decays				
$\gamma\eta_c(1S)$		(1.3 ±0.4) %		116
$\gamma\pi^+\pi^-2\pi^0$		(8.3 ±3.1) × 10^{-3}		1518
$\gamma\eta\pi\pi$		(6.1 ±1.0) × 10^{-3}		1487
$\gamma\eta(1440) \to \gamma K\overline{K}\pi$	[p]	(9.1 ±1.8) × 10^{-4}		1223
$\gamma\eta(1440) \to \gamma\gamma\rho^0$		(6.4 ±1.4) × 10^{-5}		1223
$\gamma\rho\rho$		(4.5 ±0.8) × 10^{-3}		1343
$\gamma\eta'(958)$		(4.31±0.30) × 10^{-3}		1400
$\gamma 2\pi^+2\pi^-$		(2.8 ±0.5) × 10^{-3}	S=1.9	1517
$\gamma f_4(2050)$		(2.7 ±0.7) × 10^{-3}		874
$\gamma\omega\omega$		(1.59±0.33) × 10^{-3}		1337
$\gamma\eta(1440) \to \gamma\rho^0\rho^0$		(1.7 ±0.4) × 10^{-3}	S=1.3	1223
$\gamma f_2(1270)$		(1.38±0.14) × 10^{-3}		1286
$\gamma f_J(1710) \to \gamma K\overline{K}$		(9.7 ±1.2) × 10^{-4}		1075
$\gamma\eta$		(8.6 ±0.8) × 10^{-4}		1500

Meson Summary Table

$\gamma f_1(1420) \rightarrow \gamma K\overline{K}\pi$	(8.3 ±1.5) × 10^{-4}		1220
$\gamma f_1(1285)$	(6.5 ±1.0) × 10^{-4}		1283
$\gamma f'_2(1525)$	(6.3 ±1.0) × 10^{-4}		1173
$\gamma\phi\phi$	(4.0 ±1.2) × 10^{-4}	S=2.1	1166
$\gamma p\overline{p}$	(3.8 ±1.0) × 10^{-4}		1232
$\gamma\eta(2225)$	(2.9 ±0.6) × 10^{-4}		834
$\gamma\eta(1760) \rightarrow \gamma\rho^0\rho^0$	(1.3 ±0.9) × 10^{-4}		1048
$\gamma\pi^0$	(3.9 ±1.3) × 10^{-5}		1546
$\gamma p\overline{p}\pi^+\pi^-$	< 7.9 × 10^{-4}	CL=90%	1107
$\gamma\gamma$	< 5 × 10^{-4}	CL=90%	1548
$\gamma\Lambda\overline{\Lambda}$	< 1.3 × 10^{-4}	CL=90%	1074
3γ	< 5.5 × 10^{-5}	CL=90%	1548
$\gamma f_0(1370)$	(3.4 ±0.7) × 10^{-4}		–
$\gamma f_0(1500)$	(8.2 ±1.5) × 10^{-4}		1184

$\chi_{c0}(1P)$

$I^G(J^{PC}) = 0^+(0^{++})$

Mass m = 3415.1 ± 1.0 MeV
Full width Γ = 14 ± 5 MeV

$\chi_{c0}(1P)$ DECAY MODES	Fraction (Γ_i/Γ)	Confidence level	p (MeV/c)
Hadronic decays			
$2(\pi^+\pi^-)$	(3.7±0.7) %		1679
$\pi^+\pi^- K^+K^-$	(3.0±0.7) %		1580
$\rho^0\pi^+\pi^-$	(1.6±0.5) %		1608
$3(\pi^+\pi^-)$	(1.5±0.5) %		1633
$K^+\overline{K}^*(892)^0\pi^- +$ c.c.	(1.2±0.4) %		1522
$\pi^+\pi^-$	(7.5±2.1) × 10^{-3}		1702
K^+K^-	(7.1±2.4) × 10^{-3}		1635
$\pi^+\pi^- p\overline{p}$	(5.0±2.0) × 10^{-3}		1320
$\pi^0\pi^0$	(3.1±0.6) × 10^{-3}		1702
$\eta\eta$	(2.5±1.1) × 10^{-3}		1617
$p\overline{p}$	< 9.0 × 10^{-4}	90%	1427
Radiative decays			
$\gamma J/\psi(1S)$	(6.6±1.8) × 10^{-3}		303
$\gamma\gamma$	(4.0±2.3) × 10^{-4}		1708

$\chi_{c1}(1P)$

$I^G(J^{PC}) = 0^+(1^{++})$

Mass m = 3510.53 ± 0.12 MeV
Full width Γ = 0.88 ± 0.14 MeV

$\chi_{c1}(1P)$ DECAY MODES	Fraction (Γ_i/Γ)	p (MeV/c)
Hadronic decays		
$3(\pi^+\pi^-)$	(2.2±0.8) %	1683
$2(\pi^+\pi^-)$	(1.6±0.5) %	1727
$\pi^+\pi^- K^+K^-$	(9 ±4) × 10^{-3}	1632
$\rho^0\pi^+\pi^-$	(3.9±3.5) × 10^{-3}	1659
$K^+\overline{K}^*(892)^0\pi^- +$ c.c.	(3.2±2.1) × 10^{-3}	1576
$\pi^+\pi^- p\overline{p}$	(1.4±0.9) × 10^{-3}	1381
$p\overline{p}$	(8.6±1.2) × 10^{-5}	1483
$\pi^+\pi^- + K^+K^-$	< 2.1 × 10^{-3}	–
Radiative decays		
$\gamma J/\psi(1S)$	(27.3±1.6) %	389

$\chi_{c2}(1P)$

$I^G(J^{PC}) = 0^+(2^{++})$

Mass m = 3556.17 ± 0.13 MeV
Full width Γ = 2.00 ± 0.18 MeV

$\chi_{c2}(1P)$ DECAY MODES	Fraction (Γ_i/Γ)	Confidence level	p (MeV/c)
Hadronic decays			
$2(\pi^+\pi^-)$	(2.2 ±0.5) %		1751
$\pi^+\pi^- K^+K^-$	(1.9 ±0.5) %		1656
$3(\pi^+\pi^-)$	(1.2 ±0.8) %		1707
$\rho^0\pi^+\pi^-$	(7 ±4) × 10^{-3}		1683
$K^+\overline{K}^*(892)^0\pi^- +$ c.c.	(4.8 ±2.8) × 10^{-3}		1601
$\pi^+\pi^- p\overline{p}$	(3.3 ±1.3) × 10^{-3}		1410
$\pi^+\pi^-$	(1.9 ±1.0) × 10^{-3}		1773
K^+K^-	(1.5 ±1.1) × 10^{-3}		1708
$p\overline{p}$	(10.0 ±1.0) × 10^{-5}		1510
$\pi^0\pi^0$	(1.10±0.28) × 10^{-3}		1773
$\eta\eta$	(8 ±5) × 10^{-4}		1692
$J/\psi(1S)\pi^+\pi^-\pi^0$	< 1.5 %	90%	185
Radiative decays			
$\gamma J/\psi(1S)$	(13.5 ±1.1) %		430
$\gamma\gamma$	(1.6 ±0.5) × 10^{-4}		1778

$\psi(2S)$

$I^G(J^{PC}) = 0^-(1^{--})$

Mass m = 3686.00 ± 0.09 MeV
Full width Γ = 277 ± 31 keV (S = 1.1)
Γ_{ee} = 2.14 ± 0.21 keV (Assuming $\Gamma_{ee} = \Gamma_{\mu\mu}$)

$\psi(2S)$ DECAY MODES	Fraction (Γ_i/Γ)	Scale factor/ Confidence level	p (MeV/c)
hadrons	(98.10±0.30) %		–
virtual $\gamma \rightarrow$ hadrons	(2.9 ±0.4) %		–
e^+e^-	(8.8 ±1.3) × 10^{-3}		1843
$\mu^+\mu^-$	(7.7 ±1.7) × 10^{-3}		1840
Decays into $J/\psi(1S)$ and anything			
$J/\psi(1S)$ anything	(57 ±4) %		–
$J/\psi(1S)$ neutrals	(23.2 ±2.6) %		–
$J/\psi(1S)\pi^+\pi^-$	(32.4 ±2.6) %		477
$J/\psi(1S)\pi^0\pi^0$	(18.4 ±2.7) %		481
$J/\psi(1S)\eta$	(2.7 ±0.4) %	S=1.7	200
$J/\psi(1S)\pi^0$	(9.7 ±2.1) × 10^{-4}		527
Hadronic decays			
$3(\pi^+\pi^-)\pi^0$	(3.5 ±1.6) × 10^{-3}		1746
$2(\pi^+\pi^-)\pi^0$	(3.1 ±0.7) × 10^{-3}		1799
$\pi^+\pi^- K^+K^-$	(1.6 ±0.4) × 10^{-3}		1726
$\pi^+\pi^- p\overline{p}$	(8.0 ±2.0) × 10^{-4}		1491
$K^+\overline{K}^*(892)^0\pi^- +$ c.c.	(6.7 ±2.5) × 10^{-4}		1673
$2(\pi^+\pi^-)$	(4.5 ±1.0) × 10^{-4}		1817
$\rho^0\pi^+\pi^-$	(4.2 ±1.5) × 10^{-4}		1751
$\overline{p}p$	(1.9 ±0.5) × 10^{-4}		1586
$3(\pi^+\pi^-)$	(1.5 ±1.0) × 10^{-4}		1774
$\overline{p}p\pi^0$	(1.4 ±0.5) × 10^{-4}		1543
K^+K^-	(1.0 ±0.7) × 10^{-4}		1776
$\pi^+\pi^-\pi^0$	(9 ±5) × 10^{-5}		1830
$\pi^+\pi^-$	(8 ±5) × 10^{-5}		1838
$\Lambda\overline{\Lambda}$	< 4 × 10^{-4}	CL=90%	1467
$\Xi^-\overline{\Xi}^+$	< 2 × 10^{-4}	CL=90%	1285
$\rho\pi$	< 8.3 × 10^{-5}	CL=90%	1760
$K^+K^-\pi^0$	< 2.96 × 10^{-5}	CL=90%	1754
$K^+\overline{K}^*(892)^- +$ c.c.	< 5.4 × 10^{-5}	CL=90%	1698
Radiative decays			
$\gamma\chi_{c0}(1P)$	(9.3 ±0.8) %		261
$\gamma\chi_{c1}(1P)$	(8.7 ±0.8) %		171
$\gamma\chi_{c2}(1P)$	(7.8 ±0.8) %		127
$\gamma\eta_c(1S)$	(2.8 ±0.6) × 10^{-3}		639
$\gamma\pi^0$	< 5.4 × 10^{-3}	CL=95%	1841
$\gamma\eta'(958)$	< 1.1 × 10^{-3}	CL=90%	1719
$\gamma\gamma$	< 1.6 × 10^{-4}	CL=90%	1843
$\gamma\eta(1440) \rightarrow \gamma K\overline{K}\pi$	< 1.2 × 10^{-4}	CL=90%	1569

$\psi(3770)$

$I^G(J^{PC}) = ?^?(1^{--})$

Mass m = 3769.9 ± 2.5 MeV (S = 1.8)
Full width Γ = 23.6 ± 2.7 MeV (S = 1.1)
Γ_{ee} = 0.26 ± 0.04 keV (S = 1.2)

$\psi(3770)$ DECAY MODES	Fraction (Γ_i/Γ)	Scale factor	p (MeV/c)
$D\overline{D}$	dominant		242
e^+e^-	(1.12±0.17) × 10^{-5}	1.2	1885

$\psi(4040)$ [iii]

$I^G(J^{PC}) = ?^?(1^{--})$

Mass m = 4040 ± 10 MeV
Full width Γ = 52 ± 10 MeV
Γ_{ee} = 0.75 ± 0.15 keV

$\psi(4040)$ DECAY MODES	Fraction (Γ_i/Γ)	p (MeV/c)
e^+e^-	(1.4±0.4) × 10^{-5}	2020
$D^0\overline{D}^0$	seen	777
$D^*(2007)^0\overline{D}^0 +$ c.c.	seen	578
$D^*(2007)^0\overline{D}^*(2007)^0$	seen	232

$\psi(4160)$ [iii]

$I^G(J^{PC}) = ?^?(1^{--})$

Mass $m = 4159 \pm 20$ MeV
Full width $\Gamma = 78 \pm 20$ MeV
$\Gamma_{ee} = 0.77 \pm 0.23$ keV

$\psi(4160)$ DECAY MODES	Fraction (Γ_i/Γ)	p (MeV/c)
e^+e^-	$(10\pm4)\times10^{-6}$	2079

$\psi(4415)$ [iii]

$I^G(J^{PC}) = ?^?(1^{--})$

Mass $m = 4415 \pm 6$ MeV
Full width $\Gamma = 43 \pm 15$ MeV (S = 1.8)
$\Gamma_{ee} = 0.47 \pm 0.10$ keV

$\psi(4415)$ DECAY MODES	Fraction (Γ_i/Γ)	p (MeV/c)
hadrons	dominant	–
e^+e^-	$(1.1\pm0.4)\times10^{-5}$	2207

$b\bar{b}$ MESONS

$\Upsilon(1S)$

$I^G(J^{PC}) = 0^-(1^{--})$

Mass $m = 9460.37 \pm 0.21$ MeV (S = 2.7)
Full width $\Gamma = 52.5 \pm 1.8$ keV
$\Gamma_{ee} = 1.32 \pm 0.05$ keV

$\Upsilon(1S)$ DECAY MODES	Fraction (Γ_i/Γ)	Scale factor/ Confidence level	p (MeV/c)
$\tau^+\tau^-$	$(2.67^{+0.14}_{-0.16})$ %		4384
e^+e^-	(2.52 ± 0.17) %		4730
$\mu^+\mu^-$	(2.48 ± 0.07) %	S=1.1	4729
Hadronic decays			
$J/\psi(1S)$ anything	$(1.1\ \pm0.4\ )\times10^{-3}$		4223
$\rho\pi$	< 2 $\times10^{-4}$	CL=90%	4698
$\pi^+\pi^-$	< 5 $\times10^{-4}$	CL=90%	4728
K^+K^-	< 5 $\times10^{-4}$	CL=90%	4704
$p\bar{p}$	< 5 $\times10^{-4}$	CL=90%	4636
Radiative decays			
$\gamma 2h^+2h^-$	$(7.0\ \pm1.5\ )\times10^{-4}$		4720
$\gamma 3h^+3h^-$	$(5.4\ \pm2.0\ )\times10^{-4}$		4703
$\gamma 4h^+4h^-$	$(7.4\ \pm3.5\ )\times10^{-4}$		4679
$\gamma\pi^+\pi^-K^+K^-$	$(2.9\ \pm0.9\ )\times10^{-4}$		4686
$\gamma 2\pi^+2\pi^-$	$(2.5\ \pm0.9\ )\times10^{-4}$		4720
$\gamma 3\pi^+3\pi^-$	$(2.5\ \pm1.2\ )\times10^{-4}$		4703
$\gamma 2\pi^+2\pi^-K^+K^-$	$(2.4\ \pm1.2\ )\times10^{-4}$		4658
$\gamma\pi^+\pi^-p\bar{p}$	$(1.5\ \pm0.6\ )\times10^{-4}$		4604
$\gamma 2\pi^+2\pi^-p\bar{p}$	$(4\ \ \pm6\ \ )\times10^{-5}$		4563
$\gamma 2K^+2K^-$	$(2.0\ \pm2.0\ )\times10^{-5}$		4601
$\gamma\eta'(958)$	< 1.3 $\times10^{-3}$	CL=90%	4682
$\gamma\eta$	< 3.5 $\times10^{-4}$	CL=90%	4714
$\gamma f_2'(1525)$	< 1.4 $\times10^{-4}$	CL=90%	4607
$\gamma f_2(1270)$	< 1.3 $\times10^{-4}$	CL=90%	4644
$\gamma\eta(1440)$	< 8.2 $\times10^{-5}$	CL=90%	4624
$\gamma f_J(1710) \to \gamma K\overline{K}$	< 2.6 $\times10^{-4}$	CL=90%	4576
$\gamma f_0(2200) \to \gamma K^+K^-$	< 2 $\times10^{-4}$	CL=90%	4475
$\gamma f_J(2220) \to \gamma K^+K^-$	< 1.5 $\times10^{-5}$	CL=90%	4469
$\gamma\eta(2225) \to \gamma\phi\phi$	< 3 $\times10^{-3}$	CL=90%	4469
γX	< 3 $\times10^{-5}$	CL=90%	–
X = pseudoscalar with $m<7.2$ GeV)			
$\gamma X\overline{X}$	< 1 $\times10^{-3}$	CL=90%	–
$X\overline{X}$ = vectors with $m<3.1$ GeV)			

$\chi_{b0}(1P)$ [iii]

$I^G(J^{PC}) = 0^+(0^{++})$
J needs confirmation.

Mass $m = 9859.8 \pm 1.3$ MeV

$\chi_{b0}(1P)$ DECAY MODES	Fraction (Γ_i/Γ)	Confidence level	p (MeV/c)
$\gamma\Upsilon(1S)$	<6 %	90%	391

$\chi_{b1}(1P)$ [iii]

$I^G(J^{PC}) = 0^+(1^{++})$
J needs confirmation.

Mass $m = 9891.9 \pm 0.7$ MeV

$\chi_{b1}(1P)$ DECAY MODES	Fraction (Γ_i/Γ)	p (MeV/c)
$\gamma\Upsilon(1S)$	(35±8) %	422

$\chi_{b2}(1P)$ [iii]

$I^G(J^{PC}) = 0^+(2^{++})$
J needs confirmation.

Mass $m = 9913.2 \pm 0.6$ MeV

$\chi_{b2}(1P)$ DECAY MODES	Fraction (Γ_i/Γ)	p (MeV/c)
$\gamma\Upsilon(1S)$	(22±4) %	443

$\Upsilon(2S)$

$I^G(J^{PC}) = 0^-(1^{--})$

Mass $m = 10.02330 \pm 0.00031$ GeV
Full width $\Gamma = 44 \pm 7$ keV
$\Gamma_{ee} = 0.52 \pm 0.03$ keV

$\Upsilon(2S)$ DECAY MODES	Fraction (Γ_i/Γ)	Confidence level	p (MeV/c)
$\Upsilon(1S)\pi^+\pi^-$	(18.5 ±0.8) %		475
$\Upsilon(1S)\pi^0\pi^0$	(8.8 ±1.1) %		480
$\tau^+\tau^-$	(1.7 ±1.6) %		4686
$\mu^+\mu^-$	(1.31±0.21) %		5011
e^+e^-	seen		5012
$\Upsilon(1S)\pi^0$	< 8 $\times10^{-3}$	90%	531
$\Upsilon(1S)\eta$	< 2 $\times10^{-3}$	90%	127
$J/\psi(1S)$ anything	< 6 $\times10^{-3}$	90%	4533
Radiative decays			
$\gamma\chi_{b1}(1P)$	(6.7 ±0.9) %		131
$\gamma\chi_{b2}(1P)$	(6.6 ±0.9) %		110
$\gamma\chi_{b0}(1P)$	(4.3 ±1.0) %		162
$\gamma f_J(1710)$	< 5.9 $\times10^{-4}$	90%	4866
$\gamma f_2'(1525)$	< 5.3 $\times10^{-4}$	90%	4896
$\gamma f_2(1270)$	< 2.41 $\times10^{-4}$	90%	4931

$\chi_{b0}(2P)$ [iii]

$I^G(J^{PC}) = 0^+(0^{++})$
J needs confirmation.

Mass $m = 10.2321 \pm 0.0006$ GeV

$\chi_{b0}(2P)$ DECAY MODES	Fraction (Γ_i/Γ)	p (MeV/c)
$\gamma\Upsilon(2S)$	(4.6±2.1) %	210
$\gamma\Upsilon(1S)$	(9 ±6) $\times10^{-3}$	746

$\chi_{b1}(2P)$ [iii]

$I^G(J^{PC}) = 0^+(1^{++})$
J needs confirmation.

Mass $m = 10.2552 \pm 0.0005$ GeV
$m_{\chi_{b1(2P)}} - m_{\chi_{b0(2P)}} = 23.5 \pm 1.0$ MeV

$\chi_{b1}(2P)$ DECAY MODES	Fraction (Γ_i/Γ)	Scale factor	p (MeV/c)
$\gamma\Upsilon(2S)$	(21 ±4) %	1.5	229
$\gamma\Upsilon(1S)$	(8.5±1.3) %	1.3	764

$\chi_{b2}(2P)$ [iii]

$I^G(J^{PC}) = 0^+(2^{++})$
J needs confirmation.

Mass $m = 10.2685 \pm 0.0004$ GeV
$m_{\chi_{b2(2P)}} - m_{\chi_{b1(2P)}} = 13.5 \pm 0.6$ MeV

$\chi_{b2}(2P)$ DECAY MODES	Fraction (Γ_i/Γ)	p (MeV/c)
$\gamma\Upsilon(2S)$	(16.2±2.4) %	242
$\gamma\Upsilon(1S)$	(7.1±1.0) %	776

Meson Summary Table

$\Upsilon(3S)$

$I^G(J^{PC}) = 0^-(1^{--})$

Mass $m = 10.3553 \pm 0.0005$ GeV
Full width $\Gamma = 26.3 \pm 3.5$ keV

$\Upsilon(3S)$ DECAY MODES	Fraction (Γ_i/Γ)	Scale factor	p (MeV/c)
$\Upsilon(2S)$ anything	(10.6 ±0.8) %		296
$\Upsilon(2S)\pi^+\pi^-$	(2.8 ±0.6) %	2.2	177
$\Upsilon(2S)\pi^0\pi^0$	(2.00±0.32) %		190
$\Upsilon(2S)\gamma\gamma$	(5.0 ±0.7) %		327
$\Upsilon(1S)\pi^+\pi^-$	(4.48±0.21) %		814
$\Upsilon(1S)\pi^0\pi^0$	(2.06±0.28) %		816
$\mu^+\mu^-$	(1.81±0.17) %		5177
e^+e^-	seen		5177
Radiative decays			
$\gamma\chi_{b2}(2P)$	(11.4 ±0.8) %	1.3	87
$\gamma\chi_{b1}(2P)$	(11.3 ±0.6) %		100
$\gamma\chi_{b0}(2P)$	(5.4 ±0.6) %	1.1	123

$\Upsilon(4S)$ or $\Upsilon(10580)$

$I^G(J^{PC}) = ?^?(1^{--})$

Mass $m = 10.5800 \pm 0.0035$ GeV
Full width $\Gamma = 21 \pm 4$ MeV (S = 2.3)
$\Gamma_{ee} = 0.248 \pm 0.031$ keV (S = 1.3)

$\Upsilon(4S)$ DECAY MODES	Fraction (Γ_i/Γ)	Confidence level	p (MeV/c)
$B\overline{B}$	dominant		–
e^+e^-	$(2.8\pm0.7)\times10^{-5}$		5290
$J/\psi(3097)$ anything	$(2.2\pm0.7)\times10^{-3}$		–
D^{*+} anything + c.c.	< 7.4 %	90%	5099
ϕ anything	$< 2.3 \times 10^{-3}$	90%	5240
$\Upsilon(1S)$ anything	$< 4 \times 10^{-3}$	90%	1053
non-$B\overline{B}$	< 4 %	95%	–

$\Upsilon(10860)$

$I^G(J^{PC}) = ?^?(1^{--})$

Mass $m = 10.865 \pm 0.008$ GeV (S = 1.1)
Full width $\Gamma = 110 \pm 13$ MeV
$\Gamma_{ee} = 0.31 \pm 0.07$ keV (S = 1.3)

$\Upsilon(10860)$ DECAY MODES	Fraction (Γ_i/Γ)	p (MeV/c)
e^+e^-	$(2.8\pm0.7)\times10^{-6}$	5432

$\Upsilon(11020)$

$I^G(J^{PC}) = ?^?(1^{--})$

Mass $m = 11.019 \pm 0.008$ GeV
Full width $\Gamma = 79 \pm 16$ MeV
$\Gamma_{ee} = 0.130 \pm 0.030$ keV

$\Upsilon(11020)$ DECAY MODES	Fraction (Γ_i/Γ)	p (MeV/c)
e^+e^-	$(1.6\pm0.5)\times10^{-6}$	5509

NOTES

In this Summary Table:

When a quantity has "(S = ...)" to its right, the error on the quantity has been enlarged by the "scale factor" S, defined as $S = \sqrt{\chi^2/(N-1)}$, where N is the number of measurements used in calculating the quantity. We do this when $S > 1$, which often indicates that the measurements are inconsistent. When $S > 1.25$, we also show in the Particle Listings an ideogram of the measurements. For more about S, see the Introduction.

A decay momentum p is given for each decay mode. For a 2-body decay, p is the momentum of each decay product in the rest frame of the decaying particle. For a 3-or-more-body decay, p is the largest momentum any of the products can have in this frame.

[a] See the "Note on $\pi^\pm \to \ell^\pm\nu\gamma$ and $K^\pm \to \ell^\pm\nu\gamma$ Form Factors" in the $\pi^\pm$ Particle Listings for definitions and details.

[b] Measurements of $\Gamma(e^+\nu_e)/\Gamma(\mu^+\nu_\mu)$ always include decays with γ's, and measurements of $\Gamma(e^+\nu_e\gamma)$ and $\Gamma(\mu^+\nu_\mu\gamma)$ never include low-energy γ's. Therefore, since no clean separation is possible, we consider the modes with γ's to be subreactions of the modes without them, and let $[\Gamma(e^+\nu_e) + \Gamma(\mu^+\nu_\mu)]/\Gamma_{\rm total} = 100\%$.

[c] See the $\pi^\pm$ Particle Listings for the energy limits used in this measurement; low-energy γ's are not included.

[d] Derived from an analysis of neutrino-oscillation experiments.

[e] Astrophysical and cosmological arguments give limits of order 10^{-13}; see the π^0 Particle Listings.

[f] See the "Note on the Decay Width $\Gamma(\eta \to \gamma\gamma)$" in our 1994 edition, Phys. Rev. **D50**, 1 August 1994, Part I, p. 1451.

[g] See the "Note on η Decay Parameters" in the η Particle Listings.

[h] C parity forbids this to occur as a single-photon process.

[i] See the "Note on scalar mesons" in the $f_0(1370)$ Particle Listings.

[j] See the "Note on $\rho(770)$" in the $\rho(770)$ Particle Listings.

[k] The e^+e^- branching fraction is from $e^+e^- \to \pi^+\pi^-$ experiments only. The $\omega\rho$ interference is then due to $\omega\rho$ mixing only, and is expected to be small. If $e\mu$ universality holds, $\Gamma(\rho^0 \to \mu^+\mu^-) = \Gamma(\rho^0 \to e^+e^-) \times 0.99785$.

[l] This is only an educated guess; the error given is larger than the error on the average of the published values. See the Particle Listings for details.

[m] See the "Note on $a_1(1260)$" in the $a_1(1260)$ Particle Listings.

[n] See the "Note on the $f_1(1420)$" in the $f_1(1420)$ Particle Listings.

[o] See also the $\omega(1600)$ Particle Listings.

[p] See the "Note on the $\eta(1440)$" in the $\eta(1440)$ Particle Listings.

[q] See the "Note on the $\rho(1450)$ and the $\rho(1700)$" in the $\rho(1700)$ Particle Listings.

[r] See the "Note on non-$q\overline{q}$ mesons" in the Particle Listings (see the index for the page number).

[s] See also the $\omega(1420)$ Particle Listings.

[t] See the "Note on $f_J(1710)$" in the $f_J(1710)$ Particle Listings.

[u] See the note in the $K^\pm$ Particle Listings.

[v] The definition of the slope parameter g of the $K \to 3\pi$ Dalitz plot is as follows (see also "Note on Dalitz Plot Parameters for $K \to 3\pi$ Decays" in the $K^\pm$ Particle Listings):

$$|M|^2 = 1 + g(s_3 - s_0)/m^2_{\pi^+} + \cdots .$$

[w] For more details and definitions of parameters see the Particle Listings.

[x] See the $K^\pm$ Particle Listings for the energy limits used in this measurement.

[y] Most of this radiative mode, the low-momentum γ part, is also included in the parent mode listed without γ's.

[z] Direct-emission branching fraction.

[aa] Structure-dependent part.

[bb] Derived from measured values of ϕ_{+-}, ϕ_{00}, $|\eta|$, $\tau_{K^0_S}$, and $|m_{K^0_L} - m_{K^0_S}|$, as described in the introduction to "Tests of Conservation Laws."

[cc] The *CP*-violation parameters are defined as follows (see also "Note on *CP* Violation in $K_S \to 3\pi$" and "Note on *CP* Violation in K_L^0 Decay" in the Particle Listings):

$$\eta_{+-} = |\eta_{+-}|e^{i\phi_{+-}} = \frac{A(K_L^0 \to \pi^+\pi^-)}{A(K_S^0 \to \pi^+\pi^-)} = \epsilon + \epsilon'$$

$$\eta_{00} = |\eta_{00}|e^{i\phi_{00}} = \frac{A(K_L^0 \to \pi^0\pi^0)}{A(K_S^0 \to \pi^0\pi^0)} = \epsilon - 2\epsilon'$$

$$\delta = \frac{\Gamma(K_L^0 \to \pi^-\ell^+\nu) - \Gamma(K_L^0 \to \pi^+\ell^-\nu)}{\Gamma(K_L^0 \to \pi^-\ell^+\nu) + \Gamma(K_L^0 \to \pi^+\ell^-\nu)},$$

$$\mathrm{Im}(\eta_{+-0})^2 = \frac{\Gamma(K_S^0 \to \pi^+\pi^-\pi^0)^{CP\ \mathrm{viol.}}}{\Gamma(K_L^0 \to \pi^+\pi^-\pi^0)},$$

$$\mathrm{Im}(\eta_{000})^2 = \frac{\Gamma(K_S^0 \to \pi^0\pi^0\pi^0)}{\Gamma(K_L^0 \to \pi^0\pi^0\pi^0)}.$$

where for the last two relations *CPT* is assumed valid, *i.e.*, $\mathrm{Re}(\eta_{+-0}) \simeq 0$ and $\mathrm{Re}(\eta_{000}) \simeq 0$.

[dd] See the K_S^0 Particle Listings for the energy limits used in this measurement.

[ee] Calculated from K_L^0 semileptonic rates and the K_S^0 lifetime assuming $\Delta S = \Delta Q$.

[ff] ϵ'/ϵ is derived from $|\eta_{00}/\eta_{+-}|$ measurements using theoretical input on phases.

[gg] The value is for the sum of the charge states of particle/antiparticle states indicated.

[hh] See the K_L^0 Particle Listings for the energy limits used in this measurement.

[ii] $m_{e^+e^-} > 470$ MeV.

[jj] Allowed by higher-order electroweak interactions.

[kk] Violates *CP* in leading order. Test of direct *CP* violation since the indirect *CP*-violating and *CP*-conserving contributions are expected to be suppressed.

[ll] See the "Note on $f_0(1370)$" in the $f_0(1370)$ Particle Listings and in the 1994 edition.

[mm] See the note in the $L(1770)$ Particle Listings in Reviews of Modern Physics **56** No. 2 Pt. II (1984), p. S200. See also the "Note on $K_2(1770)$ and the $K_2(1820)$" in the $K_2(1770)$ Particle Listings.

[nn] See the "Note on $K_2(1770)$ and the $K_2(1820)$" in the $K_2(1770)$ Particle Listings.

[oo] This is a weighted average of $D^\pm$ (44%) and D^0 (56%) branching fractions. See "D^+ and $D^0 \to$ (η anything) / (total D^+ and D^0)" under "D^+ Branching Ratios" in the Particle Listings.

[pp] This value averages the e^+ and μ^+ branching fractions, after making a small phase-space adjustment to the μ^+ fraction to be able to use it as an e^+ fraction; hence our ℓ^+ is really an e^+.

[qq] ℓ indicates e or μ mode, not sum over modes.

[rr] The branching fractions for this mode may differ from the sum of the submodes that contribute to it, due to interference effects. See the relevant papers in the Particle Listings.

[ss] The two experiments determining this ratio are in serious disagreement. See the Particle Listings.

[tt] This mode is not a useful test for a $\Delta C=1$ weak neutral current because both quarks must change flavor in this decay.

[uu] The D_1^0-D_2^0 limits are inferred from the D^0-$\overline{D}^0$ mixing ratio $\Gamma(K^+\pi^-$ or $K^+\pi^-\pi^+\pi^-$ via $\overline{D}^0)$ / $\Gamma(K^-\pi^+$ or $K^-\pi^+\pi^+\pi^-)$.

[vv] This value is calculated from the ratio $\Gamma(K^-\mu^+\nu_\mu)/\Gamma(\mu^+$ anything) in the D^0 Particle Listings.

[ww] The experiments on the division of this charge mode amongst its submodes disagree, and the submode branching fractions here add up to considerably more than the charged-mode fraction.

[xx] For now, we average together measurements of the $\phi e^+\nu_e$ and $\phi\mu^+\nu_\mu$ branching fractions. This is the *average*, not the *sum*.

[yy] This branching fraction is calculated from appropriate fractions of the next three branching fractions.

[zz] This value includes only K^+K^- decays of the $f_J(1710)$, because branching fractions of this resonance are not known.

[aaa] This mode is not a useful test for a $\Delta C=1$ weak neutral current because both quarks must change flavor in this decay.

[bbb] B^0 and B_s^0 contributions not separated. Limit is on weighted average of the two decay rates.

[ccc] These values are model dependent. See 'Note on Semileptonic Decays' in the B^+ Particle Listings.

[ddd] D^{**} stands for the sum of the $D(1\,^1P_1)$, $D(1\,^3P_0)$, $D(1\,^3P_1)$, $D(1\,^3P_2)$, $D(2\,^1S_0)$, and $D(2\,^1S_1)$ resonances.

[eee] Inclusive branching fractions have a multiplicity definition and can be greater than 100%.

[fff] D_J represents an unresolved mixture of pseudoscalar and tensor D^{**} (P-wave) states.

[ggg] Not a pure measurement. See note at head of B_s^0 Decay Modes.

[hhh] Includes $p\overline{p}\pi^+\pi^-\gamma$ and excludes $p\overline{p}\eta$, $p\overline{p}\omega$, $p\overline{p}\eta'$.

[iii] J^{PC} known by production in e^+e^- via single photon annihilation. I^G is not known; interpretation of this state as a single resonance is unclear because of the expectation of substantial threshold effects in this energy region.

[jjj] Spectroscopic labeling for these states is theoretical, pending experimental information.

Baryon Summary Table

N BARYONS ($S = 0$, $I = 1/2$)

p, $N^+ = uud$; n, $N^0 = udd$

p

$I(J^P) = \frac{1}{2}(\frac{1}{2}^+)$

Mass $m = 938.27231 \pm 0.00028$ MeV [a]
$= 1.007276470 \pm 0.000000012$ u
$|\frac{q_{\overline{p}}}{m_{\overline{p}}}|/(\frac{q_p}{m_p}) = 1.0000000015 \pm 0.0000000011$
$|q_p + q_{\overline{p}}|/e < 2 \times 10^{-5}$
$|q_p + q_e|/e < 1.0 \times 10^{-21}$ [b]
Magnetic moment $\mu = 2.79284739 \pm 0.00000006\ \mu_N$
Electric dipole moment $d = (-4 \pm 6) \times 10^{-23}$ ecm
Electric polarizability $\overline{\alpha} = (12.1 \pm 0.9) \times 10^{-4}$ fm^3
Magnetic polarizability $\overline{\beta} = (2.1 \pm 0.9) \times 10^{-4}$ fm^3
Mean life $\tau > 1.6 \times 10^{25}$ years (independent of mode)
$=> 10^{31} - 5 \times 10^{32}$ years [c] (mode dependent)

Below, for N decays, p and n distinguish proton and neutron partial lifetimes. See also the "Note on Nucleon Decay" in our 1994 edition (Phys. Rev. **D50**, 1673) for a short review.

The "partial mean life" limits tabulated here are the limits on τ/B_i, where τ is the total mean life and B_i is the branching fraction for the mode in question.

p DECAY MODES	Partial mean life (10^{30} years)	Confidence level	p (MeV/c)
Antilepton + meson			
$N \to e^+\pi$	> 130 (n), > 550 (p)	90%	459
$N \to \mu^+\pi$	> 100 (n), > 270 (p)	90%	453
$N \to \nu\pi$	> 100 (n), > 25 (p)	90%	459
$p \to e^+\eta$	> 140	90%	309
$p \to \mu^+\eta$	> 69	90%	296
$n \to \nu\eta$	> 54	90%	310
$N \to e^+\rho$	> 58 (n), > 75 (p)	90%	153
$N \to \mu^+\rho$	> 23 (n), > 110 (p)	90%	119
$N \to \nu\rho$	> 19 (n), > 27 (p)	90%	153
$p \to e^+\omega$	> 45	90%	142
$p \to \mu^+\omega$	> 57	90%	104
$n \to \nu\omega$	> 43	90%	144
$N \to e^+K$	> 1.3 (n), > 150 (p)	90%	337
$p \to e^+K^0_S$	> 76	90%	337
$p \to e^+K^0_L$	> 44	90%	337
$N \to \mu^+K$	> 1.1 (n), > 120 (p)	90%	326
$p \to \mu^+K^0_S$	> 64	90%	326
$p \to \mu^+K^0_L$	> 44	90%	326
$N \to \nu K$	> 86 (n), > 100 (p)	90%	339
$p \to e^+K^*(892)^0$	> 52	90%	45
$N \to \nu K^*(892)$	> 22 (n), > 20 (p)	90%	45
Antilepton + mesons			
$p \to e^+\pi^+\pi^-$	> 21	90%	448
$p \to e^+\pi^0\pi^0$	> 38	90%	449
$n \to e^+\pi^-\pi^0$	> 32	90%	449
$p \to \mu^+\pi^+\pi^-$	> 17	90%	425
$p \to \mu^+\pi^0\pi^0$	> 33	90%	427
$n \to \mu^+\pi^-\pi^0$	> 33	90%	427
$n \to e^+K^0\pi^-$	> 18	90%	319
Lepton + meson			
$n \to e^-\pi^+$	> 65	90%	459
$n \to \mu^-\pi^+$	> 49	90%	453
$n \to e^-\rho^+$	> 62	90%	154
$n \to \mu^-\rho^+$	> 7	90%	120
$n \to e^-K^+$	> 32	90%	340
$n \to \mu^-K^+$	> 57	90%	330
Lepton + mesons			
$p \to e^-\pi^+\pi^+$	> 30	90%	448
$n \to e^-\pi^+\pi^0$	> 29	90%	449
$p \to \mu^-\pi^+\pi^+$	> 17	90%	425
$n \to \mu^-\pi^+\pi^0$	> 34	90%	427
$p \to e^-\pi^+K^+$	> 20	90%	320
$p \to \mu^-\pi^+K^+$	> 5	90%	279
Antilepton + photon(s)			
$p \to e^+\gamma$	> 460	90%	469
$p \to \mu^+\gamma$	> 380	90%	463
$n \to \nu\gamma$	> 24	90%	470
$p \to e^+\gamma\gamma$	> 100	90%	469
Three leptons			
$p \to e^+e^+e^-$	> 510	90%	469
$p \to e^+\mu^+\mu^-$	> 81	90%	457
$p \to e^+\nu\nu$	> 11	90%	469
$n \to e^+e^-\nu$	> 74	90%	470
$n \to \mu^+e^-\nu$	> 47	90%	464
$n \to \mu^+\mu^-\nu$	> 42	90%	458
$p \to \mu^+e^+e^-$	> 91	90%	464
$p \to \mu^+\mu^+\mu^-$	> 190	90%	439
$p \to \mu^+\nu\nu$	> 21	90%	463
$p \to e^-\mu^+\mu^+$	> 6	90%	457
$n \to 3\nu$	> 0.0005	90%	470
Inclusive modes			
$N \to e^+$ anything	> 0.6 (n, p)	90%	–
$N \to \mu^+$ anything	> 12 (n, p)	90%	–
$N \to e^+\pi^0$ anything	> 0.6 (n, p)	90%	–
$\Delta B = 2$ dinucleon modes			
The following are lifetime limits per iron nucleus.			
$pp \to \pi^+\pi^+$	> 0.7	90%	–
$pn \to \pi^+\pi^0$	> 2	90%	–
$nn \to \pi^+\pi^-$	> 0.7	90%	–
$nn \to \pi^0\pi^0$	> 3.4	90%	–
$pp \to e^+e^+$	> 5.8	90%	–
$pp \to e^+\mu^+$	> 3.6	90%	–
$pp \to \mu^+\mu^+$	> 1.7	90%	–
$pn \to e^+\overline{\nu}$	> 2.8	90%	–
$pn \to \mu^+\overline{\nu}$	> 1.6	90%	–
$nn \to \nu_e\overline{\nu}_e$	> 0.000012	90%	–
$nn \to \nu_\mu\overline{\nu}_\mu$	> 0.000006	90%	–

$\overline{p}$ DECAY MODES

$\overline{p}$ DECAY MODES	Partial mean life (years)	Confidence level	p (MeV/c)
$\overline{p} \to e^-\gamma$	> 1848	95%	469
$\overline{p} \to e^-\pi^0$	> 554	95%	459
$\overline{p} \to e^-\eta$	> 171	95%	309
$\overline{p} \to e^-K^0_S$	> 29	95%	337
$\overline{p} \to e^-K^0_L$	> 9	95%	337

n

$I(J^P) = \frac{1}{2}(\frac{1}{2}^+)$

Mass $m = 939.56563 \pm 0.00028$ MeV [a]
$= 1.008664904 \pm 0.000000014$ u
$m_n - m_p = 1.293318 \pm 0.000009$ MeV
$= 0.001388434 \pm 0.000000009$ u
Mean life $\tau = 887.0 \pm 2.0$ s (S = 1.3)
$c\tau = 2.659 \times 10^8$ km
Magnetic moment $\mu = -1.9130428 \pm 0.0000005\ \mu_N$
Electric dipole moment $d < 1.1 \times 10^{-25}$ ecm, CL = 95%
Electric polarizability $\alpha = (0.98^{+0.19}_{-0.23}) \times 10^{-3}$ fm^3 (S = 1.1)
Charge $q = (-0.4 \pm 1.1) \times 10^{-21}\ e$
Mean $n\overline{n}$-oscillation time > 1.2×10^8 s, CL = 90% [d] (bound n)
> 0.86×10^8 s, CL = 90% (free n)

Decay parameters [e]

$pe^-\overline{\nu}_e$	$g_A/g_V = -1.2601 \pm 0.0025$ (S = 1.1)
"	$A = -0.1139 \pm 0.0011$ (S = 1.3)
"	$B = 0.990 \pm 0.008$
"	$a = -0.102 \pm 0.005$
"	$\phi_{AV} = (180.07 \pm 0.18)°$ [f]
"	$D = (-0.5 \pm 1.4) \times 10^{-3}$

n DECAY MODES	Fraction (Γ_i/Γ)	Confidence level	p (MeV/c)
$pe^-\overline{\nu}_e$	100 %		1.19
Charge conservation (Q) violating mode			
$p\nu_e\overline{\nu}_e$	$Q < 9 \times 10^{-24}$	90%	1.29

N(1440) P_{11}

$I(J^P) = \frac{1}{2}(\frac{1}{2}^+)$

Mass m = 1430 to 1470 (≈ 1440) MeV
Full width Γ = 250 to 450 (≈ 350) MeV
p_{beam} = 0.61 GeV/c $4\pi\lambda^2$ = 31.0 mb

N(1440) DECAY MODES	Fraction (Γ_i/Γ)	p (MeV/c)
$N\pi$	60–70 %	397
$N\pi\pi$	30–40 %	342
$\Delta\pi$	20–30 %	143
$N\rho$	<8 %	†
$N(\pi\pi)^{I=0}_{S\text{-wave}}$	5–10 %	–
$p\gamma$	0.035–0.048 %	414
$p\gamma$, helicity=1/2	0.035–0.048 %	414
$n\gamma$	0.009–0.032 %	413
$n\gamma$, helicity=1/2	0.009–0.032 %	413

N(1520) D_{13}

$I(J^P) = \frac{1}{2}(\frac{3}{2}^-)$

Mass m = 1515 to 1530 (≈ 1520) MeV
Full width Γ = 110 to 135 (≈ 120) MeV
p_{beam} = 0.74 GeV/c $4\pi\lambda^2$ = 23.5 mb

N(1520) DECAY MODES	Fraction (Γ_i/Γ)	p (MeV/c)
$N\pi$	50–60 %	456
$N\pi\pi$	40–50 %	410
$\Delta\pi$	15–25 %	228
$N\rho$	15–25 %	†
$N(\pi\pi)^{I=0}_{S\text{-wave}}$	<8 %	–
$p\gamma$	0.46–0.56 %	470
$p\gamma$, helicity=1/2	0.001–0.034 %	470
$p\gamma$, helicity=3/2	0.44–0.53 %	470
$n\gamma$	0.30–0.53 %	470
$n\gamma$, helicity=1/2	0.04–0.10 %	470
$n\gamma$, helicity=3/2	0.25–0.45 %	470

N(1535) S_{11}

$I(J^P) = \frac{1}{2}(\frac{1}{2}^-)$

Mass m = 1520 to 1555 (≈ 1535) MeV
Full width Γ = 100 to 250 (≈ 150) MeV
p_{beam} = 0.76 GeV/c $4\pi\lambda^2$ = 22.5 mb

N(1535) DECAY MODES	Fraction (Γ_i/Γ)	p (MeV/c)
$N\pi$	35–55 %	467
$N\eta$	30–55 %	182
$N\pi\pi$	1–10 %	422
$\Delta\pi$	<1 %	242
$N\rho$	<4 %	†
$N(\pi\pi)^{I=0}_{S\text{-wave}}$	<3 %	–
$N(1440)\pi$	<7 %	†
$p\gamma$	0.08–0.27 %	481
$p\gamma$, helicity=1/2	0.08–0.27 %	481
$n\gamma$	0.004–0.29 %	480
$n\gamma$, helicity=1/2	0.004–0.29 %	480

N(1650) S_{11}

$I(J^P) = \frac{1}{2}(\frac{1}{2}^-)$

Mass m = 1640 to 1680 (≈ 1650) MeV
Full width Γ = 145 to 190 (≈ 150) MeV
p_{beam} = 0.96 GeV/c $4\pi\lambda^2$ = 16.4 mb

N(1650) DECAY MODES	Fraction (Γ_i/Γ)	p (MeV/c)
$N\pi$	55–90 %	547
$N\eta$	3–10 %	346
ΛK	3–11 %	161
$N\pi\pi$	10–20 %	511
$\Delta\pi$	1–7 %	344
$N\rho$	4–12 %	†
$N(\pi\pi)^{I=0}_{S\text{-wave}}$	<4 %	–
$N(1440)\pi$	<5 %	147
$p\gamma$	0.04–0.18 %	558
$p\gamma$, helicity=1/2	0.04–0.18 %	558
$n\gamma$	0.003–0.17 %	557
$n\gamma$, helicity=1/2	0.003–0.17 %	557

N(1675) D_{15}

$I(J^P) = \frac{1}{2}(\frac{5}{2}^-)$

Mass m = 1670 to 1685 (≈ 1675) MeV
Full width Γ = 140 to 180 (≈ 150) MeV
p_{beam} = 1.01 GeV/c $4\pi\lambda^2$ = 15.4 mb

N(1675) DECAY MODES	Fraction (Γ_i/Γ)	p (MeV/c)
$N\pi$	40–50 %	563
ΛK	<1 %	209
$N\pi\pi$	50–60 %	529
$\Delta\pi$	50–60 %	364
$N\rho$	< 1–3 %	†
$p\gamma$	0.004–0.023 %	575
$p\gamma$, helicity=1/2	0.0–0.015 %	575
$p\gamma$, helicity=3/2	0.0–0.011 %	575
$n\gamma$	0.02–0.12 %	574
$n\gamma$, helicity=1/2	0.006–0.046 %	574
$n\gamma$, helicity=3/2	0.01–0.08 %	574

N(1680) F_{15}

$I(J^P) = \frac{1}{2}(\frac{5}{2}^+)$

Mass m = 1675 to 1690 (≈ 1680) MeV
Full width Γ = 120 to 140 (≈ 130) MeV
p_{beam} = 1.01 GeV/c $4\pi\lambda^2$ = 15.2 mb

N(1680) DECAY MODES	Fraction (Γ_i/Γ)	p (MeV/c)
$N\pi$	60–70 %	567
$N\pi\pi$	30–40 %	532
$\Delta\pi$	5–15 %	369
$N\rho$	3–15 %	†
$N(\pi\pi)^{I=0}_{S\text{-wave}}$	5–20 %	–
$p\gamma$	0.21–0.32 %	578
$p\gamma$, helicity=1/2	0.001–0.011 %	578
$p\gamma$, helicity=3/2	0.20–0.32 %	578
$n\gamma$	0.021–0.046 %	577
$n\gamma$, helicity=1/2	0.004–0.029 %	577
$n\gamma$, helicity=3/2	0.01–0.024 %	577

N(1700) D_{13}

$I(J^P) = \frac{1}{2}(\frac{3}{2}^-)$

Mass m = 1650 to 1750 (≈ 1700) MeV
Full width Γ = 50 to 150 (≈ 100) MeV
p_{beam} = 1.05 GeV/c $4\pi\lambda^2$ = 14.5 mb

N(1700) DECAY MODES	Fraction (Γ_i/Γ)	p (MeV/c)
$N\pi$	5–15 %	580
ΛK	<3 %	250
$N\pi\pi$	85–95 %	547
$N\rho$	<35 %	†
$p\gamma$	0.01–0.05 %	591
$p\gamma$, helicity=1/2	0.0–0.024 %	591
$p\gamma$, helicity=3/2	0.002–0.026 %	591
$n\gamma$	0.01–0.13 %	590
$n\gamma$, helicity=1/2	0.0–0.09 %	590
$n\gamma$, helicity=3/2	0.01–0.05 %	590

Baryon Summary Table

$N(1710)\ P_{11}$ $I(J^P) = \frac{1}{2}(\frac{1}{2}^+)$

Mass m = 1680 to 1740 (≈ 1710) MeV
Full width Γ = 50 to 250 (≈ 100) MeV
p_{beam} = 1.07 GeV/c $4\pi\lambda^2$ = 14.2 mb

N(1710) DECAY MODES	Fraction (Γ_i/Γ)	p (MeV/c)
$N\pi$	10–20 %	587
ΛK	5–25 %	264
$N\pi\pi$	40–90 %	554
$\Delta\pi$	15–40 %	393
$N\rho$	5–25 %	48
$N(\pi\pi)^{I=0}_{S\text{-wave}}$	10–40 %	–
$p\gamma$	0.002–0.05%	598
$p\gamma$, helicity=1/2	0.002–0.05%	598
$n\gamma$	0.0–0.02%	597
$n\gamma$, helicity=1/2	0.0–0.02%	597

$N(1720)\ P_{13}$ $I(J^P) = \frac{1}{2}(\frac{3}{2}^+)$

Mass m = 1650 to 1750 (≈ 1720) MeV
Full width Γ = 100 to 200 (≈ 150) MeV
p_{beam} = 1.09 GeV/c $4\pi\lambda^2$ = 13.9 mb

N(1720) DECAY MODES	Fraction (Γ_i/Γ)	p (MeV/c)
$N\pi$	10–20 %	594
ΛK	1–15 %	278
$N\pi\pi$	>70 %	561
$N\rho$	70–85 %	104
$p\gamma$	0.003–0.10 %	604
$p\gamma$, helicity=1/2	0.003–0.08 %	604
$p\gamma$, helicity=3/2	0.001–0.03 %	604
$n\gamma$	0.002–0.39 %	603
$n\gamma$, helicity=1/2	0.0–0.002 %	603
$n\gamma$, helicity=3/2	0.001–0.39 %	603

$N(2190)\ G_{17}$ $I(J^P) = \frac{1}{2}(\frac{7}{2}^-)$

Mass m = 2100 to 2200 (≈ 2190) MeV
Full width Γ = 350 to 550 (≈ 450) MeV
p_{beam} = 2.07 GeV/c $4\pi\lambda^2$ = 6.21 mb

N(2190) DECAY MODES	Fraction (Γ_i/Γ)	p (MeV/c)
$N\pi$	10–20 %	888

$N(2220)\ H_{19}$ $I(J^P) = \frac{1}{2}(\frac{9}{2}^+)$

Mass m = 2180 to 2310 (≈ 2220) MeV
Full width Γ = 320 to 550 (≈ 400) MeV
p_{beam} = 2.14 GeV/c $4\pi\lambda^2$ = 5.97 mb

N(2220) DECAY MODES	Fraction (Γ_i/Γ)	p (MeV/c)
$N\pi$	10–20 %	905

$N(2250)\ G_{19}$ $I(J^P) = \frac{1}{2}(\frac{9}{2}^-)$

Mass m = 2170 to 2310 (≈ 2250) MeV
Full width Γ = 290 to 470 (≈ 400) MeV
p_{beam} = 2.21 GeV/c $4\pi\lambda^2$ = 5.74 mb

N(2250) DECAY MODES	Fraction (Γ_i/Γ)	p (MeV/c)
$N\pi$	5–15 %	923

$N(2600)\ I_{1,11}$ $I(J^P) = \frac{1}{2}(\frac{11}{2}^-)$

Mass m = 2550 to 2750 (≈ 2600) MeV
Full width Γ = 500 to 800 (≈ 650) MeV
p_{beam} = 3.12 GeV/c $4\pi\lambda^2$ = 3.86 mb

N(2600) DECAY MODES	Fraction (Γ_i/Γ)	p (MeV/c)
$N\pi$	5–10 %	1126

Δ BARYONS ($S = 0$, $I = 3/2$)

$\Delta^{++} = uuu$, $\Delta^+ = uud$, $\Delta^0 = udd$, $\Delta^- = ddd$

$\Delta(1232)\ P_{33}$ $I(J^P) = \frac{3}{2}(\frac{3}{2}^+)$

Mass m = 1230 to 1234 (≈ 1232) MeV
Full width Γ = 115 to 125 (≈ 120) MeV
p_{beam} = 0.30 GeV/c $4\pi\lambda^2$ = 94.8 mb

Δ(1232) DECAY MODES	Fraction (Γ_i/Γ)	p (MeV/c)
$N\pi$	>99 %	227
$N\gamma$	0.54–0.61 %	259
$N\gamma$, helicity=1/2	0.12–0.14 %	259
$N\gamma$, helicity=3/2	0.41–0.47 %	259

$\Delta(1600)\ P_{33}$ $I(J^P) = \frac{3}{2}(\frac{3}{2}^+)$

Mass m = 1550 to 1700 (≈ 1600) MeV
Full width Γ = 250 to 450 (≈ 350) MeV
p_{beam} = 0.87 GeV/c $4\pi\lambda^2$ = 18.6 mb

Δ(1600) DECAY MODES	Fraction (Γ_i/Γ)	p (MeV/c)
$N\pi$	10–25 %	512
$N\pi\pi$	75–90 %	473
$\Delta\pi$	40–70 %	301
$N\rho$	<25 %	†
$N(1440)\pi$	10–35 %	74
$N\gamma$	0.001–0.02 %	525
$N\gamma$, helicity=1/2	0.0–0.02 %	525
$N\gamma$, helicity=3/2	0.001–0.005 %	525

$\Delta(1620)\ S_{31}$ $I(J^P) = \frac{3}{2}(\frac{1}{2}^-)$

Mass m = 1615 to 1675 (≈ 1620) MeV
Full width Γ = 120 to 180 (≈ 150) MeV
p_{beam} = 0.91 GeV/c $4\pi\lambda^2$ = 17.7 mb

Δ(1620) DECAY MODES	Fraction (Γ_i/Γ)	p (MeV/c)
$N\pi$	20–30 %	526
$N\pi\pi$	70–80 %	488
$\Delta\pi$	30–60 %	318
$N\rho$	7–25 %	†
$N\gamma$	0.004–0.044 %	538
$N\gamma$, helicity=1/2	0.004–0.044 %	538

$\Delta(1700)\ D_{33}$ $I(J^P) = \frac{3}{2}(\frac{3}{2}^-)$

Mass m = 1670 to 1770 (≈ 1700) MeV
Full width Γ = 200 to 400 (≈ 300) MeV
p_{beam} = 1.05 GeV/c $4\pi\lambda^2$ = 14.5 mb

Δ(1700) DECAY MODES	Fraction (Γ_i/Γ)	p (MeV/c)
$N\pi$	10–20 %	580
$N\pi\pi$	80–90 %	547
$\Delta\pi$	30–60 %	385
$N\rho$	30–55 %	†
$N\gamma$	0.12–0.26 %	591
$N\gamma$, helicity=1/2	0.08–0.16 %	591
$N\gamma$, helicity=3/2	0.025–0.12 %	591

$\Delta(1900)\ S_{31}$ $I(J^P) = \frac{3}{2}(\frac{1}{2}^-)$

Mass m = 1850 to 1950 (≈ 1900) MeV
Full width Γ = 140 to 240 (≈ 200) MeV
p_{beam} = 1.44 GeV/c $4\pi\lambda^2$ = 9.71 mb

Δ(1900) DECAY MODES	Fraction (Γ_i/Γ)	p (MeV/c)
$N\pi$	10–30 %	710

Δ(1905) F_{35}

$I(J^P) = \frac{3}{2}(\frac{5}{2}^+)$

Mass m = 1870 to 1920 (≈ 1905) MeV
Full width Γ = 280 to 440 (≈ 350) MeV
p_{beam} = 1.45 GeV/c $4\pi\lambda^2$ = 9.62 mb

Δ(1905) DECAY MODES	Fraction (Γ_i/Γ)	p (MeV/c)
$N\pi$	5–15 %	713
$N\pi\pi$	85–95 %	687
$\Delta\pi$	<25 %	542
$N\rho$	>60 %	421
$N\gamma$	0.01–0.03 %	721
$N\gamma$, helicity=1/2	0.0–0.1 %	721
$N\gamma$, helicity=3/2	0.004–0.03 %	721

Δ(1910) P_{31}

$I(J^P) = \frac{3}{2}(\frac{1}{2}^+)$

Mass m = 1870 to 1920 (≈ 1910) MeV
Full width Γ = 190 to 270 (≈ 250) MeV
p_{beam} = 1.46 GeV/c $4\pi\lambda^2$ = 9.54 mb

Δ(1910) DECAY MODES	Fraction (Γ_i/Γ)	p (MeV/c)
$N\pi$	15–30 %	716
$N\gamma$	0.0–0.2 %	725
$N\gamma$, helicity=1/2	0.0–0.2 %	725

Δ(1920) P_{33}

$I(J^P) = \frac{3}{2}(\frac{3}{2}^+)$

Mass m = 1900 to 1970 (≈ 1920) MeV
Full width Γ = 150 to 300 (≈ 200) MeV
p_{beam} = 1.48 GeV/c $4\pi\lambda^2$ = 9.37 mb

Δ(1920) DECAY MODES	Fraction (Γ_i/Γ)	p (MeV/c)
$N\pi$	5–20 %	722

Δ(1930) D_{35}

$I(J^P) = \frac{3}{2}(\frac{5}{2}^-)$

Mass m = 1920 to 1970 (≈ 1930) MeV
Full width Γ = 250 to 450 (≈ 350) MeV
p_{beam} = 1.50 GeV/c $4\pi\lambda^2$ = 9.21 mb

Δ(1930) DECAY MODES	Fraction (Γ_i/Γ)	p (MeV/c)
$N\pi$	10–20 %	729
$N\gamma$	0.0–0.02 %	737
$N\gamma$, helicity=1/2	0.0–0.01 %	737
$N\gamma$, helicity=3/2	0.0–0.01 %	737

Δ(1950) F_{37}

$I(J^P) = \frac{3}{2}(\frac{7}{2}^+)$

Mass m = 1940 to 1960 (≈ 1950) MeV
Full width Γ = 290 to 350 (≈ 300) MeV
p_{beam} = 1.54 GeV/c $4\pi\lambda^2$ = 8.91 mb

Δ(1950) DECAY MODES	Fraction (Γ_i/Γ)	p (MeV/c)
$N\pi$	35–40 %	741
$N\pi\pi$		716
$\Delta\pi$	20–30 %	574
$N\rho$	<10 %	469
$N\gamma$	0.08–0.13 %	749
$N\gamma$, helicity=1/2	0.03–0.055 %	749
$N\gamma$, helicity=3/2	0.05–0.075 %	749

Δ(2420) $H_{3,11}$

$I(J^P) = \frac{3}{2}(\frac{11}{2}^+)$

Mass m = 2300 to 2500 (≈ 2420) MeV
Full width Γ = 300 to 500 (≈ 400) MeV
p_{beam} = 2.64 GeV/c $4\pi\lambda^2$ = 4.68 mb

Δ(2420) DECAY MODES	Fraction (Γ_i/Γ)	p (MeV/c)
$N\pi$	5–15 %	1023

Λ BARYONS ($S = -1$, $I = 0$)

$\Lambda^0 = uds$

Λ

$I(J^P) = 0(\frac{1}{2}^+)$

Mass m = 1115.684 ± 0.006 MeV
Mean life $\tau = (2.632 \pm 0.020) \times 10^{-10}$ s (S = 1.6)
$c\tau$ = 7.89 cm
Magnetic moment $\mu = -0.613 \pm 0.004\ \mu_N$
Electric dipole moment $d < 1.5 \times 10^{-16}$ $e$cm, CL = 95%

Decay parameters

$p\pi^-$	$\alpha_- = 0.642 \pm 0.013$
"	$\phi_- = (-6.5 \pm 3.5)^\circ$
"	$\gamma_- = 0.76$ [g]
"	$\Delta_- = (8 \pm 4)^\circ$ [g]
$n\pi^0$	$\alpha_0 = +0.65 \pm 0.05$
$pe^-\overline{\nu}_e$	$g_A/g_V = -0.718 \pm 0.015$ [e]

Λ DECAY MODES	Fraction (Γ_i/Γ)	p (MeV/c)
$p\pi^-$	(63.9 ±0.5) %	101
$n\pi^0$	(35.8 ±0.5) %	104
$n\gamma$	(1.75±0.15) × 10^{-3}	162
$p\pi^-\gamma$	[h] (8.4 ±1.4) × 10^{-4}	101
$pe^-\overline{\nu}_e$	(8.32±0.14) × 10^{-4}	163
$p\mu^-\overline{\nu}_\mu$	(1.57±0.35) × 10^{-4}	131

Λ(1405) S_{01}

$I(J^P) = 0(\frac{1}{2}^-)$

Mass m = 1407 ± 4 MeV
Full width Γ = 50.0 ± 2.0 MeV
Below $\overline{K}N$ threshold

Λ(1405) DECAY MODES	Fraction (Γ_i/Γ)	p (MeV/c)
$\Sigma\pi$	100 %	152

Λ(1520) D_{03}

$I(J^P) = 0(\frac{3}{2}^-)$

Mass m = 1519.5 ± 1.0 MeV [i]
Full width Γ = 15.6 ± 1.0 MeV [i]
p_{beam} = 0.39 GeV/c $4\pi\lambda^2$ = 82.8 mb

Λ(1520) DECAY MODES	Fraction (Γ_i/Γ)	p (MeV/c)
$N\overline{K}$	45 ± 1%	244
$\Sigma\pi$	42 ± 1%	267
$\Lambda\pi\pi$	10 ± 1%	252
$\Sigma\pi\pi$	0.9 ± 0.1%	152
$\Lambda\gamma$	0.8 ± 0.2%	351

Λ(1600) P_{01}

$I(J^P) = 0(\frac{1}{2}^+)$

Mass m = 1560 to 1700 (≈ 1600) MeV
Full width Γ = 50 to 250 (≈ 150) MeV
p_{beam} = 0.58 GeV/c $4\pi\lambda^2$ = 41.6 mb

Λ(1600) DECAY MODES	Fraction (Γ_i/Γ)	p (MeV/c)
$N\overline{K}$	15–30 %	343
$\Sigma\pi$	10–60 %	336

Baryon Summary Table

$\Lambda(1670)\ S_{01}$ $I(J^P) = 0(\frac{1}{2}^-)$

Mass m = 1660 to 1680 ($\approx$ 1670) MeV
Full width Γ = 25 to 50 ($\approx$ 35) MeV
p_{beam} = 0.74 GeV/c $4\pi\lambda^2$ = 28.5 mb

$\Lambda(1670)$ DECAY MODES	Fraction (Γ_i/Γ)	p (MeV/c)
$N\overline{K}$	15–25 %	414
$\Sigma\pi$	20–60 %	393
$\Lambda\eta$	15–35 %	64

$\Lambda(1690)\ D_{03}$ $I(J^P) = 0(\frac{3}{2}^-)$

Mass m = 1685 to 1695 ($\approx$ 1690) MeV
Full width Γ = 50 to 70 ($\approx$ 60) MeV
p_{beam} = 0.78 GeV/c $4\pi\lambda^2$ = 26.1 mb

$\Lambda(1690)$ DECAY MODES	Fraction (Γ_i/Γ)	p (MeV/c)
$N\overline{K}$	20–30 %	433
$\Sigma\pi$	20–40 %	409
$\Lambda\pi\pi$	$\sim$ 25 %	415
$\Sigma\pi\pi$	$\sim$ 20 %	350

$\Lambda(1800)\ S_{01}$ $I(J^P) = 0(\frac{1}{2}^-)$

Mass m = 1720 to 1850 ($\approx$ 1800) MeV
Full width Γ = 200 to 400 ($\approx$ 300) MeV
p_{beam} = 1.01 GeV/c $4\pi\lambda^2$ = 17.5 mb

$\Lambda(1800)$ DECAY MODES	Fraction (Γ_i/Γ)	p (MeV/c)
$N\overline{K}$	25–40 %	528
$\Sigma\pi$	seen	493
$\Sigma(1385)\pi$	seen	345
$N\overline{K}^*(892)$	seen	†

$\Lambda(1810)\ P_{01}$ $I(J^P) = 0(\frac{1}{2}^+)$

Mass m = 1750 to 1850 ($\approx$ 1810) MeV
Full width Γ = 50 to 250 ($\approx$ 150) MeV
p_{beam} = 1.04 GeV/c $4\pi\lambda^2$ = 17.0 mb

$\Lambda(1810)$ DECAY MODES	Fraction (Γ_i/Γ)	p (MeV/c)
$N\overline{K}$	20–50 %	537
$\Sigma\pi$	10–40 %	501
$\Sigma(1385)\pi$	seen	356
$N\overline{K}^*(892)$	30–60 %	†

$\Lambda(1820)\ F_{05}$ $I(J^P) = 0(\frac{5}{2}^+)$

Mass m = 1815 to 1825 ($\approx$ 1820) MeV
Full width Γ = 70 to 90 ($\approx$ 80) MeV
p_{beam} = 1.06 GeV/c $4\pi\lambda^2$ = 16.5 mb

$\Lambda(1820)$ DECAY MODES	Fraction (Γ_i/Γ)	p (MeV/c)
$N\overline{K}$	55–65 %	545
$\Sigma\pi$	8–14 %	508
$\Sigma(1385)\pi$	5–10 %	362

$\Lambda(1830)\ D_{05}$ $I(J^P) = 0(\frac{5}{2}^-)$

Mass m = 1810 to 1830 ($\approx$ 1830) MeV
Full width Γ = 60 to 110 ($\approx$ 95) MeV
p_{beam} = 1.08 GeV/c $4\pi\lambda^2$ = 16.0 mb

$\Lambda(1830)$ DECAY MODES	Fraction (Γ_i/Γ)	p (MeV/c)
$N\overline{K}$	3–10 %	553
$\Sigma\pi$	35–75 %	515
$\Sigma(1385)\pi$	>15 %	371

$\Lambda(1890)\ P_{03}$ $I(J^P) = 0(\frac{3}{2}^+)$

Mass m = 1850 to 1910 ($\approx$ 1890) MeV
Full width Γ = 60 to 200 ($\approx$ 100) MeV
p_{beam} = 1.21 GeV/c $4\pi\lambda^2$ = 13.6 mb

$\Lambda(1890)$ DECAY MODES	Fraction (Γ_i/Γ)	p (MeV/c)
$N\overline{K}$	20–35 %	599
$\Sigma\pi$	3–10 %	559
$\Sigma(1385)\pi$	seen	420
$N\overline{K}^*(892)$	seen	233

$\Lambda(2100)\ G_{07}$ $I(J^P) = 0(\frac{7}{2}^-)$

Mass m = 2090 to 2110 ($\approx$ 2100) MeV
Full width Γ = 100 to 250 ($\approx$ 200) MeV
p_{beam} = 1.68 GeV/c $4\pi\lambda^2$ = 8.68 mb

$\Lambda(2100)$ DECAY MODES	Fraction (Γ_i/Γ)	p (MeV/c)
$N\overline{K}$	25–35 %	751
$\Sigma\pi$	$\sim$ 5 %	704
$\Lambda\eta$	<3 %	617
ΞK	<3 %	483
$\Lambda\omega$	<8 %	443
$N\overline{K}^*(892)$	10–20 %	514

$\Lambda(2110)\ F_{05}$ $I(J^P) = 0(\frac{5}{2}^+)$

Mass m = 2090 to 2140 ($\approx$ 2110) MeV
Full width Γ = 150 to 250 ($\approx$ 200) MeV
p_{beam} = 1.70 GeV/c $4\pi\lambda^2$ = 8.53 mb

$\Lambda(2110)$ DECAY MODES	Fraction (Γ_i/Γ)	p (MeV/c)
$N\overline{K}$	5–25 %	757
$\Sigma\pi$	10–40 %	711
$\Lambda\omega$	seen	455
$\Sigma(1385)\pi$	seen	589
$N\overline{K}^*(892)$	10–60 %	524

$\Lambda(2350)\ H_{09}$ $I(J^P) = 0(\frac{9}{2}^+)$

Mass m = 2340 to 2370 ($\approx$ 2350) MeV
Full width Γ = 100 to 250 ($\approx$ 150) MeV
p_{beam} = 2.29 GeV/c $4\pi\lambda^2$ = 5.85 mb

$\Lambda(2350)$ DECAY MODES	Fraction (Γ_i/Γ)	p (MeV/c)
$N\overline{K}$	$\sim$ 12 %	915
$\Sigma\pi$	$\sim$ 10 %	867

Σ BARYONS
($S = -1$, $I = 1$)

$\Sigma^+ = uus$, $\Sigma^0 = uds$, $\Sigma^- = dds$

Σ^+

$I(J^P) = 1(\frac{1}{2}^+)$

Mass $m = 1189.37 \pm 0.07$ MeV (S = 2.2)
Mean life $\tau = (0.799 \pm 0.004) \times 10^{-10}$ s
$c\tau = 2.396$ cm
Magnetic moment $\mu = 2.458 \pm 0.010\ \mu_N$ (S = 2.1)
$\Gamma(\Sigma^+ \to n\ell^+\nu)/\Gamma(\Sigma^- \to n\ell^-\overline{\nu}) < 0.043$

Decay parameters

$p\pi^0$	$\alpha_0 = -0.980^{+0.017}_{-0.015}$
"	$\phi_0 = (36 \pm 34)^\circ$
"	$\gamma_0 = 0.16$ [g]
"	$\Delta_0 = (187 \pm 6)^\circ$ [g]
$n\pi^+$	$\alpha_+ = 0.068 \pm 0.013$
"	$\phi_+ = (167 \pm 20)^\circ$ (S = 1.1)
"	$\gamma_+ = -0.97$ [g]
"	$\Delta_+ = (-73^{+133}_{-10})^\circ$ [g]
$p\gamma$	$\alpha_\gamma = -0.76 \pm 0.08$

Σ^+ DECAY MODES		Fraction (Γ_i/Γ)	Confidence level	p (MeV/c)
$p\pi^0$		(51.57±0.30) %		189
$n\pi^+$		(48.31±0.30) %		185
$p\gamma$		(1.23±0.05) × 10^{-3}		225
$n\pi^+\gamma$	[h]	(4.5 ±0.5) × 10^{-4}		185
$\Lambda e^+\nu_e$		(2.0 ±0.5) × 10^{-5}		71
$\Delta S = \Delta Q$ (SQ) violating modes or $\Delta S = 1$ weak neutral current ($S1$) modes				
$ne^+\nu_e$	SQ	< 5 × 10^{-6}	90%	224
$n\mu^+\nu_\mu$	SQ	< 3.0 × 10^{-5}	90%	202
pe^+e^-	$S1$	< 7 × 10^{-6}		225

Σ^0

$I(J^P) = 1(\frac{1}{2}^+)$

J^P not measured; assumed to be the same as for the Σ^+ and Σ^-.
Mass $m = 1192.55 \pm 0.08$ MeV (S = 1.2)
$m_{\Sigma^-} - m_{\Sigma^0} = 4.88 \pm 0.08$ MeV (S = 1.2)
$m_{\Sigma^0} - m_\Lambda = 76.87 \pm 0.08$ MeV (S = 1.2)
Mean life $\tau = (7.4 \pm 0.7) \times 10^{-20}$ s
$c\tau = 2.22 \times 10^{-11}$ m
Transition magnetic moment $|\mu_{\Sigma\Lambda}| = 1.61 \pm 0.08\ \mu_N$

Σ^0 DECAY MODES		Fraction (Γ_i/Γ)	Confidence level	p (MeV/c)
$\Lambda\gamma$		100 %		74
$\Lambda\gamma\gamma$		< 3 %	90%	74
Λe^+e^-	[j]	5×10^{-3}		74

Σ^-

$I(J^P) = 1(\frac{1}{2}^+)$

Mass $m = 1197.436 \pm 0.033$ MeV (S = 1.2)
$m_{\Sigma^-} - m_{\Sigma^+} = 8.07 \pm 0.08$ MeV (S = 1.9)
$m_{\Sigma^-} - m_\Lambda = 81.752 \pm 0.034$ MeV (S = 1.2)
Mean life $\tau = (1.479 \pm 0.011) \times 10^{-10}$ s (S = 1.3)
$c\tau = 4.434$ cm
Magnetic moment $\mu = -1.160 \pm 0.025\ \mu_N$ (S = 1.7)

Decay parameters

$n\pi^-$	$\alpha_- = -0.068 \pm 0.008$
"	$\phi_- = (10 \pm 15)^\circ$
"	$\gamma_- = 0.98$ [g]
"	$\Delta_- = (249^{+12}_{-120})^\circ$ [g]
$ne^-\overline{\nu}_e$	$g_A/g_V = 0.340 \pm 0.017$ [e]
"	$f_2(0)/f_1(0) = 0.97 \pm 0.14$
"	$D = 0.11 \pm 0.10$
$\Lambda e^-\overline{\nu}_e$	$g_V/g_A = 0.01 \pm 0.10$ [e] (S = 1.5)
"	$g_{WM}/g_A = 2.4 \pm 1.7$ [e]

Σ^- DECAY MODES	Fraction (Γ_i/Γ)	p (MeV/c)
$n\pi^-$	(99.848±0.005) %	193
$n\pi^-\gamma$	[h] (4.6 ±0.6) × 10^{-4}	193
$ne^-\overline{\nu}_e$	(1.017±0.034) × 10^{-3}	230
$n\mu^-\overline{\nu}_\mu$	(4.5 ±0.4) × 10^{-4}	210
$\Lambda e^-\overline{\nu}_e$	(5.73 ±0.27) × 10^{-5}	79

$\Sigma(1385)\ P_{13}$

$I(J^P) = 1(\frac{3}{2}^+)$

$\Sigma(1385)^+$ mass $m = 1382.8 \pm 0.4$ MeV (S = 2.0)
$\Sigma(1385)^0$ mass $m = 1383.7 \pm 1.0$ MeV (S = 1.4)
$\Sigma(1385)^-$ mass $m = 1387.2 \pm 0.5$ MeV (S = 2.2)
$\Sigma(1385)^+$ full width $\Gamma = 35.8 \pm 0.8$ MeV
$\Sigma(1385)^0$ full width $\Gamma = 36 \pm 5$ MeV
$\Sigma(1385)^-$ full width $\Gamma = 39.4 \pm 2.1$ MeV (S = 1.7)
Below $\overline{K}N$ threshold

$\Sigma(1385)$ DECAY MODES	Fraction (Γ_i/Γ)	p (MeV/c)
$\Lambda\pi$	88±2 %	208
$\Sigma\pi$	12±2 %	127

$\Sigma(1660)\ P_{11}$

$I(J^P) = 1(\frac{1}{2}^+)$

Mass $m = 1630$ to 1690 (≈ 1660) MeV
Full width $\Gamma = 40$ to 200 (≈ 100) MeV
$p_{\text{beam}} = 0.72$ GeV/c $4\pi\lambda^2 = 29.9$ mb

$\Sigma(1660)$ DECAY MODES	Fraction (Γ_i/Γ)	p (MeV/c)
$N\overline{K}$	10–30 %	405
$\Lambda\pi$	seen	439
$\Sigma\pi$	seen	385

$\Sigma(1670)\ D_{13}$

$I(J^P) = 1(\frac{3}{2}^-)$

Mass $m = 1665$ to 1685 (≈ 1670) MeV
Full width $\Gamma = 40$ to 80 (≈ 60) MeV
$p_{\text{beam}} = 0.74$ GeV/c $4\pi\lambda^2 = 28.5$ mb

$\Sigma(1670)$ DECAY MODES	Fraction (Γ_i/Γ)	p (MeV/c)
$N\overline{K}$	7–13 %	414
$\Lambda\pi$	5–15 %	447
$\Sigma\pi$	30–60 %	393

$\Sigma(1750)\ S_{11}$

$I(J^P) = 1(\frac{1}{2}^-)$

Mass $m = 1730$ to 1800 (≈ 1750) MeV
Full width $\Gamma = 60$ to 160 (≈ 90) MeV
$p_{\text{beam}} = 0.91$ GeV/c $4\pi\lambda^2 = 20.7$ mb

$\Sigma(1750)$ DECAY MODES	Fraction (Γ_i/Γ)	p (MeV/c)
$N\overline{K}$	10–40 %	486
$\Lambda\pi$	seen	507
$\Sigma\pi$	<8 %	455
$\Sigma\eta$	15–55 %	81

Baryon Summary Table

$\Sigma(1775)\ D_{15}$ $I(J^P) = 1(\frac{5}{2}^-)$

Mass $m = 1770$ to 1780 (≈ 1775) MeV
Full width $\Gamma = 105$ to 135 (≈ 120) MeV
$p_{\text{beam}} = 0.96$ GeV/c $4\pi\lambda^2 = 19.0$ mb

$\Sigma(1775)$ DECAY MODES	Fraction (Γ_i/Γ)	p (MeV/c)
$N\overline{K}$	37–43%	508
$\Lambda\pi$	14–20%	525
$\Sigma\pi$	2–5%	474
$\Sigma(1385)\pi$	8–12%	324
$\Lambda(1520)\pi$	17–23%	198

$\Sigma(1915)\ F_{15}$ $I(J^P) = 1(\frac{5}{2}^+)$

Mass $m = 1900$ to 1935 (≈ 1915) MeV
Full width $\Gamma = 80$ to 160 (≈ 120) MeV
$p_{\text{beam}} = 1.26$ GeV/c $4\pi\lambda^2 = 12.8$ mb

$\Sigma(1915)$ DECAY MODES	Fraction (Γ_i/Γ)	p (MeV/c)
$N\overline{K}$	5–15 %	618
$\Lambda\pi$	seen	622
$\Sigma\pi$	seen	577
$\Sigma(1385)\pi$	<5 %	440

$\Sigma(1940)\ D_{13}$ $I(J^P) = 1(\frac{3}{2}^-)$

Mass $m = 1900$ to 1950 (≈ 1940) MeV
Full width $\Gamma = 150$ to 300 (≈ 220) MeV
$p_{\text{beam}} = 1.32$ GeV/c $4\pi\lambda^2 = 12.1$ mb

$\Sigma(1940)$ DECAY MODES	Fraction (Γ_i/Γ)	p (MeV/c)
$N\overline{K}$	<20 %	637
$\Lambda\pi$	seen	639
$\Sigma\pi$	seen	594
$\Sigma(1385)\pi$	seen	460
$\Lambda(1520)\pi$	seen	354
$\Delta(1232)\overline{K}$	seen	410
$N\overline{K}^*(892)$	seen	320

$\Sigma(2030)\ F_{17}$ $I(J^P) = 1(\frac{7}{2}^+)$

Mass $m = 2025$ to 2040 (≈ 2030) MeV
Full width $\Gamma = 150$ to 200 (≈ 180) MeV
$p_{\text{beam}} = 1.52$ GeV/c $4\pi\lambda^2 = 9.93$ mb

$\Sigma(2030)$ DECAY MODES	Fraction (Γ_i/Γ)	p (MeV/c)
$N\overline{K}$	17–23 %	702
$\Lambda\pi$	17–23 %	700
$\Sigma\pi$	5–10 %	657
ΞK	<2 %	412
$\Sigma(1385)\pi$	5–15 %	529
$\Lambda(1520)\pi$	10–20 %	430
$\Delta(1232)\overline{K}$	10–20 %	498
$N\overline{K}^*(892)$	<5 %	438

$\Sigma(2250)$ $I(J^P) = 1(?^?)$

Mass $m = 2210$ to 2280 (≈ 2250) MeV
Full width $\Gamma = 60$ to 150 (≈ 100) MeV
$p_{\text{beam}} = 2.04$ GeV/c $4\pi\lambda^2 = 6.76$ mb

$\Sigma(2250)$ DECAY MODES	Fraction (Γ_i/Γ)	p (MeV/c)
$N\overline{K}$	<10 %	851
$\Lambda\pi$	seen	842
$\Sigma\pi$	seen	803

Ξ BARYONS ($S = -2$, $I = 1/2$)

$\Xi^0 = uss$, $\Xi^- = dss$

Ξ^0 $I(J^P) = \frac{1}{2}(\frac{1}{2}^+)$

P is not yet measured; + is the quark model prediction.
Mass $m = 1314.9 \pm 0.6$ MeV
$m_{\Xi^-} - m_{\Xi^0} = 6.4 \pm 0.6$ MeV
Mean life $\tau = (2.90 \pm 0.09) \times 10^{-10}$ s
$c\tau = 8.71$ cm
Magnetic moment $\mu = -1.250 \pm 0.014\ \mu_N$

Decay parameters

$\Lambda\pi^0$	$\alpha = -0.411 \pm 0.022$ (S = 2.1)
"	$\phi = (21 \pm 12)°$
"	$\gamma = 0.85$ [g]
"	$\Delta = (218^{+12}_{-19})°$ [g]
$\Lambda\gamma$	$\alpha = 0.4 \pm 0.4$
$\Sigma^0\gamma$	$\alpha = 0.20 \pm 0.32$

Ξ^0 DECAY MODES		Fraction (Γ_i/Γ)		Confidence level	p (MeV/c)
$\Lambda\pi^0$		(99.54 ± 0.05) %			135
$\Lambda\gamma$		(1.06 ± 0.16)	$\times 10^{-3}$		184
$\Sigma^0\gamma$		(3.5 ± 0.4)	$\times 10^{-3}$		117
$\Sigma^+ e^- \overline{\nu}_e$		< 1.1	$\times 10^{-3}$	90%	120
$\Sigma^+ \mu^- \overline{\nu}_\mu$		< 1.1	$\times 10^{-3}$	90%	64
$\Delta S = \Delta Q$ (SQ) violating modes or $\Delta S = 2$ forbidden ($S2$) modes					
$\Sigma^- e^+ \nu_e$	SQ	< 9	$\times 10^{-4}$	90%	112
$\Sigma^- \mu^+ \nu_\mu$	SQ	< 9	$\times 10^{-4}$	90%	49
$p\pi^-$	$S2$	< 4	$\times 10^{-5}$	90%	299
$p e^- \overline{\nu}_e$	$S2$	< 1.3	$\times 10^{-3}$		323
$p\mu^- \overline{\nu}_\mu$	$S2$	< 1.3	$\times 10^{-3}$		309

Ξ^- $I(J^P) = \frac{1}{2}(\frac{1}{2}^+)$

P is not yet measured; + is the quark model prediction.
Mass $m = 1321.32 \pm 0.13$ MeV
Mean life $\tau = (1.639 \pm 0.015) \times 10^{-10}$ s
$c\tau = 4.91$ cm
Magnetic moment $\mu = -0.6507 \pm 0.0025\ \mu_N$

Decay parameters

$\Lambda\pi^-$	$\alpha = -0.456 \pm 0.014$ (S = 1.8)
"	$\phi = (4 \pm 4)°$
"	$\gamma = 0.89$ [g]
"	$\Delta = (188 \pm 8)°$ [g]
$\Lambda e^- \overline{\nu}_e$	$g_A/g_V = -0.25 \pm 0.05$ [e]

Ξ^- DECAY MODES		Fraction (Γ_i/Γ)		Confidence level	p (MeV/c)
$\Lambda\pi^-$		(99.887 ± 0.035) %			139
$\Sigma^-\gamma$		(1.27 ± 0.23)	$\times 10^{-4}$		118
$\Lambda e^- \overline{\nu}_e$		(5.63 ± 0.31)	$\times 10^{-4}$		190
$\Lambda\mu^- \overline{\nu}_\mu$		(3.5 $^{+3.5}_{-2.2}$)	$\times 10^{-4}$		163
$\Sigma^0 e^- \overline{\nu}_e$		(8.7 ± 1.7)	$\times 10^{-5}$		122
$\Sigma^0 \mu^- \overline{\nu}_\mu$		< 8	$\times 10^{-4}$	90%	70
$\Xi^0 e^- \overline{\nu}_e$		< 2.3	$\times 10^{-3}$	90%	6
$\Delta S = 2$ forbidden ($S2$) modes					
$n\pi^-$	$S2$	< 1.9	$\times 10^{-5}$	90%	303
$n e^- \overline{\nu}_e$	$S2$	< 3.2	$\times 10^{-3}$	90%	327
$n\mu^- \overline{\nu}_\mu$	$S2$	< 1.5	%	90%	314
$p\pi^-\pi^-$	$S2$	< 4	$\times 10^{-4}$	90%	223
$p\pi^- e^- \overline{\nu}_e$	$S2$	< 4	$\times 10^{-4}$	90%	304
$p\pi^-\mu^-\overline{\nu}_\mu$	$S2$	< 4	$\times 10^{-4}$	90%	250
$p\mu^-\mu^-$	L	< 4	$\times 10^{-4}$	90%	272

Ξ(1530) P_{13}

$I(J^P) = \frac{1}{2}(\frac{3}{2}^+)$

$\Xi(1530)^0$ mass $m = 1531.80 \pm 0.32$ MeV (S = 1.3)
$\Xi(1530)^-$ mass $m = 1535.0 \pm 0.6$ MeV
$\Xi(1530)^0$ full width $\Gamma = 9.1 \pm 0.5$ MeV
$\Xi(1530)^-$ full width $\Gamma = 9.9^{+1.7}_{-1.9}$ MeV

Ξ(1530) DECAY MODES	Fraction (Γ_i/Γ)	Confidence level	p (MeV/c)
$\Xi\pi$	100 %		152
$\Xi\gamma$	<4 %	90%	200

Ξ(1690)

$I(J^P) = \frac{1}{2}(?^?)$

Mass $m = 1690 \pm 10$ MeV [f]
Full width $\Gamma < 50$ MeV

Ξ(1690) DECAY MODES	Fraction (Γ_i/Γ)	p (MeV/c)
$\Lambda\overline{K}$	seen	240
$\Sigma\overline{K}$	seen	51
$\Xi^-\pi^+\pi^-$	possibly seen	214

Ξ(1820) D_{13}

$I(J^P) = \frac{1}{2}(\frac{3}{2}^-)$

Mass $m = 1823 \pm 5$ MeV [f]
Full width $\Gamma = 24^{+15}_{-10}$ MeV [f]

Ξ(1820) DECAY MODES	Fraction (Γ_i/Γ)	p (MeV/c)
$\Lambda\overline{K}$	large	400
$\Sigma\overline{K}$	small	320
$\Xi\pi$	small	413
$\Xi(1530)\pi$	small	234

Ξ(1950)

$I(J^P) = \frac{1}{2}(?^?)$

Mass $m = 1950 \pm 15$ MeV [f]
Full width $\Gamma = 60 \pm 20$ MeV [f]

Ξ(1950) DECAY MODES	Fraction (Γ_i/Γ)	p (MeV/c)
$\Lambda\overline{K}$	seen	522
$\Sigma\overline{K}$	possibly seen	460
$\Xi\pi$	seen	518

Ξ(2030)

$I(J^P) = \frac{1}{2}(\geq \frac{5}{2}^?)$

Mass $m = 2025 \pm 5$ MeV [f]
Full width $\Gamma = 20^{+15}_{-5}$ MeV [f]

Ξ(2030) DECAY MODES	Fraction (Γ_i/Γ)	p (MeV/c)
$\Lambda\overline{K}$	~ 20 %	589
$\Sigma\overline{K}$	~ 80 %	533
$\Xi\pi$	small	573
$\Xi(1530)\pi$	small	421
$\Lambda\overline{K}\pi$	small	501
$\Sigma\overline{K}\pi$	small	430

Ω BARYONS ($S = -3, I = 0$)

$\Omega^- = sss$

Ω⁻

$I(J^P) = 0(\frac{3}{2}^+)$

J^P is not yet measured; $\frac{3}{2}^+$ is the quark model prediction.

Mass $m = 1672.45 \pm 0.29$ MeV
Mean life $\tau = (0.822 \pm 0.012) \times 10^{-10}$ s
$c\tau = 2.46$ cm
Magnetic moment $\mu = -2.02 \pm 0.05\ \mu_N$

Decay parameters

ΛK^-	$\alpha = -0.026 \pm 0.026$
$\Xi^0\pi^-$	$\alpha = 0.09 \pm 0.14$
$\Xi^-\pi^0$	$\alpha = 0.05 \pm 0.21$

Ω⁻ DECAY MODES	Fraction (Γ_i/Γ)	Confidence level	p (MeV/c)
ΛK^-	(67.8±0.7) %		211
$\Xi^0\pi^-$	(23.6±0.7) %		294
$\Xi^-\pi^0$	(8.6±0.4) %		290
$\Xi^-\pi^+\pi^-$	$(4.3^{+3.4}_{-1.3}) \times 10^{-4}$		190
$\Xi(1530)^0\pi^-$	$(6.4^{+5.1}_{-2.0}) \times 10^{-4}$		17
$\Xi^0 e^-\overline{\nu}_e$	$(5.6\pm2.8) \times 10^{-3}$		319
$\Xi^-\gamma$	$< 4.6 \times 10^{-4}$	90%	314
$\Delta S = 2$ forbidden ($S2$) modes			
$\Lambda\pi^-$	$S2$ $< 1.9 \times 10^{-4}$	90%	449

Ω(2250)⁻

$I(J^P) = 0(?^?)$

Mass $m = 2252 \pm 9$ MeV
Full width $\Gamma = 55 \pm 18$ MeV

Ω(2250)⁻ DECAY MODES	Fraction (Γ_i/Γ)	p (MeV/c)
$\Xi^-\pi^+K^-$	seen	531
$\Xi(1530)^0K^-$	seen	437

CHARMED BARYONS ($C = +1$)

$\Lambda_c^+ = udc$, $\Sigma_c^{++} = uuc$, $\Sigma_c^+ = udc$, $\Sigma_c^0 = ddc$,
$\Xi_c^+ = usc$, $\Xi_c^0 = dsc$, $\Omega_c^0 = ssc$

Λ_c^+

$I(J^P) = 0(\frac{1}{2}^+)$

J not confirmed; $\frac{1}{2}$ is the quark model prediction.

Mass $m = 2284.9 \pm 0.6$ MeV
Mean life $\tau = (0.206 \pm 0.012) \times 10^{-12}$ s
$c\tau = 61.8\ \mu$m

Decay asymmetry parameters

$\Lambda\pi^+$	$\alpha = -0.98 \pm 0.19$
$\Sigma^+\pi^0$	$\alpha = -0.45 \pm 0.32$
$\Lambda\ell^+\nu_\ell$	$\alpha = -0.82^{+0.11}_{-0.07}$

Λ_c^+ DECAY MODES	Fraction (Γ_i/Γ)	Scale factor/ Confidence level	p (MeV/c)
Hadronic modes with a p and one $\overline{K}$			
$p\overline{K}^0$	(2.2 ± 0.4) %		872
$pK^-\pi^+$	(4.4 ± 0.6) %		822
$p\overline{K}^*(892)^0$	[k] (1.6 ± 0.4) %		681
$\Delta(1232)^{++}K^-$	(7 ± 4) × 10^{-3}		709
$\Lambda(1520)\pi^+$	[k] $(4.0 \pm {}^{2.0}_{1.7}) \times 10^{-3}$		626
$pK^-\pi^+$ nonresonant	$(2.5 \pm {}^{0.5}_{0.6})$ %		822
$p\overline{K}^0\eta$	(1.10± 0.29) %		567

Baryon Summary Table

$p\overline{K}^0\pi^+\pi^-$		(2.1 ± 0.8) %	753
$pK^-\pi^+\pi^0$		seen	758
$pK^*(892)^-\pi^+$	[k]	(9 ± 5) × 10^{-3}	579
$p(K^-\pi^+)_{\text{nonresonant}}\pi^0$		(3.2 ± 0.7) %	758
$\Delta(1232)\overline{K}^*(892)$		seen	416
$pK^-\pi^+\pi^+\pi^-$		(10 ± 7) × 10^{-4}	670
$pK^-\pi^+\pi^0\pi^0$		(7.0 ± 3.5) × 10^{-3}	676
$pK^-\pi^+\pi^0\pi^0\pi^0$		(4.4 ± 2.8) × 10^{-3}	573
Hadronic modes with a p and zero or two K's			
$p\pi^+\pi^-$		(3.0 ± 1.6) × 10^{-3}	926
$pf_0(980)$	[k]	(2.4 ± 1.6) × 10^{-3}	621
$p\pi^+\pi^+\pi^-\pi^-$		(1.6 ± 1.0) × 10^{-3}	851
pK^+K^-		(2.0 ± 0.6) × 10^{-3}	615
$p\phi$	[k]	(1.06± 0.33) × 10^{-3}	589
Hadronic modes with a hyperon			
$\Lambda\pi^+$		(7.9 ± 1.8) × 10^{-3}	863
$\Lambda\pi^+\pi^0$		(3.2 ± 0.9) %	843
$\Lambda\rho^0$		< 4 % CL=95%	638
$\Lambda\pi^+\pi^+\pi^-$		(2.9 ± 0.6) %	806
$\Lambda\pi^+\eta$		(1.5 ± 0.4) %	690
$\Sigma(1385)^+\eta$	[k]	(7.5 ± 2.4) × 10^{-3}	569
$\Lambda K^+\overline{K}^0$		(5.3 ± 1.4) × 10^{-3}	441
$\Sigma^0\pi^+$		(8.8 ± 2.0) × 10^{-3}	824
$\Sigma^+\pi^0$		(8.8 ± 2.2) × 10^{-3}	826
$\Sigma^+\eta$		(4.8 ± 1.7) × 10^{-3}	712
$\Sigma^+\pi^+\pi^-$		(3.0 ± 0.6) %	803
$\Sigma^+\rho^0$		< 1.2 % CL=95%	578
$\Sigma^-\pi^+\pi^+$		(1.6 ± 0.6) %	798
$\Sigma^0\pi^+\pi^0$		(1.6 ± 0.6) %	802
$\Sigma^0\pi^+\pi^+\pi^-$		(9.2 ± 3.4) × 10^{-3}	762
$\Sigma^+\pi^+\pi^-\pi^0$			766
$\Sigma^+\omega$	[k]	(2.4 ± 0.7) %	568
$\Sigma^+\pi^+\pi^+\pi^-\pi^-$		(2.6 $^{+\ 3.5}_{-\ 1.8}$) × 10^{-3}	707
$\Sigma^+K^+K^-$		(3.1 ± 0.8) × 10^{-3}	346
$\Sigma^+\phi$	[k]	(3.0 ± 1.3) × 10^{-3}	292
$\Sigma^+K^+\pi^-$		(5.7 $^{+\ 5.3}_{-\ 3.2}$) × 10^{-3}	668
Ξ^0K^+		(3.4 ± 0.9) × 10^{-3}	652
$\Xi^-K^+\pi^+$		(4.3 ± 1.1) × 10^{-3}	564
$\Xi(1530)^0K^+$	[k]	(2.3 ± 0.7) × 10^{-3}	471
Semileptonic modes			
$\Lambda\ell^+\nu_\ell$	[l]	(2.3 ± 0.5) %	–
e^+ anything		(4.5 ± 1.7) %	–
pe^+ anything		(1.8 ± 0.9) %	–
Λe^+ anything		(1.6 ± 0.6) %	–
$\Lambda\mu^+$ anything		(1.5 ± 0.9) %	–
Inclusive modes			
p anything		(50 ±16) %	–
p anything (no Λ)		(12 ±19) %	–
n anything		(50 ±16) %	–
n anything (no Λ)		(29 ±17) %	–
Λ anything		(35 ±11) % S=1.4	–
$\Sigma^\pm$ anything	[m]	(10 ± 5) %	–
$\Delta C = 1$ weak neutral current ($C1$) modes, or Lepton number (L) violating modes			
$p\mu^+\mu^-$	$C1$	< 3.4 × 10^{-4} CL=90%	936
$\Sigma^-\mu^+\mu^+$	L	< 7.0 × 10^{-4} CL=90%	811

$\Lambda_c(2593)^+$

$I(J^P) = 0(\frac{1}{2}^-)$

The spin-parity follows from the fact that $\Sigma_c(2455)\pi$ decays, with little available phase space, dominate.

Mass $m = 2593.6 \pm 1.0$ MeV (S = 1.2)
$m - m_{\Lambda_c^+} = 308.6 \pm 0.8$ MeV (S = 1.3)
Full width $\Gamma = 3.9^{+2.4}_{-1.6}$ MeV

$\Lambda_c^+\pi\pi$ and $\Sigma_c(2455)\pi$ — the latter just barely — are the only strong decays allowed to an excited Λ_c^+ having this mass; and the $\Lambda_c^+\pi^+\pi^-$ mode seems to be largely via $\Sigma_c^{++}\pi^-$ or $\Sigma_c^0\pi^+$.

$\Lambda_c(2593)^+$ DECAY MODES	Fraction (Γ_i/Γ)	p (MeV/c)
$\Lambda_c^+\pi^+\pi^-$	seen	124
$\Sigma_c(2455)^{++}\pi^-$	large	17
$\Sigma_c(2455)^0\pi^+$	large	23
$\Lambda_c^+\pi^+\pi^-$ 3-body	small	124
$\Lambda_c^+\pi^0$	not seen	261
$\Lambda_c^+\gamma$	not seen	290

$\Lambda_c(2625)^+$

$I(J^P) = 0(?^?)$

J^P is expected to be $3/2^-$.

Mass $m = 2626.4 \pm 0.9$ MeV (S = 1.3)
$m - m_{\Lambda_c^+} = 341.5 \pm 0.8$ MeV (S = 1.9)
Full width $\Gamma < 1.9$ MeV, CL = 90%

$\Lambda_c^+\pi\pi$ and $\Sigma(2455)\pi$ are the only strong decays allowed to an excited Λ_c^+ having this mass.

$\Lambda_c(2625)^+$ DECAY MODES	Fraction (Γ_i/Γ)	p (MeV/c)
$\Lambda_c^+\pi^+\pi^-$	seen	184
$\Sigma_c(2455)^{++}\pi^-$	small	100
$\Sigma_c(2455)^0\pi^+$	small	101
$\Lambda_c^+\pi^+\pi^-$ 3-body	large	184
$\Lambda_c^+\pi^0$	not seen	293
$\Lambda_c^+\gamma$	not seen	319

$\Sigma_c(2455)$

$I(J^P) = 1(\frac{1}{2}^+)$

J^P not confirmed; $\frac{1}{2}^+$ is the quark model prediction.

$\Sigma_c(2455)^{++}$ mass $m = 2452.9 \pm 0.6$ MeV
$\Sigma_c(2455)^+$ mass $m = 2453.5 \pm 0.9$ MeV
$\Sigma_c(2455)^0$ mass $m = 2452.1 \pm 0.7$ MeV
$m_{\Sigma_c^{++}} - m_{\Lambda_c^+} = 167.95 \pm 0.25$ MeV
$m_{\Sigma_c^+} - m_{\Lambda_c^+} = 168.5 \pm 0.7$ MeV (S = 1.1)
$m_{\Sigma_c^0} - m_{\Lambda_c^+} = 167.2 \pm 0.4$ MeV (S = 1.1)
$m_{\Sigma_c^{++}} - m_{\Sigma_c^0} = 0.79 \pm 0.33$ MeV (S = 1.2)
$m_{\Sigma_c^+} - m_{\Sigma_c^0} = 1.4 \pm 0.6$ MeV

$\Lambda_c^+\pi$ is the only strong decay allowed to a Σ_c having this mass.

$\Sigma_c(2455)$ DECAY MODES	Fraction (Γ_i/Γ)	p (MeV/c)
$\Lambda_c^+\pi$	≈ 100 %	90

Ξ_c^+

$I(J^P) = \frac{1}{2}(\frac{1}{2}^+)$

$I(J^P)$ not confirmed; $\frac{1}{2}(\frac{1}{2}^+)$ is the quark model prediction.

Mass $m = 2465.6 \pm 1.4$ MeV
Mean life $\tau = (0.35^{+0.07}_{-0.04}) \times 10^{-12}$ s
$c\tau = 106\ \mu$m

Ξ_c^+ DECAY MODES	Fraction (Γ_i/Γ)	p (MeV/c)
$\Lambda K^-\pi^+\pi^+$	seen	784
$\Lambda\overline{K}^*(892)^0\pi^+$	not seen	601
$\Sigma(1385)^+K^-\pi^+$	not seen	676
$\Sigma^+K^-\pi^+$	seen	808
$\Sigma^+\overline{K}^*(892)^0$	seen	653
$\Sigma^0K^-\pi^+\pi^+$	seen	733
$\Xi^0\pi^+$	seen	875
$\Xi^-\pi^+\pi^+$	seen	850
$\Xi(1530)^0\pi^+$	not seen	748
$\Xi^0\pi^+\pi^0$	seen	854
$\Xi^0\pi^+\pi^+\pi^-$	seen	817
$\Xi^0e^+\nu_e$	seen	882

Ξ_c^0

$I(J^P) = \frac{1}{2}(\frac{1}{2}^+)$

$I(J^P)$ not confirmed; $\frac{1}{2}(\frac{1}{2}^+)$ is the quark model prediction.

Mass $m = 2470.3 \pm 1.8$ MeV (S = 1.3)
$m_{\Xi_c^0} - m_{\Xi_c^+} = 4.7 \pm 2.1$ MeV (S = 1.2)
Mean life $\tau = (0.098^{+0.023}_{-0.015}) \times 10^{-12}$ s
$c\tau = 29$ μm

Ξ_c^0 DECAY MODES	Fraction (Γ_i/Γ)	p (MeV/c)
$\Lambda \overline{K}^0$	seen	864
$\Xi^- \pi^+$	seen	875
$\Xi^- \pi^+ \pi^+ \pi^-$	seen	816
$p K^- \overline{K}^*(892)^0$	seen	406
$\Omega^- K^+$	seen	522
$\Xi^- e^+ \nu_e$	seen	882
$\Xi^- \ell^+$ anything	seen	–

$\Xi_c(2645)$

$I(J^P) = ?(?^?)$

Mass $m = 2643.8 \pm 1.8$ MeV
$m_{\Xi_c(2645)^0} - m_{\Xi_c^+} = 178.2 \pm 1.1$ MeV
Full width $\Gamma < 5.5$ MeV, CL = 90%

$\Xi_c \pi$ is the only strong decay allowed to a Ξ_c resonance having this mass.

$\Xi_c(2645)$ DECAY MODES	Fraction (Γ_i/Γ)	p (MeV/c)
$\Xi_c^+ \pi^-$	seen	107

Ω_c^0

$I(J^P) = 0(\frac{1}{2}^+)$

$I(J^P)$ not confirmed; $0(\frac{1}{2}^+)$ is the quark model prediction.

Mass $m = 2704 \pm 4$ MeV (S = 1.8)
Mean life $\tau = (0.064 \pm 0.020) \times 10^{-12}$ s
$c\tau = 19$ μm

Ω_c^0 DECAY MODES	Fraction (Γ_i/Γ)	p (MeV/c)
$\Sigma^+ K^- K^- \pi^+$	seen	697
$\Xi^- K^- \pi^+ \pi^+$	seen	838
$\Omega^- \pi^+$	seen	827
$\Omega^- \pi^- \pi^+ \pi^+$	seen	759

BOTTOM (BEAUTY) BARYONS ($B = -1$)

$\Lambda_b^0 = udb$, $\Xi_b^0 = usb$, $\Xi_b^- = dsb$

Λ_b^0

$I(J^P) = 0(\frac{1}{2}^+)$

$I(J^P)$ not yet measured; $0(\frac{1}{2}^+)$ is the quark model prediction.

Mass $m = 5641 \pm 50$ MeV
Mean life $\tau = (1.14 \pm 0.08) \times 10^{-12}$ s
$c\tau = 342$ μm

These branching fractions are actually an average over weakly decaying b-baryons weighted by their production rates in Z decay (or high-energy $p\overline{p}$), branching ratios, and detection efficiencies. They scale with the LEP Λ_b production fraction $B(b \rightarrow \Lambda_b)$ and are evaluated for our value $B(b \rightarrow \Lambda_b) = (13.2 \pm 4.1)\%$.

The branching fractions $B(\Lambda_b^0 \rightarrow \Lambda \ell^- \overline{\nu}_\ell \text{ anything})$ and $B(\Lambda_b^0 \rightarrow \Lambda_c^+ \ell^- \overline{\nu}_\ell \text{ anything})$ are not pure measurements because the underlying measured products of these with $B(b \rightarrow \Lambda_b)$ were used to determine $B(b \rightarrow \Lambda_b)$, as described in the note "Production and Decay of b-Flavored Hadrons."

Λ_b^0 DECAY MODES	Fraction (Γ_i/Γ)	p (MeV/c)
$J/\psi(1S)\Lambda$	(1.4± 0.9) %	1756
$p D^0 \pi^-$	seen	2383
$\Lambda_c^+ \pi^+ \pi^- \pi^-$	seen	2336
$p \mu^- \overline{\nu}$ anything	(3.7± 1.7) %	–
$\Lambda \ell^- \overline{\nu}_\ell$ anything	[n] (2.5± 0.5) %	–
$\Lambda_c^+ \ell^- \overline{\nu}_\ell$ anything	[n] (10.0± 3.0) %	–
$\Lambda/\overline{\Lambda}$ anything	(17 $^{+11}_{-8}$) %	–

NOTES

This Summary Table only includes established baryons. The Particle Listings include evidence for other baryons. The masses, widths, and branching fractions for the resonances in this Table are Breit-Wigner parameters. The Particle Listings also give, where available, pole parameters. See, in particular, the *Note on N and Δ Resonances*.

For most of the resonances, the parameters come from various partial-wave analyses of more or less the same sets of data, and it is not appropriate to treat the results of the analyses as independent or to average them together. Furthermore, the systematic errors on the results are not well understood. Thus, we usually only give ranges for the parameters. We then also give a best guess for the mass (as part of the name of the resonance) and for the width. The *Note on N and Δ Resonances* and the *Note on Λ and Σ Resonances* in the Particle Listings review the partial-wave analyses.

When a quantity has "(S = ...)" to its right, the error on the quantity has been enlarged by the "scale factor" S, defined as $S = \sqrt{\chi^2/(N-1)}$, where N is the number of measurements used in calculating the quantity. We do this when S > 1, which often indicates that the measurements are inconsistent. When S > 1.25, we also show in the Particle Listings an ideogram of the measurements. For more about S, see the Introduction.

A decay momentum p is given for each decay mode. For a 2-body decay, p is the momentum of each decay product in the rest frame of the decaying particle. For a 3-or-more-body decay, p is the largest momentum any of the products can have in this frame. For any resonance, the *nominal* mass is used in calculating p. A dagger ("†") in this column indicates that the mode is forbidden when the nominal masses of resonances are used, but is in fact allowed due to the nonzero widths of the resonances.

[*a*] The masses of the p and n are most precisely known in u (unified atomic mass units). The conversion factor to MeV, 1 u = 931.49432 ± 0.00028 MeV, is less well known than are the masses in u.

[*b*] The limit is from neutrality-of-matter experiments; it assumes $q_n = q_p + q_e$. See also the charge of the neutron.

[*c*] The first limit is geochemical and independent of decay mode. The second entry, a range of limits, assumes the dominant decay modes are among those investigated. For antiprotons the best limit, inferred from the observation of cosmic ray $\overline{p}$'s is $\tau_{\overline{p}} > 10^7$ yr, the cosmic-ray storage time, but this limit depends on a number of assumptions. The best direct observation of stored antiprotons gives $\tau_{\overline{p}}/B(\overline{p} \rightarrow e^- \gamma) > 1848$ yr.

[*d*] There is some controversy about whether nuclear physics and model dependence complicate the analysis for bound neutrons (from which the best limit comes). The second limit here is from reactor experiments with free neutrons.

[*e*] The parameters g_A, g_V, and g_{WM} for semileptonic modes are defined by $\overline{B}_f[\gamma_\lambda(g_V + g_A\gamma_5) + i(g_{WM}/m_{B_i})\,\sigma_{\lambda\nu}\,q^\nu]B_i$, and ϕ_{AV} is defined by $g_A/g_V = |g_A/g_V|e^{i\phi_{AV}}$. See the "Note on Baryon Decay Parameters" in the neutron Particle Listings.

[*f*] Time-reversal invariance requires this to be 0° or 180°.

[*g*] The decay parameters γ and Δ are calculated from α and ϕ using

$$\gamma = \sqrt{1-\alpha^2}\cos\phi\,, \qquad \tan\Delta = -\frac{1}{\alpha}\sqrt{1-\alpha^2}\sin\phi\,.$$

See the "Note on Baryon Decay Parameters" in the neutron Particle Listings.

[*h*] See the Particle Listings for the pion momentum range used in this measurement.

[*i*] The error given here is only an educated guess. It is larger than the error on the weighted average of the published values.

[*j*] A theoretical value using QED.

[*k*] This branching fraction includes all the decay modes of the final-state resonance.

[*l*] ℓ indicates e or μ mode, not sum over modes.

[*m*] The value is for the sum of the charge states of particle/antiparticle states indicated.

[*n*] Not a pure measurement. See note at head of Λ_b^0 Decay Modes.

Searches Summary Table

MONOPOLES, SUPERSYMMETRY, COMPOSITENESS, etc., SEARCHES FOR

Magnetic Monopole Searches

Isolated candidate events have not been confirmed. Most experiments obtain negative results.

Supersymmetric Particle Searches

Limits are based on the Minimal Supersymmetric Standard Model. Assumptions include: 1) $\widetilde{\chi}_1^0$ (or $\widetilde{\gamma}$) is lightest supersymmetric particle; 2) R-parity is conserved; 3) $m_{\widetilde{f}_L} = m_{\widetilde{f}_R}$, and all scalar quarks (except $\widetilde{t}_L$ and $\widetilde{t}_R$) are degenerate in mass.

See the Particle Listings for a Note giving details of supersymmetry.

$\widetilde{\chi}_i^0$ — neutralinos (mixtures of $\widetilde{\gamma}$, $\widetilde{Z}^0$, and $\widetilde{H}_i^0$)

Mass $m_{\widetilde{\gamma}} > 15$ GeV, CL = 90% [if $m_{\widetilde{f}} = 100$ GeV (from cosmology)]
Mass $m_{\widetilde{\chi}_1^0} > 23$ GeV, CL = 95% [$\tan\beta > 3$]
Mass $m_{\widetilde{\chi}_2^0} > 52$ GeV, CL = 95% [$\tan\beta > 3$]
Mass $m_{\widetilde{\chi}_3^0} > 84$ GeV, CL = 95% [$\tan\beta > 3$]
Mass $m_{\widetilde{\chi}_4^0} > 127$ GeV, CL = 95% [$\tan\beta > 3$]

$\widetilde{\chi}_i^\pm$ — charginos (mixtures of $\widetilde{W}^\pm$ and $\widetilde{H}_i^\pm$)

Mass $m_{\widetilde{\chi}_1^\pm} > 45$ GeV, CL = 95% [all $m_{\widetilde{\chi}_1^0}$]
Mass $m_{\widetilde{\chi}_2^\pm} > 99$ GeV, CL = 95% [GUT relations assumed]

$\widetilde{\nu}$ — scalar neutrino (sneutrino)

Mass $m > 37.1$ GeV, CL = 95% [one flavor]
Mass $m > 41.8$ GeV, CL = 95% [three degenerate flavors]

$\widetilde{e}$ — scalar electron (selectron)

Mass $m > 65$ GeV, CL = 95% [if $m_{\widetilde{\gamma}} = 0$]
Mass $m > 50$ GeV, CL = 95% [if $m_{\widetilde{\gamma}} < 5$ GeV]
Mass $m > 45$ GeV, CL = 95% [if $m_{\widetilde{\chi}_1^0} < 41$ GeV]

$\widetilde{\mu}$ — scalar muon (smuon)

Mass $m > 45$ GeV, CL = 95% [if $m_{\widetilde{\chi}_1^0} < 41$ GeV]

$\widetilde{\tau}$ — scalar tau (stau)

Mass $m > 45$ GeV, CL = 95% [if $m_{\widetilde{\chi}_1^0} < 38$ GeV]

$\widetilde{q}$ — scalar quark (squark)

These limits include the effects of cascade decays, evaluated assuming a fixed value of the parameters μ and $\tan\beta$. The limits are weakly sensitive to these parameters over much of parameter space. Limits assume GUT relations between gaugino masses and the gauge coupling; in particular that for $|\mu|$ not small, $m_{\widetilde{\chi}_1^0} \approx m_{\widetilde{g}}/6$.

Mass $m > 176$ GeV, CL = 95% [any $m_{\widetilde{g}} < 300$ GeV, $\mu = -250$ GeV, $\tan\beta = 2$]
Mass $m > 224$ GeV, CL = 95% [$m_{\widetilde{g}} \leq m_{\widetilde{q}}$, $\mu = -400$ GeV, $\tan\beta = 4$]

$\widetilde{g}$ — gluino

There is some controversy about a low-mass window ($1 \lesssim m_{\widetilde{g}} \lesssim 4$ GeV). Several experiments cast doubt on the existence of this window.

These limits include the effects of cascade decays, evaluated assuming a fixed value of the parameters μ and $\tan\beta$. The limits are weakly sensitive to these parameters over much of parameter space. Limits assume GUT relations between gaugino masses and the gauge coupling; in particular that for $|\mu|$ not small, $m_{\widetilde{\chi}_1^0} \approx m_{\widetilde{g}}/6$.

Mass $m > 154$ GeV, CL = 95% [$m_{\widetilde{g}} \leq m_{\widetilde{q}}$, $\mu = -400$ GeV, $\tan\beta = 4$]
Mass $m > 212$ GeV, CL = 95% [$m_{\widetilde{g}} \geq m_{\widetilde{q}}$, $\mu = -250$ GeV, $\tan\beta = 2$]

Quark and Lepton Compositeness, Searches for

Scale Limits Λ for Contact Interactions (the lowest dimensional interactions with four fermions)

If the Lagrangian has the form

$$\pm \frac{g^2}{2\Lambda^2} \overline{\psi}_L \gamma_\mu \psi_L \overline{\psi}_L \gamma^\mu \psi_L$$

(with $g^2/4\pi$ set equal to 1), then we define $\Lambda \equiv \Lambda_{LL}^\pm$. For the full definitions and for other forms, see the Note in the Listings on Searches for Quark and Lepton Compositeness in the full *Review* and the original literature.

$\Lambda_{LL}^+(eeee) > 1.6$ TeV, CL = 95%
$\Lambda_{LL}^-(eeee) > 3.6$ TeV, CL = 95%
$\Lambda_{LL}^+(ee\mu\mu) > 2.6$ TeV, CL = 95%
$\Lambda_{LL}^-(ee\mu\mu) > 1.9$ TeV, CL = 95%
$\Lambda_{LL}^+(ee\tau\tau) > 1.9$ TeV, CL = 95%
$\Lambda_{LL}^-(ee\tau\tau) > 2.9$ TeV, CL = 95%
$\Lambda_{LL}^+(\ell\ell\ell\ell) > 3.5$ TeV, CL = 95%
$\Lambda_{LL}^-(\ell\ell\ell\ell) > 2.8$ TeV, CL = 95%
$\Lambda_{LL}^+(eeqq) > 2.3$ TeV, CL = 95%
$\Lambda_{LL}^-(eeqq) > 2.2$ TeV, CL = 95%
$\Lambda_{LL}^+(\mu\mu qq) > 1.4$ TeV, CL = 95%
$\Lambda_{LL}^-(\mu\mu qq) > 1.6$ TeV, CL = 95%
$\Lambda_{LR}^\pm(\nu_\mu \nu_e \mu e) > 3.1$ TeV, CL = 90%
$\Lambda_{LL}^\pm(qqqq) > 1.4$ TeV, CL = 95%

Recent CDF measurements of the inclusive jet cross section in $p\overline{p}$ collisions could be interpreted as tentative evidence for a four-quark contact interaction with $\Lambda_{LL}^\pm(qqqq) \sim 1.6$ TeV. However, CDF notes that uncertainty in the parton distribution functions, higher-order QCD corrections, and detector calibration may possibly account for the effect.

Excited Leptons

The limits from $\ell^{*+}\ell^{*-}$ do not depend on λ (where λ is the $\ell\ell^*$ transition coupling). The λ-dependent limits assume chiral coupling, except for the third limit for e^* which is for nonchiral coupling. For chiral coupling, this limit corresponds to $\lambda_\gamma = \sqrt{2}$.

$e^{*\pm}$ — excited electron

Mass $m > 46.1$ GeV, CL = 95% (from $e^{*+}e^{*-}$)
Mass $m > 91$ GeV, CL = 95% (if $\lambda_Z > 1$)
Mass $m > 146$ GeV, CL = 95% (if $\lambda_\gamma = 1$)

$\mu^{*\pm}$ — excited muon

Mass $m > 46.1$ GeV, CL = 95% (from $\mu^{*+}\mu^{*-}$)
Mass $m > 91$ GeV, CL = 95% (if $\lambda_Z > 1$)

$\tau^{*\pm}$ — excited tau

Mass $m > 46.0$ GeV, CL = 95% (from $\tau^{*+}\tau^{*-}$)
Mass $m > 90$ GeV, CL = 95% (if $\lambda_Z > 0.18$)

ν^* — excited neutrino

Mass $m > 47$ GeV, CL = 95% (from $\nu^*\overline{\nu}^*$)
Mass $m > 91$ GeV, CL = 95% (if $\lambda_Z > 1$)

q^* — excited quark

Mass $m > 45.6$ GeV, CL = 95% (from $q^*\overline{q}^*$)
Mass $m > 88$ GeV, CL = 95% (if $\lambda_Z > 1$)
Mass $m > 570$ GeV, CL = 95% ($p\overline{p} \rightarrow q^*X$)

Color Sextet and Octet Particles

Color Sextet Quarks (q_6)

Mass $m > 84$ GeV, CL = 95% (Stable q_6)

Color Octet Charged Leptons (ℓ_8)

Mass $m > 86$ GeV, CL = 95% (Stable ℓ_8)

Color Octet Neutrinos (ν_8)

Mass $m > 110$ GeV, CL = 90% ($\nu_8 \rightarrow \nu g$)

TESTS OF CONSERVATION LAWS

Revised by L. Wolfenstein and T.G. Trippe, June 1996.

In keeping with the current interest in tests of conservation laws, we collect together a Table of experimental limits on all weak and electromagnetic decays, mass differences, and moments, and on a few reactions, whose observation would violate conservation laws. The Table is given only in the full *Review of Particle Physics*, not in the Particle Physics Booklet. For the benefit of Booklet readers, we include the best limits from the Table in the following text. The Table is in two parts: "Discrete Space-Time Symmetries," *i.e.*, C, P, T, CP, and CPT; and "Number Conservation Laws," *i.e.*, lepton, baryon, hadronic flavor, and charge conservation. The references for these data can be found in the the Particle Listings in the *Review*. A discussion of these tests follows.

CPT INVARIANCE

General principles of relativistic field theory require invariance under the combined transformation CPT. The simplest tests of CPT invariance are the equality of the masses and lifetimes of a particle and its antiparticle. The best test comes from the limit on the mass difference between K^0 and $\overline{K}^0$. Any such difference contributes to the CP-violating parameter ϵ. Assuming CPT invariance, ϕ_ϵ, the phase of ϵ should be very close to 44°. (See the "Note on CP Violation in K_L^0 Decay" in the Particle Listings.) In contrast, if the entire source of CP violation in K^0 decays were a $K^0 - \overline{K}^0$ mass difference, ϕ_ϵ would be 44° + 90°. It is possible to deduce that [1]

$$m_{\overline{K}^0} - m_{K^0} \approx \frac{2(m_{K_L^0} - m_{K_S^0})\,|\eta|\,(\frac{2}{3}\phi_{+-} + \frac{1}{3}\phi_{00} - \phi_\epsilon)}{\sin\phi_\epsilon}\,.$$

Using our best values of the CP-violation parameters, we get $|(m_{\overline{K}^0} - m_{K^0})/m_{K^0}| \leq 9 \times 10^{-19}$ (CL = 90%). Limits can also be placed on specific CPT-violating decay amplitudes. Given the small value of $(1-|\eta_{00}/\eta_{+-}|)$, the value of $\phi_{00}-\phi_{+-}$ provides a measure of CPT violation in $K_L^0 \to 2\pi$ decay. Results from CERN [1] and Fermilab [2] indicate no CPT-violating effect.

CP AND T INVARIANCE

Given CPT invariance, CP violation and T violation are equivalent. So far the only evidence for CP or T violation comes from the measurements of η_{+-}, η_{00}, and the semileptonic decay charge asymmetry for K_L, *e.g.*, $|\eta_{+-}| = |A(K_L^0 \to \pi^+\pi^-)/A(K_S^0 \to \pi^+\pi^-)| = (2.285 \pm 0.019) \times 10^{-3}$ and $[\Gamma(K_L^0 \to \pi^- e^+ \nu) - \Gamma(K_L^0 \to \pi^+ e^- \overline{\nu})]/[\text{sum}] = (0.333 \pm 0.014)\%$. Other searches for CP or T violation divide into (a) those that involve weak interactions or parity violation, and (b) those that involve processes otherwise allowed by the strong or electromagnetic interactions. In class (a) the most sensitive are probably the searches for an electric dipole moment of the neutron, measured to be $< 1.1 \times 10^{-25}$ e cm (95% CL), and the electron $(-0.3 \pm 0.8) \times 10^{-26}$ e cm. A nonzero value requires both P and T violation. Class (b) includes the search for C violation in η decay, believed to be an electromagnetic process, *e.g.*, as measured by $\Gamma(\eta \to \mu^+\mu^-\pi^0)/\Gamma(\eta \to \text{all}) < 5 \times 10^{-6}$, and searches for T violation in a number of nuclear and electromagnetic reactions.

CONSERVATION OF LEPTON NUMBERS

Present experimental evidence and the standard electroweak theory are consistent with the absolute conservation of three separate lepton numbers: electron number L_e, muon number L_μ, and tau number L_τ. Searches for violations are of the following types:

a) $\Delta L = 2$ for one type of lepton. The best limit comes from the search for neutrinoless double beta decay $(Z, A) \to (Z+2, A) + e^- + e^-$. The best laboratory limit is $t_{1/2} > 5.6 \times 10^{24}$ yr (CL=90%) for ^{76}Ge.

b) Conversion of one lepton type to another. For purely leptonic processes, the best limits are on $\mu \to e\gamma$ and $\mu \to 3e$, measured as $\Gamma(\mu \to e\gamma)/\Gamma(\mu \to \text{all}) < 5 \times 10^{-11}$ and $\Gamma(\mu \to 3e)/\Gamma(\mu \to \text{all}) < 1.0 \times 10^{-12}$. For semileptonic processes, the best limit comes from the coherent conversion process in a muonic atom, $\mu^- + (Z, A) \to e^- + (Z, A)$, measured as $\Gamma(\mu^-\text{Ti} \to e^-\text{Ti})/\Gamma(\mu^-\text{Ti} \to \text{all}) < 4 \times 10^{-12}$. Of special interest is the case in which the hadronic flavor also changes, as in $K_L \to e\mu$ and $K^+ \to \pi^+ e^- \mu^+$, measured as $\Gamma(K_L \to e\mu)/\Gamma(K_L \to \text{all}) < 3.3 \times 10^{-11}$ and . Limits on the conversion of τ into e or μ are found in τ decay and are much less stringent than those for $\mu \to e$ conversion, *e.g.*, $\Gamma(\tau \to \mu\gamma)/\Gamma(\tau \to \text{all}) < 4.2 \times 10^{-6}$ and $\Gamma(\tau \to e\gamma)/\Gamma(\tau \to \text{all}) < 1.1 \times 10^{-4}$.

c) Conversion of one type of lepton into another type of antilepton. The case most studied is $\mu^- + (Z, A) \to e^+ + (Z-2, A)$, the strongest limit being $\Gamma(\mu^-\text{Ti} \to e^+\text{Ca})/\Gamma(\mu^-\text{Ti} \to \text{all}) < 9 \times 10^{-11}$.

d) Relation to neutrino mass. If neutrinos have mass, then it is expected even in the standard electroweak theory that the lepton numbers are not separately conserved, as a consequence of lepton mixing analogous to Cabibbo quark mixing. However, in this case lepton-number-violating processes such as $\mu \to e\gamma$ are expected to have extremely small probability. For small neutrino masses, the lepton-number violation would be observed first in neutrino oscillations, which have been the subject of extensive experimental searches. For example, searches for $\overline{\nu}_e$ disappearance, which we label as $\overline{\nu}_e \not\to \overline{\nu}_e$, give measured limits $\Delta(m^2) < 0.0075$ eV^2 for $\sin^2(2\theta) = 1$, and $\sin^2(2\theta) < 0.02$ for large $\Delta(m^2)$, where θ is the neutrino mixing angle. Searches for $\nu_\mu \to \nu_e$ limit $\sin^2(2\theta) < 0.0025$ for large $\Delta(m^2)$. For larger neutrino masses ($\gg 1$ keV), lepton-number violation is searched for by looking for anomalous decays such as $\pi \to e\nu_x$, where ν_x is a massive neutrino. If the $\Delta L = 2$ type of violation occurs, it is expected that neutrinos will have a nonzero mass of the Majorana type.

CONSERVATION OF HADRONIC FLAVORS

In strong and electromagnetic interactions, hadronic flavor is conserved, *i.e.* the conversion of a quark of one flavor (d, u, s, c, b, t) into a quark of another flavor is forbidden. In the Standard Model, the weak interactions violate these conservation laws in a manner described by the Cabibbo-Kobayashi-Maskawa mixing (see the section "Cabibbo-Kobayashi-Maskawa Mixing Matrix"). The way in which these conservation laws are violated is tested as follows:

a) $\Delta S = \Delta Q$ rule. In the semileptonic decay of strange particles, the strangeness change equals the change in charge of the hadrons. Tests come from limits on decay rates such as $\Gamma(\Sigma^+ \to ne^+\nu)/\Gamma(\Sigma^+ \to \text{all}) < 5 \times 10^{-6}$, and from a detailed analysis of $K_L \to \pi e \nu$, which yields the parameter x, measured to be $(\text{Re}\,x,\ \text{Im}\,x) = (0.006 \pm 0.018,\ -0.003 \pm 0.026)$. Corresponding rules are $\Delta C = \Delta Q$ and $\Delta B = \Delta Q$.

b) Change of flavor by two units. In the Standard Model this occurs only in second-order weak interactions. The classic example is $\Delta S = 2$ via $K^0 - \overline{K}^0$ mixing, which is directly measured by $m(K_S) - m(K_L) = (3.491 \pm 0.009) \times 10^{-12}$ MeV. There

is now evidence for $B^0 - \overline{B}^0$ mixing ($\Delta B = 2$), with the corresponding mass difference between the eigenstates ($m_{B^0_H} - m_{B^0_L}$) $= (0.73 \pm 0.05)\Gamma_{B^0} = (3.12 \pm 0.21) \times 10^{-10}$ MeV, and for B^0_s–$\overline{B}^0_s$ mixing, with ($m_{B^0_{sH}} - m_{B^0_{sL}}$) $> 9.5\Gamma_{B^0_s}$ or $> 4 \times 10^{-9}$ MeV. No evidence exists for $D^0 - \overline{D}^0$ mixing, which is expected to be much smaller in the Standard Model.

c) Flavor-changing neutral currents. In the Standard Model the neutral-current interactions do not change flavor. The low rate $\Gamma(K_L \to \mu^+\mu^-)/\Gamma(K_L \to \text{all}) = (7.2 \pm 0.5) \times 10^{-9}$ puts limits on such interactions; the nonzero value for this rate is attributed to a combination of the weak and electromagnetic interactions. The best test should come from a limit on $K^+ \to \pi^+\nu\overline{\nu}$, which occurs in the Standard Model only as a second-order weak process with a branching fraction of (1 to 8)$\times 10^{-10}$. The current limit is $\Gamma(K^+ \to \pi^+\nu\overline{\nu})/\Gamma(K^+ \to \text{all}) < 2.4 \times 10^{-9}$. Limits for charm-changing or bottom-changing neutral currents are much less stringent: $\Gamma(D^0 \to \mu^+\mu^-)/\Gamma(D^0 \to \text{all}) < 8 \times 10^{-6}$ and $\Gamma(B^0 \to \mu^+\mu^-)/\Gamma(B^0 \to \text{all}) < 5.9 \times 10^{-6}$. One cannot isolate flavor-changing neutral current (FCNC) effects in non leptonic decays. For example, the FCNC transition $s \to d + (\overline{u} + u)$ is equivalent to the charged-current transition $s \to u + (\overline{u} + d)$. Tests for FCNC are therefore limited to hadron decays into lepton pairs. Such decays are expected only in second-order in the electroweak coupling in the Standard Model.

References

1. R. Carosi *et al.*, Phys. Lett. **B237**, 303 (1990).
2. M. Karlsson *et al.*, Phys. Rev. Lett. **64**, 2976 (1990); L.K. Gibbons *et al.*, Phys. Rev. Lett. **70**, 1199 (1993).
3. B. Schwingenheuer *et al.*, Phys. Rev. Lett. **74**, 4376 (1995).

1. PHYSICAL CONSTANTS

Table 1.1. Reviewed 1995 by B.N. Taylor, NIST. Based mainly on the "1986 Adjustment of the Fundamental Physical Constants" by E.R. Cohen and B.N. Taylor, Rev. Mod. Phys. **59**, 1121 (1987). The last group of constants (beginning with the Fermi coupling constant) comes from the Particle Data Group. The figures in parentheses after the values give the 1-standard-deviation uncertainties in the last digits; the corresponding uncertainties in parts per million (ppm) are given in the last column. This set of constants (aside from the last group) is recommended for international use by CODATA (the Committee on Data for Science and Technology).

Since the 1986 adjustment, new experiments have yielded improved values for a number of constants, including the Rydberg constant R_∞, the Planck constant h, the fine-structure constant α, and the molar gas constant R, and hence also for constants directly derived from these, such as the Boltzmann constant k and Stefan-Boltzmann constant σ. The new results and their impact on the 1986 recommended values are discussed extensively in "Recommended Values of the Fundamental Physical Constants: A Status Report," B.N. Taylor and E.R. Cohen, J. Res. Natl. Inst. Stand. Technol. **95**, 497 (1990); see also E.R. Cohen and B.N. Taylor, "The Fundamental Physical Constants," Phys. Today, August 1995 Part 2, BG9. In general, the new results give uncertainties for the affected constants that are 5 to 7 times smaller than the 1986 uncertainties, but the changes in the values themselves are smaller than twice the 1986 uncertainties. Because the output values of a least-squares adjustment are correlated, the new results cannot readily be incorporated with the 1986 values. Until the next complete adjustment of the constants, the 1986 CODATA set, given (in part) below, remains the set of choice.

Quantity	Symbol, equation	Value	Uncert. (ppm)
speed of light in vacuum	c	299 792 458 m s^{-1}	exact*
Planck constant	h	$6.626\ 075\ 5(40)\times10^{-34}$ J s	0.60
Planck constant, reduced	$\hbar \equiv h/2\pi$	$1.054\ 572\ 66(63)\times10^{-34}$ J s	0.60
		$= 6.582\ 122\ 0(20)\times10^{-22}$ MeV s	0.30
electron charge magnitude	e	$1.602\ 177\ 33(49)\times10^{-19}$ C $= 4.803\ 206\ 8(15)\times10^{-10}$ esu	0.30, 0.30
conversion constant	$\hbar c$	197.327 053(59) MeV fm	0.30
conversion constant	$(\hbar c)^2$	0.389 379 66(23) GeV^2 mbarn	0.59
electron mass	m_e	0.510 999 06(15) MeV/c^2 $= 9.109\ 389\ 7(54)\times10^{-31}$ kg	0.30, 0.59
proton mass	m_p	938.272 31(28) MeV/c^2 $= 1.672\ 623\ 1(10)\times10^{-27}$ kg	0.30, 0.59
		$= 1.007\ 276\ 470(12)$ u $= 1836.152\ 701(37)\ m_e$	0.012, 0.020
deuteron mass	m_d	1875.613 39(57) MeV/c^2	0.30
unified atomic mass unit (u)	(mass ^{12}C atom)/12 = (1 g)/(N_A mol)	931.494 32(28) MeV/c^2 $= 1.660\ 540\ 2(10)\times10^{-27}$ kg	0.30, 0.59
permittivity of free space	ϵ_0	8.854 187 817 ... $\times10^{-12}$ F m^{-1}	exact
permeability of free space	μ_0 ; $\epsilon_0\mu_0 = 1/c^2$	$4\pi \times 10^{-7}$ N A^{-2} $= 12.566\ 370\ 614\ ... \times10^{-7}$ N A^{-2}	exact
fine-structure constant	$\alpha = e^2/4\pi\epsilon_0\hbar c$	$1/137.035\ 989\ 5(61)^\dagger$	0.045
classical electron radius	$r_e = e^2/4\pi\epsilon_0 m_e c^2$	$2.817\ 940\ 92(38)\times10^{-15}$ m	0.13
electron Compton wavelength	$\lambda\!\!\!^{-}_e = \hbar/m_e c = r_e\alpha^{-1}$	$3.861\ 593\ 23(35)\times10^{-13}$ m	0.089
Bohr radius ($m_{\rm nucleus} = \infty$)	$a_\infty = 4\pi\epsilon_0\hbar^2/m_e e^2 = r_e\alpha^{-2}$	$0.529\ 177\ 249(24)\times10^{-10}$ m	0.045
wavelength of 1 eV/c particle	hc/e	$1.239\ 842\ 44(37)\times10^{-6}$ m	0.30
Rydberg energy	$hcR_\infty = m_e e^4/2(4\pi\epsilon_0)^2\hbar^2 = m_e c^2\alpha^2/2$	13.605 698 1(40) eV	0.30
Thomson cross section	$\sigma_T = 8\pi r_e^2/3$	0.665 246 16(18) barn	0.27
Bohr magneton	$\mu_B = e\hbar/2m_e$	$5.788\ 382\ 63(52)\times10^{-11}$ MeV T^{-1}	0.089
nuclear magneton	$\mu_N = e\hbar/2m_p$	$3.152\ 451\ 66(28)\times10^{-14}$ MeV T^{-1}	0.089
electron cyclotron freq./field	$\omega^e_{\rm cycl}/B = e/m_e$	$1.758\ 819\ 62(53)\times10^{11}$ rad s^{-1} T^{-1}	0.30
proton cyclotron freq./field	$\omega^p_{\rm cycl}/B = e/m_p$	$9.578\ 830\ 9(29)\times10^{7}$ rad s^{-1} T^{-1}	0.30
gravitational constant	G_N	$6.672\ 59(85)\times10^{-11}$ m^3 kg^{-1} s^{-2}	128
		$= 6.707\ 11(86)\times10^{-39}$ $\hbar c$ $(GeV/c^2)^{-2}$	128
standard grav. accel., sea level	g	9.806 65 m s^{-2}	exact
Avogadro constant	N_A	$6.022\ 136\ 7(36)\times10^{23}$ mol^{-1}	0.59
Boltzmann constant	k	$1.380\ 658(12)\times10^{-23}$ J K^{-1}	8.5
		$= 8.617\ 385(73)\times10^{-5}$ eV K^{-1}	8.4
molar volume, ideal gas at STP	$N_A k(273.15\ {\rm K})/(101\ 325\ {\rm Pa})$	$22.414\ 10(19)\times10^{-3}$ m^3 mol^{-1}	8.4
Wien displacement law constant	$b = \lambda_{\rm max}T$	$2.897\ 756(24)\times10^{-3}$ m K	8.4
Stefan-Boltzmann constant	$\sigma = \pi^2 k^4/60\hbar^3 c^2$	$5.670\ 51(19)\times10^{-8}$ W m^{-2} K^{-4}	34
Fermi coupling constant‡	$G_F/(\hbar c)^3$	$1.166\ 39(2)\times10^{-5}$ GeV^{-2}	20
weak mixing angle	$\sin^2\widehat{\theta}(M_Z)$ $(\overline{\rm MS})$	0.2315(4)	2200
$W^\pm$ boson mass	m_W	80.33(15) GeV/c^2	1900
Z^0 boson mass	m_Z	91.187(7) GeV/c^2	77
strong coupling constant	$\alpha_s(m_Z)$	0.118(3)	25000

$\pi = 3.141\ 592\ 653\ 589\ 793\ 238$ $\quad e = 2.718\ 281\ 828\ 459\ 045\ 235$ $\quad \gamma = 0.577\ 215\ 664\ 901\ 532\ 861$

1 in $\equiv$ 0.0254 m $\quad$ 1 G $\equiv 10^{-4}$ T $\quad$ 1 eV $= 1.602\ 177\ 33(49) \times 10^{-19}$ J $\quad$ kT at 300 K $= [38.681\ 49(33)]^{-1}$ eV

1 Å $\equiv$ 0.1nm $\quad$ 1 dyne $\equiv 10^{-5}$ N $\quad$ 1 eV/$c^2 = 1.782\ 662\ 70(54) \times 10^{-36}$ kg $\quad$ 0 °C $\equiv$ 273.15 K

1 barn $\equiv 10^{-28}$ m^2 $\quad$ 1 erg $\equiv 10^{-7}$ J $\quad$ $2.997\ 924\ 58 \times 10^9$ esu $= 1$ C $\quad$ 1 atmosphere $\equiv$ 760 torr $\equiv$ 101 325 Pa

* The meter is the length of the path traveled by light in vacuum during a time interval of 1/299 792 458 of a second.

† At $Q^2 = 0$. At $Q^2 \approx m_W^2$ the value is approximately 1/128.

‡ See discussion in Sec. 10 "Standard Model of electroweak interactions."

2. ASTROPHYSICAL CONSTANTS

Table 2.1. Written and revised with the help of K.R. Lang, K.A. Olive, J. Primack, S. Rudaz, E.M. Standish, Jr., and M.S. Turner. The figures in parentheses after some values give the 1-standard deviation uncertainties in the last digit(s). While every effort has been made to obtain the most accurate current values of the listed quantities, the table does not represent a critical review or adjustment of the constants, and is not intended as a primary reference.

Quantity	Symbol, equation	Value	Reference
speed of light	c	299 792 458 m s^{-1}	defined [1]
Newtonian gravitational constant	G_N	$6.672\,59(85) \times 10^{-11}$ $m^3\,kg^{-1}\,s^{-2}$	[2]
astronomical unit	AU	$1.495\,978\,706\,6(2) \times 10^{11}$ m	[3,4]
tropical year (equinox to equinox) (1994)	yr	31 556 925.2 s	[3]
sidereal year (fixed star to fixed star) (1994)		31 558 149.8 s	[3]
mean sidereal day		$23^h\,56^m\,04^s.090\,53$	[3]
Jansky	Jy	10^{-26} W $m^{-2}\,Hz^{-1}$	
Planck mass	$\sqrt{\hbar c/G_N}$	$1.221\,047(79) \times 10^{19}$ GeV/c^2	uses [2]
		$= 2.176\,71(14) \times 10^{-8}$ kg	
parsec (1 AU/1 arc sec)	pc	$3.085\,677\,580\,7(4) \times 10^{16}$ m = 3.262... ly	[5]
light year (deprecated unit)	ly	0.306 6... pc = 0.946 1... $\times 10^{16}$ m	
Schwarzschild radius of the Sun	$2G_N M_\odot/c^2$	2.953 250 08 km	[6]
solar mass	$M_\odot$	$1.988\,92(25) \times 10^{30}$ kg	[7]
solar luminosity	$L_\odot$	3.846×10^{26} W	[8]
solar equatorial radius	$R_\odot$	6.96×10^8 m	[3]
Earth equatorial radius	$R_\oplus$	$6.378\,140 \times 10^6$ m	[3]
Earth mass	$M_\oplus$	$5.973\,70(76) \times 10^{24}$ kg	[9]
luminosity conversion	L	$3.02 \times 10^{28} \times 10^{-0.4\,M_b}$ W	[10]
		(M_b = absolute bolometric magnitude	
		= bolometric magnitude at 10 pc)	
flux conversion	$\mathscr{F}$	$2.52 \times 10^{-8} \times 10^{-0.4\,m_b}$ W m^{-2}	from above
		(m_b = apparent bolometric magnitude)	
$v_\odot$ around center of Galaxy	Θ_o	220(20) km s^{-1}	[11]
solar distance from galactic center	R_o	8.0(5) kpc	[12]
Hubble constant†	H_0	$100\,h_0$ km s^{-1} Mpc^{-1}	
		$= h_0 \times (9.778\,13\ \mathrm{Gyr})^{-1}$	[13]
normalized Hubble constant†	h_0	$0.5 < h_0 < 0.85$	[14,15,16]
critical density of the universe†	$\rho_c = 3H_0^2/8\pi G_N$	$2.775\,366\,27 \times 10^{11}\,h_0^2\,M_\odot Mpc^{-3}$	
		$= 1.878\,82(24) \times 10^{-29}\,h_0^2$ g cm^{-3}	
		$= 1.053\,94(13) \times 10^{-5}\,h_0^2$ GeV cm^{-3}	
local disk density	$\rho_{\,\mathrm{disk}}$	$3\text{–}12 \times 10^{-24}$ g $cm^{-3} \approx 2\text{–}7$ GeV/c^2 cm^{-3}	[17]
local halo density	$\rho_{\,\mathrm{halo}}$	$2\text{–}13 \times 10^{-25}$ g $cm^{-3} \approx 0.1\text{–}0.7$ GeV/c^2 cm^{-3}	[18]
density parameter of the universe†	$\Omega_0 \equiv \rho_0/\rho_c$	$0.1 < \Omega_0 < 2$	[19]
scaled cosmological constant†	$\lambda_0 = \Lambda c^2/3H_0^2$	$-1 < \lambda_0 < 2$	[20,21]
scale factor for cosmological constant†	$c^2/3H_0^2$	$2.853 \times 10^{51}\,h_0^{-2}$ m^2	
age of the universe†	t_0	15(5) Gyr	[10]
	$\Omega_0 h_0^2$	≤ 2.4 for $t_0 \geq 10$ Gyr	[10]
		≤ 1 for $t_0 \geq 10$ Gyr, $h_0 > 0.4$	[10]
cosmic background radiation (CBR) temperature†	T_0	2.726 ± 0.005 K	[22,23]
solar velocity with respect to CBR		369.5 ± 3.0 km s^{-1}	[23,24]
energy density of CBR	ρ_γ	$4.647\,7 \times 10^{-34}\,(T/2.726)^4$ g cm^{-3}	[10,23]
		$= 0.260\,71\,(T/2.726)^4$ eV cm^{-3}	
number density of CBR photons	n_γ	$410.89\,(T/2.726)^3$ cm^{-3}	[10,23]
entropy density/Boltzmann constant	s/k	$2\,892.4\,(T/2.726)^3$ cm^{-3}	[10]

† Subscript 0 indicates present-day values.

References:

1. B.W. Petley, Nature **303**, 373 (1983).
2. E.R. Cohen and B.N. Taylor, Rev. Mod. Phys. **59**, 1121 (1987). The set of constants resulting from this adjustment has been recommended for international use by CODATA (Committee on Data for Science and Technology).
3. *The Astronomical Almanac for the year 1994*, U.S. Government Printing Office, Washington, and Her Majesty's Stationary Office, London (1993). Where possible, the values as adjusted for the fitting of the ephemerides to all the observational data are used.
4. JPL Planetary Ephemerides, E. Myles Standish, Jr., private communication (1989).
5. 1 AU divided by $\pi/648\,000$; quoted error is from the JPL Planetary Ephemerides value of the AU [4].
6. Heliocentric gravitational constant from Ref. 3 times $2/c^2$. The given 9-place accuracy appears to be consistent with uncertainties in actually defining the earth's orbital parameters.
7. Obtained from the heliocentric gravitational constant [3] and G_N [2]. The error is the 128 ppm standard deviation quoted for G_N.
8. It is surprisingly difficult to find a definitive value for this important constant. In all cases, the solar luminosity is calculated as $4\pi \times (1\ \mathrm{AU})^2$ times the solar constant (or total solar irradiance, TSI). The luminosity given is reduced from TSI $= 1367.51 \pm 0.01$ W m^{-2}, obtained from SMM/ACRIMI spacecraft measurements during the interval 2/80–6/89 [25]. While the time constant for energy production by the sun is very long, radiation from the surface might be modulated or otherwise modified by sunspots; this has apparently not been taken into account. Accordingly, we quote 4-place accuracy. We do not know the actual error, but suppose it might be 5 or 10 in the last place. Sackmann *et al.* [26] use TSI $= 1370 \pm 2$ W m^{-2}, but conclude that the solar luminosity ($L_\odot = 3.853 \times 10^{26}$ J s^{-1}) has an uncertainty of 1.5%. Their value is based on three 1977–83 papers, and they comment that the error is based on scatter among the reported values, which is substantially in excess of that expected from the individual quoted errors. The conclusion of the 1971 review by Thekaekara and Drummond [27] ($1353 \pm 1\%$ W m^{-2}) is often quoted [28], and a luminosity based on this value was tabulated in the last two editions of this Review. The conversion to luminosity is not given in the Thekaekara and Drummond paper, and we cannot exactly reproduce the solar luminosity given in Ref. 28. Finally, a value based on the 1954 spectral curve due to Johnson [29] ($1395 \pm 1\%$ W m^{-2}, or $L_\odot = 3.92 \times 10^{26}$ J s^{-1}) has been used widely, and may be the basis for higher value of the solar luminosity and corresponding lower value of the solar absolute bolometric magnitude (4.72) still common in the literature [10].
9. Obtained from the geocentric gravitational constant [3] and G_N [2]. The error is the 128 ppm standard deviation quoted for G_N.
10. E.W. Kolb and M.S. Turner, *The Early Universe*, Addison-Wesley (1990).
11. F.J. Kerr and D. Lynden-Bell, Mon. Not. R. Astr. Soc. **221**, 1023–1038 (1985). "On the basis of this review these [$R_\circ = 8.5 \pm 1.1$ kpc and $\Theta_\circ = 220 \pm 20$ km s^{-1}] were adopted by resolution of IAU Commission 33 on 1985 November 21 at Delhi".
12. M.J. Reid, Annu. Rev. Astron. Astrophys. **31**, 345–372 (1993). Note that $\Theta_\circ$ from the 1985 IAU Commission 33 recommendations is adopted in this review, although the new value for $R_\circ$ is smaller.
13. Conversion using length of tropical year.
14. P.J.E. Peebles, *Principles of Physical Cosmology,* Princeton University Press (1993.).
15. Kolb and Turner [10] give the more conservative limits $0.4 < h_0 < 1$. For other conclusions, see the recent reviews by Jacoby *et al.* [30], who say "Using the weighted or unweighted Virgo distances to bootstrap to the Coma cluster, we find the Hubble constant to be either 80 ± 11 or 73 ± 11 km s^{-1} Mpc^{-1}, respectively," and Huchra [31], who concludes that "Values are still clustered about two numbers, but these numbers are now 50 and 85. A preponderance of the newest local estimates favors the higher value of 85 km s^{-1} Mpc^{-1}...".
16. See the section on the Hubble Constant (Sec. 17 of this *Review*).
17. G. Gilmore, R.F.G. Wyse, and K. Kuijken, Annu. Rev. Astron. Astrophys. **27**, 555 (1989).
18. E.I. Gates, G. Gyuk, and M.S. Turner (Astrophys. J. **449**, L133 (1995)) find the local halo density to be $9.2^{+3.8}_{-3.1} \times 10^{-25}$ g cm^{-3}, but also comment that previously published estimates are in the range $1\text{–}10 \times 10^{-25}$ g cm^{-3}.
    The value 0.3 GeV/c^2 has been taken as "standard" in several papers setting limits on WIMP mass limits, *e.g.* in M. Mori *et al.*, Phys. Lett. **B289**, 463 (1992).
19. Tonry gives $0.2 < \Omega_0 < 2$ [20]. We extend the lower limit so as not to exclude the absence of nonbaryonic dark matter.
20. J. L. Tonry, in *Proc. Texas/PASCOS 92: Relativistic Astrophysics and Particle Cosmology*, ed. C.W. Akerlof and M. Srednicki (Ann. NY Acad. Sci. **688**, 113 (1993).
21. S.M. Carroll and W. H. Press, Annu. Rev. Astron. Astrophys. **30**, 499 (1992).
22. J. C. Mather *et al.*, Astrophy. J. **420**, 439 (1994). Error quoted here is $1\,\sigma$.
23. See the section on Cosmic Background Radiation (Sec. 19 of this *Review*).
24. A. Kogut *et al.*, Astrophy. J. **419**, 1 (1993).
25. R.C. Willson, pp 5–18 in *Atlas of Satellite Observations Related to Global Change*, ed. J.L. Foster and C.L. Parkinson, Cambridge University Press, (1993).
26. I.-J. Sackmann, A.I. Boothroyd, and K.E. Kraemer, Astrophy. J. **418**, 457 (1993).
27. M.P. Thekaekara and A.J. Drummond, Nature Phys. Sci. **229**, 6 (1971).
28. K.R. Lang, *Astrophysical Formulae*, Springer-Verlag (1974);
    K.R. Lang, *Astrophysical Data: Planets and Stars*, Springer-Verlag (1992).
29. F.S. Johnson, J. Meterol. **11**, 431 (1954).
30. G.H. Jacoby *et al.*, J. Astron. Soc. Pacific **104**, 599–662 (1992).
31. J.P. Huchra, Science **256**, 321–325 (1992).

6. ATOMIC AND NUCLEAR PROPERTIES OF MATERIALS

Table 6.1. Table revised May 1996. Gases are evaluated at 20°C and 1 atm (in parentheses) or at STP [square brackets]. Densities and refractive indices without parentheses or brackets are for solids or liquids, or are for cryogenic liquids at the indicated boiling point (BP) at 1 atm. Refractive indices are evaluated at the sodium D line.

Material	Z	A	Nuclear[a] total cross section σ_T {barn}	Nuclear[b] inelastic cross section σ_I {barn}	Nuclear[c] collision length λ_T {g/cm^2}	Nuclear[c] interaction length λ_I {g/cm^2}	$dE/dx\|_{\rm min}$[d] $\left\{\frac{\rm MeV}{\rm g/cm^2}\right\}$	Radiation length[e] X_0 {g/cm^2}	{cm}	Density {g/cm^2} ({g/ℓ} for gas)	Refractive index n ($(n-1)\times10^6$ for gas)
H_2 gas	1	1.01	0.0387	0.033	43.3	50.8	(4.103)	63.05	(752300)	(0.0838)[0.0899]	[139.2]
H_2 (BP 20.39 K)	1	1.01	0.0387	0.033	43.3	50.8	4.045[f]	63.05	890	0.0708	1.112
D_2 (BP 23.65 K)	1	2.01	0.073	0.061	45.7	54.7	(2.052)	125.98	754	0.169[0.179]	1.128 [138]
He (BP 4.224 K)	2	4.00	0.133	0.102	49.9	65.1	(1.937)	94.32	756	0.1248[0.1786]	1.024 [34.9]
Li	3	6.94	0.211	0.157	54.6	73.4	1.639	82.76	155	0.534	—
Be	4	9.01	0.268	0.199	55.8	75.2	1.594	65.19	35.3	1.848	—
C	6	12.01	0.331	0.231	60.2	86.3	1.745	42.70	18.8	2.265[g]	—
N_2 (BP 77.36 K)	7	14.01	0.379	0.265	61.4	87.8	(1.825)	37.99	47.1	0.8073[1.250]	1.205 [298]
O_2 (BP 90.18 K)	8	16.00	0.420	0.292	63.2	91.0	(1.801)	34.24	30.0	1.141[1.428]	1.22 [296]
Ne (BP 27.09 K)	10	20.18	0.507	0.347	66.1	96.6	(1.724)	28.94	24.0	1.206[0.9003]	1.092 [67.1]
Al	13	26.98	0.634	0.421	70.6	106.4	1.615	24.01	8.9	2.70	—
Si	14	28.09	0.660	0.440	70.6	106.0	1.664	21.82	9.36	2.33	—
Ar (BP 87.28 K)	18	39.95	0.868	0.566	76.4	117.2	(1.519)	19.55	14.0	1.393[1.782]	1.233 [283]
Ti	22	47.88	0.995	0.637	79.9	124.9	1.476	16.17	3.56	4.54	—
Fe	26	55.85	1.120	0.703	82.8	131.9	1.451	13.84	1.76	7.87	—
Cu	29	63.55	1.232	0.782	85.6	134.9	1.403	12.86	1.43	8.96	—
Ge	32	72.59	1.365	0.858	88.3	140.5	1.371	12.25	2.30	5.323	—
Sn	50	118.69	1.967	1.21	100.2	163	1.264	8.82	1.21	7.31	—
Xe (BP 165.0 K)	54	131.29	2.120	1.29	102.8	169	(1.255)	8.48	2.40	3.52[5.858]	[701]
W	74	183.85	2.767	1.65	110.3	185	1.145	6.76	0.35	19.3	—
Pt	78	195.08	2.861	1.708	113.3	189.7	1.129	6.54	0.305	21.45	—
Pb	82	207.19	2.960	1.77	116.2	194	1.123	6.37	0.56	11.35	—
U	92	238.03	3.378	1.98	117.0	199	1.082	6.00	≈0.32	≈18.95	—
Air, (20°C, 1 atm.), [STP]					62.0	90.0	(1.815)	36.66	[30420]	(1.205)[1.2931]	(273) [293]
H_2O					60.1	84.9	1.991	36.08	36.1	1.00	1.33
CO_2					62.4	90.5	(1.819)	36.2	[18310]	[1.977]	[410]
Shielding concrete[h]					67.4	99.9	1.711	26.7	10.7	2.5	—
Borosilicate glass (Pyrex)[i]					66.2	97.6	1.695	28.3	12.7	2.23	1.474
SiO_2 (fused quartz)					67.0	99.2	1.70[j]	27.05	12.3	2.20[k]	1.458
Methane (CH_4) (BP 111.7 K)					54.7	74.0	(2.417)	46.5	[64850]	0.4241[0.717]	[444]
Ethane (C_2H_6) (BP 184.5 K)					55.73	75.71	(2.304)	45.66	[34035]	0.509(1.356)[ℓ]	(1.038)[ℓ]
Propane (C_3H_8) (BP 231.1 K)					—	—	(2.262)	—	—	(1.879)	
Isobutane ($(CH_3)_2CHCH_3$) (BP 261.42 K)					56.3	77.4	(2.239)	45.2	[16930]	[2.67]	[1900]
Octane, liquid ($CH_3(CH_2)_6CH_3$)					—	—	2.123	—	—	0.703	
Paraffin wax ($CH_3(CH_2)_nCH_3$, $\langle n\rangle \approx 25$)					—	—	2.087	—	—	0.93	
Nylon, type 6					—	—	1.974	—	—	1.14	
Polycarbonate (Lexan)					—	—	1.886	—	—	1.200	
Polyethylene terephthlate (Mylar) ($C_5H_4O_2$)					60.2	85.7	1.848	39.95	28.7	1.39	—
Polyethylene (monomer $CH_2=CH_2$)					56.9	78.8	2.076	44.8	≈47.9	0.92–0.95	—
Polyimide film (Kapton)					—	—	1.820	—	—	1.420	
Polymethylmethacralate (Lucite, Plexiglas) (monomer ($CH_2=C(CH_3)CO_2CH_3$))					59.2	83.6	1.929	40.55	≈34.4	1.16–1.20	≈1.49
Polystyrene, scintillator (monomer $C_6H_5CH=CH_2$)					58.4	82.0	1.936	43.8	42.4	1.032	1.581
Polytetrafluoroethylene (Teflon) (monomer $CF_2=CF_2$)					—	—	1.671	—	—	2.20	
Polyvinyltolulene, scintillator (monomer 2-$CH_3C_6H_4CH=CH_2$)					—	—	1.956	—	—	1.032	
Barium fluoride (BaF_2)					92.1	146	1.303	9.91	2.05	4.89	1.56
Bismuth germanate (BGO) ($Bi_4Ge_3O_{12}$)					97.4	156	1.251	7.98	1.12	7.1	2.15
Cesium iodide (CsI)					—	167	1.243	8.38	1.85	4.53	1.80
Lithium fluoride (LiF)					62.00	88.24	1.614	39.25	14.91	2.632	1.392
Sodium fluoride (NaF)					66.78	97.57	1.69	29.87	11.68	2.558	1.336
Sodium iodide (NaI)					94.8	152	1.305	9.49	2.59	3.67	1.775
Silica Aerogel[m]					65.5	95.7	1.83	29.85	≈150	0.1–0.3	1.0+0.25ρ
NEMA G10 plate[n]					62.6	90.2	1.87	33.0	19.4	1.7	—

Material	Dielectric constant ($\kappa = \epsilon/\epsilon_0$) () is $(\kappa-1)\times10^6$ for gas	Young's modulus [10^6 psi]	Coeff. of thermal expansion [10^{-6}cm/cm-°C]	Specific heat [cal/g-°C]	Electrical resistivity [$\mu\Omega$cm(@°C)]	Thermal conductivity [cal/cm-°C-sec]
H_2	(253.9)	—	—	—	—	—
He	(64)	—	—	—	—	—
Li	—	—	56	0.86	8.55(0°)	0.17
Be	—	37	12.4	0.436	5.885(0°)	0.38
C	—	0.7	0.6–4.3	0.165	1375(0°)	0.057
N_2	(548.5)	—	—	—	—	—
O_2	(495)	—	—	—	—	—
Ne	(127)	—	—	—	—	—
Al	—	10	23.9	0.215	2.65(20°)	0.53
Si	11.9	16	2.8–7.3	0.162	—	0.20
Ar	(517)	—	—	—	—	—
Ti	—	16.8	8.5	0.126	50(0°)	—
Fe	—	28.5	11.7	0.11	9.71(20°)	0.18
Cu	—	16	16.5	0.092	1.67(20°)	0.94
Ge	16.0	—	5.75	0.073	—	0.14
Sn	—	6	20	0.052	11.5(20°)	0.16
Xe	—	—	—	—	—	—
W	—	50	4.4	0.032	5.5(20°)	0.48
Pt	—	21	8.9	0.032	9.83(0°)	0.17
Pb	—	2.6	29.3	0.038	20.65(20°)	0.083
U	—	—	36.1	0.028	29(20°)	0.064

σ_T, σ_I, λ_T, and λ_I are energy dependent. Values quoted apply to high energy range given in footnote *a* or *b*, where energy dependence is weak.

a. σ_{total} at 80–240 GeV for neutrons ($\approx \sigma$ for protons) from Murthy *et al.*, Nucl. Phys. **B92**, 269 (1975). This scales approximately as $A^{0.77}$.

b. $\sigma_{\text{inelastic}} = \sigma_{\text{total}} - \sigma_{\text{elastic}} - \sigma_{\text{quasielastic}}$; for neutrons at 60–375 GeV from Roberts *et al.*, Nucl. Phys. **B159**, 56 (1979). For protons and other particles, see Carroll *et al.*, Phys. Lett. **80B**, 319 (1979); note that $\sigma_I(p) \approx \sigma_I(n)$. σ_I scales approximately as $A^{0.71}$.

c. Mean free path between collisions (λ_T) or inelastic interactions (λ_I), calculated from $\lambda = A/(N \times \sigma)$, where N is Avogadro's number.

d. For minimum-ionizing heavy particles (calculated for pions; results are very slightly different for other particles). Minimum dE/dx calculated in 1994, using density effect correction coefficients from R. M. Sternheimer, M. J. Berger, and S. M. Seltzer, Atomic Data and Nuclear Data Tables **30**, 261–271 (1984). For electrons and positrons see S.M. Seltzer and M.J. Berger, Int. J. Appl. Radiat. **35**, 665–676 (1984). Ionization energy loss is discussed in Sec. 22.

e. From Y.S. Tsai, Rev. Mod. Phys. **46**, 815 (1974); X_0 data for all elements up to uranium are given. Corrections for molecular binding applied for H_2 and D_2.

f. Density effect constants evaluated for $\rho = 0.0600$ g/cm^3 (H_2 bubble chamber?).

g. For pure graphite; industrial graphite density may vary 2.1–2.3 g/cm^3.

h. Standard shielding blocks, typical composition O_2 52%, Si 32.5%, Ca 6%, Na 1.5%, Fe 2%, Al 4%, plus reinforcing iron bars. The attenuation length, $\ell = 115 \pm 5$ g/cm^2, is also valid for earth (typical $\rho = 2.15$), from CERN-LRL-RHEL Shielding exp., UCRL-17841 (1968).

i. Main components: 80% SiO_2 + 12% B_2O_3 + 5% Na_2O.

j. Calculated using Sternheimer's density effect parameterization for $\rho = 2.32$ g cm^{-3}. Actual value may be slightly lower.

k. For typical fused quartz. The specific gravity of crystalline quartz is 2.64.

ℓ. Solid ethane density at −60°C; gaseous refractive index at 0°C, 546 mm pressure.

m. $n(SiO_2) + 2n(H_2O)$ used in Čerenkov counters, ρ = density in g/cm^3. From M. Cantin *et al.*, Nucl. Instr. and Meth. **118**, 177 (1974).

n. G10-plate, typical 60% SiO_2 and 40% epoxy.

9. QUANTUM CHROMODYNAMICS

9.1. The QCD Lagrangian

Prepared August 1995 by I. Hinchliffe.

Quantum Chromodynamics (QCD), the gauge field theory which describes the strong interactions of colored quarks and gluons, is one of the components of the SU(3)×SU(2)×U(1) Standard Model. A quark of specific flavor (such as a charm quark) comes in 3 colors; gluons come in eight colors; hadrons are color-singlet combinations of quarks, anti-quarks, and gluons. The Lagrangian describing the interactions of quarks and gluons is (up to gauge-fixing terms)

$$L_{\rm QCD} = -\frac{1}{4}F^{(a)}_{\mu\nu}\,F^{(a)\mu\nu} + i\sum_q \overline{\psi}^i_q\,\gamma^\mu\,(D_\mu)_{ij}\,\psi^j_q - \sum_q m_q\,\overline{\psi}^i_q\,\psi_{qi}\ , \tag{9.1}$$

$$F^{(a)}_{\mu\nu} = \partial_\mu\,A^a_\nu - \partial_\nu\,A^a_\mu + g_s\,f_{abc}\,A^b_\mu\,A^c_\nu\ , \tag{9.2}$$

$$(D_\mu)_{ij} = \delta_{ij}\,\partial_\mu - ig_s\sum_a \frac{\lambda^a_{i,j}}{2}A^a_\mu\ , \tag{9.3}$$

where g_s is the QCD coupling constant, and the f_{abc} are the structure constants of the SU(3) algebra (the λ matrices and values for f_{abc} can be found in "SU(3) Isoscalar Factors and Representation Matrices," Sec. 32 of this *Review*). The $\psi^i_q(x)$ are the 4-component Dirac spinors associated with each quark field of (3) color i and flavor q, and the $A^a_\mu(x)$ are the (8) Yang-Mills (gluon) fields. A complete list of the Feynman rules which derive from this Lagrangian, together with some useful color-algebra identities, can be found in Ref. 1.

The principle of "asymptotic freedom" (see below) determines that the renormalized QCD coupling is small only at high energies, and it is only in this domain that high-precision tests—similar to those in QED—can be performed using perturbation theory. Nonetheless, there has been in recent years much progress in understanding and quantifying the predictions of QCD in the nonperturbative domain, for example, in soft hadronic processes and on the lattice [2]. This short review will concentrate on QCD at short distances (large momentum transfers), where perturbation theory is the standard tool. It will discuss the processes that are used to determine the coupling constant of QCD. Other recent reviews of the coupling constant measurements may be consulted for a different perspective [3].

9.2. The QCD coupling and renormalization scheme

The renormalization scale dependence of the effective QCD coupling $\alpha_s = g_s^2/4\pi$ is controlled by the β-function:

$$\mu\frac{\partial\alpha_s}{\partial\mu} = -\frac{\beta_0}{2\pi}\,\alpha_s^2 - \frac{\beta_1}{4\pi^2}\,\alpha_s^3 - \frac{\beta_2}{64\pi^3}\,\alpha_s^4 - \cdots\ , \tag{9.4a}$$

$$\beta_0 = 11 - \frac{2}{3}n_f\ , \tag{9.4b}$$

$$\beta_1 = 51 - \frac{19}{3}n_f\ , \tag{9.4c}$$

$$\beta_2 = 2857 - \frac{5033}{9}n_f + \frac{325}{27}n_f^2\ ; \tag{9.4d}$$

where n_f is the number of quarks with mass less than the energy scale μ. In solving this differential equation for α_s, a constant of integration is introduced. This constant is the one fundamental constant of QCD that must be determined from experiment. The most sensible choice for this constant is the value of α_s at a fixed-reference scale μ_0, but it is more conventional to introduce the dimensional parameter Λ, since this provides a parametrization of the μ dependence of α_s. The definition of Λ is arbitrary. One way to define it (adopted here) is to write a solution of Eq. (9.4) as an expansion in inverse powers of $\ln(\mu^2)$:

$$\alpha_s(\mu) = \frac{4\pi}{\beta_0\,\ln(\mu^2/\Lambda^2)}\left[1 - \frac{2\beta_1}{\beta_0^2}\,\frac{\ln\left[\ln(\mu^2/\Lambda^2)\right]}{\ln(\mu^2/\Lambda^2)} + \frac{4\beta_1^2}{\beta_0^4\ln^2(\mu^2/\Lambda^2)} \times\left(\left(\ln\left[\ln(\mu^2/\Lambda^2)\right] - \frac{1}{2}\right)^2 + \frac{\beta_2\beta_0}{8\beta_1^2} - \frac{5}{4}\right)\right]\ . \tag{9.5a}$$

The last term in this expansion is

$$\mathcal{O}\left(\frac{\ln^2\left[\ln(\mu^2/\Lambda^2)\right]}{\ln^3(\mu^2/\Lambda^2)}\right)\ , \tag{9.5b}$$

and is usually neglected in the definition of Λ. We choose to include it even though its effect on $\alpha_s(\mu)$ is smaller than the experimental errors. For a fixed value of $\alpha_s(M_Z)$, the inclusion of this term shifts the value of Λ by ~ 15 MeV. This solution illustrates the *asymptotic freedom* property: $\alpha_s \to 0$ as $\mu \to \infty$. Alternative definitions of Λ are possible. We adopt this as the standard. Values given by experiments using other definitions are adjusted as needed to meet our definition.

Consider a "typical" QCD cross section which, when calculated perturbatively, starts at $\mathcal{O}(\alpha_s)$:

$$\sigma = A_1\,\alpha_s + A_2\,\alpha_s^2 + \cdots\ . \tag{9.6}$$

The coefficients A_1, A_2 come from calculating the appropriate Feynman diagrams. In performing such calculations, various divergences arise, and these must be regulated in a consistent way. This requires a particular renormalization scheme (RS). The most commonly used one is the modified minimal subtraction ($\overline{\rm MS}$) scheme [4]. This involves continuing momentum integrals from 4 to $4{-}2\epsilon$ dimensions, and then subtracting off the resulting $1/\epsilon$ poles and also $(\ln 4\pi - \gamma_E)$, which is another artifact of continuing the dimension. (Here γ_E is the Euler-Mascheroni constant.) To preserve the dimensionless nature of the coupling, a mass scale μ must also be introduced: $g \to \mu^\epsilon g$. The finite coefficients A_i thus obtained depend implicitly on the renormalization convention used and explicitly on the scale μ.

The first two coefficients (β_0, β_1) in Eq. (9.4) are independent of the choice of RS's. In contrast, the coefficients of terms proportional to α_s^n for $n > 3$ *are* RS-dependent. The form given above for β_2 is in the $\overline{\rm MS}$ scheme. It has become conventional to use the $\overline{\rm MS}$ scheme for calculating QCD cross sections beyond leading order.

The fundamental theorem of RS dependence is straightforward. Physical quantities, in particular the cross section, calculated to all orders in perturbation theory, do not depend on the RS. It follows that a truncated series *does* exhibit RS dependence. In practice, QCD cross sections are known to leading order (LO), or to next-to-leading order (NLO), or in a few cases, to next-to-next-to-leading order (NNLO); and it is only the latter two cases, which have reduced RS dependence, that are useful for precision tests. At NLO the RS dependence is completely given by one condition which can be taken to be the value of the renormalization scale μ. At NNLO this is not sufficient, and μ is no longer equivalent to a choice of scheme; both must now be specified. One, therefore, has to address the question of what is the "best" choice for μ. There is no definite answer to this question—higher-order corrections do not "fix" the scale, rather they render the theoretical predictions less sensitive to its variation.

One could imagine that choosing a scale μ characteristic of the typical energy scale (E) in the process would be most appropriate. In general, a poor choice of scale generates terms of order $\ln(E/\mu)$ in the A_i's. Various methods have been proposed including choosing: the scale for which the next-to-leading-order correction vanishes ("Fastest Apparent Convergence [5]"); the scale for which the next-to-leading-order prediction is stationary [6], (*i.e.*, the value of μ where $d\sigma/d\mu = 0$); or the scale dictated by the effective charge scheme [7] or by the BLM scheme [8]. By comparing the values of α_s that different reasonable schemes give, an estimate of theoretical errors can be obtained.

An important corollary is that if the higher-order corrections are naturally small, then the additional uncertainties introduced by the μ dependence are likely to be less than the experimental measurement errors. There are some processes, however, for which the choice of scheme *can* influence the extracted value of $\Lambda_{\overline{\rm MS}}$. There is no resolution to this problem other than to try to calculate even more terms in the perturbation series. It is important to note that, since the perturbation series is an asymptotic expansion, there is a limit to the precision with which any theoretical quantity can be

calculated. In some processes, the highest-order perturbative terms may be comparable in size to nonperturbative corrections (sometimes called higher-twist or renormalon effects, for a discussion see [9]); an estimate of these terms and their uncertainties is required if a value of α_s is to be extracted.

In the cases where the higher-order corrections to a process are known and are large, some caution should be exercised when quoting the value of α_s. In what follows, we will attempt to indicate the size of the theoretical uncertainties on the extracted value of α_s. There are two simple ways to determine this error. First, we can estimate it by comparing the value of $\alpha_s(\mu)$ obtained by fitting data using the QCD formula to highest known order in α_s, and then comparing it with the value obtained using the next-to-highest-order formula (μ is chosen as the typical energy scale in the process). The corresponding Λ's are then obtained by evolving $\alpha_s(\mu)$ to $\mu = m_Z$ using Eq. (9.4) to the same order in α_s as the fit, and then converting to $\Lambda^{(4)}$ using Eq. (9.7). Alternatively, we can vary the value of μ over a reasonable range, extracting a value of Λ for each choice of μ. This method is of its nature imprecise, since "reasonable" involves a subjective judgment. In either case, if the perturbation series is well behaved, the resulting error on Λ will be small.

In the above discussion we have ignored quark-mass effects, *i.e.*, we have assumed an idealized situation where quarks of mass greater than μ are neglected completely. In this picture, the β-function coefficients change by discrete amounts as flavor thresholds are crossed when integrating the differential equation for α_s. It follows that, for a relationship such as Eq. (9.5) to remain valid for all values of μ, Λ must also change as flavor thresholds are crossed. This leads to the concept of a different Λ for each range of μ corresponding to an effective number of massless quarks: $\Lambda \to \Lambda^{(n_f)}$. There is some arbitrariness in how this relationship is set up. As an idealized case, consider QCD with $n_f - 1$ massless quarks and one quark of mass M. Now imagine an experiment at energy scale μ; for example, this could be $e^+e^- \to$ *hadrons* at center-of-mass energy μ. If $\mu \gg M$, the mass M is negligible and the process is well described by QCD with n_f massless flavors and its parameter $\Lambda^{(n_f)}$ up to terms of order M^2/μ^2. Conversely if $\mu \ll M$, the heavy quark plays no role and the process is well described by QCD with $n_f - 1$ massless flavors and its parameter $\Lambda^{(n_f-1)}$ up to terms of order μ^2/M^2. If $\mu \sim M$, the effects of the quark mass are process-dependent and cannot be absorbed into the running coupling.

A mass scale μ' is chosen where the relationship between $\Lambda^{(n_f-1)}$ and $\Lambda^{(n_f)}$ will be fixed. μ' should be of order M and the relationship should not depend on it. A prescription has been given [10] which has this property. We use this procedure choosing $\mu' = M_Q$, where M_Q is the mass of the value of the running quark mass defined in the $\overline{\rm MS}$ scheme (see the note on "Quark Masses" in the Particle Listings for more details), *i.e.*, where $M_{\overline{\rm MS}}(M_Q) = M_Q$. Then [10]

$$\begin{aligned}
\beta_0^{n_f-1} \ln\left(\frac{\Lambda^{(n_f)}}{\Lambda^{(n_f-1)}}\right)^2 &= (\beta_0^{n_f} - \beta_0^{n_f-1}) \ln\left(\frac{M_Q}{\Lambda^{(n_f)}}^2\right) \\
&+ 2\left(\frac{\beta_1^{n_f}}{\beta_0^{n_f}} - \frac{\beta_1^{n_f-1}}{\beta_0^{n_f-1}}\right) \ln\left[\ln\left(\frac{M_Q}{\Lambda^{(n_f)}}\right)^2\right] \\
&- \frac{2\beta_1^{n_f-1}}{\beta_0^{n_f-1}} \ln\left(\frac{\beta_0^{n_f}}{\beta_0^{n_f-1}}\right) \\
&+ \frac{4\frac{\beta_1^{n_f}}{(\beta_0^{n_f})^2}\left(\frac{\beta_1^{n_f}}{\beta_0^{n_f}} - \frac{\beta_1^{n_f-1}}{\beta_0^{n_f-1}}\right) \ln\left[\ln\left(\frac{M_Q}{\Lambda^{n_f}}\right)^2\right]}{\ln\left(\frac{M_Q}{\Lambda^{(n_f)}}\right)^2} \\
&+ \frac{\frac{1}{\beta_0^{n_f}}\left[\left(\frac{2\beta_1^{n_f}}{\beta_0^{n_f}}\right)^2 - \left(\frac{2\beta_1^{n_f-1}}{\beta_0^{n_f-1}}\right)^2 - \frac{2\beta_2^{n_f}}{\beta_0^{n_f}} + \frac{2\beta_2^{n_f-1}}{\beta_0^{n_f-1}} - \frac{14}{9}\right]}{\ln\left(\frac{M_Q}{\Lambda^{(n_f)}}\right)^2} .
\end{aligned} \tag{9.7}$$

This result is valid to order α_s^3 (or alternatively to terms of order $1/\ln^2[(M_Q/\Lambda^{(n_f)})^2]$).

An alternative matching procedure can be used [11]. This procedure requires the equality $\alpha_s(\mu)^{(n_f)} = \alpha_s(\mu)^{(n_f-1)}$ for $\mu = M_Q$. This matching is somewhat arbitrary; a different relation between $\Lambda^{(n_f)}$ and $\Lambda^{(n_f-1)}$ would result if $\mu = M_Q/2$ were used. In practice, the differences between these procedures are very small. $\Lambda^{(5)} = 200$ MeV corresponds to $\Lambda^{(4)} = 289$ MeV in the scheme of Ref. 11 and $\Lambda^{(4)} = 280$ MeV in the scheme adopted above. Note that the differences between $\Lambda^{(5)}$ and $\Lambda^{(4)}$ are numerically very significant.

Data from deep-inelastic scattering are in a range of energy where the bottom quark is not readily excited, and hence, these experiments quote $\Lambda^{(4)}_{\overline{\rm MS}}$. Most data from PEP, PETRA, TRISTAN, LEP, and SLC quote a value of $\Lambda^{(5)}_{\overline{\rm MS}}$ since these data are in an energy range where the bottom quark is light compared to the available energy. We have converted it to $\Lambda^{(4)}_{\overline{\rm MS}}$ as required. A few measurements, including the lattice gauge theory values from the ψ system and from τ decay are at sufficiently low energy that $\Lambda^{(3)}_{\overline{\rm MS}}$ is appropriate.

We turn now to a discussion of renormalization-scheme dependence in QCD. Although necessarily rather technical, this discussion is vital to understanding how α_s (or Λ) values can be measured and compared. See the review by Duke and Roberts [12] for further details.

In order to compare the values of α_s from various experiments, they must be evolved using the renormalization group to a common scale. For convenience, this is taken to be the mass of the Z boson. This evolution uses third-order perturbation theory and can introduce additional errors particularly if extrapolation from very small scales is used. The variation in the charm and bottom quark masses ($m_b = 4.3 \pm 0.2$ and $m_c = 1.3 \pm 0.3$ are used) can also introduce errors. These result in a fixed value of $\alpha_s(2$ GeV), giving an uncertainty in $\alpha_s(M_Z) = \pm 0.001$ if only perturbative evolution is used. There could be additional errors from nonperturbative effects that enter at low energy. All values are in the $\overline{\rm MS}$ scheme unless otherwise noted.

9.3. QCD in deep-inelastic scattering

The original and still one of the most powerful quantitative tests of perturbative QCD is the breaking of Bjorken scaling in deep-inelastic lepton-hadron scattering. In the leading-logarithm approximation, the measured structure functions $F_i(x, Q^2)$ are related to the quark distribution functions $q_i(x, Q^2)$ according to the naive parton model, by the formulae in "Cross-section Formulae for Specific Processes," Sec. 35 of this *Review*. (In that section, q_i is denoted by the notation f_q). In describing the way in which scaling is broken in QCD, it is convenient to define nonsinglet and singlet quark distributions:

$$F^{NS} = q_i - q_j \qquad F^S = \sum_i (q_i + \overline{q}_i) . \tag{9.8}$$

The nonsinglet structure functions have nonzero values of flavor quantum numbers such as isospin or baryon number. The variation with Q^2 of these is described by the so-called DGLAP equations [13,14]:

$$Q^2 \frac{\partial F^{NS}}{\partial Q^2} = \frac{\alpha_s(|Q|)}{2\pi} P^{qq} * F^{NS} \tag{9.9a}$$

$$Q^2 \frac{\partial}{\partial Q^2}\begin{pmatrix} F^S \\ G \end{pmatrix} = \frac{\alpha_s(|Q|)}{2\pi}\begin{pmatrix} P^{qq} & 2n_f P^{qg} \\ P^{gq} & P^{gg} \end{pmatrix} * \begin{pmatrix} F^S \\ G \end{pmatrix} \tag{9.9b}$$

where $*$ denotes a convolution integral:

$$f * g = \int_x^1 \frac{dy}{y} f(y)\, g\left(\frac{x}{y}\right) . \tag{9.10}$$

The leading-order Altarelli-Parisi [14] splitting functions are

$$P^{qq} = \frac{4}{3}\left[\frac{1+x^2}{(1-x)_+}\right] + 2\delta(1-x) \ , \tag{9.11a}$$

$$P^{qg} = \frac{1}{2}\left[x^2 + (1-x)^2\right] \ , \tag{9.11b}$$

$$P^{gq} = \frac{4}{3}\left[\frac{1+(1-x)^2}{x}\right] \ , \tag{9.11c}$$

$$P^{gg} = 6\left[\frac{1-x}{x} + x(1-x) + \frac{x}{(1-x)_+} + \frac{11}{12}\delta(1-x)\right] - \frac{n_f}{3}\delta(1-x) \ . \tag{9.11d}$$

Here the gluon distribution $G(x,Q^2)$ has been introduced and $1/(1-x)_+$ means

$$\int_0^1 dx \frac{f(x)}{(1-x)_+} = \int_0^1 dx \, \frac{f(x)-f(1)}{(1-x)} \ . \tag{9.12}$$

The precision of contemporary experimental data demands that higher-order corrections also be included [15]. The above results are for massless quarks. Algorithms exist for the inclusion of nonzero quark masses [16]. At low Q^2 values, there are also important "higher-twist" (HT) contributions of the form:

$$F_i(x,Q^2) = F_i^{(LT)}(x,Q^2) + \frac{F_i^{(HT)}(x,Q^2)}{Q^2} + \cdots \ . \tag{9.13}$$

Leading twist (LT) indicates a term whose behavior is predicted by perturbative QCD. These corrections are numerically important only for $Q^2 < \mathcal{O}(10\,\mathrm{GeV}^2)$ except for x very close to 1.

A detailed review of the current status of the experimental data can be found, for example, in Refs. [17–20], and only a brief summary will be presented here. We shall only include determinations of Λ from the recently published results; the earlier editions of this *Review* should be consulted for the earlier data. In any event, the recent results will dominate the average since their errors are smaller. Data have now appeared from HERA at much smaller values of x than the previous data. They provide valuable information about the shape of the antiquark and gluon distribution functions at $x \sim 10^{-3}$ [21].

From Eq. (9.9), it is clear that a nonsinglet structure function offers in principle the most precise test of the theory, since the Q^2 evolution is independent of the unmeasured gluon distribution. The CCFR collaboration fit to the Gross-Llewellyn Smith sum rule [22] is known to order α_s^3 [23]

$$\int_0^1 dx (F_3^{\overline{p}p}(x,Q^2) + F_3^{\nu p}(x,Q^2)) = 3\left[(1 - \frac{\alpha_s}{\pi}(1 + 3.58\frac{\alpha_s}{\pi} + 19.0(\frac{\alpha_s}{\pi})^2) - \Delta HT\right] \ , \tag{9.14}$$

where the higher-twist contribution $\Delta HT = (0.09 \pm 0.045)/Q^2$ [23,24]. Using the CCFR data [25], this gives α_s (1.76 GeV) $= 0.26 \pm 0.035$ (expt.) ± 0.03 (theory). The error from higher-twist terms dominates the theoretical error, the higher-twist term being approximately 50% larger than the α_s^3 term.

A measurement of Λ has been made using F_3 in neutrino scattering [27]. The result is $\Lambda^{(4)}_{\overline{\mathrm{MS}}} = 179 \pm 36 \pm 41$ MeV. The errors are statistical and systematic but do not include (theoretical) errors arising from the choice of μ^2. Measurements involving singlet-dominated structure functions, such as F_2, result in correlated measurements of $\Lambda^{(4)}_{\overline{\mathrm{MS}}}$ and the gluon distribution. By utilizing high-statistics data at large x (> 0.25) and large Q^2, where F_2 behaves like an nonsinglet and F_3 at smaller x, a nonsinglet fit can be performed with better statistical precision, and hence, the error on the measured value of $\Lambda^{(4)}_{\overline{\mathrm{MS}}}$ is much reduced. CCFR gives $\Lambda^{(4)}_{\overline{\mathrm{MS}}} = 210 \pm 28 \pm 41$ MeV [27] from $F_2(\nu N)$ and $F_3(\nu N)$. There is an additional uncertainty of ± 59 MeV from the choice of scale. The NMC collaboration [28] gives $\alpha_s(7\ \mathrm{GeV}^2) = 0.264 \pm 0.018(\mathrm{stat.}) \pm 0.070(\mathrm{syst.}) \pm 0.013(\ \mathrm{higher\text{-}twist})$. The systematic error is larger than the CCFR result, partially because the data are at smaller values of x and the gluon distribution is more important. A reanalysis [29] of EMC data [30] gives $\Lambda^{(4)}_{\overline{\mathrm{MS}}} = 211 \pm 80 \pm 80$ MeV from $F_2(\nu N)$. Finally a combined analysis [31] of SLAC [32] and BCDMS [33] data gives $\Lambda^{(4)}_{\overline{\mathrm{MS}}} = 263 \pm 42 \pm 55$ MeV. Here the systematic error is an estimate of the uncertainty due to the choice of Q^2 used in the argument of α_s, and in the scale at which the structure functions (factorization scale) used in the QCD calculation are evaluated.

The results from Refs. [27–29] and [31] can be combined to give $\alpha_s(M_Z) = 0.112 \pm 0.002 \pm 0.004$, or equivalently $\Lambda^{(4)}_{\overline{\mathrm{MS}}} = 234 \pm 26 \pm 50$ MeV. Here the first error is a combination of statistical and systematic errors, and the second error is due to the scale uncertainty. This result is an average of the results weighted by their statistical and systematic errors. The scale error which is common to all is then reapplied to the average.

The spin-dependent structure functions can also be used to determine α_s. Here the values of $Q^2 \sim 2.5$ GeV^2 are small and higher-twist corrections are again important. The values extracted are consistent with the average quote below [26].

At very small values of x and large Q^2, the x-dependence of the structure functions is predicted by perturbative QCD [34]. Here terms to all orders in $\alpha_s \ln(1/x)$ are summed. The data from HERA [21] on $F_2^{ep}(x,Q^2)$ have been fitted to the this form [35], including the NLO terms which are required to fix the Q^2 scale. The data are dominated by 4 GeV$^2 < Q^2 < 100$ GeV^2. The fit gives $\alpha_s(M_Z) = 0.120 \pm 0.005$ (expt.) ± 0.009 (theory). The dominant part of the theoretical error is from the scale dependence. The fit neglects terms which are suppressed by $1/\ln(1/x)$. Hence, the uncertainties from this source cannot be estimated and are not included in the quoted error. This result is not averaged with the other ones from scaling violations, since the values there are derived from the Q^2 dependence alone, and this possible source of error is not present.

Typically, Λ is extracted from the data by parametrizing the parton densities in a simple analytic way at some Q_0^2, evolving to higher Q^2 using the next-to-leading-order evolution equations, and fitting globally to the measured structure functions to obtain $\Lambda^{(4)}_{\overline{\mathrm{MS}}}$. Thus, an important by-product of such studies is the extraction of parton densities at a fixed-reference value of Q_0^2. These can then be evolved in Q^2 and used as input for phenomenological studies in hadron-hadron collisions (see below). To avoid having to evolve from the starting Q_0^2 value each time, a parton density is required; it is useful to have available a simple analytic approximation to the densities valid over a range of x and Q^2 values. A package is available from the CERN computer library that includes an exhaustive set of fits [36]. Some of these fits are obsolete. In using a parameterization to predict event rates, a next-to-leading order fit must be used if the process being calculated is known to next-to-leading order in QCD perturbation theory. In such a case, there is an additional scheme dependence; this scheme dependence is reflected in the $\mathcal{O}(\alpha_s)$ corrections that appear in the relations between the structure functions and the quark distribution functions. There are two common schemes: a deep-inelastic scheme where there are no order α_s corrections in the formula for $F_2(x,Q^2)$ and the minimal subtraction scheme. It is important when these next-to-leading order fits are used in other processes (see below), that the same scheme is used in the calculation of the partonic rates.

9.4. QCD in decays of the τ lepton

The semi-leptonic branching ratio of the tau ($\tau \to \nu_\tau + hadrons$, R_τ) is an inclusive quantity. It is related to the contribution of hadrons to the imaginary part of the W self energy ($\Pi(s)$). However, it is more inclusive than R since it involves an integral

$$R_\tau \sim \int_0^{m_\tau^2} \frac{ds}{m_\tau^2}(1 - \frac{s}{m_\tau^2})^2 \ \mathrm{Im}\,(\Pi(s)) \ .$$

Since the scale involved is low, one must take into account nonperturbative (higher-twist) contributions which are suppressed by

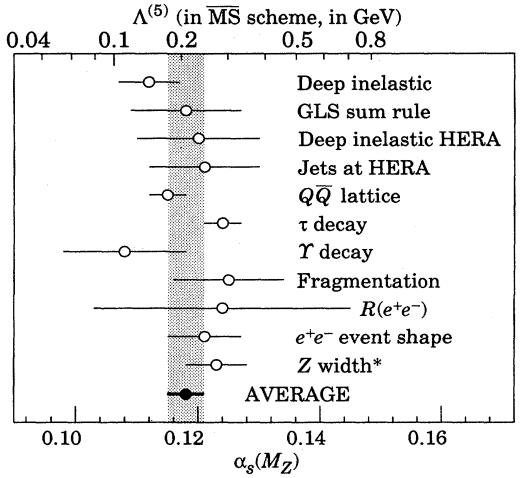

Figure 9.1: Summary of the values of $\alpha_s(M_Z)$ and $\Lambda^{(5)}$ from various processes ordered from top to bottom by increasing energy scale of the measurements. The values shown indicate the process and the measured value of α_s extrapolated up to $\mu = M_Z$. The error shown is the *total* error including theoretical uncertainties. The value denoted by '*' is not used in the average (see text).

powers of the τ mass.

$$R_\tau = 3.058\left[1 + \frac{\alpha_s(m_\tau)}{\pi} + 5.2\left(\frac{\alpha_s(m_\tau)}{\pi}\right)^2 + 26.4\left(\frac{\alpha_s(m_\tau)}{\pi}\right)^3 + a\frac{m^2}{m_\tau^2} + b\frac{m\bar{\psi}\psi}{m_\tau^4} + c\frac{\bar{\psi}\psi\bar{\psi}\psi}{m_\tau^6} + \cdots\right]. \quad (9.15)$$

Here a, b, and c are dimensionless constants and m is a light quark mass. The term of order $1/m_\tau^2$ is a kinematical effect due to the light quark masses and is consequently very small. The nonperturbative terms are estimated using sum rules [37]. In total, they are estimated to be -0.007 ± 0.004 [38]. This estimate relies on there being no term of order Λ^2/m_τ^2 $\left(\text{note that } \frac{\alpha_s(m_\tau)}{\pi} \sim (\frac{0.5\ \text{GeV}}{m_\tau})^2\right)$. The a, b, and c can be determined from the data [39] by fitting to moments of the $\Pi(s)$. The values so extracted [40,41] are consistent with the theoretical estimates. If the nonperturbative terms are omitted from the fit, the extracted value of $\alpha_s(m_\tau)$ decreases by ~ 0.02.

For $\alpha_s(m_\tau) = 0.37$ the perturbative series for R_τ is $R_\tau \sim 3.058(1 + 0.118 + 0.072 + 0.043)$. The size (estimated error) of the nonperturbative term is 20% (7%) of the size of the order α_s^3 term. The perturbation series in not very well convergent; if the order α_s^3 term is omitted, the extracted value of $\alpha_s(m_\tau)$ increases by 0.05. R_τ, can be extracted from the semi-leptonic branching ratio from the relation $R_\tau = 1/(\mathrm{B}(\tau \to e\nu\overline{\nu}) - 1.97256$; where $\mathrm{B}(\tau \to e\nu\overline{\nu})$ is measured directly or extracted from the lifetime, the muon mass and the muon lifetime assuming universality of lepton couplings. Using the average lifetime of 291.3 ± 1.6 fs [42] and a τ mass of $1.776.96 \pm 0.30$ [43] gives $R_\tau = 3.633 \pm 0.031$. Assuming e/μ universality, the data give $\mathrm{B}(\tau \to e\nu\overline{\nu}) = 0.1780 \pm 0.0006$ [44]. Averaging these yields $\alpha_s(m_\tau) = 0.370 \pm 0.008$ using the experimental error alone. This result is consistent with measurements reported recently by other collaborations [45,46]. The value of $\alpha_s(m_\tau) = 0.306 \pm 0.017$ quoted by CLEO [41] uses the measured moments and the average value $\mathrm{B}(\tau \to e\nu\overline{\nu}) = 0.1810 \pm 0.0012$ from the 1992 edition of this review. We assign a theoretical error equal to 1/2 of the contribution from the order α^3 term and all of the nonperturbative contributions. This then gives $\alpha_s(m_\tau) = 0.370 \pm 0.033$ for the final result. Note that the theoretical errors are dominant. The small theoretical errors have been criticized [47].

9.5. QCD in high-energy hadron collisions

There are many ways in which perturbative QCD can be tested in high-energy hadron colliders. The quantitative tests are only useful if the process in question has been calculated beyond leading order in QCD perturbation theory. The production of hadrons with large transverse momentum in hadron-hadron collisions provides a direct probe of the scattering of quarks and gluons: $qq \to qq$, $qg \to qg$, $gg \to gg$, *etc.* The present generation of $p\overline{p}$ colliders provide center-of-mass energies which are sufficiently high that these processes can be unambiguously identified in two-jet production at large transverse momentum. Recent higher-order QCD calculations of the jet rates [48] and shapes are in impressive agreement with data [49]. As an example, Fig. 36.7 in this *Review* shows the inclusive jet cross section at zero pseudorapidity as a function of the jet transverse momentum for $p\overline{p}$ collisions. The QCD prediction combines the parton distributions with the leading-order $2 \to 2$ parton scattering amplitudes. Data are also available on the angular distribution of jets; these are also in agreement with QCD expectations [50,51].

QCD corrections to Drell-Yan type cross sections (*i.e.*, the production in hadron collisions by quark-antiquark annihilation of lepton pairs of invariant mass Q from virtual photons, or of real W or Z bosons), are known [52]. These $\mathcal{O}(\alpha_s)$ QCD corrections are sizable at small values of Q.

It is interesting to note that the corresponding correction to W and Z production, as measured in $p\overline{p}$ collisions at $\sqrt{s} = 0.63$ TeV and $\sqrt{s} = 1.8$ TeV, has essentially the same theoretical form and is of order 30%.

The production of W and Z bosons and photons at large transverse momentum can also be used to determine α_s. The leading-order QCD subprocesses are $q\overline{q} \to \gamma g$ and $qg \to \gamma q$. If the parton distributions are taken from other processes and a value of $\Lambda^{(4)}_{\overline{\rm MS}}$ assumed, then an absolute prediction is obtained. Conversely, the data can be used to extract information on quark and gluon distributions and on the value of $\Lambda^{(4)}_{\overline{\rm MS}}$. The next-to-leading-order QCD corrections are known [53,54] (for photons), and for W/Z production [55], and so a precision test is possible in principle. Data exist from the CDF and DØ collaborations [56,57]. The UA2 collaboration [58] has extracted a value of $\alpha_s(M_W) = 0.123 \pm 0.018(\text{stat.}) \pm 0.017(\text{syst.})$ from the measured ratio $R_W = \dfrac{\sigma(W + 1jet)}{\sigma(W + 0jet)}$. The result depends on the algorithm used to define a jet, and the dominant systematic errors due to fragmentation and corrections for underlying events (the former causes jet energy to be lost, the latter causes it to be increased) are connected to the algorithm. The scale at which $\alpha_s(M)$ is to be evaluated is not clear. A change from $\mu = M_W$ to $\mu = M_W/2$ causes a shift of 0.01 in the extracted α_s. The quoted error should be increased to take this into account. There is dependence on the parton distribution functions, and hence, α_s appears explicitly in the formula for R_W, and implicitly in the distribution functions. The DØ collaboration has performed an analysis similar to UA2. They are unable to obtain a fit where the two values of α_s are consistent with one another, and do not quote a value of α_s [59]. The values from this process are no longer used in determining the overall average value of α_s.

9.6. QCD in heavy-quarkonium decay

Under the assumption that the hadronic and leptonic decay widths of heavy $Q\overline{Q}$ resonances can be factorized into a nonperturbative part—dependent on the confining potential—and a calculable perturbative part, the ratios of partial decay widths allow measurements of α_s at the heavy-quark mass scale. The most precise data come from the decay widths of the 1^{--} $J/\psi(1S)$ and Υ resonances. The total decay width of the Υ is predicted by perturbative QCD [60]

$$R_\Upsilon = \frac{\Gamma(\Upsilon \to \text{hadrons})}{\Gamma(\Upsilon \to \mu^+\mu^-)}$$
$$= \frac{10(\pi^2-9)\alpha_s^3(M)}{9\pi\alpha_{\rm em}^2}$$
$$\times \left[1 + \frac{\alpha_s}{\pi}\left(-19.4 + \frac{3\beta_0}{2}\left(1.162 + \ln\left(\frac{2M}{M_\Upsilon}\right)\right)\right)\right] . \quad (9.16)$$

Data are available for the Υ, Υ', Υ'' and ψ. The result is very sensitive to α_s and the data are sufficiently precise ($R_\mu(\Upsilon) = 32.5 \pm 0.9$) [61] that the theoretical errors will dominate. There are theoretical corrections to this simple formula due to the relativistic nature of the $Q\overline{Q}$ system; $v^2/c^2 \sim 0.1$ for the Υ. They are more severe for the ψ. There are also nonperturbative corrections of the form Λ^2/m_Υ^2; again these are more severe for the ψ. A fit to Υ, Υ', and Υ'' [62] gives $\alpha_s(M_Z) = 0.108 \pm 0.001$ (expt.). The results from each state separately and also from the ψ are consistent with each other. There is an uncertainty of order ± 0.005 from the choice of scale; the error from v^2/c^2 corrections is a little larger. $\alpha_s(M_Z) = 0.108 \pm 0.010$ is a fair representation of the total error including the possibility of nonperturbative corrections.

9.7. Perturbative QCD in e^+e^- collisions

The total cross section for $e^+e^- \to$ hadrons is obtained (at low values of $\sqrt{s}$) by multiplying the muon-pair cross section by the factor $R = 3\Sigma_q e_q^2$. The higher-order QCD corrections to this quantity have been calculated, and the results can be expressed in terms of the factor:

$$R = R^{(0)}\left[1 + \frac{\alpha_s}{\pi} + C_2\left(\frac{\alpha_s}{\pi}\right)^2 + C_3\left(\frac{\alpha_s}{\pi}\right)^3 + \cdots\right] , \quad (9.17)$$

where $C_2 = 1.411$ and $C_3 = -12.8$ [63].

$R^{(0)}$ can be obtained from the formula for $d\sigma/d\Omega$ for $e^+e^- \to f\overline{f}$ by integrating over Ω. The formula is given in Sec. 35.2 of this *Review*. This result is only correct in the zero-quark-mass limit. The $\mathcal{O}(\alpha_s)$ corrections are also known for massive quarks [64]. The principal advantage of determining α_s from R in e^+e^- annihilation is that there is no dependence on fragmentation models, jet algorithms, *etc.*

A comparison of the theoretical prediction of Eq. (9.17) (corrected for the b-quark mass), with all the available data at values of $\sqrt{s}$ between 20 and 65 GeV, gives [65] $\alpha_s(35\text{ GeV}) = 0.146 \pm 0.030$. The size of the order α_s^3 term is of order 40% of that of the order α_s^2 and 3% of the order α_s. If the order α_s^3 term is not included, a fit to the data yields α_s (34 GeV) $= 0.142 \pm 0.03$, indicating that the theoretical uncertainty is smaller than the experimental error.

Measurements of the ratio of hadronic to leptonic width of the Z at LEP and SLC, Γ_h/Γ_μ probe the same quantity as R. Using the average of $\Gamma_h/\Gamma_\mu = 20.788 \pm 0.032$ gives $\alpha_s(M_Z) = 0.123 \pm 0.004 \pm 0.002$ [66]. There are theoretical errors arising from the values of the top-quark and Higgs masses which enter due to electroweak corrections to the Z width and from the choice of scale.

While this method has small theoretical uncertainties from QCD itself, it relies sensitively on the electroweak couplings of the Z to quarks [67]. The experimental results on $\Gamma(Z \to b\overline{b})$ and $\Gamma(Z \to c\overline{c})$ are not in agreement with the Standard Model [68]. If these widths are taken from experiment (rather than from the Standard Model), the extracted vale of $\alpha_s(M_Z)$ is 0.183. If the Standard Model is used for $\Gamma(Z \to c\overline{c})$, $\alpha_s(M_Z) = 0.104$ results. In view of these problems, the value from Γ_h/Γ_μ is not included in the final average.

An alternative method of determining α_s in e^+e^- annihilation is from measuring quantities that are sensitive to the relative rates of two-, three-, and four-jet events. A recent review should be consulted for more details [69] of the issues mentioned briefly here. In addition to simply counting jets, there are many possible choices of such "shape variables": thrust [70], energy-energy correlations [71], planar triple-energy correlations [72], average jet mass, *etc.* All of these are infrared safe, which means they can be reliably calculated in perturbation theory. The starting point for all these quantities is the multijet cross section. For example, at order α_s, for the process $e^+e^- \to qqg$:

$$\frac{1}{\sigma}\frac{d^2\sigma}{dx_1 dx_2} = \frac{2\alpha_s}{3\pi}\frac{x_1^2 + x_2^2}{(1-x_1)(1-x_2)} , \quad (9.18)$$

where

$$x_i = \frac{2E_i}{\sqrt{s}} \quad (9.19)$$

are the center-of-mass energy fractions of the final-state (massless) quarks. A distribution in a "three-jet" variable, such as those listed above, is obtained by integrating this differential cross section over an appropriate phase space region for a fixed value of the variable. The order α_s^2 corrections to this process have been computed, as well as the 4-jet final states such as $e^+e^- \to qqgg$ [73].

There are many methods used by the e^+e^- experimental groups to determine α_s from the event topology. The jet-counting algorithm, originally introduced by the JADE collaboration [74], has been used by the LEP groups. Here, particles of momenta p_i and p_j are combined into a pseudo-particle of momentum $p_i + p_j$ if the invariant mass of the pair is less than $y_0\sqrt{s}$. The process is then iterated until no more pairs of particles or pseudo-particles remain. The remaining number is then defined to be the number of jets in the event, and can be compared to the QCD prediction. The Durham algorithm is slightly different: in computing the mass of a pair of partons, it uses $M^2 = 2\min(E_1^2, E_2^2)(1 - \cos\theta_{ij})$ for partons of energies E_i and E_j separated by angle θ_{ij} [75].

There are theoretical ambiguities in the way this process is carried out. Quarks and gluons are massless, whereas the observed hadrons are not, so that the massive jets that result from this scheme (the so-called E-0 scheme) cannot be compared directly to the massless jets of perturbative QCD. Different recombination schemes have been tried, for example combining 3-momenta and then rescaling the energy of the cluster so that it remains massless (p scheme). These schemes result in the same data giving a slightly different values [76,77] of α_s. These differences can be used to determine a systematic error. In addition, since what is observed are hadrons rather than quarks and gluons, a model is needed to describe the evolution of a partonic final state into one involving hadrons, so that detector corrections can be applied. The QCDmatrix elements are combined with a parton-fragmentation model. This model can then be used to correct the data for a direct comparison with the parton calculation. The different hadronization models that are used [78–81] model the dynamics that are controlled by nonperturbative QCD effects which we cannot yet calculate. The fragmentation parameters of these Monte Carlos are tuned to get agreement with the observed data. The differences between these models contribute to the systematic errors. The systematic errors from recombination schemes and fragmentation effects dominate over the statistical and other errors of the LEP/SLD experiments.

The scale M at which $\alpha_s(M)$ is to be evaluated is not clear. The invariant mass of a typical jet (or $\sqrt{sy_0}$) is probably a more appropriate choice than the e^+e^- center-of-mass energy. If the value is allowed to float in the fit to the data, the data tend to prefer values of order $\sqrt{s}/10$ [82]; the exact value depends on the variable that is fitted. The dominant uncertainties arise from the choice of M and from the freedom in the fragmentation Monte Carlos.

The perturbative QCD formulae can break down in special kinematical configurations. For example, the thrust distribution contains terms of the type $\alpha_s \ln^2(1-T)$. The higher orders in the perturbation expansion contain terms of order $\alpha_s^n \ln^m(1-T)$. For $T \sim 1$ (the region populated by 2-jet events), the perturbation expansion is unreliable. The terms with $n \le m$ can be summed to all orders in α_s [83]. If the jet recombination methods are used higher-order terms involve $\alpha_s^n \ln^m y_0$), these too can be resummed [84]. The resummed results give better agreement with the data at large values of T. Some caution should be exercised in using these resummed results because of the possibility of overcounting; the showering Monte Carlos that are used for the fragmentation corrections also generate

some of these leading-log corrections. Different schemes for combining the order α_s^2 and the resummations are available [85]. These different schemes result in shifts in α_s of order ± 0.002 [86].

An average of the recent results from SLD [86], OPAL [87], L3 [88], ALEPH [89], and DELPHI [90], using the combined α_s^2 and resummation fitting to a large set of shape variables, gives $\alpha_s(M_Z) = 0.122 \pm 0.007$. The errors in the values of $\alpha_s(M_Z)$ from these shape variables are totally dominated by the theoretical uncertainties associated with the choice of scale, and the effects of hadronization Monte Carlos on the different quantities fitted.

Similar studies on event shapes have been undertaken at TRISTAN, at PEP/PETRA, and at CLEO. A combined result from various shape parameters by the TOPAZ collaboration gives α_s (58 GeV) $= 0.125 \pm 0.009$, using the fixed order QCD result, and α_s (58 GeV) $= 0.132 \pm 0.008$ (corresponding to $\alpha_s(M_Z) = 0.123 \pm 0.007$), using the same method as in the SLD and LEP average [91].

The measurements of event shapes at PEP/PETRA are summarized in earlier editions of this note. The results are consistent with those from Z decay, but have larger errors. We use α_s (34 GeV) $= 0.14 \pm 0.02$ [92]. A recent analysis by the TPC group [93] gives α_s (29 GeV) $= 0.160 \pm 0.012$, using the same method as TOPAZ. This value corresponds to $\alpha_s(M_Z) = 0.131 \pm 0.010$

The CLEO collaboration fits to the order α_s^2 results for the two jet fraction at $\sqrt{s} = 10.53$ GeV, and obtains $\alpha_s(10.93) = 0.164 \pm 0.004$ (expt.) ± 0.014 (theory) [94]. The dominant systematic error arises from the choice of scale (μ), and is determined from the range of α_s that results from fit with $\mu = 10.53$ GeV, and a fit where μ is allowed to vary to get the lowest χ^2. The latter results in $\mu = 1.2$ GeV. Since the quoted result corresponds to $\alpha_s(1.2) = 0.35$, it is by no means clear that the perturbative QCD expression is reliable and the resulting error should, therefore, be treated with caution. A fit to many different variables as is done in the LEP/SLC analyses would give added confidence to the quoted error.

Since the errors in the event shape measurements are dominantly systematic, and are common to the experiments, the results from PEP/PETRA, TRISTAN, LEP, SLC, and CLEO are combined to give $\alpha_s(M_Z) = 0.122 \pm 0.007$. This result is used in forming the final average value of α_s.

The total cross section $e^+e^- \to b\bar{b} + X$ near threshold can be used to determine α_s [95]. The result quoted is $\alpha_s(M_Z) = 0.109 \pm 0.001$. The relevant process is only calculated to leading order and the BLM scheme [8] is used. This results in $\alpha_s(0.632\ m_b)$. If $\alpha_s(m_b)$ is used, the resulting $\alpha_s(M_Z)$ shifts to ~ 0.117. This result is not used in the average.

9.8. Scaling violations in fragmentation functions

Measurements of the fragmentation function $d_i(z, E)$, being the probability that a hadron of type i be produced with energy zE in e^+e^- collisions at $\sqrt{s} = 2E$, can be used to determine α_s. As in the case of scaling violations in structure functions, QCD predicts only the E dependence. Hence, measurements at different energies are needed to extract a value of α_s. Because the QCD evolution mixes the fragmentation functions for each quark flavor with the gluon fragmentation function, it is necessary to determine each of these before α_s can be extracted. The ALEPH collaboration has used data from energies ranging from $\sqrt{s} = 22$ GeV to $\sqrt{s} = 91$ GeV. A flavor tag is used to discriminate between different quark species, and the longitudinal and transverse cross sections are used to extract the gluon fragmentation function [96]. The result obtained is $\alpha_s(M_Z) = 0.126 \pm 0.007$ (expt.) ± 0.006 (theory) [97]. The theory error is due mainly to the choice of scale. The OPAL collaboration [98] has also extracted the separate fragmentation functions. DELPHI [99] has also performed a similar analysis using data from other experiments at lower energy with the result $\alpha_s(M_Z) = 0.122 \pm 0.012 \pm 0.006$ (theory). An earlier analysis by this collaboration [100], is consistent with this result, but used fixed order QCD. The older result is not used in the average, which is determined to be $\alpha_s(M_Z) = 0.125 \pm 0.006 \pm 0.006$ (theory)

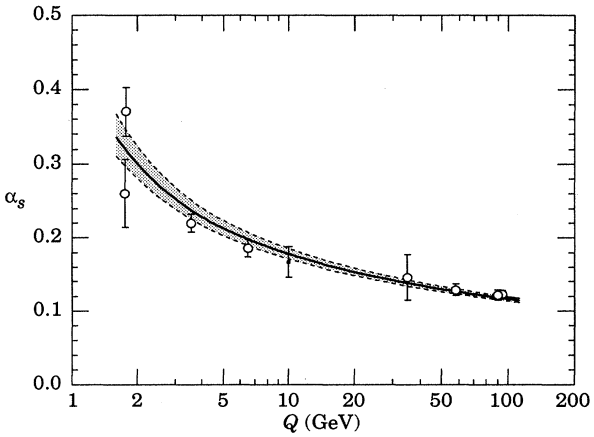

Figure 9.2: Summary of the values of $\alpha_s(Q)$ at the values of Q where they are measured. The lines show the central values and the $\pm 1\sigma$ limits of our average. The figure clearly shows the decrease in $\alpha_s(Q)$ with increasing Q.

9.9. Jet rates in *ep* collisions

At lowest order in α_s, the *ep* scattering process produces a final state of (1+1) jets, one from the proton fragment and the other from the quark knocked out by the process $e + quark \to e + quark$. At next order in α_s, a gluon can be radiated, and hence a (2+1) jet final state produced. By comparing the rates for these (1+1) and (1+2) jet processes, a value of α_s can be obtained. A NLO QCD calculation is available [101]. The basic methodology is similar to that used in the jet counting experiments in e^+e^- annihilation discussed above. Unlike those measurements, the ones in *ep* scattering are not at a fixed value of Q^2. In addition to the systematic errors associated with the jet definitions, there are additional ones since the structure functions enter into the rate calculations. Results from H1 [102] and ZEUS [103] can be combined to give $\alpha_s(M_Z) = 0.121 \pm 0.004$ (stat.) ± 0.008 (syst.). The contributions to the systematic errors from experimental effects (mainly the hadronic energy scale) are comparable to the theoretical ones arising from scale choice, structure functions, and jet definitions. These errors are common to the two measurements; therefore, we have not reduced the systematic error after forming the average.

9.10. Lattice QCD

Lattice gauge theory calculations can be used to calculate the energy levels of a $Q\overline{Q}$ system and then extract α_s. The masses of the $Q\overline{Q}$ states depend only on the quark mass and on α_s. A limitation is that calculations cannot be performed for three light quark flavors. Results are available for zero (quenched approximation) and two light flavors, which allow extrapolation to three. The coupling constant so extracted is in a lattice renormalization scheme, and must be converted to the $\overline{\rm MS}$ scheme for comparison with other results. Using the mass differences of Υ and Υ' and Υ and χ_b, Davies *et al.* [104] extract a value of $\alpha_s(M_Z) = 0.115 \pm 0.002$. The result is consistent with an earlier result by the same group based on quenched approximation ($\alpha_s(M_Z) = 0.112 \pm 0.004$) [105]. The error is dominated by the conversion between the coupling constants, which is performed at next-to-leading order in perturbation theory. It is estimated by making an assumption about the size of the NNLO term in this conversion. If it is estimated as one-half of the NLO term, then the resulting value is $\alpha_s(M_Z) = 0.115 \pm 0.003$.

A similar result with larger errors is reported by [106], where results are consistent with $\alpha_s(M_Z) = 0.111 \pm 0.006$. This result confirms that obtained in quenched approximation by [107]. A calculation [108] using the strength of the force between two heavy quarks computed in the quenched approximation obtains a value of $\alpha_s(5$ GeV) that is consistent with these results.

The result with a more conservative error $\alpha_s(M_Z) = 0.115 \pm 0.003$ will be used in the average, although a recent reviewer quotes an error of ± 0.007 [109].

9.11. Conclusions

The need for brevity has meant that many other important topics in QCD phenomenology have had to be omitted from this review. One should mention in particular the study of exclusive processes (form factors, elastic scattering, ...), the behavior of quarks and gluons in nuclei, the spin properties of the theory, the interface of soft and hard QCD as manifest, for example, by minijet production and hard diffractive processes, and QCD effects in hadron spectroscopy.

In this short review, we have focused on those high-energy processes which currently offer the most quantitative tests of perturbative QCD. Figure 9.1 shows the values of $\alpha_s(M_Z)$ deduced from the various experiments. Figure 9.2 shows the values and the values of Q where they are measured. This figure clearly shows the experimental evidence for the variation of $\alpha_s(Q)$ with Q.

An average of the values in Fig. 9.1 (except the one from the width of the Z) gives $\alpha_s(M_z) = 0.118$, with a total χ^2 of 9.1 for ten fitted points, showing good consistency among the data. The error on the average, assuming that all of the errors in the contributing results are uncorrelated, is ± 0.0017, and is surely an underestimate. All the values are dominated by systematic, usually theoretical, errors. The two results with the smallest errors (± 0.003) are the ones from τ decay and lattice gauge theory. If these errors are increased to ± 0.006, the average is unchanged. There has been discussion of systematic differences in the data. The measurements which are dominated by low-energy (deep-inelastic scattering (not including HERA), τ decay, Υ width, lattice) average to $\alpha_s(M_z) = 0.118$ ($\chi^2 = 8.3$ for 5 points). Results from space-like momentum transfers (all ep results) average to $\alpha_s(M_z) = 0.114 \pm 0.004$, which might indicate some lack of theoretical understanding in comparing the data. Since, in most cases, the dominant error is systematic (mainly theoretical), a more conservative estimate of the final error is obtained by using the smallest of the individual errors on the experimental results, *i.e.*, ± 0.003. Our average value is then $\alpha_s(M_z) = 0.118 \pm 0.003$, which corresponds to $\Lambda^{(5)} = 209^{+39}_{-33}$ MeV.

References:

1. F.J. Yndurain, "Quantum Chromodynamics: an Introduction to the Theory of Quarks and Gluons", (Springer, New York, 1983); CTEQ Collaboration, Rev. Mod. Phys. **67**, 157 (1995).
2. For a recent review, see for example A.S. Kronfeld and P.B. Mackenzie, Ann. Rev. Nucl. and Part. Sci. **43**, 793 (1993).
3. For example see, B.R. Webber, in *Proceedings of the XXVII International Conference on High Energy Physics*, Glasgow, Scotland (July 1994); S. Bethke, at QCD94, Montpellier, France (July 1994).
4. W.A. Bardeen *et al.*, Phys. Rev. **D18**, 3998 (1978).
5. G. Grunberg, Phys. Lett. **95B**, 70 (1980), and Phys. Rev. **D29**, 2315 (1984).
6. P.M. Stevenson, Phys. Rev. **D23**, 2916 (1981), and Nucl. Phys. **B203**, 472 (1982).
7. S. Brodsky and H.J. Lu SLAC-PUB-6389 (Nov. 1993).
8. S. Brodsky, G.P. Lepage, and P.B. Mackenzie, Phys. Rev. **D28**, 228 (1983).
9. A.H. Mueller, Phys. Lett. **B308**, 355, (1993).
10. W. Bernreuther, Annals of Physics 151,127(1983).
11. W. Marciano, Phys. Rev. **D29**, 580 (1984).
12. D.W. Duke and R.G. Roberts, Phys. Reports **120**, 275 (1985).
13. V.N. Gribov and L.N. Lipatov, Sov. J. Nucl. Phys. **15**, 438 (1972); Yu.L. Dokshitzer, Sov. Phys. JETP **46**, 641 (1977).
14. G. Altarelli and G. Parisi, Nucl. Phys. **B126**, 298 (1977).
15. G. Curci, W. Furmanski, and R. Petronzio, Nucl. Phys. **B175**, 27 (1980); W. Furmanski and R. Petronzio, Phys. Lett. **97B**, 437 (1980), and Z. Phys. **C11**, 293 (1982); E.G. Floratos, C. Kounnas, and R. Lacaze, Phys. Lett. **98B**, 89 (1981), Phys. Lett. **98B**, 285 (1981), and Nucl. Phys. **B192**, 417 (1981); R.T. Herrod and S. Wada, Phys. Lett. **96B**, 195 (1981), and Z. Phys. **C9**, 351 (1981).
16. M. Glück *et al.*, Z. Phys. **C13**, 119 (1982).
17. M. Virchaux, Saclay preprint, DAPHNIA/SPP 92-30, in *Proceedings of the "QCD 20 years later" Workshop*, Aachen Germany, p. 205 (June 9–13, 1992).
18. R. Voss, in *Proceedings of the 1993 International Symposium on Lepton and Photon Interactions at High Energies, Ithaca, NY*, p. 144 (July 1993).
19. J. Feltese, in *Proceedings of the XXVII International Conference on High Energy Physics*, Glasgow, Scotland, July 1994.
20. F. Eisele, at the European Physical Society meeting, Brussels, (July 1995).
21. M. Derrick *et al.*, Phys. Lett. **B345**, 576 (1995); S. Aid *et al.*, Phys. Lett. **B354**, 494 (1995).
22. D. Gross, and Llewellyn Smith, Nucl. Phys. **B14**, 337 (1969).
23. J. Chyla and A.L. Kataev, Phys. Lett. **B297**, 385 (1992).
24. V.M. Braun and A.V. Kolesnichenko, Nucl. Phys. **B283**, 723 (1987).
25. W.C. Leung *et al.*, Phys. Lett. **B317**, 655 (1993); J. Kim at the European Physical Society meeting, Brussels, (July 1995).
26. J. Ellis and M. Karliner, Phys. Lett. **B341**, 397 (1995).
27. P.Z. Quintas *et al.*, Phys. Rev. Lett. **71**, 1307 (1993); J.P. Berge *et al.*, Z. Phys. **C49**, 187 (1991).
28. M. Arneodo *et al.*, Phys. Lett. **B309**, 222 (1993).
29. K. Bazizi and S.J. Wimpenny, UCR/DIS/91-02.
30. J.J. Aubert *et al.*, Nucl. Phys. **B333**, 1 (1990); Nucl. Phys. **293**, 740 (1987); Nucl. Phys. **B272**, 158 (1986); and Nucl. Phys. **B145**, 189 (1985).
31. M. Virchaux and A. Milsztajn, Phys. Lett. **B274**, 221 (1992).
32. L.W. Whitlow, Ph.D thesis, SLAC Report 357 (1990).
33. A.C. Benvenuti *et al.*, Phys. Lett. **B195**, 97 (1987); Phys. Lett. **B223**, 490 (1989); Phys. Lett. **B223**, 485, (1989); Phys. Lett. **B237**, 592 (1990); and Phys. Lett. **B237**, 599 (1990).
34. E.A. Kurayev, L.N. Lipatov, and V.S. Fadin, Sov. Phys. JETP **45**, 119 (1977); Ya.Ya. Balitsky, and L.N. Lipatov, Sov. J. Nucl. Phys. **28**, 882 (1978).
35. R.D. Ball and S. Forte, CERN-TH/95-148 (1995).
36. H. Plothow-Besch, Comp. Phys. Comm. **75**, 396 (1993).
37. M.A. Shifman, A.I Vainshtein, and V.I. Zakharov Nucl. Phys. **B147**, 385 (1979).
38. S. Narison and A. Pich, Phys. Lett. **B211**, 183 (1988); E. Braaten, S. Narison, and A. Pich, Nucl. Phys. **B373**, 581 (1992).
39. F. Le Diberder and A. Pich, Phys. Lett. **B289**, 165 (1992).
40. D. Buskulic *et al.*, Phys. Lett. **B307**, 209 (1993).
41. T. Coan *et al.*, CLNS 95/1332 (1995).
42. S.R. Wasserbaech, Aleph number PUB 95-06, Talk given at the Workshop on the Tau/Charm Factory, (June 1995, Argonne).
43. J.Z. Bai *et al.*, SLAC-PUB-95-6930 (1995).
44. G. Rahal-Callot, talk at European Physical Society meeting, Brussels (July 1995).
45. D. Buskulic *et al.*, Nucl. Phys. **B** (Proc. Suppl.) Vol. **40** (1995).
46. R. Akers *et al.*, CERN-PPE/95-06 (1995).
47. G. Altarelli, CERN-TH 7493/94 (1994); G. Altarelli, P. Nason, and G. Ridolfi, Z. Phys. **C68**, 257 (1995).
48. S.D. Ellis, Z. Kunszt,and D.E. Soper, Phys. Rev. Lett. **64**, 2121 (1991); W.T. Giele, E.W.N. Glover, and D. Kosower, Phys. Rev. Lett. **73**, 2019 (1994).

49. F. Abe *et al.*, Phys. Rev. Lett. **68**, 1104 (1992).
50. UA1 Collaboration: G. Arnison *et al.*, Phys. Lett. **B177**, 244 (1986).
51. F. Abe *et al.*, Phys. Rev. Lett. **64**, 157 (1990).
52. G. Altarelli, R.K. Ellis, and G. Martinelli, Nucl. Phys. **B143**, 521 (1978).
53. P. Aurenche, R. Baier, and M. Fontannaz, Phys. Rev. **D42**, 1440 (1990);
    P. Aurenche *et al.*, Phys. Lett. **140B**, 87 (1984);
    P. Aurenche *et al.*, Nucl. Phys. **B297**, 661 (1988).
54. H. Baer, J. Ohnemus, and J.F. Owens, Phys. Lett. **B234**, 127 (1990).
55. H. Baer and M.H. Reno, Phys. Rev. **D43**, 2892 (1991);
    P.B. Arnold and M.H. Reno, Nucl. Phys. **B319**, 37 (1989).
56. F. Abe *et al.*, Phys. Rev. Lett. **73**, 2662 (1994).
57. S. Abachi *et al.*, FERMILAB-CONF-95-215E (1995).
58. J. Alitti *et al.*, Phys. Lett. **B263**, 563 (1991).
59. DØ Collaboration, submitted to European Physical Society meeting, Brussels, (July 1995).
60. R. Barbieri *et al.*, Phys. Lett. **95B**, 93 (1980);
    B.P. Mackenzie and G.P. Lepage, Phys. Rev. Lett. **47**, 1244 (1981).
61. M. Kobel *et al.*, Z. Phys. **C53**, 193 (1992).
62. M. Kobel DESY-F31-91-03.
63. S.G. Gorishny, A. Kataev, and S.A. Larin, Phys. Lett. **B259**, 114 (1991);
    L.R. Surguladze and M.A. Samuel, Phys. Rev. Lett. **66**, 560 (1991).
64. K.G. Chetyrkin, J.H. Kuhn (Karlsruhe U., ITTP) Phys. Lett. **B308**, 127 (1993).
65. D. Haidt, in *Directions in High Energy Physics*, vol. 14, p. 201 Ed. P. Langacker (World Scientific, 1995).
66. A. Olchevsi, at the European Physical Society meeting, Brussels, (July 1995).
67. A. Blondel and C. Verzgrassi, Phys. Lett. **B311**, 346 (1993);
    G. Altarelli *et al.*, Nucl. Phys. **B405**, 3 (1993).
68. See the sections on "Constraints on New Physics from Electroweak Analyses" (Sec. 14) and "Standard Model of Electroweak Interactions" (Sec. 10) in this *Review*.
69. S. Bethke and J. Pilcher, Ann. Rev. Nucl. and Part. Sci. **42**, 251 (1992).
70. E. Farhi, Phys. Rev. Lett. **39**, 1587 (1977).
71. C.L. Basham *et al.*, Phys. Rev. **D17**, 2298 (1978).
72. F. Csikor *et al.*, Phys. Rev. **D31**, 1025 (1985).
73. R.K. Ellis, D.A. Ross, T. Terrano, Phys. Rev. Lett. **45**, 1226 (1980);
    Z. Kunszt and P. Nason, ETH-89-0836 (1989).
74. S. Bethke *et al.*, Phys. Lett. **B213**, 235 (1988).
75. S. Bethke *et al.*, Nucl. Phys. **B370**, 310 (1992).
76. M.Z. Akrawy *et al.*, Z. Phys. **C49**, 375 (1991).
77. K. Abe *et al.*, Phys. Rev. Lett. **71**, 2578 (1993).
78. B. Andersson *et al.*, Phys. Reports **97**, 33 (1983).
79. A. Ali *et al.*, Nucl. Phys. **B168**, 409 (1980);
    A. Ali and R. Barreiro, Phys. Lett. **118B**, 155 (1982).
80. B.R. Webber, Nucl. Phys. **B238**, 492 (1984).
81. T. Sjostrand and M. Bengtsson, Comp. Phys. Comm. **43**, 367 (1987).
82. O. Adriani *et al.*, Phys. Lett. **B284**, 471 (1992);
    M. Akrawy *et al.*, Z. Phys. **C47**, 505 (1990);
    B. Adeva *et al.*, Phys. Lett. **B248**, 473 (1990);
    P. Abreu *et al.*Z. Phys. **C54**, 55 (1992);
    D. Decamp *et al.*, Phys. Lett. **B255**, 623 (1991).
83. S. Catani *et al.*, Phys. Lett. **B263**, 491 (1991).
84. S. Catani *et al.*, Phys. Lett. **B269**, 432 (1991);
    S. Catani, B.R. Webber, and G. Turnock, Phys. Lett. **B272**, 368 (1991);
    N. Brown and J. Stirling, Z. Phys. **C53**, 629 (1992).
85. G. Turnock, Cavendish preprint HEP-92/3;
    G. Catani, G. Turnock, and B.R. Webber CERN-TH-6570/92 (1992);
    S. Catani *et al.*, Phys. Lett. **B269**, 432 (1991).
86. K. Abe *et al.*, Phys. Rev. **D51**, 962 (1995).
87. P.D. Acton *et al.*, Z. Phys. **C55**, 1 (1992).
88. O. Adriani *et al.*, Phys. Lett. **B284**, 471 (1992).
89. D. Decamp *et al.*, Phys. Lett. **B284**, 163 (1992).
90. P. Abreu *et al.*, Z. Phys. **C59**, 21 (1993).
91. Y. Onishi *et al.*, Phys. Lett. **B313**, 475 (1993).
92. W.J. Stirling and M.R. Whalley, Durham-RAL Database Publication RAL/87/107 (1987).
93. D.A. Bauer *et al.*, SLAC-PUB-5618.
94. L. Gibbons *et al.*, CLNS 95-1323 (1995).
95. M.B. Voloshin, Int. J. Mod. Phys. **A10**, 2865 (1995).
96. P. Nason and B.R. Webber Nucl. Phys. **B421**, 473 (1994).
97. D. Buskulic *et al.*, CERN-PPE-95-096, to appear in Phys. Lett. (1995).
98. OPAL Collaboaration, CERN-PPE/95-57 to appear in Zeit. fur Physik C (1995).
99. DELPHI Collaboration, DELPH 95-93, submitted to the European Physical Society meeting, Brussels, (July 1995).
100. P. Abreu *et al.*, Phys. Lett. **B311**, 408 (1993).
101. D. Graudenz, Phys. Rev. **D49**, 3921 (1994), J.G. Korner, E. Mirkes, and G.A. Schuler, Int. J. Mod. Phys. **A4**, 1781, (1989).
102. H1 Collaboration submitted to the European Physical Society meeting, Brussels, (July 1995).
103. ZEUS Collaboration submitted to the European Physical Society meeting, Brussels, (July 1995);
    S.L. Wu, in *Proceedings of the 1987 International Symposium on Lepton and Photon Interactions at High Energies, Hamburg*, 27–31 July 1987, ed. by W. Bartel and R. Ruckl (North-Holland, Amsterdam, 1988), p. 39;
    W.J. Stirling, in *Proceedings of the 1987 International Symposium on Lepton and Photon Interactions at High Energies, Hamburg*, 27–31 July 1987, ed. by W. Bartel and R. Ruckl (North-Holland, Amsterdam, 1988), p. 715.
104. C.T.H. Davies *et al.*, Phys. Lett. **B345**, 42 (1995).
105. G.P. Lepage and J. Sloan presented at 1993 Lattice conference, hep-lat/9312070.
106. S. Aoki *et al.*, Phys. Rev. Lett. **74**, 222 (1995).
107. A.X. El-Khadra *et al.*, Phys. Rev. Lett. **69**, 729 (1992);
    A.X. El-Khadra, presented at 1993 Lattice conference, OHSTPY-HEP-T-93-020 (1993);
    A.X. El-Khadra *et al.*, FNAL 94-091/T (1994).
108. M. Luscher *et al.*, CERN-TH 6996/93 (1993).
109. C. Michael presented at the 1995 Lepton-Photon Symposium, Beijing, China.

10. STANDARD MODEL OF ELECTROWEAK INTERACTIONS

This section prepared July 1995 by P. Langacker and J. Erler.

The standard electroweak model is based on the gauge group [1] SU(2) × U(1), with gauge bosons W^i_μ, $i = 1,2,3$, and B_μ for the SU(2) and U(1) factors, respectively, and the corresponding gauge coupling constants g and g'. The left-handed fermion fields $\psi_i = \begin{pmatrix} \nu_i \\ \ell_i^- \end{pmatrix}$ and $\begin{pmatrix} u_i \\ d_i' \end{pmatrix}$ of the i^{th} fermion family transform as doublets under SU(2), where $d_i' \equiv \sum_j V_{ij}\, d_j$, and V is the Cabibbo-Kobayashi-Maskawa mixing matrix. (Constraints on V are discussed in the section on the Cabibbo-Kobayashi-Maskawa mixing matrix.) The right-handed fields are SU(2) singlets. In the minimal model there are three fermion families and a single complex Higgs doublet $\phi \equiv \begin{pmatrix} \phi^+ \\ \phi^0 \end{pmatrix}$.

After spontaneous symmetry breaking the Lagrangian is

$$\begin{aligned}\mathscr{L}_F = &\sum_i \overline{\psi}_i \left(i\, \partial\!\!\!/ - m_i - \frac{g m_i H}{2M_W} \right) \psi_i \\ &- \frac{g}{2\sqrt{2}} \sum_i \overline{\psi}_i\, \gamma^\mu\, (1-\gamma^5)(T^+\, W_\mu^+ + T^-\, W_\mu^-)\, \psi_i \\ &- e \sum_i q_i\, \overline{\psi}_i\, \gamma^\mu\, \psi_i\, A_\mu \\ &- \frac{g}{2\cos\theta_W} \sum_i \overline{\psi}_i\, \gamma^\mu (g_V^i - g_A^i \gamma^5)\, \psi_i\, Z_\mu\ . \end{aligned} \tag{10.1}$$

$\theta_W \equiv \tan^{-1}(g'/g)$ is the weak angle; $e = g \sin\theta_W$ is the positron electric charge; and $A \equiv B\cos\theta_W + W^3 \sin\theta_W$ is the (massless) photon field. $W^\pm \equiv (W^1 \mp i W^2)/\sqrt{2}$ and $Z \equiv -B\sin\theta_W + W^3 \cos\theta_W$ are the massive charged and neutral weak boson fields, respectively. T^+ and T^- are the weak isospin raising and lowering operators. The vector and axial couplings are

$$g_V^i \equiv t_{3L}(i) - 2 q_i \sin^2\theta_W \tag{10.2}$$

$$g_A^i \equiv t_{3L}(i)\ , \tag{10.3}$$

where $t_{3L}(i)$ is the weak isospin of fermion i ($+1/2$ for u_i and ν_i; $-1/2$ for d_i and e_i) and q_i is the charge of ψ_i in units of e.

The second term in $\mathscr{L}_F$ represents the charged-current weak interaction [2]. For example, the coupling of a W to an electron and a neutrino is

$$-\frac{e}{2\sqrt{2}\sin\theta_W} \left[W_\mu^-\ \overline{e}\, \gamma^\mu (1-\gamma^5)\nu + W_\mu^+\ \overline{\nu}\, \gamma^\mu\, (1-\gamma^5) e \right]\ . \tag{10.4}$$

For momenta small compared to M_W, this term gives rise to the effective four-fermion interaction with the Fermi constant given (at tree level, *i.e.*, lowest order in perturbation theory) by $G_F/\sqrt{2} = g^2/8M_W^2$. CP violation is incorporated in the Standard Model by a single observable phase in V_{ij}. The third term in $\mathscr{L}_F$ describes electromagnetic interactions (QED), and the last is the weak neutral-current interaction.

In Eq. (10.1), m_i is the mass of the i^{th} fermion ψ_i. For the quarks these are the current masses. For the light quarks, as described in the Particle Listings, $m_u \approx$ 2–8 MeV, $m_d \approx$ 5–15 MeV, and $m_s \approx$ 100–300 MeV (these are running masses evaluated at 1 GeV). For the heavier quarks, the "pole" masses are $m_c \approx$ 1.2–1.9 GeV and $m_b \approx$ 4.5–4.9 GeV. The average of the recent CDF [4] and DØ [5] values for m_t is 180 ± 12 GeV. See "The Note on Quark Masses" in the Particle Listings for more information.

H is the physical neutral Higgs scalar which is the only remaining part of ϕ after spontaneous symmetry breaking. The Yukawa coupling of H to ψ_i, which is flavor diagonal in the minimal model, is $g m_i/2M_W$. The H mass is not predicted by the model. Experimental limits are given in the Higgs section. In nonminimal models there are additional charged and neutral scalar Higgs particles [6].

10.1. Renormalization and radiative corrections

The Standard Model has three parameters (not counting M_H and the fermion masses and mixings). A particularly useful set is:

(*a*) The fine structure constant $\alpha = 1/137.036$, determined from the quantum Hall effect. In most electroweak-renormalization schemes, it is convenient to define a running α dependent on the energy scale of the process, with $\alpha^{-1} \sim 137$ appropriate at low energy. At energies of order M_Z, $\alpha^{-1} \sim 128$. For example, in the modified minimal subtraction ($\overline{\rm MS}$) scheme, one has $\widehat{\alpha}(M_Z)^{-1} = 127.90 \pm 0.09$ [7], while the conventional (on-shell) QED renormalization yields [8] $\alpha(M_Z)^{-1} = 128.90 \pm 0.09$, which differs by finite constants from $\widehat{\alpha}(M_Z)^{-1}$. The uncertainty, due to the low-energy hadronic contribution to vacuum polarization, is the dominant theoretical uncertainty in the interpretation of precision data. The values include recent reevaluations [8–12] of this effect, which, following a correction to [11], are now in reasonable agreement. Further improvement will require improved measurements of the cross section for $e^+e^- \to$ hadrons at low energy.

(*b*) The Fermi constant, $G_F = 1.16639(2) \times 10^{-5}$ GeV^{-2}, determined from the muon lifetime formula [13]:

$$\tau_\mu^{-1} = \frac{G_F^2 m_\mu^5}{192\pi^3}\, F\left(\frac{m_e^2}{m_\mu^2}\right) \left(1 + \frac{3}{5}\frac{m_\mu^2}{M_W^2}\right) \times \left[1 + \frac{\alpha(m_\mu)}{2\pi}\left(\frac{25}{4} - \pi^2\right)\right]\ , \tag{10.5a}$$

where

$$F(x) = 1 - 8x + 8x^3 - x^4 - 12x^2 \ln x \tag{10.5b}$$

and

$$\alpha(m_\mu)^{-1} = \alpha^{-1} - \frac{2}{3\pi}\ln\left(\frac{m_\mu}{m_e}\right) + \frac{1}{6\pi} \approx 136\ . \tag{10.5c}$$

The uncertainty in G_F from the input quantities is 1.1×10^{-10} GeV^{-2}. The quoted uncertainty of 2×10^{-10} is dominated by second order radiative corrections, estimated from the magnitude of the known $\alpha^2 \ln(m_\mu/m_e)$ term to be $\sim 1.8 \times 10^{-10}$ (alternately, one can view Eq. (10.5) as the exact definition of G_F; then the theoretical uncertainty appears instead in the formulae for quantities derived from G_F).

(*c*) $\sin^2\theta_W$, determined from the Z mass and other Z-pole observables, the W mass, and neutral-current processes [14]. The value of $\sin^2\theta_W$ depends on the renormalization prescription. There are a number of popular schemes [16–21] leading to $\sin^2\theta_W$ values which differ by small factors which depend on m_t and M_H. The notation for these schemes is shown in Table 10.1. Discussion of the schemes follows the table.

Table 10.1: Notations used to indicate the various schemes discussed in the text. Each definition of $\sin\theta_W$ leads to values that differ by small factors depending on m_t and M_H.

Scheme	Notation
On-shell	$s_W = \sin\theta_W$
NOV	$s_{M_Z} = \sin\theta_W$
$\overline{\rm MS}$	$\widehat{s}_Z = \sin\theta_W$
$\overline{\rm MS}$ ND	$\widehat{s}_{ND} = \sin\theta_W$
Effective angle	$\overline{s}_f = \sin\theta_W$

(*i*) The on-shell scheme promotes the tree-level formula $\sin^2\theta_W = 1 - M_W^2/M_Z^2$ to a definition of the renormalized $\sin^2\theta_W$ to all orders in perturbation theory, *i.e.*, $\sin^2\theta_W \to s_W^2 \equiv 1 - M_W^2/M_Z^2$. This scheme is simple conceptually. However, M_W is known much less precisely than M_Z and in practice one extracts s_W^2 from M_Z alone using

$$M_W = \frac{A_0}{s_W(1-\Delta r)^{1/2}} \tag{10.6a}$$

$$M_Z = \frac{M_W}{c_W}\ , \tag{10.6b}$$

where $s_W \equiv \sin\theta_W$, $c_W \equiv \cos\theta_W$, $A_0 = (\pi\alpha/\sqrt{2}G_F)^{1/2} = 37.2802$ GeV, and Δr includes the radiative corrections relating α, $\alpha(M_Z)$, G_F, M_W, and M_Z. One finds $\Delta r \sim \Delta r_0 - \rho_t/\tan^2\theta_W$, where $\Delta r_0 \approx 1 - \alpha/\alpha(M_Z) \approx 0.06$ is due to the running of α and $\rho_t = 3G_F\, m_t^2/8\sqrt{2}\pi^2 \approx 0.0100\ (m_t/180\ \text{GeV})^2$ represents the dominant (quadratic) m_t dependence. There are additional contributions to Δr from bosonic loops, including those which depend logarithmically on the Higgs mass M_H. One has $\Delta r = 0.0376 \pm 0.0025 \pm 0.0007$ for $(m_t, M_H) = (180 \pm 7, 300)$, where the second uncertainty is from $\alpha(M_Z)$. Thus the value of s_W^2 extracted from M_Z includes a large uncertainty (~ 0.0008) from the currently allowed range of m_t.

(*ii*) A more precisely determined quantity $s^2_{M_Z}$ can be obtained from M_Z by removing the (m_t, M_H) dependent term from Δr [17], *i.e.*,

$$s^2_{M_Z} c^2_{M_Z} \equiv \frac{\pi\alpha(M_Z)}{\sqrt{2}\,G_F\,M_Z^2}\ . \tag{10.7}$$

This yields $s^2_{M_Z} = 0.2311 \pm 0.0002$, with most of the uncertainty from α rather than M_Z. Scheme (*ii*) is equivalent to using M_Z rather than $\sin^2\theta_W$ as the third fundamental parameter. However, it recognizes that $s^2_{M_Z}$ is still a useful derived quantity. The small uncertainty in $s^2_{M_Z}$ compared to other schemes is because the m_t dependence has been removed by definition. However, the m_t uncertainty reemerges when other quantities (*e.g.*, M_W or other Z-pole observables) are predicted in terms of M_Z.

Both s_W^2 and $s^2_{M_Z}$ depend not only on the gauge couplings but also on the spontaneous-symmetry breaking, and both definitions are awkward in the presence of any extension of the Standard Model which perturbs the value of M_Z (or M_W). Other definitions are motivated by the tree-level coupling constant definition $\theta_W = \tan^{-1}(g'/g)$.

(*iii*) In particular, the modified minimal subtraction ($\overline{\text{MS}}$) scheme introduces the quantity $\sin^2\widehat{\theta}_W(\mu) \equiv \widehat{g}'^2(\mu)/[\widehat{g}^2(\mu) + \widehat{g}'^2(\mu)]$, where the couplings $\widehat{g}$ and $\widehat{g}'$ are defined by modified minimal subtraction and the scale μ is conveniently chosen to be M_Z for electroweak processes. The value of $\widehat{s}^2_Z = \sin^2\widehat{\theta}_W(M_Z)$ extracted from M_Z is less sensitive than s_W^2 to m_t (by a factor of $\tan^2\theta_W$), and is less sensitive to most types of new physics than s_W^2 or $s^2_{M_Z}$. It is also very useful for comparing with the predictions of grand unification. There are actually several variant definitions of $\sin^2\widehat{\theta}_W(M_Z)$, differing according to whether or how finite $\alpha\ln(m_t/M_Z)$ terms are decoupled (subtracted from the couplings). One cannot entirely decouple the $\alpha\ln(m_t/M_Z)$ terms from all electroweak quantities because $m_t \gg m_b$ breaks SU(2) symmetry. The scheme that will be adopted here decouples the $\alpha\ln(m_t/M_Z)$ terms from the $\gamma - Z$ mixing [7,18], essentially eliminating any $\ln(m_t/M_Z)$ dependence in the formulae for asymmetries at the Z pole when written in terms of $\widehat{s}^2_Z$. The various definitions are related by

$$\widehat{s}^2_Z = c\,(m_t, M_H) s_W^2 = \overline{c}\,(m_t, M_H)\, s^2_{M_Z}\ , \tag{10.8}$$

where $c = 1.035 \pm 0.003$ for $m_t = 180 \pm 7$ GeV and $M_H = 300$ GeV. Similarly $\overline{c} = 1.002 \pm 0.001$. The quadratic m_t dependence is given by $c \sim 1 + \rho_t/\tan^2\theta_W$. The expressions for M_W and M_Z in the $\overline{\text{MS}}$ scheme are

$$M_W = \frac{A_0}{\widehat{s}_Z(1-\Delta\widehat{r}_W)^{1/2}} \tag{10.9a}$$

$$M_Z = \frac{M_W}{\widehat{\rho}^{1/2}\widehat{c}_Z}\ . \tag{10.9b}$$

One predicts $\Delta\widehat{r}_W = 0.0705 \pm 0.0001 \pm 0.0007$ for $m_t = 180 \pm 7$ GeV and $M_H = 300$ GeV. $\Delta\widehat{r}_W$ has no quadratic m_t dependence, because shifts in M_W are absorbed into the observed G_F, so that $\Delta\widehat{r}_W$ is dominated by $\Delta r_0 = 1 - \alpha/\alpha(M_Z)$. Similarly, $\widehat{\rho} \sim 1 + \rho_t$. Including bosonic loops, $\widehat{\rho} = 0.0103 \pm 0.0008$ for $m_t = 180 \pm 7$ GeV.

(*iv*) A variant $\overline{\text{MS}}$ quantity $\widehat{s}^2_{\text{ND}}$ (used in the 1992 edition of this *Review*) does not decouple the $\alpha\ln(m_t/M_Z)$ terms [19]. It is related to $\widehat{s}^2_Z$ by

$$\widehat{s}^2_Z = \widehat{s}^2_{\text{ND}}/\Big(1 + \frac{\widehat{\alpha}}{\pi}d\Big) \tag{10.10a}$$

$$d = \frac{1}{3}\Big(\frac{1}{\widehat{s}^2} - \frac{8}{3}\Big)\left[(1 + \frac{\widehat{\alpha}_s}{\pi})\ln\frac{m_t}{M_Z} - \frac{15\widehat{\alpha}_s}{\pi}\right]\ , \tag{10.10b}$$

where $\widehat{\alpha}_s$ is the QCD coupling at M_Z. Thus, $\widehat{s}^2_Z - \widehat{s}^2_{\text{ND}} \sim -0.0002$ for $(m_t,\ M_H) = (180, 300)$ GeV.

(*v*) Yet another definition, the effective angle [20,21] $\overline{s}^2_f$ for Z coupling to fermion f, is described below.

Experiments are now at such a level of precision that complete $\mathcal{O}(\alpha)$ radiative corrections must be applied. For neutral-current and Z-pole processes, these corrections are conveniently divided into two classes:

1. QED diagrams involving the emission of real photons or the exchange of virtual photons in loops, but not including vacuum polarization diagrams. These graphs yield finite and gauge-invariant contributions to observable processes. However, they are dependent on energies, experimental cuts, *etc.*, and must be calculated individually for each experiment.
2. Electroweak corrections, including $\gamma\gamma$, γZ, ZZ, and WW vacuum polarization diagrams, as well as vertex corrections, box graphs, *etc.*, involving virtual W's and Z's. Many of these corrections are absorbed into the renormalized Fermi constant defined in Eq. (10.5). Others modify the tree-level expressions for Z-pole observables and neutral-current amplitudes in several ways [14]. One-loop corrections are included for all processes. In addition, certain two-loop corrections are also important. In particular, two-loop corrections involving the top-quark [22] modify ρ_t in $\widehat{\rho}$, Δr, and elsewhere by

$$\rho_t \to \rho_t[1 + R(M_H/m_t)\rho_t/3]\ , \tag{10.11}$$

where $-3.8 > R > -11.8$ is strongly dependent on M_H/m_t: $R = -3.8$ for M_H at its lower direct limit and $R = -7.8$ for $M_H = 1.7m_t \approx 300$ GeV. -11.8 is in absolute lower bound for R which is assumed for large M_H. Mixed QCD-electroweak loops of order $\alpha\alpha_s m_t^2$ [23] and $\alpha\alpha_s^2 m_t^2$ [24] multiply ρ_t by $1 - 2\ \alpha_s(0.3m_t)(\pi^2 + 3)/9\pi \sim 0.88$, where the three-loop result is included through the use of a lower scale for α_s. These mixed corrections increase the predicted value of m_t by 6%. Analogous electroweak and mixed two-loop terms are also known for the $Z \to b\overline{b}$ vertex [22,25].

10.2. Cross section and asymmetry formulas

It is convenient to write the four-fermion interactions relevant to ν-hadron, νe, and parity-violating e-hadron neutral-current processes in a form that is valid in an arbitrary gauge theory (assuming massless left-handed neutrinos). One has

$$-\mathscr{L}^{\nu\text{Hadron}} = \frac{G_F}{\sqrt{2}}\,\overline{\nu}\,\gamma^\mu\,(1-\gamma^5)\nu \times\sum_i\left[\epsilon_L(i)\,\overline{q}_i\,\gamma_\mu(1-\gamma^5)q_i+\epsilon_R(i)\,\overline{q}_i\,\gamma_\mu(1+\gamma^5)q_i\right]\,, \quad (10.12)$$

$$-\mathscr{L}^{\nu e} = \frac{G_F}{\sqrt{2}}\,\overline{\nu}_\mu\,\gamma^\mu(1-\gamma^5)\nu_\mu\,\overline{e}\,\gamma_\mu(g_V^{\nu e}-g_A^{\nu e}\gamma^5)e \quad (10.13)$$

(for $\nu_e e$ or $\overline{\nu}_e e$, the charged-current contribution must be included), and

$$-\mathscr{L}^{e\text{Hadron}} = -\frac{G_F}{\sqrt{2}} \times\sum_i\left[C_{1i}\,\overline{e}\,\gamma_\mu\,\gamma^5\,e\,\overline{q}_i\,\gamma^\mu\,q_i+C_{2i}\,\overline{e}\,\gamma_\mu\,e\,\overline{q}_i\,\gamma^\mu\,\gamma^5\,q_i\right] \quad (10.14)$$

(One must add the parity-conserving QED contribution.)

The Standard Model expressions for $\epsilon_{L,R}(i)$, $g_{V,A}^{\nu e}$, and C_{ij} are given in Table 10.2. Note that $g_{V,A}^{\nu e}$ and the other quantities are coefficients of effective four-fermi operators, which differ from the quantities defined in Eq. (10.2) and Eq. (10.3) in the radiative corrections and in the presence of possible physics beyond the Standard Model.

A precise determination of the on-shell s_W^2, which depends only very weakly on m_t and M_H, is obtained from deep inelastic neutrino scattering from (approximately) isoscalar targets [26]. The ratio $R_\nu \equiv \sigma_{\nu N}^{NC}/\sigma_{\nu N}^{CC}$ of neutral- to charged-current cross sections has been measured to 1% accuracy by the CDHS [27] and CHARM [28] collaborations [29,30] at CERN, and the CCFR collaboration at Fermilab [31] has obtained an even more precise result, so it is important to obtain theoretical expressions for R_ν and $R_{\overline{\nu}} \equiv \sigma_{\overline{\nu}N}^{NC}/\sigma_{\overline{\nu}N}^{CC}$ (as functions of $\sin^2\theta_W$) to comparable accuracy. Fortunately, most of the uncertainties from the strong interactions and neutrino spectra cancel in the ratio.

A simple zeroth-order approximation is

$$R_\nu = g_L^2 + g_R^2 r \quad (10.15a)$$

$$R_{\overline{\nu}} = g_L^2 + \frac{g_R^2}{r}\,, \quad (10.15b)$$

where

$$g_L^2 \equiv \epsilon_L\,(u)^2 + \epsilon_L\,(d)^2 \approx \frac{1}{2} - \sin^2\theta_W + \frac{5}{9}\sin^4\theta_W \quad (10.16a)$$

$$g_R^2 \equiv \epsilon_R\,(u)^2 + \epsilon_R\,(d)^2 \approx \frac{5}{9}\sin^4\theta_W\,, \quad (10.16b)$$

and $r \equiv \sigma_{\overline{\nu}N}^{CC}/\sigma_{\nu N}^{CC}$ is the ratio of $\overline{\nu}$ and ν charged-current cross sections, which can be measured directly. [In the simple parton model, ignoring hadron energy cuts, $r \approx (\frac{1}{3}+\epsilon)/(1+\frac{1}{3}\epsilon)$, where $\epsilon \sim 0.125$ is the ratio of the fraction of the nucleon's momentum carried by antiquarks to that carried by quarks.] In practice, Eq. (10.15) must be corrected for quark mixing, the s and c seas, c-quark threshold effects, nonisoscalar target effects, W-Z propagator differences, and radiative corrections (which lower the extracted value of $\sin^2\theta_W$ by ~ 0.009). Details of the neutrino spectra, experimental cuts, x and Q^2 dependence of structure functions, and longitudinal structure functions enter only at the level of these corrections and therefore lead to very small uncertainties. The largest theoretical uncertainty is associated with the c threshold, which mainly affects σ^{CC}. Using the slow rescaling prescription [14] the central value of $\sin^2\theta_W$ varies as 0.013 [m_c(GeV)−1.3], where m_c is the effective mass. For $m_c = 1.31 \pm 0.24$ GeV (determined from ν-induced dimuon production [31]) this contributes ± 0.003 to the total theoretical uncertainty $\Delta\sin^2\theta_W \sim \pm 0.004$. This would require a high-energy neutrino beam for improvement. (The experimental uncertainty is ± 0.003). The CCFR group quotes $s_W^2 = 0.2218 \pm 0.0059$ for $(m_t, M_H) = (150, 100)$, but this result is insensitive to (m_t, M_H). Combining all of the precise deep-inelastic measurements, one obtains $s_W^2 = 0.2259 \pm 0.0043$ for (m_t, M_H) in the allowed range.

Table 10.2: Standard Model expressions for the neutral-current parameters for ν-hadron, νe, and e-hadron processes. If radiative corrections are ignored, $\rho = \kappa = 1$, $\lambda = 0$. At $\mathcal{O}(\alpha)$ in the on-shell scheme, $\rho_{\nu N}^{NC} = 1.0095$, $\kappa_{\nu N} = 1.0382$, $\lambda_{u_L} = -0.0032$, $\lambda_{d_L} = -0.0026$, and $\lambda_{u_R} = 1/2\,\lambda_{d_R} = 3.6\times10^{-5}$ for $m_t = 180$ GeV, $M_H = 300$ GeV, $M_Z = 91.1884$ GeV, and $\langle Q^2\rangle = 20$ GeV^2. For νe scattering, $\kappa_{\nu e} = 1.0385$ and $\rho_{\nu e} = 1.0143$ (at $\langle Q^2\rangle = 0$.). For atomic parity violation, $\rho'_{eq} = 0.9884$ and $\kappa'_{eq} = 1.036$. For the SLAC polarized electron experiment, $\rho'_{eq} = 0.979$, $\kappa'_{eq} = 1.034$, $\rho_{eq} = 1.002$, and $\kappa_{eq} = 1.06$ after incorporating additional QED corrections, while $\lambda_{2u} = -0.013$, $\lambda_{2d} = 0.003$. The dominant m_t dependence is given by $\rho \sim 1 + \rho_t$, while $\kappa \sim 1 + \rho_t/\tan^2\theta_W$ (on-shell) or $\kappa \sim 1(\overline{\text{MS}})$.

Quantity	Standard Model Expression
$\epsilon_L(u)$	$\rho_{\nu N}^{NC}\left(\frac{1}{2} - \frac{2}{3}\kappa_{\nu N}\,\sin^2\theta_W + \lambda_{uL}\right)$
$\epsilon_L(d)$	$\rho_{\nu N}^{NC}\left(-\frac{1}{2} + \frac{1}{3}\kappa_{\nu N}\,\sin^2\theta_W + \lambda_{dL}\right)$
$\epsilon_R(u)$	$\rho_{\nu N}^{NC}\left(-\frac{2}{3}\kappa_{\nu N}\,\sin^2\theta_W + \lambda_{uR}\right)$
$\epsilon_R(d)$	$\rho_{\nu N}^{NC}\left(\frac{1}{3}\kappa_{\nu N}\,\sin^2\theta_W + \lambda_{dR}\right)$
$g_V^{\nu e}$	$\rho_{\nu e}\left(-\frac{1}{2} + 2\kappa_{\nu e}\,\sin^2\theta_W\right)$
$g_A^{\nu e}$	$\rho_{\nu e}\left(-\frac{1}{2}\right)$
C_{1u}	$\rho'_{eq}\left(-\frac{1}{2} + \frac{4}{3}\kappa'_{eq}\,\sin^2\theta_W\right)$
C_{1d}	$\rho'_{eq}\left(\frac{1}{2} - \frac{2}{3}\kappa'_{eq}\,\sin^2\theta_W\right)$
C_{2u}	$\rho_{eq}\left(-\frac{1}{2} + 2\kappa_{eq}\,\sin^2\theta_W\right) + \lambda_{2u}$
C_{2d}	$\rho_{eq}\left(\frac{1}{2} - 2\kappa_{eq}\,\sin^2\theta_W\right) + \lambda_{2d}$

The laboratory cross section for $\nu_\mu e \to \nu_\mu e$ or $\overline{\nu}_\mu e \to \overline{\nu}_\mu e$ elastic scattering is

$$\frac{d\sigma_{\nu_\mu,\overline{\nu}_\mu}}{dy} = \frac{G_F^2 m_e E_\nu}{2\pi} \times\left[(g_V^{\nu e} \pm g_A^{\nu e})^2+(g_V^{\nu e} \mp g_A^{\nu e})^2(1-y)^2 -(g_V^{\nu e2} - g_A^{\nu e2})\frac{y\,m_e}{E_\nu}\right]\,, \quad (10.17)$$

where the upper (lower) sign refers to $\nu_\mu(\overline{\nu}_\mu)$, and $y \equiv E_e/E_\nu$ [which runs from 0 to $(1+m_e/2E_\nu)^{-1}$] is the ratio of the kinetic energy of the recoil electron to the incident ν or $\overline{\nu}$ energy. For $E_\nu \gg m_e$ this yields a total cross section

$$\sigma = \frac{G_F^2\,m_e\,E_\nu}{2\pi}\left[(g_V^{\nu e} \pm g_A^{\nu e})^2 + \frac{1}{3}(g_V^{\nu e} \mp g_A^{\nu e})^2\right]\,. \quad (10.18)$$

The most accurate leptonic measurements [32–34] of $\sin^2\theta_W$ are from the ratio $R \equiv \sigma_{\nu_\mu e}/\sigma_{\overline{\nu}_\mu e}$ in which many of the systematic uncertainties cancel. Radiative corrections (other than m_t effects) are small compared to the precision of present experiments and have negligible effect on the extracted $\sin^2\theta_W$. The most precise (CHARM II) experiment [34] determined not only $\sin^2\theta_W$ but $g_{V,A}^{\nu e}$ as well. The cross sections for $\nu_e e$ and $\overline{\nu}_e e$ may be obtained from

Eq. (10.17) by replacing $g_{V,A}^{\nu e}$ by $g_{V,A}^{\nu e} + 1$, where the 1 is due to the charged-current contribution.

The SLAC polarized-electron experiment [35] measured the parity-violating asymmetry

$$A = \frac{\sigma_R - \sigma_L}{\sigma_R + \sigma_L} , \tag{10.19}$$

where $\sigma_{R,L}$ is the cross section for the deep-inelastic scattering of a right- or left-handed electron: $e_{R,L}N \to e\mathrm{X}$. In the quark parton model

$$\frac{A}{Q^2} = a_1 + a_2 \frac{1-(1-y)^2}{1+(1-y)^2} , \tag{10.20}$$

where $Q^2 > 0$ is the momentum transfer and y is the fractional energy transfer from the electron to the hadrons. For the deuteron or other isoscalar target, one has, neglecting the s quark and antiquarks,

$$a_1 = \frac{3G_F}{5\sqrt{2}\pi\alpha}\left(C_{1u} - \frac{1}{2}C_{1d}\right) \approx \frac{3G_F}{5\sqrt{2}\pi\alpha}\left(-\frac{3}{4} + \frac{5}{3}\sin^2\theta_W\right) \tag{10.21a}$$

$$a_2 = \frac{3G_F}{5\sqrt{2}\pi\alpha}\left(C_{2u} - \frac{1}{2}C_{2d}\right) \approx \frac{9G_F}{5\sqrt{2}\pi\alpha}\left(\sin^2\theta_W - \frac{1}{4}\right) . \tag{10.21b}$$

Radiative corrections (other than m_t effects) lower the extracted value of $\sin^2\theta_W$ by $\sim$ 0.005.

There are now precise experiments measuring atomic parity violation [36] in cesium [37], bismuth [38], lead [39], and thallium [40]. The uncertainties associated with atomic wave functions are quite small for cesium, for which the theoretical uncertainty is $\sim 1\%$ [41] but somewhat larger for the other atoms. For heavy atoms one determines the "weak charge"

$$\begin{aligned} Q_W &= -2\left[C_{1u}\,(2Z+N) + C_{1d}(Z+2N)\right] \\ &\approx Z(1-4\sin^2\theta_W) - N . \end{aligned} \tag{10.22}$$

Radiative corrections increase the extracted $\sin^2\theta_W$ by ~ 0.008.

In the future it should be possible to reduce the theoretical wave function uncertainties by taking the ratios of parity violation in different isotopes [36,42]. There would still be some residual uncertainties from differences in the neutron charge radii, however [43].

The forward-backward asymmetry for $e^+e^- \to \ell\bar{\ell}$, $\ell = \mu$ or τ, is defined as

$$A_{FB} \equiv \frac{\sigma_F - \sigma_B}{\sigma_F + \sigma_B} , \tag{10.23}$$

where $\sigma_F(\sigma_B)$ is the cross section for ℓ^- to travel forward (backward) with respect to the e^- direction. A_{FB} and R, the total cross section relative to pure QED, are given by

$$R = F_1 \tag{10.24}$$

$$A_{FB} = 3F_2/4F_1 , \tag{10.25}$$

where

$$F_1 = 1 - 2\chi_0\, g_V^e\, g_V^\ell\, \cos\delta_R + \chi_0^2\left(g_V^{e2} + g_A^{e2}\right)\left(g_V^{\ell 2} + g_A^{\ell 2}\right) \tag{10.26a}$$

$$F_2 = -2\chi_0\, g_A^e\, g_A^\ell\, \cos\delta_R + 4\chi_0^2\, g_A^e\, g_A^\ell\, g_V^e\, g_V^\ell , \tag{10.26b}$$

where

$$\tan\delta_R = \frac{M_Z\Gamma_Z}{M_Z^2 - s} \tag{10.27}$$

$$\chi_0 = \frac{G_F}{2\sqrt{2}\pi\alpha}\,\frac{sM_Z^2}{\left[(M_Z^2-s)^2 + M_Z^2\Gamma_Z^2\right]^{1/2}} \tag{10.28}$$

and $\sqrt{s}$ is the CM energy. Eq. (10.26) is valid at tree level. If the data are radiatively corrected for QED effects (as described above), then the remaining electroweak corrections can be incorporated [44] (in an approximation adequate for existing PEP, PETRA, and TRISTAN data, which are well below the Z pole) by replacing χ_0 by $\chi(s) \equiv (1+\rho_t)\chi_0(s)\alpha/\alpha(s)$, where $\alpha(s)$ is the running QED coupling, and evaluating g_V in the $\overline{\mathrm{MS}}$ scheme. Formulas for $e^+e^- \to$ *hadrons* may be found in Ref. 45.

At LEP and SLC, there are high-precision measurements of various Z-pole observables [46–49]. These include the Z mass and total width Γ_Z, and partial widths $\Gamma(f\bar{f})$ for $Z \to f\bar{f}$ for fermion f ($f = e$, μ, τ, hadrons, b, c, and ν). The data is consistent with lepton-family universality $\Gamma(e^+e^-) = \Gamma(\mu^+\mu^-) = \Gamma(\tau^+\tau^-)$, so one may work with an average width $\Gamma(\ell\bar{\ell})$. It is convenient to use the variables M_Z, Γ_Z, $R \equiv \Gamma(\mathrm{had})/\Gamma(\ell\bar{\ell})$, $\sigma_{\mathrm{had}} \equiv 12\pi\Gamma(e^+e^-)\Gamma(\mathrm{had})/M_Z^2\,\Gamma_Z^2$, $R_b \equiv \Gamma(b\bar{b})/\Gamma(\mathrm{had})$, and $R_c \equiv \Gamma(c\bar{c})/\Gamma(\mathrm{had})$, most of which are weakly correlated experimentally. ($\Gamma(\mathrm{had})$ is the partial width into hadrons.) The largest correlation coefficient of -0.35 occurs between R_b and R_c. R is insensitive to m_t except for $Z \to b\bar{b}$ vertex and final state corrections and the implicit dependence through $\sin^2\theta_W$. Thus it is especially useful for constraining α_s. The width for invisible decays, $\Gamma(\mathrm{inv}) = \Gamma_Z - 3\Gamma(\ell\bar{\ell}) - \Gamma(\mathrm{had}) = 499.9 \pm 2.5$ MeV, can be used to determine the number of neutrino flavors lighter than $M_Z/2$, $N_\nu = \Gamma_{\mathrm{inv}}/\Gamma(\nu\bar{\nu}) = 2.991 \pm 0.016$.

There are also measurements of various asymmetries. These include the polarization or left-right asymmetry

$$A_{LR} \equiv \frac{\sigma_L - \sigma_R}{\sigma_L + \sigma_R} , \tag{10.29}$$

where $\sigma_L(\sigma_R)$ is the cross section for a left- (right)-handed incident electron. A_{LR} has been measured precisely by the SLD collaboration at SLC [48] and has the advantages of being extremely sensitive to $\sin^2\theta_W$ and insensitive to QED radiative corrections. Other asymmetries are the forward-backward asymmetries $A_{FB}^{(0,f)}$ for $f = e$, μ, τ, b, c ($A_{FB}^{(0,e)}$, $A_{FB}^{(0,\mu)}$, $A_{FB}^{(0,\tau)}$ are consistent with lepton-family universality, allowing an average value $A_{FB}^{(0,\ell)}$), the hadronic-charge asymmetry, the τ polarization P_τ, and its angular distribution. Further details, including references to the data from the LEP experiments (ALEPH, DELPHI, L3, OPAL) may be found in the Particle Listings in the 'Note on the Z Boson' and in [46–49]. At tree level and neglecting QED effects and terms of order $(\Gamma_Z/M_Z)^2$, one has

$$A_{FB}^{(0,f)} \approx \frac{3}{4}A_f\,\frac{A_e + P_e}{1 + P_eA_e} \tag{10.30}$$

$$A_{LR} \approx A_eP_e , \tag{10.31}$$

where P_e is the initial e^- polarization and

$$A_f \equiv \frac{2g_V^f\, g_A^f}{g_V^{f2} + g_A^{f2}} . \tag{10.32}$$

Similarly, A_τ is given by the negative total τ polarization, and A_e can be extracted from the angular distribution of the polarization. In addition, the SLD collaboration [49] has extracted the final-state couplings A_b and A_c from the left-right forward-backward asymmetry, using

$$\frac{\sigma_{LF} - \sigma_{LB} - \sigma_{RF} + \sigma_{RB}}{\sigma_{LF} + \sigma_{LB} + \sigma_{RF} + \sigma_{RB}} = A_f , \tag{10.33}$$

where, for example, σ_{LF} is the cross section for a left-handed incident electron to produce a fermion f traveling in the forward hemisphere.

It has become customary for the experimental groups to present corrected asymmetries A^0, in which photon exchange and γ-Z interference, QED corrections, and corrections for $\sqrt{s} \neq M_Z$ are removed from the data, leaving the pure electroweak asymmetries. Ignoring negligible electroweak boxes, these corrected asymmetries are expressed using effective tree-level expression *e.g.*, $A_{FB}^{(0,f)} = \frac{3}{4}\overline{A}_f\overline{A}_e$ (for $P_e = 0$) and $A_{LR}^0 = \overline{A}_e$, where

$$\overline{A}_f = \frac{2\overline{g}_V^f\,\overline{g}_A^f}{\overline{g}_V^{f2} + \overline{g}_A^{f2}} , \tag{10.34a}$$

and

$$\overline{g}_V^f = \sqrt{\rho_f}\,(t_{3L}^{(f)} - 2q_f\kappa_f \sin^2\theta_W) \tag{10.34b}$$

$$\overline{g}_A^f = \sqrt{\rho_f}\,t_{3L}^{(f)}\ . \tag{10.34c}$$

The electroweak-radiative corrections have been absorbed into corrections $\rho_f - 1$ and $\kappa_f - 1$, which depend on the fermion f and on the renormalization scheme. In the on-shell scheme, the quadratic m_t dependence is given by $\rho_f \sim 1 + \rho_t$, $\kappa_f \sim \kappa_f^{os} \sim 1 + \rho_t/\tan^2\theta_W$, while in $\overline{\rm MS}$, $\rho_f \sim \widehat{\rho}$, $\kappa_f \equiv \widehat{\kappa}_f \sim 1$. In practice, additional bosonic loops, vertex corrections, *etc.*, must be included. For example, in the $\overline{\rm MS}$ scheme one has, for $(m_t, M_H) = (180, 300)$, $\rho_\ell = 1.0053$ and $\widehat{\kappa}_\ell = 1.0012$. It is convenient to define an effective angle $\overline{s}_f^2 \equiv \sin^2\overline{\theta}_{Wf} \equiv \widehat{\kappa}_f \widehat{s}_Z^2 = \kappa_f^{os} s_W^2$, in terms of which $\overline{g}_V^f$ and $\overline{g}_A^f$ are given by $\sqrt{\rho_f}$ times their tree-level formulae. Because $\overline{g}_V^\ell$ is very small, not only A_{LR}^0 $A_{FB}^{(0,\ell)}$, and P_τ^0, but also $A_{FB}^{(0,b)}$, $A_{FB}^{(0,c)}$, and the hadronic-charge asymmetry are mainly sensitive to $\overline{s}_\ell^2$. One finds that $\widehat{\kappa}_f$ is almost independent of (m_t, M_H), so that

$$\overline{s}_\ell^2 \sim \widehat{s}_Z^2 + 0.00028 \tag{10.35}$$

using Ref. 20, or $\overline{s}_\ell^2 \sim \widehat{s}_Z^2 + 0.0002$ from Ref. 21 (the small difference is an indication of theoretical uncertainties from higher-order terms, *etc.*). In any case, the asymmetries determine values of $\overline{s}_\ell^2$ and $\widehat{s}_Z^2$ almost independent of m_t, while the κ's for the other schemes are m_t dependent.

10.3. W and Z decays

The partial decay width for gauge bosons to decay into massless fermions $f_1\overline{f}_2$ is

$$\Gamma(W^+ \to e^+\nu_e) = \frac{G_F M_W^3}{6\sqrt{2}\pi} \approx 226 \pm 1 \text{ MeV} \tag{10.36a}$$

$$\Gamma(W^+ \to u_i\overline{d}_j) = \frac{C G_F M_W^3}{6\sqrt{2}\pi}\,|V_{ij}|^2 \approx (705 \pm 4)\,|V_{ij}|^2 \text{ MeV} \tag{10.36b}$$

$$\Gamma(Z \to \psi_i\overline{\psi}_i) = \frac{C G_F M_Z^3}{6\sqrt{2}\pi}\left[g_V^{i2} + g_A^{i2}\right] \tag{10.36c}$$

$$\approx \begin{cases} 167.2 \pm 0.1 \text{ MeV } (\nu\overline{\nu}),\ \ 84.0 \pm 0.1 \text{ MeV } (e^+e^-), \\ 300.6 \pm 0.3 \text{ MeV } (u\overline{u}),\ \ 383.3 \pm 0.3 \text{ MeV } (d\overline{d}), \\ 375.9 \mp 0.2 \text{ MeV } (b\overline{b}). \end{cases}$$

For leptons $C = 1$, while for quarks $C = 3\Big(1 + \alpha_s(M_V)/\pi + 1.409\alpha_s^2/\pi^2 - 12.77\alpha_s^3/\pi^3\Big)$, where the 3 is due to color and the factor in parentheses represents the universal QCD corrections for massless quarks [50]. The $Z \to f\overline{f}$ widths contain a number of additional corrections [51]: universal (non-singlet) top-mass contributions [52]; fermion mass effects and further QCD corrections proportional to m_q^2 [53] (m_q is the running quark mass evaluated at the Z scale) which are different for vector and axial-vector partial widths; and singlet contributions starting from two loop order which are large, strongly top-mass dependent, family universal and flavor non-universal [54]. All QCD effects are known and included up to three loop order with the exception of order $\alpha_s^3 m_b^2$ corrections which are very small. The QED factor $1 + 3\alpha q_f^2/4\pi$ and order $\alpha\alpha_s$ corrections [55] have to be included, as well. Expressing the widths in terms of $G_F M_{W,Z}^3$ incorporates the bulk of the low-energy radiative corrections [16,56]. The electroweak corrections are incorporated by replacing $g_{V,A}^{i2}$ by $\overline{g}_{V,A}^{i2}$. Hence, the widths are proportional to $\rho_i \sim 1 + \rho_t$. There is additional (negative) quadratic m_t dependence in the $Z \to b\overline{b}$ vertex corrections [57] which causes $\Gamma(b\overline{b})$ to decrease with m_t. The dominant effect is to multiply $\Gamma(b\overline{b})$ by the vertex correction $1 + \delta\rho_{b\overline{b}}$, where $\delta\rho_{b\overline{b}} \sim 10^{-2}(-\frac{1}{2}\frac{m_t^2}{M_Z^2} + \frac{1}{5})$. In practice, the corrections are included in ρ_b and κ_b.

For 3 fermion families the total widths are predicted to be

$$\Gamma_Z \approx 2.497 \pm 0.002 \text{ GeV} \tag{10.37}$$

$$\Gamma_W \approx 2.09 \pm 0.01 \text{ GeV}\ . \tag{10.38}$$

The numerical values for the widths assume $M_Z = 91.1884 \pm 0.0022$ GeV, $M_W = 80.26 \pm 0.16$ GeV, $\alpha_s = 0.123$, and $m_t = 180 \pm 7$ GeV, where the α_s and m_t values are predicted by the global fits for $M_H = 300$ GeV. The uncertainties for Γ_W and Γ_Z are dominated by ΔM_W and Δm_t, respectively. The uncertainty in α_s, ± 0.004, introduces an additional uncertainty of 0.13% in the hadronic widths, corresponding to ± 2 MeV in Γ_Z.

These predictions are to be compared with the experimental results $\Gamma_Z = 2.4963 \pm 0.0032$ GeV and $\Gamma_W = 2.08 \pm 0.07$ GeV.

10.4. Experimental results

The values of the principal Z-pole observables are listed in Table 10.3, along with the Standard Model predictions for $M_Z = 91.1884 \pm 0.0022$, $m_t = 180 \pm 7$ GeV (for $M_H = 300$ GeV), 60 GeV $< M_H <$ 1 TeV, and $\alpha_s = 0.123 \pm 0.004$. Note that, the values of the Z-pole observables (as well as M_W) differ from those in the Particle Listings because they include recent preliminary results [47,49,59]. The values and predictions of M_W [59], the Q_W for cesium [36,41], and recent results from deep inelastic and $\nu_\mu e$ scattering are also listed. The agreement is generally excellent. Major exceptions are $R_b = \Gamma(b\overline{b})/\Gamma(\text{had})$ which is 3.7σ above the Standard Model prediction, and $R_c = \Gamma(c\overline{c})/\Gamma(\text{had})$ which is 2.4σ below. These are strongly correlated: if R_c is fixed at the Standard Model value of 0.172, then one obtains [47] $R_b = 0.2205 \pm 0.0016$, which is still 3.0σ too high. Within the Standard Model framework, these values must be considered large statistical fluctuations or systematic errors. However, R_b tends to favor small values of m_t, and when combined with other observables, small values for M_H. Many types of new physics could contribute to R_b (see also Sec. 14 on "Constraints on New Physics from Electroweak Analyses" in this *Review*). The implications of this possiblity for the value of $\alpha_s(M_Z)$ extracted from the fits are discussed below. The left-right asymmetry $A_{LR}^0 = 0.1551 \pm 0.0040$ [49] based on all data from 1992–1995 has moved closer to the Standard Model expectation of 0.144 ± 0.003 than the previous value 0.1637 ± 0.0075, from 1992–1993. However, because of the smaller error A_{LR}^0 is still 2.3σ above the Standard Model prediction. There is also an experimental difference of $\sim 1.5\sigma$ between the SLD value of $A_e^0 = A_{LR}^0$ and the LEP value $A_{\ell\text{LEP}}^0 \sim 0.147 \pm 0.004$ obtained from $A_{FB}^{(0,\ell)}$, $A_e^0(P_\tau)$, $A_\tau^0(P_\tau)$ assuming lepton family universality. Finally, the forward-backward asymmetry into τ's, $A_{FB}^{0\tau} = 0.0206 \pm 0.0023$ [47], is 2.2σ above the Standard Model prediction and 1.6σ above the average 0.0162 ± 0.0014 of A_{FB}^{0e} and $A_{FB}^{0\mu}$. This is small enough to be a fluctuation, so lepton-family universality will be assumed. The observables in Table 10.3 (including correlations on the LEP observables), as well as all low-energy neutral-current data [14,15], are used in the global fits described below. The parameter $\sin^2\theta_W$ can be determined from the Z-pole observables and M_W, and from a variety of neutral-current processes spanning a very wide Q^2 range. The results [14], shown in Table 10.4, are in impressive agreement with each other, indicating the quantitative success of the Standard Model. The one discrepancy is the value $\widehat{s}_Z^2 = 0.2302 \pm 0.0005$ from A_{LR}^0 which is 2.1σ below the value (0.2315 ± 0.0004) from the global fit to all data and 2.6σ below the value 0.2318 ± 0.0004 obtained from all data other than A_{LR}^0.

The data allow a simultaneous determination of $\sin^2\theta_W$, m_t, and the strong coupling $\alpha_s(M_Z)$. The latter is determined mainly from Γ_Z and R, and is only weaky correlated with the other variables. The global fit to all data, including the CDF/DØ value $m_t = 180 \pm 12$ GeV, yields

$$\begin{aligned} \widehat{s}_Z^2 &= 0.2315 \pm 0.0002 \pm 0.0003 \\ m_t &= 180 \pm 7^{+12}_{-13} \text{ GeV} \\ \alpha_s(M_Z) &= 0.123 \pm 0.004 \pm 0.002\ , \end{aligned} \tag{10.39}$$

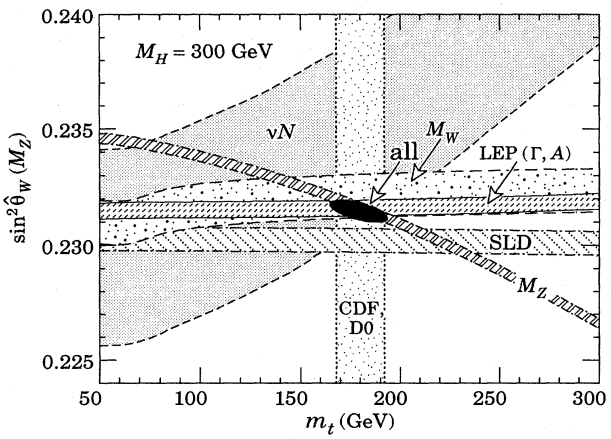

Figure 10.1: One-standard-deviation uncertainties in $\sin^2\hat{\theta}_W$ as a function of m_t, the direct CDF and DØ range 180 ± 12 GeV, and the 90% CL region in $\sin^2\hat{\theta}_W - m_t$ allowed by all data, assuming $M_H = 300$ GeV.

where the central values are for a Higgs mass of 300 GeV, and the second error bars are for $M_H \to 1000(+)$ or $60(-)$ GeV. In all fits, the errors include full statistical, systematic, and theoretical uncertainties. The $\hat{s}^2_Z$ error is dominated by m_t, and $\hat{s}^2_Z$ and m_t have a strong negative correlation of ~ -0.62. In the on-shell scheme one has $s^2_W = 0.2236 \pm 0.0008$, the larger error due to the stronger sensitivity to m_t. The extracted value of α_s is based on a formula which has almost no theoretical uncertainty (if one assumes the exact validity of the Standard Model), and is in excellent agreement with the values 0.122 ± 0.007 from jet-event shapes in e^+e^- annihilation, and the average 0.118 ± 0.003 from all data (including the Z-lineshape data), as described in our Section 9 on "Quantum Chromodynamics" in this *Review*. However, it is higher than some of the individual values extracted from low-energy data, such as deep-inelastic scattering (0.112 ± 0.002 (exp) ± 0.004 (scale)) or lattice calculations of the $b\bar{b}$ and $c\bar{c}$ spectra (0.115 ± 0.003). It has been suggested [60] that there is a real discrepancy. However, caution is requred since most of the determinations are dominated by theory errors.

The value of R_b is more than 3σ above the Standard Model expectation. If this is not just a fluctuation but is due to a new physics contribution to the $Z \to b\bar{b}$ vertex (many types would couple preferentially to the third family), the value of $\alpha_s(M_Z)$ extracted from the hadronic Z width would be reduced [15]. Allowing for this possibility one obtains $\alpha_s(M_Z) = 0.101 \pm 0.008$. (See also Sec. 14 on "Constraints on New Physics from Electroweak Analyses." in this *Review*)

In principle the low value of R_c could also be due to new physics. However, allowing for new physics contributions to R_c alone, one obtains $\alpha_s(M_Z) = 0.19 \pm 0.03$, which is clearly inconsistent with low-energy determinations. Allowing new contributions to both R_b and R_c yields the slightly lower but still high value of $\alpha_s(M_Z) = 0.16 \pm 0.04$. We will, therefore, take the view that the R_c value is a fluctuation. We keep the experimental values $R_b = 0.2219(17)$ and $R_c = 0.1540(74)$ and their correlation (-0.35) in all fits, but do not allow any special vertex corrections for $Z \to c\bar{c}$. This is effectively equivalent to using the lower value 0.2205(16) that the LEP experimenters obtain for R_b when they constrain R_c to the Standard Model value of 0.172.

One can also carry out a fit to the indirect data alone, *i.e.*, without including the value $m_t = 180 \pm 12$ GeV observed directly by CDF and DØ. (The indirect prediction is for the pole mass, which should correspond approximately to the kinematic mass extracted from the collider events.) One obtains $m_t = 179 \pm 8^{+17}_{-20}$ GeV, with little change in the $\sin^2\theta_W$ and α_s values, in remarkable agreement with the direct CDF/DØ value. The results of fits to various combinations of the data are shown in Table 10.5 and the relation between $\hat{s}^2_Z$ and m_t for various observables in Fig. 10.1.

The data indicate a preference for a small Higgs mass. This is because there is a strong correlation between the quadratic ρ_t terms and logarithmic M_H effects in all of the indirect data except the $Z \to b\bar{b}$ vertex. The latter favor a smaller m_t and therefore a smaller M_H. The difference in χ^2 for the global fit is $\Delta\chi^2 = \chi^2(M_H = 1000 \text{ GeV}) - \chi^2(M_H = 60 \text{ GeV}) = 7.9$. Hence, the data favor a small value of M_H, as in supersymmetric extensions of the Standard Model, and m_t on the lower side of the allowed range; including the direct constraint $M_H \geq 60$ GeV, the best fit is for $M_H = 60$ GeV, with the limit $M_H < 320(430)$ GeV at 90(95)% CL. However, one should be cautious because the M_H constraint is driven almost entirely by R_b and A_{LR}, both of which deviate from the Standard Model prediction. Using $\alpha(M_Z)$ and $\hat{s}^2_Z$ as inputs, one can predict $\alpha_s(M_Z)$ assuming grand unification. One predicts [61] $\alpha_s(M_Z) = 0.130 \pm 0.001 \pm 0.01$ for the simplest theories based on the minimal supersymmetric extension of the Standard Model, where the first (second) uncertainty is from the inputs (thresholds). This is consistent with the experimental $\alpha_s(M_Z) = 0.121(4)(1)$ from the Z-lineshape (using the lower M_H range appropriate for supersymmetry) and with the average 0.118 ± 0.003 (see our Section 9 on "Quantum Chromodynamics" in this *Review*), but is high compared to some low-energy determinations of α_s [60]. Nonsupersymmetric unified theories predict the low value $\alpha_s(M_Z) = 0.073 \pm 0.001 \pm 0.001$.

One can also determine the radiative correction parameters Δr: including the CDF and DØ data, one obtains $\Delta r = 0.039 \pm 0.003$ and $\Delta\hat{r}_W = 0.068 \pm 0.0013$, where the error includes m_t and M_H, in excellent agreement with the predictions 0.038 ± 0.005 and 0.0705 ± 0.0007.

Table 10.4: Values obtained for s^2_W (on-shell) and $\hat{s}^2_Z(\overline{\text{MS}})$ from various reactions assuming the global best fit value $m_t = 180 \pm 07$ GeV (for $M_H = 300$ GeV), and $\alpha_s = 0.123 \pm 0.004$. The uncertainties include the effect of 60 GeV $< M_H <$ 1 TeV. The determination from Γ_Z, R, and σ_{had} uses the experimental value of M_Z, so that the values obtained are from the vertices and not the overall scale.

Reaction	s^2_W	$\hat{s}^2_Z$
M_Z	0.2237 ± 0.0010	0.2316 ± 0.0005
M_W	0.2242 ± 0.0011	0.2321 ± 0.0009
Γ_Z, R, σ_{had}	0.2239 ± 0.0013	0.2317 ± 0.0013
$A_{FB}^{(0,\ell)}$	0.2228 ± 0.0009	0.2307 ± 0.0007
LEP asymmetries	0.2237 ± 0.0007	0.2316 ± 0.0003
A^0_{LR}	0.2223 ± 0.0008	0.2302 ± 0.0005
$\overline{A}_b$, $\overline{A}_c$	0.250 ± 0.021	0.259 ± 0.022
Deep inelastic (isocalar)	0.226 ± 0.004	0.234 ± 0.005
$\nu_\mu(\overline{\nu}_\mu)p \to \nu_\mu(\overline{\nu}_\mu)p$	0.205 ± 0.030	0.212 ± 0.031
$\nu_\mu(\overline{\nu}_\mu)e \to \nu_\mu(\overline{\nu}_\mu)e$	0.221 ± 0.007	0.228 ± 0.008
atomic parity violation	0.216 ± 0.008	0.223 ± 0.008
SLAC eD	0.216 ± 0.017	0.223 ± 0.018
All data	0.2236 ± 0.0008	0.2315 ± 0.0004

10.5. Deviations from the Standard Model

The Z pole, W mass, and neutral-current data can be used to search for and set limits on deviations from the Standard Model.

For example, the relation between M_W and M_Z is modified if there are Higgs multiplets with weak isospin $> 1/2$ with significant vacuum expectation values. In order to calculate to higher orders in such theories one must define a set of four fundamental renormalized parameters. It is convenient to take these as α, G_F, M_Z, and M_W,

Table 10.3: Principal LEP and other recent observables, compared with the Standard Model predictions for $M_Z = 91.1884 \pm 0.0022$ GeV, 60 GeV $< M_H <$ 1 TeV, the global best fit value $m_t = 180 \pm 7$ GeV (for $M_H = 300$ GeV), $\alpha_s = 0.123 \pm 0.004$, and $\alpha_s(M_Z)^{-1} = 128.90 \pm 0.09$. The LEP averages [58] of the ALEPH, DELPHI, L3, and OPAL results include common systematic errors and correlations [58]. $\overline{s}^2_\ell(A^{(0,q)}_{FB})$ is the effective angle extracted from the hadronic-charge asymmetry. A^0_{LR} includes all data from 1992–1995 [48,49]. The values of $\Gamma(\ell\bar{\ell})$, Γ(had), and Γ(inv) are not independent of Γ_Z, R, and $\sigma_{\rm had}$. The M_W value is from CDF, UA2, and DØ [59]. M_W and M_Z are correlated, but the effect is negligible due to the tiny M_Z error. The two values of s^2_W from deep-inelastic scattering are from CCFR [31] and the global average, respectively. The $g^{\nu e}_{V,A}$ are from CHARM II [34]. The second error in Q_W (for cesium) is theoretical [41]. Older low-energy results are not listed but are included in the fits. In the Standard Model predictions, the first uncertainty is from M_Z and Δr, while the second is from m_t and M_H. The $\Delta\alpha_s = 0.004$ uncertainty leads to additional errors of 0.002 (Γ_Z), 0.02 (R), 0.02 (σ), 2.0 (Γ(had)).

Quantity	Value	Standard Model
M_Z (GeV)	91.1884 ± 0.0022	input
Γ_Z (GeV)	2.4963 ± 0.0032	$2.497 \pm 0.001 \pm 0.002$
R	20.788 ± 0.032	$20.77 \pm 0.004 \pm 0.002$
$\sigma_{\rm had}(nb)$	41.488 ± 0.078	$41.45 \pm 0.002 \pm 0.004$
R_b	0.2219 ± 0.0017	$0.2156 \pm 0 \pm 0.0003$
R_c	0.1540 ± 0.0074	$0.172 \pm 0 \pm 0$
$A^{(0,\ell)}_{FB}$	0.0172 ± 0.0012	$0.0155 \pm 0.0004 \pm 0.0004$
$A^0_\tau(P_\tau)$	0.1418 ± 0.0075	$0.144 \pm 0.002 \pm 0.002$
$A^0_e(P_\tau)$	0.1390 ± 0.0089	$0.144 \pm 0.002 \pm 0.002$
$A^{(0,b)}_{FB}$	0.0997 ± 0.0031	$0.101 \pm 0.001 \pm 0.001$
$A^{(0,c)}_{FB}$	0.0729 ± 0.0058	$0.072 \pm 0.001 \pm 0.001$
A^0_{LR}	0.1551 ± 0.0040	$0.144 \pm 0.002 \pm 0.002$
$\overline{A}_b$	0.841 ± 0.053	$0.934 \pm 0 \pm 0$
$\overline{A}_c$	0.606 ± 0.090	$0.667 \pm 0.001 \pm 0.001$
$\overline{s}^2_\ell(A^{(0,q)}_{FB})$	0.2325 ± 0.0013	$0.2319 \pm 0.0002 \pm 0.0002$
$\Gamma(\ell\bar{\ell})$ (MeV)	83.93 ± 0.14	$83.97 \pm 0.01 \pm 0.06$
Γ(had) (MeV)	1744.8 ± 3.0	$1743.8 \pm 0.2 \pm 1.2$
Γ(inv) (MeV)	499.9 ± 2.5	$501.6 \pm 0 \pm 0.3$
M_W (GeV)	80.26 ± 0.16	$80.34 \pm 0.01 \pm 0.04$
Q_W	$-71.04 \pm 1.58 \pm 0.88$	$-72.88 \pm 0.05 \pm 0.03$
$s^2_W = 1 - \dfrac{M^2_W}{M^2_Z}$	0.2218 ± 0.0059 0.2260 ± 0.0048	$0.2237 \pm 0.0002 \pm 0.0008$
$g^{\nu e}_A$	-0.503 ± 0.017	$-0.507 \pm 0 \pm 0.0004$
$g^{\nu e}_V$	-0.035 ± 0.017	$-0.037 \pm 0.0005 \pm 0.0003$

since M_W and M_Z are directly measurable. Then $\widehat{s}^2_Z$ and ρ_0 can be considered dependent parameters defined by

$$\widehat{s}^2_Z \equiv A^2_0/M^2_W(1 - \Delta\widehat{r}_W) \tag{10.40}$$

and

$$\rho_0 \equiv M^2_W/(M^2_Z\,\widehat{c}^2_Z\,\widehat{\rho}) \ . \tag{10.41}$$

Provided that the new physics which yields $\rho_0 \neq 1$ is a small perturbation which does not significantly affect the radiative corrections, ρ_0 can be regarded as a phenomenological parameter which multiplies G_F in Eqs. (10.12)–(10.14), (10.28), and Γ_Z in Eq. (10.36). (Also, the expression for M_Z is divided by $\sqrt{\rho_0}$;

Table 10.5: Values of $\widehat{s}^2_Z$ and s^2_W (in parentheses), α_s, and m_t for various combinations of observables. The central values are for $M_H = 300$ GeV, and the second set of errors is for $M_H \to 1000(+), 60(-)$.

Data	$\widehat{s}^2_Z$ (s^2_W)	α_s (M_Z)	m_t (GeV)
Indirect + CDF + DØ	0.2315(2)(3) (0.2236 ± 0.0008)	0.123(4)(2)	$180 \pm 7^{+12}_{-13}$
All indirect	0.2315(2)(2) (0.2236 ± 0.0009)	0.123(4)(2)	$179 \pm 8^{+17}_{-20}$
All LEP	0.2318(3)(2) (0.2246 ± 0.0011)	0.124(4)(2)	$171 \pm 10^{+18}_{-20}$
SLD + M_Z	0.2302(5)(0) (0.2184 ± 0.0020)	—	220^{+14+19}_{-15-24}
Z pole (LEP + SLD)	0.2314(3)(1) (0.2234 ± 0.0010)	0.123(4)(2)	181^{+8+18}_{-9-20}

the M_W formula is unchanged.) There is now enough data to determine ρ_0, $\sin^2\theta_W$, m_t, and α_s simultaneously. In particular, R_b and the direct CDF and DØ events yield m_t independent of ρ_0, the asymmetries yield $\widehat{s}^2_Z$, R gives α_s, and M_Z and the widths constrain ρ_0. From the global fit (including CDF and DØ),

$$\rho_0 = 1.0012 \pm 0.0013 \pm 0.0018 \tag{10.42}$$

$$\widehat{s}^2_Z = 0.2314 \pm 0.0002 \pm 0.0002 \tag{10.43}$$

$$\alpha_s = 0.121 \pm 0.004 \pm 0.001 \tag{10.44}$$

$$m_t = 171 \pm 12 \ , \tag{10.45}$$

where the second error is from M_H. This is in remarkable agreement with the Standard Model expectation $\rho_0 = 1$, and constrains any higher-dimensional Higgs representation to have vacuum expectation values of less than a few percent of those of the doublets. The allowed regions in the $\rho_0 - \widehat{s}^2_Z$ plane are shown in Fig. 10.2. Allowing for new physics in R_b, one obtains $\rho_0 = 1.0002(14)(18)$ and $\alpha_s = 0.101(8)(1)$. The effects of other types of new physics are described in Sec. 14 on "Constraints on New Physics from Electroweak Analyses" in this *Review*.

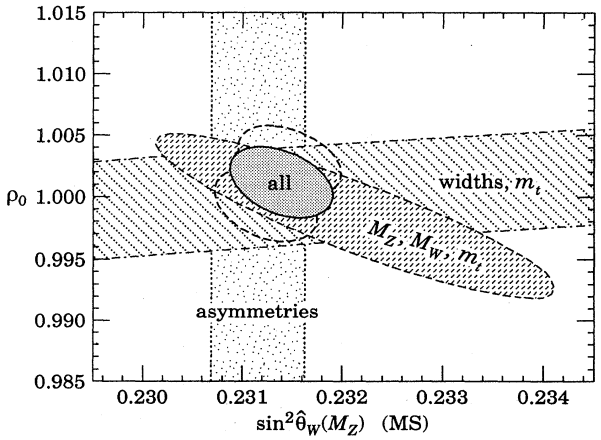

Figure 10.2: The allowed regions in $\sin^2\widehat{\theta}_W - \rho_0$ at 90% CL. m_t is a free parameter and $M_H = 300$ GeV is assumed. (The upper (lower) dashed contours are for $M_H = 1000$ (60) GeV.) The horizontal (width) band uses the experimental value of M_Z in Eq. (10.36).

Most of the parameters relevant to ν-hadron, νe, e-hadron, and e^+e^- processes are determined uniquely and precisely from the data in "model independent" fits (*i.e.*, fits which allow for an arbitrary electroweak gauge theory). The values for the parameters defined in Eqs. (10.12)–(10.14) are given in Table 10.6 along with the predictions of the Standard Model. The agreement is excellent. The low-energy e^+e^- results are difficult to present in a model-independent way because Z-propagator effects are non-negligible at TRISTAN, PETRA, and PEP energies. However, assuming e-μ-τ universality, the lepton asymmetries imply [45] $4(g_A^e)^2 = 0.99 \pm 0.05$, in good agreement with the Standard Model prediction $\simeq 1$. The much more precisely measured Z-pole parameters in Table 10.3 are in excellent agreement with the Standard Model.

Table 10.6: Values of the model-independent neutral-current parameters, compared with the Standard Model prediction using $M_Z = 91.1884$ GeV for $m_t = 180 \pm 7$ GeV and $M_H = 300$ GeV. There is a second $g_{V,A}^{\nu e}$ solution, given approximately by $g_V^{\nu e} \leftrightarrow g_A^{\nu e}$, which is eliminated by e^+e^- data under the assumption that the neutral current is dominated by the exchange of a single Z. θ_i, $i = L$ or R, is defined as $\tan^{-1}[\epsilon_i(u)/\epsilon_i(d)]$.

Quantity	Experimental Value	Standard Model Prediction		Correlation
$\epsilon_L(u)$	0.332 ± 0.016	0.345 ± 0.0003		
$\epsilon_L(d)$	-0.438 ± 0.012	-0.429 ± 0.0004		non-
$\epsilon_R(u)$	-0.178 ± 0.013	-0.156		Gaussian
$\epsilon_R(d)$	$-0.026\ ^{+0.075}_{-0.048}$	0.078		
g_L^2	0.3017 ± 0.0033	0.303 ± 0.0005		
g_R^2	0.0326 ± 0.0033	0.030		small
θ_L	2.50 ± 0.035	2.46		
θ_R	$4.58\ ^{+0.46}_{-0.28}$	5.18		
$g_A^{\nu e}$	-0.507 ± 0.014	-0.507 ± 0.0004		-0.04
$g_V^{\nu e}$	-0.041 ± 0.015	-0.037 ± 0.0003		
C_{1u}	-0.214 ± 0.046	-0.190 ± 0.0005	-0.995	-0.79
C_{1d}	0.359 ± 0.041	0.342 ± 0.0004		0.79
$C_{2u} - \frac{1}{2}C_{2d}$	-0.04 ± 0.13	-0.052 ± 0.0009		

References:

1. S. Weinberg, Phys. Rev. Lett. **19**, 1264 (1967);
   A. Salam in *Elementary Particle Theory*, ed. N. Svartholm (Almquist and Wiksells, Stockholm, 1969) p. 367;
   S.L. Glashow, J. Iliopoulos, and L. Maiani, Phys. Rev. **D2**, 1285 (1970).
2. For reviews, see G. Barbiellini and C. Santoni, Riv. Nuovo Cimento **9(2)**, 1 (1986);
   E.D. Commins and P.H. Bucksbaum, *Weak Interactions of Leptons and Quarks* (Cambridge Univ. Press, Cambridge, 1983);
   W. Fetscher and H.J. Gerber, p. 657 of Ref. 3;
   J. Deutsch and P. Quin, p. 706 of Ref. 3.
3. *Precision Tests of the Standard Electroweak Model*, ed. P. Langacker (World, Singapore, 1995).
4. CDF: F. Abe *et al.*, Phys. Rev. Lett. **74**, 2626 (1995).
5. DØ: S. Abachi *et al.*, Phys. Rev. Lett. **74**, 2632 (1995).
6. For reviews, see J. Gunion *et al.*, *The Higgs Hunter's Guide*, (Addison-Wesley, Redwood City, 1990);
   M. Sher, Phys. Reports **179**, 273 (1989).
7. S. Fanchiotti, B. Kniehl, and A. Sirlin, Phys. Rev. **D48**, 307 (1993) and references therein.
8. $\alpha(M_Z)^{-1} = 128.896 \pm 0.090$, S. Eidelman and F. Jegerlehner, Z. Phys. **C67**, 585 (1995).
9. $\alpha(M_Z)^{-1} = 128.99 \pm 0.06$, A.D. Martin and D. Zeppenfeld, Phys. Lett. **B345**, 558 (1995).
10. $\alpha(M_Z)^{-1} = 128.89 \pm 0.09$, H. Burkhardt and B. Pietrzyk, Phys. Lett. **B356**, 398 (1995).
11. $\alpha(M_Z)^{-1} = 128.96 \pm 0.06$, (corrected from an original 129.08 ± 0.10), M.L. Swartz, SLAC-PUB-95-7001.
12. N.V. Krasnikov, Mod. Phys. Lett. **A9**, 2825 (1994).
13. W.J. Marciano and A. Sirlin, Phys. Rev. Lett. **61**, 1815 (1988).
14. The results given here are updated from U. Amaldi *et al.*, Phys. Rev. **D36**, 1385 (1987);
    P. Langacker and M. Luo, Phys. Rev. **D44**, 817 (1991);
    Very similar conclusions are reached in an analysis by G. Costa *et al.*, Nucl. Phys. **B297**, 244 (1988);
    Deep inelastic scattering is considered by G.L. Fogli and D. Haidt, Z. Phys. **C40**, 379 (1988). For recent analyses, see Ref. 15.
15. P. Langacker, p. 883 of Ref. 3;
    J. Erler and P. Langacker, Phys. Rev. **D52**, 441 (1995).
16. A. Sirlin, Phys. Rev. **D22**, 971 (1980); **D29**, 89 (1984);
    W. Hollik, Fortsch. Phys. **38**, 165 (1990);
    D.C. Kennedy *et al.*, Nucl. Phys. **B321**, 83 (1989);
    D.C. Kennedy and B.W. Lynn, Nucl. Phys. **B322**, 1 (1989);
    D.Yu Bardin *et al.*, Z. Phys. **C44**, 493 (1989);
    For recent reviews, see the articles by W. Hollik, pp. 37,117 and W. Marciano, p. 170 in Ref. 3. Extensive references to other papers are given in Ref. 14.
17. W. Hollik in [16] and references therein;
    V.A. Novikov, L.B. Okun, and M.I. Vysotsky, Nucl. Phys. **B397**, 35 (1993).
18. W.J. Marciano and J.L. Rosner, Phys. Rev. Lett. **65**, 2963 (1990).
19. G. Degrassi, S. Fanchiotti, and A. Sirlin, Nucl. Phys. **B351**, 49 (1991).
20. P. Gambino and A. Sirlin, Phys. Rev. **D49**, 1160 (1994).
21. Zfitter: D. Bardin *et al.*, CERN-TH.6443/92, and references therein.
22. R. Barbieri *et al.*, Phys. Lett. **B288**, 95 (1992);
    Nucl. Phys. **B409**, 105 (1993).
23. A. Djouadi and C. Verzegnassi, Phys. Lett. **B195**, 265 (1987);
    A. Djouadi, Nuovo Cimento **100A**, 357 (1988);
    B.A. Kniehl, Nucl. Phys. **B347**, 86 (1990).
24. K.G. Chetyrkin, J.H. Kühn and M. Steinhauser, Phys. Lett. **B351**, 331 (1995);
    L. Avdeev, J. Fleischer, S. Mikhailov and O. Tarasov, Phys. Lett. **B336**, 560 (1994), **B349**, 597(E) (1995).
25. J. Fleischer *et al.*, Phys. Lett. **B293**, 437 (1992);
    K.G. Chetyrkin *et al.*, Mod. Phys. Lett. **A8**, 2785 (1993).
26. For a review, see F. Perrier, p. 385 of Ref. 3.
27. CDHS: H. Abramowicz *et al.*, Phys. Rev. Lett. **57**, 298 (1986);
    A. Blondel *et al.*, Z. Phys. **C45**, 361 (1990).
28. CHARM: J.V. Allaby *et al.*, Z. Phys. **C36**, 611 (1987).
29. BEBC: D. Allasia *et al.*, Nucl. Phys. **B307**, 1 (1988).
30. Previous Fermilab results are CCFR:P.G. Reutens *et al.*, Z. Phys. **C45**, 539 (1990);
    FMM: T.S. Mattison *et al.*, Phys. Rev. **D42**, 1311 (1990).
31. CCFR: C.G. Arroyo *et al.*, Phys. Rev. Lett. **72**, 3452 (1994).
32. CHARM I: J. Dorenbosch *et al.*, Z. Phys. **C41**, 567 (1989).
33. BNL E734: L.A. Ahrens *et al.*, Phys. Rev. **D41**, 3297 (1990).
34. CHARM II: P. Vilain *et al.*, Phys. Lett. **B335**, 246 (1994). See also J. Panman, p. 504 of Ref. 3.
35. C.Y. Prescott *et al.*, Phys. Lett. **84B**, 524 (1979). For a review, see P. Souder, p. 599 of Ref. 3.

36. For reviews and references to earlier work, see B.P. Masterson and C.E. Wieman, p. 545 of Ref. 3;
M.A. Bouchiat and L. Pottier, Science **234**, 1203 (1986).
37. Cesium (Boulder): M.C. Noecker *et al.*, Phys. Rev. Lett. **61**, 310 (1988).
38. Bismuth (Oxford): M.J.D. Macpherson *et al.*, Phys. Rev. Lett. **67**, 2784 (1991).
39. Lead (Seattle): D.M. Meekhof *et al.*, Phys. Rev. Lett. **71**, 3442 (1993).
40. Thallium (Oxford): N.H. Edwards *et al.*, Phys. Rev. Lett. **74**, 2654 (1995);
(Seattle): P.A. Vetter *et al.*, Phys. Rev. Lett. **74**, 2658 (1995).
41. S.A. Blundell, W.R. Johnson, and J. Sapirstein, Phys. Rev. Lett. **65**, 1411 (1990) and p. 577 of Ref. 3;
V.A. Dzuba *et al.*, Phys. Lett. **141A**, 147 (1989).
42. J.L. Rosner, hepph-9507375.
43. S.J. Pollock *et al.*, Phys. Rev. **C46**, 2587 (1992);
B.Q. Chen and P. Vogel, Phys. Rev. **C48**, 1392 (1993).
44. B.W. Lynn and R.G. Stuart, Nucl. Phys. **B253**, 216 (1985);
Physics at LEP, ed. J. Ellis and R. Peccei, CERN 86-02, Vol. I.
45. R. Marshall, Z. Phys. **C43**, 607 (1989);
C. Kiesling, *Tests of the Standard Theory of Electroweak Interactions* (Springer-Verlag, NY, 1988);
Y. Mori *et al.*, Phys. Lett. **B218**, 499 (1989);
D. Haidt, p. 203 of Ref. 3.
46. For reviews, see D. Schaile, p. 215, and A. Blondel, p. 277 of Ref. 3.
47. Recent LEP results, including preliminary results from the 1994 run, are given in the LEP Electroweak Working Group report LEPEWWG/95-02.
48. SLD: K. Abe *et al.*, Phys. Rev. Lett. **73**, 25 (1994).
49. Preliminary SLD results including those from the 1994–1995 run were presented at the 1995 EPS meeting, Brussels, contributions eps 0654, 0222, 0248–0251.
50. J. Schwinger, *Particles, Sources and Fields, Vol.* II (Addison-Wesley, New York, 1973);
K.G. Chetyrkin, A.L. Kataev, and F.V. Tkachev, Phys. Lett. **B85**, 277 (1979);
M. Dine and J. Sapirstein, Phys. Rev. Lett. **43**, 668 (1979);
W. Celmaster, R.J. Gonsalves, Phys. Rev. Lett. **44**, 560 (1980);
S.G. Gorishny, A.L. Kataev, and S.A. Larin, Phys. Lett. **B212**, 238 (1988) and **B259**, 144 (1991);
L.R. Surguladze and M.A. Samuel, Phys. Rev. Lett. **66**, 560 (1991) and 2416 (E);
A comprehensive report and further references can be found in K.G. Chetyrkin, J.H. Kühn, and A. Kwiatkowski, CERN yellow report CERN 95-03, Part II.
51. For a recent review, see B.A. Kniehl, Int. J. Mod. Phys. **A10**, 443 (1995).
52. W. Bernreuther and W. Wetzel, Z. Phys. **11**, 113 (1981) and Phys. Rev. **D24**, 2724 (1982);
B.A. Kniehl, Phys. Lett. **B237**, 127 (1990);
K.G. Chetyrkin, Phys. Lett. **B307**, 169 (1993);
A.H. Hoang, M. Jezabek, J.H. Kühn, and T. Teubner, Phys. Lett. **B338**, 330 (1994);
S.A. Larin, T. van Ritbergen, and J.A.M. Vermaseren, Nucl. Phys. **B438**, 278 (1995).
53. T.H. Chang, K.J.F. Gaemers, and W.L. van Neerven, Nucl. Phys. **B202**, 407 (1980);
J. Jersak, E. Laermann, and P.M. Zerwas, Phys. Lett. **B98**, 363 (1981) and Phys. Rev. **D25**, 1218 (1982);
S.G. Gorishny, A.L. Kataev, and S.A. Larin, Nuovo Cimento **92**, 117 (1986);
K.G. Chetyrkin and J.H. Kühn, Phys. Lett. **B248**, 359 (1990);
K.G. Chetyrkin, J.H. Kühn, and A. Kwiatkowski, Phys. Lett. **B282**, 221 (1992);
see also the last reference in Ref. 50.
54. B.A. Kniehl and J.H. Kühn, Phys. Lett. **B224**, 229 (1990) and Nucl. Phys. **B329**, 547 (1990);
K.G. Chetyrkin and A. Kwiatkowski, Phys. Lett. **B305**, 285 (1993) and **B319**, 307 (1993);
S.A. Larin, T. van Ritbergen, and J.A.M. Vermaseren, Phys. Lett. **B320**, 159 (1994);
K.G. Chetyrkin and O.V. Tarasov, Phys. Lett. **B327**, 114 (1994).
55. A.L. Kataev, Phys. Lett. **B287**, 209 (1992).
56. D. Albert *et al.*, Nucl. Phys. **B166**, 460 (1980);
F. Jegerlehner, Z. Phys. **C32**, 425 (1986);
A. Djouadi *et al.*, Z. Phys. **C46**, 411 (1990);
A. Borrelli *et al.*, Nucl. Phys. **B333**, 357 (1990);
see also Ref. 57.
57. W. Beenakker and W. Hollik, Z. Phys. **C40**, 141 (1988);
A.A. Akhundov *et al.*, Nucl. Phys. **B276**, 1 (1986);
B.W. Lynn and R.G. Stuart, Phys. Lett. **B352**, 676 (1990);
J. Bernabeu, A. Pich, and A. Santamaria, Nucl. Phys. **B363**, 326 (1991).
58. See the Z-Boson Listings and Refs. 46 and 47.
59. CDF: F. Abe *et al.*, Phys. Rev. Lett. **75**, 1ℓ (1995);
UA2: S. Alitti *et al.*, Phys. Lett. **B276**, 354 (1992);
DØ: C.K. Jung, presented at the 27th International Conference of High Energy Physics, Glasgow (1994).
60. M. Shifman, Mod. Phys. Lett. **A10**, 605 (1995);
see also Ref. 15.
61. P. Langacker and N. Polonsky, Phys. Rev. **D52**, 3081 (1995) and references therein.

11. THE CABIBBO-KOBAYASHI-MASKAWA MIXING MATRIX

Updated 1995 by F.J. Gilman, K. Kleinknecht, and B. Renk.

In the Standard Model with SU(2) × U(1) as the gauge group of electroweak interactions, both the quarks and leptons are assigned to be left-handed doublets and right-handed singlets. The quark mass eigenstates are not the same as the weak eigenstates, and the matrix relating these bases was defined for six quarks and given an explicit parametrization by Kobayashi and Maskawa [1] in 1973. It generalizes the four-quark case, where the matrix is parametrized by a single angle, the Cabibbo angle [2].

By convention, the three charge $2e/3$ quarks (u, c, and t) are unmixed, and all the mixing is expressed in terms of a 3×3 unitary matrix V operating on the charge $-e/3$ quarks (d, s, and b):

$$\begin{pmatrix} d' \\ s' \\ b' \end{pmatrix} = \begin{pmatrix} V_{ud} & V_{us} & V_{ub} \\ V_{cd} & V_{cs} & V_{cb} \\ V_{td} & V_{ts} & V_{tb} \end{pmatrix} \begin{pmatrix} d \\ s \\ b \end{pmatrix} . \tag{11.1}$$

The values of individual matrix elements can in principle all be determined from weak decays of the relevant quarks, or, in some cases, from deep inelastic neutrino scattering. Using the constraints discussed below together with unitarity, and assuming only three generations, the 90% confidence limits on the magnitude of the elements of the complete matrix are:

$$\begin{pmatrix} 0.9745 \text{ to } 0.9757 & 0.219 \text{ to } 0.224 & 0.002 \text{ to } 0.005 \\ 0.218 \text{ to } 0.224 & 0.9736 \text{ to } 0.9750 & 0.036 \text{ to } 0.046 \\ 0.004 \text{ to } 0.014 & 0.034 \text{ to } 0.046 & 0.9989 \text{ to } 0.9993 \end{pmatrix} . \tag{11.2}$$

The ranges shown are for the individual matrix elements. The constraints of unitarity connect different elements, so choosing a specific value for one element restricts the range of others.

There are several parametrizations of the Cabibbo-Kobayashi-Maskawa matrix. In view of the need for a "standard" parametrization in the literature, we advocate:

$$V = \begin{pmatrix} c_{12}c_{13} & s_{12}c_{13} & s_{13}e^{-i\delta_{13}} \\ -s_{12}c_{23} - c_{12}s_{23}s_{13}e^{i\delta_{13}} & c_{12}c_{23} - s_{12}s_{23}s_{13}e^{i\delta_{13}} & s_{23}c_{13} \\ s_{12}s_{23} - c_{12}c_{23}s_{13}e^{i\delta_{13}} & -c_{12}s_{23} - s_{12}c_{23}s_{13}e^{i\delta_{13}} & c_{23}c_{13} \end{pmatrix} \tag{11.3}$$

proposed by Chau and Keung [3]. The choice of rotation angles follows earlier work of Maiani [4], and the placement of the phase follows that of Wolfenstein [5]. The notation used is that of Harari and Leurer [6] who, along with Fritzsch and Plankl [7], proposed this parametrization as a particular case of a form generalizable to an arbitrary number of "generations." The general form was also put forward by Botella and Chau [8]. Here $c_{ij} = \cos\theta_{ij}$ and $s_{ij} = \sin\theta_{ij}$, with i and j being "generation" labels, $\{i, j = 1, 2, 3\}$. In the limit $\theta_{23} = \theta_{13} = 0$ the third generation decouples, and the situation reduces to the usual Cabibbo mixing of the first two generations with θ_{12} identified with the Cabibbo angle [2].

The real angles θ_{12}, θ_{23}, θ_{13} can all be made to lie in the first quadrant by an appropriate redefinition of quark field phases. Then all s_{ij} and c_{ij} are positive, $|V_{us}| = s_{12}c_{13}$, $|V_{ub}| = s_{13}$, and $|V_{cb}| = s_{23}c_{13}$. As c_{13} is known to deviate from unity only in the fifth decimal place, $|V_{us}| = s_{12}$, $|V_{ub}| = s_{13}$, and $|V_{cb}| = s_{23}$ to an excellent approximation. The phase δ_{13} lies in the range $0 \le \delta_{13} < 2\pi$, with non-zero values generally breaking CP invariance for the weak interactions. The generalization to the n generation case contains $n(n-1)/2$ angles and $(n-1)(n-2)/2$ phases [6,7,8]. The range of matrix elements in Eq. (11.2) corresponds to 90% CL limits on the angles of $s_{12} = 0.219$ to $0.223, s_{23} = 0.036$ to 0.046, and $s_{13} = 0.002$ to 0.005.

Kobayashi and Maskawa [1] originally chose a parametrization involving the four angles, θ_1, θ_2, θ_3, δ:

$$\begin{pmatrix} d' \\ s' \\ b' \end{pmatrix} = \begin{pmatrix} c_1 & -s_1c_3 & -s_1s_3 \\ s_1c_2 & c_1c_2c_3 - s_2s_3e^{i\delta} & c_1c_2s_3 + s_2c_3e^{i\delta} \\ s_1s_2 & c_1s_2c_3 + c_2s_3e^{i\delta} & c_1s_2s_3 - c_2c_3e^{i\delta} \end{pmatrix} \begin{pmatrix} d \\ s \\ b \end{pmatrix} , \tag{11.4}$$

where $c_i = \cos\theta_i$ and $s_i = \sin\theta_i$ for $i = 1, 2, 3$. In the limit $\theta_2 = \theta_3 = 0$, this reduces to the usual Cabibbo mixing with θ_1 identified (up to a sign) with the Cabibbo angle [2]. Slightly different forms of the Kobayashi-Maskawa parametrization are found in the literature. The CKM matrix used in the 1982 *Review of Particle Properties* is obtained by letting $s_1 \to -s_1$ and $\delta \to \delta + \pi$ in the matrix given above. An alternative is to change Eq. (11.4) by $s_1 \to -s_1$ but leave δ unchanged. With this change in s_1, the angle θ_1 becomes the usual Cabibbo angle, with the "correct" sign (*i.e.* $d' = d\cos\theta_1 + s\sin\theta_1$) in the limit $\theta_2 = \theta_3 = 0$. The angles θ_1, θ_2, θ_3 can, as before, all be taken to lie in the first quadrant by adjusting quark field phases. Since all these parametrizations are referred to as "the" Kobayashi-Maskawa form, some care about which one is being used is needed when the quadrant in which δ lies is under discussion.

Other parametrizations, mentioned above, are due to Maiani [4] and to Wolfenstein [5]. Still other parametrizations [9] have come into the literature in connection with attempts to define "maximal CP violation". No physics can depend on which of the above parametrizations (or any other) is used as long as a single one is used consistently and care is taken to be sure that no other choice of phases is in conflict.

Our present knowledge of the matrix elements comes from the following sources:

(1) New analyses have been performed comparing nuclear beta decay to muon decay. The previous radiative corrections [10] already included order $Z\alpha^2$ effects and more recent results [11–15] concentrate on nuclear mismatch and structure-dependent radiative corrections. The results in Ref. 15 violate CVC, and the updated [13] average ft values for superallowed 0^+ to 0^+ transitions of Refs. 11 and 12 do not agree with each other within the estimated uncertainties:

$$\begin{aligned} ft &= 3150.8 \pm 1.7 \text{ sec} \quad \text{(Refs. 11 and 13)} , \\ ft &= 3145.7 \pm 1.5 \text{ sec} \quad \text{(Refs. 12 and 13)} , \end{aligned} \tag{11.5}$$

The common experimental error is ±0.82. We have taken an average of the above values and scaled up the error to take account of the uncertainty in the nuclear structure dependent radiative corrections and corresponding inconsistency of the theoretical results. This transforms to

$$|V_{ud}| = 0.9736 \pm 0.0010 , \tag{11.6}$$

which is almost one standard deviation smaller than the result in the previous *Review of Particle Physics*. It is consistent with the result $|V_{ud}| = 0.9734 \pm 0.0007$ from the update in Ref. 14.

(2) Analysis of K_{e3} decays yields [16]

$$|V_{us}| = 0.2196 \pm 0.0023 . \tag{11.7}$$

With isospin violation taken into account in K^+ and K^0 decays, the extracted values of $|V_{us}|$ are in agreement at the 1% level. A reanalysis [13] obtains essentially the same value, but quotes a somewhat smaller error which is only statistical. The analysis of hyperon decay data has larger theoretical uncertainties because of first order SU(3) symmetry breaking effects in the axial-vector couplings, but due account of symmetry breaking [17] applied to the WA2 data [18] gives a corrected value [19] of 0.222 ± 0.003. We average these two results to obtain:

$$|V_{us}| = 0.2205 \pm 0.0018 . \tag{11.8}$$

(3) The magnitude of $|V_{cd}|$ may be deduced from neutrino and antineutrino production of charm off valence d quarks. The dimuon production cross sections of the CDHS group [20] yield $\overline{B}_c\,|V_{cd}|^2 = 0.41 \pm 0.07 \times 10^{-2}$, where $\overline{B}_c$ is the semileptonic branching fraction of the charmed hadrons produced. The corresponding value from a more recent Tevatron experiment [21], where a next-to-leading-order

QCD analysis has been carried out, is $0.534 \pm 0.021^{+0.025}_{-0.051} \times 10^{-2}$, where the last error is from the scale uncertainty. Assuming a similar scale error for the CDHS result and averaging these two results gives $0.49 \pm 0.05 \times 10^{-2}$. Supplementing this with data [22] on the mix of charmed particle species produced by neutrinos and PDG values for their semileptonic branching fractions to give [21] $\overline{B}_c = 0.099 \pm 0.012$, yields

$$|V_{cd}| = 0.224 \pm 0.016 \tag{11.9}$$

(4) Values of $|V_{cs}|$ from neutrino production of charm are dependent on assumptions about the strange quark density in the parton-sea. The most conservative assumption, that the strange-quark sea does not exceed the value corresponding to an SU(3) symmetric sea, leads to a lower bound [20], $|V_{cs}| > 0.59$. It is more advantageous to proceed analogously to the method used for extracting $|V_{us}|$ from K_{e3} decay; namely, we compare the experimental value for the width of D_{e3} decay with the expression [23] that follows from the standard weak interaction amplitude:

$$\Gamma(D \to \overline{K} e^+ \nu_e) = |f_+^D(0)|^2 \, |V_{cs}|^2 \, (1.54 \times 10^{11} \text{ s}^{-1}) \, . \tag{11.10}$$

Here $f_+^D(q^2)$, with $q = p_D - p_K$, is the form factor relevant to D_{e3} decay; its variation has been taken into account with the parametrization $f_+^D(t)/f_+^D(0) = M^2/(M^2 - t)$ and $M = 2.1$ GeV/c^2, a form and mass consistent with Mark III and E691 measurements [24,25]. Combining data on branching ratios for D_{e3} decays from Mark III, E691, and CLEO experiments [24–26] with accurate values [27] for τ_{D^+} and τ_{D^0}, yields $(0.762 \pm 0.055) \times 10^{11}$ s^{-1} for $\Gamma(D \to \overline{K} e^+ \nu_e)$. Therefore

$$|f_+^D(0)|^2 \, |V_{cs}|^2 = 0.495 \pm 0.036 \, . \tag{11.11}$$

A very conservative assumption is that $|f_+^D(0)| < 1$, from which it follows that $|V_{cs}| > 0.62$. Calculations of the form factor either performed [28,29] directly at $q^2 = 0$, or done [30] at the maximum value of $q^2 = (m_D - m_K)^2$ and interpreted at $q^2 = 0$ using the measured q^2 dependence, gives the value $f_+^D(0) = 0.7 \pm 0.1$. It follows that

$$|V_{cs}| = 1.01 \pm 0.18 \, . \tag{11.12}$$

The constraint of unitarity when there are only three generations gives a much tighter bound (see below).

(5) The ratio $|V_{ub}/V_{cb}|$ can be obtained from the semileptonic decay of B mesons produced on the $\Upsilon(4S)$ $b\bar{b}$ resonance by measuring the lepton energy spectrum above the endpoint of the $b \to c\ell\nu$ spectrum. There the $b \to u\ell\nu$ decay rate can be obtained by subtracting the background from nonresonant e^+e^- reactions. This continuum background is determined from auxiliary measurements off the $\Upsilon(4S)$. Both the CLEO [31] and ARGUS [32] collaborations have reported evidence for $b \to u$ transitions in semileptonic B decays. The interpretation of the result in terms of $|V_{ub}/V_{cb}|$ depends fairly strongly on the theoretical model used to generate the lepton energy spectrum, especially for $b \to u$ transitions [29,30,33]. Combining the experimental and theoretical uncertainties, we quote

$$|V_{ub}/V_{cb}| = 0.08 \pm 0.02 \, . \tag{11.13}$$

(6) The heavy quark effective theory [34](HQET) provides a nearly model-independent treatment of B semileptonic decays to charmed mesons. From measurements [35–37] of the exclusive decay $B \to \overline{D}^* \ell \nu_\ell$, the value $|V_{cb}| = 0.041 \pm 0.003 \pm 0.002$ has been extracted [38] using corrections based on the HQET. A new analysis of inclusive decays [39], where the measured semileptonic bottom hadron partial width is assumed to be that of a b quark decaying through the usual $V - A$ interaction, gives $|V_{cb}| \cdot (\tau_b/1.5 \text{ ps})^{1/2} = 0.041 \pm 0.002$. Using a value [40] for the b lifetime $\tau_b = 1.55 \pm 0.06$ ps and combining with the exclusive result, we obtain

$$|V_{cb}| = 0.041 \pm 0.003 \, . \tag{11.14}$$

The results for three generations of quarks, from Eqs. 11.6, 11.8, 11.9, 11.12, 11.13, and 11.14 plus unitarity, are summarized in the matrix in Eq. (11.2). The ranges given there are different from those given in Eqs. (11.6)–(11.14) because of the inclusion of unitarity, but are consistent with the one-standard-deviation errors on the input matrix elements. Note in particular that the unitarity constraint has pushed $|V_{ud}|$ about one standard deviation higher than given in Eq. (11.6).

The data do not preclude there being more than three generations. Moreover, the entries deduced from unitarity might be altered when the CKM matrix is expanded to accommodate more generations. Conversely, the known entries restrict the possible values of additional elements if the matrix is expanded to account for additional generations. For example, unitarity and the known elements of the first row require that any additional element in the first row have a magnitude $|V_{ub'}| < 0.08$. When there are more than three generations the allowed ranges (at 90% CL) of the matrix elements connecting the first three generations are

$$\begin{pmatrix} 0.9720 \text{ to } 0.9752 & 0.217 \text{ to } 0.223 & 0.002 \text{ to } 0.005 & \dots \\ 0.199 \text{ to } 0.234 & 0.818 \text{ to } 0.975 & 0.036 \text{ to } 0.046 & \dots \\ 0 \text{ to } 0.11 & 0 \text{ to } 0.52 & 0 \text{ to } 0.9993 & \dots \\ \vdots & \vdots & \vdots & \end{pmatrix} , \tag{11.15}$$

where we have used unitarity (for the expanded matrix) and Eqs. 11.6, 11.8, 11.9, 11.12, 11.13, and 11.14.

Further information, particularly on CKM matrix elements involving the top quark, can be obtained from flavor-changing processes that occur at the one-loop level. We have not used this information in the discussion above since the derivation of values for V_{td} and V_{ts} in this manner from, for example, B mixing, $b \to s\gamma$, or $K \to \pi\nu\overline{\nu}$, requires an additional assumption that the top-quark loop, rather than new physics, gives the dominant contribution to the process in question.

The measured value [41] of $\Delta M_d = 0.496 \pm 0.032$ ps^{-1} from $B_d^0 - \overline{B}_d^0$ mixing can be turned in this way into information on $|V_{tb}^* V_{td}|$. Using $\widehat{B}_{B_d} f_{B_d}^2 = (1.2 \pm 0.2)(173 \pm 40 \text{ MeV})^2$ from lattice QCD calculations [42], next-to-leading-order QCD corrections 43 and $m_t = 174 \pm 16$ GeV as input,

$$|V_{tb}^* \, V_{td}| = 0.009 \pm 0.003 \, , \tag{11.16}$$

where the error bar comes primarily from the theoretical uncertainty in the hadronic matrix elements.

In the ratio of B_s to B_d mass differences, many of the factors (such as the QCD correction and dependence on the t-quark mass) cancel, and we have

$$\frac{\Delta M_{B_s}}{\Delta M_{B_d}} = \frac{\widehat{B}_{B_s} f_{B_s}^2}{\widehat{B}_{B_d} f_{B_d}^2} \, \frac{|V_{tb}^* \cdot V_{ts}|^2}{|V_{tb}^* \cdot V_{td}|^2} \, . \tag{11.17}$$

With $\widehat{B}_{B_s} \approx \widehat{B}_{B_d}$ and $f_{B_s}/f_{B_d} = 1.16 \pm 0.10$ from lattice QCD [42] and the experimental limit [41] $\Delta M_{B_s}/\Delta M_{B_d} > 11.6$,

$$|V_{td}|/|V_{ts}| < 0.37 \, . \tag{11.18}$$

The CLEO observation [44] of $b \to s\gamma$ can be translated [45] similarly into $|V_{ts}|/|V_{cb}| = 1.1 \pm 0.43$, where the large uncertainty is again dominantly theoretical. Ultimately $K \to \pi\nu\overline{\nu}$ decays offer high precision because the matrix elements can be directly measured, but experiment is presently several orders of magnitude away from the requisite sensitivity. All these additional indirect constraints are consistent with the matrix elements obtained from the direct measurements plus unitarity, assuming three generations; adding the indirect constraints to the fit leaves the ranges of CKM matrix elements in Eq. (11.2) essentially unchanged.

Direct and indirect information on the CKM matrix is neatly summarized in terms of the "unitarity triangle." The name arises since unitarity of the 3×3 CKM matrix applied to the first and third columns yields

$$V_{ud} \, V_{ub}^* + V_{cd} \, V_{cb}^* + V_{td} V_{tb}^* = 0 \, . \tag{11.19}$$

The unitarity triangle is just a geometrical presentation of this equation in the complex plane [46]. We can always choose to orient the triangle so that $V_{cd}\,V_{cb}^*$ lies along the horizontal; in the parametrization we have chosen, V_{cb} is real, and V_{cd} is real to a very good approximation in any case. Setting cosines of small angles to unity, Eq. (11.19) becomes

$$V_{ub}^* + V_{td} = s_{12}\,V_{cb}^* \ , \tag{11.20}$$

which is shown as the unitarity triangle in Fig. 11.1(a). Rescaling the triangle by a factor $[1/|s_{12}\,V_{cb}|]$, the coordinates of the vertices become

$$A\big(\mathrm{Re}(V_{ub})/|s_{12}\,V_{cb}|, -\mathrm{Im}(V_{ub})/|s_{12}\,V_{cb}|\big) \ , \ B(1,0) \ , \ C(0,0) \ . \tag{11.21}$$

In the approximation of the Wolfenstein parametrization [5], with matrix elements expressed in powers of the Cabibbo angle, $\lambda \sim s_{12}$:

$$\begin{aligned} V_{us} &\sim \lambda \\ V_{ub} &\sim \lambda^3 A(\rho - i\eta) \\ V_{cb} &\sim \lambda^2 A \\ V_{td} &\sim \lambda^3 A(1 - \rho - i\eta) \ , \end{aligned} \tag{11.22}$$

the coordinates of the vertex A of the unitarity triangle are simply (ρ, η), as shown in Fig. 11.1(b).

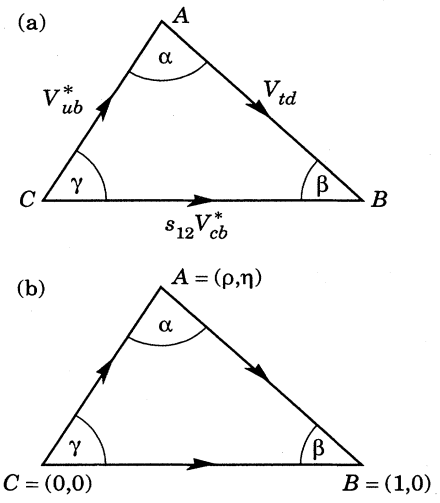

Figure 11.1: (a) Representation in the complex plane of the triangle formed by the CKM matrix elements V_{ub}^*, V_{td}, and $s_{12}\,V_{cb}^*$. (b) Rescaled triangle with vertices $A(\rho,\eta)$, $B(1,0)$, and $C(0,0)$.

CP-violating processes will involve the phase in the CKM matrix, assuming that the observed CP violation is solely related to a nonzero value of this phase. This allows additional constraints to be brought to bear. More specifically, a necessary and sufficient condition for CP violation with three generations can be formulated in a parametrization-independent manner in terms of the non-vanishing of the determinant of the commutator of the mass matrices for the charge $2e/3$ and charge $-e/3$ quarks [47]. CP violating amplitudes or differences of rates all are proportional to the CKM factor in this quantity. This is the product of factors $s_{12}s_{13}s_{23}c_{12}c_{13}^2c_{23}s_{\delta_{13}}$ in the parametrization adopted above, and is $s_1^2 s_2 s_3 c_1 c_2 c_3 s_\delta$ in that of Ref. 1. With the approximation of setting cosines to unity, this is just twice the area of the unitarity triangle. While hadronic matrix elements whose values are imprecisely known generally now enter, the constraints from CP violation in the neutral kaon system are tight enough to very much restrict the range of angles and the phase of the CKM matrix. For example, the constraint obtained from the CP-violating parameter ϵ in the neutral K system corresponds to the vertex A of the unitarity triangle lying on a hyperbola for fixed values of the hadronic matrix elements. [48] For CP-violating asymmetries of neutral B mesons decaying to CP eigenstates, there is a direct relationship between the magnitude of the asymmetry in a given decay and $\sin 2\phi$, where $\phi = \alpha$, β, γ is an appropriate angle of the unitarity triangle [46].

The combination of all the direct and indirect information can be used to find the overall constraints on the CKM matrix and thence the implications for future measurements of CP violation in the B system [48].

References:

1. M. Kobayashi and T. Maskawa, Prog. Theor. Phys. **49**, 652 (1973).
2. N. Cabibbo, Phys. Rev. Lett. **10**, 531 (1963).
3. L.-L. Chau and W.-Y. Keung, Phys. Rev. Lett. **53**, 1802 (1984).
4. L. Maiani, Phys. Lett. **62B**, 183 (1976) and in *Proceedings of the 1977 International Symposium on Lepton and Photon Interactions at High Energies* (DESY, Hamburg, 1977), p. 867.
5. L. Wolfenstein, Phys. Rev. Lett. **51**, 1945 (1983).
6. H. Harari and M. Leurer, Phys. Lett. **181B**, 123 (1986).
7. H. Fritzsch and J. Plankl, Phys. Rev. **D35**, 1732 (1987).
8. F.J. Botella and L.-L. Chau, Phys. Lett. **168B**, 97 (1986). A generalization to an arbitrary number of generalizations was also proposed by H. Terazawa, Prog. Theor. Phys. **63**, 1779 (1980).
9. See, for example, M. Gronau and J. Schechter, Phys. Rev. Lett. **54**, 385 (1985), where various parametrizations are discussed, including one equivalent to that in Eq. (11.3).
10. W.J. Marciano and A. Sirlin, Phys. Rev. Lett. **56**, 22 (1986); A. Sirlin and R. Zucchini, Phys. Rev. Lett. **57**, 1994 (1986); W. Jaus and G. Rasche, Phys. Rev. **D35**, 3420 (1987); A. Sirlin, Phys. Rev. **D35**, 3423 (1987).
11. B.A. Brown and W.E. Ormand, Phys. Rev. Lett. **62**, 866 (1989).
12. E. Hagberg *et al.*, Nucl. Phys. **A509**, 429 (1990).
13. F.C. Barker, Nucl. Phys. **A540**, 501 (1992).
14. I.S. Towner, Nucl. Phys. **A540**, 478 (1992).
15. F.C. Barker, Nucl. Phys. **A579**, 62 (1994).
16. H. Leutwyler and M. Roos, Z. Phys. **C25**, 91 (1984); See also the earlier work of R.E. Shrock and L.L. Wang, Phys. Rev. Lett. **41**, 1692 (1978).
17. J.F. Donoghue, B.R. Holstein, and S.W. Klimt, Phys. Rev. **D35**, 934 (1987).
18. M. Bourquin *et al.*, Z. Phys. **C21**, 27 (1983).
19. J.M. Gaillard and G. Sauvage, private communication; Using different SU(3) symmetry breaking corrections, a somewhat higher value of $|V_{us}|$ is obtained by A. Garcia, R. Huerta, and P. Kielanowski, Phys. Rev. **D45**, 879 (1992).
20. H. Abramowicz *et al.*, Z. Phys. **C15**, 19 (1982).
21. S.A. Rabinowitz *et al.*, Phys. Rev. Lett. **70**, 134 (1993); A.O. Bazarko *et al.*, Z. Phys. **C65**, 189 (1995).
22. N. Ushida *et al.*, Phys. Lett. **B206**, 375 (1988).
23. The result for $M = 2.2$ GeV is found in F. Bletzacker, H.T. Nieh, and A. Soni, Phys. Rev. **D16**, 732 (1977).
24. CLEO: A. Bean *et al.*, Phys. Lett. **B317**, 647 (1993).
25. Mark III: Z. Bai *et al.*, Phys. Rev. Lett. **66**, 1011 (1991).
26. Mark III: J. Adler *et al.*, Phys. Rev. Lett. **62**, 1821 (1989).
27. E691: J.R. Raab *et al.*, Phys. Rev. **D37**, 2391 (1988); E687: P.L. Frabetti *et al.*, Phys. Lett. **B263**, 584 (1991).
28. T.M. Aliev *et al.*, Yad. Fiz. **40**, 823 (1984) [Sov. J. Nucl. Phys. **40**, 527 (1984)].
29. M. Bauer, B. Stech, and M. Wirbel, Z. Phys. **C29**, 637 (1985).

30. B. Grinstein, N. Isgur, and M.B. Wise, Phys. Rev. Lett. **56**, 298 (1986);
    B. Grinstein, N. Isgur, D. Scora, and M.B. Wise, Phys. Rev. **D39**, 799 (1989).
31. F. Bartelt *et al.*, Phys. Rev. Lett. **71**, 4111 (1993).
32. H. Albrecht *et al.*, Phys. Lett. **B255**, 297 (1991).
33. G. Altarelli *et al.*, Nucl. Phys. **B208**, 365 (1982).
34. N. Isgur and M.B. Wise, Phys. Lett. **B232**, 113 (1989); **B237**, 527 (1990);
    E. Eichten and B. Hill, Phys. Lett. **B234**, 511 (1990);
    M.E. Luke, Phys. Lett. **B252**, 447 (1990).
35. H. Albrecht *et al.*, Z. Phys. **C57**, 533 (1993).
36. I.J. Scott *et al.*, *Proceedings of the XXVII International Conference on High-Energy Physics*, Glasgow, Scotland, July 20–27, 1994, edited by P.J. Bussey and I.G. Knowles (Institute of Physics, Bristol, 1995), Vol. II, p. 1121.
37. T.E. Browder *et al.*, Phys. Rev. **D51**, 1014 (1995).
38. M. Neubert, CERN preprint CERN-TH/95-107 (1995) (unpublished).
39. P. Ball, M.N. Beneke, and V.M. Brown, CERN preprint CERN-TH/95-65 (1995) (unpublished).
40. See the review of J.R. Patterson in *Proceedings of the XXVII International Conference on High-Energy Physics*, Glasgow, Scotland, July 20–27, 1994, edited by P.J. Bussey and I.G. Knowles (Institute of Physics, Bristol, 1995), Vol. I, p. 149.
41. See the review of R. Forty in *Proceedings of the XXVII International Conference on High-Energy Physics*, Glasgow, Scotland, July 20–27, 1994, edited by P.J. Bussey and I.G. Knowles (Institute of Physics, Bristol, 1995), Vol. I, p. 171.
42. A. Soni, plenary talk at the *1994 International Workshop on B Physics*, Nagoya, Japan, October 1994 and Brookhaven preprint BNL-61378 (1995) (unpublished).
43. A.J. Buras, M. Jamin, and P. Weisz, Nucl. Phys. **B347**, 491 (1990).
44. M.S. Alam *et al.*, Phys. Rev. Lett. **74**, 2885 (1995).
45. A. Ali and C. Greub, DESY preprint DESY-95-117 (1995) (unpublished). See also P.A. Griffin, M. Maslip, and M. McGuigan, Phys. Rev. **D50**, 5751 (1994) for extraction within large errors of a value for $|V_{ts}|$ using the exclusive decay $B \to K^*(892)\,\gamma$.
46. L.-L. Chau and W.-Y. Keung, Ref. 3;
    J.D. Bjorken, private communication and Phys. Rev. **D39**, 1396 (1989);
    C. Jarlskog and R. Stora, Phys. Lett. **B208**, 268 (1988);
    J.L. Rosner, A.I. Sanda, and M.P. Schmidt, in *Proceedings of the Workshop on High Sensitivity Beauty Physics at Fermilab*, Fermilab, November 11–14, 1987, edited by A.J. Slaughter, N. Lockyer, and M. Schmidt (Fermilab, Batavia, IL, 1988), p. 165;
    C. Hamzaoui, J.L. Rosner and A.I. Sanda, *ibid*, p. 215.
47. C. Jarlskog, Phys. Rev. Lett. **55**, 1039 (1985) and Z. Phys. **C29**, 491 (1985).
48. C.O. Dib *et al.*, Phys. Rev. **D41**, 1522 (1990);
    A.I. Sanda, invited talk at the *KEK Topical Conference on Electron-Positron Collision Physics*, Tsukuba, Japan, May 17–19, 1989 (KEK, Tsukuba, 1989), p. 437;
    C.S. Kim, J.L. Rosner, and C.-P. Yuan, Phys. Rev. **D42**, 96 (1990).

12. QUARK MODEL

12.1. Quantum numbers of the quarks

Each quark has spin 1/2 and baryon number 1/3. Table 12.1 gives the additive quantum numbers (other than baryon number) of the three generations of quarks. Our convention is that the *flavor* of a quark (I_z, S, C, B, or T) has the same sign as its *charge*. With this convention, any flavor carried by a *charged* meson has the same sign as its charge; *e.g.*, the strangeness of the K^+ is +1, the bottomness of the B^+ is +1, and the charm *and* strangeness of the D_s^- are each −1.

By convention, each quark is assigned positive parity. Then each antiquark has negative parity.

Table 12.1: Additive quantum numbers of the quarks.

Property \ Quark	d	u	s	c	b	t
Q – electric charge	$-\frac{1}{3}$	$+\frac{2}{3}$	$-\frac{1}{3}$	$+\frac{2}{3}$	$-\frac{1}{3}$	$+\frac{2}{3}$
I_z – isospin z-component	$-\frac{1}{2}$	$+\frac{1}{2}$	0	0	0	0
S – strangeness	0	0	−1	0	0	0
C – charm	0	0	0	+1	0	0
B – bottomness	0	0	0	0	−1	0
T – topness	0	0	0	0	0	+1

12.2. Mesons: $q\bar{q}$ states

Nearly all known mesons are bound states of a quark q and an antiquark $\bar{q}'$ (the flavors of q and q' may be different). If the orbital angular momentum of the $q\bar{q}'$ state is L, then the parity P is $(-1)^{L+1}$. A state $q\bar{q}$ of a quark and its own antiquark is also an eigenstate of charge conjugation, with $C = (-1)^{L+S}$, where the spin S is 0 or 1. The $L = 0$ states are the pseudoscalars, $J^P = 0^-$, and the vectors, $J^P = 1^-$. Assignments for many of the known mesons are given in Table 12.2. States in the "normal" spin-parity series, $P = (-1)^J$, must, according to the above, have $S = 1$ and hence $CP = +1$. Thus mesons with normal spin-parity and $CP = -1$ are forbidden in the $q\bar{q}'$ model. The $J^{PC} = 0^{--}$ state is forbidden as well. Mesons with such J^{PC} may exist, but would lie outside the $q\bar{q}'$ model.

The nine possible $q\bar{q}'$ combinations containing u, d, and s quarks group themselves into an octet and a singlet:

$$\mathbf{3} \otimes \overline{\mathbf{3}} = \mathbf{8} \oplus \mathbf{1} \tag{12.1}$$

States with the same IJ^P and additive quantum numbers can mix. (If they are eigenstates of charge conjugation, they must also have the same value of C.) Thus the $I = 0$ member of the ground-state pseudoscalar octet mixes with the corresponding pseudoscalar singlet to produce the η and η'. These appear as members of a nonet, which is shown as the middle plane in Fig. 12.1(a). Similarly, the ground-state vector nonet appears as the middle plane in Fig. 12.1(b).

A fourth quark such as charm can be included in this scheme by extending the symmetry to SU(4), as shown in Fig. 12.1. Bottom extends the symmetry to SU(5); to draw the multiplets would require four dimensions.

For the pseudoscalar mesons, the Gell-Mann-Okubo formula is

$$m_\eta^2 = \frac{1}{3}(4m_K^2 - m_\pi^2) \ , \tag{12.2}$$

assuming no octet-singlet mixing. However, the octet η_8 and singlet η_1 mix because of SU(3) breaking. In general, the mixing angle is mass dependent and becomes complex for resonances of finite width.

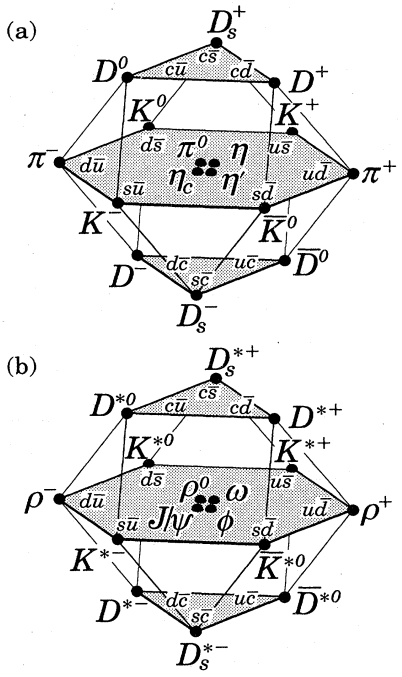

Figure 12.1: SU(4) 16-plets for the (a) pseudoscalar and (b) vector mesons made of u, d, s, and c quarks. The nonets of light mesons occupy the central planes, to which the $c\bar{c}$ states have been added. The neutral mesons at the centers of these planes are mixtures of $u\bar{u}$, $d\bar{d}$, $s\bar{s}$, and $c\bar{c}$ states.

Neglecting this, the physical states η and η' are given in terms of a mixing angle θ_P by

$$\eta = \eta_8 \cos\theta_P - \eta_1 \sin\theta_P \tag{12.3a}$$

$$\eta' = \eta_8 \sin\theta_P + \eta_1 \cos\theta_P \ . \tag{12.3b}$$

These combinations diagonalize the mass-squared matrix

$$M^2 = \begin{pmatrix} M_{11}^2 & M_{18}^2 \\ M_{18}^2 & M_{88}^2 \end{pmatrix} \ , \tag{12.4}$$

where $M_{88}^2 = \frac{1}{3}(4m_K^2 - m_\pi^2)$. It follows that

$$\tan^2\theta_P = \frac{M_{88}^2 - m_\eta^2}{m_{\eta'}^2 - M_{88}^2} \ . \tag{12.5}$$

The sign of θ_P is meaningful in the quark model. If

$$\eta_1 = (u\bar{u} + d\bar{d} + s\bar{s})/\sqrt{3} \tag{12.6a}$$

$$\eta_8 = (u\bar{u} + d\bar{d} - 2s\bar{s})/\sqrt{6} \ , \tag{12.6b}$$

then the matrix element M_{18}^2, which is due mostly to the strange quark mass, is negative. From the relation

$$\tan\theta_P = \frac{M_{88}^2 - m_\eta^2}{M_{18}^2} \ , \tag{12.7}$$

we find that $\theta_P < 0$. However, caution is suggested in the use of the η-η' mixing-angle formulas, as they are extremely sensitive to SU(3)

Table 12.2: Suggested $q\bar{q}$ quark-model assignments for most of the known mesons. Some assignments, especially for the 0^{++} multiplet and for some of the higher multiplets, are controversial. Mesons in bold face are included in the Meson Summary Table. Of the light mesons in the Summary Table, the $f_1(1420)$, $f_0(1500)$, $f_J(1710)$, $f_2(2300)$, $f_2(2340)$, and the two peaks in the $\eta(1440)$ entry are not in this table. Within the $q\bar{q}$ model, it is especially hard to find a place for the first three of these f mesons and for one of the $\eta(1440)$ peaks. See the "Note on Non-$q\bar{q}$ Mesons" at the end of the Meson Listings.

$N\,^{2S+1}L_J$	J^{PC}	$u\bar{d}$, $u\bar{u}$, $d\bar{d}$ $I=1$	$u\bar{u}$, $d\bar{d}$, $s\bar{s}$ $I=0$	$c\bar{c}$ $I=0$	$b\bar{b}$ $I=0$	$\bar{s}u$, $\bar{s}d$ $I=1/2$	$c\bar{u}$, $c\bar{d}$ $I=1/2$	$c\bar{s}$ $I=0$	$\bar{b}u$, $\bar{b}d$ $I=1/2$	$\bar{b}s$ $I=0$
$1\,^1S_0$	0^{-+}	π	η, η'	η_c		K	D	D_s	B	B_s
$1\,^3S_1$	1^{--}	ρ	ω, ϕ	$J/\psi(1S)$	$\Upsilon(1S)$	$K^*(892)$	$D^*(2010)$	$D_s^*(2110)$	$B^*(5330)$	
$1\,^1P_1$	1^{+-}	$b_1(1235)$	$h_1(1170)$, $h_1(1380)$	$h_c(1P)$		K_{1B}†	$D_1(2420)$	$D_{s1}(2536)$		
$1\,^3P_0$	0^{++}	*	*	$\chi_{c0}(1P)$	$\chi_{b0}(1P)$	$K_0^*(1430)$				
$1\,^3P_1$	1^{++}	$a_1(1260)$	$f_1(1285)$, $f_1(1510)$	$\chi_{c1}(1P)$	$\chi_{b1}(1P)$	K_{1A}†				
$1\,^3P_2$	2^{++}	$a_2(1320)$	$f_2(1270)$, $f_2'(1525)$	$\chi_{c2}(1P)$	$\chi_{b2}(1P)$	$K_2^*(1430)$	$D_2^*(2460)$			
$1\,^1D_2$	2^{-+}	$\pi_2(1670)$				$K_2(1770)$				
$1\,^3D_1$	1^{--}	$\rho(1700)$	$\omega(1600)$	$\psi(3770)$		$K^*(1680)$‡				
$1\,^3D_2$	2^{--}					$K_2(1820)$				
$1\,^3D_3$	3^{--}	$\rho_3(1690)$	$\omega_3(1670)$, $\phi_3(1850)$			$K_3^*(1780)$				
$1\,^3F_4$	4^{++}	$a_4(2040)$	$f_4(2050)$, $f_4(2220)$			$K_4^*(2045)$				
$2\,^1S_0$	0^{-+}	$\pi(1300)$	$\eta(1295)$	$\eta_c(2S)$		$K(1460)$				
$2\,^3S_1$	1^{--}	$\rho(1450)$	$\omega(1420)$, $\phi(1680)$	$\psi(2S)$	$\Upsilon(2S)$	$K^*(1410)$‡				
$2\,^3P_2$	2^{++}		$f_2(1810)$, $f_2(2010)$		$\chi_{b2}(2P)$	$K_2^*(1980)$				
$3\,^1S_0$	0^{-+}	$\pi(1770)$	$\eta(1760)$			$K(1830)$				

* See our scalar minireview in the Particle Listings. The candidates for the $I=1$ states are $a_0(980)$ and $a_0(1450)$, while for $I=0$ they are: $f_0(400$–$1200)$, $f_0(980)$, and $f_0(1370)$. The light scalars are problematic, since there may be two poles for one $q\bar{q}$ state and $a_0(980)$, $f_0(980)$ may be $K\overline{K}$ bound states.

† The K_{1A} and K_{1B} are nearly equal (45°) mixes of the $K_1(1270)$ and $K_1(1400)$.

‡The $K^*(1410)$ could be replaced by the $K^*(1680)$ as the $2\,^3S_1$ state.

If we allow $M_{88}^2 = \frac{1}{3}(4m_K^2 - m_\pi^2)\ (1+\Delta)$, the mixing angle is determined by

$$\tan^2\theta_P = 0.0319(1+17\Delta) \tag{12.8}$$

$$\theta_P = -10.1°(1+8.5\Delta) \tag{12.9}$$

to first order in Δ. A small breaking of the Gell-Mann-Okubo relation can produce a major modification of θ_P.

For the vector mesons, $\pi \to \rho$, $K \to K^*$, $\eta \to \phi$, and $\eta' \to \omega$, so that

$$\phi = \omega_8 \cos\theta_V - \omega_1 \sin\theta_V \tag{12.10}$$

$$\omega = \omega_8 \sin\theta_V + \omega_1 \cos\theta_V\ . \tag{12.11}$$

For "ideal" mixing, $\phi = s\bar{s}$, so $\tan\theta_V = 1/\sqrt{2}$ and $\theta_V = 35.3°$. Experimentally, θ_V is near 35°, the sign being determined by a formula like that for $\tan\theta_P$. Following this procedure we find the mixing angles given in Table 12.3.

Table 12.3: Singlet-octet mixing angles for several nonets, neglecting possible mass dependence and imaginary parts. The sign conventions are given in the text. The values of $\theta_{\rm quad}$ are obtained from the equations in the text, while those for $\theta_{\rm lin}$ are obtained by replacing m^2 by m throughout. Of the two isosinglets in a nonet, the mostly octet one is listed first.

J^{PC}	Nonet members	$\theta_{\rm quad}$	$\theta_{\rm lin}$
0^{-+}	π, K, η, η'	$-10°$	$-23°$
1^{--}	ρ, $K^*(892)$, ϕ, ω	39°	36°
2^{++}	$a_2(1320)$, $K_2^*(1430)$, $f_2'(1525)$, $f_2(1270)$	28°	26°
3^{--}	$\rho_3(1690)$, $K_3^*(1780)$, $\phi_3(1850)$, $\omega_3(1670)$	29°	28°

In the quark model, the coupling of neutral mesons to two photons is proportional to $\sum_i Q_i^2$, where Q_i is the charge of the i-th quark. This provides an alternative characterization of mixing. For example, defining

$$\text{Amp}\,[P \to \gamma(k_1)\,\gamma(k_2)] = M\epsilon^{\mu\nu\alpha\beta}\,\epsilon^*_{1\mu}\,k_{1\nu}\,\epsilon^*_{2\alpha}\,k_{2\beta}\;, \tag{12.12}$$

where $\epsilon_{i\lambda}$ is the λ component of the polarization vector of the i^{th} photon, one finds

$$\frac{M(\eta \to \gamma\gamma)}{M(\pi^0 \to \gamma\gamma)} = \frac{1}{\sqrt{3}}(\cos\theta_P - 2\sqrt{2}\sin\theta_P) = \frac{1.73 \pm 0.18}{\sqrt{3}} \tag{12.13a}$$

$$\frac{M(\eta' \to \gamma\gamma)}{M(\pi^0 \to \gamma\gamma)} = 2\sqrt{2/3}\left(\cos\theta_P + \frac{\sin\theta_P}{2\sqrt{2}}\right) = 2\sqrt{2/3}\,(0.78 \pm 0.04)\;, \tag{12.13b}$$

where the numbers with errors are experimental. These data favor $\theta_P \approx -20°$, which is compatible with the quadratic mass mixing formula with about 12% SU(3) breaking in M_{88}^2.

12.3. Baryons: qqq states

All the established baryons are apparently 3-quark (qqq) states, and each such state is an SU(3) color singlet, a completely antisymmetric state of the three possible colors. Since the quarks are fermions, the state function for any baryon must be antisymmetric under interchange of any two equal-mass quarks (up and down quarks in the limit of isospin symmetry). Thus the state function may be written as

$$|\,qqq\,\rangle_A = |\,\text{color}\,\rangle_A \times |\,\text{space, spin, flavor}\,\rangle_S\;, \tag{12.14}$$

where the subscripts S and A indicate symmetry or antisymmetry under interchange of any two of the equal-mass quarks. Note the contrast with the state function for the three nucleons in ^{3}H or ^{3}He:

$$|\,NNN\,\rangle_A = |\,\text{space, spin, isospin}\,\rangle_A\;. \tag{12.15}$$

This difference has major implications for internal structure, magnetic moments, *etc.* (For a nice discussion, see Ref. 1.)

The "ordinary" baryons are made up of u, d, and s quarks. The three flavors imply an approximate flavor SU(3), which requires that baryons made of these quarks belong to the multiplets on the right side of

$$\mathbf{3} \otimes \mathbf{3} \otimes \mathbf{3} = \mathbf{10}_S \oplus \mathbf{8}_M \oplus \mathbf{8}_M \oplus \mathbf{1}_A \tag{12.16}$$

(see Sec. 33, on "SU(n) Multiplets and Young Diagrams"). Here the subscripts indicate symmetric, mixed-symmetry, or antisymmetric states under interchange of any two quarks. The **1** is a uds state (Λ_1) and the octet contains a similar state (Λ_8). If these have the same spin and parity they can mix. An example is the mainly octet D_{03} $\Lambda(1690)$ and mainly singlet D_{03} $\Lambda(1520)$. In the ground state multiplet, the SU(3) flavor singlet Λ is forbidden by Fermi statistics. The mixing formalism is the same as for η-η' or ϕ-ω (see above), except that for baryons the mass M instead of M^2 is used. Section 32, on "SU(3) Isoscalar Factors and Representation Matrices", shows how relative decay rates in, say, $\mathbf{10} \to \mathbf{8} \otimes \mathbf{8}$ decays may be calculated. A summary of results of fits to the observed baryon masses and decay rates for the best-known SU(3) multiplets is given in Appendix II of our 1982 edition [2].

The addition of the c quark to the light quarks extends the flavor symmetry to SU(4). Figures 12.2(a) and 12.2(b) show the (badly broken) SU(4) baryon multiplets that have as their "ground floors" the SU(3) octet that contains the nucleons and the SU(3) decuplet that contains the $\Delta(1232)$. All the particles in a given SU(4) multiplet have the same spin and parity. The only charmed baryons that have been discovered each contain one charmed quark. These belong to the first floor of the multiplet shown in Fig. 12.2(a); for details, see

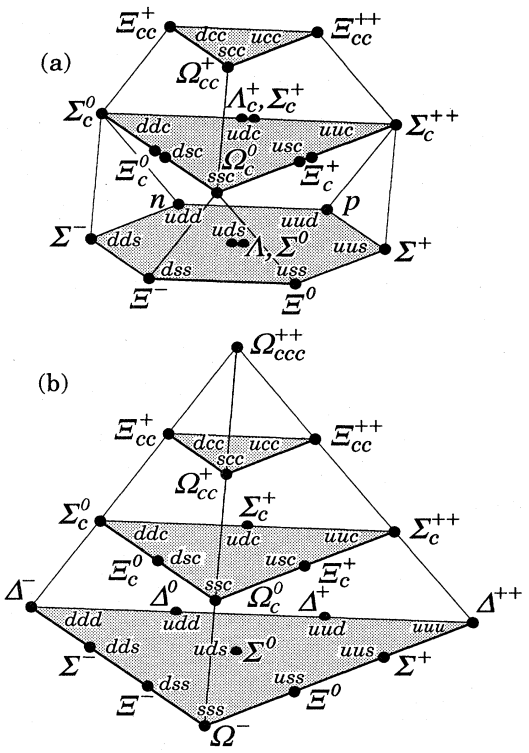

Figure 12.2: SU(4) multiplets of baryons made of u, d, s, and c quarks. (a) The 20-plet with an SU(3) octet. (b) The 20-plet with an SU(3) decuplet.

the "Note on Charmed Baryons" in the Baryon Particle Listings. The addition of a b quark extends the flavor symmetry to SU(5); it would require four dimensions to draw the multiplets.

For the "ordinary" baryons, flavor and spin may be combined in an approximate flavor-spin SU(6) in which the six basic states are $d\uparrow$, $d\downarrow$, $\cdots$, $s\downarrow$ ($\uparrow$, $\downarrow$ = spin up, down). Then the baryons belong to the multiplets on the right side of

$$\mathbf{6} \otimes \mathbf{6} \otimes \mathbf{6} = \mathbf{56}_S \oplus \mathbf{70}_M \oplus \mathbf{70}_M \oplus \mathbf{20}_A\;. \tag{12.17}$$

These SU(6) multiplets decompose into flavor SU(3) multiplets as follows:

$$\mathbf{56} = {}^4\mathbf{10} \oplus {}^2\mathbf{8} \tag{12.18a}$$

$$\mathbf{70} = {}^2\mathbf{10} \oplus {}^4\mathbf{8} \oplus {}^2\mathbf{8} \oplus {}^2\mathbf{1} \tag{12.18b}$$

$$\mathbf{20} = {}^2\mathbf{8} \oplus {}^4\mathbf{1}\;, \tag{12.18c}$$

where the superscript $(2S+1)$ gives the net spin S of the quarks for each particle in the SU(3) multiplet. The $J^P = 1/2^+$ octet containing the nucleon and the $J^P = 3/2^+$ decuplet containing the $\Delta(1232)$ together make up the "ground-state" 56-plet in which the orbital angular momenta between the quark pairs are zero (so that the spatial part of the state function is trivially symmetric). The **70** and **20** require some excitation of the spatial part of the state function in order to make the overall state function symmetric. States with nonzero orbital angular momenta are classified in SU(6)⊗O(3) supermultiplets. Physical baryons with the same quantum numbers do not belong to a single supermultiplet, since SU(6) is broken by spin-dependent interactions, differences in quark masses, *etc.* Nevertheless, the SU(6)⊗O(3) basis provides a suitable framework for describing baryon state functions.

It is useful to classify the baryons into bands that have the same number N of quanta of excitation. Each band consists of a number of

supermultiplets, specified by (D, L_N^P), where D is the dimensionality of the SU(6) representation, L is the total quark orbital angular momentum, and P is the total parity. Supermultiplets contained in bands up to $N = 12$ are given in Ref. 3. The $N = 0$ band, which contains the nucleon and $\Delta(1232)$, consists only of the $(56,0_0^+)$ supermultiplet. The $N = 1$ band consists only of the $(70,1_1^-)$ multiplet and contains the negative-parity baryons with masses below about 1.9 GeV. The $N = 2$ band contains five supermultiplets: $(56,0_2^+)$, $(70,0_2^+)$, $(56,2_2^+)$, $(70,2_2^+)$, and $(20,1_2^+)$. Baryons belonging to the $(20,1_2^+)$ supermultiplet are not ever likely to be observed, since a coupling from the ground-state baryons requires a two-quark excitation. Selection rules are similarly responsible for the fact that many other baryon resonances have not been observed [4].

In Table 12.4, quark-model assignments are given for many of the established baryons whose SU(6)⊗O(3) compositions are relatively unmixed. We note that the unestablished resonances $\Sigma(1480)$, $\Sigma(1560)$, $\Sigma(1580)$, $\Sigma(1770)$, and $\Xi(1620)$ in our Baryon Particle Listings are too low in mass to be accommodated in most quark models [4,5].

Table 12.4: Quark-model assignments for many of the known baryons in terms of a flavor-spin SU(6) basis. Only the dominant representation is listed. Assignments for some states, especially for the $\Lambda(1810)$, $\Lambda(2350)$, $\Xi(1820)$, and $\Xi(2030)$, are merely educated guesses.

J^P	(D, L_N^P)	S	Octet members				Singlets
$1/2^+$	$(56,0_0^+)$	1/2	$N(939)$	$\Lambda(1116)$	$\Sigma(1193)$	$\Xi(1318)$	
$1/2^+$	$(56,0_2^+)$	1/2	$N(1440)$	$\Lambda(1600)$	$\Sigma(1660)$	$\Xi(?)$	
$1/2^-$	$(70,1_1^-)$	1/2	$N(1535)$	$\Lambda(1670)$	$\Sigma(1620)$	$\Xi(?)$	$\Lambda(1405)$
$3/2^-$	$(70,1_1^-)$	1/2	$N(1520)$	$\Lambda(1690)$	$\Sigma(1670)$	$\Xi(1820)$	$\Lambda(1520)$
$1/2^-$	$(70,1_1^-)$	3/2	$N(1650)$	$\Lambda(1800)$	$\Sigma(1750)$	$\Xi(?)$	
$3/2^-$	$(70,1_1^-)$	3/2	$N(1700)$	$\Lambda(?)$	$\Sigma(?)$	$\Xi(?)$	
$5/2^-$	$(70,1_1^-)$	3/2	$N(1675)$	$\Lambda(1830)$	$\Sigma(1775)$	$\Xi(?)$	
$1/2^+$	$(70,0_2^+)$	1/2	$N(1710)$	$\Lambda(1810)$	$\Sigma(1880)$	$\Xi(?)$	$\Lambda(?)$
$3/2^+$	$(56,2_2^+)$	1/2	$N(1720)$	$\Lambda(1890)$	$\Sigma(?)$	$\Xi(?)$	
$5/2^+$	$(56,2_2^+)$	1/2	$N(1680)$	$\Lambda(1820)$	$\Sigma(1915)$	$\Xi(2030)$	
$7/2^-$	$(70,3_3^-)$	1/2	$N(2190)$	$\Lambda(?)$	$\Sigma(?)$	$\Xi(?)$	$\Lambda(2100)$
$9/2^-$	$(70,3_3^-)$	3/2	$N(2250)$	$\Lambda(?)$	$\Sigma(?)$	$\Xi(?)$	
$9/2^+$	$(56,4_4^+)$	1/2	$N(2220)$	$\Lambda(2350)$	$\Sigma(?)$	$\Xi(?)$	
			Decuplet members				
$3/2^+$	$(56,0_0^+)$	3/2	$\Delta(1232)$	$\Sigma(1385)$	$\Xi(1530)$	$\Omega(1672)$	
$1/2^-$	$(70,1_1^-)$	1/2	$\Delta(1620)$	$\Sigma(?)$	$\Xi(?)$	$\Omega(?)$	
$3/2^-$	$(70,1_1^-)$	1/2	$\Delta(1700)$	$\Sigma(?)$	$\Xi(?)$	$\Omega(?)$	
$5/2^+$	$(56,2_2^+)$	3/2	$\Delta(1905)$	$\Sigma(?)$	$\Xi(?)$	$\Omega(?)$	
$7/2^+$	$(56,2_2^+)$	3/2	$\Delta(1950)$	$\Sigma(2030)$	$\Xi(?)$	$\Omega(?)$	
$11/2^+$	$(56,4_4^+)$	3/2	$\Delta(2420)$	$\Sigma(?)$	$\Xi(?)$	$\Omega(?)$	

The quark model for baryons is extensively reviewed in Ref. 6 and 7.

12.4. Dynamics

Many specific quark models exist, but most contain the same basic set of dynamical ingredients. These include:

i) A confining interaction, which is generally spin-independent.

ii) A spin-dependent interaction, modeled after the effects of gluon exchange in QCD. For example, in the S-wave states, there is a spin-spin hyperfine interaction of the form

$$H_{HF} = -\alpha_S M \sum_{i>j} (\vec{\sigma}\lambda_a)_i (\vec{\sigma}\lambda_a)_j \ , \tag{12.19}$$

where M is a constant with units of energy, λ_a $(a = 1, \cdots, 8,)$ is the set of SU(3) unitary spin matrices, defined in Sec. 32, on "SU(3) Isoscalar Factors and Representation Matrices," and the sum runs over constituent quarks or antiquarks. Spin-orbit interactions, although allowed, seem to be small.

iii) A strange quark mass somewhat larger than the up and down quark masses, in order to split the SU(3) multiplets.

iv) In the case of isoscalar mesons, an interaction for mixing $q\bar{q}$ configurations of different flavors (*e.g.*, $u\bar{u} \leftrightarrow d\bar{d} \leftrightarrow s\bar{s}$), in a manner which is generally chosen to be flavor independent.

These four ingredients provide the basic mechanisms that determine the hadron spectrum.

References:

1. F.E. Close, in *Quarks and Nuclear Forces* (Springer-Verlag, 1982), p. 56.
2. Particle Data Group, Phys. Lett. **111B** (1982).
3. R.H. Dalitz and L.J. Reinders, in *Hadron Structure as Known from Electromagnetic and Strong Interactions, Proceedings of the Hadron '77 Conference* (Veda, 1979), p. 11.
4. N. Isgur and G. Karl, Phys. Rev. **D18**, 4187 (1978); ibid. **D19**, 2653 (1979); ibid. **D20**, 1191 (1979);
   K.-T. Chao, N. Isgur, and G. Karl, Phys. Rev. **D23**, 155 (1981).
5. C.P. Forsyth and R.E. Cutkosky, Z. Phys. **C18**, 219 (1983).
6. A.J.G. Hey and R.L. Kelly, Phys. Reports **96**, 71 (1983). Also see S. Gasiorowicz and J.L. Rosner, Am. J. Phys. **49**, 954 (1981).
7. N. Isgur, Int. J. Mod. Phys. **E1**, 465 (1992);
   G. Karl, Int. J. Mod. Phys. **E1**, 491 (1992).

THE TOP QUARK

(by M. Mangano at CERN and T. Trippe at LBNL)

A. Introduction: The top quark is the $Q = 2/3$, $T_3 = +1/2$ member of the weak-isospin doublet containing the bottom quark (see our review on the "Standard Model of Electroweak Interactions" for more information). The existence of a sixth quark has been expected since the discovery of the bottom quark itself and has become an absolute theoretical necessity within the Standard Model (SM) after the measurement of the $T_3 = -1/2$ weak isospin of the bottom quark [1]. While models with additional quarks but quantum numbers different from the top quark have been constructed, the simplest hypothesis that the weak doublet containing the bottom be completed into a family structure similar to the first two generations has always been the most appealing. This idea has finally been confirmed with the recent announcement of the top discovery by the CDF and DØ experiments at the Fermilab 1.8 TeV Tevatron proton-antiproton collider.

We start this note by presenting a brief historical survey of top searches. Then we discuss in more detail the essential features of top production and decay properties which were exploited to perform the discovery. Finally, we discuss the experimental and theoretical issues involved in the determination of its parameters (mass, production cross section, decay branching ratios, *etc.*) and conclude with the prospects for future improvements.

B. Some history: The first expectations for the value of the top mass used a naive extrapolation of the up- to down-type quark mass ratios in the first two generations, leading to values in the range of 10–20 GeV. Direct searches for $t\bar{t}$ pair production in e^+e^- collisions in this mass range were performed beginning in the late 70's at DESY and SLAC (see the compilation of limits in our 1990 edition [2]). These searches looked for a sudden increase in the ratio $R = \sigma(e^+e^- \to \text{hadrons})/\sigma(e^+e^- \to \mu^+\mu^-)$ or for anomalies in the distributions of thrust and acoplanarity in hadronic events. The lower limit on the top mass was increased to 30 GeV and then to approximately 46 GeV between the end of the 80's and the beginning of the 90's, when the more powerful Tristan, SLC and LEP e^+e^- colliders began operations (see the t-Quark Particle Listings in the current edition).

In parallel to the searches in e^+e^- collisions, direct searches were performed during the 80's by the UA1 and UA2 experiments at the CERN $S\overline{p}pS$ proton-antiproton collider, $\sqrt{s} = 630$ GeV. At this energy, and at the available luminosities, the CERN experiments were sensitive to top mass values not exceeding 70 GeV, the top quark being mostly produced via an intermediate on-shell W, decaying to $t\bar{b}$. A top quark with mass below the Wb threshold was then expected to undergo a 3-body weak decay to a $bf\overline{f}'$ final state, with $f\overline{f}'$ being a weak isospin doublet such as $\nu_\ell\bar{\ell}$ or $u\bar{d}$.

Because of the overwhelming QCD background to the detection of the purely hadronic final states, the experiments looked for final states including a high momentum isolated lepton, missing transverse energy (E_T), and one or more jets. No evidence for top production was obtained (see the t-Quark Particle Listings in the current edition for the references): the 95% CL mass limits went from 41 GeV (UA1, 1988), to 60 GeV (UA1, 1990), to 69 GeV (UA2, 1990). The first limits from CDF at the Fermilab Tevatron also appeared in 1990: $m_t > 72$ GeV from searches in the $e\mu$ final states, and $m_t > 77$ GeV from searches in the e plus jets and missing E_T final states.

Further indications of a large top mass had come from the measurement of a significant B^0–$\overline{B}^0$ mixing, performed in 1986 by UA1 and Argus.

Mass limits independent of the decay mode were also set in the range $m_t > 40$ GeV via the determination of the W boson width, from the measurement in hadronic collisions of the ratio $\sigma(W \to \ell\nu_\ell)/\sigma(Z \to \ell^+\ell^-)$. With the advent of high-precision electroweak data (from deep-inelastic scattering, M_W, atomic parity violation and, most importantly, from the study of the Z-boson couplings at SLC and LEP), global fits of the SM parameters have become possible, and have provided significant indirect constraints on the value of the top mass, once more indicating a large value (see our review "Standard Model of Electroweak Interactions" in the current edition for more information).

In this edition we have shortened the Particle Listings of indirect top mass limits by omitting superseded limits and reviews published before 1994. For more complete listings see our 1994 edition [3].

C. Top quark searches at the Tevatron: The first direct limits on the top mass exceeding the threshold for the decay into real W and a bottom quark came in the early 90's from the Fermilab Tevatron collider: $m_t > 91$ GeV (CDF, 1992) and $m_t > 131$ GeV (D0, 1994).

At the Tevatron energy, 1.8 TeV, a top quark above the W mass is dominantly produced in pairs from pure QCD processes: $q\bar{q} \to t\bar{t}$ and $gg \to t\bar{t}$. For a top mass around 100 GeV, the production cross section is expected to be of the order of 100 pb and is evenly shared between the two above channels. At 150 (175, 200) GeV the cross section is about 10 (5, 2.5) pb, with approximately 80% (90%, 95%) of it due to the light quark annihilation.

For masses above the Wb threshold, and neglecting terms of order m_b^2/m_t^2, the top quark decay width is predicted in the SM to be [4]:

$$\Gamma_t = \frac{G_F m_t^3}{8\pi\sqrt{2}}\left(1 - \frac{M_W^2}{m_t^2}\right)^2\left(1 + 2\frac{M_W^2}{m_t^2}\right)\left[1 - \frac{2\alpha_s}{3\pi}\left(\frac{2\pi^2}{3} - \frac{5}{2}\right)\right].$$

The use of G_F in this equation accounts for the largest part of the 1-loop electroweak radiative corrections, providing an expression accurate to better than 2%. The width values increase from 302 MeV (for $m_t = 120$ GeV) to 1.04 GeV ($m_t = 160$ GeV) and 2.23 GeV ($m_t = 200$ GeV). With such a correspondingly short lifetime, the top quark is expected to decay before top-favoured hadrons or $t\bar{t}$ quarkonium bound states can form.

The top quark decay is expected to be largely dominated by the Wb final state. The Ws and Wd final states are suppressed relatively to Wb by the square of the CKM matrix elements V_{ts} and V_{td}, whose values can be estimated under the assumption of unitarity of the three-generation CKM matrix to be less than 0.046 and 0.014, respectively (see our review "The Cabibbo-Kobayashi-Maskawa Mixing Matrix" in the current edition for more information).

Typical final states therefore belong to three classes:

A. $t\bar{t} \to W\,b\,W\,\bar{b} \to q\,\overline{q}'\,b\,q''\,\overline{q}'''\,\bar{b}$,

B. $t\bar{t} \to W\,b\,W\,\bar{b} \to q\,\overline{q}'\,b\,\ell\,\overline{\nu}_\ell\,\bar{b}$,

C. $t\bar{t} \to W\,b\,W\,\bar{b} \to \bar{\ell}\,\nu_\ell\,b\,\ell'\,\overline{\nu}_{\ell'}\,\bar{b}$.

The final state quarks emit radiation and evolve into jets of hadrons. The precise number of jets reconstructed by the detectors varies event by event, as it depends on the decay

kinematics, as well as on the precise definition of jet used in the analysis. The neutrinos are reconstructed via the large imbalance in detected transverse momentum of the event (missing E_T).

The $t\bar{t}$ production signature is by itself quite clear in all possible decay channels, due to the many kinematical constraints imposed by the sequential decay via a real W. However, the combination of the limited experimental resolution and of the large cross section for the production of 6 jets in the QCD continuum (several nb) make the search in the purely hadronic channel very difficult. Since the detection of τ leptons has small efficiency, studies have therefore mostly concentrated on final states where one (or both) W decays to either an electron or a muon. Potential physics backgrounds still exist, mainly due to associated production of one (or two) W and several jets, with the W decaying leptonically. The gain in the S/B ratio is by an approximate factor of 10 for each W which is required to decay leptonically.

The theoretical estimates of the physics backgrounds have large uncertainties, since only leading order QCD calculations are available for most of the relevant processes (W+3 and 4 jets, or WW+2 jets). While this limitation is known to affect the estimates of the overall production rates, it is believed that the LO determination of the event kinematics and of the fraction of W plus multi-jet events containing b quarks is rather accurate. In particular, one expects the E_T spectrum of these jets to fall rather steeply, the jet direction to point preferentially at small angles from the beams, and the fraction of events with b quarks to be of the order of few percent. In the case of the top signal, *vice versa*, the b fraction is $\sim 100\%$ and the jets are rather energetic, since they come from the decay of a massive object. It is therefore possible to improve the S/B ratio by either requiring the presence of a b quark, or by selecting very energetic and central kinematical configurations.

A detailed study of control samples with features similar to those of the relevant backgrounds, but free from possible top contamination (*e.g.*, a sample of Z plus multi-jet events), is required to provide a reliable check on the background estimates.

D. Top observation at CDF and DØ: The CDF experiment and the DØ experiment independently observed the production and decay of the top quark at the Fermilab Tevatron collider in $p\bar{p}$ collisions at $\sqrt{s} = 1.8$ TeV.

The CDF experiment published the first direct experimental evidence for the top quark in 1994 [5]. They found 12 events consistent with top, containing 6 silicon vertex tags, 7 low-p_T lepton tags, and 3 dilepton events (these categories are discussed below in more detail) with estimated backgrounds of 2.3 ± 0.3, 3.1 ± 0.3, and $0.56^{+0.25}_{-0.13}$ respectively. The combined excess signal was inconsistent with backgrounds by 2.8 σ, not enough to firmly establish the existence of the top quark. Interpreting the excess events as top, they found a $t\bar{t}$ production cross section of $13.9^{+6.1}_{-4.8}$ pb, larger than the expected QCD cross section discussed below. A mass analysis of seven of these events yielded $m_t = 174 \pm 10^{+13}_{-12}$ GeV. A sample of events selected according to the expected kinematical properties of top provided additional support for the top interpretation [6].

The DØ experiment [7] found nine top candidates in their data taken during the same Tevatron run with an estimated background of 3.8 ± 0.9. They found a probability of 2.7% that this yield was consistent with backgrounds, corresponding to a 1.9 σ effect. If they assumed that the observed excess was top production, they obtained a $t\bar{t}$ production cross section of 8.2 ± 5.1 pb at $m_t = 180$ GeV.

After accumulating more than three times the amount of data, both CDF and DØ reported in 1995 [8,9] that they had conclusively observed the top quark.

The CDF experiment [8] observed top signals in two classes of events: $\ell\ell + jets$ events, which have two high-p_T leptons (e or μ) of opposite charge, large missing E_T, and at least two jets; and $\ell + jets/b$-tag events, which have one high-p_T lepton, large missing E_T, and at least three jets, of which at least one is tagged as a b jet. They tagged b jets by finding secondary vertices from b-quark decay with their silicon vertex detector or by finding low-p_T leptons from semileptonic b decay.

In 67 pb^{-1} integrated luminosity, CDF observed 37 $\ell + jets/b$-tag) events containing 27 secondary vertex b tags and 23 low-p_T lepton b tags with estimated backgrounds of 6.7 ± 2.1 and 15.4 ± 2.0 respectively. They also observed 6 $\ell\ell$ events with an estimated background of 1.3 ± 0.3 events. The combined excess signal observed in these three categories is inconsistent with the background prediction by 4.8 σ.

The DØ experiment [9] observed top signals in three classes of events: $\ell\ell + jets$ events, $\ell + jets$ events, and $\ell + jets/b$-tag events. These classes differ from those of CDF in the details of their selection cuts, but the main differences are that DØ imposes topological cuts, includes $\ell + jets$ events without a b tag if they have at least four jets, and uses soft-muon b tagging only. The topological cuts, mainly H_T, which is the scalar sum of transverse energies of the jets (and, in dilepton events, the leading electron), are very effective since the top quark is heavy, and hence top events are more spherical than background events and are produced more centrally in the detector.

In an integrated luminosity of approximately 50 pb^{-1} DØ observed 3 $\ell\ell + jets$ events, 8 $\ell + jets$ events, and 6 $\ell + jets/b$-tag events, a total of 17 top candidates. The total estimated background in these events is 3.8 ± 0.6 events. The excess signal is inconsistent with the background prediction by 4.6 σ.

E. Measured top properties: CDF and DØ both measured the top mass using single lepton events with four or more jets. Each event was subjected to a two-constraint kinematic fit to the hypothesis $t\bar{t} \rightarrow W^+ b W^- \bar{b} \rightarrow \ell \nu_\ell q \bar{q}' b \bar{b}$, assuming that the four highest E_T jets were the $t\bar{t}$ daughters. All permutations of these jets were tried, with the restriction that b-tagged jets were assigned to b quarks in the fit.

CDF found that of their 37 $\ell + jets/b$-tag events, 19 events had four or more jets. Of these 19, $6.9^{+2.5}_{-1.9}$ were expected to be background. A fit to the mass distribution of the 19 events by the sum of the expected distributions for the $W + jets$ background and a top quark yielded $m_t = 176 \pm 8 \pm 10$ GeV where the second error is the estimated systematic uncertainty.

DØ found that of their 14 $\ell + jets$ (with and without b-tags) events, 11 had four or more jets and passed the fit. To increase the statistics and reduce mass biases, the H_T requirement was removed, yielding 27 $\ell + 4jets$ events, of which 24 passed the fit. A fit of the mass distribution to top and background contributions yielded $m_t = 199^{+19}_{-21} \pm 22$ GeV, where the second error is the estimated systematic error.

Preliminary results for the top mass based on the full (Run Ia+Ib) data set have been presented by CDF and DØ at conferences in early 1996 and are given in Table 1. Since these are preliminary results, we do not average them or include them in the data listings or summary tables.

Table 1: Preliminary top masses presented at conferences in early 1996. See for example Ref. 10 for CDF results and Ref. 11 for DØ results.

top quark mass	Expt.	Channel
$175.6 \pm 5.7 \pm 7.1$ GeV	CDF	lepton + jets
$159^{+24}_{-22} \pm 17$ GeV	CDF	dilepton
$187 \pm 8 \pm 12$ GeV	CDF	hadronic
$170 \pm 15 \pm 10$ GeV	DØ	lepton + jets
$158 \pm 24 \pm 10$ GeV	DØ	$e\mu$

The current average of the CDF and DØ published results is $m_t = 180 \pm 12$ GeV, where statistical and systematic errors have been combined in quadrature and where CDF and DØ systematic errors have been assumed to be independent.

Given the experimental technique used to extract the top mass, this value should be taken as representing the top *pole mass* (see our review "Note on Quark Masses" in the current edition).

The extraction of the value of the top mass from the analyses described requires, in addition to an understanding of the absolute energy calibration and resolution of the detectors, also an *a priori* knowledge of the structure of the final state. Given the hardness of a $t\bar{t}$ production process, jets can in fact arise not only from the top decays, but also from the initial state gluon radiation. Furthermore, quarks from the top decays can radiate additional jets. The presence of these additional jets will affect the shape of the mass spectrum, depending on the details of how the samples used for the mass determination were defined. QCD calculations used to model top production and decay are expected to be rather reliable, but residual uncertainties remain and are accounted for in the overall systematic error on the top mass.

CDF [8] and DØ [9] determined the $t\bar{t}$ cross section in $p\bar{p}$ collisions at $\sqrt{s} = 1.8$ TeV from their numbers of top candidates, their estimated background, their $t\bar{t}$ acceptance, and their integrated luminosity. The evaluation was done under the assumption of SM decays $t \to Wb$, with unity branching ratio. Based on their number of secondary-vertex b-tagged events, CDF determined the $t\bar{t}$ cross section to be $6.8^{+3.6}_{-2.4}$ pb at $m_t = 175$ GeV. The next-to-leading-order QCD prediction [12], allowing for a variation of the renormalization and factorization scales μ in the range $0.5 < \mu/m_t < 2$ and using the MRSA set of parton densities [13], gives $4.3 < \sigma_{t\bar{t}}(\text{pb}) < 5.0$ at $m_t = 175$ GeV.

Based on their 17 top candidates, DØ determined the $t\bar{t}$ cross section to be 6.4 ± 2.2 pb at their central mass value of 199 GeV or 8.2 ± 2.9 pb at 180 GeV. The QCD predictions are: $2.0 < \sigma_{t\bar{t}}(\text{pb}) < 2.4$ ($m_t = 199$ GeV), and $3.6 < \sigma_{t\bar{t}}(\text{pb}) < 4.3$ ($m_t = 180$ GeV).

More recent preliminary values of the $t\bar{t}$ cross section were given at early 1996 conferences CDF found $7.5^{+1.9}_{-1.7}$ pb at 175 GeV [14] and DØ found 5.2 ± 1.8 pb at 170 GeV [15].

The measurement of other properties of the top quark has just started. CDF reported the first direct measurement of the $t \to Wb$ branching ratio [16]. Their preliminary result, obtained by comparing the number of events with 1 and 2 tagged-b jets and using the known tagging efficiency, is: $R = \text{B}(t \to Wb)/\sum_{q=d,s,b} \text{B}(t \to Wq) = 0.87^{+0.13+0.13}_{-0.30-0.11}$.

F. The future: With the discovery of the top quark, future studies will follow two main tracks. Theoretically, it is hoped that the large top mass, and the tantalizing coincidence between its current value and the fundamental scale of the electroweak symmetry breaking, will lead to some understanding of the structure of fermion masses and of the symmetry breaking mechanism itself. Experimentally, the work will concentrate on reducing the errors on the mass and cross section determinations and on the measurement of more specific properties of the top quark, namely its decay branching ratios and its couplings. With a smaller error on the top mass, and with yet improved measurements of the electroweak parameters, it will be possible to get important constraints on the value of the Higgs mass. Current global fits performed within the SM and its minimal supersymmetric extension, provide indications for a relatively light Higgs (see the "H^0 Indirect Mass Limits from Electroweak Analysis" in the Particle Listings of the current edition), possibly within the range of the upcoming LEP2 experiments.

The current Tevatron data, once fully analysed, should allow the first determination of limits on rare top decay modes, such as $t \to \gamma c$ or $t \to Zc$. Studies of the decay angular distributions will allow a first direct analysis of the $V - A$ nature of the Wtb coupling, as well as providing direct information on the relative coupling of longitudinal and transverse W bosons to the top. In the SM, the fraction of decays to transversely polarized W bosons is expected to be $1/(1 + m_t^2/2M_W^2)$ (29% for $m_t = 180$ GeV). Deviations from this value would challenge the Higgs mechanism of spontaneous symmetry breaking.

Over the longer term, a direct measurement of the Wtb coupling constant will be possible when enough data will be accumulated to detect the less frequent single-top production processes, such as $q\bar{q}' \to W^* \to t\bar{b}$ and $qb \to q't$ via W exchange.

A precise determination of the top production cross section will test the current theoretical understanding of the production mechanisms. The current state of the art amounts to complete calculations at the next-to-leading order in QCD [12], as well as efforts to resum classes of potentially large logarithmic corrections coming from multiple soft gluon emission in the intial state [17]. A precise understanding of top production at the Tevatron is important for the extrapolation to the higher energies of future colliders, like the LHC, where the expected large cross section will enable more extensive studies.

Discrepancies in rate between theory and data, on the other hand, would be more exciting and might indicate the presence of exotic production channels, as predicted in some models. In this case, one should also expect a modification of kinematical distributions such as the invariant mass of the top pair or the top quark transverse momentum.

As discussed in the previous sections, some of the current uncertainty in the determination of the top mass from the reconstruction of its final state jets arises from theoretical uncertainties in the modeling of the radiation in these very hard events. The current data, once fully analyzed, will presumably help improve our theoretical understanding. At the same time, the larger samples that will become available in the future will allow more strict selection criteria, leading to purer samples of top quarks. For example, requesting the presence of two secondary-vertex b tags in the event, in addition to two and only two central jets of high-E_T, should largely reduce the possibility of erroneously including jets not coming from the top decays into the mass reconstruction. This will significantly improve the mass resolution and will make it less sensitive to the theoretical uncertainties.

Finally, the large mass of the top quark leaves open the possibility of top decays into yet unobserved particles beyond the SM. For example, current limits on the masses of a charged Higgs (H^+) or of a supersymmetric scalar top quark ($\tilde{t}$) and neutralino ($\tilde{\chi}^0$), cannot exclude the existence of decays such as $t \to H^+ b$ or $t \to \tilde{t}\tilde{\chi}^0$. The first channel, in particular, has been used extensively in the past in direct top searches (see the Particle Listings in the current edition). Both these exotic modes are currently under investigation at CDF and DØ.

References

1. W. Bartel *et al.*, Phys. Lett. **B146**, 437 (1984).
2. Particle Data Group, *Review of Particle Properties*, Phys. Lett. **B239**, P. VII. 167 (1990).
3. Particle Data Group, *Review of Particle Properties*, Phys. Rev. **D50**, 1173 (1994).
4. C.S. Li, R.J. Oakes, and T.C. Yuan, Phys. Rev. **D43**, 3759 (1991);
   A. Denner and T. Sack, Nucl. Phys. **B358**, 46 (1991).
5. F. Abe *et al.*, Phys. Rev. **D50**, 2966 (1994).
6. F. Abe *et al.*, Phys. Rev. **D51**, 4623 (1995).
7. S. Abachi *et al.*, Phys. Rev. Lett. **74**, 2422 (1995).
8. F. Abe *et al.*, Phys. Rev. Lett. **74**, 2626 (1995).
9. S. Abachi *et al.*, Phys. Rev. Lett. **74**, 2632 (1995).
10. L. Galtieri, (for the CDF Collaboration), presented at Les Rencontres de Moriond, Hadronic session, Les Arcs, France (Mar. 23–30, 1996).
11. M. Narain, (for the DØ Collaboration), presented at Les Rencontres de Physique de La Vallee D'Aoste, La Thuile, Italy (Mar. 1996).
12. P. Nason, S. Dawson, and R.K. Ellis, Nucl. Phys. **B303**, 607 (1988);
    W. Beenakker, H. Kuijf, W.L. van Neerven, and J. Smith, Phys. Rev. **D40**, 54 (1989);
    G. Altarelli, M. Diemoz, G. Martinelli, and P. Nason, Nucl. Phys. **B308**, 724 (1988);
    R.K. Ellis, Phys. Lett. **B259**, 492 (1991).
13. A.D. Martin, R.G. Roberts, and W.J. Stirling, Phys. Rev. **D50**, 6723 (1994).
14. F. Tartarelli (for the CDF Collaboration), presented at Rencontres de Moriond, Electroweak session, Les Arcs, France (Mar. 16–23, 1996).
15. Q. Li-Demarteau (for the DØ Collaboration), presented at 1996 Aspen Winter Physics Conference, Aspen, Colorado, USA (Jan. 1996).
16. F. Abe *et al.*, FERMILAB-CONF-95-237-E, Jul 1995. 8pp. Presented at 6th International Symposium on Heavy Flavor Physics, Pisa, Italy, 6-9 Jun 1995.
17. E. Laenen, J. Smith, and W.L. van Neerven, Nucl. Phys. **B369**, 543 (1992);
    E.L. Berger and H. Contopanagos, Phys. Lett. **B361**, 115 (1995);
    S. Catani, M. Mangano, P. Nason, and L. Trentadue, CERN-TH/96-21, hep-ph/9602208.

PSEUDOSCALAR-MESON DECAY CONSTANTS

(by M. Suzuki, LBNL)

Charged mesons

The decay constant f_P for a charged pseudoscalar meson P is defined by

$$\langle 0|A_\mu(0)|P(\mathbf{q})\rangle = i f_P\, q_\mu \ ,$$

where A_μ is the axial-vector part of the charged weak current after a Cabibbo-Kobayashi-Maskawa mixing-matrix element $V_{qq'}$ has been removed. The state vector is normalized by $\langle P(\mathbf{q})|P(\mathbf{q}')\rangle = (2\pi)^3\, 2E_q\, \delta(\mathbf{q}-\mathbf{q}')$, and its phase is chosen to make f_P real and positive. Note, however, that in many theoretical papers our $f_P/\sqrt{2}$ is denoted by f_P.

In determining f_P experimentally, radiative corrections must be taken into account. Since the photon-loop correction introduces an infrared divergence that is canceled by soft-photon emission, we can determine f_P only from the combined rate for $P^\pm \to \ell^\pm \nu_\ell$ and $P^\pm \to \ell^\pm \nu_\ell \gamma$. This rate is given by

$$\Gamma\left(P \to \ell\nu_\ell + \ell\nu_\ell\gamma\right) = \frac{G_F^2 |V_{qq'}{}^2|}{8\pi} f_P^2\, m_\ell^2\, m_P \left(1 - \frac{m_\ell^2}{m_P^2}\right)^2 \left[1 + \mathcal{O}(\alpha)\right] \ .$$

Radiative corrections include inner bremsstrahlung, which is independent of the structure of the meson [1–3], and also a structure-dependent term [4,5]. After radiative corrections are made, there are ambiguities in extracting f_P from experimental measurements. In fact, the definition of f_P is no longer unique.

It is desirable to define f_P such that it depends only on the properties of the pseudoscalar meson, not on the final decay products. The short-distance corrections to the fundamental electroweak constants like $G_F|V_{qq'}|$ should be separated out. Following Marciano and Sirlin [6], we define f_P with the following form for the $\mathcal{O}(\alpha)$ corrections:

$$1 + \mathcal{O}(\alpha) = \left[1 + \frac{2\alpha}{\pi}\ln\left(\frac{m_Z}{m_\rho}\right)\right]\left[1 + \frac{\alpha}{\pi}F(x)\right]$$
$$\times\left\{1 - \frac{\alpha}{\pi}\left[\frac{3}{2}\ln\left(\frac{m_\rho}{m_P}\right) + C_1 + C_2\frac{m_\ell^2}{m_\rho^2}\ln\left(\frac{m_\rho^2}{m_\ell^2}\right) + C_3\frac{m_\ell^2}{m_\rho^2} + \ldots\right]\right\} \ .$$

Here

$$F(x) = 3\ln x + \frac{13 - 19x^2}{8(1-x^2)} - \frac{8 - 5x^2}{2(1-x^2)^2}\, x^2 \ln x$$
$$-2\left(\frac{1+x^2}{1-x^2}\ln x + 1\right)\ln(1-x^2) + 2\left(\frac{1+x^2}{1-x^2}\right)L(1-x^2) \ ,$$

with

$$x \equiv m_\ell/m_P \ , \qquad L(z) \equiv \int_0^z \frac{\ln(1-t)}{t}\, dt \ .$$

The first bracket in the expression for $1+\mathcal{O}(\alpha)$ is the short-distance electroweak correction. The QCD correction reduces this factor by 0.00033. The second bracket together with the term $-(3\alpha/2\pi)\ln(m_\rho/m_P)$ in the third bracket corresponds to the radiative corrections to the point-like pion decay ($\Lambda_{\rm cutoff} \approx m_\rho$) [2]. The rest of the corrections in the third bracket are expanded in powers of m_ℓ/m_ρ. The expansion coefficients C_1, C_2, and C_3 depend on the hadronic structure of the pseudoscalar meson and in most cases cannot be computed accurately. In particular, C_1 absorbs the uncertainty in the matching energy scale between short- and long-distance strong interactions and thus is the main source of uncertainty in determining f_{π^+} accurately.

With the experimental value for the decay $\pi \to \mu\nu_\mu + \mu\nu_\mu\gamma$, one obtains

$$f_{\pi^+} = 130.7 \pm 0.1 \pm 0.36 \text{ MeV} ,$$

where the first error comes from the experimental uncertainty on $|V_{ud}|$ and the second comes from the uncertainty on C_1 ($= 0 \pm 0.24$) [6]. Similarly, one obtains from the decay $K \to \mu\nu_\mu + \mu\nu_\mu\gamma$ the decay constant

$$f_{K^+} = 159.8 \pm 1.4 \pm 0.44 \text{ MeV} ,$$

where the first error is due to the uncertainty on $|V_{us}|$.

For the heavy pseudoscalar mesons, uncertainties in the experimental values for the decay rates are much larger than the radiative corrections. For the D^+, only an upper bound can be obtained from the published data:

$$f_{D^+} < 310 \text{ MeV (CL} = 90\%) .$$

Three groups have measured the $D_s^+ \to \mu^+\nu_\mu$ branching fraction, leading to the following values of the decay constant:

$$f_{D_s^+} = 232 \pm 45 \pm 20 \pm 48 \text{ MeV} \quad [7] ,$$

$$f_{D_s^+} = 344 \pm 37 \pm 52 \pm 42 \text{ MeV} \quad [8] ,$$

$$f_{D_s^+} = 430^{+150}_{-130} \pm 40 \text{ MeV} \quad [9] ,$$

where the first errors are statistical, the second errors are systematic, and the third errors are uncertainties involved in extracting the branching fraction $\mathrm{B}(D_s^+ \to \mu^+\nu_\mu)$. We must wait for more data before drawing a conclusion on $f_{D_s^+}$.

There have been many attempts to extract f_P from spectroscopy and nonleptonic decays using theoretical models. Since it is difficult to estimate uncertainties for them, we have listed here only values of decay constants that are obtained directly from the observation of $P^\pm \to \ell^\pm\nu_\ell$.

Light neutral mesons

The decay constants for the light neutral pseudoscalar mesons π^0, η, and η' are defined by

$$\langle 0|A_\mu(0)|P^0(\mathbf{q})\rangle = \mathrm{i}(f_P/\sqrt{2})q_\mu ,$$

where A_μ is a neutral axial-vector current of octet or singlet. Values of f_P can be obtained from the two-photon decay $P^0 \to \gamma\gamma$, since in the $m_P = 0$ limit the decay matrix element is determined by the Adler-Bell-Jackiw anomaly [10,11]. However, large uncertainties enter values of f_P through extrapolation to the physical mass and, in the case of η and η', through the mixing angle, too.

The CELLO Collaboration has obtained the values [12]

$$f_{\pi^0} = 119 \pm 4 \text{ MeV}$$

$$f_\eta = 133 \pm 10 \text{ MeV}$$

$$f_{\eta'} = 126 \pm 7 \text{ MeV} ,$$

while the TPC/2γ Collaboration has obtained [13]

$$f_\eta = 129 \pm 8 \text{ MeV}$$

$$f_{\eta'} = 110 \pm 7 \text{ MeV} .$$

(We have multiplied the published values by $\sqrt{2}$ to be in accord with our definition of f_P.)

References

1. S. Berman, Phys. Rev. Lett. **1**, 468 (1958).
2. T. Kinoshita, Phys. Rev. Lett. **2**, 477 (1959).
3. A. Sirlin, Phys. Rev. **D5**, 436 (1972).
4. M.V. Terent'ev, Yad. Fiz. **18**, 870 (1973) [Sov. J. Nucl. Phys. **18**, 449 (1974)].
5. T. Goldman and W.J. Wilson, Phys. Rev. **D15**, 709 (1977).
6. W.J. Marciano and A. Sirlin, Phys. Rev. Lett. **71**, 3629 (1993).
7. S. Aoki *et al.*, Prog. Theor. Phys. **89**, 131 (1993).
8. D. Acosta *et al.*, Phys. Rev. **D49**, 5690 (1993).
9. J.Z. Bai *et al.*, Phys. Rev. Lett. **74**, 4599 (1995).
10. S.L. Adler, Phys. Rev. **177**, 2426 (1969).
11. J.S. Bell and R. Jackiw, Nuovo Cimento **60A**, 46 (1969).
12. H.-J. Behrend *et al.*, Z. Phys. **C49**, 401 (1991).
13. H. Aihara *et al.*, Phys. Rev. Lett. **64**, 172 (1990).

PRODUCTION AND DECAY OF *b*-FLAVORED HADRONS

K. Honscheid, Ohio State University, Columbus

In the two years since the last edition of this review our understanding of the physics of B mesons and b-flavored baryons has significantly improved. 1995 was another record setting year for the CLEO experiment as well as the Cornell e^+e^- storage ring (CESR) which reached an instantaneous luminosity of 3.3×10^{32} cm^{-2}s^{-1}. More than 4 fb^{-1} have been logged by the CLEO Collaboration. At CERN, the Z program has been completed and each of the four LEP experiments has recorded data samples containing about 3 million Z decays, corresponding to approximately 0.7×10^6 produced $b\bar{b}$ quark pairs. The FNAL $p\bar{p}$ collider run continued throughout most of 1995 and the CDF and DØ experiments have collected close to 100 pb^{-1} of new data. SLD has begun to contribute to B physics. Using the excellent resolution of their vertex detector they have obtained precise measurements of B-meson lifetimes. New results in this edition include:

- The first observation of exclusive semileptonic $b \to u$ transitions.
- The determination of the decay rate for inclusive $b \to s\gamma$ transitions.
- Updated lifetimes and masses for b-flavored hadrons.
- Improved measurements of B^0–$\overline{B}^0$ and B_s^0–$\overline{B}_s^0$ oscillations.
- A new set of inclusive branching ratios for B mesons.
- Updated limits on rare B decays including new results on $b \to s$ gluon.

Weak decays of heavy quarks test the Standard Model and can be used to determine its parameters, in particular the weak-mixing angles of the Cabibbo-Kobayashi-Maskawa matrix. Experiments with B mesons may lead to the first precise determination of the fourth CKM parameter, the complex phase. While the underlying decay of the heavy quark is governed by the weak interaction, it is the strong force that is responsible for the formation of the hadrons that are observed by experimenters. Hence, in order to extract the Standard Model parameters from the experimental data, an understanding of the interplay of the weak and strong interaction is needed.

Production and spectroscopy

Elementary particles are characterized by their masses, lifetimes, and internal quantum numbers. The bound states with a b quark and a $\overline{u}$ or $\overline{d}$ antiquark are referred to as the B_d ($\overline{B^0}$) and the B_u (B^-) mesons, respectively. The first radial excitation is called the B^* meson. B^{**} is the generic name for the four orbitally excited ($L = 1$) B meson states that correspond to the P-wave mesons in the charm system, D^{**}.

Experimental studies of b decay are performed at the $\Upsilon(4S)$ resonance near the production threshold as well as at higher energies in proton-antiproton collisions and Z decays. For quantitative analyses of B decays the initial composition of the data sample must be known. At the threshold experiments this is determined by the ratio of charged to neutral decays of the $\Upsilon(4S)$. This ratio is denoted

$$\frac{f_+}{f_0} = \frac{\Upsilon(4S) \to B^+B^-}{\Upsilon(4S) \to B^0\overline{B}^0} \tag{1}$$

The $\Upsilon(4S)$ resonance decays only to $B^0\overline{B}^0$ and B^+B^- pairs, while heavier states such as B_s or B_c are not accessible. The current experimental limit for non-$B\overline{B}$ decays of the $\Upsilon(4S)$ is less than 4% at the 95% confidence level [1]. CLEO has measured the production ratio using semileptonic B decays and found [2]

$$\frac{f_+}{f_0} = 1.13 \pm 0.14 \pm 0.13 \pm 0.06 \tag{2}$$

where the last error is due to the uncertainties in the ratio of B^0 and B^+ lifetimes. This is consistent with equal production of B^+B^- and $B^0\overline{B}^0$ pairs and unless explicitly stated otherwise we will assume $f_+/f_0 = 1$. This assumption is further supported by the near equality of the B^+ and B^0 masses.

At high energy collider experiments the b quarks hadronize as B_d, B_u, B_s, and B_c mesons or as baryons containing b quarks. The composition of the initial sample is not very precisely known although over the last year significant improvements have been achieved. Several methods have been developed to determine f_{B_s} and f_{Λ_b}, the fractions of B_s mesons, and b-flavored baryons produced in $Z \to b\overline{b}$ decays. ALEPH use their measurement of the product branching fraction, $f_{B_s} \times \mathrm{B}(\overline{B}_s^0 \to D_s^+\ell^-\overline{\nu}_\ell \text{ anything}) = 0.82 \pm 0.09^{+0.13}_{-0.14}\%$ [3]. Under the assumption of equal semileptonic partial widths for b-flavored hadrons results from the $\Upsilon(4S)$ experiments can be used to obtain an estimate for $\mathrm{B}(\overline{B}_s^0 \to D_s^+\ell^-\overline{\nu}_\ell)$. Using these results ALEPH [4] extract the fraction of b quarks that hadronize to B_s mesons to[†]

$$f_{B_s} = 11.1^{+2.5}_{-2.6}\% \tag{3}$$

A similar procedure is followed to obtain an estimate for the fraction of b baryons [5]:

$$f_{\Lambda_b} = 13.2 \pm 2.4 \pm 3.3\% \tag{4}$$

An alternative methods to determine f_{B_s} starts with the time integrated mixing parameter

$$\overline{\chi} = f_{B_s}\chi_s + f_{B^0}\chi_d \tag{5}$$

Assuming $\chi_s = 0.5$ and using the measured value for χ_d the fraction of B_s mesons can be extracted [6]

$$f_{B_s} = 11.3^{+2.5}_{-2.6}\% \tag{6}$$

Averaging the two measurements of f_{B_s} with correlated systematics taken into account yields

$$< f_{B_s} >= 11.2^{+1.8}_{-1.9}\% \tag{7}$$

Assuming that $f_{B^0} = f_{B^+}$ and $f_{B^0} + f_{B^+} + f_{B_s} + f_{\Lambda_b} = 1$ we obtain the results listed in Table 1.

Table 1: Fractions of weakly decaying b-hadron species in $Z \to b\overline{b}$ decay.

b-hadron	Fraction [%]
B^+	37.8 ± 2.2
B^0	37.8 ± 2.2
B_s	$11.2^{+1.8}_{-1.9}$
Λ_b	13.2 ± 4.1

To date, the existence of four b-flavored mesons (B^-, $\overline{B}^0$, B^*, B_s) has been established. The LEP experiments have provided evidence for excited B^{**} and B_s^{**} states. The B_c is still not observed. The Λ_b baryon has been exclusively reconstructed by CDF and the LEP experiments. First indications of Σ_b and Ξ_b production have been presented by the LEP collaborations [7]. DELPHI has measured the Σ_b^*–Σ_b hyperfine splitting to 56 ± 16 MeV [8].

Lifetimes

The lifetime of a b-flavored hadron is given by its hadronic and semileptonic decay rates

$$\frac{1}{\tau_B} = \Gamma_{\mathrm{tot}} = \Gamma_{\mathrm{hadronic}} + \Gamma_{\mathrm{semileptonic}} \tag{8}$$

In the naive spectator model the heavy quark can decay only via the external spectator mechanism and thus the lifetimes of all mesons and baryons containing b quarks would be equal. Non-spectator effects such as the interference between contributing amplitudes modify this simple picture and give rise to a lifetimes hierarchy for b-flavored hadrons similar to the charm sector. However, since the lifetime differences are expected to scale as $1/m_Q^2$, where m_Q is the mass of the heavy quark, the variation in the b system should be significantly smaller, of order 10% or less [9]. For the b system we expect

$$\tau(B^-) \geq \tau(\overline{B}^0) \approx \tau(B_s) > \tau(\Lambda_b^0) \tag{9}$$

Measurements of lifetimes for the various b-flavored hadrons thus provide a means to determine the importance of nonspectator mechanisms in the b sector.

The experimental errors on individual B-lifetime measurements are approaching the 5–10% level. However, in order to reach the precision necessary to test theoretical predictions, the results from different experiments need to be averaged. Using the conventional approach of weighting the measurements according to their error does not take into account the underlying exponential lifetime distribution. If a measurement fluctuates low then its weight in the average will increase, leading to a bias towards low values. Combining lifetime measurements correctly is a difficult task that requires detailed knowledge of common systematic uncertainties and correlations between the results from different experiments. The average lifetimes for b-flavored hadrons given in this edition have been determined

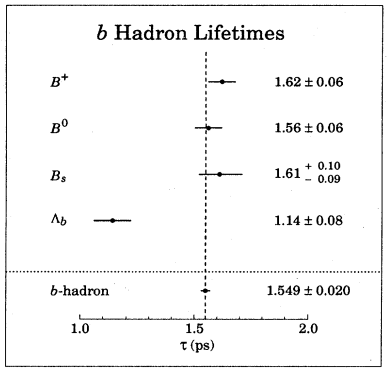

Figure 1: Summary of lifetime measurements for individual b hadrons and for the b-hadron admixture at high energy (LEP and CDF).

by L. Di Ciaccio (DELPHI) and the LEP B Lifetimes Working Group. Among other things, they considered uncertainties in the composition of the b sample and background, correlation in the b momentum estimation and common errors in b and c branching fractions. A detailed description of their procedures and the treatment of correlated and uncorrelated errors can be found in [10]. The experimental papers used in this calculation are given in the Particle Listing sections on b-flavored mesons and baryons. A summary of the average b-hadron lifetimes is shown in Fig. 1. The pattern of measured lifetimes follows the theoretical expectations outlined above and nonspectator effects are observed to be small. However, the Λ_b baryon lifetime is unexpectedly short. As has been noted by several authors, the observed value of the Λ_b lifetime is quite difficult to accommodate theoretically [11,12].

Semileptonic decays and mixing

Measurements of semileptonic B decays are important for the determination of the weak couplings $|V_{cb}|$ and $|V_{ub}|$ and test our understanding of the dynamics of heavy quark decay. A measurement technique using events with two leptons was introduced by the ARGUS experiment [13] which significantly reduces the model dependence associated with the subtraction of the $b \to c \to \ell$ cascade component. A high momentum lepton is selected ($p_\ell > 1.4$ GeV) which tags a $b\overline{b}$ event. This primary lepton is then combined with an additional lepton candidate which has a momentum above 0.5 GeV. In the absence of mixing, if the second lepton has a charge opposite to the tagging lepton it is a primary lepton from the b decay, while if the second lepton has the same sign as the tag it is a cascade lepton. Models of semileptonic B decay are only needed for the small extrapolation to zero lepton momentum. Using this method, CLEO II finds

$$\mathrm{B_{sl}} = (10.49 \pm 0.17 \pm 0.43)\,\% \qquad (10)$$

consistent with the conventional single lepton analysis.

Assuming the semileptonic decay width is the same for all b-flavored hadrons, the semileptonic branching ratio should be slightly different at LEP since other b particles are produced:

$$\mathrm{B_{sl}}(\Upsilon(4S)) = \frac{\Gamma_{\mathrm{sl}}}{\Gamma_{\mathrm{tot}}} = \Gamma_{\mathrm{sl}} \times \frac{(\tau_{B^+} + \tau_{B^0})}{2} \qquad (11)$$

while

$$\mathrm{B_{sl}}(Z) = \Gamma_{\mathrm{sl}} \times \tau_b \qquad (12)$$

Using the world averages for the B lifetimes and the CLEO semileptonic branching fraction this gives

$$\mathrm{B_{sl}}(Z) = \frac{2\tau_b}{(\tau_{B^+} + \tau_{B^0})} \times \mathrm{B_{sl}}(\Upsilon(4S)) = 10.2 \pm 0.4\% \qquad (13)$$

Note that the contribution of other hadrons *reduces* the expected average semileptonic branching fraction at the Z. This is below the experimental average from LEP, $\mathrm{B_{sl}}(Z) = 10.9 \pm 0.1 \pm 0.3$, but the errors are still too large to draw any conclusions.

It is interesting to compare the inclusive semileptonic branching fraction to the sum of branching fractions for exclusive modes. CLEO and the LEP collaborations have updated their measurements of $\mathrm{B}(B \to D\ell\nu_\ell)$ and $\mathrm{B}(B \to D^*\ell\nu_\ell)$. Including the recent observations of $B \to D^{**}(2420)\ell\nu_\ell$ and $B \to D^{**}(2460)$ by OPAL and ALEPH the sum of exclusive semileptonic branching fractions amounts to $8.81 \pm 0.1\%$. The remaining decays may correspond to $B \to D^{**}\ell\nu_\ell$ where D^{**} denotes a p-wave charmed meson with a large width (*e.g.* the very broad but as of now unobserved $1^3P_1(2490)$ and $1^3P_0(2440)$ states). It is also possible that the other missing decays are $B \to D\pi\ell^-\nu_\ell$ where the $D\pi$ system is nonresonant or originates from the decay of a broad excited charm meson. These possibilities are difficult to check experimentally. It is also conceivable that the difference between the sum of the exclusive modes and the inclusive semileptonic rate is due to a systematic error in the D meson absolute branching fraction scale.

The ALEPH, DELPHI, OPAL, and CDF experiments have performed explicit measurements of $\mathrm{Prob}(B^0 \to \overline{B^0})$ as a function of time to obtain the parameter $x_d = \Delta m_d/\Gamma$ [6]. The initial state b quark flavor is tagged either using leptons or jet charge, while the flavor of the final state b quark is tagged using either $\overline{B}_d \to D^{*+}\ell^-X$, $\overline{B}_d \to D^{*+}X$, or $\overline{B}_d \to \ell^-X$. If the final state is not fully reconstructed, as is the case for the analyses using dileptons, then the decay time must be determined using a topological vertexing technique where the lepton from the B decay and the other tracks in the same jet hemisphere are combined. The boost is determined using the observed energy, missing momentum and a correction factor determined from a Monte Carlo simulation. Averaging these results gives $\Delta m_d = 0.458 \pm 0.020$ ps^{-1} which is statistically superior to the results obtained from time integrated measurements by experiments at the $\Upsilon(4S)$.

The measurement of the mixing parameter $x_s = \Delta m_s/\Gamma$ for the B_s meson combined with the results on B^0–$\overline{B}^0$ oscillations allows the determination of the ratio of the CKM matrix elements $|V_{td}|^2/|V_{ts}|^2$ with significantly reduced theoretical uncertainties. Experimentally the measurement of x_s is a challenge. For large values, as expected for the B_s meson, time integrated measurements of B_s mixing become insensitive to x_s and one must make time dependent measurements in order to extract this parameter. These are very difficult because of the rapid oscillation rate of the B_s meson. Using an event sample with a lepton and a tag based on a jet charge technique where each track is weighted by its rapidity, ALEPH has searched for a high frequency component in their fit to the proper time distribution. They find $\Delta m_s > 6$ ps^{-1} or $x_s > 8.8$ at the 95% confidence level [6].

Hadronic decays

CLEO has presented a set of new measurements of inclusive B-meson decay rates that can be used to test the parton level expectation that most B decays proceed via a $b \to c$ transition. If we neglect the small contributions from $b \to u$ and penguin transitions, we expect about 1.15 charm quarks to be produced per B decay. The additional 15% is due to

the fact that the virtual W forms a $s\bar{c}$ quark pair with a probability of approximately 0.15. This expectation can be verified experimentally by adding all inclusive $b \to c$ branching fractions. Using the world averages for the $b \to c$ branching fractions we find [14]:

$$\begin{aligned}\text{Charm yield} &= \mathrm{B}(B \to D^0 X) + \mathrm{B}(B \to D^+ X) + \mathrm{B}(B \to D_s X) \\ &+ \mathrm{B}(B \to \Lambda_c X) + \mathrm{B}(B \to \Xi_c^+ X) + \mathrm{B}(B \to \Xi_c^0 X) \\ &+ 2 \times \mathrm{B}(B \to \psi X) + 2 \times \mathrm{B}(B \to \psi' X) \\ &+ 2 \times \mathrm{B}(B \to \chi_{c1} X) + 2 \times \mathrm{B}(B \to \chi_{c2} X) \\ &+ 2 \times \mathrm{B}(B \to \eta_c X \text{ (incl. other } c\bar{c})) \\ &= 1.15 \pm 0.05 \end{aligned} \tag{14}$$

The factor of 2 which multiplies $\mathrm{B}(B \to c\bar{c}X)$ accounts for the two charm quarks produced in $b \to c\bar{c}s$ transitions. Wherever possible the branching fractions for direct production are used. The contribution of $B \to \eta_c X$ and other charmonia is generously taken to be at the CLEO 90% confidence level upper limit $\mathrm{B}(B \to \eta_c X) < 0.90\%$.

Another interesting quantity is the fraction of B decays in which two charm quarks are produced. In a parton level calculation, Palmer and Stech [15] find that $\mathrm{B}(B \to X_{c\bar{c}}) = 19 \pm 1\%$ where the theoretical error is the uncertainty due to the choice of quark masses. This can be compared to the sum of the experimental measurements [14]

$$\begin{aligned}\mathrm{B}(B \to X_{c\bar{c}}) &= \mathrm{B}(B \to D_s X) + \mathrm{B}(B \to \psi X) + \mathrm{B}(B \to \psi' X) \\ &+ \mathrm{B}(B \to \chi_{c1} X) + \mathrm{B}(B \to \chi_{c2} X) + \mathrm{B}(B \to \Xi_c X) \\ &+ \mathrm{B}(B \to \eta_c X \text{ (incl. other } \bar{c})) \\ &= (15.8 \pm 2.8)\% \end{aligned} \tag{15}$$

where the direct $B \to \psi$ and $B \to \chi_{c1}$ branching fraction have been used. The contribution from $B \to \Xi_c^0 X$ is reduced by 1/3 to take into account the fraction that is not produced by the $b \to c\bar{c}s$ subprocess but by $b \to c\bar{u}d + s\bar{s}$ quark popping.

A possible contribution of $B \to D\overline{D}KX$ decays, which corresponds to the quark level process $b \to c\bar{c}s$ with popping of a light quark pair, is not included in the sum calculated above. Buchalla, Dunietz, and Yamamoto have recently suggested that the latter mechanism may be significant [16]. This possibility leads to wrong sign D–ℓ correlations and is currently under investigation at CLEO. Preliminary results [17] indicate a significant branching fraction on the order of 10% for $B \to \overline{D}_{\text{upper vertex}} X$.

The charm yield per B-meson decay is related to an intriguing puzzle in B physics: the experimental value for the semileptonic branching ratio of B mesons is significantly below the theoretical lower bound $\mathrm{B} > 12.5\%$ from QCD calculations within the parton model [18]. An enhanced hadronic decay rate would resolve this discrepancy and several explanations have been proposed. The theoretically preferred solution calls for an enhancement of the $b \to c\bar{c}s$ channel [19]. Increasing the $b \to c\bar{c}s$ component, however, would increase the average number of c quarks produced per b-quark decay and lead to another interesting problem: the predicted number of charm quarks per b decay would rise to 1.3 while the current experimental value for this number is 1.15 ± 0.05. Moreover, as noted above, $\mathrm{B}(B \to X_{c\bar{c}}) = 15.8 \pm 2.8$ is far below the required 30%. A systematic study of inclusive hadronic B decays to mesons and baryons and more precise measurements of charm meson branching fractions will be required to resolve this problem.

Measurements of exclusive hadronic B decays have reached sufficient precision to challenge our understanding of the dynamics of these decays. The factorization hypothesis has been experimentally confirmed for decays with large energy release. By comparing hadronic B^- and $\overline{B}^0$ decays, the relative contributions from external and internal spectator decays have been disentangled. For all decay modes studied the B^- branching ratio was found to be larger than the corresponding $\overline{B}^0$ branching ratio indicating constructive interference between the external and internal spectator amplitudes. This came as a surprise since destructive interference was observed in hadronic charm decay. However, the B^- modes analyzed so far comprise only a small fraction of the total hadronic rate. Further experimental study is required to determine at what level constructive interference is present in the remainder of hadronic B^- decays.

Rare decays

All B meson decays that do not occur through the usual $b \to c$ transition are known as rare B decays. The simplest diagram for a rare B decay is obtained by replacing the $b \to c$ transition by a CKM suppressed $b \to u$ transition. These decays probe the small CKM matrix element V_{ub}, the magnitude of which sets bounds on the combination $\rho^2 + \eta^2$ in the Wolfenstein parameterization of the CKM matrix. So far the only measurement of the magnitude of V_{ub} has been obtained from measurements of inclusive semileptonic B decays [20]. Last year CLEO reported the observation of exclusive semileptonic transitions. Using their large data sample and employing the excellent hermiticity of the CLEO II detector they were able to measure (using the BSW model) $\mathrm{B}(B^0 \to \pi^- \ell^+ \nu_\ell) = (1.63 \pm 0.46 \pm 0.34) \times 10^{-4}$ and $\mathrm{B}(B^0 \to \rho^- \ell^+ \nu_\ell) = (3.88 \pm 0.54 \pm 0.34) \times 10^{-4}$ [21].

While the errors are still large these results are an important step towards establishing a reliable value of $|V_{ub}|$.

Exclusive hadronic $b \to u$ transitions still await experimental discovery. CLEO sees a significant signal in the combined $B^0 \to \pi^+\pi^-$, $K^+\pi^-$ channels but detector resolution and statistics are not sufficient to separate the two modes.

The observation of the decay $B \to K^*(892)\gamma$, reported in 1993 by the CLEO II experiment, provided first evidence for the 1-loop penguin diagram [22]. The observed branching fractions were used to constrain a large class of Standard Model extensions [23]. However, due to the uncertainties in the hadronization, only the inclusive $b \to s\gamma$ rate can be reliably compared with theoretical calculations. This rate can be measured from the endpoint of the inclusive photon spectrum in B decay. CLEO found $\mathrm{B}(b \to s\gamma) = (2.32 \pm 0.54 \pm 0.35) \times 10^{-4}$.

A larger total rate is expected for gluonic penguins, the counterpart of $b \to s\gamma$ with the photon replaced by a gluon. However, it is a major experimental challenge to measure the inclusive $b \to sg$ rate, where the virtual gluon hadronizes as a $q\bar{q}$ pair. Since the coupling of gluons to quark-antiquark pairs is flavor independent, it is expected that except for modifications due to phase space $b \to s\bar{s}s$ will be comparable to $b \to s\bar{u}u$, $b \to s\bar{d}d$. A recent CLEO search revealed no signal for exclusive $b \to s\bar{s}s$ decays such as $\overline{B} \to \phi K^{(*)}$ nor did they find an excess in the endpoint of the ϕ momentum spectrum for inclusive $B \to \phi$ transitions.

Outlook

With the end of the Fermilab collider run and the change of the LEP beam energies CLEO and SLD will be the only collider experiments in the next few years to collect data.

While this might slow down the current rate of rapid progress in our understanding of heavy flavor physics there are still many answers hidden in the large data samples collected by CDF and the LEP collaborations. This combined with the ever-growing CLEO data sample will provide many new insights into all aspects of B physics.

The one exception is a measurement of the complex phase in CKM matrix. Data samples at least one order of magnitude larger than those available at present are needed to observe CP asymmetries in the B-meson system and to perform one of the most fundamental consistency check of the Standard Model. This is the justification for the construction of high luminosity e^+e^- storage rings (PEP II/BaBar, CESR III/CLEO III, TRISTAN II/BELLE) as well as a dedicated fixed target experiment at the HERA ring at DESY. Hadron collider experiments dedicated to the study of CP violation have also been proposed at Fermilab and at CERN.

Notes and References

† The results given in this section have been obtained by O. Hayes (ALEPH) and M. Jimack (OPAL). Their analysis is based on the average branching ratio, mixing parameters, and lifetimes listed in this compilation.

1. CLEO Collaboration, Cornell Preprint CLNS 1362, (submitted to Phys. Rev. Lett.).
2. CLEO Collaboration, Phys. Rev. **D51**, 1014 (1995).
3. ALEPH Collaboration, Phys. Lett. **B361**, 221 (1995).
4. ALEPH Collaboration, Phys. Lett. **B359**, 236 (1995).
5. ALEPH Collaboration, Phys. Lett. **B357**, 685 (1995); OPAL Collaboration, Z. Phys. **C69**, 195 (1996); DELPHI Collaboration, Z. Phys. **C68**, 375 (1995).
6. Sau Lan Wu, contribution to the Proceedings of 17th International Symposium on Lepton-Photon Interactions, Beijing.
7. M. Feindt, contribution to the proceedings of the Hadron 95 conference, Manchester, UK.
8. DELPHI Collaboration, EPS0565, contribution to the 1995 Europhysics Conference, Brussels, Belgium and the Beijing Lepton-Photon Symposium, 1995.
9. See I.I. Bigi, B. Blok, M. Shifman, N. Uraltsev, and A. Vainshtein for a review of the current theoretical situation, contribution to B Decays ed. S. Stone, World Scientific (1994) and also available as CERN-TH-7132/94 (1994).
10. L. Di Ciaccio *et al.*, "Averaging Lifetimes for B Hadron Species", Oxford University preprint OUNP 96-05 (1996), Rome University preprint ROM2F/96/09 (1996), Max Planck Institute Munich MPI-PhE/96-05 (1996). The information is also available on the World Wide Web at `http://wwwcn.cern.ch/~claires/lepblife.html`.
11. M. Neubert and C.T. Sachrajda, CERN-TH/96-19.
12. J. Rosner, preprint CERN-TH-96/24, EFI-96-03, hep-ph/9602265, submitted to Physics Letters B.
13. H. Albrecht *et al.* (ARGUS Collaboration), Phys. Lett. **B318**, 397 (1993).
14. T. Browder, K. Honscheid, D. Pedrini, OHSTPY-HEP-E-96-003, to be published in Annual Review of Nuclear and Particle Science, 1996.
15. W.F. Palmer and B. Stech, Phys. Rev. **D48**, 4174 (1993).
16. G. Buchalla, I. Dunietz, H. Yamamoto, Phys. Lett. **B364**, 188 (1995).
17. Y. Kwon, contribution to the Proceedings of the Rencontres de Moriond, March 1996, World Scientific.
18. I. Bigi, B. Blok, M.A. Shifman, and A.I. Vainshtein, Phys. Lett. **B323**, 408 (1994).
19. E. Bagan, P. Ball, V.M. Braun, and P. Gosdzinsky, Phys. Lett. **B42**, 362 (1995).
20. J. Bartelt *et al.* (CLEO Collaboration), Phys. Rev. Lett. **71**, 511 (1993); S. Stone "Semileptonic B Decays", B decays, ed. S. Stone, World Scientific (1994).
21. The first observation of this decay mode is described in L.K. Gibbons (CLEO II Collaboration), contribution to the Proceedings of the Rencontres de Moriond, March 1995, World Scientific. Updated branching fractions are given in D.M. Asner *et al.* (CLEO Collaboration), CLEO-CONF 95-7, paper submitted to the EPS and Lepton Photon conferences. Also see E.H. Thorndike and L.K. Gibbons,contribution to the Proceedings of 1995 Brussels Europhysics Conference.
22. R. Ammar *et al.* (CLEO Collaboration), Phys. Rev. Lett. **71**, 674 (1993).
23. J.L. Hewett, Phys. Rev. Lett. **70**, 1045 (1993).

QUARK MASSES

(by A. Manohar, University of California, San Diego)

A. Introduction

This note discusses some of the theoretical issues involved in the determination of quark masses. Unlike the leptons, quarks are confined inside hadrons and are not observed as physical particles. Quark masses cannot be measured directly, but must be determined indirectly through their influence on hadron properties. As a result, the values of the quark masses depend on precisely how they are defined; there is no one definition that is the obvious choice. Though one often speaks loosely of quark masses as one would of the electron or muon mass, any careful statement of a quark mass value must make reference to a particular computational scheme that is used to extract the mass from observations. It is important to keep this scheme dependence in mind when using the quark mass values tabulated in the data listings.

The simplest way to define the mass of a quark is by making a fit of the hadron mass spectrum to a nonrelativistic quark model. The quark masses are defined as the values obtained from the fit. The resulting masses only make sense in the limited context of a particular quark model. They depend on the phenomenological potential used, and on how relativistic effects are modelled. The quark masses used in potential models also cannot be connected with the quark mass parameters in the QCD Lagrangian. Fortunately, there exist other definitions of the quark mass that have a more general significance, though they also depend on the method of calculation. The purpose of this review is to explain the most important such definitions and their interrelations.

B. Mass parameters and the QCD Lagrangian

The QCD Lagrangian for N_F quark flavors is

$$\mathcal{L} = \sum_{k=1}^{N_F} \overline{q}_k \left(i \not{D} - m_k \right) q_k - \tfrac{1}{4} G_{\mu\nu} G^{\mu\nu} \ , \qquad (1)$$

where $\not{D} = (\partial_\mu - i g A_\mu)\, \gamma^\mu$ is the gauge covariant derivative, A_μ is the gluon field, $G_{\mu\nu}$ is the gluon field strength, m_k is the mass parameter of the k^{th} quark, and q_k is the quark Dirac field. The QCD Lagrangian Eq. (1) gives finite scattering amplitudes after renormalization, a procedure that invokes a subtraction scheme to render the amplitudes finite, and requires the introduction of

a dimensionful scale parameter μ. The mass parameters in the QCD Lagrangian Eq. (1) depend on the renormalization scheme used to define the theory, and also on the scale parameter μ. The most commonly used renormalization scheme for QCD perturbation theory is the $\overline{\rm MS}$ scheme.

The QCD Lagrangian has a chiral symmetry in the limit that the quark masses vanish. This symmetry is spontaneously broken by dynamical chiral symmetry breaking, and explicitly broken by the quark masses. The nonperturbative scale of dynamical chiral symmetry breaking, Λ_χ, is around 1 GeV. It is conventional to call quarks heavy if $m > \Lambda_\chi$, so that explicit chiral symmetry breaking dominates, and light if $m < \Lambda_\chi$, so that spontaneous chiral symmetry breaking dominates. The c, b, and t quarks are heavy, and the u, d and s quarks are light. The computations for light quarks involve an expansion in m_q/Λ_χ about the limit $m_q = 0$, whereas for heavy quarks, they involve an expansion in Λ_χ/m_q about $m_q = \infty$. The corrections are largest for the s and c quarks, which are the heaviest light quark and the lightest heavy quark, respectively.

At high energies or short distances, nonperturbative effects such as chiral symmetry breaking are unimportant, and one can in principle analyze mass-dependent effects using QCD perturbation theory to extract the quark mass values. The QCD computations are conventionally performed using the $\overline{\rm MS}$ scheme at a scale $\mu \gg \Lambda_\chi$, and give the $\overline{\rm MS}$ "running" mass $\overline{m}(\mu)$. The μ dependence of $\overline{m}(\mu)$ at short distances can be calculated using the renormalization group equations.

For heavy quarks, one can obtain useful information on the quark masses by studying the spectrum and decays of hadrons containing heavy quarks. One method of calculation uses the heavy quark effective theory (HQET), which defines a HQET quark mass m_Q. Other commonly used definitions of heavy quark masses such as the pole mass are discussed in Sec. C. QCD perturbation theory at the heavy quark scale $\mu = m_Q$ can be used to relate the various heavy quark masses to the $\overline{\rm MS}$ mass $\overline{m}(\mu)$, and to each other.

For light quarks, one can obtain useful information on the quark mass ratios by studying the properties of the light pseudoscalar mesons using chiral perturbation theory, which utilizes the symmetries of the QCD Lagrangian Eq. (1). The quark mass ratios determined using chiral perturbation theory are those in a subtraction scheme that is independent of the quark masses themselves, such as the $\overline{\rm MS}$ scheme.

A more detailed discussion of the masses for heavy and light quarks is given in the next two sections. The $\overline{\rm MS}$ scheme applies to both heavy and light quarks. It is also commonly used for predictions of quark masses in unified theories, and for computing radiative corrections in the Standard Model. For this reason, we use the $\overline{\rm MS}$ scheme as the standard scheme in reporting quark masses. One can easily convert the $\overline{\rm MS}$ masses into other schemes using the formulæ given in this review.

C. Heavy quarks

The commonly used definitions of the quark mass for heavy quarks are the pole mass, the $\overline{\rm MS}$ mass, the Georgi-Politzer mass, the potential model mass used in ψ and Υ spectroscopy, and the HQET mass.

The strong interaction coupling constant at the heavy quark scale is small, and one can compute the heavy quark propagator using QCD perturbation theory. For an observable particle such as the electron, the position of the pole in the propagator is the definition of the particle mass. In QCD this definition of the quark mass is known as the pole mass m_P, and is independent of the renormalization scheme used. It is known that the on-shell quark propagator has no infrared divergences in perturbation theory [1], so this provides a perturbative definition of the quark mass. The pole mass cannot be used to arbitrarily high accuracy because of nonperturbative infrared effects in QCD. The full quark propagator has no pole because the quarks are confined, so that the pole mass cannot be defined outside of perturbation theory.

The $\overline{\rm MS}$ running mass $\overline{m}(\mu)$ is defined by regulating the QCD theory using dimensional regularization, and subtracting the divergences using the modified minimal subtraction scheme. The $\overline{\rm MS}$ scheme is particularly convenient for Feynman diagram computations, and is the most commonly used subtraction scheme.

The Georgi-Politzer mass $\widehat{m}$ is defined using the momentum space subtraction scheme at the spacelike point $-p^2 = \widehat{m}^2$ [2]. A generalization of the Georgi-Politzer mass that is often used in computations involving QCD sum rules [3] is $\widehat{m}(\xi)$, defined at the subtraction point $p^2 = -(\xi + 1)m_P^2$. QCD sum rules are discussed in more detail in the next section on light quark masses.

Lattice gauge theory calculations can be used to obtain heavy quark masses from ψ and Υ spectroscopy. The quark masses are obtained by comparing a nonperturbative computation of the meson spectrum with the experimental data. The lattice quark mass values can then be converted into quark mass values in the continuum QCD Lagrangian Eq. (1) using lattice perturbation theory at a scale given by the inverse lattice spacing. A recent computation determines the b-quark pole mass to be 5.0 ± 0.2 GeV, and the $\overline{\rm MS}$ mass to be 4.0 ± 0.1 GeV [4].

Potential model calculations of the hadron spectrum also involve the heavy quark mass. There is no way to relate the quark mass as defined in a potential model to the quark mass parameter of the QCD Lagrangian, or to the pole mass. Even in the heavy quark limit, the two masses can differ by nonperturbative effects of order $\Lambda_{\rm QCD}$. There is also no reason why the potential model quark mass should be independent of the particular form of the potential used.

Recent work on the heavy quark effective theory [5–9] has provided a definition of the quark mass for a heavy quark that is valid when one includes nonperturbative effects and will be called the HQET mass m_Q. The HQET mass is particularly useful in the analysis of the $1/m_Q$ corrections in HQET. The HQET mass agrees with the pole mass to all orders in perturbation theory when only one quark flavor is present, but differs from the pole mass at order α_s^2 when there are additional flavors [10]. Physical quantities such as hadron masses can in principle be computed in the heavy quark effective theory in terms of the HQET mass m_Q. The computations cannot be done analytically in practice because of nonperturbative effects in QCD, which also prevent a direct extraction of the quark masses from the original QCD Lagrangian, Eq. (1). Nevertheless, for heavy quarks, it is possible to parametrize the nonperturbative effects to a given order in the $1/m_Q$ expansion in terms of a few unknown constants that can be obtained from experiment. For example, the B and D meson masses in the heavy quark effective theory are given in terms of a single nonperturbative parameter $\overline{\Lambda}$,

$$M(B) = m_b + \overline{\Lambda} + \mathcal{O}\left(\frac{\overline{\Lambda}^2}{m_b}\right) ,$$

$$M(D) = m_c + \overline{\Lambda} + \mathcal{O}\left(\frac{\overline{\Lambda}^2}{m_c}\right) . \qquad (2)$$

This allows one to determine the mass difference $m_b - m_c = M(B) - M(D) = 3.4$ GeV up to corrections of order $\overline{\Lambda}^2/m_b - \overline{\Lambda}^2/m_c$. The extraction of the individual quark masses m_b and m_c requires some knowledge of $\overline{\Lambda}$. An estimate of $\overline{\Lambda}$ using QCD sum rules gives $\overline{\Lambda} = 0.57 \pm 0.07$ GeV [11]. The HQET masses with this value of $\overline{\Lambda}$ are $m_b = 4.74 \pm 0.14$ GeV and $m_c = 1.4 \pm 0.2$ GeV, where the spin averaged meson masses $(3M(B^*) + M(B))/4$ and $(3M(D^*) + M(D))/4$ have been used to eliminate the spin-dependent $\mathcal{O}(\overline{\Lambda}^2/m_Q)$ correction terms. The errors reflect the uncertainty in $\overline{\Lambda}$ and the unknown spin-averaged $\mathcal{O}(\overline{\Lambda}^2/m_Q)$ correction. The errors do not include any theoretical uncertainty in the QCD sum rules, which could be large. A quark model estimate suggests that $\overline{\Lambda}$ is the constituent quark mass (≈ 350 MeV), which differs significantly from the sum rule estimate. In HQET, the $1/m_Q$ corrections to heavy meson decay form-factors are also given in terms of $\overline{\Lambda}$. Thus an accurate enough measurement of these form-factors could be used to extract $\overline{\Lambda}$ directly from experiment, which then determines the quark masses up to corrections of order $1/m_Q$.

The quark mass m_Q of HQET can be related to other quark mass parameters using QCD perturbation theory at the scale m_Q. The relation between m_Q and $\widehat{m}(\xi)$ at one loop is [12]

$$m_Q = \widehat{m}(\xi)\left[1 + \frac{\widehat{\alpha}_s(\xi)}{\pi}\frac{\xi+2}{\xi+1}\log(\xi+2)\right], \tag{3}$$

where $\widehat{\alpha}_s(\xi)$ is the strong interaction coupling constant in the momentum space subtraction scheme. The relation between m_Q and the $\overline{\rm MS}$ mass $\overline{m}$ is known to two loops [13],

$$m_Q = \overline{m}(m_Q)\left[1 + \frac{4\overline{\alpha}_s(m_Q)}{3\pi} + \left(16.11 - 1.04\sum_k\left(1 - \frac{m_{Q_k}}{m_Q}\right)\right)\left(\frac{\overline{\alpha}_s(m_Q)}{\pi}\right)^2\right], \tag{4}$$

where $\overline{\alpha}_s(\mu)$ is the strong interaction coupling constants in the $\overline{\rm MS}$ scheme, and the sum on k extends over all flavors Q_k lighter than Q. For the b-quark, Eq. (4) reads

$$m_b = \overline{m}_b(m_b)\,[1 + 0.09 + 0.06], \tag{5}$$

where the contributions from the different orders in α_s are shown explicitly. The two loop correction is comparable in size and has the same sign as the one loop term. There is presumably an error of order 0.05 in the relation between m_b and $\overline{m}_b(m_b)$ from the uncalculated higher order terms.

D. Light quarks

For light quarks, one can use the techniques of chiral perturbation theory to extract quark mass ratios. The light quark part of the QCD Lagrangian Eq. (1) has a chiral symmetry in the limit that the light quark masses are set to zero, under which left- and right-handed quarks transform independently. The mass term explicitly breaks the chiral symmetry, since it couples the left- and right-handed quarks to each other. A systematic analysis of this explicit chiral symmetry breaking provides some information on the light quark masses.

It is convenient to think of the three light quarks u, d and s as a three component column vector Ψ, and to write the mass term for the light quarks as

$$\overline{\Psi} M \Psi = \overline{\Psi}_L M \Psi_R + \overline{\Psi}_R M \Psi_L, \tag{6}$$

where M is the quark mass matrix M,

$$M = \begin{pmatrix} m_u & 0 & 0 \\ 0 & m_d & 0 \\ 0 & 0 & m_s \end{pmatrix}. \tag{7}$$

The mass term $\overline{\Psi} M \Psi$ is the only term in the QCD Lagrangian that mixes left- and right-handed quarks. In the limit that $M \to 0$, there is an independent SU(3) flavor symmetry for the left- and right-handed quarks. This $G_\chi = {\rm SU}(3)_L \times {\rm SU}(3)_R$ chiral symmetry of the QCD Lagrangian is spontaneously broken, which leads to eight massless Goldstone bosons, the π's, K's, and η, in the limit $M \to 0$. The symmetry G_χ is only an approximate symmetry, since it is explicitly broken by the quark mass matrix M. The Goldstone bosons acquire masses which can be computed in a systematic expansion in M in terms of certain unknown nonperturbative parameters of the theory. For example, to first order in M one finds that [14,15]

$$\begin{aligned} m_{\pi^0}^2 &= B(m_u + m_d)\ , \\ m_{\pi^\pm}^2 &= B(m_u + m_d) + \Delta_{em}\ , \\ m_{K^0}^2 = m_{\overline{K}^0}^2 &= B(m_d + m_s)\ , \\ m_{K^\pm}^2 &= B(m_u + m_s) + \Delta_{em}\ , \\ m_\eta^2 &= \frac{1}{3}B(m_u + m_d + 4m_s)\ , \end{aligned} \tag{8}$$

with two unknown parameters B and Δ_{em}, the electromagnetic mass difference. From Eq. (8), one can determine the quark mass ratios [14]

$$\begin{aligned} \frac{m_u}{m_d} &= \frac{2m_{\pi^0}^2 - m_{\pi^+}^2 + m_{K^+}^2 - m_{K^0}^2}{m_{K^0}^2 - m_{K^+}^2 + m_{\pi^+}^2} = 0.56\ , \\ \frac{m_s}{m_d} &= \frac{m_{K^0}^2 + m_{K^+}^2 - m_{\pi^+}^2}{m_{K^0}^2 + m_{\pi^+}^2 - m_{K^+}^2} = 20.1\ , \end{aligned} \tag{9}$$

to lowest order in chiral perturbation theory. The error on these numbers is the size of the second-order corrections, which are discussed at the end of this section. Chiral perturbation theory cannot determine the overall scale of the quark masses, since it uses only the symmetry properties of M, and any multiple of M has the same G_χ transformation law as M. This can be seen from Eq. (8), where all quark masses occur only in the form Bm, so that B and m cannot be determined separately.

The mass parameters in the QCD Lagrangian have a scale dependence due to radiative corrections, and are renormalization scheme dependent. Since the mass ratios extracted using chiral perturbation theory use the symmetry transformation property of M under the chiral symmetry G_χ, it is important to use a renormalization scheme for QCD that does not change this transformation law. Any quark mass independent subtraction scheme such as $\overline{\rm MS}$ is suitable. The ratios of quark masses are scale independent in such a scheme.

The absolute normalization of the quark masses can be determined by using methods that go beyond chiral perturbation theory, such as QCD sum rules [3]. Typically, one writes a sum rule for a quantity such as B in terms of a spectral integral over all states with certain quantum numbers. This spectral integral is then evaluated by assuming it is dominated by one (or two) of the lowest resonances, and using the experimentally measured resonance parameters [16]. There are many subtleties involved, which cannot be discussed here [16].

Another method for determining the absolute normalization of the quark masses, is to assume that the strange quark mass is equal to the SU(3) mass splitting in the baryon multiplets [14,16]. There is an uncertainty in this method since in the baryon octet one can use either the Σ–N or the Λ–N mass difference, which differ by about 75 MeV, to estimate the strange quark mass. But more importantly, there is no way to

relate this normalization to any more fundamental definition of quark masses.

One can extend the chiral perturbation expansion Eq. (8) to second order in the quark masses M to get a more accurate determination of the quark mass ratios. There is a subtlety that arises at second order [17], because

$$M\left(M^\dagger M\right)^{-1}\det M^\dagger \tag{10}$$

transforms in the same way under G_χ as M. One can make the replacement $M \to M(\lambda) = M + \lambda M\left(M^\dagger M\right)^{-1}\det M^\dagger$ in all formulæ,

$$M(\lambda) = \mathrm{diag}\,(m_u(\lambda),\ m_d(\lambda),\ m_s(\lambda))$$

$$= \mathrm{diag}\,(m_u + \lambda m_d m_s,\ m_d + \lambda m_u m_s,\ m_s + \lambda m_u m_d)\ , \tag{11}$$

so it is not possible to determine λ by fitting to data. One can only determine the ratios $m_i(\lambda)/m_j(\lambda)$ using second-order chiral perturbation theory, not the desired ratios $m_i/m_j = m_i(\lambda=0)/m_j(\lambda=0)$.

Dimensional analysis can be used to estimate [18] that second-order corrections in chiral perturbation theory due to the strange quark mass are of order $\lambda m_s \sim 0.25$. The ambiguity due to the redefinition Eq. (11) (which corresponds to a second-order correction) can produce a sizeable uncertainty in the ratio m_u/m_d. The lowest-order value $m_u/m_d = 0.56$ gets corrections of order $\lambda m_s(m_d/m_u - m_u/m_d) \sim 30\%$, whereas m_s/m_d gets a smaller correction of order $\lambda m_s(m_u/m_d - m_u m_d/m_s^2) \sim 15\%$. A more quantitative discussion of second-order effects can be found in Refs. 17,19,20. Since the second-order terms have a single parameter ambiguity, the value of m_u/m_d is related to the value of m_s/m_d.

The ratio m_u/m_d is of great interest since there is no strong CP problem if $m_u = 0$. To determine m_u/m_d requires fixing λ in the mass redefinition Eq. (11). There has been considerable effort to determine the chiral Lagrangian parameters accurately enough to determine m_u/m_d, for example from the analysis of the decays $\psi' \to \psi + \pi^0, \eta$, the decay $\eta \to 3\pi$, using sum rules, and from the heavy meson mass spectrum [16,21–24]. A recent paper giving a critique of these estimates is Ref. 25.

Eventually, lattice gauge theory methods will be accurate enough to be able to compute meson masses directly from the QCD Lagrangian Eq. (1), and thus determine the light quark masses. For a reliable determination of quark masses, these computations will have to be done with dynamical fermions, and with a small enough lattice spacing that one can accurately compute the relation between lattice and continuum Lagrangians.

The quark masses for light quarks discussed so far are often referred to as current quark masses. Nonrelativistic quark models use constituent quark masses, which are of order 350 MeV for the u and d quarks. Constituent quark masses model the effects of dynamical chiral symmetry breaking, and are not related to the quark mass parameters m_k of the QCD Lagrangian Eq. (1). Constituent masses are only defined in the context of a particular hadronic model.

E. Numerical values and caveats

The quark masses in the particle data listings have been obtained by using the wide variety of theoretical methods outlined above. Each method involves its own set of approximations and errors. In most cases, the errors are a best guess at the size of neglected higher-order corrections. The expansion parameter for the approximations is not much smaller than unity (for example it is $m_K^2/\Lambda_\chi^2 \approx 0.25$ for the chiral expansion), so an unexpectedly large coefficient in a neglected higher-order term could significantly alter the results. It is also important to note that the quark mass values can be significantly different in the different schemes. For example, assuming that the b-quark pole mass is 5.0 GeV, and $\overline{\alpha}_s(m_b) \approx 0.22$ gives the $\overline{\rm MS}$ b-quark mass $\overline{m}_b(\mu = m_b) = 4.6$ GeV using the one-loop term in Eq. (4), and $\overline{m}_b(\mu = m_b) = 4.3$ GeV including the one-loop and two-loop terms. The heavy quark masses obtained using HQET, QCD sum rules, or lattice gauge theory are consistent with each other if they are all converted into the same scheme. When using the data listings, it is important to remember that the numerical value for a quark mass is meaningless without specifying the particular scheme in which it was obtained. All non-$\overline{\rm MS}$ quark masses have been converted to $\overline{\rm MS}$ values in the data listings using one-loop formulæ, unless an explicit two-loop conversion is given by the authors in the original article.

References

1. R. Tarrach, Nucl. Phys. **B183**, 384 (1981).
2. H. Georgi and H.D. Politzer, Phys. Rev. **D14**, 1829 (1976).
3. M.A. Shifman, A.I. Vainshtein, and V.I. Zakharov, Nucl. Phys. **B147**, 385 (1979).
4. C.T.H. Davies, *et al.*, Phys. Rev. Lett. **73**, 2654 (1994).
5. N. Isgur and M.B. Wise, Phys. Lett. **B232**, 113 (1989), *ibid* **B237**, 527 (1990);
   M.B. Voloshin and M. Shifman, Sov. J. Nucl. Phys. **45**, 292 (1987), *ibid* **47**, 511 (1988);
   S. Nussinov and W. Wetzel, Phys. Rev. **D36**, 130 (1987).
6. H. Georgi, Phys. Lett. **B240**, 447 (1990).
7. E. Eichten and B. Hill, Phys. Lett. **B234**, 511 (1990).
8. H. Georgi, in *Perspectives of the Standard Model*, ed. R.K. Ellis, C.T. Hill, and J.D. Lykken (World Scientific, Singapore, 1992);
   B. Grinstein, in *High Energy Phenomenology*, ed. R. Huerta and M.A. Pérez (World Scientific, Singapore, 1992).
9. A.F. Falk, M. Neubert, and M.E. Luke, Nucl. Phys. **B388**, 363 (1992).
10. A.V. Manohar and M.B. Wise, (unpublished).
11. M. Neubert, Phys. Reports **245**, 259 (1994).
12. S. Narison, Phys. Lett. **B197**, 405 (1987).
13. N. Gray, D.J. Broadhurst, W. Grafe, and K. Schilcher, Z. Phys. **C48**, 673 (1990).
14. S. Weinberg, Trans. N.Y. Acad. Sci. **38**, 185 (1977).
15. See for example, H. Georgi, *Weak Interactions and Modern Particle Theory* (Benjamin/Cummings, Menlo Park, 1984).
16. J. Gasser and H. Leutwyler, Phys. Reports **87**, 77 (1982).
17. D.B. Kaplan and A.V. Manohar, Phys. Rev. Lett. **56**, 2004 (1986).
18. A. Manohar and H. Georgi, Nucl. Phys. **B234**, 189 (1984).
19. J. Gasser and H. Leutwyler, Nucl. Phys. **B250**, 465 (1985).
20. H. Leutwyler, Nucl. Phys. **B337**, 108 (1990).
21. P. Langacker and H. Pagels, Phys. Rev. **D19**, 2070 (1979);
    H. Pagels and S. Stokar, Phys. Rev. **D22**, 2876 (1980);
    H. Leutwyler, Nucl. Phys. **B337**, 108 (1990);
    J. Donoghue and D. Wyler, Phys. Rev. Lett. **69**, 3444 (1992);
    K. Maltman, T. Goldman and G.L. Stephenson Jr., Phys. Lett. **B234**, 158 (1990).
22. K. Choi, Nucl. Phys. **B383**, 58 (1992).
23. J. Donoghue and D. Wyler, Phys. Rev. **D45**, 892 (1992).
24. M.A. Luty and R. Sundrum, e-print hep-ph/9502398.
25. T. Banks, Y. Nir, and N. Seiberg, *Proceedings of the 2nd IFT Workshop on Yukawa Couplings and the Origins of Mass*, Gainesville, Florida (1994).

SOLAR NEUTRINOS

(by K. Nakamura, KEK, National Laboratory for High-Energy Physics, Japan)

The Sun is a main-sequence star at a stage of stable hydrogen burning. It produces an intense flux of electron neutrinos as a consequence of nuclear fusion reactions which generate solar energy, and whose combined effect is

$$4p + 2e^- \rightarrow {}^4\mathrm{He} + 2\nu_e + 26.73\ \mathrm{MeV} - E_\nu\ , \qquad (1)$$

where E_ν represents the energy taken away by neutrinos, with an average value being $\langle E_\nu \rangle \sim 0.6$ MeV. Each neutrino-producing reaction and the resulting flux predicted by the two recent standard solar model (SSM) calculations [1,2] are listed in Table 1. Figure 1 shows the energy spectra of solar neutrinos from these reactions quoted from the SSM calculation by Bahcall and Ulrich [3]. All SSM calculations give essentially the same results for the same input parameters and physics. The Bahcall and Pinsonneault model [1] and the Turck-Chièze and Lopes model [2] listed in Table 1 differ primarily in that Bahcall and Pinsonneault include helium diffusion [4].

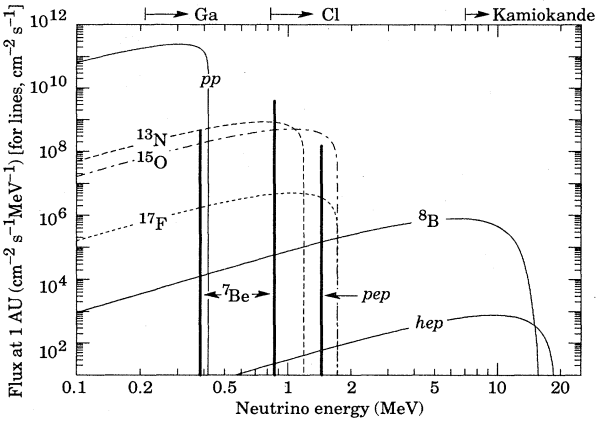

Figure 1: The solar neutrino spectrum predicted by the standard solar model. The neutrino fluxes from continuum sources are given in units of number $\mathrm{cm^{-2}s^{-1}MeV^{-1}}$ at one astronomical unit, and the line fluxes are given in number $\mathrm{cm^{-2}s^{-1}}$. Spectra for the *pp* chain are shown by solid lines, and those for the CNO chain by dotted or dashed lines. (Courtesy of J.N. Bahcall, 1995.)

Observations of solar neutrinos directly addresses the SSM and, more generally, the theory of stellar structure and evolution which is the basis of the SSM. The Sun as a well defined neutrino source also provides extremely important opportunities to investigate nontrivial neutrino properties such as nonzero mass and mixing, because of the wide range of matter density and the very long distance from the Sun to the Earth. In fact, the currently available solar-neutrino data seem to require such neutrino properties, if one tries to understand them consistently.

Table 1: Neutrino-producing reactions in the Sun (the first column) and their abbreviations (second column). The neutrino fluxes predicted by Bahcall and Pinsonneault (B-P) [1] and by Turck-Chièze and Lopes (T-C-L) [2] are listed in the third and fourth columns, respectively. The errors associated with the B-P calculation are "theoretical" 3 standard deviations according to the authors.

Reaction	Abbr.	B-P	T-C-L
$pp \rightarrow d\,e^+\,\nu$	*pp*	$6.00(1 \pm 0.02)$E10	6.02E10
$pe^-p \rightarrow d\,\nu$	*pep*	$1.43(1 \pm 0.04)$E8	1.3E8
$^3\mathrm{He}\ p \rightarrow {}^4\mathrm{He}\ e^+\nu$	*hep*	1.23E3	
$^7\mathrm{Be}\ e^- \rightarrow {}^7\mathrm{Li}\ \nu + (\gamma)$	^{7}Be	$4.89(1 \pm 0.18)$E9	4.33E9
$^8\mathrm{B} \rightarrow {}^8\mathrm{B}^*\ e^+\nu$	^{8}B	$5.69(1 \pm 0.43)$E6	4.43E9
$^{13}\mathrm{N} \rightarrow {}^{13}\mathrm{C}\ e^+\nu$	^{13}N	$4.92(1 \pm 0.51)$E8	3.83E8
$^{15}\mathrm{O} \rightarrow {}^{15}\mathrm{N}\ e^+\nu$	^{15}O	$4.26(1 \pm 0.58)$E8	3.15E8
$^{17}\mathrm{F} \rightarrow {}^{17}\mathrm{O}\ e^+\nu$	^{17}F	$5.39(1 \pm 0.48)$E6	

At present, four solar-neutrino experiments are taking data. Three of them are radiochemical experiments using ^{37}Cl (Homestake in USA) or ^{71}Ga (GALLEX at Gran Sasso in Italy and SAGE at Baksan in Russia) to capture neutrinos: $^{37}\mathrm{Cl}\ \nu_e \rightarrow {}^{37}\mathrm{Ar}\ e^-$ (threshold 814 keV) or $^{71}\mathrm{Ga}\ \nu_e \rightarrow {}^{71}\mathrm{Ge}\ e^-$ (threshold 233 keV). The produced ^{37}Ar and ^{71}Ge are both radioactive nuclei with half lives ($\tau_{1/2}$) of 34.8 days and 11.43 days, respectively. After an exposure of the detector for two to three times $\tau_{1/2}$, the reaction products are extracted and introduced into a low-background proportional counter, and are counted for a sufficiently long period to determine the exponentially decaying signal and a constant background. In the chlorine experiment, the dominant contribution comes from ^{8}B neutrinos, but ^{7}Be, *pep*, ^{13}N, and ^{15}O neutrinos also contribute. At present, the most abundant *pp* neutrinos can be detected only in gallium experiments. Even so, almost half of the capture rate in these experiments is due to other solar neutrinos.

The fourth is a real-time experiment utilizing νe scattering in a large water-Čerenkov detector (Kamiokande in Japan). This experiment takes advantage of the directional correlation between the incoming neutrino and the recoil electron. This feature greatly helps the clear separation of the solar-neutrino signal from the background. Due to its high threshold (7 MeV at present), Kamiokande observes pure ^{8}B solar neutrinos (*hep* neutrinos have too small a flux to be observed in the present generation of solar neutrino experiments.)

Solar neutrinos were first observed in the Homestake chlorine experiment around 1970. From the very beginning, it was recognized that the observed capture rate was significantly smaller than the SSM prediction. This deficit has been called "the solar-neutrino problem." The Kamiokande-II Collaboration started observing the ^{8}B solar neutrinos at the beginning of 1987. Because of the strong directional correlation of νe scattering, this result gave the first direct evidence that the Sun emits neutrinos (no directional information is available in radiochemical solar-neutrino experiments.) The observed solar-neutrino flux was also significantly less than the SSM prediction. In addition, Kamiokande-II obtained the energy spectrum of recoil electrons and the fluxes separately measured in the day time and nighttime. GALLEX presented the first evidence of *pp* solar-neutrino observation in 1992. Here also, the observed capture rate is significantly less than the SSM prediction. SAGE, after initial confusion which is ascribed to statistics by the group, observes a similar capture rate to that of GALLEX. The most recent results on the average capture rates or flux from these experiments [5–8] are compared with the recent SSM calculations [1,2] in Table 2.

Table 2: Recent results from the four solar-neutrino experiments. For Homestake [5], GALLEX [6], and SAGE [7], the data are capture rates given in SNU (Solar Neutrino Units; 1 SNU $= 10^{-36}$ capture per atom per second). For Kamiokande [8], the datum is ^{8}B solar-neutrino flux given in units of 10^6 cm^{-2} s^{-1}. The first errors are statistical and the second errors are systematic. The SSM predictions by Bahcall and Pinsonneault (B-P) [1] and by Turck-Chièze and Lopes (T-C-L) [2] are listed in the third and fourth columns, respectively. The errors associated with the B-P calculation are "theoretical" 3 standard deviations according to the authors.

Experiment	Data	B-P	T-C-L
Homestake	$2.55 \pm 0.17 \pm 0.18$	8.0 ± 3.0	6.4
GALLEX	$79 \pm 10 \pm 6$	131.5^{+21}_{-17}	122.5
SAGE	73^{+18+5}_{-16-7}	131.5^{+21}_{-17}	122.5
Kamiokande	$2.89^{+0.22}_{-0.21} \pm 0.35$	5.7 ± 2.4	4.4

There was a controversy concerning whether the ^{37}Cl capture rate showed time variation, anticorrelated with the sunspot numbers which represent the 11-year solar-activity cycle. However, more than 7 years of the Kamiokande-II solar-neutrino observation does not show evidence for a statistically significant correlation or anticorrelation between the solar-neutrino flux and sunspot number.

All results from the present solar-neutrino experiments indicate significantly less flux than expected from the SSM calculations. Is there any possible consistent explanation of all the results of solar-neutrino observations in the framework of the standard solar model? This is difficult because the Homestake result and the Kamiokande result, taken at face value, are mutually inconsistent if one assumes standard neutrino spectra. That is, with the reduction factor of the ^{8}B solar-neutrino flux as determined from the Kamiokande result, the Homestake ^{37}Cl capture rate would be oversaturated, and there would be no room to accommodate the ^{7}Be solar neutrinos. Several authors made more elaborate analyses using the constraint of observed solar luminosity, and found that not only the SSM but also nonstandard solar models are incompatible with the observed data. Now it is a common understanding that the solar-neutrino problem is not only the deficit of the ^{8}B solar-neutrino flux, but also the deficit of ^{7}Be solar-neutrino flux. The latter problem stems from the incompatibility between the Homestake and Kamiokande results and this makes astrophysical solutions untenable. There is another solar-neutrino problem concerning the low gallium capture rate observed by GALLEX and SAGE.

In view of the above situation, it is attractive to invoke nontrivial neutrino properties. Neutrino oscillation in matter (MSW mechanism) is particularly attractive in explaining all the experimental data on the average solar-neutrino flux consistently, without any a priori assumptions or fine tuning. Several authors made extensive MSW analyses using all the existing data and ended up with similar results. For example, Hata and Langacker [9] analyzed the solar-neutrino data as of mid-1993. They obtained solutions for various standard and nonstandard solar models taking the Earth effect and the Kamiokande day-night data into account. Assuming the Bahcall-Pinsonneault SSM [1], the small-mixing solution ($\Delta m^2 \sim 6 \times 10^{-6}$ eV^2 and $\sin^2 2\theta \sim 7 \times 10^{-3}$) gives an excellent fit to the data, but the large-mixing solution ($\Delta m^2 \sim 9 \times 10^{-6}$ eV^2 and $\sin^2 2\theta \sim 0.6$) is marginally allowed at 90% confidence level.

Assuming that the solution to the solar-neutrino problem be provided by some nontrivial neutrino properties, how can one discriminate various scenarios? There are at least two very important things to do experimentally. One is the measurement of energy spectrum of the solar neutrinos and the other is the measurement of the solar-neutrino flux by utilizing neutral-current reactions. Two high-statistics solar-neutrino experiments which are under construction, SuperKamiokande and Sudbury Neutrino Observatory (SNO) are expected to provide such results within a few years. A 50 kton water-Čerenkov detector, SuperKamiokande is sensitive to the solar-neutrino spectrum through measurement of recoil electron energy. SNO will use 1,000 tons of heavy water (D_2O) to measure solar neutrinos through both inverse beta decay ($\nu_e d \rightarrow e^- pp$) and neutral current interactions ($\nu_x d \rightarrow \nu_x pn$). In addition, νe scattering events will also be measured. The Borexino experiment with 300 tons of ultra-pure liquid scintillator is approved for the Gran Sasso. The primary purpose of this experiment is the measurement of the ^{7}Be solar neutrino flux, where possible deficit is now a key question, by lowering the detection threshold for the recoil electrons to 250 keV. It is hoped that these experiments will finally provide the key to solving the solar-neutrino problem.

References

1. J.N. Bahcall and M.H. Pinsonneault, Rev. Mod. Phys. **64**, 885 (1992).
2. S. Turck-Chièze and I. Lopes, Astrophys. J. **408**, 347 (1993).
3. J.N. Bahcall and R.K. Ulrich, Rev. Mod. Phys. **60**, 297 (1988).
4. J.N. Bahcall, private communication (1995).
5. B.T. Cleveland *et al.*, Nucl. Phys. (Proc. Supp.) **B38**, 47 (1995).
6. P. Anselmann *et al.*, Phys. Lett. **B327**, 377 (1994).
7. J.N. Abdurashitov *et al.*, Nucl. Phys. (Proc. Supp.) **B38**, 60 (1995).
8. Y. Suzuki, Nucl. Phys. (Proc. Supp.) **B38**, 54 (1995).
9. N. Hata and P. Langacker, Phys. Rev. **D50**, 632 (1994).

THE HIGGS BOSON

(by I. Hinchliffe, LBNL)

The Standard Model [1] contains one neutral scalar Higgs boson, which is a remnant of the mechanism that breaks the SU(2) × U(1) symmetry and generates the W and Z boson masses. The Higgs couples to quarks and leptons of mass m_f with a strength $gm_f/2M_W$. Its coupling to W and Z bosons is of strength g, where g is the coupling constant of the SU(2) gauge theory. Consequently its coupling to stable matter is very small, and its production and detection in experiments is difficult. An exception is its production in the decay of the Z boson. Since large numbers of Z's can be produced and the coupling of the Z to the Higgs is unsuppressed, experiments at LEP are now able to rule out a significant range of Higgs masses. The branching ratio of the Higgs boson into various final states is shown in Fig. 1.

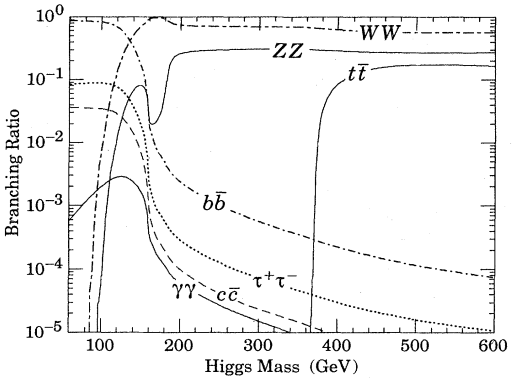

Figure 1: The branching ratio of the Higgs boson into $\gamma\gamma$, $\tau\overline{\tau}$, $b\bar{b}$, $t\bar{t}$, $c\bar{c}$, ZZ, and WW as a function of the Higgs mass. In the latter cases, if $M_H < 2M_Z$ (or $M_H < 2M_W$), the value indicated is the rate to ZZ^* (or WW^*) where Z^* (W^*) denotes a virtual Z (W). The $c\overline{c}$ rate depends sensitively on the poorly-determined charmed quark mass.

If the Higgs mass is very large, the couplings of the Higgs to itself and to longitudinally polarized gauge bosons become large. Requiring that these couplings remain weak enough so that perturbation theory is applicable implies that $M_H \lesssim 1$ TeV [2]. While this is not an absolute bound, it is an indication of the mass scale at which one can no longer speak of an elementary Higgs boson. This fact is made more clear if one notes that the width of the Higgs boson is proportional to the cube of its mass (for $M_H > 2M_Z$) and that a boson of mass 1 TeV has a width of 500 GeV.

It is believed that scalar field theories of the type used to describe Higgs self-interactions can only be effective theories valid over a limited range of energies if the Higgs self-coupling and hence Higgs mass is nonzero. A theory of this type that is valid at all energy scales must have zero coupling. The range of energies over which the interacting theory is valid is a function of the Higgs self-coupling and hence its mass. An upper bound on the Higgs mass can then be determined by requiring that the theory be valid (*i.e.*, have a nonzero value of the renormalized Higgs self-coupling) at all scales up to the Higgs mass [3]. Nonperturbative calculations using lattice [4] gauge theory that can be used to compute at arbitrary values of the Higgs mass indicate that $M_H \lesssim 770$ GeV.

If the Higgs mass were small, then the vacuum (ground) state with the correct value of M_W would cease to be the true ground state of the theory [5]. A theoretical constraint can then be obtained from the requirement that this is not the case, *i.e.*, that our universe is in the true minimum of the Higgs potential. The constraint depends upon the top quark mass and upon the scale (Λ) up to which the Standard Model remains valid. This scale must be at least 1 TeV, resulting in the constraint [7] $M_H > 72$ GeV$+0.9$ ($m_{\rm top}$–174 GeV). The bound increases monotonically with the scale, for $\Lambda = 10^{19}$ GeV, $M_H > 135$ GeV $+ 2.1$ ($m_{\rm top}$–174 GeV). This constraint may be too restrictive. Strictly speaking we can only require that the predicted lifetime of our universe, if it is not at the true minimum of the Higgs potential, be longer than its observed age [8,9]. For $\Lambda = 1$ TeV there is no constraint; and for $\Lambda = 10^{19}$ GeV $M_H > 120$ GeV $+ 2.3$ ($m_{\rm top} - 174$ GeV) [10].

Experiments at LEP are able to exclude a large range of Higgs masses. They search for the decay $Z \to HZ^*$. Here Z^* refers to a virtual Z boson that can appear in the detector as e^+e^-, $\mu^+\mu^-$, $\tau^+\tau^-$, $\nu\overline{\nu}$ (*i.e.*, missing energy) or hadrons. The experimental searches have considered both $H \to$ hadrons and $H \to \tau^+\tau^-$. The best limits are shown in the Particle Listings below.

Precision measurement of electroweak parameters such as M_W and the various asymmetries at LEP and SLC are becoming sensitive enough that they can in principle constrain the Higgs mass through its effect in radiative corrections. Currently, the precision tests allow the entire range from the direct LEP limit ($M_H \gtrsim 60$ GeV) to 1 TeV [11] at 95% confidence level although fits prefer the lower end of this range. The recent determination of the top mass has improved the constraint on M_H. See the article in this volume on the "Standard Model of Electroweak Interactions."

The search range for Higgs bosons will expand shortly when LEP begins operation at higher energy. The process $e^+e^- \to ZH$ [12] should enable neutral Higgs bosons of masses up to ~ 0.97 ($\sqrt{s} - M_Z$) to be discovered [13]. If the Higgs is heavier than this, its discovery will probably have to wait until experiments at the LHC have data. If the neutral Higgs boson has mass greater than $2M_Z$, it will likely be discovered via its decay to ZZ and the subsequent decay of the Z's to charged leptons (electrons or muons) or of one Z to charged leptons and the other to neutrinos. A challenging region is that between the ultimate limit of LEP and $2M_Z$. At the upper end of this range the decay to a real and a virtual Z, followed by the decay to charged leptons is available. The decay rate of the Higgs boson into this channel falls rapidly as M_H is reduced and becomes too small for $M_H \lesssim 140$ GeV. For masses below this, the decays $H \to \gamma\gamma$ and possibly $H \to b\bar{b}$ [14] are expected to be used. The former has a small branching ratio and large background,

the latter has a large branching ratio, larger background and a final state that is difficult to fully reconstruct [15].

Extensions of the Standard Model, such as those based on supersymmetry [16], can have more complicated spectra of Higgs bosons. The simplest extension has two Higgs doublets whose neutral components have vacuum expectation values v_1 and v_2, both of which contribute to the W and Z masses. The physical particle spectrum contains one charged Higgs boson ($H^{\pm}$), two neutral scalars (H_1, H_2),* and one pseudoscalar (A). In the simplest version of the supersymmetric model, the mass the lightest of these scalars depends upon the top quark mass, the ratio v_2/v_1, and the masses of the other supersymmetric particles. For $m_t = 174$ GeV, there is a bound $M_{H_1} \lesssim 125$ GeV [18,19]. In models where all fermions of the same electric charge receive their masses from only one of the two doublets (v_2 gives mass to the charge 2/3 quarks, while v_1 gives mass to the charged leptons and the charge 1/3 quarks), there are, as in the Standard Model, no flavor-changing neutral currents at lowest order in perturbation theory. The H_1, H_2^0, and A couplings to fermions depend on v_2/v_1 and are either enhanced or suppressed relative to the couplings in the Standard Model. Experiments at LEP are able to exclude ranges of masses for neutral Higgs particles in these models. These ranges depend on the values of v_2/v_1. See the Particle Listings below on H_1^0, Mass Limits in Supersymmetric Models.

Charged Higgs bosons can be pair produced in e^+e^- annihilation. Searches for charged Higgs bosons depend on the assumed branching fractions to $\nu\tau$, $c\bar{s}$, and $c\bar{b}$. Data from LEP now exclude charged Higgs bosons of mass less than 43.5 GeV [20]. See the Particle Listings for details of the $H^{\pm}$ Mass Limit.

A charged Higgs boson could be produced in the decay of a top quark, $t \to H^+b$. Searches for this decay at hadron colliders should be possible [21].

Notes and References

*H_1 and H_2 are usually called h and H in the literature.

1. S. Weinberg, Phys. Rev. Lett. **19**, 1264 (1967);
   A. Salam, in "Elementary Particle Theory," W. Svartholm, ed., Almquist and Wiksell, Stockholm (1968);
   S.L. Glashow, J. Iliopoulos, and L. Maiani, Phys. Rev. **D2**, 1285 (1970).
2. M. Veltman, Ann. Phys. (NY) **B8**, 475 (1977);
   B.W. Lee, C. Quigg, and H. Thacker, Phys. Rev. **D16**, 1519 (1977);
   D. Picus and V. Mather, Phys. Rev. **D7**, 3111 (1978).
3. L. Maiani, G. Parisi, and R. Petronzio, Nucl. Phys. **B136**, 115 (1978);
   R. Dashen and H. Neuberger, Phys. Rev. Lett. **50**, 1897 (1983).
4. U. M. Heller, M. Klomfass, H. Neuberger, and Pavlos Vranas Nucl. Phys. **B405**, 555 (1993);
   J. Kuti, L. Lin, and Y. Shen, Phys. Rev. Lett. **61**, 678 (1988);
   M. Gockeler, K. Jansen, and T. Neuhaus, Phys. Lett. **B273**, 450 (1991);
   U.M. Heller, H. Neuberger, and P. Vranas, Phys. Lett. **B283**, 355 (1992).
5. A.D. Linde, JETP Lett. **23**, 64 (1976) [Pis'ma Zh. Eksp. Teor. Fiz. **23**, 73 (1976)];
   S. Weinberg, Phys. Rev. Lett. **36**, 294 (1976).
6. M. Lindner, M. Sher, and H.W. Zaglauer, Phys. Lett. **B228**, 527 (1988).
7. M.J. Duncan, R. Phillipe, and M. Sher, Phys. Lett. **153B**, 165 (1985);
   G. Altarelli and I. Isidori, Phys. Lett. **B337**, 141 (1994);
   J.A. Casas, J.R. Espinosa, and M. Quiros, Phys. Lett. **B342**, 171 (1995).
8. G. Anderson, Phys. Lett. **B243**, 265 (1990).
9. P.B. Arnold, Phys. Rev. **D40**, 613 (1989).
10. J.R. Espinosa and M. Quiros, Phys. Lett. **B353**, 257 (1995).
11. D. Schaile, in *Proceedings of the XXVII International Conference on High Energy Physics*, Glasgow (Institute of Physics, 1995).
12. J. Ellis, M.K. Gaillard, D.V. Nanopoulous, Nucl. Phys. **B106**, 292 (1976);
    J.D. Bjorken, in *Weak Interactions at High Energies and the Production of New Particles*, SLAC report 198 (1976);
    B.I. Ioffe and V.A. Khoze, Sov. J. Part. Nucl. **9**, 50 (1978).
13. LEP-2 report, CERN PPE/95-78 (1995).
14. A. Stange, W. Marciano, S. Willenbrock Phys. Rev. **D50**, 4491 (1994);
    A. Stange, W. Marciano, S. Willenbrock J.F. Gunion, and T. Han, Phys. Rev. **D41**, 1051 (1995).
15. ATLAS technical proposal, CERN/LHCC/94-43, CMS technical proposal CERN/LHCC/94-38.
16. For a review of these models see, for example, I. Hinchliffe, Ann. Rev. Nucl. and Part. Sci. **36**, 505 (1986).
17. J.F. Gunion, H.E. Haber, G.L. Kane, and S. Dawson, *The Higgs Hunter's Guide* (Addison-Wesley, Redwood City, CA, 1990).
18. J. Ellis, G. Ridolfi, and F. Zwirner, Phys. Lett. **B257**, 83 (1991).
19. M. Carena, J.R. Espinosa, M. Quiros, and C.E.M. Wagner, Phys. Lett. **B355**, 209 (1995).
20. M. Pieri, in *Proceedings of XXVII International Conference on High Energy Physics*, Glasgow (1994);
    R. Barbieri, F. Caravaglios, and M. Frigeni, Phys. Lett. **B258**, 167 (1991);
    P.H. Chankowski, S. Pokorski, and T. Rosiek, Phys. Lett. **B274**, 191 (1991);
    Y. Okada, M. Yamaguchi, and T. Yanagida, Prog. Theor. Phys. **85**, 1 (1991);
    H.E. Haber and R. Hempfling, Phys. Rev. Lett. **66**, 1815 (1991).
21. R.M. Barnett, *et al.*, in *Research Directions for the Decade*, Snowmass 1990, World Scientific (1990).

SUPERSYMMETRY

(by H.E. Haber, Univ. of California, Santa Cruz)

A. Introduction: Supersymmetry is a generalization of the space-time symmetries of quantum field theory that transforms fermions into bosons and vice versa. It also provides a framework for the unification of particle physics and gravity, which takes place at an energy of order the Planck scale ($\approx 10^{19}$ GeV) [1–3]. However, supersymmetry is clearly not an exact symmetry of nature, and therefore must be broken. In theories of "low-energy" supersymmetry, the effective scale of supersymmetry breaking is tied to the electroweak scale [4–6]. In this way, it is hoped that supersymmetry will ultimately explain the origin of the large hierarchy between the W and Z masses and the Planck scale. At present, there are no unambiguous experimental results that require the existence of low-energy supersymmetry. However, if experimentation at future colliders uncovers evidence for supersymmetry, this would have a profound effect on the study of TeV-scale physics and the development of a more fundamental theory of mass and symmetry-breaking phenomena in particle physics.

B. Structure of the MSSM: The minimal supersymmetric extension of the Standard Model (MSSM) consists of taking the Standard Model and adding the corresponding supersymmetric partners [7]. In addition, the MSSM contains two hypercharge $Y = \pm 1$ Higgs doublets, which is the minimal structure for the Higgs sector of an anomaly-free supersymmetric extension of the Standard Model. The supersymmetric structure of the theory also requires (at least) two Higgs doublets to generate mass for both "up"-type and "down"-type quarks (and charged leptons) [8,9]. All renormalizable supersymmetric interactions consistent with (global) B–L conservation (B =baryon number and L =lepton number) are included. Finally, the most general soft-supersymmetry-breaking terms are added [10].

If supersymmetry is relevant for explaining the scale of electroweak interactions, then the mass parameters that occur in the soft-supersymmetry-breaking terms must be of order 1 TeV or below [11]. Some bounds on these parameters exist due to the absence of supersymmetric-particle production at current accelerators (see the Particle Listings following this note). Additional constraints arise from limits on the contributions of virtual supersymmetric particle exchange to a variety of Standard Model processes [12]. The impact of precision electroweak measurements at LEP and SLC on the MSSM parameter space is discussed briefly at the end of this note.

As a consequence of B–L invariance, the MSSM possesses a discrete R-parity invariance, where $R = (-1)^{3(B-L)+2S}$ for a particle of spin S [13]. Note that this formula implies that all the ordinary Standard Model particles have even R-parity, whereas the corresponding supersymmetric partners have odd R-parity. The conservation of R-parity in scattering and decay processes has a crucial impact on supersymmetric phenomenology. For example, starting from an initial state involving ordinary (R-even) particles, it follows that supersymmetric particles must be produced in pairs. In general, these particles are highly unstable and decay quickly into lighter states. However, R-parity invariance also implies that the lightest supersymmetric particle (LSP) is absolutely stable, and must eventually be produced at the end of a decay chain initiated by the decay of a heavy unstable supersymmetric particle.

In order to be consistent with cosmological constraints, the LSP is almost certainly electrically and color neutral [14]. Consequently, the LSP is weakly-interacting in ordinary matter, *i.e.* it behaves like a stable heavy neutrino and will escape detectors without being directly observed. Thus, the canonical signature for (R-parity conserving) supersymmetric theories is missing (transverse) energy, due to the escape of the LSP.

Some model builders attempt to relax the assumption of R-parity conservation. Models of this type must break B–L and are therefore strongly constrained by experiment [15]. Nevertheless, it is still important to allow for the possibility of R-parity violating processes in the search for supersymmetry. In such models, the LSP is unstable and supersymmetric particles can be singly produced and destroyed in association with B or L violation. These features lead to a phenomenology of broken-R-parity models that is very different from that of the MSSM.

In the MSSM, supersymmetry breaking is accomplished by including the soft-supersymmetry breaking terms mentioned earlier. These terms parametrize our ignorance of the fundamental mechanism of supersymmetry breaking. If this breaking occurs spontaneously, then (in the absence of supergravity) a massless Goldstone fermion called the *goldstino* ($\widetilde{G}$) must exist. The goldstino would then be the LSP and could play an important role in supersymmetric phenomenology [16]. In models that incorporate supergravity, this picture changes. If supergravity is spontaneously broken, the goldstino is absorbed ("eaten") by the *gravitino* ($g_{3/2}$), the spin-3/2 partner of the graviton [17]. By this super-Higgs mechanism, the gravitino acquires a mass ($m_{3/2}$). In many models, the gravitino mass is of order the electroweak-symmetry-breaking scale, while its couplings are gravitational in strength [1,18]. Such a gravitino would play no role in supersymmetric phenomenology at colliders.

The parameters of the MSSM are conveniently described by considering separately the supersymmetry-conserving sector and the supersymmetry-breaking sector. A careful discussion of the conventions used in defining the MSSM parameters can be found in Ref. 19. Among the parameters of the supersymmetry conserving sector are: (i) gauge couplings: g_s, g, and g', corresponding to the Standard Model gauge group SU(3)×SU(2)×U(1) respectively; (ii) Higgs-Yukawa couplings: λ_e, λ_u, and λ_d (which are 3×3 matrices in flavor space); and (iii) a supersymmetry-conserving Higgs mass parameter μ.

The supersymmetry-breaking sector contains the following set of parameters: (i) gaugino Majorana masses M_3, M_2 and M_1 associated with the SU(3), SU(2), and U(1) subgroups of the Standard Model; (ii) scalar mass matrices for the squarks and sleptons; (iii) Higgs-squark-squark trilinear interaction terms (the so-called "A-parameters") and corresponding terms involving the sleptons; and (iv) three scalar Higgs mass parameters—two diagonal and one off-diagonal mass terms for

the two Higgs doublets. These three mass parameters can be re-expressed in terms of the two Higgs vacuum expectation values, v_1 and v_2, and one physical Higgs mass. Here, v_1 (v_2) is the vacuum expectation value of the Higgs field which couples exclusively to down-type (up-type) quarks and leptons. Note that $v_1^2 + v_2^2 = (246\ \text{GeV})^2$ is fixed by the W mass (or equivalently by the Fermi constant G_F), while the ratio

$$\tan\beta = v_2/v_1 \tag{1}$$

is a free parameter of the model.

The supersymmetric constraints imply that the MSSM Higgs sector is automatically CP-conserving (at tree-level). Thus, $\tan\beta$ is a real parameter (conventionally chosen to be positive), and the physical neutral Higgs scalars are CP-eigenstates. Nevertheless, the MSSM does contain a number of possible new sources of CP violation. For example, gaugino-mass parameters, the A-parameters, and μ may be complex. Some combination of these complex phases must be less than of order 10^{-2}–10^{-3} (for a supersymmetry-breaking scale of 100 GeV) to avoid generating electric dipole moments for the neutron, electron, and atoms in conflict with observed data [20]. However, these complex phases have little impact on the direct searches for supersymmetric particles, and are usually ignored in experimental analyses.

C. The Higgs sector of the MSSM: Before describing the supersymmetric-particle sector, let us consider the Higgs sector of the MSSM [21]. There are five physical Higgs particles in this model: a charged Higgs pair ($H^\pm$), two CP-even neutral Higgs bosons (denoted by H_1^0 and H_2^0 where $m_{H_1^0} \leq m_{H_2^0}$) and one CP-odd neutral Higgs boson (A^0). The properties of the Higgs sector are determined by the Higgs potential which is made up of quadratic terms [whose squared-mass coefficients were mentioned above Eq. (1)] and quartic interaction terms. The strengths of the interaction terms are directly related to the gauge couplings by supersymmetry (and are not affected at tree-level by supersymmetry-breaking). As a result, $\tan\beta$ [defined in Eq. (1)] and one Higgs mass determine: the Higgs spectrum, an angle α [which indicates the amount of mixing of the original $Y = \pm 1$ Higgs doublet states in the physical CP-even scalars], and the Higgs boson couplings.

When one-loop radiative corrections are incorporated, additional parameters of the supersymmetric model enter via virtual loops. The impact of these corrections can be significant [22,23]. For example, at tree-level, the MSSM predicts $m_{H_1^0} \leq m_Z$ [8,9]. If true, this would imply that experiments to be performed at LEP-2 operating at its maximum energy and luminosity would rule out the MSSM if H_1^0 were not found. However, this Higgs mass bound can be violated when the radiative corrections are incorporated. For example, in Ref. 22, the following approximate upper bound was obtained for $m_{H_1^0}$ (assuming $m_{A^0} > m_Z$) in the limit of $m_Z \ll m_t \ll M_{\widetilde{t}}$ [where top-squark ($\widetilde{t}_L$–$\widetilde{t}_R$) mixing is neglected]

$$m_{H_1^0}^2 \lesssim m_Z^2 + \frac{3g^2 m_Z^4}{16\pi^2 m_W^2} \times \left\{ \ln\left(\frac{M_{\widetilde{t}}^2}{m_t^2}\right)\left[\frac{2m_t^4 - m_t^2 m_Z^2}{m_Z^4}\right] + \frac{m_t^2}{3m_Z^2} \right\}. \tag{2}$$

More refined computations (which include the effects of top-squark mixing, renormalization group improvement, and the leading two-loop contributions) yield $m_{H_1^0} \lesssim 125$ GeV for $m_t = 175$ GeV and a top-squark mass of $M_{\widetilde{t}} = 1$ TeV [24]. Clearly, the radiative corrections to the Higgs masses have a significant impact on the search for the Higgs bosons of the MSSM at LEP [25].

D. Supersymmetric-particle spectrum: Consider next the supersymmetric-particle sector of the MSSM. The supersymmetric partners of the gauge and Higgs bosons are fermions, whose names are obtained by appending "ino" at the end of the corresponding Standard Model particle name. The *gluino* is the color octet Majorana fermion partner of the gluon with mass $M_{\widetilde{g}} = |M_3|$. The supersymmetric partners of the electroweak gauge and Higgs bosons (the *gauginos* and *Higgsinos*) can mix. As a result, the physical mass eigenstates are model-dependent linear combinations of these states, called *charginos* and *neutralinos*, which are obtained by diagonalizing the corresponding mass matrices. The chargino-mass matrix depends on M_2, μ, $\tan\beta$ and m_W [26].

The corresponding chargino-mass eigenstates are denoted by $\widetilde{\chi}_1^+$ and $\widetilde{\chi}_2^+$, with masses

$$M^2_{\widetilde{\chi}_1^+,\widetilde{\chi}_2^+} = \tfrac{1}{2}\Big\{ |\mu|^2 + |M_2|^2 + 2m_W^2 \mp \Big[\left(|\mu|^2 + |M_2|^2 + 2m_W^2\right)^2 - 4|\mu|^2|M_2|^2 - 4m_W^4 \sin^2 2\beta + 8m_W^2 \sin 2\beta\, \mathrm{Re}(\mu M_2) \Big]^{1/2} \Big\}, \tag{3}$$

where the states are ordered such that $M_{\widetilde{\chi}_1^+} \leq M_{\widetilde{\chi}_2^+}$. If CP-violating effects are ignored (in which case, M_2 and μ are real parameters), then one can choose a convention where $\tan\beta$ and M_2 are positive. (Note that the relative sign of M_2 and μ is meaningful. The sign of μ is convention-dependent; the reader is warned that both sign conventions appear in the literature.) The sign convention for μ implicit in Eq. (3) is used by the LEP collaborations [27] in their plots of exclusion contours in the M_2 *vs.* μ plane derived from the non-observation of $Z \to \widetilde{\chi}_1^+\widetilde{\chi}_1^-$. The neutralino mass matrix depends on M_1, M_2, μ, $\tan\beta$, m_Z, and the weak mixing angle θ_W [26]. The corresponding neutralino eigenstates are usually denoted by $\widetilde{\chi}_i^0$ ($i = 1, \ldots 4$), according to the convention that $M_{\widetilde{\chi}_1^0} \leq M_{\widetilde{\chi}_2^0} \leq M_{\widetilde{\chi}_3^0} \leq M_{\widetilde{\chi}_4^0}$. If a chargino or neutralino eigenstate approximates a particular gaugino or Higgsino state, it may be convenient to use the corresponding nomenclature. For example, if M_1 and M_2 are small compared to m_Z (and μ), then the lightest neutralino $\widetilde{\chi}_1^0$ will be nearly a pure photino, $\widetilde{\gamma}$ (the supersymmetric partner of the photon).

It is common practice in the literature to reduce the supersymmetric parameter freedom by requiring that all three gaugino-mass parameters are equal at some grand unification scale. Then, at the electroweak scale, the gaugino-mass parameters can be expressed in terms of one of them (say, M_2). The other two gaugino-mass parameters are given by

$$M_3 = (g_s^2/g^2)M_2\,, \qquad M_1 = (5g'^2/3g^2)M_2\,. \tag{4}$$

Having made this assumption, the chargino and neutralino masses and mixing angles depend only on three unknown parameters: the gluino mass, μ, and $\tan\beta$. However, the assumption of gaugino-mass unification could prove false and must eventually be tested experimentally.

The supersymmetric partners of the quarks and leptons are spin-zero bosons: the *squarks*, charged *sleptons*, and *sneutrinos*. For a given fermion f, there are two supersymmetric partners $\widetilde{f}_L$ and $\widetilde{f}_R$ which are scalar partners of the corresponding left and right-handed fermion. (There is no $\widetilde{\nu}_R$.) However, in general, $\widetilde{f}_L$ and $\widetilde{f}_R$ are not mass-eigenstates since there is $\widetilde{f}_L$-$\widetilde{f}_R$ mixing which is proportional in strength to the corresponding element of the scalar mass-squared matrix [28]:

$$M^2_{LR} = \begin{cases} m_d(A_d - \mu\tan\beta), & \text{for "down"-type } f \\ m_u(A_u - \mu\cot\beta), & \text{for "up"-type } f, \end{cases} \tag{5}$$

where m_d (m_u) is the mass of the appropriate "down" ("up") type quark or lepton. Here, A_d and A_u are (unknown) soft-supersymmetry-breaking A–parameters and μ and $\tan\beta$ have been defined earlier. The signs of the A parameters are also convention-dependent; see Ref. 19. Due to the appearance of the *fermion* mass in Eq. (5), one expects M_{LR} to be small compared to the diagonal squark and slepton masses, with the possible exception of the top-squark, since m_t is large, and the bottom-squark and tau-slepton if $\tan\beta \gg 1$.

The (diagonal) L- and R-type squark and slepton masses are given by [2]

$$M^2_{u_L} = M^2_{\widetilde{Q}} + m_u^2 + m_Z^2\cos 2\beta(\tfrac{1}{2} - \tfrac{2}{3}\sin^2\theta_W) \tag{6}$$

$$M^2_{u_R} = M^2_{\widetilde{U}} + m_u^2 + \tfrac{2}{3}m_Z^2\cos 2\beta\sin^2\theta_W \tag{7}$$

$$M^2_{d_L} = M^2_{\widetilde{Q}} + m_d^2 - m_Z^2\cos 2\beta(\tfrac{1}{2} - \tfrac{1}{3}\sin^2\theta_W) \tag{8}$$

$$M^2_{d_R} = M^2_{\widetilde{D}} + m_d^2 - \tfrac{1}{3}m_Z^2\cos 2\beta\sin^2\theta_W \tag{9}$$

$$M^2_{\nu} = M^2_{\widetilde{L}} + \tfrac{1}{2}m_Z^2\cos 2\beta \tag{10}$$

$$M^2_{e_L} = M^2_{\widetilde{L}} + m_e^2 - m_Z^2\cos 2\beta(\tfrac{1}{2} - \sin^2\theta_W) \tag{11}$$

$$M^2_{e_R} = M^2_{\widetilde{E}} + m_e^2 - m_Z^2\cos 2\beta\sin^2\theta_W\,. \tag{12}$$

The soft-supersymmetry-breaking parameters: $M_{\widetilde{Q}}$, $M_{\widetilde{U}}$, $M_{\widetilde{D}}$, $M_{\widetilde{L}}$, and $M_{\widetilde{E}}$ are unknown parameters. In the equations above, the notation of first generation fermions has been used and generational indices have been suppressed. Further complications such as intergenerational mixing are possible, although there are some constraints from the nonobservation of flavor-changing neutral currents (FCNC) [29].

E. Reducing the MSSM parameter freedom: One way to guarantee the absence of significant FCNC's mediated by virtual supersymmetric-particle exchange is to posit that the diagonal soft-supersymmetry-breaking scalar squared-masses are universal in flavor space at some energy scale (normally taken to be at or near the Planck scale) [5,30,31]. Renormalization group evolution is used to determine the low-energy values for the scalar mass parameters listed above. This assumption substantially reduces the MSSM parameter freedom. For example, supersymmetric grand unified models with universal scalar masses at the Planck scale typically give [32] $M_{\widetilde{L}} \approx M_{\widetilde{E}} < M_{\widetilde{Q}} \approx M_{\widetilde{U}} \approx M_{\widetilde{D}}$ with the squark masses somewhere between a factor of 1–3 larger than the slepton masses (neglecting generational distinctions). More specifically, the first two generations are thought to be nearly degenerate in mass, while $M_{\widetilde{Q}_3}$ and $M_{\widetilde{U}_3}$ are typically reduced by a factor of 1–3 from the other soft-supersymmetry-breaking masses because of renormalization effects due to the heavy top quark mass.

As a result, four flavors of squarks (with two squark eigenstates per flavor) and $\widetilde{b}_R$ will be nearly mass-degenerate and somewhat heavier than six flavors of nearly mass-degenerate sleptons (with two per flavor for the charged sleptons and one per flavor for the sneutrinos). On the other hand, the $\widetilde{b}_L$ mass and the diagonal $\widetilde{t}_L$ and $\widetilde{t}_R$ masses are reduced compared to the common squark mass of the first two generations. In addition, third generation squark masses and tau-slepton masses are sensitive to the strength of the respective $\widetilde{f}_L$–$\widetilde{f}_R$ mixing as discussed below Eq. (5).

Two additional theoretical frameworks are often introduced to reduce further the MSSM parameter freedom [1,2,33]. The first involves grand unified theories (GUTs) and the desert hypothesis (*i.e* no new physics between the TeV-scale and the GUT-scale). Perhaps one of the most compelling hints for low-energy supersymmetry is the unification of SU(3)×SU(2)×U(1) gauge couplings predicted by supersymmetric GUT models [5,34] (with the supersymmetry breaking scale of order 1 TeV or below). The unification, which takes place at an energy scale of order 10^{16} GeV, is quite robust (and depends weakly on the details of the GUT-scale theory). For example, a recent analysis [35] finds that supersymmetric GUT unification implies that $\alpha_s(m_Z) = 0.129 \pm 0.010$, not including threshold corrections due to GUT-scale particles (which could diminish the value of $\alpha_s(m_Z)$). This result is compatible with the world average of $\alpha_s(m_Z) = 0.118 \pm 0.003$ as quoted by the Particle Data Group. In contrast, gauge coupling unification in the simplest nonsupersymmetric GUT models fails by many standard deviations [36].

Grand unification can impose additional constraints through the unification of Higgs-fermion Yukawa couplings (λ_f). There is some evidence that $\lambda_b = \lambda_\tau$ leads to good low-energy phenomenology [37], and an intriguing possibility that in the MSSM (in the parameter regime where $\tan\beta \simeq m_t/m_b$) $\lambda_b = \lambda_\tau = \lambda_t$ may be phenomenologically viable [38]. However, such unification constraints are GUT-model dependent, and do not address the origin of the first and second generation fermion masses and the CKM mixing matrix. Finally, grand unification imposes constraints on the soft-supersymmetry-breaking parameters. For example, gaugino-mass unification leads to the relations given in Eq. (4). Diagonal squark and slepton soft-supersymmetry-breaking scalar masses may also be unified at the GUT scale (analogous to the unification of Higgs-fermion Yukawa couplings).

In order to further reduce the number of independent soft-supersymmetry-breaking parameters (with or without grand

unification), an additional simplifying assumption is required. In the minimal supergravity theory, the soft-supersymmetry-breaking parameters are often taken to have the following simple form. Referring to the parameter list given above Eq. (1), the Planck-scale values of the soft-supersymmetry-breaking terms depend on the following minimal set of parameters: (i) a universal gaugino mass $m_{1/2}$; (ii) a universal diagonal scalar-mass parameter m_0 [whose consequences were described at the beginning of this section]; (iii) a universal A-parameter, A_0; and (iv) three scalar Higgs mass parameters—two common diagonal-squared masses given by $|\mu_0|^2 + m_0^2$ and an off-diagonal-squared mass given by $B_0\mu_0$ (which defines the Planck-scale supersymmetry-breaking parameter B_0), where μ_0 is the Planck-scale value of the μ-parameter.

As before, renormalization group evolution is used to compute the low-energy values of the supersymmetry-breaking parameters and determines the supersymmetric-particle spectrum. Moreover, in this approach, electroweak symmetry breaking is induced radiatively if one of the Higgs diagonal-squared masses is forced negative by the evolution. This occurs in models with a large Higgs-top quark Yukawa coupling (*i.e.* large m_t). As a result, the two Higgs vacuum expectation values (or equivalently, m_Z and $\tan\beta$) can be expressed as a function of the Planck-scale supergravity parameters. The simplest procedure [32] is to remove μ_0 and B_0 in favor of m_Z and $\tan\beta$ (the sign of μ_0 is not fixed in this process). In this case, the MSSM spectrum and its interactions are determined by m_0, A_0, $m_{1/2}$, $\tan\beta$, and the sign of μ_0 (in addition to the parameters of the Standard Model). However, the minimal approach above is probably too restrictive. Theoretical considerations suggest that the universality of Planck-scale soft-supersymmetry breaking parameters is not generic [39]. In the absence of a fundamental theory of supersymmetry breaking, further progress will require a detailed knowledge of the supersymmetric-particle spectrum in order to determine the nature of the Planck-scale parameters. Of course, any of the theoretical assumptions described in this section could be wrong and must eventually be tested experimentally.

F. The MSSM and precision of electroweak data: The MSSM (with or without constraints imposed from the theory near the Planck scale) provides a framework that can be tested by precision electroweak data. The level of accuracy of the measured Z decay observables at LEP and SLC is sufficient to test the structure of the one-loop radiative corrections of the electroweak model [40], and is thus potentially sensitive to the virtual effects of undiscovered particles. Combining the most recent LEP and SLC electroweak results [41] with the recent top-quark mass measurement at the Tevatron [42], a weak preference is found [41,43] for a light Higgs boson mass of order m_Z, which is consistent with the MSSM Higgs mass upper bound previously noted. Moreover, for Z decay observables, the effects of virtual supersymmetric-particle exchange are suppressed by a factor of $m_Z^2/M_{\rm SUSY}^2$, and therefore decouple in the limit of large supersymmetric-particle masses. It follows that for $M_{\rm SUSY}^2 \gg m_Z$ (in practice, it is sufficient to have all supersymmetric-particle masses above 200 GeV) the MSSM yields an equally good fit to the precision electroweak data as compared to the Standard Model fit.

On the other hand, there are a few tantalizing hints in the data for deviations from Standard Model predictions. Indeed, if $R_b \equiv \Gamma(Z \to b\bar{b})/\Gamma(Z \to \text{hadrons})$ is confirmed to lie above its Standard Model prediction due to the presence of new physics, then a plausible candidate for the new physics would be the MSSM with some light supersymmetric particles (*e.g.* a light chargino and top-squark and/or a light CP-odd scalar, A^0) close in mass to their present LEP bounds [44,45]. Such a scenario would be tested by the search for supersymmetric particles at LEP-2 and the Tevatron.

G. Beyond the MSSM: Nonminimal versions of low-energy supersymmetry can also be constructed. These models add additional matter and/or gauge super-multiplets to the MSSM (at the TeV scale or below). Experimental and theoretical constraints place some restrictions on these approaches, although no comprehensive treatment has yet appeared in the literature.

References

1. H.P. Nilles, Phys. Reports **110**, 1 (1984).
2. P. Nath, R. Arnowitt, and A. H. Chamseddine, *Applied $N = 1$ Supergravity* (World Scientific, Singapore, 1984).
3. M.B. Green, J.S. Schwarz, and E. Witten, *Superstring Theory* (Cambridge University Press, Cambridge, 1987).
4. E. Witten, Nucl. Phys. **B188**, 513 (1981).
5. S. Dimopoulos and H. Georgi, Nucl. Phys. **B193**, 150 (1981).
6. L. Susskind, Phys. Reports **104**, 181 (1984); N. Sakai, Z. Phys. **C11**, 153 (1981); See also, R.K. Kaul, Phys. Lett. **109B**, 19 (1982).
7. H.E. Haber and G.L. Kane, Phys. Reports **117**, 75 (1985).
8. K. Inoue, A. Kakuto, H. Komatsu, and S. Takeshita, Prog. Theor. Phys. **68**, 927 (1982) [E: **70,** 330 (1983)]; **71,** 413 (1984); R. Flores and M. Sher, Ann. Phys. (NY) **148**, 95 (1983).
9. J.F. Gunion and H.E. Haber, Nucl. Phys. **B272**, 1 (1986); [E. **B402**, 567 (1993)].
10. L. Girardello and M. Grisaru, Nucl. Phys. **B194**, 65 (1982).
11. See, *e.g.*, R. Barbieri and G.F. Giudice, Nucl. Phys. **B305**, 63 (1988); G.W. Anderson and D.J. Castano, Phys. Lett. **B347**, 300 (1995); Phys. Rev. **D52**, 1693 (1995).
12. See, *e.g.*, S. Bertolini, F. Borzumati, A. Masiero, and G. Ridolfi, Nucl. Phys. **B353**, 591 (1991).
13. P. Fayet, Phys. Lett. **69B**, 489 (1977); G. Farrar and P. Fayet, Phys. Lett. **76B**, 575 (1978).
14. J. Ellis, J.S. Hagelin, D.V. Nanopoulos, K. Olive, and M. Srednicki, Nucl. Phys. **B238**, 453 (1984).
15. See, *e.g.*, V. Barger, T. Han, and G.F. Giudice, Phys. Rev. **D40**, 2987 (1989); S. Dimopoulos, R. Esmailzadeh, L.J. Hall, and G.D. Starkman, Phys. Rev. **D41**, 2099 (1990); H. Dreiner and G.G. Ross, Nucl. Phys. **B365**, 597 (1991).
16. P. Fayet, Phys. Lett. **84B**, 421 (1979); Phys. Lett. **86B**, 272 (1979).
17. S. Deser and B. Zumino, Phys. Rev. Lett. **38**, 1433 (1977).
18. A.B. Lahanas and D.V. Nanopoulos, Phys. Reports **145**, 1 (1987).

19. H.E. Haber, "Introductory Low-Energy Supersymmetry," in *Recent Directions in Particle Theory*, Proceedings of the 1992 Theoretical Advanced Study Institute in Particle Physics, edited by J. Harvey and J. Polchinski (World Scientific, Singapore, 1993) pp. 589–686.
20. W. Fischler, S. Paban, and S. Thomas, Phys. Lett. **B289**, 373 (1992);
S.M. Barr, Int. J. Mod. Phys. **A8**, 209 (1993).
21. J.F. Gunion, H.E. Haber, G. Kane, and S. Dawson, *The Higgs Hunter's Guide* (Addison-Wesley Publishing Company, Redwood City, CA, 1990).
22. H.E. Haber and R. Hempfling, Phys. Rev. Lett. **66**, 1815 (1991).
23. Y. Okada, M. Yamaguchi, and T. Yanagida, Prog. Theor. Phys. **85**, 1 (1991);
J. Ellis, G. Ridolfi, and F. Zwirner, Phys. Lett. **B257**, 83 (1991).
24. M. Carena, J.R. Espinosa, M. Quiros, and C.E.M. Wagner, Phys. Lett. **B335**, 209 (1995);
H.E. Haber, R. Hempfling, and A.H. Hoang, CERN-TH-95-216 (1995).
25. G. Altarelli *et al.*, "Interim Report on the Physics Motivations for an Energy Upgrade of LEP2", CERN-TH/95-151 and CERN-PPE/95-78 (1995).
26. Explicit forms for the chargino and neutralino mass matrices can be found in Appendix A of Ref. 9; see also Ref. 19.
27. See, *e.g.*, D. Decamp *et al.* [ALEPH Collaboration], Phys. Reports **216**, 253 (1992).
28. J. Ellis and S. Rudaz, Phys. Lett. **128B**, 248 (1983).
29. For recent works and references to the original literature, see: J. Hagelin, S. Kelley, and T. Tanaka, Nucl. Phys. **B415**, 293 (1994);
D. Choudhury *et al.*, Phys. Lett. **B342**, 1980 (1995).
30. See *e.g.*, M. Dine, R. Leigh, and A. Kagan, Phys. Rev. **D48**, 4269 (1993).
31. Other mechanisms for avoiding potentially dangerous FCNC's have been proposed. For example, non-universal scalar masses are not dangerous if squark and slepton mass matrices are diagonal in the same basis as the corresponding fermion mass matrices. See, *e.g.*, Y. Nir and N. Seiberg, Phys. Lett. **B309**, 337 (1993);
S. Dimopoulos, G.F. Giudice, and N. Tetradis, CERN-TH/95-90 (1995).
32. For a recent review, see M. Drees and S.P. Martin, MADPH-95-879 [hep-ph/9504324], to appear in *Electroweak Symmetry Breaking and New Physics at the TeV Scale*, edited by T. Barklow, S. Dawson, H.E. Haber, and J. Siegrist (World Scientific, Singapore).
33. For a recent review, see R. Arnowitt and P. Nath, in *Particles and Fields*, Proceedings of the 7th Summer School Jorge Andre Swieca, Sao Paulo, Brazil, 10–23 January 1993, edited by O.J.P. Eboli and V.O. Rivelles (World Scientific, Singapore, 1994);
W. de Boer, Prog. in Part. Nucl. Phys. **33**, 201 (1994).
34. M.B. Einhorn and D.R.T. Jones, Nucl. Phys. **B196**, 475 (1982);
W.J. Marciano and G. Senjanovic, Phys. Rev. **D25**, 3092 (1982).
35. P. Langacker and N. Polonsky, Phys. Rev. **D52**, 3081 (1995). Recent related work can be found in: R. Barbieri, P. Ciafaloni, and A. Strumia, Nucl. Phys. **B442**, 461 (1995);
J. Bagger, K. Matchev, and D. Pierce, Phys. Lett. **B348**, 443 (1995);
P.H. Chankowski, Z. Pluciennik and S. Pokorski, Nucl. Phys. **B349**, 23 (1995).
36. For a recent review comparing unification in supersymmetric and nonsupersymmetric GUTS, see S. Dimopoulos, CERN-TH-7531-94 [hep-ph/9412297].
37. H. Arason *et al.*, Phys. Rev. Lett. **67**, 2933 (1991);
Phys. Rev. **D46**, 3945 (1992);
V. Barger, M.S. Berger, and P. Ohmann, Phys. Rev. **D47**, 1093 (1993);
M. Carena, S. Pokorski, and C.E.M. Wagner, Nucl. Phys. **B406**, 59 (1993);
P. Langacker and N. Polonsky, Phys. Rev. **D49**, 1454 (1994).
38. M. Olechowski and S. Pokorski, Phys. Lett. **B214**, 393 (1988);
B. Ananthanarayan, G. Lazarides and Q. Shafi, Phys. Rev. **D44**, 1613 (1991);
S. Dimopoulos, L.J. Hall, and S. Raby, Phys. Rev. Lett. **68**, 1984 (1992);
L.J. Hall, R. Rattazzi, and U. Sarid, Phys. Rev. **D50**, 7048 (1994);
M. Carena, M. Olechowski, S. Pokorski, and C.E.M. Wagner, Nucl. Phys. **B426**, 269 (1994).
39. L.E. Ibáñez and D. Lüst, Nucl. Phys. **B382**, 305 (1992);
B. de Carlos, J.A. Casas and C. Munoz, Phys. Lett. **B299**, 234 (1993);
V. Kaplunovsky and J. Louis, Phys. Lett. **B306**, 269 (1993);
A. Brignole, L.E. Ibáñez, and C. Munoz, Nucl. Phys. **B422**, 125 (1994) [E: **B436**, 747 (1995)].
40. D. Bardin, W. Hollik, and G. Passarino, editors, "Report of the Working Group on Precision Calculations for the Z Resonance", CERN Yellow Report 95-03 (1995).
41. P. Antilogus *et al.* [LEP Electroweak Working Group], LEPEWWG/95-02 (1995), contributions of the LEP Experiments to the 1995 International Europhysics Conference on High Energy Physics, 27 July–2 August, 1995, Brussels, Belgium, and the 17th International Symposium on Lepton-Photon Interactions, 10–15 August, 1995, Beijing, China.
42. F. Abe *et al.* [CDF Collaboration], Phys. Rev. Lett. **74**, 2626 (1995);
S. Abachi *et al.* [D0 Collaboration], Phys. Rev. Lett. **74**, 2632 (1995).
43. P.H. Chankowski and S. Pokorski, Phys. Lett. **B356**, 307 (1995);
J.Ellis, G.L. Fogli, and E. Lisi, CERN-TH/95-202 [hep-ph/9507424].
44. M. Boulware and D. Finnel, Phys. Rev. **D44**, 2054 (1991);
A. Djouadi *et al.*, Nucl. Phys. **B349**, 48 (1991);
G. Altarelli, R. Barbieri, and F. Caravaglios, Nucl. Phys. **B405**, 3 (1993);
J.D. Wells, C. Kolda, and G.L. Kane, Phys. Lett. **B338**, 219 (1994).
45. Recent analyses along these lines can be found in: D. Garcia, R.A. Jiménez and J. Solà, Phys. Lett. **B347**, 321 (1995) [E: **B351**, 602 (1995)];
D. Garcia and H. Solà, Phys. Lett. **B354**, 335 (1995);
G.L. Kane, R.G. Stuart, and J.D. Wells, Phys. Lett. **B354**, 350 (1995);
A. Dabelstein, W. Hollik and W. Mösle, KA-THEP-5-1995 [hep-ph/9506251];
P.H. Chankowski and S. Pokorski, IFT-95/5 [hep-ph/9505304];
X. Wang, J.L. Lopez, and D.V. Nanopoulos, CTP-TAMU-25/95 [hep-ph/9506217].

NON-$q\bar{q}$ MESONS

The existence of gluon self coupling in QCD suggests that gluonia (or glueballs) and hybrids ($q\bar{q}g$) might exist. Another possible kind of non-$q\bar{q}$ mesons is multiquark states. For detailed reviews, see HEUSCH 86, CLOSE 87, TOKI 88, and BURNETT 90. Among the signatures naively expected for glueballs are (i) no place in $q\bar{q}$ nonets, (ii) flavor-singlet couplings, (iii) enhanced production in gluon-rich channels such as $J/\psi(1S)$ decay, and (iv) reduced $\gamma\gamma$ coupling. However, mixing effects with $q\bar{q}$ states, and other dynamical effects such as form factors, may obscure these simple signatures. If mixing is large, only the finding of more states than are predicted by the $q\bar{q}$ quark model remains as a clear signal for non-exotic non-$q\bar{q}$ states.

Lattice gauge theory calculations in the quenched approximation (without quark loops) predict the lightest glueball to be a scalar with a mass of typically 1550±95 MeV (BALI 93). The same calculations find a tensor glueball mass of 2270±100 MeV, and glueballs with other spin-parities are predicted to be still heavier. A more recent lattice calculation (SEXTON 95) predicts a slightly higher mass, 1740 ± 71 MeV. Including dynamical quarks will, however, change the predicted masses.

Hybrid mesons are $q\bar{q}$ states combined with a gluonic excitation (BARNES 82, CHANOWITZ 83, ISGUR 85, CLOSE 95). Hybrids span flavor nonets, may have exotic (non-$q\bar{q}$) quantum numbers (a $J^{PC} = 1^{-+}$ state is expected in all models), and are predicted to have characteristic decay modes (LEYAOUANC 85, CLOSE 95). The masses of the lightest hybrids are typically predicted to be in the range 1500 to 2000 MeV. Charm hybrids ($c\bar{c}g$) are attractive experimentally since they may appear as supernumerary states in the predictable charmonium spectrum. The $\psi(4040)$ and $\psi(4160)$ are possibly mixtures of $c\bar{c}$ and $c\bar{c}g$ states (CLOSE 96).

The third class of non-$q\bar{q}$ states, the multiquark states, can be either baglike or clusters of mesons (VOLOSHIN 76, JAFFE 77, GUTBROD 79). A subclass of the latter are the deuteronlike meson-meson bound states, or deusons, where the long-range pion exchange is the major source of binding (TORNQVIST 91 and 94, ERICSON 93, MANOHAR 93). Many of the best non-$q\bar{q}$ candidates discussed below lie close to important thresholds, which suggests that they might be bound states of a meson pair. Examples include the $f_0(980)$ and $a_0(980)$ (close to the $K\overline{K}$ threshold), the $f_1(1420)$ (above the $K\overline{K}^*$ threshold, thus not a bound state but perhaps a threshold enhancement), the $f_0(1500)$ and $f_2(1520)$ ($\omega\omega$ and $\rho\rho$), the $f_J(1710)$ ($K^*\overline{K}^*$), and the $\psi(4040)$ ($D^*\overline{D}^*$). Many suggestions for such mesonium candidates, involving both light and heavy quarks and binding mechanisms, have appeared (WEINSTEIN 90, DOVER 91, BARNES 92, DOOLEY 92).

The candidates we discuss below are chosen because they are difficult to interpret as conventional $q\bar{q}$ states. We do not see it as our task to discuss theoretical interpretations of the candidates, but merely to catalogue the observations of possible relevance.

Scalar mesons: There are four known isoscalars with $J^{PC} = 0^{++}$: the $f_0(400\text{–}1200)$, a very broad structure around 800 MeV, the $f_0(980)$, the $f_0(1370)$, and the $f_0(1500)$; the spin of another established isoscalar, the $f_J(1710)$, may be 0 or 2. In the quark model, one expects two 1^3P_0 states and one 2^3P_0 ($u\bar{u} + d\bar{d}$)-like state below 1.8 GeV. Thus, there are too many scalars to find a place in the quark model.

However, for scalar resonances, naive quark model expectations, in particular ideal mixing, could be strongly broken by the opening of inelastic thresholds. Thus, the physical scalar $q\bar{q}$ spectrum may be very much distorted from naive expectations. For a detailed discussion of this sector, see our Note under the $f_0(1370)$.

In this edition, we have merged the $f_0(1590)$ observed in π^-p interactions at high energies with the $f_0(1525)$ observed in $\overline{p}p$ annihilations, under the new name $f_0(1500)$. The $\pi\pi$ and $\eta\eta$ S-waves have a T-matrix pole at $m - i\Gamma/2 \sim 1500 - i60$ MeV, which corresponds to the physical mass and width (AMSLER 95B, AMSLER 95C), while a simple Breit-Wigner description gives a slightly higher mass and width (AMSLER 92, ALDE 88). For consistency, we average the mass and width determined by the T-matrix poles. A coupled-channel analysis taking unitarity constraints into account has been performed in $\overline{p}p$ (AMSLER 95D) but not in π^-p. Thus, we do not view the apparent discrepancies in the decay branching ratios to $\pi^0\pi^0$, $\eta\eta$, and $\eta\eta'$ between the $\overline{p}p$ and π^-p experiments to be serious.

In the model of AMSLER 95E and AMSLER 96, the (nearly ideally mixed) ground state scalar $q\bar{q}$ nonet consists of the $a_0(1450)$, the $K_0^*(1430)$, the $f_0(1370)$, and the still missing isoscalar $s\bar{s}$ state, which cannot be the $f_0(1500)$ due to its comparatively narrow width and low $K\overline{K}$ decay branching ratio. The $f_0(1500)$ is interpreted as a scalar glueball mixed with the two nearby $q\bar{q}$ isoscalars.

The $f_J(1710)$ (whose spin is uncertain) has been seen mainly in the gluon-rich $J/\psi(1S)$ radiative decay, where it is copiously produced. Before 1991, the spin of the $f_J(1710)$ was believed to be 2, and the subsequent spin-0 determination in $J/\psi(1S)$ radiative decay (CHEN 91) has not been confirmed. In central production, the WA76 experiment (ARMSTRONG 89D) on 300 GeV/c pp interactions sees a structure at the same mass, but favors spin 2. The $f_J(1710)$ has not been seen in hadronic production ($K^-p \to K\overline{K}\Lambda$) (ASTON 88D), nor in $\gamma\gamma$ fusion. The ratio of the branching fractions in $J/\psi(1S) \to \omega f_J$ and $J/\psi(1S) \to \phi f_J$ suggests that nonstrange and strange components are both important in this state. Its mass and width are consistent with the prediction for the ground-state glueball, according to the most recent lattice gauge calculations (SEXTON 95), if one assumes that the spin is indeed zero.

Pseudoscalar mesons: The established isoscalars with $J^{PC} = 0^{-+}$ are the η, the $\eta'(958)$, the $\eta(1295)$, and the $\eta(1440)$ [which may be two pseudoscalar resonances, an $\eta(1410)$ and an $\eta(1490)$; see the Note under the $\eta(1440)$]. In the $q\bar{q}$ model, one expects two 1^1S_0 and two 2^1S_0 pseudoscalars between 500 and 1800 MeV.

Identifying the $\eta(1280)$ with the 2^1S_0 ($u\bar{u} + d\bar{d}$) state is natural, but it is more problematic to identify one of the two peaks in the $\eta(1440)$ region with the 2^1S_0 $s\bar{s}$ state. The $\eta(1440)$ is observed in $s\bar{s}$-depleted reactions like $\pi^-p \to \eta\pi\pi n$ (ANDO 86), $p\overline{p}$ annihilation (BAILLON 67, AMSLER 95F, BERTIN 95), and $\pi^-p \to a_0(980)\pi p$ (CHUNG 85, BIRMAN 88), and is not seen in the $s\bar{s}$-enriched channels like $K^-p \to K^*(892)\overline{K}\Lambda$ (ASTON 87). The fact that ANDO 86 sees the $\eta(1440)$ and $\eta(1280)$ with similar intensities argues that these states are of a similar nature, *e.g.*, radial excitations of the η and $\eta'(958)$. However, as there are suggestions that the $\eta(1440)$ is in fact two η's, the situation remains confused.

The $\pi(1770)$ (BERDNIKOV 94, AMELIN 95B) has a surprisingly narrow width (if interpreted as the second radial excitation of the π), a large coupling to $K\overline{K}$, and decays to a pair of mesons, one with $\ell(q\overline{q}) = 0$, the other with $\ell(q\overline{q}) = 1$. This is the signature expected for a hybrid meson (CLOSE 95).

Axial-vector mesons: The $q\overline{q}$ model predicts a nonet that includes two isoscalar 1^3P_1 states with masses below about 1.6 GeV. Three such 1^{++} states are known, the $f_1(1285)$, the $f_1(1420)$, and the $f_1(1530)$, which suggests that one of these is a non-$q\overline{q}$ meson. The $f_1(1420)$ is the most likely candidate: see CALDWELL 90 and the Note under the $f_1(1420)$. The proximity of the $K\overline{K}^*$ threshold suggests this may be a dominantly $K\overline{K}^*$ mesonium resonance or a threshold enhancement (LONGACRE 90, TORNQVIST 91).

Tensor mesons: The two 1^3P_2 $q\overline{q}$ states are very likely the well-known $f_2(1270)$ and $f_2'(1525)$. There are several other states, which have been suggested as $J^{PC} = 2^{++}$ non-$q\overline{q}$ candidates: the $f_2(1430)$, $f_2(1520)$, $f_J(1710)$, $f_2(1810)$, $f_2(2010)$, $f_2(2150)$, $f_2(2300)$, and $f_2(2340)$.

The $f_2(1520)$ is observed by the ASTERIX Collaboration (MAY 89) in $p\overline{p}$ P-wave annihilation in the $\pi^+\pi^-\pi^0$ channel and by the Crystal Barrel Collaboration (ANISOVICH 94, AMSLER 95B) in $3\pi^0$, close to the $\rho\rho$ and $\omega\omega$ thresholds. It has no place in a $q\overline{q}$ scheme, since all nearby $q\overline{q}$ states are already accounted for. Similarly, the $f_J(1710)$ could be composed of $K^*\overline{K}^*$ and $\omega\phi$ (DOOLEY 92), since it lies close to these thresholds.

Of the heavier states, the $f_2(1810)$ is likely to be the 2^3P_2, and among those above 2 GeV one expects the 2^3P_2 $s\bar{s}$, 1^3F_2 $s\bar{s}$, and 3^2P_2 $s\bar{s}$, but a gluonium interpretation of one of the four states is not excluded. These three f_2 resonances have been observed in the OZI-rule forbidden process $\pi p \to \phi\phi n$ (ETKIN 88), which has been claimed as favoring the gluonium interpretation.

A similar $\phi\phi$ mass spectrum is seen by ARMSTRONG 89B in the Ω spectrometer. The DM2 and MARK-III collaborations see threshold $\phi\phi$ production, but favor $J^P = 0^-$, not 2^+.

In $\gamma\gamma \to 4\pi$ near the $\rho\rho$ threshold, TASSO (BRANDELIK 80B, ALTHOFF 82), MARK2 (BURKE 81), CELLO (BEHREND 84E), PLUTO (BERGER 88B), SLAC TPC (AIHARA 88), and ARGUS (ALBRECHT 91F) observe a resonance-like structure. This is dominated by $\rho^0\rho^0$, and the cross section peaks a little above the $f_2(1520)$. This process has not been explained by models in which only conventional resonances dominate. The fact that the $\gamma\gamma \to \rho^+\rho^-$ is small (ALBRECHT 91F quotes 1/4 for the $\rho^+\rho^-/\rho^0\rho^0$ ratio) requires both isospin 0 and 2 for the $\rho\rho$ system. A resonance interpretation in terms of $q^2\overline{q}^2$ states thus requires the presence of a flavor exotic $I = 2$ resonance (ACHASOV 82, 87, 90). The 2^{++} partial wave is found to dominate the $\rho\rho$ structure (BERGER 88B, ALBRECHT 91F), with some 0^{++} at the low- energy end, while $J^P = 0^-$ and 2^- contribute very little.

In $\gamma\gamma \to \omega\rho$ and $\phi\rho$, there are also broad enhancements that peak near 1.7 GeV. The dominant partial wave is 2^{++} in $\omega\rho$, while 2^{-+} is favored in $\phi\rho$ (ALBRECHT 94Z).

Other exotic or non-$q\overline{q}$ candidates: An isovector $\phi\pi^0$ resonance at 1480 MeV has been reported by BITYUKOV 87 in $\pi^-p \to \phi\pi^0 n$ (listed under the $\rho(1450)$). Preliminary indications favor the nonexotic $J^{PC} = 1^{--}$, but the large OZI-rule violating branching ratio $\phi\pi$:$\omega\pi$ seems peculiar for a $(u\overline{u}$-$d\overline{d})$ $I=1$ $q\overline{q}$ object. However, ACHASOV 88 shows that the threshold effect from the two-step process $\rho(1600) \to K\overline{K}^* \to \pi\phi$ can violate the rule, especially near threshold. No sign of this candidate is seen in $\pi\omega$ (FUKUI 91). In addition, the small coupling to the photon makes an identification with the $\rho(1450)$ difficult (CLEGG 88). More recently DONNACHIE 93, analyzing e^+e^--annihilation and diffractive-photoproduction data, suggests there may be 4-quark states near 1100 and 1300 MeV.

Another exotic candidate is the $\hat{\rho}(1405)$ (ALDE 88B, IDDIR 88), seen in the GAMS experiment under the $a_2(1320)$ in $\pi^-p \to \eta\pi^0 n$ with the exotic quantum numbers $J^{PC} = 1^{-+}$. The analysis of ALDE 88B has, however, been questioned by PROKOSHKIN 95B, 95C. Although the forward-backward asymmetry demands an $\eta\pi$ P-wave, it may be due to a nonresonant amplitude. The Crystal Barrel Collaboration has reported results on the corresponding P-wave in $\eta\pi$ seen in $p\overline{p} \to \eta\pi\pi$; they see a much broader effect, which can be explained as nonresonant or as a resonance with $\Gamma \approx 600$ MeV (AMSLER 94D). AOYAGI 93 also notes the $\eta\pi$ P-wave, but its interpretation is unclear.

Another possible 1^{-+} candidate is the isosinglet $X(1910)$ (ALDE 89), which seems to decay to $\eta\eta'$ but not to $\pi^0\pi^0$ or $\eta\eta$ (ALDE 89). An enhancement with quantum numbers 1^{-+}, decaying to $f_1(1285)$, has also been reported around 1900 MeV (LEE 94).

A narrow resonance, listed under the $K_J(3100)$, has been reported at about 3100 MeV (BOURQUIN 86, ALEEV 93) in several $\Lambda\overline{p}$ + pions and $\overline{\Lambda}p$ + pions states. The observation of the doubly-charged states $\Lambda\overline{p}\pi^-$ and $\overline{\Lambda}p\pi^+$ implies, assuming the decay is strong, $I = 3/2$, clearly not a $q\overline{q}$ state. In addition, a narrow peak is observed at about 3250 MeV, listed under the $X(3250)$, in the hidden strangeness combinations containing a baryon-antibaryon pair (ALEEV 93). However, all these observations need confirmation.

For all references, see the full *Review of Particle Physics*, Phys. Rev. **D54**, 1 (1996).

15. BIG-BANG COSMOLOGY

Revised November 1993 by K.A. Olive.

At early times, and today on a sufficently large scale, our Universe is very nearly homogeneous and isotropic. The most general space-time metric for a homogeneous, isotropic space is the Friedmann-Robertson-Walker metric (with $c = 1$) [1,2,3]:

$$ds^2 = dt^2 - R^2(t)\left[\frac{dr^2}{1-\kappa r^2} + r^2\,(d\theta^2 + \sin^2\theta\, d\phi^2)\right] . \qquad (15.1)$$

$R(t)$ is a scale factor for distances in comoving coordinates. With appropriate rescaling of the corrdinates, κ can be chosen to be $+1$, -1, or 0, corresponding to closed, open, or spatially flat geometries. Einstein's equations lead to the Friedmann equation

$$H^2 \equiv \left(\frac{\dot R}{R}\right)^2 = \frac{8\pi\, G_N\, \rho}{3} - \frac{\kappa}{R^2} + \frac{\Lambda}{3} , \qquad (15.2)$$

as well as to

$$\frac{\ddot R}{R} = \frac{\Lambda}{3} - \frac{4\pi G_N}{3}\ (\rho + 3p) , \qquad (15.3)$$

where $H(t)$ is the Hubble parameter, ρ is the total mass-energy density, p is the isotropic pressure, and Λ is the cosmological constant. (For limits on Λ, see the Table of Astrophysical Constants; we will assume here $\Lambda = 0$.) The Friedmann equation serves to define the density parameter Ω_0 (subscript 0 indicates present-day values):

$$\kappa/R_0^2 = H_0^2(\Omega_0 - 1) , \qquad \Omega_0 = \rho_0/\rho_c ; \qquad (15.4)$$

and the critical density is defined as

$$\rho_c \equiv \frac{3H^2}{8\pi\, G_N} = 1.88 \times 10^{-29}\, h^2 \text{ g cm}^{-3} , \qquad (15.5)$$

with

$$H_0 = 100\, h_0 \text{ km s}^{-1} \text{ Mpc}^{-1} = h_0/(9.78 \text{ Gyr}) . \qquad (15.6)$$

Observational bounds give $0.4 < h_0 < 1$. The three curvature signatures $\kappa = +1, -1$, and 0 correspond to $\Omega_0 > 1$, < 1, and $= 1$. Knowledge of Ω_0 is even poorer than that of h_0. Luminous matter (stars and associated material) contribute $\Omega_{\rm lum} \leq 0.01$. There is no lack of evidence for copious amounts of dark matter: rotation curves of spiral galaxies, virial estimates of cluster masses, gravitational lensing by clusters and individual galaxies, and so on. The minimum amount of dark matter required to explain the flat rotation curves of spiral galaxies only amounts to $\Omega_0 \sim 0.1$, while estimates for Ω_0 based upon cluster virial masses suggests $\Omega_0 \sim 0.2 - 0.4$. The highest estimates for the mass density come from studies of the peculiar motions of galaxies (including our own); estimates for Ω_0 obtained by relating peculiar velocity measurements to the distribution galaxies within a few hundred Mpc approach unity. A conservative range for the mass density is: $0.1 \leq \Omega_0 \leq 2$. The excess of Ω_0 over $\Omega_{\rm lum}$ leads to the inference that most of the matter in the Universe is nonluminous dark matter.

In an expanding universe, the wavelength of light emitted from a distant source is shifted towards the red. The redshift z is defined such that $1 + z$ is the ratio of the detected wavelength (λ) to emitted (laboratory) wavelength ($\lambda_{\rm e}$) of some electromagnetic spectral feature. It follows from the metric given in Eq. (15.1) that

$$1 + z = \lambda/\lambda_{\rm e} = R_0/R_{\rm e} \qquad (15.7)$$

where $R_{\rm e}$ is the value of the scale factor at the time the light was emitted. For light emitted in the not too distant past, one can expand $R_{\rm e}$ and write $R_{\rm e} \simeq R_0 + (t_{\rm e} - t_0)\dot R_0$. For small (compared to H_0^{-1}) $\Delta t = (t_{\rm e} - t_0)$, Eq. (15.7) takes the form of Hubble's law

$$z \approx \Delta t \frac{\dot R_0}{R_0} \approx \ell H_0 , \qquad (15.8)$$

where ℓ is the distance to the source.

Energy conservation implies that

$$\dot\rho = -3(\dot R/R)(\rho + p) , \qquad (15.9)$$

so that for a matter-dominated ($p = 0$) universe $\rho \propto R^{-3}$, while for a radiation-dominated ($p = \rho/3$) universe $\rho \propto R^{-4}$. Thus the less singular curvature term κ/R^2 in the Friedmann equation can be neglected at early times when R is small. If the Universe expands adiabatically, the entropy per comoving volume ($\equiv R^3 s$) is constant, where the entropy density is $s = (\rho + p)/T$ and T is temperature. The energy density of radiation can be expressed (with $\hbar = c = 1$) as

$$\rho_r = \frac{\pi^2}{30} N(T)(kT)^4 , \qquad (15.10)$$

where $N(T)$ counts the effectively massless degrees of freedom of bosons and fermions:

$$N(T) = \sum_B g_B + \frac{7}{8}\sum_F g_F . \qquad (15.11)$$

For example, for $m_\mu > kT > m_e$, $N(T) = g_\gamma + 7/8\,(g_e + 3g_\nu) = 2 + 7/8\,[4 + 3(2)] = 43/4$. For $m_\pi > kT > m_\mu$, $N(T) = 57/4$. At temperatures less than about 1 MeV, neutrinos have decoupled from the thermal background, *i.e.*, the weak interaction rates are no longer fast enough compared with the expansion rate to keep neutrinos in equilibrium with the remaining thermal bath consisting of $\gamma, e^\pm$. Furthermore, at temperatures $kT < m_e$, by entropy conservation, the ratio of the neutrino temperature to the photon temperature is given by $(T_\nu/T_\gamma)^3 = g_\gamma/(g_\gamma + \frac{7}{8}g_e) = 4/11$.

In the early Universe when $\rho \approx \rho_r$, then $\dot R \propto 1/R$, so that $R \propto t^{1/2}$ and $Ht \to 1/2$ as $t \to 0$. The time-temperature relationship at very early times can then be found from the above equations:

$$t = \frac{2.42}{\sqrt{N(T)}}\left(\frac{1\text{ MeV}}{kT}\right)^2 \text{ sec} . \qquad (15.12)$$

At later times, since the energy density in radiation falls off as R^{-4} and the energy density in non-relativistic matter falls off as R^{-3}, the Universe eventually became matter dominated. The epoch of matter-radiation density equality is determined by equating the matter density at $t_{\rm eq}$, $\rho_m = \Omega_0\rho_c(R_0/R_{\rm eq})^3$ to the radiation density, $\rho_r = (\pi^2/30)[2 + (21/4)(4/11)^{4/3}](kT_0)^4(R_0/R_{\rm eq})^4$ where T_0 is the present temperature of the microwave background (see below). Solving for $(R_0/R_{\rm eq}) = 1 + z_{\rm eq}$ gives

$$\begin{aligned} z_{\rm eq} + 1 &= \Omega_0 h_0^2/4.2 \times 10^{-5} = 2.4 \times 10^4\, \Omega_0 h_0^2 ; \\ kT_{\rm eq} &= 5.6\, \Omega_0 h_0^2\, \text{eV} ; \\ t_{\rm eq} &\approx 0.39(\Omega_0 H_0^2)^{-1/2}(1 + z_{\rm eq})^{-3/2} \\ &= 3.2 \times 10^{10}(\Omega_0 h_0^2)^{-2}\, \text{sec} . \end{aligned} \qquad (15.13)$$

Prior to this epoch the density was dominated by radiation (relativistic particles; see Eq. (15.10)), and at later epochs matter density dominated. Atoms formed at $z \approx 1300$, and by $z_{\rm dec} \approx 1100$ the free electron density was low enough that space became essentially transparent to photons and matter and radiation were decoupled. These are the photons observed in the microwave background today.

The age of the Universe today, t_0, is related to both the Hubble parameter and the value of Ω_0 (still assuming that $\Lambda = 0$). In the Standard Model, $t_0 \gg t_{\rm eq}$ and we can write

$$t_0 = H_0^{-1}\int_0^1 \left(1 - \Omega_0 + \Omega_0 x^{-1}\right)^{-1/2} dx . \qquad (15.14)$$

Constraints on t_0 yield constraints on the combination $\Omega_0 h_0^2$. For example, $t_0 \geq 13 \times 10^9$ yr implies that $\Omega_0 h_0^2 \leq 0.25$ for $h_0 \geq 0.5$,

or $\Omega_0 h_0^2 \leq 0.45$ for $h_0 \geq 0.4$, while $t_0 \geq 10 \times 10^9$ yr implies that $\Omega_0 h_0^2 \leq 0.8$ for $h_0 \geq 0.5$, or $\Omega_0 h_0^2 \leq 1.1$ for $h_0 \geq 0.4$.

The present temperature of the microwave background is $T_0 = 2.726 \pm 0.005$ K as measured by COBE [4], and the number density of photons $n_\gamma = (2\zeta(3)/\pi^2)(kT_0)^3 \approx 411$ cm^{-3}. The energy density in photons (for which $g_\gamma = 2$) is $\rho_\gamma = (\pi^2/15)(kT_0)^4$. At the present epoch, $\rho_\gamma = 4.65 \times 10^{-34}$ g cm^{-3} $= 0.26$ eV cm^{-3}. For nonrelativistic matter (such as baryons) today, the energy density is $\rho_B = m_B n_B$ with $n_B \propto R^{-3}$, so that for most of the history of the Universe n_B/s is constant. Today, the entropy density is related to the photon density by $s = (4/3)(\pi^2/30)[2 + (21/4)(4/11)](kT_0)^3 = 7.0\, n_\gamma$. Big Bang nucleosynthesis calculations limit $\eta = n_B/n_\gamma$ to $2.8 \times 10^{-10} \leq \eta \leq 4.0 \times 10^{-10}$. The parameter η is also related to the portion of Ω in baryons

$$\Omega_B = 3.66 \times 10^7 \eta\, h_0^{-2}\, (T_0/2.726\ \mathrm{K})^3\ , \tag{15.15}$$

so that $0.010 < \Omega_B\, h_0^2 < 0.015$, and hence the Universe cannot be closed by baryons.

References:

1. S. Weinberg, *Gravitation and Cosmology*, John Wiley and Sons (1972).
2. G. Börner, *The Early Universe: Facts and Fiction*, Springer-Verlag (1988).
3. E.W. Kolb and M.S. Turner, *The Early Universe*, Addison-Wesley (1990).
4. J.C. Mather *et al.*, Astrophys. J. **420**, 439 (1994). Error quoted here is 1σ.

16. BIG-BANG NUCLEOSYNTHESIS

Written July 1995 by K.A. Olive and D.N. Schramm.

Among the successes of the standard big-bang model is the agreement between the predictions of big-bang nucleosynthesis (BBN) for the abundances of the light elements, D, ^{3}He, ^{4}He, and ^{7}Li, and the primordial abundances inferred from observational data (see [1–3] for a more complete discussion). These abundances span some nine orders of magnitude: ^{4}He has an abundance by number relative to hydrogen of about 0.08 (accounting for about 25% of the baryonic mass), while ^{7}Li, the least abundant of the elements with a big-bang origin, has a abundance by number relative to hydrogen of about $\sim 10^{-10}$.

16.1. Big-bang nucleosynthesis theory

The BBN theory matches the observationally determined abundances with a single well-defined parameter, the baryon-to-photon ratio, η. All the light-element abundances can be explained with η in the relatively narrow range $(2.8\text{–}4.5) \times 10^{-10}$, or $\eta_{10} \equiv \eta \times 10^{10} = 2.8\text{–}4.5$. (When possible systematic errors are allowed to take extreme values, the range becomes $\eta_{10} = 1.5\text{–}6.3$ [4]. We shall always quote this extreme range parenthetically following the best range.) Equivalently, this range can be expressed as the allowed range for the baryon mass density, $\rho_B = 1.9\text{–}3.1\ (1.0\text{–}4.3) \times 10^{-31}$ g cm^{-3}, and can be converted to the fraction of the critical density, Ω.

The synthesis of the light elements was affected by conditions in the early Universe at temperatures $T \lesssim 1$ MeV, corresponding to an age as early as 1 s. At somewhat higher temperatures, weak-interaction rates were in equilibrium, thus fixing the ratio of the neutron and proton number densities. At $T \gg 1$ MeV, $n/p \approx 1$, since the ratio was given approximately by the Boltzmann factor, $n/p \approx e^{-Q/T}$, where Q is the neutron-proton mass difference. As the temperature fell, the Universe approached the point ("freeze-out") where the weak-interaction rates were no longer fast enough to maintain equilibrium. The final abundance of ^{4}He is very sensitive to the n/p ratio at freeze-out.

The nucleosynthesis chain begins with the formation of deuterium in the process $pn \to \mathrm{D}\gamma$. However, photo-dissociation by the high number density of photons ($n_\gamma/n_B = \eta^{-1} \sim 10^{10}$) delays production of deuterium (and other complex nuclei) well past the point where T reaches the binding energy of deuterium, $E_B = 2.2$ MeV. (The average photon energy in a blackbody is $\overline{E}_\gamma \approx 2.7\ T$.) When the quantity $\eta^{-1}\exp(-E_B/T)$ reaches about 1 (at $T \approx 0.1$ MeV), the photo-dissociation rate finally falls below the nuclear production rate.

The 25% fraction of mass in ^{4}He due to BBN is easily estimated by counting the number of neutrons present when nucleosynthesis begins. When the weak-interaction rates freeze-out at about $T \approx 0.8$ MeV, the n-to-p ratio is about 1/6. When free-neutron decays prior to deuterium formation are taken into account, the ratio drops to $n/p \lesssim 1/7$. Then simple counting yields a primordial ^{4}He mass fraction

$$Y_p = \frac{2(n/p)}{1 + n/p} \lesssim 0.25\ . \tag{16.1}$$

In the Standard Model, the ^{4}He mass fraction depends primarily on the baryon-to-photon ratio η, as it is this quantity that determines when nucleosynthesis via deuterium production may begin. But because the n/p ratio depends only weakly on η, the ^{4}He mass fraction is relatively flat as a function of η. The effect of the uncertainty in the neutron half-life, $\tau_n = 887 \pm 2$ s, is small. Lesser amounts of the other light elements are produced: D and ^{3}He at the level of a few times 10^{-5} by number relative to H, and ^{7}Li/H at the level of about 10^{-10}, when η is in the range $1 - 10 \times 10^{-10}$.

When we go beyond the Standard Model, the ^{4}He abundance is very sensitive to changes in the expansion rate, which can be related to the effective number of neutrino flavors. This will be discussed below.

The calculated abundances of the light elements are shown in Fig. 16.1 as a function of η_{10}. The curves for the ^{4}He mass fraction, Y_p, bracket the range based on the uncertainty of the neutron mean-life, $\tau_n = 887 \pm 2$ s. The spread in the ^{7}Li curves is due to the 1σ uncertainties in nuclear cross sections leading to ^{7}Li and ^{7}Be which subsequently decays to ^{7}Li [4,5,6]. The uncertainties in the D and ^{3}He predictions are small and have been neglected here. The boxes show to the observed abundances, discussed below. Since the observational boxes line up on top of each other, there is an overall agreement between theory and observations for η_{10} in the range 2.8–4.5 (1.5–6.3).

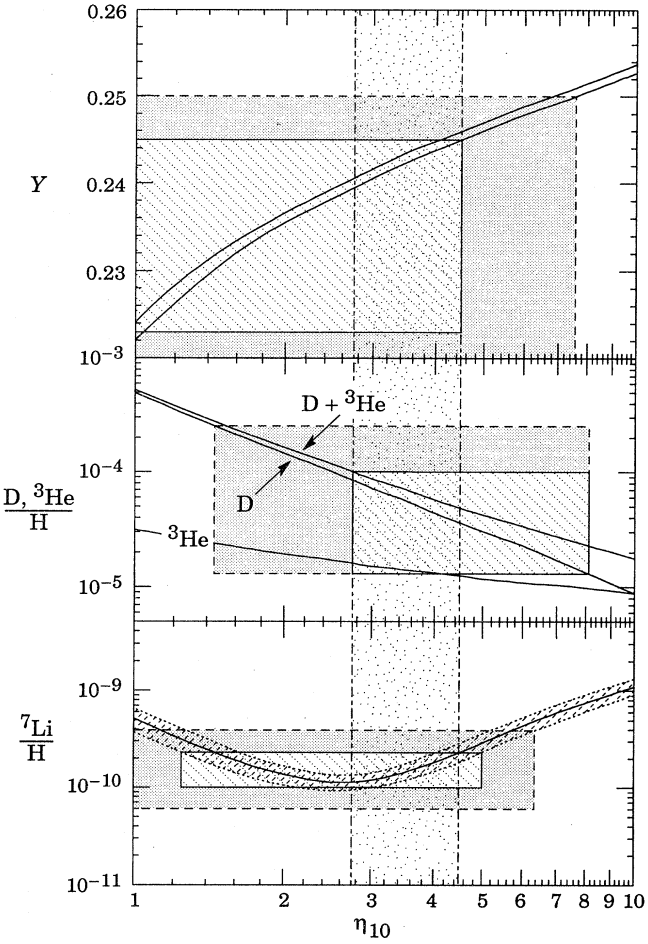

Figure 16.1: The abundances of D, ^{3}He, ^{4}He and ^{7}Li as predicted by the standard model of big-bang nucleosynthesis. Also shown by a series of boxes is the comparison between these predictions and the observational determination of the light element abundances. See text for details.

16.2. Observations

Because stars produce helium as well as heavier elements, one must search for primordial helium in regions where stellar processing has been minimal, *i.e.*, in regions where abundances of elements such as carbon, nitrogen, and oxygen are very low. There are extensive compilations of observed abundances of ^{4}He, N, and O in many different extra-galactic regions of ionized H [7,8,9]. Extrapolating the ^{4}He abundances from the data leads to a observational estimate for Y_p of [10,11]

$$Y_p = 0.234 \pm 0.003 \pm 0.005\ . \tag{16.2}$$

(Here and elsewhere, the first error is the statistical standard deviation, and the second systematic.) The large box in Fig. 16.1 bracketing the

^{4}He curves covers the range 0.223 to 0.245, where the half height is conservatively given as twice the statistical error plus the systematic error. There has been some debate on the size of systematic errors [4] and the dashed box is obtained using a larger systematic error of 0.01.

Observations for deuterium and ^{3}He abundances present larger problems. All deuterium is primordial [12], but some of the primordial deuterium has been destroyed. Thus, as can be seen in the figure, the present deuterium abundance gives an upper limit to η. However, to get more information requires either an understanding of galactic chemical evolution of deuterium or a direct measurement of primordial deuterium. Even more problematical is ^{3}He: Not only is primordial ^{3}He destroyed in stars but it is very likely that low-mass stars are net producers of ^{3}He. Neither the galactic chemical evolution of ^{3}He nor the production of ^{3}He in stars is well understood.

It appears that D/H has decreased over the age of the galaxy. Samples obtained deep inside meteorites provide measurements of the true (pre)-solar system abundance of ^{3}He, while measurements on meteoritic near-surface samples, the solar wind, and lunar soil samples also contain ^{3}He converted from deuterium in the early pre-main-sequence stage of the sun. The best current values are [13]

$$\left(\frac{\mathrm{D}+{}^3\mathrm{He}}{\mathrm{H}}\right)_\odot = (4.1 \pm 1.0) \times 10^{-5} ,$$

$$\left(\frac{{}^3\mathrm{He}}{\mathrm{H}}\right)_\odot = (1.5 \pm 0.3) \times 10^{-5} . \qquad (16.3)$$

The difference between these, D/H $\approx (2.6 \pm 1.0) \times 10^{-5}$, is the pre-solar D abundance.

On the other hand, the present interstellar-medium abundance of D/H is [14]

$$\mathrm{D/H} = 1.60 \pm 0.09^{+0.05}_{-0.10} \times 10^{-5} . \qquad (16.4)$$

It is this lowest value of D/H that provides the most robust upper bound on η, since D is only destroyed. It is shown (decreased by $2\sigma_{\rm stat} + \sigma_{\rm syst}$) as the lower side of the D and ^{3}He box in Fig. 16.1. If η_{10} is in the range 2.8–4.5 (1.5–6.3) then the primordial abundance of D/H is between 3.6–8 (2–25) $\times 10^{-5}$, and it would appear that significant destruction of deuterium has occurred. The upper side of the box in Fig. 16.1 comes from the upper limit on $(\mathrm{D} + {}^3\mathrm{He})_\odot$ under the assumption that at least 25% of a star's initial D + ^{3}He is returned to the interstellar medium [15].

Deuterium may have been detected in high-redshift, low-metallicity quasar absorption systems [16,17,18]. These measured abundances should represent the primordial value, but, they are not entirely consistent: One [16] gives D/H ≈ 1.9–2.5×10^{-4} while the other [17] gives D/H ≈ 1–2×10^{-5}. Most recently, measurements in three absorption systems show consistent values of D/H around $10^{-4.0 \pm 0.25}$ [18] and corresponds to a value of η in good agreement with that discussed in the previous section. The upper limit on D/H from the first observation is shown by the dashed box in Fig. 16.1. As one can see, the corresponding value of Y_p (at the same value of η as inferred by the observation of a high D/H) is in excellent agreement with the data. ^{7}Li is also acceptable at this value as well. However, due to the still somewhat preliminary status of this observation, it is premature to use it to fix the primordial abundance. A high value for the D abundance would require an even greater degree of D destruction over the age of the galaxy. The lower measurement for D/H is problematic for both ^{4}He and ^{7}Li and requires that systematics all work in the same direction to give a marginal overlap with this data.

Finally, we turn to ^{7}Li. In old, hot, population-II stars, ^{7}Li is found to have a very nearly uniform abundance. For stars with a surface temperature $T > 5500$ K and a metallicity less than about 1/20th solar (so that effects such as stellar convection may not be important), the abundances show little or no dispersion beyond that consistent with the errors of individual measurements. Much data has been obtained recently from a variety of sources, and the best estimate for the mean ^{7}Li abundance and its statistical uncertainty in halo stars is [19](the estimate of the systematic uncertainty discussed below is our own)

$$\mathrm{Li/H} = (1.6 \pm 0.1^{+0.4+1.6}_{-0.3-0.5}) \times 10^{-10} . \qquad (16.5)$$

The first error is statistical, and the second is a systematic uncertainty that covers the range of abundances derived by various methods. The box in Fig. 16.1 corresponds to these errors (as before, with a half height of $2\sigma_{\rm stat} + \sigma_{\rm syst}$). The third set of errors in Eq. (16.5) accounts for the possibility that as much as half of the primordial ^{7}Li has been destroyed in stars, and that as much as 30% of the observed ^{7}Li was produced in cosmic ray collisions rather than in the Big Bang. These uncertainties are shown by the dashed box in Fig. 16.1. Observations of ^{6}Li, Be, and B help constrain the degree to which these effects play a role [20,21,22].

16.3. A consistent value for η

For the standard model of BBN to be deemed successful, theory and observation of the light element abundances must agree using a single value of η. We summarize the constraints on η from each of the light elements. From the ^{4}He mass fraction, $Y_p < 0.240$ (0.245–0.250), we have $\eta_{10} < 2.9$ (4.5–7.6) as a 2σ upper limit (the highest values use possible systematic errors up to their extreme range). Because of the sensitivity to the assumed upper limit on Y_p, the upper limit on η from D/H, is still of value. From D/H $> 1.3 \times 10^{-5}$, we have $\eta_{10} < 8.1$.

The lower limit on η_{10} comes from the upper limit on D + ^{3}He and is $\eta_{10} \gtrsim 2.8$ if one ignores ^{3}He production. We stress, however, that the upper limit on D + ^{3}He depends critically on models of galactic chemical evolution, which are far from being understood, and that one of the two measurements of D/H in quasar absorption systems indicates that $\eta_{10} \sim 1.5$.

Finally, ^{7}Li allows a broad range for η_{10} consistent with the other elements. When uncertainties in the reaction rates and systematic uncertainties in the observed abundances are both taken into account, ^{7}Li allows values of η_{10} between 1.3–5.0 (1–6.3). The resulting overall consistent range for η_{10} becomes 2.8–4.5 (1.5–6.3). These bounds on η_{10} constrain the fraction of critical density in baryons, Ω_B, to be

$$0.010 < \Omega_B h_0^2 < 0.016 \;\; (0.005 < \Omega_B h_0^2 < 0.023) \qquad (16.6)$$

for a Hubble parameter, h_0, between 0.4 and 1.0. The corresponding range for Ω_B is 0.01–0.10 (0.005–0.14).

16.4. Beyond the Standard Model

Limits on particle physics beyond the Standard Model come mainly from the observational bounds on the ^{4}He abundance. As discussed earlier, the neutron-to-proton ratio is fixed by its equilibrium value at the freeze-out of the weak-interaction rates at a temperature $T_f \sim 1$ MeV, with corrections for free neutron decay. Furthermore, freeze-out is determined by the competition between the weak-interaction rates and the expansion rate of the Universe,

$$G_F{}^2 T_f{}^5 \sim \Gamma_{\rm wk}(T_f) = H(T_f) \sim \sqrt{G_N N(T_f)}\, T_f{}^2 , \qquad (16.7)$$

where $N(T_f)$ counts the total (equivalent) number of relativistic particle species. The presence of additional neutrino flavors (or of any other relativistic species) at the time of nucleosynthesis increases the energy density of the Universe and hence the expansion rate, leading to a larger value of T_f, n/p, and ultimately Y_p. It is clear that just as one can place limits [23] on N, any changes in the weak or gravitational coupling constants can be similarly constrained.

In the Standard Model, the number of particle species can be written as $N = 5.5 + \frac{7}{4} N_\nu$ at $T_f = 1$ MeV; 5.5 accounts for photons and $e^\pm$; and N_ν is the number of light neutrino flavors. The helium curves in Fig. 16.1 were computed assuming $N_\nu = 3$, and the computed ^{4}He abundance scales roughly as $\Delta Y_{\rm BBN} \approx 0.012$–$0.014\ \Delta N_\nu$. Clearly the central value for N_ν from BBN will depend on η. If the best value for the observed primordial ^{4}He abundance is 0.234, then, for $\eta_{10} \sim 1.7$, the central value for N_ν is very close to 3. For $\eta_{10} > 2.8$ the central value for N_ν is less than 2.5. However, because of the uncertainties in the abundances, and thus in η, the upper limit on N_ν is more important here than the central value of N_ν. A straightforward propagation of errors leads to a 2σ upper limit of about 3.1 (3.5) on N_ν when systematic errors are included [10,24]. Other prescriptions,

which involve renormalization of the probability distributions when the central value of N_ν falls below 3, give even higher upper limits to N_ν [25].

The limits on N_ν can be translated into limits on other types of particles or particle masses that would affect the expansion rate of the Universe just prior to nucleosynthesis. In some cases, it is the interaction strengths of new particles which are constrained. Particles with less than full weak strength interactions contribute less to the energy density than particles that remain in equilibrium up to the time of nucleosynthesis [26].

We close with a simple example. Suppose there exist three right-handed neutrinos with only right-handed interactions of strength $G_R < G_F$. The standard left-handed neutrinos are no longer in equilibrium at temperatures below ~ 1 MeV. Particles with weaker interactions decouple at higher temperatures, and their number density ($\propto T^3$) relative to neutrinos is reduced by the annihilations of particles more massive than 1 MeV. If we use the upper bound $N_\nu < 3.1$, then the three right-handed neutrinos must have a temperature $3(T_{\nu_R}/T_{\nu_L})^4 < 0.1$. Since the temperature of the decoupled ν_R's is determined by entropy conservation, $T_{\nu_R}/T_{\nu_L} = [(43/4)/N(T_f)]^{1/3} < 0.4$, where T_f is the freeze-out temperature of the ν_R's. Thus $N(T_f) > 100$ and decoupling must have occurred at $T_f > M_W$ (since in the Standard Model, $N(T > M_W) = 106.75$). Finally, the decoupling temperature is related to G_R by $(G_R/G_F)^2 \sim (T_f/3\ \mathrm{MeV})^{-3}$, where 3 MeV corresponds to the decoupling temperature for ν_L. This yields a limit $G_R \lesssim 10^{-7}\ G_F$. Clearly these limits are strongly dependent on the assumed upper limit to N_ν; for $N_\nu < 3.5$, the limit on G_R is relaxed to $G_R < 0.002\ G_F$, since T_f is constrained only to be larger than the temperature corresponding to the QCD transition in the early Universe.

References:

1. D.N. Schramm and R.V. Wagoner, Ann. Rev. Nucl. and Part. Sci. **27**, 37 (1977).
2. A. Boesgard and G. Steigman, Ann. Rev. Astron. Astrophys. **23**, 319 (1985).
3. T.P. Walker, G. Steigman, D.N. Schramm, K.A. Olive, and H.-S. Kang, Astrophys. J. **376**, 51 (1991).
4. C.J. Copi, D.N. Schramm, and M.S. Turner, Science **267**, 192 (1995).
5. L.M. Krauss and P. Romanelli, Astrophys. J. **358**, 47 (1990).
6. N. Hata, R.J. Scherrer, G. Steigman, D. Thomas, and T.P. Walker, APJ Lett., in press (1995).
7. B.E.J. Pagel, E.A. Simonson, R.J. Terlevich, and M. Edmunds, MNRAS **255**, 325 (1992).
8. E. Skillman *et al.*, Astrophys. J. Lett. (in preparation) 199 5.
9. Y.I. Izatov, T.X. Thuan, and V.A. Lipovetsky, Astrophys. J. **435**, 647 (1994).
10. K.A. Olive and G. Steigman, Astrophys. J. Supp. **97**, 49 (1995).
11. K.A. Olive and S.T. Scully, Int. J. Mod. Phys. A (in press, 1995).
12. H. Reeves, J. Audouze, W. Fowler, and D.N. Schramm, Astrophys. J. **179**, 909 (1973).
13. J. Geiss, in *Origin and Evolution of the Elements*, eds. N. Prantzos, E. Vangioni-Flam, and M. Cassé (Cambridge: Cambridge University Press, 1993), p. 89.
14. J.L. Linsky, *et al.*, Astrophys. J. **402**, 695 (1993);
    J.L. Linsky, *et al.*, Astrophys. J. (in press, 1995).
15. J. Yang, M.S. Turner, G. Steigman, D.N. Schramm, and K.A. Olive, Astrophys. J. **281**, 493 (1984).
16. R.F. Carswell, M. Rauch, R.J. Weymann, A.J. Cooke, J.K. Webb, MNRAS **268**, L1 (1994);
    A. Songaila, L.L. Cowie, C. Hogan, M. Rugers, Nature **368**, 599 (1994).
17. D. Tytler and X.-M. Fan, BAAS **26**, 1424 (1995).
18. M. Rugers and C.J. Hogan Astrophys. J. (in press, 1995).
19. P. Molaro, F. Primas, and P. Bonifacio, Astron. & Astrophys. **295**, L47 (1995).
20. T.P. Walker, G. Steigman, D.N. Schramm, K.A. Olive,and B. Fields, Astrophys. J. **413**, 562 (1993).
21. K.A. Olive, and D.N. Schramm, Nature **360**, 439 (1993).
22. G. Steigman, B. Fields, K.A. Olive, D.N. Schramm, and T.P. Walker, Astrophys. J. **415**, L35 (1993).
23. G. Steigman, D.N. Schramm, and J. Gunn, Phys. Lett. **B66**, 202 (1977).
24. P. Kernan and L.M. Krauss, Phys. Rev. Lett. **72**, 3309 (1994).
25. K.A. Olive and G. Steigman, Phys. Lett. **B354**, 357 (1995).
26. G. Steigman, K.A. Olive, and D.N. Schramm, Phys. Rev. Lett. **43**, 239 (1979);
    K.A. Olive, D.N. Schramm, and G. Steigman, Nucl. Phys. **B180**, 497 (1981).

17. THE HUBBLE CONSTANT

Written August 1995 by C.J. Hogan, University of Washington.

In a uniform expanding universe, the position $\boldsymbol{r}$ and velocity $\boldsymbol{v}$ of any particle relative to another obey Hubble's relation $\boldsymbol{v} = H_0\boldsymbol{r}$, where H_0 is Hubble's constant.* As cosmological distances are measured in Mpc, the natural unit for H_0 is km s^{-1} Mpc^{-1}, which has the dimensions of inverse time: [100 km s^{-1} Mpc^{-1}]$^{-1}$ = 9.78 × 10^9 yr.

The real universe is nonuniform on small scales, and its motion obeys the Hubble relation only as a large scale average. But as typical non-Hubble motions ("peculiar velocities") are less than about 500 km s^{-1}, on scales more than about 5,000 km s^{-1} the deviations from Hubble flow are less than about 10%, so the notion of a global Hubble constant is well defined. The value of H_0 averaged over the local 15,000 km s^{-1} volume is known to lie within 10% of its global value even if H_0 itself is not known this precisely [1–3].

The Hubble constant is only meaningful on very large scales, but very large distances can only be measured indirectly. Distance ratios are measured with selected uniform types of astronomical systems ("Standard Candles") some examples of which are given below. These are used to tie distances to an absolute scale, either the nearby one based on trigonometric parallax or to some system where a physical model is precise enough to yield a distance directly from observed properties. There are many different ways to combine these tools to calibrate large distance, some of which are reviewed here. More complete reviews can be found in Refs. [4–7].

Using stars as standard candles and the Earth's orbit as a baseline, it is possible to tie distances throughout the Galaxy directly to trigonometric parallax measurements. A good landmark point for extragalactic studies is the Large Magellanic Cloud (LMC), a satellite galaxy of our Galaxy whose distance (50 kpc) is known to about 7% and provides confirmation and calibration of other measures. Beyond that, other galaxies in the Local Group (within about 1 Mpc) and other nearby groups provide stepping stones to the Virgo cluster (about 17 Mpc distant), and finally to the Coma cluster (about 100 Mpc distant) and others where the peculiar velocities introduce only small ambiguities. Most of the effort thus lies in obtaining an accurate ratio of distances in the range between Coma (or other similarly distant clusters) and the LMC.

Table 17.1 lists several candles and calibrators with a typical range of distance accessible to each. Usually the ends of the range are not precisely defined; the near end is plagued by small numbers of accessible objects and the far end by signal to noise. The precision quoted is a typical guideline which also varies depending on the sample used; it indicates the error in a distance ratio between an object and some standard reference, not including uncertainties in the absolute calibration of the reference distance (except for the first entry, which lists the typical absolute distance uncertainty in the Cepheid distance to a galaxy.) (The units are astronomical "distance modulus," given by $\mu = 5\log_{10}(\textit{distance in parsecs}) - 5.0$; a ± 0.1 magnitude error in magnitude or distance modulus corresponds to a 5% error in distance.) The verification of this precision is made by cross-checking against some other indicator on a galaxy-by-galaxy basis. This provides a control of systematic errors, since we do not expect detailed correlations between (for example) supernova brightness and host-galaxy rotation. Some examples are given in the next column, along with options often used for absolute calibration. The Hubble relation itself is included here, as it is the most precise indication of relative distance for large distances, and is used to verify the standardization of the other candles. As velocities are easy to measure at the relevant precision, a measurement of the Hubble constant is obtained from a calibrated distance measurement at a sufficiently large distance that the Hubble relation itself is precisely defined.

Table 17.1: Selected extragalactic distance indicators.†

Technique	Range of distance	Precision	Verification/ calibration
Cepheids	<LMC to 17 Mpc	0.15 mag	LMC/MWG
SNIa	4 Mpc to 2 Gpc	0.1-0.2 mag	Hubble/Model, Cepheid
EPM/SNII	LMC to 200 Mpc	0.4 mag	Hubble/Model, Cepheid
PNLF	1 Mpc to 20 Mpc	0.1 mag	SBF/Cepheid
SBF	1 Mpc to 60 Mpc	0.1 mag	PNLF/Cepheid
TF	1 Mpc to 100 Mpc	0.3 mag	Hubble/Cepheid
D_n–σ	10 Mpc to 60 Mpc	0.4 mag	Hubble/SBF
BCG	50 Mpc to 1 Gpc	0.2-0.3 mag	Hubble
GCLF	<LMC to 100 Mpc	0.4 mag	SBF/MWG
SZ	100 Mpc to > 1 Gpc	—	Hubble/Model
GL	∼5 Gpc	—	Model
Hubble	20 Mpc to $\gtrsim$1Gpc	500 km s^{-1} ÷ H_0D	BCG, SNeIa/H_0

MWG = Milky Way Galaxy
†Extracted from [4-7].

17.1. Cepheid variables

The best studied and most trusted of the standard candles, Cepheids are bright stars undergoing overstable oscillations driven by the variation of helium opacity with temperature. The period of oscillation is tightly correlated with the absolute brightness of the star. The calibration of this "period-luminosity relation" ties galaxies to geometrical parallax measurements with about 0.15 mag or 7% precision [8]. There may be some indications of nonuniformity in different populations, but no evidence yet that they are significant. Cepheids have been identified in the Galaxy, the LMC, and in galaxies as distant as M100 in the Virgo cluster, at 17.1 ± 1.8 Mpc [9]. More measurements at large distances are expected from Hubble Space Telescope data. This is an important development because it allows direct absolute calibration of the best distant indicator, SNIa, as well as other methods, to better than 10% accuracy.

17.2. Type Ia supernovae (SNIa)

A SNIa occurs when a degenerate dwarf, of the order of a solar mass and of CNO composition, undergoes explosive detonation or deflagration by nuclear burning to iron-group elements (Ni, Co, Fe). Their uniformity arises because the degenerate material only becomes unstable when it is gravitationally compressed to where the electrons become close to relativistic, which requires nearly a Chandrasekhar mass (1.4 solar masses). Theoretical models of the explosion predict approximately the right peak brightness, but cannot be relied upon for a precise calibration. SNIa are very bright, so their brightness distribution can be studied using the distant Hubble flow as a reference. Indeed, the Hubble diagram of distant SNIa (as well as cases of two SNIa in a single galaxy) shows that they can serve as remarkably precise standard candles; even though they display large variations in brightness, with detailed knowledge of the shape of the light curve, the relative intrinsic brightness of a single SNIa can be predicted to $\Delta m = 0.15$ mag or better and its distance estimated to better than 7% accuracy [10–12]. (Note that distant SNIa can even measure deviation from a linear Hubble law with precision $\Delta q_0 \simeq \Delta m/z$.) Supernovae of all types are fairly rare events, occurring in a typical galaxy every hundred years, so it is only recently that a direct absolute calibration to SNIa host galaxies with Cepheids has been possible.

17.3. Type II supernovae (SNII)

A SNII occurs when a massive star has accumulated 1.4 solar masses of iron group elements in its core; there is then no source of nuclear energy and the core collapses by the Chandrasekhar instability. The collapse to a neutron star releases a large gravitational binding energy, some of which powers an explosion. The large variety of envelopes around collapsing cores means that SNII are not at all uniform in their properties. However, their distances can be calibrated absolutely by the fairly reliable "expanding photosphere method" (EPM). The principle is most easily understood for an expanding spherical blackbody. Even if the disk is unresolved, the continuum spectrum yields the angular size from spectral temperature and absolute flux. Spectral lines yield the expansion velocity, which from knowledge of the elapsed time gives a physical size and hence a distance. Models of real photospheres are not so simple but yield individual distances accurate to about 20% [13]. This is in principle an independent absolute distance, but is precisely verified by comparison with Cepheids in several cases, the distant Hubble diagram and Tully Fisher distance ratios (described below) in several others, and by multiple-epoch fits of the same object.

17.4. Planetary nebula luminosity function (PNLF)

A planetary nebula (PN) forms when the gaseous envelope is ejected from a low-mass star as its core collapses to a white dwarf. We see bright fluorescent radiation from the ejected gas shell, excited by UV light from the hot new white dwarf. The line radiation makes PN's easy to find and measure even in far-away galaxies; a bright galaxy can have tens of thousands, of which hundreds are bright enough to use to construct a PNLF. It is found empirically that the range of PN brightnesses has a sharp upper cutoff that appears to provide a good empirical standard candle, verified by comparison with SBF distance ratios.

17.5. Surface brightness fluctuations (SBF)

When galaxies are farther away than the Local Group, atmospheric blurring causes stellar images to blend together. However, with modern linear detectors, it is still possible to measure the moments of the distribution of stellar brightness in a population (in particular, the brightness-weighted average stellar brightness) through spatial fluctuations in the light. Stellar populations in elliptical galaxies appear to be universal enough for this to be a remarkably good standard candle, as verified by comparison with PNLF distance ratios. Note the problem of absolute calibration: as there are no elliptical galaxies with Cepheids, instead one uses the bulge components of nearby spirals, which have similar populations.

17.6. Tully-Fisher (TF)

The TF relation refers to a correlation of the properties of whole spiral galaxies, between rotational velocity and total luminosity. In rough terms, the relation can be understood as a relation between mass and luminosity, but given the variation in structural properties and stellar populations the narrow relation is a surprisingly good standard candle. Looking at a whole galaxy gives a long range and wide applicability. The TF distance ratios and precision have been verified by cross-checking against all of the above candles, and against the Hubble flow, particularly galaxy cluster averages, which permit greater precision. The absolute calibration of TF is traditionally made by a handful of local galaxies, with Cepheid calibration, and a major thrust now is to extend Cepheid measurements to a larger, more representative, and more distant sample, especially to galaxies in the Virgo cluster.

17.7. D_n–σ

A rough equivalent to TF for elliptical galaxies, D_n–σ is a correlation between galaxy size and velocity dispersion. It has a larger dispersion than TF and less opportunity for local calibration, but it is particularly useful for verifying distance ratios of galaxy clusters, whose cores contain almost no spirals.

17.8. Brightest cluster galaxies (BCG)

As a result of agglomeration, rich clusters of galaxies have accumulated the largest and brightest galaxies in the universe in their centers. They are very nearly all the same brightness; when account is taken of their light profiles, they are even more uniform. These provide the best check on the approach to uniform Hubble flow on large scales. (Quasars, which are even brighter, are far too variable to be good standard candles).

17.9. Globular cluster luminosity function (GCLF)

Many galaxies have systems of globular clusters orbiting them, each of which contain hundreds of thousands of stars and hence is visible at large distances. It is assumed that similar galaxies ought to have similar distributions of globular cluster luminosity, and current work is centered on verifying the precision of this assumption.

17.10. Sunyaev-Zeldovich effect (SZ)

The electron density and temperature of the hot plasma in a cluster of galaxies can be measured in two ways which depend differently on distance: the thermal x-ray emission, which is mostly bremsstrahlung by hot electrons, and the Sunyaev-Zeldovich effect on the microwave background, caused by Compton scattering off the electrons. This provides in principle an absolute calibration. Although the model has other unconstrained parameters, such as the gas geometry, which limit the precision and reliability of distances, in the handful of cases which have been studied most recently the distances are broadly in accord with those obtained by the other techniques.

17.11. Gravitational lenses (GL)

The time delay δt between different images of a high redshift gravitationally lensed quasar is $\delta t = C(z_Q, z_l)\delta\theta^2/H_0 \approx 1$ yr for image separations $\delta\theta$ of the order of arcseconds, with a numerical factor C of order unity determined by the specific lens geometry (the angular distribution of the lensing matter) and background cosmology. Variability of the double quasar 0957+561 has permitted measurements of δt from time series correlation, but these remain controversial and ambiguous, yielding correlation peaks at both 415 and 540 days. Although lensing does not yet provide a precise measurement, it is an amazing sanity check that this system, which relies on no other intermediate steps for its calibration, gives estimates on the scale of the Hubble length which are broadly consistent with local measures of H_0.

17.12. Estimates of H_0

The central idea is to find "landmark" systems whose distance is given by more than one technique. Systems are not always well defined, however. For example, the LMC size is a few percent of its distance, introducing errors of this order for any calibration based on an individual object within it. Nor are galaxy clusters as compact and well defined as individual galaxies; using galaxy clusters as calibrating systems often requires some assumptions and models about cluster membership (the most important example being the Virgo cluster, whose structure is somewhat amorphous, creating a ±20% or more distance ambiguity in some arguments). The best way to avoid this is to cross-correlate calibrators on a galaxy-by-galaxy basis, but this introduces problems of bias associated with sample selection that must be modeled. The basic difficulty remains that the nearby calibrators of any sort remain few and possibly anomalous.

The reason for the variable estimates of the Hubble constant lies in the many different ways to combine these techniques to obtain an absolute distance calibration in the Hubble flow, each involving several, usually individually reasonable, assumptions. Nevertheless there is broad agreement within the errors among a wide variety of independent ladders with different systematics. As examples, we cite a variety of (somewhat arbitrarily chosen) independent methods, which illustrate some of the choices and tradeoffs, summarized in Table 17.2.

1. Expanding photosphere method (EPM) distances give an absolute calibration to objects in the distant Hubble flow. A small sample of these direct distances with small flow corrections gives $H_0 = 73 \pm 6$ (statistical) ± 7 (systematic).The distance estimates and limits on the systematic error component are verified by Cepheid distances in three cases, where the Cepheid/EPM distances come out to 1.02 ± 0.08 (LMC), $1.01^{+0.23}_{-0.17}$ (M101) and 1.13 ± 0.28 (M100).
2. With HST, it is now possible to calibrate SNIa directly with Cepheid distances to host galaxies. The light from brighter SNIa decays more slowly than from faint ones, so the best fits to the distant Hubble diagram include information about the light curve shape ("LCS") rather than simply assuming uniformity; low values of H_0 arise in the latter case. There are several options for empirical calibration, among them: (a) Three individual SNIa host galaxy distances have been calibrated directly with Cepheids. There is evidence from their light curves that two of these calibrators may indeed be unusually bright, which explains why the value of H_0 depends on whether or not the LCS correction is applied (a fourth, SN 1990N in N4639 is appearing as this goes to press, with more on the way). (b) Alternatively, assuming that the mean of six well-studied SNIa in the Virgo cluster lies at the Cepheid Virgo distance of 17 Mpc yields $H_0 = 71 \pm 7$ km s^{-1} Mpc^{-1}.
3. The distance to Virgo or any other local cluster is tied to H_0 via the distant Hubble diagram for TF or D_n–σ distances for galaxies in distant clusters. This can be done with a large scale flow model fit to many clusters. Using a Virgo distance of 17 Mpc yields $H_0 = 82 \pm 11$ km s^{-1} Mpc^{-1}. Alternatively, we can use the distance ratio to a fiducial reference such as the Coma cluster, for which such models predict almost vanishing peculiar velocity, and which is in any case distant enough for flow to be unimportant. (The flow models give its Hubble velocity as 7170 ± 125 km s^{-1}; relative to the CMBR its velocity is 7197 ± 73 km s^{-1}.) If (as estimated from TF, D_n–σ, SNeI) the Coma to Virgo ratio lies in the range 5.5 to 5.75, 17 Mpc for Virgo leads to $H_0 = 77$ to 73 km s^{-1} Mpc^{-1}, subject to uncertainty over the Virgo depth. Nearly the same TF calibration is given by six local Cepheid calibrators, and by several more in the M101 group. This avoids the Virgo depth uncertainty, but replaces it with doubts about whether all of the local calibrators might be anomalous (although the apparent uniformity of galaxies elsewhere argues against this being a large effect.)
4. TF comparison with distant field galaxies in the Hubble flow (after corrections for Malmquist bias in the samples, which is worse than in cluster samples) yield $H_0 = 80 \pm 10$ km s^{-1} Mpc^{-1}.
5. For completeness, some recent SZ and GL estimates are shown. The GL estimate in the best model [25] depends on the convergence κ added to the main galaxy lens by the cluster potential; κ probably lies between 0.1 and 0.2, and must be greater than zero, providing a firm upper limit on H_0 and an estimate squarely in the range of the other techniques.

The central values by most reliably calibrated methods lie in the range $H_0 = 65$ to 85 km s^{-1} Mpc^{-1}, and indeed this corresponds roughly with the range of estimates expected from the internally estimated errors. Thus systematic errors are at least not dominant, although they could well be comparable to internal errors. The simplicity and apparent precision of the new Cepheid + SNIa ladder lead one to suspect a true value in the lower end of this range.

Footnote and References:

* To first order in v. For discussion of the second-order term, including the "deceleration parameter" q_0, see the Big-Bang Cosmology section (Sec. 15).

1. J. Kristian, A. Sandage, and J. Westphal, Astrophys. J. **221**, 383 (1978).
2. T. Lauer and M. Postman, Astrophys. J. Lett. **400**, L47 (1992).
3. T. Lauer and M. Postman, Astrophys. J. **425**, 418 (1994).
4. G.H. Jacoby *et al.*, Pub. Astron. Soc. Pac. **104**, 599 (1992).
5. S. van den Bergh, Pub. Astron. Soc. Pac. **104**, 861 (1992).
6. S. van den Bergh, Pub. Astron. Soc. Pac. **106**, 1113 (1994).
7. M. Fukugita, C.J. Hogan, and P.J.E. Peebles, Nature **366**, 309 (1993).
8. B. Madore and W. Freedman, Pub. Astron. Soc. Pac. **103**, 933 (1991).
9. W. Freedman *et al.*, Nature **371**, 757 (1994).
10. M. Phillips, Astrophys. J. Lett. **413**, L105 (1993).
11. M. Hamuy *et al.*, Astrophys. J. **109**, 1 (1995).
12. A. Riess, W. Press, and R. Kirshner, Astrophys. J. Lett. **438**, L17 (1994).
13. B. Schmidt *et al.*, Astrophys. J. **432**, 42 (1994).
14. J. Mould *et al.*, Astrophys. J. **449**, 413 (1995).
15. A. Saha *et al.*, Astrophys. J. **438**, 8 (1995).
16. G.H. Jacoby and M.J. Pierce, Astron. J., (November 1995).
17. A. Saha *et al.*, Astrophys. J. **425**, 14 (1994).
18. I have used the photometric compilation and LCS correction from B.E. Schaefer, Astrophys. J. **449**, L9 (1995), and the Cepheid distance from Ref. 19.
19. A. Saha *et al.*, private communication, give $(m - M)_0 = 31.05 \pm 0.15$.
20. N. Tanvir *et al.*, Nature **377**, 27 (1995).
21. T. Ichihawa and M. Fukugita, Astrophys. J. **394**, 61 (1992).
22. M. Birkinshaw and J.P. Hughes, Astrophys. J. **420**, 33 (1994).
23. T. Herbig, C.R. Lawrence, and A.C.S. Readhead, Astrophys. J. Lett. **449**, L5 (1995).
24. J. Pelt, R. Kayser, S. Refsdal, and T. Schramm, Astron. Astrophys., in press (1995).
25. N.A. Grogin and R. Narayan, astro-phys 9512156, submitted to Astrophys. J. (1995).
26. M. Pierce *et al.*, Nature **371**, 385 (1994).

Table 17.2: Some recent estimates of Hubble's constant

Technique	Calibration*	Ties to Hubble flow	Result* (km s^{-1} Mpc^{-1})	Ref.
EPM	Expanding photosphere model	Direct EPM Hubble Diagram + Flow model or TF	$73 \pm 6 \pm 7$	[13]
	Cepheids in 3 SNII hosts		same × [0.88, 1.26]	[14]
SNeIa		Direct SNIa Hubble Diagram		
	Cepheids (N5253 + SN1972E)	Direct + LCS correction	$62 - 67$	[11]
	Cepheids (N5253 + SN1972E)	Direct + LCS correction	67 ± 7	[12]
	Cepheids (N5253 + SN1972E)	Direct	54 ± 8	[15]
	Cepheids (IC4182 + SN1937C)	Direct + LCS correction	$68\text{–}74 \pm 6$	[16]
	Cepheids (IC4182 + SN1937C)	Direct	52 ± 9	[17]
	Cepheids (N4536 + SN1981B)	Direct + LCS correction	67 ± 6	[18,19]
	Virgo mean (M100) + six Virgo SN hosts	Direct	$71 \pm 7^{\dagger}$	[14]
Clusters	Virgo mean (M100 Cepheids) + local + M101 Cepheids	Virgo infall model	$81 \pm 11^{\dagger}$	[14]
		Virgo/Coma ratio	$73\text{–}77 \pm 10^{\dagger}$	[14]
		Cluster TF + LS flow model fit	$82 \pm 11^{\dagger}$	[14]
	M96 Cepheids	LeoI to Virgo and Coma	$69 \pm 8^{\dagger}$	[20]
Field TF	Local Cepheids‡	Field TF Hubble Diagram + Malmquist bias correction	$\approx 80 \pm 10$	[21]
SZ	SZ model + X-ray maps + SZ maps	Direct single cluster velocities:		
		A2218	65 ± 25	[22]
		A2218,A665	55 ± 17	[22]
		Coma	74 ± 29	[23]
Gravitational lensing	Lens model, time delay	Direct, Q0957+561	<70	[24]
			$82.5^{+5.9}_{-3.0}(1-\kappa)\,(\delta t/1.1\mathrm{yr})^{-1}$	[25]

* For all methods based on Cepheids, add a common multiplicative error of ±0.15 mag or 7% in H_0.

† plus Virgo depth uncertainty (scales with M100/Virgo ratio)

‡ TF calibration from 6 local Cepheid calibration is verified by M101 group galaxies and (less directly) by M100 and NGC 4571 distance to Virgo TF galaxies [9,14,26].

18. DARK MATTER

Written September 1995 by M. Srednicki, University of California, Santa Barbara

There is strong evidence from a variety of different observations for a large amount of dark matter in the universe [1]. The phrase "dark matter" means matter whose existence has been inferred only through its gravitational effects. There is also extensive circumstantial evidence that at least some of this dark matter is nonbaryonic: that is, composed of elementary particles other than protons, neutrons, and electrons. These particles must have survived from the Big Bang, and therefore must either be stable or have lifetimes in excess of the current age of the universe.

The abundance of dark matter is usually quoted in terms of its mass density $\rho_{\rm dm}$ in units of the critical density, $\Omega_{\rm dm} = \rho_{\rm dm}/\rho_{\rm c}$; the critical density $\rho_{\rm c}$ is defined in Eq. (15.5) (in Section 15 on "Big-Bang Cosmology" in this *Review*). The total amount of visible matter (that is, matter whose existence is inferred from its emission or absorption of photons) is roughly $\Omega_{\rm vis} \simeq 0.005$, with an uncertainty of at least a factor of two.

The strongest evidence for dark matter is from the rotation curves of spiral galaxies [1,2]. In these observations, the circular velocity $v_{\rm c}$ of hydrogen clouds surrounding the galaxy is measured (via Doppler shift) as a function of radius r. If there were no dark matter, at large r we would find $v_{\rm c}^2 \simeq G_N M_{\rm vis}/r$, since the visible mass $M_{\rm vis}$ of a spiral galaxy is concentrated at its center. However, observations of many spiral galaxies instead indicate a velocity $v_{\rm c}$ which is independent of r at large r, with a typical value $v_{\rm c} \sim 200\,{\rm km\ s^{-1}}$. Such a "flat rotation curve" implies that the total mass within radius r grows linearly with r, $M_{\rm tot}(r) \simeq G_N^{-1} v_{\rm c}^2 r$. A self-gravitating ball of ideal gas at a uniform temperature of $kT = \frac{1}{2} m_{\rm dm} v_{\rm c}^2$ would have this mass profile; here $m_{\rm dm}$ is the mass of one dark matter particle. The rotation curves are measured out to some tens of kiloparsecs, implying a total mass within this radius which is typically about ten times the visible mass. This would imply $\Omega_{\rm dm} \gtrsim 10\,\Omega_{\rm vis} \simeq 0.05$. In our own galaxy, estimates of the local density of dark matter typically give $\rho_{\rm dm} \simeq 0.3\,{\rm GeV\ cm^{-3}}$, but this result depends sensitively on how the halo of dark matter is modeled.

Other indications of the presence of dark matter come from observations of the motion of galaxies and hot gas in clusters of galaxies [3]. The overall result is that $\Omega_{\rm dm} \sim 0.2$. Studies of large-scale velocity fields result in $\Omega_{\rm dm} \gtrsim 0.3$ [4]. However, these methods of determining $\Omega_{\rm dm}$ require some astrophysical assumptions about how galaxies form.

None of these observations give us any direct indication of the nature of the dark matter. If it is baryonic, the forms it can take are severely restricted, since most forms of ordinary matter readily emit and absorb photons in at least one observable frequency band [5]. Possible exceptions include remnants (white dwarfs, neutron stars, black holes) of an early generation of massive stars, or smaller objects which never initiated nuclear burning (and would therefore have masses less than about $0.1\,M_\odot$). These massive compact halo objects are collectively called machos. Preliminary results [6] of a search for machos via gravitational lensing effects indicate that a standard halo has a mass fraction of no more than 0.66 of machos with mass less than $0.1\,M_\odot$ at the 95% confidence level, but it is possible to construct models of an all-macho halo which are consistent with all observations.

There are, however, several indirect arguments which argue for a substantial amount of nonbaryonic dark matter. First, nucleosynthesis gives the limits $0.010 \le \Omega_{\rm b} h_0^2 \le 0.016$ for the total mass of baryons; h_0 is defined in Eq. (15.6) (in Section 15 on "Big-Bang Cosmology" in this *Review*). The upper limit on $\Omega_{\rm b}$ is substantially below the value $\Omega_{\rm dm} \gtrsim 0.3$ given by large scale measurements, even if h_0 is near the lower end of its optimistically allowed range, $0.4 \le h_0 \le 1.0$. A second, purely theoretical argument is that inflationary models (widely regarded as providing explanations of a number of otherwise puzzling paradoxes) generically predict $\Omega_{\rm total} = 1$. Finally, without nonbaryonic dark matter it is difficult to construct a model of galaxy formation that predicts sufficiently small fluctuations in the cosmic microwave background radiation [7].

For purposes of galaxy formation models, nonbaryonic dark matter is classified as "hot" or "cold," depending on whether the dark matter particles were relativistic or nonrelativistic at the time when the horizon of the universe enclosed enough matter to form a galaxy. If the dark matter particles are in thermal equilibrium with the baryons and radiation, then only the mass of a dark matter particle is relevant to knowing whether the dark matter is hot or cold, with the dividing line being $m_{\rm dm} \sim 1\,{\rm keV}$. In addition, specifying a model requires giving the power spectrum of initial density fluctuations. Inflationary models generically predict a power spectrum which is nearly scale invariant. Given this, models with only cold dark matter are much more successful than models with only hot dark matter at reproducing the observed structure of our universe. Some lingering discrepancies in the cold dark matter model are removed in models with both kinds of dark matter [8]. Another class of models uses mass fluctuations due to topological defects, but these are much harder to analyze with comparable quantitative detail [9].

The best candidate for hot dark matter is one of the three neutrinos, endowed with a Majorana mass m_ν. Such a neutrino would contribute $\Omega_\nu = 0.56\,G_N T_0^3 H_0^{-2} m_\nu = m_\nu/(92\,h_0^2\,{\rm eV})$, where T_0 is the present temperature of the cosmic microwave background radiation. There is another constraint on neutrinos (or any light fermions) if they are to comprise the halos of dwarf galaxies: the Pauli exclusion principle restricts the number that can fit into the phase space of a halo [10], which puts a lower limit on the neutrino mass of $m_\nu \gtrsim 80\,{\rm eV}$.

There are no presently known particles which could be cold dark matter. However, many proposed extensions of the Standard Model predict a stable (or sufficiently long lived) particle. The key question then becomes the predicted value of $\Omega_{\rm dm}$.

If the particle is its own antiparticle (or there are particles and antiparticles present in equal numbers), and these particles were in thermal equilibrium with radiation at least until they became nonrelativistic, then their relic abundance is determined by their annihilation cross section $\sigma_{\rm ann}$: $\Omega_{\rm dm} \sim G_N^{3/2} T_0^3 H_0^{-2} \langle \sigma_{\rm ann} v_{\rm rel} \rangle^{-1}$. Here $v_{\rm rel}$ is the relative velocity of the two incoming dark matter particles, and the angle brackets denote an averaging over a thermal distribution of velocities for each at the freezeout temperature $T_{\rm fr}$ when the dark matter particles go out of thermal equilibrium with radiation; typically $T_{\rm fr} \simeq \frac{1}{20} m_{\rm dm}$. One then finds (putting in appropriate numerical factors) that $\Omega_{\rm dm} h_0^2 \simeq 3 \times 10^{-27}\,{\rm cm^3\,s^{-1}}/\langle \sigma_{\rm ann} v_{\rm rel} \rangle$. The value of $\langle \sigma_{\rm ann} v_{\rm rel} \rangle$ needed for $\Omega_{\rm dm} \simeq 1$ is remarkably close to what one would expect for a weakly interacting massive particle (wimp) with a mass of $m_{\rm dm} = 100\,{\rm GeV}$: $\langle \sigma_{\rm ann} v_{\rm rel} \rangle \sim \alpha^2/8\pi m_{\rm dm}^2 \sim 3 \times 10^{-27}\,{\rm cm^3\,s^{-1}}$.

If the dark matter particle is not its own antiparticle, and the number of particles minus antiparticles is conserved, then an initial asymmetry in the abundances of particles and antiparticles will be preserved, and can give relic abundances much larger than those predicted above.

If the dark matter particles were never in thermal equilibrium with radiation, then their abundance today must be calculated in some other way, and will in general depend on the precise initial conditions which are assumed.

The two best known and most studied cold dark matter candidates are the neutralino and the axion. The neutralino is predicted by supersymmetric extensions of the Standard Model [11,12]. It qualifies as a wimp, with a theoretically expected mass in the range of tens to hundreds of GeV. The axion is predicted by extensions of the Standard Model which resolve the strong CP problem [13]. Its mass must be approximately $10^{-5}\,{\rm eV}$ if it is to be a significant component of the dark matter. Axions can occur in the early universe in the form of a Bose condensate which never comes into thermal equilibrium; these axions are always nonrelativistic, despite their small mass.

There are prospects for direct experimental detection of both these candidates (and other wimp candidates as well). Wimps will scatter off nuclei at a calculable rate, and produce observable nuclear recoils [12,14]. This technique has been used to show that all the dark matter cannot consist of massive Dirac neutrinos or scalar neutrinos (predicted by supersymmetric models) with masses in the

range of $10\,\mathrm{GeV} \lesssim m_{\mathrm{dm}} \lesssim 4\,\mathrm{TeV}$ [15]. The neutralino is harder to detect because its scattering cross section with nuclei is considerably smaller. The axion can be detected by axion to photon conversion in an inhomogeneous magnetic field, and limits on the allowed axion-photon coupling have been set (which, however, do not exclude the theoretically favored value) [13]. Both types of detection experiments are in progress.

Wimp candidates can have indirect signatures as well, via present-day annihilations into particles which can be detected as cosmic rays [12]. The most promising possibility arises from the fact that wimps collect at the centers of the sun and the earth, thus greatly increasing their annihilation rate, and producing high energy neutrinos which can escape and arrive at the earth's surface in potentially observable numbers.

References:

1. *Dark Matter in the Universe: IAU Symposium No. 117*, ed. J. Kormendy and G.R. Knapp (Reidel, Dordrecht, 1987);
   Proceedings 23rd Rencontre de Moriond: Dark Matter, ed. J. Audouze and J. Tran Thanh Van (Editions Frontieres, Gif-sur-Yvette, 1988);
   Particle Physics and Cosmology: Dark Matter, ed. M. Srednicki (North-Holland, Amsterdam, 1990);
   Baryonic Dark Matter, ed. D. Lynden-Bell and G. Gilmore (Kluwer, Dordrecht, 1990).
2. K.G. Begeman, A.H. Broeils, and R.H. Sanders, Mon. Not. R. Astr. Soc. **259**, L31 (1991).
3. *Clusters and Superclusters of Galaxies*, ed. A.C. Fabian (Kluwer, Dordrecht, 1992);
   S.D.M. White *et al.*, Nature **366**, 429 (1993).
4. A. Deckel, Ann. Rev. Astron. Astrophys. **32**, 371 (1994).
5. D.J. Hegyi and K.A. Olive, Phys. Lett. **126B**, 28 (1983); Astrophys. J. **303**, 56 (1986).
6. C. Alcock *et al.*, Phys. Rev. Lett. **74**, 2867 (1995); astro-ph/9506113, Astrophys. J., in press.
7. M. White, D. Scott, and J. Silk, Ann. Rev. Astron. Astrophys. **32**, 319 (1994);
   W. Hu and N. Sugiyama, Astrophys. J. **436**, 456 (1994).
8. A. Klypin, R. Nolthenius, and J.R. Primack, astro-ph/9502062, Astrophys. J., in press.
9. R. Brandenberger, astro-ph/941109, in *TASI–94*, ed. J. Donoghue (World Scientific, Singapore, 1995).
10. S. Tremaine and J.E. Gunn, Phys. Rev. Lett. **42**, 407 (1979);
    O.E. Gerhard and D.N. Spergel, Astrophys. J. **389**, L1 (1992).
11. H.E. Haber and G.L. Kane, Phys. Rep. **117**, 75 (1985).
12. G. Jungman, M. Kamionkowski, and K. Griest, hep-ph/9506380, Phys. Rep., in press.
13. M.S. Turner, Phys. Rep. **197**, 67 (1990);
    P. Sikivie, Int. J. Mod. Phys. D **3** (supp.), 1 (1994);
    K. van Bibber *et al.*, Int. J. Mod. Phys. D **3** (supp.), 33 (1994).
14. J.R. Primack, B. Sadoulet, and D. Seckel, Ann. Rev. Nucl. and Part. Sci. **38**, 751 (1988);
    P.F. Smith and J.D. Lewin, Phys. Rep. **187**, 203 (1990).
15. D.O. Caldwell, in *Proceedings 27th International Conference on High-Energy Physics*, ed. P.J. Bussey and I G. Knowles (IOP, Bristol, 1995).

19. COSMIC BACKGROUND RADIATION

Revised February 1996 by G.F. Smoot and D. Scott

19.1. Introduction

The observed cosmic microwave background (CMB) radiation provides strong evidence for the hot big bang. The success of primordial nucleosynthesis calculations (see Sec. 16, "Big-bang nucleosynthesis") requires a cosmic background radiation (CBR) characterized by a temperature $kT \sim 1\,\mathrm{MeV}$ at a redshift of $z \simeq 10^9$. In their pioneering work, Gamow, Alpher, and Herman [1] realized this and predicted the existence of a faint residual relic, primordial radiation, with a present temperature of a few degrees. The observed CMB is interpreted as the current manifestation of the hypothesized CBR.

The CMB was serendipitously discovered by Penzias and Wilson [2] in 1965. Its spectrum is well characterized by a $2.73 \pm 0.01\,\mathrm{K}$ black-body (Planckian) spectrum over more than three decades in frequency (see Fig. 19.1). A non-interacting Planckian distribution of temperature T_i at redshift z_i transforms with the universal expansion to another Planckian distribution at redshift z_r with temperature $T_r/(1+z_r) = T_i/(1+z_i)$. Hence thermal equilibrium, once established (e.g. at the nucleosynthesis epoch), is preserved by the expansion, in spite of the fact that photons decoupled from matter at early times. Because there are about 10^9 photons per nucleon, the transition from the ionized primordial plasma to neutral atoms at $z \sim 1000$ does not significantly alter the CBR spectrum [3].

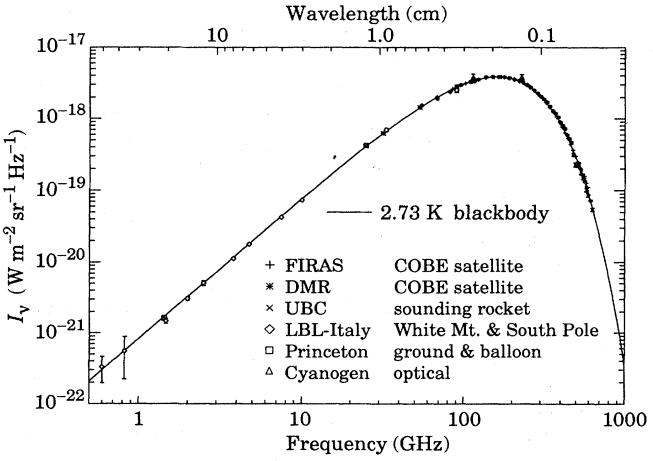

Figure 19.1: Precise measurements of the CMB spectrum. The line represents a 2.73 K blackbody, which describes the spectrum very well, especially around the peak of intensity. The spectrum is less well constrained at 10 cm and longer wavelengths. (References for this figure are at the end of this section under "CMB Spectrum References.")

19.2. Theoretical spectral distortions

The remarkable precision with which the CMB spectrum is fitted by a Planckian distribution provides limits on possible energy releases in the early Universe, at roughly the fractional level of 10^{-4} of the CBR energy, for redshifts $\lesssim 10^7$ (corresponding to epochs $\gtrsim 1$ year). The following three important classes of spectral distortions (see Fig. 19.2) generally correspond to energy releases at different epochs. The distortion results from the CBR photon interactions with a hot electron gas at temperature T_e.

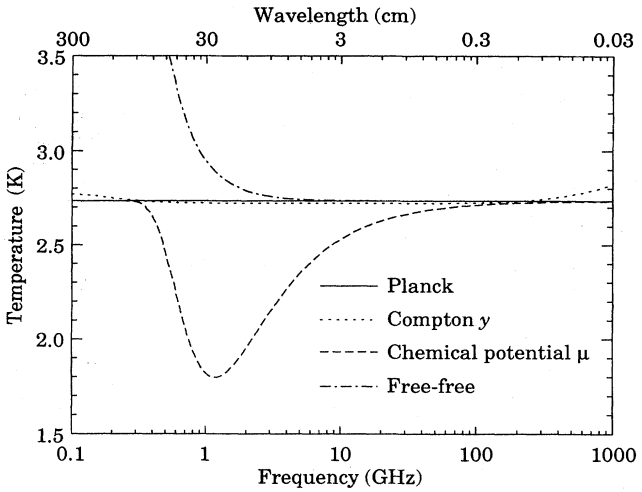

Figure 19.2: The shapes of expected, but so far unobserved, CMB distortions, resulting from energy-releasing processes at different epochs.

19.2.1. ***Compton distortion***: Late energy release ($z \lesssim 10^5$). Compton scattering ($\gamma e \rightarrow \gamma' e'$) of the CBR photons by a hot electron gas creates spectral distortions by transfering energy from the electrons to the photons. Compton scattering cannot achieve thermal equilibrium for $y < 1$, where

$$y = \int_0^z \frac{kT_e(z') - kT_\gamma(z')}{m_e c^2}\, \sigma_T\, n_e(z')\, c\, \frac{dt}{dz'}\, dz' \,, \tag{19.1}$$

is the integral of the number of interactions, $\sigma_T\, n_e(z)\, c\, dt$, times the mean-fractional photon-energy change per collision [4]. For $T_e \gg T_\gamma$ y is also proportional to the integral of the electron pressure $n_e kT_e$ along the line of sight. For standard thermal histories $y < 1$ for epochs later than $z \simeq 10^5$.

The resulting CMB distortion is a temperature decrement

$$\Delta T_{\mathrm{RJ}} = -2y\, T_\gamma \tag{19.2}$$

in the Rayleigh-Jeans ($h\nu/kT \ll 1$) portion of the spectrum, and a rapid rise in temperature in the Wien ($h\nu/kT \gg 1$) region, *i.e.* photons are shifted from low to high frequencies. The magnitude of the distortion is related to the total energy transfer [4] ΔE by

$$\Delta E/E_{\mathrm{CBR}} = e^{4y} - 1 \simeq 4y \,. \tag{19.3}$$

A prime candidate for producing a Comptonized spectrum is a hot intergalactic medium. A hot ($T_e > 10^5\,\mathrm{K}$) medium in clusters of galaxies can and does produce a partially Comptonized spectrum as seen through the cluster, known as the Sunyaev-Zel'dovich effect. Based upon X-ray data, the predicted large angular scale total combined effect of the hot intracluster medium should produce $y \lesssim 10^{-6}$ [5].

19.2.2. ***Bose-Einstein or chemical potential distortion***: Early energy release ($z \sim 10^5$–10^7). After many Compton scatterings ($y > 1$), the photons and electrons will reach statistical (not thermodynamic) equilibrium, because Compton scattering conserves photon number. This equilibrium is described by the Bose-Einstein distribution with non-zero chemical potential:

$$n = \frac{1}{e^{x+\mu_0} - 1} \,, \tag{19.4}$$

where $x \equiv h\nu/kT$ and $\mu_0 \simeq 1.4\, \Delta E/E_{\mathrm{CBR}}$, with μ_0 being the dimensionless chemical potential that is required.

The collisions of electrons with nuclei in the plasma produce free-free (thermal bremsstrahlung) radiation: $eZ \rightarrow eZ\gamma$. Free-free

emission thermalizes the spectrum to the plasma temperature at long wavelengths. Including this effect, the chemical potential becomes frequency-dependent,

$$\mu(x) = \mu_0 e^{-2x_b/x} \ , \tag{19.5}$$

where x_b is the transition frequency at which Compton scattering of photons to higher frequencies is balanced by free-free creation of new photons. The resulting spectrum has a sharp drop in brightness temperature at centimeter wavelengths [6]. The minimum wavelength is determined by Ω_B.

The equilibrium Bose-Einstein distribution results from the oldest non-equilibrium processes ($10^5 < z < 10^7$), such as the decay of relic particles or primordial inhomogeneities. Note that free-free emission (thermal bremsstrahlung) and radiative-Compton scattering effectively erase any distortions [7] to a Planckian spectrum for epochs earlier than $z \sim 10^7$.

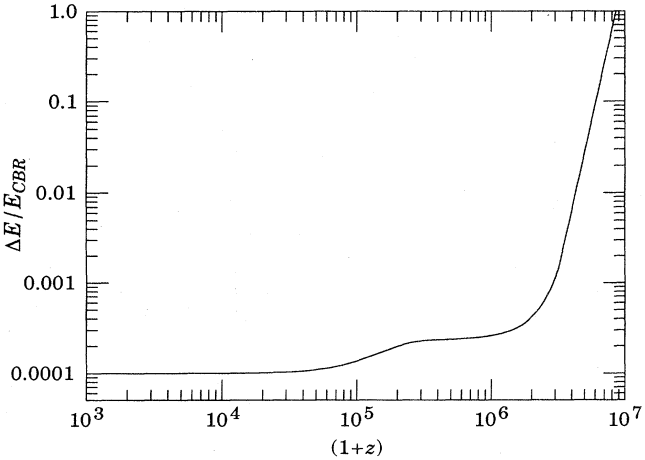

Figure 19.3: Upper Limits (95% CL) on fractional energy ($\Delta E/E_{\rm CBR}$) releases as set by lack of CMB spectral distortions resulting from processes at different epochs. These can be translated into constraints on the mass, lifetime and photon branching ratio of unstable relic particles, with some additional dependence on cosmological parameters such as Ω_B [9,10].

19.2.3. ***Free-free distortion***: Very late energy release ($z \ll 10^3$). Free-free emission can create rather than erase spectral distortion in the late universe, for recent reionization ($z < 10^3$) and from a warm intergalactic medium. The distortion arises because of the lack of Comptonization at recent epochs. The effect on the present-day CMB spectrum is described by

$$\Delta T_{ff} = T_\gamma \, Y_{ff}/x^2, \tag{19.6}$$

where T_γ is the undistorted photon temperature, x is the dimensionless frequency, and Y_{ff}/x^2 is the optical depth to free-free emission:

$$Y_{ff} = \int_0^z \frac{T_e(z') - T_\gamma(z')}{T_e(z')} \frac{8\pi e^6 h^2 n_e^2 \, g}{3 m_e (kT_\gamma)^3 \sqrt{6\pi \, m_e \, kT_e}} \frac{dt}{dz'} dz' \ . \tag{19.7}$$

Here h is Planck's constant, n_e is the electron density and g is the Gaunt factor [8].

19.2.4. ***Spectrum summary***: The CMB spectrum is consistent with a blackbody spectrum over more than three decades of frequency around the peak. A least-squares fit to all CMB measurements yields:

$$T_\gamma = 2.73 \pm 0.01 \text{ K}$$
$$n_\gamma = (2\zeta(3)/\pi^2) T_\gamma^3 \simeq 413 \, \text{cm}^{-3}$$
$$\rho_\gamma = (\pi^2/15) T_\gamma^4 \simeq 4.68 \times 10^{-34} \, \text{g cm}^{-3} \simeq 0.262 \, \text{eV cm}^{-3}$$
$$|y| < 1.5 \times 10^{-5} \quad (95\% \text{ CL})$$
$$|\mu_0| < 9 \times 10^{-5} \quad (95\% \text{ CL})$$
$$|Y_{ff}| < 1.9 \times 10^{-5} \quad (95\% \text{ CL})$$

The limits here [11] correspond to limits [11–13] on energetic processes $\Delta E/E_{\rm CBR} < 2 \times 10^{-4}$ occurring between redshifts 10^3 and 5×10^6 (see Fig. 19.3). The best-fit temperature from the COBE FIRAS experiment is $T_\gamma = 2.728 \pm 0.002$ K [11].

19.3. Deviations from isotropy

Penzias and Wilson reported that the CMB was isotropic and unpolarized to the 10% level. Current observations show that the CMB is unpolarized at the 10^{-5} level but has a dipole anisotropy at the 10^{-3} level, with smaller-scale anisotropies at the 10^{-5} level. Standard theories predict anisotropies in linear polarization well below currently achievable levels, but temperature anisotropies of roughly the amplitude now being detected.

It is customary to express the CMB temperature on the sky in a spherical harmonic expansion,

$$T(\theta, \phi) = \sum_{\ell m} a_{\ell m} Y_{\ell m}(\theta, \phi) \ , \tag{19.8}$$

and to discuss the various multipole amplitudes. The power at a given angular scale is roughly $\ell \sum_m |a_{\ell m}|^2 / 4\pi$, with $\ell \sim 1/\theta$.

19.3.1. ***The dipole***: The largest anisotropy is in the $\ell = 1$ (dipole) first spherical harmonic, with amplitude at the level of $\Delta T/T = 1.23 \times 10^{-3}$. The dipole is interpreted as the result of the Doppler shift caused by the solar system motion relative to the nearly isotropic blackbody field. The motion of the observer (receiver) with velocity $\beta = v/c$ relative to an isotropic Planckian radiation field of temperature T_0 produces a Doppler-shifted temperature

$$T(\theta) = T_0 (1 - \beta^2)^{1/2} / (1 - \beta \cos\theta)$$
$$= T_0 \left(1 + \beta \cos\theta + (\beta^2/2) \cos 2\theta + O(\beta^3)\right) \ . \tag{19.9}$$

The implied velocity [11,14] for the solar-system barycenter is $\beta = 0.001236 \pm 0.000002$ (68% CL) or $v = 371 \pm 0.5 \, \text{km s}^{-1}$, assuming a value $T_0 = 2.728 \pm 0.002$ K, towards $(\alpha, \delta) = (11.20^{\rm h} \pm 0.01^{\rm h}, -7.0° \pm 0.2°)$, or $(\ell, b) = (264.14° \pm 0.15°, 48.26° \pm 0.15°)$. Such a solar-system velocity implies a velocity for the Galaxy and the Local Group of galaxies relative to the CMB. The derived velocity is $v_{\rm LG} = 627 \pm 22 \, \text{km s}^{-1}$ toward $(\ell, b) = (276° \pm 3°, 30° \pm 3°)$, where most of the error comes from uncertainty in the velocity of the solar system relative to the Local Group.

The Doppler effect of this velocity and of the velocity of the Earth around the Sun, as well as any velocity of the receiver relative to the Earth, is normally removed for the purposes of CMB anisotropy study. The resulting high degree of CMB isotropy is the strongest evidence for the validity of the Robertson-Walker metric.

19.3.2. ***The quadrupole***: The rms quadrupole anisotropy amplitude is defined through $Q_{\rm rms}^2/T_\gamma^2 = \sum_m |a_{2m}|^2 / 4\pi$. The current estimate of its value is $4 \, \mu\text{K} \leq Q_{\rm rms} \leq 28 \, \mu\text{K}$ for a 95% confidence interval [15]. The uncertainty here includes both statistical errors and systematic errors, which are dominated by the effects of galactic emission modelling. This level of quadrupole anisotropy allows one to set precise limits on anisotropic expansion, shear, and vorticity; all such dimensionless quantities are constrained to be less than about 10^{-5}.

19.3.3. ***Smaller angular scales***: The COBE-discovered [16] higher-order ($\ell > 2$) anisotropy is interpreted as being the result of perturbations in the energy density of the early Universe, manifesting themselves at the epoch of the CMB's last scattering. Hence the detection of these anisotropies has provided evidence for the existence of the density perturbations that seeded all the structure we observe today.

In the standard scenario the last scattering takes place at a redshift of approximately 1100, at which epoch the large number of photons was no longer able to keep the hydrogen sufficiently ionized. The optical thickness of the cosmic photosphere is roughly $\Delta z \sim 100$ or about 5 arcminutes, so that features smaller than this size are damped.

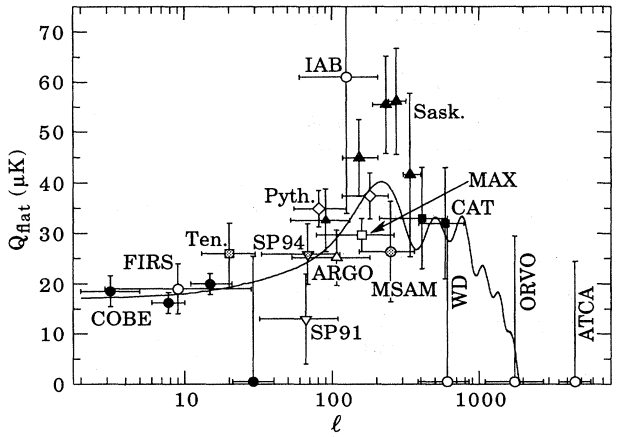

Figure 19.4: Current status of CMB anisotropy observations, adapted from Scott, Silk, & White (1995) [17]. This is a representation of the results from COBE, together with a wide range of ground- and balloon-based experiments which have operated in the last few years. Plotted are the quadrupole amplitudes for a flat (unprocessed scale-invariant spectrum of primordial perturbations, *i.e.*, a horizontal line) anisotropy spectrum that would give the observed results for each experiment. In other words each point is the normalization of a flat spectrum derived from the individual experiments. The vertical error bars represent estimates of 68% CL, while the upper limits are at 95% CL. Horizontal bars indicate the range of ℓ values sampled. The curve indicates the expected spectrum for a standard CDM model ($\Omega_0 = 1, \Omega_B = 0.05, h = 0.5$), although true comparison with models should involve convolution of this curve with each experimental filter function. (References for this figure are at the end of this section under "CMB Anisotropy References.")

Anisotropies are observed on angular scales larger than this damping scale (see Fig. 19.4), and are consistent with those expected from an initially scale-invariant power spectrum (flat = independent of scale) of potential and thus metric fluctuations. It is believed that the large scale structure in the Universe developed through the process of gravitational instability, where small primordial perturbations in energy density were amplified by gravity over the course of time. The initial spectrum of density perturbations can evolve significantly in the epoch $z > 1100$ for causally connected regions (angles $\lesssim 1^\circ\ \Omega_{\rm tot}^{1/2}$). The primary mode of evolution is through adiabatic (acoustic) oscillations, leading to a series of peaks that encode information about the perturbations and geometry of the universe, as well as information on Ω_0, Ω_B, Ω_Λ (cosmological constant), and H_0 [17]. The location of the first acoustic peak is predicted to be at $\ell \sim 220\ \Omega_{\rm tot}^{-1/2}$ or $\theta \sim 0.3^\circ\ \Omega_{\rm tot}^{1/2}$ and its amplitude increases with increasing Ω_B.

Theoretical models often predict a power spectrum in spherical harmonic amplitudes, since the models lead to primordial fluctuations and thus $a_{\ell m}$ that are Gaussian random fields, and hence the power spectrum in ℓ is sufficient to characterize the results. The power at each ℓ is $(2\ell+1)C_\ell/(4\pi)$, where $C_\ell \equiv \langle |a_{\ell m}|^2 \rangle$. For an idealized full-sky observation, the variance of each measured C_ℓ is $[2/(2\ell+1)]C_\ell^2$. This sampling variance (known as cosmic variance) comes about because each C_ℓ is chi-squared distributed with $(2\ell+1)$ degrees of freedom for our observable volume of the Universe [18].

Figure 19.5 shows the theoretically predicted anisotropy power spectrum for a sample of models, plotted as $\ell(\ell+1)C_\ell$ versus ℓ which is the power per logarithmic interval in ℓ or, equivalently, the two-dimensional power spectrum. If the initial power spectrum of perturbations is the result of quantum mechanical fluctuations produced and amplified during inflation, then the shape of the anisotropy spectrum is coupled to the ratio of contributions from density (scalar) and gravity wave (tensor) perturbations. If the energy scale of inflation at the appropriate epoch is at the level of $\simeq 10^{16}$GeV, then detection of the effect of gravitons is possible, as well as partial reconstruction of the inflaton potential. If the energy scale is $\lesssim 10^{14}$GeV, then density fluctuations dominate and less constraint is possible.

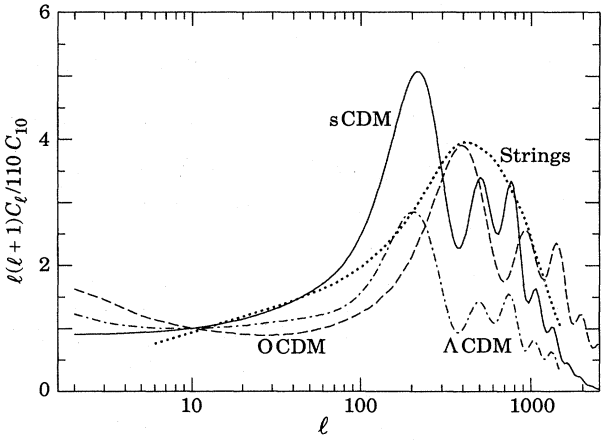

Figure 19.5: Examples of theoretically predicted $\ell(\ell+1)C_\ell$ or CMB anisotropy power spectra. **sCDM** is the standard cold dark matter model with $h = 0.5$ and $\Omega_B = 0.05$. **ΛCDM** is a model with $\Omega_{\rm tot} = \Omega_\Lambda + \Omega_0 = 1$, with $\Omega_\Lambda = 0.3$ and $h = 0.8$. **OCDM** is an open model with $\Omega_0 = 0.3$ and $h = 0.75$ (see [19] for models). **Strings** is a model where cosmic strings are the primary source of large scale structure [20]. The plot indicates that precise measurements of the CMB anisotropy power spectrum could distinguish between current models.

Fits to data over smaller angular scales are often quoted as the expected value of the quadrupole $\langle Q \rangle$ for some specific theory, *e.g.* a model with power-law initial conditions (primordial density perturbation power spectrum $P(k) \propto k^n$). The full 4-year COBE DMR data give $\langle Q \rangle = 15.3^{+3.7}_{-2.8}\ \mu$K, after projecting out the slope dependence, while the best-fit slope is $n = 1.2 \pm 0.3$, and for a pure $n = 1$ (scale-invariant potential perturbation) spectrum $\langle Q \rangle\,(n=1) = 18 \pm 1.6\,\mu$K [15,21]. The conventional notation is such that $\langle Q \rangle^2 / T_\gamma^2 = 5C_2/4\pi$. The fluctuations measured by other experiments can also be quoted in terms of $Q_{\rm flat}$, the equivalent value of the quadrupole for a flat ($n = 1$) spectrum, as presented in Fig. 19.4.

It now seems clear that there is more power at sub-degree scales than at COBE scales, which provides some model-dependent information on cosmological parameters [17,22], for example Ω_B. In terms of such parameters, fits to the COBE data alone yield $\Omega_0 > 0.34$ at 95% CL [23] and $\Omega_{\rm tot} < 1.5$ also at 95% CL [24], for inflationary models. Only somewhat weak conclusions can be drawn based on the current smaller angular scale data (see Fig. 19.4). A sample preliminary fit [25] finds $\Omega_{\rm tot} = 0.7^{+1.0}_{-0.4}$ and $30 < H_0 < 70\ {\rm km\,s^{-1}Mpc^{-1}}$ for a limited range of cosmological models.

However, new data are being acquired at an increasing rate, with a large number of improved ground- and balloon-based experiments being developed. It appears that we are not far from being able to distinguish crudely between currently favored models, and to begin a more precise determination of cosmological parameters. A vigorous suborbital and interferometric program could map out the CMB anisotropy power spectrum to about 10% accuracy and determine several parameters at the 10 to 20% level in the next few years. Ultimately, on the scale of a perhaps 5–10 years, there is the prospect of another satellite mission which could provide a precise measurement of the power spectrum down to scales of 10 arcminutes, allowing us to decode essentially all of the information that it contains [26].

References:

1. R.A. Alpher and R.C. Herman, Physics Today, Vol. 41, No. 8, p. 24 (1988).
2. A.A. Penzias and R. Wilson, Astrophys. J. **142**, 419 (1965);
   R.H. Dicke, P.J.E. Peebles, P.G. Roll, and D.T. Wilkinson, Astrophys. J. **142**, 414 (1965).
3. P.J.E. Peebles, "Principles of Physical Cosmology," Princeton U. Press, p. 168 (1993).
4. R.A. Sunyaev and Ya.B. Zel'dovich, Ann. Rev. Astron. Astrophys. **18**, 537 (1980).
5. M.T. Ceballos and X. Barcons, MNRAS **271**, 817 (1994).
6. C. Burigana, L. Danese, and G.F. De Zotti, Astron. & Astrophys. **246**, 49 (1991).
7. L. Danese and G.F. De Zotti, Astron. & Astrophys. **107**, 39 (1982);
   G. De Zotti, Prog. in Part. Nucl. Phys. **17**, 117 (1987).
8. J.G. Bartlett and A. Stebbins, Astrophys. J. **371**, 8 (1991).
9. E.L. Wright *et al.*, Astrophys. J. **420**, 450 (1994).
10. W. Hu and J. Silk, Phys. Rev. Lett. **70**, 2661 (1993).
11. D.J. Fixsen *et al.*, Astrophys. J., in press (1996).
12. J.C. Mather *et al.*, Astrophys. J. **420**, 439 (1994).
13. M. Bersanelli *et al.*, Astrophys. J. **424**, 517 (1994).
14. A. Kogut *et al.*, Astrophys. J. **419**, 1 (1993);
    C. Lineweaver *et al.*, Astrophys. J., submitted (astro-ph/9601151).
15. C.L. Bennett *et al.*, Astrophys. J., in press (1996) (astro-ph/9601067).
16. G.F. Smoot *et al.*, Astrophys. J. **396**, L1 (1992).
17. D. Scott, J. Silk, and M. White, Science **268**, 829 (1995).
18. M. White, D. Scott, and J. Silk, Ann. Rev. Astron. & Astrophys. **32**, 329 (1994).
19. M. White, Phys. Rev. **D**, in press (1996) (astro-ph/9601158).
20. A. Albrecht, D. Coulson, P. Ferreira, and J. Magueijo, Phys. Rev. Lett., in press (1995) (astro-ph/9505030).
21. K.M. Górski *et al.*, Astrophys. J., in press (1996) (astro-ph/9601063).
22. A. Kogut and G. Hinshaw, Astrophys. J. Lett., submitted (1996) (astro-ph/9601179).
23. K. Yamamoto and E.F. Bunn, Astrophys. J., in press (1996) (astro-ph/9508090).
24. M. White and D. Scott, Astrophys. J. **459**, 415 (1996).
25. S. Hancock, G. Rocha, A.N. Lasenby, and C.M. Gutiérrez, Nature, submitted (1996).
26. L. Knox, Phys. Rev. **D**, in press (1995) (astro-ph/9504054);
    A. Kosowsky and M. Turner, Phys. Rev. **D52**, 1739 (1995);
    G. Jungman, M. Kamionkowski, A. Kosowsky, and D.N. Spergel, Phys. Rev. **D**, in press (1996) (astro-ph/9512139);
    W. Hu and M. White, Phys. Rev. Lett., submitted (1996) (astro-ph/9602020).

CMB Spectrum References:

1. **FIRAS:** J.C. Mather *et al.*, Astrophys. J. **432**, L15 (1993);
   D. Fixsen *et al.*, Astrophys. J. **420**, 445 (1994);
   D. Fixsen *et al.*, Astrophys. J., in press (1996).
2. **DMR:** A. Kogut *et al.*, Astrophys. J. **419**, 1 (1993);
   A. Kogut *et al.*, Astrophys. J., submitted (1996).
3. **UBC:** H.P. Gush, M. Halpern, and E.H. Wishnow, Phys. Rev. Lett. **65**, 537 (1990).
4. **LBL-Italy:** G.F. Smoot *et al.*, Phys. Rev. Lett. **51**, 1099 (1983);
   M. Bensadoun *et al.*, Astrophys. J. **409**, 1 (1993);
   M. Bersanelli *et al.*, Astrophys. J. **424**, 517 (1994);
   M. Bersanelli *et al.*, Astrophys. Lett. and Comm. **32**, 7 (1995);
   G. De Amici *et al.*, Astrophys. J. **381**, 341 (1991);
   A. Kogut *et al.*, Astrophys. J. **335**, 102 (1990);
   N. Mandolesi *et al.*, Astrophys. J. **310**, 561 (1986);
   G. Sironi, G. Bonelli, and M. Limon, Astrophys. J. **378**, 550 (1991).
5. **Princeton:** S. Staggs *et al.*, Astrophys. Lett. & Comm. **32**, 3 (1995);
   D.G. Johnson and D.T. Wilkinson, Astrophys. J. **313**, L1 (1987).
6. **Cyanogen:** K.C. Roth, D.M. Meyer, and I. Hawkins, Astrophys. J. **413**, L67 (1993);
   K.C. Roth and D.M. Meyer, Astrophys. J. **441**, 129 (1995);
   E. Palazzi *et al.*, Astrophys. J. **357**, 14 (1990).

CMB Anisotropy References:

1. **COBE:** K.M. Górski *et al.*, Astrophys. J. **430**, L89 (1994);
   K.M. Górski *et al.*, Astrophys. J., submitted (1996) (astro-ph/9601063);
   G. Hinshaw *et al.*, Astrophys. J., in press (1996) (astro-ph/9601058).
2. **FIRS:** K. Ganga, L. Page, E. Cheng, and S. Meyers, Astrophys. J. **432**, L15 (1993).
3. **Ten.:** S. Hancock *et al.*, Nature **367**, 333 (1994).
4. **SP91:** J. Schuster *et al.*, Astrophys. J. **412**, L47 (1993). (Revised, see **SP94** reference.).
5. **SP94:** J.O. Gundersen *et al.*, Astrophys. J. **443**, L57 (1994).
6. **Sask.:** C.B. Netterfield *et al.*, Astrophys. J., submitted (1996) (astro-ph/9601197).
7. **Pyth.:** M. Dragovan *et al.*, Astrophys. J. **427**, L67 (1993);
   J. Ruhl *et al.*, Astrophys. J. **453**, L1 (1995).
8. **ARGO:** P. de Bernardis *et al.*, Astrophys. J. **422**, L33 (1994).
9. **IAB:** L. Piccirillo and P. Calisse, Astrophys. J. **413**, 529 (1993).
10. **MAX:** S.T. Tanaka *et al.*, Astrophys. J., in press (1996) (astro-ph/9512067);
    M. Lim *et al.*, Astrophys. J., submitted (1996).
11. **MSAM:** E.S. Cheng *et al.*, Astrophys. J. **456**, L71 (1996).
12. **CAT:** P.F.S. Scott *et al.*, Astrophys. J., in press (1996).
13. **WD:** G.S. Tucker, G.S. Griffin, H.T. Nguyen, and J.B. Peterson, Astrophys. J. **419**, L45 (1993).
14. **OVRO:** A.C.S. Readhead *et al.*, Astrophys. J. **346**, 566 (1989).
15. **ATCA:** R. Subrahmayan, R.D. Ekers, M. Sinclair, and J. Silk, Monthly Not. Royal Astron. Soc. **263**, 416 (1993).

20. COSMIC RAYS

Written 1995 by T.K. Gaisser and T. Stanev

20.1. Primary spectra

The cosmic radiation incident at the top of the terrestrial atmosphere includes all stable charged particles and nuclei with lifetimes of order 10^6 years or longer. Technically, "primary" cosmic rays are those particles accelerated at astrophysical sources and "secondaries" are those particles produced in interaction of the primaries with interstellar gas. Thus electrons, protons and helium, as well as carbon, oxygen, iron, and other nuclei synthesized in stars, are primaries. Nuclei such as lithium, beryllium, and boron (which are not abundant end-products of stellar nucleosynthesis) are secondaries. Antiprotons and positrons are partly, if not entirely, secondaries, but the fraction of these particles that may be primary is a question of current interest.

Apart from particles associated with solar flares, the cosmic radiation comes from outside the solar system. The incoming charged particles are "modulated" by the solar wind, the expanding magnetized plasma generated by the Sun, which decelerates and partially excludes the lower energy galactic cosmic rays from the inner solar system. There is a significant anticorrelation between solar activity (which has an eleven-year cycle) and the intensity of the cosmic rays with energies below about 10 GeV. In addition, the lower-energy cosmic rays are affected by the geomagnetic field, which they must penetrate to reach the top of the atmosphere. Thus the intensity of any component of the cosmic radiation in the GeV range depends both on the location and time.

There are four different ways to describe the spectra of the components of the cosmic radiation: (1) By particles per unit rigidity. Propagation (and probably also acceleration) through cosmic magnetic fields depends on gyroradius or *magnetic rigidity*, R, which is gyroradius multiplied by the magnetic field strength:

$$R = \frac{p\,c}{Z\,e} = r_L B\ . \tag{20.1}$$

(2) By particles per energy-per-nucleon. Fragmentation of nuclei propagating through the interstellar gas depends on energy per nucleon, since that quantity is approximately conserved when a nucleus breaks up on interaction with the gas. (3) By nucleons per energy-per-nucleon. Production of secondary cosmic rays in the atmosphere depends on the intensity of nucleons per energy-per-nucleon, approximately independently of whether the incident nucleons are free protons or bound in nuclei. (4) By particles per energy-per-nucleus. Air shower experiments that use the atmosphere as a calorimeter generally measure a quantity that is related to total energy per particle.

The units of differential intensity I are $[\mathrm{cm}^{-2}\mathrm{s}^{-1}\mathrm{sr}^{-1}\mathcal{E}^{-1}]$, where $\mathcal{E}$ represents the units of one of the four variables listed above.

The intensity of primary nucleons in the energy range from several GeV to somewhat beyond 100 TeV is given approximately by

$$I_N(E) \approx 1.8\,E^{-\alpha}\ \frac{\text{nucleons}}{\mathrm{cm}^2\ \mathrm{s}\ \mathrm{sr}\ \mathrm{GeV}}\ , \tag{20.2}$$

where E is the energy-per-nucleon (including rest mass energy) and α ($\equiv \gamma + 1$) $= 2.7$ is the differential spectral index of the cosmic ray flux and γ is the integral spectral index. About 79% of the primary nucleons are free protons and about 70% of the rest are nucleons bound in helium nuclei. The fractions of the primary nuclei are nearly constant over this energy range (possibly with small but interesting variations). Fractions of both primary and secondary incident nuclei are listed in Table 20.1. Figure 20.1 [1] shows the major components as a function of energy at a particular epoch of the solar cycle.

The spectrum of electrons and positrons incident at the top of the atmosphere is steeper than the spectra of protons and nuclei, as shown in Fig. 20.2 [2]. The positron fraction is about 10% in the region in which it is measured (< 20 GeV), but it is not yet fully understood [5].

Above 10 GeV the fraction of antiprotons to protons is about 10^{-4}, and there is evidence for the kinematic suppression at lower energy expected for secondary antiprotons [5]. There is at this time no evidence for a significant primary component of antiprotons.

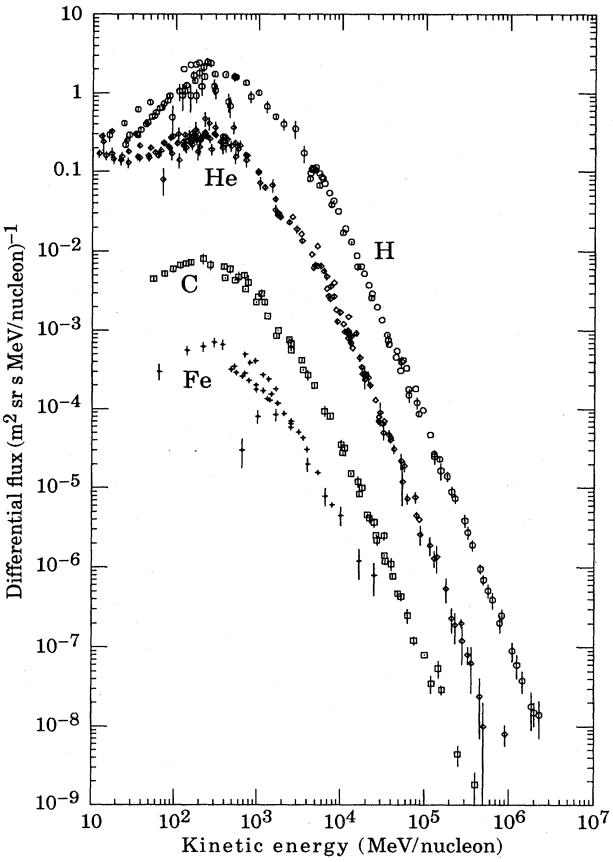

Figure 20.1: Major components of the primary cosmic radiation (from Ref. 1).

Table 20.1: Relative abundances F of cosmic-ray nuclei at 10.6 GeV/nucleon normalized to oxygen ($\equiv 1$) [3]. The oxygen flux at kinetic energy of 10.6 GeV/nucleon is 3.26×10^{-6} cm^{-2} s^{-1} sr^{-1} (GeV/nucleon)$^{-1}$. Abundances of hydrogen and helium are from Ref. 4.

Z	Element	F	Z	Element	F
1	H	730	13–14	Al-Si	0.19
2	He	34	15–16	P-S	0.03
3–5	Li-B	0.40	17–18	Cl-Ar	0.01
6–8	C-O	2.20	19–20	K-Ca	0.02
9–10	F-Ne	0.30	21–25	Sc-Mn	0.05
11–12	Na-Mg	0.22	26–28	Fe-Ni	0.12

20.2. Cosmic rays in the atmosphere

Figure 20.3 shows the vertical fluxes of the major cosmic ray components in the atmosphere in the energy region where the particles are most numerous (except for electrons, which are most numerous near their critical energy, which is about 81 MeV in air). Except for protons and electrons near the top of the atmosphere, all particles are produced in interactions of the primary cosmic rays in the air. Muons and neutrinos are products of the decay of charged mesons, while electrons and photons originate in decays of neutral mesons.

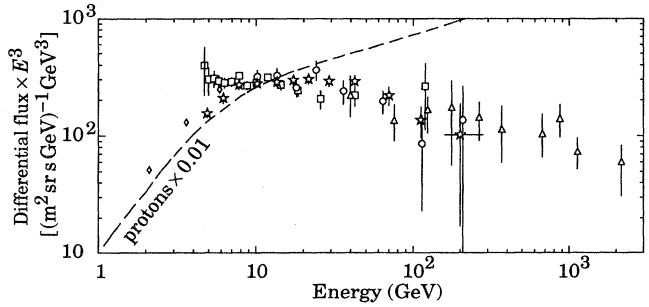

Figure 20.2: Differential spectrum of electrons plus positrons multiplied by E^3 (from Ref. 2).

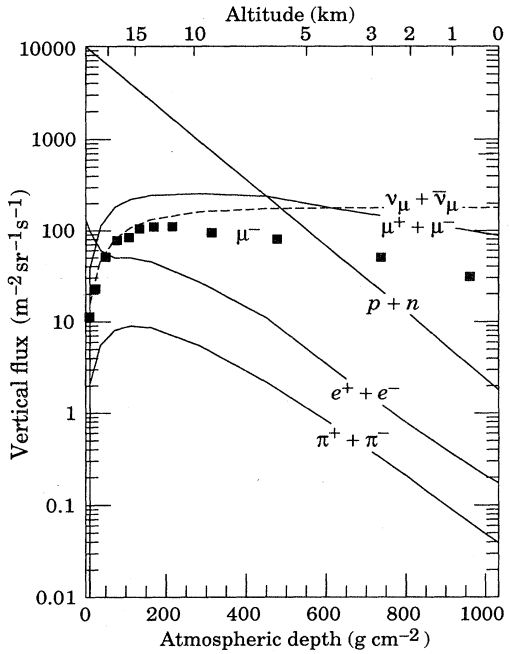

Figure 20.3: Vertical fluxes of cosmic rays in the atmosphere with $E > 1$ GeV estimated from the nucleon flux of Eq. (20.2). The points show measurements of negative muons with $E_\mu > 1$ GeV [7].

Most measurements are made at ground level or near the top of the atmosphere, but there are also measurements of muons and electrons from airplanes and balloons. Fig. 20.3 includes a recent measurement of negative muons [7]. Since $\mu^+(\mu^-)$ are produced in association with $\nu_\mu(\overline{\nu}_\mu)$, the measurement of muons near the maximum of the intensity curve for the parent pions serves to calibrate the atmospheric ν_μ beam [6]. Because muons typically lose almost two GeV in passing through the atmosphere, the comparison near the production altitude is important for the sub-GeV range of $\nu_\mu(\overline{\nu}_\mu)$ energies.

The flux of cosmic rays through the atmosphere is described by a set of coupled cascade equations with boundary conditions at the top of the atmosphere to match the primary spectrum. Numerical or Monte Carlo calculations are needed to account accurately for decay and energy-loss processes, and for the energy-dependences of the cross sections and of the primary spectral index γ. Approximate analytic solutions are, however, useful in limited regions of energy [8]. For example, the vertical intensity of nucleons at depth X (g cm^{-2}) in the atmosphere is given by

$$I_N(E, X) \approx I_N(E, 0)\, e^{-X/\Lambda} , \tag{20.3}$$

where Λ is the attenuation length of nucleons in air.

The corresponding expression for the vertical intensity of charged pions with energy $E_\pi \ll \epsilon_\pi = 115$ GeV is

$$I_\pi(E_\pi, X) \approx \frac{Z_{N\pi}}{\lambda_N} I_N(E_\pi, 0)\, e^{-X/\Lambda} \frac{X\, E_\pi}{\epsilon_\pi} . \tag{20.4}$$

This expression has a maximum at $t = \Lambda \approx 120$ g cm^{-2}, which corresponds to an altitude of 15 kilometers. The quantity $Z_{N\pi}$ is the spectrum-weighted moment of the inclusive distribution of charged pions in interactions of nucleons with nuclei of the atmosphere. The intensity of low-energy pions is much less than that of nucleons because $Z_{N\pi} \approx 0.079$ is small and because most pions with energy much less than the critical energy ϵ_π decay rather than interact.

20.3. Cosmic rays at the surface

20.3.1. ***Muons***: Muons are the most numerous charged particles at sea level (see Fig. 20.3). Most muons are produced high in the atmosphere (typically 15 km) and lose about 2 GeV to ionization before reaching the ground. Their energy and angular distribution reflect a convolution of production spectrum, energy loss in the atmosphere, and decay. For example, $E_\mu = 2.4$ GeV muons have a decay length of 15 km, which is reduced to 8.7 km by energy loss. The mean energy of muons at the ground is ≈ 4 GeV. The energy spectrum is almost flat below 1 GeV, steepens gradually to reflect the primary spectrum in the 10–100 GeV range, and steepens further at higher energies because pions with $E_\pi > \epsilon_\pi \approx 115$ GeV tend to interact in the atmosphere before they decay. Asymptotically ($E_\mu \gg 1$ TeV), the energy spectrum of atmospheric muons is one power steeper than the primary spectrum. The integral intensity of vertical muons above 1 GeV/c at sea level is ≈ 70 m^{-2}s^{-1}sr^{-1} [9,10]. Experimentalists are familiar with this number in the form $I \approx 1$ cm^{-2} min^{-1} for horizontal detectors.

The overall angular distribution of muons at the ground is $\propto \cos^2\theta$, which is characteristic of muons with $E_\mu \sim 3$ GeV. At lower energy the angular distribution becomes increasingly steeper, while at higher energy it flattens and approaches a $\sec\theta$ distribution for $E_\mu \gg \epsilon_\pi$ and $\theta < 70°$.

Figure 20.4 shows the muon energy spectrum at sea level for two angles. At large angles low energy muons decay before reaching the surface and high energy pions decay before they interact, thus the average muon energy increases. An approximate extrapolation formula valid when muon decay is negligible ($E_\mu > 100/\cos\theta$ GeV) and the curvature of the Earth can be neglected ($\theta < 70°$) is

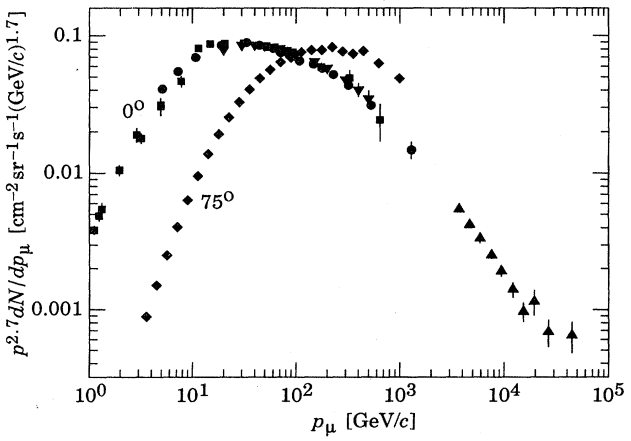

Figure 20.4: Spectrum of muons at $\theta = 0°$ (■ [12], ● [13], ▼ [14], ▲ [15]), and $\theta = 75°$ ♦ [16]).

$$\frac{dN_\mu}{dE_\mu} \approx \frac{0.14\,E^{-2.7}}{\mathrm{cm^2\ s\ sr\ GeV}} \times \left\{ \frac{1}{1+\frac{1.1E_\mu\cos\theta}{115\,\mathrm{GeV}}} + \frac{0.054}{1+\frac{1.1E_\mu\cos\theta}{850\,\mathrm{GeV}}} \right\}, \quad (20.5)$$

where the two terms give the contribution of pions and charged kaons. Eq. (20.5) neglects a small contribution from charm and heavier flavors which is negligible except at very high energy [17].

The muon charge ratio reflects the excess of π^+ over π^- in the forward fragmentation region of proton initiated interactions together with the fact that there are more protons than neutrons in the primary spectrum. The charge ratio is between 1.2 and 1.3 from 250 MeV up to 100 GeV [9].

20.3.2. ***Electromagnetic component***: At the ground, this component consists of electrons, positrons, and photons primarily from electromagnetic cascades initiated by decay of neutral and charged mesons. Muon decay is the dominant source of low-energy electrons at sea level. Decay of neutral pions is more important at high altitude or when the energy threshold is high. Knock-on electrons also make a small contribution at low energy [11]. The integral vertical intensity of electrons plus positrons is very approximately 30, 6, and 0.2 $\mathrm{m^{-2}s^{-1}sr^{-1}}$ above 10, 100, and 1000 MeV respectively [10,18], but the exact numbers depend sensitively on altitude, and the angular dependence is complex because of the different altitude dependence of the different sources of electrons [11,18,19]. The ratio of photons to electrons plus positrons is approximately 1.3 above a GeV and 1.7 below the critical energy [19].

20.3.3. ***Protons***: Nucleons above 1 GeV/c at ground level are degraded remnants of the primary cosmic radiation. The intensity is approximately represented by Eq. (20.3) with the replacement $t \to t/\cos\theta$ for $\theta < 70°$ and an attenuation length $\Lambda = 123$ g cm^{-2}. At sea level, about 1/3 of the nucleons in the vertical direction are neutrons (up from $\approx 10\%$ at the top of the atmosphere as the n/p ratio approaches equilibrium). The integral intensity of vertical protons above 1 GeV/c at sea level is ≈ 0.9 $\mathrm{m^{-2}s^{-1}sr^{-1}}$ [10,20].

20.4. Cosmic rays underground

Only muons and neutrinos penetrate to significant depths underground. The muons produce tertiary fluxes of photons, electrons, and hadrons.

20.4.1. ***Muons***: As discussed in Section 22.9 of this *Review*, muons lose energy by ionization and by radiative processes: bremsstrahlung, direct production of e^+e^- pairs, and photonuclear interactions. The total muon energy loss may be expressed as a function of the amount of matter traversed as

$$-\frac{dE_\mu}{dX} = a + b\,E_\mu\,, \quad (20.6)$$

where a is the ionization loss and b is the fractional energy loss by the three radiation processes. Both are slowly varying functions of energy. The quantity $\epsilon \equiv a/b$ (≈ 500 GeV in standard rock) defines a critical energy below which continuous ionization loss is more important the radiative losses. Table 20.2 shows a and b values for standard rock as a function of muon energy. The second column of Table 20.2 shows the muon range in standard rock ($A = 22$, $Z = 11$, $\rho = 2.65$ g cm^{-3}). These parameters are quite sensitive to the chemical composition of the rock, which must be evaluated for each experimental location.

The intensity of muons underground can be estimated from the muon intensity in the atmosphere and their rate of energy loss. To the extent that the mild energy dependence of a and b can be neglected, Eq. (20.6) can be integrated to provide the following relation between the energy $E_{\mu,0}$ of a muon at production in the atmosphere and its average energy E_μ after traversing a thickness X of rock (or ice or water):

$$E_\mu = (E_{\mu,0} + \epsilon)\,e^{-bX} - \epsilon\,. \quad (20.7)$$

Table 20.2: Average muon range R and energy loss parameters calculated for standard rock. Range is given in km-water-equivalent, or 10^5 g cm^{-2}.

E_μ	R	a	b_{pair}	b_{brems}	b_{nucl}	$\sum b_i$
GeV	km.w.e.	MeV g^{-1} cm^2	——	10^{-6} g^{-1} cm^2		——
10	0.05	2.15	0.73	0.74	0.45	1.91
100	0.41	2.40	1.15	1.56	0.41	3.12
1000	2.42	2.58	1.47	2.10	0.44	4.01
10000	6.30	2.76	1.64	2.27	0.50	4.40

Especially at high energy, however, fluctuations are important and an accurate calculation requires a simulation that accounts for stochastic energy-loss processes [21].

Fig. 20.5 shows the vertical muon intensity versus depth. In constructing this "depth-intensity curve," each group has taken account of the angular distribution of the muons in the atmosphere, the map of the overburden at each detector, and the properties of the local medium in connecting measurements at various slant depths and zenith angles to the vertical intensity. Use of data from a range of angles allows a fixed detector to cover a wide range of depths. The flat portion of the curve is due to muons produced locally by charged-current interactions of ν_μ.

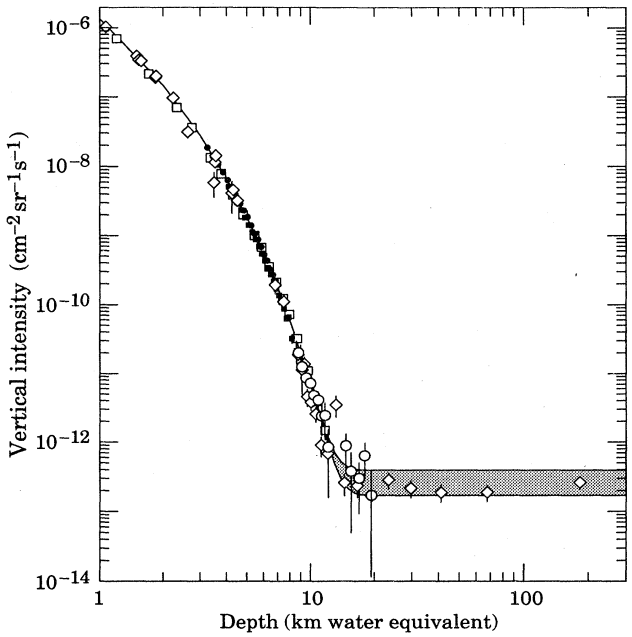

Figure 20.5: Vertical muon intensity *vs.* depth (1 km.w.e. = 10^5 g cm^{-2} of standard rock). The experimental data are from: ◇: the compilations of Crouch [29], □: Baksan [30], ○ : LVD [31], ● : MACRO [32], ■: Frejus [33]. The shaded area at large depths represents neutrino induced muons of energy above 2 GeV. The upper line is for horizontal neutrino-induced muons, the lower one for vertically upward muons.

The energy spectrum of atmospheric muons underground can be estimated from Eq. (20.7). The muon energy spectrum at slant depth X is

$$\frac{dN_\mu(X)}{dE_\mu} = \frac{dN_\mu}{dE_{\mu,0}}\,e^{bX}\,, \quad (20.8)$$

where $E_{\mu,0}$ is the solution of Eq. (20.7). For $X \ll b^{-1} \approx 2.5$ km water equivalent, $E_{\mu,0} \approx E_\mu(X) + aX$. Thus at shallow depths the differential muon energy spectrum is approximately constant for

$E_\mu < aX$ and steepens to reflect the surface muon spectrum for $E_\mu > aX$. For $X \gg b^{-1}$ the differential spectrum underground is again constant for small muon energies but steepens to reflect the surface muon spectrum for $E_\mu > \epsilon \approx 0.5$ TeV. In this regime the shape is independent of depth although the intensity decreases exponentially with depth.

20.4.2. ***Neutrinos***: Because neutrinos have small interaction cross sections, measurements of atmospheric neutrinos require a deep detector to avoid backgrounds. There are two types of measurements: contained (or semi-contained) events, in which the vertex is determined to originate inside the detector, and neutrino-induced muons. The latter are muons that enter the detector from zenith angles so large (*e.g.*, nearly horizontal or upward) that they cannot be muons produced in the atmosphere. In neither case is the neutrino flux measured directly. What is measured is a convolution of the neutrino flux and cross section with the properties of the detector (which includes the surrounding medium in the case of entering muons).

Contained events reflect the neutrinos in the GeV region where the product of increasing cross section and decreasing flux is maximum. In this energy region the neutrino flux and its angular distribution depend on the geomagnetic location of the detector and to a lesser extent on the phase of the solar cycle. Naively, we expect $\nu_\mu/\nu_e = 2$ from counting the neutrinos of the two flavors coming from the chain of pion and muon decay. This ratio is only slightly modified by the details of the decay kinematics. Experimental measurements have also to account for the ratio of $\overline{\nu}/\nu$, which have cross sections different by a factor of 3 in this energy range. In addition, detectors will generally have different efficiencies for detecting muon neutrinos and electron neutrinos. Even after correcting for these and other effects, some detectors [22,23] infer a ν_μ/ν_e ratio lower by $\approx 4\sigma$ from the expected value. (See Tables in the Particle Listings of this *Review*.) This effect is sometimes cited as possible evidence of neutrino oscillations and is a subject of current investigation. Figure 20.6 shows the data of Refs. 22,23 for the distributions of visible energy in electron-like and muon-like charged-current events, which appear to be nearly equal in number. Corrections for detection efficiencies and backgrounds are insufficient to account for the difference from the expected value of two.

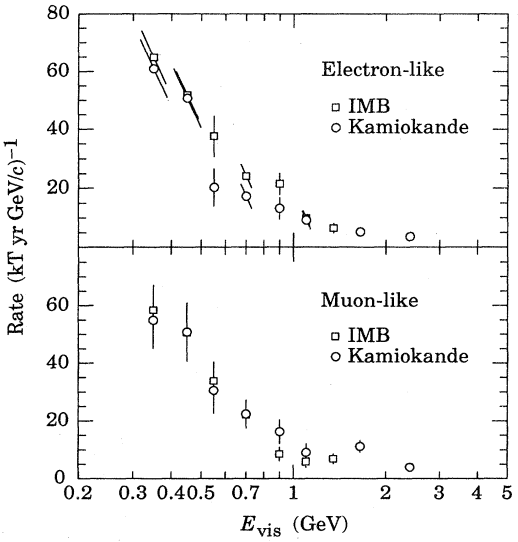

Figure 20.6: Contained neutrino interactions from IMB [23](□) and Kamiokande [22].

Muons that enter the detector from outside after production in charged-current interactions of neutrinos naturally reflect a higher energy portion of the neutrino spectrum than contained events because the muon range increases with energy as well as the cross section. The relevant energy range is $\sim 10 < E_\nu < 1000$ GeV, depending somewhat on angle. Like muons (see Eq. (20.5)), high energy neutrinos show a "secant theta" effect which causes the flux of horizontal neutrino induced muons to be approximately a factor two higher than the vertically upward flux. The upper and lower edges of the horizontal shaded region in Fig. 20.5 correspond to horizontal and vertical intensities of neutrino-induced muons. Table 20.3 gives the measured fluxes of neutrino induced muons.

Table 20.3: Measured fluxes (10^{-13} cm^{-2} s^{-1} sr^{-1}) of neutrino-induced muons as a function of the minimum muon energy E_μ.

$E_\mu >$	1 GeV	1 GeV	1 GeV	2 GeV	3 GeV
Ref.	CWI [24]	Baksan [25]	MACRO [26]	IMB [27]	Kam [28]
F_μ	2.17±0.21	2.77±0.17	2.48 ± 0.27	2.26±0.11	2.04±0.13

20.5. Air showers

So far we have discussed inclusive or uncorrelated fluxes of various components of the cosmic radiation. An air shower is caused by a single cosmic ray with energy high enough for its cascade to be detectable at the ground. The shower has a hadronic core, which acts as a collimated source of electromagnetic subshowers, generated mostly from $\pi^0 \to \gamma\gamma$. The resulting electrons and positrons are the most numerous particles in the shower. The number of muons, produced by decays of charged mesons, is an order of magnitude lower.

Air showers spread over a large area on the ground, and arrays of detectors operated for long times are useful for studying cosmic rays with primary energy $E_0 > 100$ TeV, where the low flux makes measurements with small detectors in balloons and satellites difficult.

Greisen [46] gives the following approximate expressions for the numbers and lateral distributions of particles in showers at ground level. The total number of muons N_μ with energies above 1 GeV is

$$N_\mu(> 1 \text{ GeV}) \approx 0.95 \times 10^5 \left(\frac{N_e}{10^6}\right)^{3/4} , \tag{20.9}$$

where N_e is the total number of charged particles in the shower (not just $e^\pm$). The number of muons per square meter, ρ_μ, as a function of the lateral distance r (in meters) from the center of the shower is

$$\rho_\mu = \frac{1.25\, N_\mu}{2\pi\, \Gamma(1.25)} \left(\frac{1}{320}\right)^{1.25} r^{-0.75} \left(1 + \frac{r}{320}\right)^{-2.5} , \tag{20.10}$$

where Γ is the gamma function. The number density of charged particles is

$$\rho_e = C_1(s, d, C_2)\, x^{(s-2)}(1+x)^{(s-4.5)}(1 + C_2 x^d) . \tag{20.11}$$

Here s, d, and C_2 are parameters in terms of which the overall normalization constant $C_1(s, d, C_2)$ is given by

$$C_1(s, d, C_2) = \frac{N_e}{2\pi r_1^2} \left[B(s, 4.5 - 2s) + C_2\, B(s + d,\, 4.5 - d - 2s)\right]^{-1} , \tag{20.12}$$

where $B(m, n)$ is the beta function. The values of the parameters depend on shower size (N_e), depth in the atmosphere, identity of the primary nucleus, etc. For showers with $N_e \approx 10^6$ at sea level, Greisen uses $s = 1.25$, $d = 1$, and $C_2 = 0.088$. Finally, x is r/r_1, where r_1 is the Molière radius, which depends on the density of the atmosphere and hence on the altitude at which showers are detected. At sea level $r_1 \approx 78$ m. It increases with altitude.

The lateral spread of a shower is determined largely by Coulomb scattering of the many low-energy electrons and is characterized by

the Moliere radius. The lateral spread of the muons (ρ_μ) is larger and depends on the transverse momenta of the muons at production as well as multiple scattering.

There are large fluctuations in development from shower to shower, even for showers of the same energy and primary mass—especially for small showers, which are usually well past maximum development when observed at the ground. Thus the shower size N_e and primary energy E_0 are only related in an average sense, and even this relation depends on depth in the atmosphere. One estimate of the relation is [35]

$$E_0 \sim 3.9 \times 10^6 \text{ GeV } (N_e/10^6)^{0.9} \qquad (20.13)$$

for vertical showers with $10^{14} < E < 10^{17}$ eV at 920 g cm^{-2} (965 m above sea level). Because of fluctuations, N_e as a function of E_0 is not the inverse of Eq. (20.13). As E_0 increases the shower maximum (on average) moves down into the atmosphere and the relation between N_e and E_0 changes. At the maximum of shower development, there are approximately 2/3 particles per GeV of primary energy.

Detailed simulations and cross-calibrations between different types of detectors are necessary to establish the primary energy spectrum from air-shower experiments [35,36]. Figure 20.7 shows the "all-particle" spectrum. In establishing this spectrum, efforts have been made to minimize the dependence of the analysis on the primary composition. In the energy range above 10^{17} eV, the Fly's Eye technique [48] is particularly useful because it can establish the primary energy in a model-independent way by observing most of the longitudinal development of each shower, from which E_0 is obtained by integrating the energy deposition in the atmosphere.

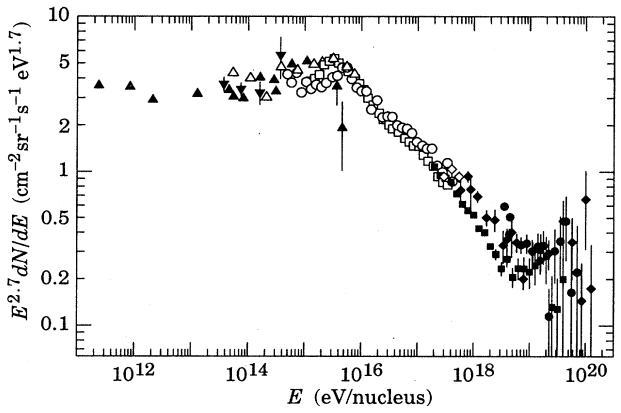

Figure 20.7: The all-particle spectrum: ▲ [37], ▼ [38], △ [39], □ [40], ○ [35], ■ [48], ● [42], ♦ [43].

In Fig. 20.7 the differential energy spectrum has been multiplied by $E^{2.7}$ in order to display the features of the steep spectrum that are otherwise difficult to discern. The steepening that occurs between 10^{15} and 10^{16} eV is known as the *knee* of the spectrum. The feature between 10^{18} and 10^{19} eV is called the *ankle* of the spectrum. Both these features are the subject of intense interest at present [44].

The *ankle* has the classical characteristic shape [45] of a higher energy population of particles overtaking a lower energy population. A possible interpretation is that the higher energy population represents cosmic rays of extragalactic origin. If this is the case and if the cosmic rays are cosmological in origin, then there should be a cutoff around 5×10^{19} eV, resulting from interactions with the microwave background [46,47]. It is therefore of special interest that several events have been assigned energies above 10^{20} eV [48,49,50].

If the cosmic ray spectrum below 10^{18} eV is of galactic origin, the *knee* could reflect the fact that some (but not all) cosmic accelerators have reached their maximum energy. Some types of expanding supernova remnants, for example, are estimated not to be able to accelerate particles above energies in the range of 10^{15} eV total energy per particle. Effects of propagation and confinement in the galaxy [51] also need to be considered.

References:

1. J.A. Simpson, Ann. Rev. Nucl. & Particle Sci. **33**, 323 (1983).
2. Dietrich Müller & Kwok-Kwong Tang, Astrophys. J. **312**, 183 (1987).
3. J.J. Engelmann *et al.*, Astron. & Astrophys. **233**, 96 (1990);
   See also *Cosmic Abundances of Matter* (ed. C. Jake Waddington) A.I.P. Conf. Proceedings No. 183 (1988) p. 111.
4. W.R. Webber, R.L. Golden and S.A. Stephens, in Proc. 20th Int. Cosmic Ray Conf. (Moscow) **1**, 325 (1987).
5. Several new experimental results on antiprotons and positrons were reported and published in the Proceedings of the 24th (Rome) **3** (1995). The positron results are: G. Basini *et al.*, p. 1, J.M. Clem *et al.*, p. 5, F. Aversa *et al.*, p. 9 and G. Tarlé *et al.*, p. 17 (See also S.W. Barwick *et al.*, Phys. Rev. Lett. **75**, 3909 (1995)). The antiproton results are: M. Hof *et al.*, p. 60, A.W. Labrador *et al.*, p. 64, J.W. Mitchell *et al.*, p. 72 and S. Orito *et al.*, p. 76.
6. D.H. Perkins, Astropart. Phys. **2**, 249 (1994).
7. R. Bellotti *et al.*, Phys. Rev. **D53**, 35 (1996).
8. T.K. Gaisser, *Cosmic Rays and Particle Physics*, Cambridge University Press (1990).
9. M.P. De Pascale *et al.*, J. Geophys. Res. **98**, 3501 (1993).
10. K. Allkofer & P.K.F. Grieder, *Cosmic Rays on Earth*, Fachinformationszentrum, Karlsruhe (1984).
11. S. Hayakawa, *Cosmic Ray Physics*, Wiley, Interscience, New York (1969).
12. O.C. Allkofer, K. Carstensen and W.D. Dau, Phys. Lett. **B36**, 425 (1971).
13. B.C. Rastin, J. Phys. **G10**, 1609 (1984).
14. C.A. Ayre *et al.*, J. Phys. **G1**, 584 (1975).
15. I.P. Ivanenko *et al.*, Proc. 19th Int. Cosmic Ray Conf. (La Jolla) **8**, 210 (1985).
16. H. Jokisch *et al.*, Phys. Rev. **D19**, 1368 (1979).
17. F. Halzen, R. Vázquez and E. Zas, Astropart. Phys. **1**, 297 (1993).
18. R.R. Daniel and S.A. Stephens, Revs. Geophysics & Space Sci. **12**, 233 (1974).
19. K.P. Beuermann and G. Wibberenz, Can. J. Phys. **46**, S1034 (1968).
20. I.S. Diggory *et al.*, J. Phys. **A7**, 741 (1974).
21. Paolo Lipari & Todor Stanev, Phys. Rev. **D44**, 3543 (1991).
22. K.S. Hirata *et al.*, (Kam-II Collaboration), Phys. Lett. **B280**, 146 (1992);
    Y. Fukuda *et al.*, Phys. Lett. **B335**, 237 (1994).
23. R. Becker-Szendy *et al.*, (IMB Collaboration), Phys. Rev. **D46**, 3720 (1992);
    See also D. Casper *et al.*, Phys. Rev. Lett. **66**, 2561 (1991).
24. F. Reines *et al.*, Phys. Rev. Lett. **15**, 429 (1965).
25. M.M. Boliev *et al.*, in Proceedings 3rd Int. Workshop on Neutrino Telescopes (ed. Milla Baldo Ceolin), 235 (1991).
26. D. Michael *et al.*, (MACRO) Nucl. Phys. **B35**, 235 (1994) (TAUP-93).
27. R. Becker-Szendy *et al.*, Phys. Rev. Lett. **69**, 1010 (1992);
    Proc. 25th Int. Conf. High-Energy Physics (Singapore, ed. K.K. Phua & Y. Yamaguchi, World Scientific, 1991) p. 662.
28. M. Mori *et al.*, Phys. Lett. **B210**, 89 (1991).
29. M. Crouch, in Proc. 20th Int. Cosmic Ray Conf. (Moscow) **6**, 165 (1987).
30. Yu.M. Andreev, V.I. Gurentzov and I.M. Kogai, in Proc. 20th Int. Cosmic Ray Conf. (Moscow) **6**, 200 (1987).
31. M. Aglietta *et al.*(LVD Collaboration), Astropart. Phys. **3**, 311 (1995).

32. M. Ambrosio *et al.*(MACRO Collaboration), Phys. Rev. **D52**, 3793 (1995).
33. Ch. Berger *et al.*(Frejus Collaboration), Phys. Rev. **D40**, 2163 (1989).
34. K. Greisen, Ann. Rev. Nucl. Sci. **10**, 63 (1960).
35. M. Nagano *et al.*, J. Phys. **G10**, 1295 (1984).
36. M. Teshima *et al.*, J. Phys. **G12**, 1097 (1986).
37. N.L. Grigorov *et al.*, Yad. Fiz. **11**, 1058 (1970) and Proc. 12th Int. Cosmic Ray Conf. (Hobart) **2**, 206 (1971).
38. K. Asakimori *et al.*, Proc. 23rd Int. Cosmic Ray Conf. (Calgary) **2**, 25 (1993);
    Proc. 22nd Int. Cosmic Ray Conf. (Dublin) **2**, 57 and 97 (1991).
39. T.V. Danilova *et al.*, Proc. 15th Int. Cosmic Ray Conf. (Plovdiv) **8**, 129 (1977).
40. Yu. A. Fomin *et al.*, Proc. 22nd Int. Cosmic Ray Conf. (Dublin) **2**, 85 (1991).
41. D.J. Bird *et al.*, Astrophys. J. **424**, 491 (1994).
42. S. Yoshida *et al.*, Astropart. Phys. **3**, 105 (1995).
43. M.A. Lawrence, R.J.O. Reid and A.A. Watson, J. Phys. **G17**, 773 (1991).
44. The most recent discussion is contained in Proc. 24th Int. Cosmic Ray Conf. (Rome) **2**, (1995) as well as the rapporteur talk of S. Petrera at the same conference (to be published). Some important information and discussion can also be found in [50] (World Scientific, Singapore, to be published).
45. B. Peters, Nuovo Cimento **22**, 800 (1961).
46. K. Greisen, Phys. Rev. Lett. **16**, 748 (1966).
47. G.T. Zatsepin and V.A. Kuz'min, Sov. Phys. JETP Lett. **4**, 78 (1966).
48. D.J. Bird *et al.*, Astrophys. J. **441**, 144 (1995).
49. N. Hayashima *et al.*, Phys. Rev. Lett. **73**, 3941 (1994).
50. A.A. Watson, *Proc. of the 1994 Summer Study on Nuclear and Particle Astrophysics and Cosmology for the Next Millenium*, Snowmass CO, 1994, ed. by E.W. Kolb *et al.* (World Scientific, Singapore, to be published, 1996).
51. V.S. Ptustkin *et al.*, Astron. & Astrophys. **268**, 726 (1993).

36. PLOTS OF CROSS SECTIONS AND RELATED QUANTITIES

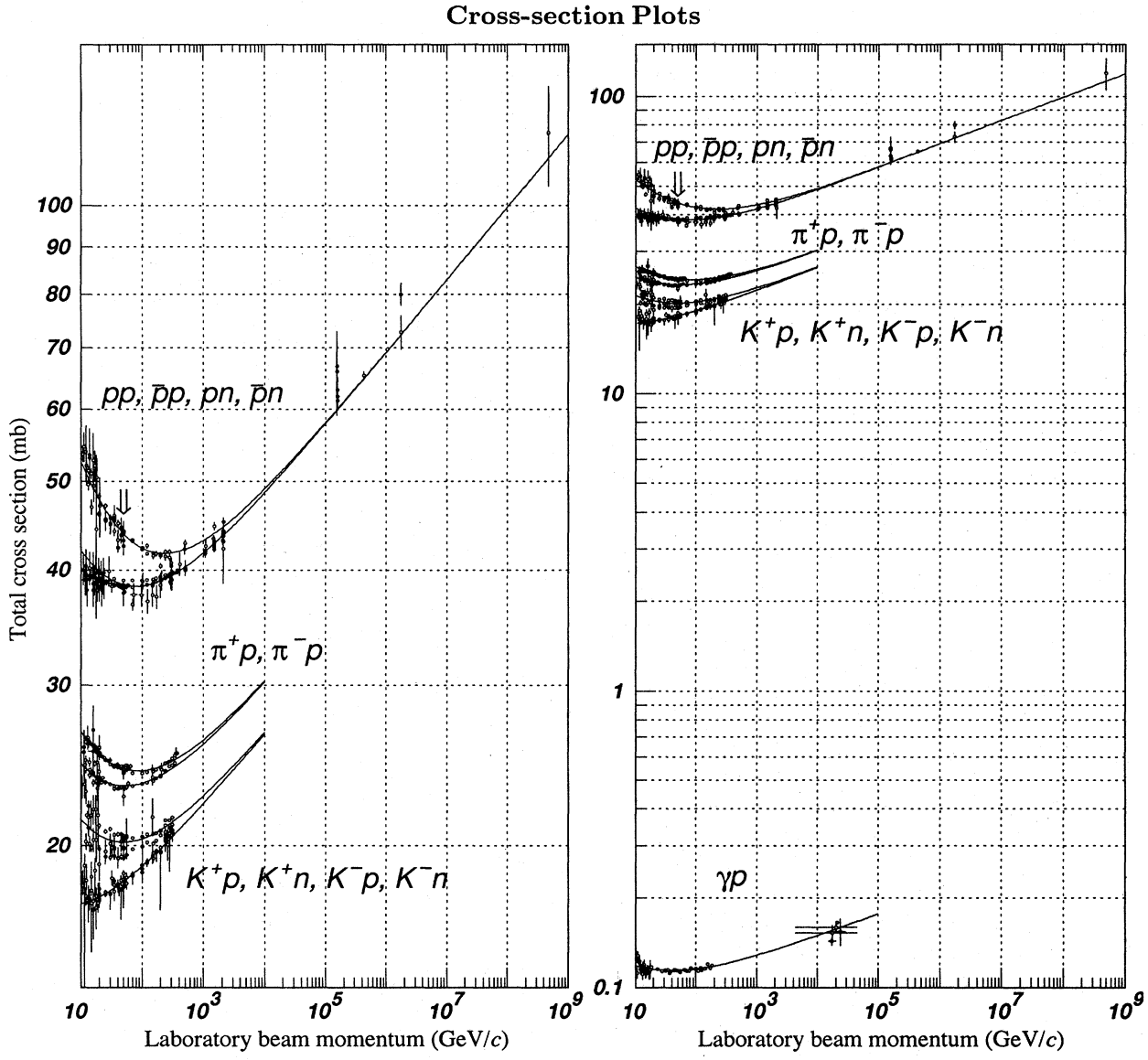

Figure 36.17: Summary of hadron-nucleon and γp total cross sections. Simple Regge pole fits of the form $\sigma_{\rm tot} = X\,s^{\epsilon} + y\,s^{-\eta}$ are shown. (Courtesy of the COMPAS Group, IHEP, Protvino, Russia, 1966.)

RARE KAON DECAYS

(by L. Littenberg, BNL and G. Valencia, Iowa State University)

A. Introduction: There are several recent reviews on rare kaon decays and related topics [1–13]. The current activity in rare kaon decays can be divided roughly into four categories:

1. Searches for explicit violations of the Standard Model
2. Measurements of Standard Model parameters
3. Searches for CP violation
4. Studies of strong interactions at low energy.

The paradigm of Category 1 is the lepton flavor violating decay $K_L \to \mu e$. Category 2 includes processes such as $K^+ \to \pi^+\nu\overline{\nu}$, which is sensitive to $|V_{td}|$. Much of the interest in Category 3 is focussed on the decays $K_L \to \pi^0\ell\overline{\ell}$, where $\ell \equiv e, \mu, \nu$. Category 4 includes reactions like $K^+ \to \pi^+\ell^+\ell^-$ which constitute a testing ground for the ideas of chiral perturbation theory. Other reactions of this type are $K_L \to \pi^0\gamma\gamma$, which also scales a CP-conserving background to CP violation in $K_L \to \pi^0\ell^+\ell^-$ and $K_L \to \gamma\ell^+\ell^-$, which could possibly shed light on long distance contributions to $K_L \to \mu^+\mu^-$.

B. Explicit violations of the Standard Model: Most of the activity here is in searches for lepton flavor violation (LFV). This is motivated by the fact that many extensions of the minimal Standard Model violate lepton flavor and by the potential to access very high scales. For example, the tree-level exchange of a LFV vector boson of mass M_X that couples to left-handed fermions with electroweak strength and without mixing angles yields $\mathrm{B}(K_L \to \mu e) = 3.3\times10^{-11}(91\ \mathrm{TeV}/M_X)^4$ [7]. This simple dimensional analysis may be used to read from Table 1 that the reaction $K_L \to \mu e$ is already probing scales of nearly 100 TeV. Table 1 summarizes the present experimental situation vis a vis LFV, along with the expected near-future progress. The decays $K_L \to \mu^\pm e^\mp$ and $K^+ \to \pi^+ e^\mp \mu^\pm$ (or $K_L \to \pi^0 e^\mp \mu^\pm$) provide complementary information on potential family number violating interactions since the former is sensitive to axial-vector (or pseudoscalar) couplings and the latter is sensitive to vector (or scalar) couplings.

Table 1: Searches for lepton flavor violation in K decay

Mode	90% CL upper limit	Exp't	Yr./Ref.	(Near-) future aim
$K^+ \to \pi^+ e\mu$	2.1E-10	BNL-777	90/14	3E-12 (BNL-865)
$K_L \to \mu e$	3.3E-11	BNL-791	93/15	2E-12 (BNL-871)
$K_L \to \pi^0 \mu e$	3.5E-9	FNAL-799	94/16	E-11 (FNAL799II)

Another forbidden decay currently being pursued is $K^+ \to \pi^+ X^0$, where X^0 is a very light, noninteracting particle (*e.g.* hyperphoton, axion, familon, etc.). The published upper limit on this process [17] is 1.7×10^{-9}, but recently this has been improved to 5.2×10^{-10} [18]. Data already collected by BNL-787 are expected to yield another substantial factor in sensitivity to this process.

C. Measurements of Standard Model parameters: Until recently searches for $K^+ \to \pi^+\nu\overline{\nu}$ have been motivated by the possibility of observing non-SM physics because the sensitivity attained was far short of the SM prediction for this decay [19] and long-distance contributions were known to be negligible [3,20]. However, BNL-787 is approaching the sensitivity at which the observation of an event could no longer be unambiguously attributed to non-SM physics. The published 90% c.l. upper limit [17] is 5.2×10^{-9}, but this has been recently improved to 2.4×10^{-9} [18], and extensive recent running with an upgraded beam and detector is expected to further improve this significantly. This reaction is now becoming interesting from the point of view of constraining SM parameters where the branching ratio is expected to be of order 10^{-10}, and can be written as [3]:

$$\mathrm{B}(K^+ \to \pi^+\nu\overline{\nu}) = \frac{\alpha^2 \mathrm{B}(K^+ \to \pi^o e^+\nu)}{V_{us}^2 2\pi^2 \sin^4\theta_W} \times \sum_{l=e,\mu,\tau} |V_{cs}^* V_{cd} X_{NL}^\ell + V_{ts}^* V_{td} X(m_t)|^2 \quad (1)$$

where $X(m_t)$ is of order 1, and X_{NL}^ℓ is several hundred times smaller. This form exhibits the strong dependence of this branching ratio on $|V_{td}|$. It also makes manifest the fact that the *a priori* unknown hadronic matrix element drops out in the comparison to the very well-measured rate of K_{e3} decay. QCD corrections, which are contained in X_{NL}^ℓ, are relatively small and now known [21] to $\leq 10\%$. Evaluating the constants in Eq. (1) with $m_t = 175$ GeV, one can cast this result in terms of the CKM parameters A, ρ and η (see our Section on "The Cabibbo-Kobayashi-Maskawa mixing matrix") [21].

$$\mathrm{B}(K^+ \to \pi^+\nu\overline{\nu}) \approx 1.2 \times 10^{-10} A^4 [\eta^2 + \frac{2}{3}(\rho_o^e - \rho)^2 + \frac{1}{3}(\rho_o^\tau - \rho)^2] \quad (2)$$

where $\rho_o^\ell \equiv 1 + \frac{X_{NL}^\ell}{A^2\lambda^4 X(m_t)}$. Thus, $\mathrm{B}(K^+ \to \pi^+\nu\overline{\nu})$ determines a circle in the ρ, η plane with center $(\rho_o, 0)$; $\rho_o \equiv \frac{2}{3}\rho_o^e + \frac{1}{3}\rho_o^\tau \approx 1.4$, and radius $\approx \frac{1}{A^2}\sqrt{\frac{\mathrm{B}(K^+\to\pi^+\nu\overline{\nu})}{1.2\times10^{-10}}}$.

The decay $K_L \to \mu^+\mu^-$ also has a short distance contribution sensitive to the CKM parameter ρ. For $m_t = 175$ GeV it is given by [21]:

$$\mathrm{B}_{\mathrm{SD}}(K_L \to \mu^+\mu^-) \approx 1.9 \times 10^{-9} A^4 (\rho_o' - \rho)^2 \quad (3)$$

where ρ_o' depends on the charm quark mass and is around 1.2. This decay, however, is dominated by a long-distance contribution from a two-photon intermediate state. The absorptive (imaginary) part of the long-distance component is calculated in terms of the measured rate for $K_L \to \gamma\gamma$ to be $\mathrm{B}_{\mathrm{abs}}(K_L \to \mu^+\mu^-) = (6.8 \pm 0.3) \times 10^{-9}$; and it almost completely saturates the observed rate $\mathrm{B}(K_L \to \mu^+\mu^-) = (7.2 \pm 0.5) \times 10^{-9}$ listed in the current edition. The difference between the observed rate and the absorptive component can be attributed to the (coherent) sum of the short-distance amplitude and the real part of the long-distance amplitude. In order to use this mode to constrain ρ it is, therefore, necessary to know the real part of the long-distance contribution. Unlike the absorptive part, the real part of the long-distance contribution cannot be derived from the measured rate for $K_L \to \gamma\gamma$. At present, it is not possible to compute this long-distance component reliably and, therefore, it is not possible to constrain ρ from this mode. It is expected that studies of the reactions $K_L \to \ell^+\ell^-\gamma$, and $K_L \to \ell^+\ell^-\ell'^+\ell'^-$ for $\ell, \ell' = e$ or μ will improve our understanding of the long distance effects in $K_L \to \mu^+\mu^-$ (the current data is parameterized in terms of α_K^*, discussed in the Form Factors section of the K_L^0 Particle Properties Listings).

D. Searches for CP violation: The mode $K_L \to \pi^0\nu\overline{\nu}$ is dominantly CP-violating and free of hadronic uncertainties [3,22]. The Standard Model predicts a branching ratio of order 10^{-10}; for $m_t = 175$ GeV it is given approximately by [21]:

$$\mathrm{B}(K_L \to \pi^0\nu\overline{\nu}) \approx 5 \times 10^{-10} A^4 \eta^2 \,. \quad (4)$$

The current upper bound is $B(K_L \to \pi^0\nu\bar{\nu}) \leq 5.8 \times 10^{-5}$ [23] and FNAL799II (KTeV) is expected to place a bound of order 10^{-8} [24].

The decay $K_L \to \pi^0 e^+ e^-$ also has sensitivity to the product $A^4\eta^2$. It has a direct CP-violating component that depends on the value of the top-quark mass, and that for $m_t = 175$ GeV is given by [25]:

$$B_{dir}(K_L \to \pi^0 e^+ e^-) \approx 7 \times 10^{-11} A^4 \eta^2 \ . \quad (5)$$

However, like $K_L \to \mu^+\mu^-$ this mode suffers from large theoretical uncertainties due to long distance strong interaction effects. It has an indirect CP-violating component given by:

$$B_{ind}(K_L \to \pi^0 e^+ e^-) = |\epsilon|^2 \frac{\tau_{K_L}}{\tau_{K_S}} B(K_S \to \pi^0 e^+ e^-) \ , \quad (6)$$

that has been estimated to be less than 10^{-12} [26], but that will not be known precisely until a measurement of $K_S \to \pi^0 e^+ e^-$ is available [6,27]. There is also a CP-conserving component dominated by a two-photon intermediate state that cannot be computed reliably at present. This component has an absorptive part that can be, in principle, determined from a detailed analysis of $K_L \to \pi^0\gamma\gamma$.

An analysis of $K_L \to \pi^0\gamma\gamma$ within chiral perturbation theory has been carried out in terms of a parameter a_V [28,29] that determines both the rate and the shape of the distribution $d\Gamma/dm_{\gamma\gamma}$. A fit to the distribution has given $-0.32 < a_V < 0.19$ [30]; a value that suggests that the absorptive part of the CP-conserving contribution to $K_L \to \pi^0 e^+ e^-$ is significantly smaller than the direct CP-violating component [30]. However, there remains some uncertainty in the interpretation of $K_L \to \pi^0\gamma\gamma$ in terms of a_V. Analyses that go beyond chiral perturbation theory have found larger values of a_V, indicating a sizable CP-conserving component for $K_L \to \pi^0 e^+ e^-$. The real part of the CP-conserving contribution to $K_L \to \pi^0 e^+ e^-$ is also unknown.

Finally, BNL-845 observed a potential background to $K_L \to \pi^0 e^+ e^-$ from the decay $K_L \to \gamma\gamma e^+ e^-$ [31]. This was later confirmed with an order of magnitude larger sample by FNAL-799 [32], which measured additional kinematic quantities. It has been estimated that this background will enter at the level of 10^{-11} [33], comparable to the signal level. Because of this, the observation of $K_L \to \pi^0 e^+ e^-$ will depend on background subtraction with good statistics.

The current upper bound for the process $K_L \to \pi^0 e^+ e^-$ is 4.3×10^{-9} [34]. For the closely related muonic process, the upper bound is $B(K_L \to \pi^0\mu^+\mu^-) \leq 5.1 \times 10^{-9}$ [35]. FNAL799II expects to reach a sensitivity $\lesssim 10^{-11}$ for both reactions [36].

E. Other long distance dominated modes: The decays $K^+ \to \pi^+\ell^+\ell^-$ ($\ell = e$ or μ) are described by chiral perturbation theory in terms of one parameter, ω^+ [37]. This parameter determines both the rate and distribution $d\Gamma/dm_{\ell\ell}$ for these processes. A careful study of these two reactions can provide a measurement of ω^+ and a test of the chiral perturbation theory description. A simultaneous fit to the rate and spectrum of $K^+ \to \pi^+ e^+ e^-$ gives: $\omega^+ = 0.89^{+0.24}_{-0.14}$; $B(K^+ \to \pi^+ e^+ e^-) = (2.99 \pm 0.22) \times 10^{-7}$ [38]. These two results satisfy the prediction of chiral perturbation theory within two standard deviations [6]. Improved statistics for this mode and a measurement of the mode $K^+ \to \pi^+\mu^+\mu^-$ are thus desired. BNL-787 has observed the process $K^+ \to \pi^+\mu^+\mu^-$ [39] at about the predicted level, but the result is not yet accurate enough to provide additional constraints.

References

1. W. Marciano, Rare Decay Symposium, Ed. D. Bryman *et al.*, World Scientific 1 (1988).
2. D. Bryman, Int. J. Mod. Phys. **A4**, 79 (1989).
3. J. Hagelin and L. Littenberg, Prog. in Part. Nucl. Phys. **23**, 1 (1989).
4. A. Buras and M. Harlander, *Review Volume on Heavy Flavors*, ed. A. Buras and M. Lindner, World Scientific, Singapore (1992).
5. R. Battiston *et al.*, Phys. Reports **214**, 293 (1992).
6. L.Littenberg and G. Valencia, Ann. Rev. Nucl. and Part. Sci. **43**, 729 (1993).
7. J. Ritchie and S. Wojcicki, Rev. Mod. Phys. **65**, 1149 (1993).
8. U. Meissner, Rept. on Prog. in Phys. **56**, 903 (1993).
9. B. Winstein and L. Wolfenstein, Rev. Mod. Phys. **65**, 1113 (1993).
10. N. Bilic and B. Guberina, Fortsch. Phys. **42**, 209 (1994).
11. G. D'Ambrosio, G. Ecker, G. Isidori and H. Neufeld, *Radiative Non-Leptonic Kaon Decays*, in The DAΦNE Physics Handbook (second edition), eds. L. Maiani, G. Pancheri and N. Paver (Frascati), Vol. I, 265 (1995).
12. E. de Rafael, *Chiral Lagrangians and Kaon CP Violation*, in *CP Violation and the Limits of the Standard Model*, Proc. TASI'94, ed. J.F. Donoghue (World Scientific, Singapore, 1995).
13. A. Pich, Rept. on Prog. in Phys. **58**, 563 (1995).
14. A. M Lee *et al.*, Phys. Rev. Lett. **64**, 165 (1990).
15. K. Arisaka *et al.*, Phys. Rev. Lett. **70**, 1049 (1993).
16. P. Gu, Albuquerque DPF Workshop, 1994.
17. M.S. Atiya *et al.*, Phys. Rev. Lett. **70**, 2521 (1993).
18. S. Adler *et al.*, Phys. Rev. Lett. **76**, 1421 (1996).
19. I. Bigi and F. Gabbiani, Nucl. Phys. **B367**, 3 (1991).
20. D. Rein and L.M. Sehgal, Phys. Rev. **D39**, 3325 (1989); M. Lu and M.B. Wise, Phys. Lett. **B324**, 461 (1994).
21. G. Buchalla and A. Buras, Nucl. Phys. **B412**, 106 (1994).
22. L. Littenberg, Phys. Rev. **D39**, 3322 (1989).
23. M. Weaver *et al.*, Phys. Rev. Lett. **72**, 3758 (1994).
24. M. Weaver, "The Albuquerque Meeting", Ed. S. Seidel, World Scientific, 1026 (1995).
25. A. Buras *et al.*, Nucl. Phys. **B423**, 349 (1994).
26. G. Ecker, A. Pich and E. de Rafael, Nucl. Phys. **B303**, 665 (1988).
27. J.F. Donoghue and F. Gabbiani, Phys. Rev. **D51**, 2187 (1995).
28. G. Ecker, A. Pich and E. de Rafael, Phys. Lett. **189B**, 363 (1987).
29. G. Ecker, A. Pich and E. de Rafael, Phys. Lett. **237B**, 481 (1990).
30. G.D. Barr *et al.*, Phys. Lett. **242B**, 523 (1990); G.D. Barr *et al.*, Phys. Lett. **284B**, 440 (1992).
31. W.M. Morse *et al.*, Phys. Rev. **D45**, 36 (1992).
32. T. Nakaya *et al.*, Phys. Rev. Lett. **73**, 2169 (1994).
33. H.B. Greenlee, Phys. Rev. **D42**, 3724 (1990).
34. D.A. Harris *et al.*, Phys. Rev. Lett. **71**, 3918 (1993).
35. D.A. Harris *et al.*, Phys. Rev. Lett. **71**, 3914 (1993).
36. "Heavy Flavor Physics and CP Violation", in *Particle Physics - Perspectives and Opportunities, Report of the DPF Committee on Long-Term Planning*, Ed. R. Peccei *et al.*, 91 (1995).
37. G. Ecker, A. Pich and E. de Rafael, Nucl. Phys. **B291**, 692 (1987).
38. C. Alliegro *et al.*, Phys. Rev. Lett. **68**, 278 (1992).
39. J.S. Haggerty, *Proceedings of the XXVII International Conference on High Energy Physics*, Ed. P.J. Bussey and I.G. Knowles, 1341 (1995); M. Ardebili, Ph D. thesis, Princeton University (1995).

13. *CP* VIOLATION

This section prepared April 1994 by L. Wolfenstein.

The symmetries C (particle-antiparticle interchange) and P (space inversion) hold for strong and electromagnetic interactions. After the discovery of large C and P violation in the weak interactions, it appeared that the product CP was a good symmetry. Then CP violation was observed in K^0 decays at a level given by the parameter $\epsilon = 2.3 \times 10^{-3}$. Larger CP-violation effects are anticipated in B^0 decays.

The eigenstates of the K^0–$\overline{K}^0$ system can be written

$$|K_S\rangle = p|K^0\rangle + q|\overline{K}^0\rangle \ , \qquad |K_L\rangle = p|K^0\rangle - q|\overline{K}^0\rangle \ . \tag{13.1}$$

If CP invariance held, we would have $q = p$ so that K_S would be CP even and K_L CP odd. (We define $|\overline{K}^0\rangle$ as $CP\ |K^0\rangle$). CP violation in K^0–$\overline{K}^0$ mixing gives

$$\frac{p}{q} = \frac{(1+\widetilde{\epsilon})}{(1-\widetilde{\epsilon})} \ . \tag{13.2}$$

CP violation can also occur in the decay amplitudes

$$A\big(K^0 \to \pi\pi(I)\big) = A_I e^{i\delta_I} \ , \qquad A\big(\overline{K}^0 \to \pi\pi(I)\big) = A_I^* e^{i\delta_I} \ , \tag{13.3}$$

where I is the isospin of $\pi\pi$, δ_I is the final-state phase shift, and A_I would be real if CP invariance held. The ratios of CP-violating to CP-conserving amplitudes $\eta_{+-} = A(K_L^0 \to \pi^+\pi^-)/A(K_S^0 \to \pi^+\pi^-)$ and $\eta_{00} = A(K_L^0 \to \pi^0\pi^0)/A(K_S^0 \to \pi^0\pi^0)$ can be written as

$$\eta_{+-} = \epsilon + \epsilon' \ , \qquad \eta_{00} = \epsilon - 2\epsilon' \ , \tag{13.4a}$$

$$\epsilon = \widetilde{\epsilon} + i\ (\mathrm{Im}\ A_0/\mathrm{Re}\ A_0) \ , \tag{13.4b}$$

$$|\sqrt{2}\epsilon'| = (\mathrm{Re}\ A_2/\mathrm{Re}\ A_0)\ (\mathrm{Im}\ A_2/\mathrm{Re}\ A_2 - \mathrm{Im}\ A_0/\mathrm{Re}\ A_0) \ . \tag{13.4c}$$

If CP violation is confined to the mass matrix, as in a superweak theory, ϵ' is zero and $\eta_{+-} = \eta_{00} = \epsilon = \widetilde{\epsilon}$. The measurement of ϵ'/ϵ has as its goal finding an effect that requires CP violation in the decay amplitude; this corresponds to a relative phase between A_2 and A_0 as seen in Eq. (13.4c).

In the Standard Model, CP violation arises as a result of a single phase entering the CKM matrix (q.v.). As a result in what is now the standard phase convention, two elements have large phases, $V_{ub} \sim e^{-i\gamma}$, $V_{td} \sim e^{-i\beta}$. Because these elements have small magnitudes and involve the third generation, CP violation in the K^0 system is small. A definite nonzero value for ϵ'/ϵ is expected but hadronic uncertainties allow theoretical values between 10^{-4} and 3×10^{-3}. On the other hand, large effects are expected in the B^0 system, which is a major motivation for B factories.

The most clearcut experiments would be those that measure asymmetries between B^0 and $\overline{B}^0$ decays. The time-dependent rate to a CP eigenstate a is given by

$$\Gamma_a \sim e^{-\Gamma t}\Big(\big[1+|r_a|^2\big] \pm \big[1-|r_a|^2\big]\ \cos(\Delta M t) \mp 2\eta_a \mathrm{Im}\ r_a\ \sin(\Delta M t)\Big) \ , \tag{13.5}$$

where the top sign is for B^0 and the bottom for $\overline{B}^0$, η_a is the CP eigenvalue and

$$r_a = (q_B/p_B)\ \overline{A}_a/A_a \ . \tag{13.6}$$

The quantity (q_B/p_B) comes from the analogue for B^0 of Eq. (13.1); however, for B^0 the eigenstates have a negligible lifetime difference and are distinguished only by the mass difference ΔM; also as a result $|q_B/p_B| \approx 1$ so that $\widetilde{\epsilon}_B$ is purely imaginary. A_a ($\overline{A}_a$) are the decay amplitudes to a for B^0 ($\overline{B}^0$). If only one quark weak transition contributes to the decay $|\overline{A}_a/A_a| = 1$ so that $|r_a| = 1$ and the $\cos(\Delta M t)$ term vanishes. The basic goal of the B factories is to observe the asymmetric $\sin(\Delta M t)$ term. For B^0 ($\overline{B}^0$) $\to \psi K_s$ from the transition $b \to c\bar{c}s$, one finds in the Standard Model the asymmetry parameter

$$-2\mathrm{Im}\ r_a = \sin 2\beta \ . \tag{13.7}$$

The asymmetry is given directly in terms of a CKM phase with no hadronic uncertainty and is expected to be between 0.2 and 0.8. For B^0 ($\overline{B}^0$) $\to \pi^+\pi^-$ from the transition $b \to u\bar{u}d$

$$-2\mathrm{Im}\ r_a = \sin 2(\beta+\gamma) \ . \tag{13.8}$$

(This result has some hadronic uncertainty due to penguin contributions, but these should be able to be estimated from other observations.) While either of these asymmetries could be ascribed to $B^0 - \overline{B}^0$ mixing (q_B/p_B or $\widetilde{\epsilon}_B$), the difference between the two asymmetries is evidence for direct CP violation. From Eq. (13.6) (with $\overline{A}_a/A_a = 1$) it is seen this corresponds to a phase difference between $A_{\psi K_S}$ and $A_{\pi^+\pi^-}$. Thus this is analogous to ϵ'. In the standard phase convention 2β in Eq. (13.7) and (13.8) arises from $B^0 - \overline{B}^0$ mixing whereas the 2γ comes from V_{bu} in the transition $b \to u\bar{u}d$.

CP violation in the decay amplitude is also revealed by the $\cos(\Delta M t)$ in Eq. (13.5) or by a difference in rates of B^+ and B^- to charge-conjugate states. These effects, however, require two contributing amplitudes to the decay (such as a tree amplitude plus a penguin) and also require final-state interaction phases. Predicted effects are very uncertain and are generally small.

For further details, see the notes on CP violation in the K_L^0, K_S^0, and B^0 Particle Listings of this *Review*.